

Water Science and Technology Library

Thirugnanasambandham Karchiyappan
Rama Rao Karri
Mohammad Hadi Dehghani *Editors*

Industrial Wastewater Treatment

Emerging Technologies
for Sustainability

 Springer

Water Science and Technology Library

Volume 106

Editor-in-Chief

V. P. Singh, Department of Biological and Agricultural Engineering & Zachry
Department of Civil and Environmental Engineering, Texas A&M University,
College Station, TX, USA

Editorial Board

R. Berndtsson, Lund University, Lund, Sweden

L. N. Rodrigues, Embrapa Cerrados, Brasília, Brazil

Arup Kumar Sarma, Department of Civil Engineering, Indian Institute of
Technology Guwahati, Guwahati, Assam, India

M. M. Sherif, Civil and Environmental Engineering Department, UAE University,
Al-Ain, United Arab Emirates

B. Sivakumar, School of Civil and Environmental Engineering, The University of
New South Wales, Sydney, NSW, Australia

Q. Zhang, Faculty of Geographical Science, Beijing Normal University, Beijing,
China

The aim of the *Water Science and Technology Library* is to provide a forum for dissemination of the state-of-the-art of topics of current interest in the area of water science and technology. This is accomplished through publication of reference books and monographs, authored or edited. Occasionally also proceedings volumes are accepted for publication in the series. *Water Science and Technology Library* encompasses a wide range of topics dealing with science as well as socio-economic aspects of water, environment, and ecology. Both the water quantity and quality issues are relevant and are embraced by *Water Science and Technology Library*. The emphasis may be on either the scientific content, or techniques of solution, or both. There is increasing emphasis these days on processes and *Water Science and Technology Library* is committed to promoting this emphasis by publishing books emphasizing scientific discussions of physical, chemical, and/or biological aspects of water resources. Likewise, current or emerging solution techniques receive high priority. Interdisciplinary coverage is encouraged. Case studies contributing to our knowledge of water science and technology are also embraced by the series. Innovative ideas and novel techniques are of particular interest.

Comments or suggestions for future volumes are welcomed.

Vijay P. Singh, Department of Biological and Agricultural Engineering & Zachry Department of Civil and Environment Engineering, Texas A & M University, USA
Email: vsingh@tamu.edu

All contributions to an edited volume should undergo standard peer review to ensure high scientific quality, while monographs should also be reviewed by at least two experts in the field.

Manuscripts that have undergone successful review should then be prepared according to the Publisher's guidelines manuscripts: <https://www.springer.com/gp/authors-editors/book-authors-editors/book-manuscript-guidelines>

More information about this series at <https://link.springer.com/bookseries/6689>

Thirugnanasambandham Karchiyappan ·
Rama Rao Karri · Mohammad Hadi Dehghani
Editors

Industrial Wastewater Treatment

Emerging Technologies for Sustainability

 Springer

Editors

Thirugnanasambandham Karchiyappan
Department of Molecular Engineering
Lodz University of Technology
Lodz, Poland

Rama Rao Karri
Petroleum and Chemical Engineering
Universiti Teknologi Brunei
Bandar Seri Begawan, Brunei Darussalam

Mohammad Hadi Dehghani
Department of Environmental Health
Engineering, School of Public Health
and Institute for Environmental Research
Center for Solid Waste Research
Tehran University of Medical Sciences
Tehran, Iran

ISSN 0921-092X

ISSN 1872-4663 (electronic)

Water Science and Technology Library

ISBN 978-3-030-98201-0

ISBN 978-3-030-98202-7 (eBook)

<https://doi.org/10.1007/978-3-030-98202-7>

© The Editor(s) (if applicable) and The Author(s), under exclusive license to Springer Nature Switzerland AG 2022

This work is subject to copyright. All rights are solely and exclusively licensed by the Publisher, whether the whole or part of the material is concerned, specifically the rights of translation, reprinting, reuse of illustrations, recitation, broadcasting, reproduction on microfilms or in any other physical way, and transmission or information storage and retrieval, electronic adaptation, computer software, or by similar or dissimilar methodology now known or hereafter developed.

The use of general descriptive names, registered names, trademarks, service marks, etc. in this publication does not imply, even in the absence of a specific statement, that such names are exempt from the relevant protective laws and regulations and therefore free for general use.

The publisher, the authors and the editors are safe to assume that the advice and information in this book are believed to be true and accurate at the date of publication. Neither the publisher nor the authors or the editors give a warranty, expressed or implied, with respect to the material contained herein or for any errors or omissions that may have been made. The publisher remains neutral with regard to jurisdictional claims in published maps and institutional affiliations.

This Springer imprint is published by the registered company Springer Nature Switzerland AG
The registered company address is: Gewerbestrasse 11, 6330 Cham, Switzerland

Contents

Recent Developments in Membrane Filtration for Wastewater Treatment	1
Muhammad Salman, Muhammad Shakir, and Muhammad Yaseen	
Spent Filter Backwash Water Treatment by Coagulation Followed by Ultrafiltration	27
K. Sukanya, N. Sivarajasekar, and K. Saranya	
Ultrafiltration Integrated Photocatalytic Treatment Systems for Water and Wastewater	41
C. Nirmala Rani and S. Karthikeyan	
Application of Electrospun Polymeric Nanofibrous Membranes for Water Treatment	75
Sankha Chakraborty, Jayato Nayak, and Prasenjit Chakraborty	
Biosorbents in Industrial Wastewater Treatment	101
Ali Nematollahzadeh and Zahra Vaseghi	
Nanoparticles in Industrial Wastewater Treatment: An Overview	133
Rekha Pachaiappan, Saravanan Rajendran, and Lorena Cornejo Ponce	
Green Magnetic Nanoparticles in Industrial Wastewater Treatment: An Overview	187
Laiza Bergamasco Beltran, Anna Carla Ribeiro, Elizabeth da Costa Neves Fernandes de Almeida Duarte, Rosângela Bergamasco, and Angélica Marquetotti Salcedo Vieira	
Nanocellulose in Industrial Wastewater Treatment: An Overview	209
Vartika Srivastava	
Synthesis and Applications of Polymer–Nano Clay Composites in Wastewater Treatment: A Review	237
Priyanka Pareek and Lalita Ledwani	

Polymeric Composites for Industrial Water Treatment: An Overview	257
Jordana Bortoluz, Mário César Vebber, Nayrim Brizuela Guerra, Janaina da Silva Crespo, and Marcelo Giovanela	
Optimisation and Modeling Approaches for the Textile Industry Water Treatment Plants	285
M. Magesh Kumar	
UV-Chlorination and Treatment of Oily Wastewater in Batch Ozone Reactor	309
Thirugnanasambandham Karchiyappan and Rama Rao Karri	
Sol-gel Synthesis of Kaolin/TiO₂ Nanocomposites for Photocatalytic Degradation of Tannery Wastewater	323
S. Mustapha, J. O. Tijani, T. C. Egbosiuba, A. Sumaila, T. A. Amigun, A. B. Salihu, Y. O. Ibrahim, M. M. Ndamitso, and S. A. Abdulkareem	
Microbial Biofilm Reactor for Sustained Waste Water Treatment and Reuse	345
Shaon Ray Chaudhuri	
Life Cycle Assessment of Emerging Technologies in Industrial Wastewater Treatment and Desalination	369
Arash Khosravi, Benyamin Bordbar, and Ali Ahmadi Orkomi	
Photoelectrochemical Water Treatment of Sewage	399
Priya Chandulal Vithalani and Nikhil Sumantray Bhatt	
Solar Energy in Water Treatment Processes—An Overview	421
Ashish Unnarkat, Ayush Bhavsar, Samyak Ostwal, Pancham Vashi, and Swapnil Dharaskar	
Quantification of Potential Savings in Drinking Water Treatment Plants: Benchmarking Energy Efficiency	447
Shalini Nakkasunchi	

About the Editors

Dr. Thirugnanasambandham Karchiyappan completed Ph.D. (Environmental Chemistry-Water purification) in Anna University, India. After that, he has worked as a Post-Doctoral Fellow in State University of Maringa (CAPES Postdoctoral Fellowship), Brazil; Sun Yat Sen University (NSF Postdoctoral Fellowship), China; and Dublin City University (Marie Curie Postdoctoral Fellowship), Ireland. Now, he is presently working as Post-Doctoral Fellow in department of molecular engineering, Lodz University of Technology, Lodz, Poland in Ulam NAWA project (PPN/U LM/2020/1/00017/U/00001/A/00001). Also, he is presently working as an Assistant Professor in Chemistry Department (Excel College of Engineering and Technology, Tamil Nadu, India) for about 8 months. During his Ph.D., he has worked in University Grants Commission (UGC)-Major Research Project. Overall, he has published more than 25 international journals. Also, he visited various countries like United Kingdom, Italy, and Denmark for career development.

Dr. Rama Rao Karri is a Professor (Sr. Asst) in the Faculty of Engineering, Universiti Teknologi Brunei, Brunei Darussalam. He has completed Ph.D. from the Indian Institute of Technology (IIT) Delhi, Masters from IIT Kanpur and BTech from Andhra University College of Engineering, Visakhapatnam, all in Chemical Engineering. He has worked as a Post-Doctoral Research Fellow at NUS, Singapore for about six years and has over 19 years of working experience in Academics, Industry, and Research. He has experience working in multidisciplinary fields and has expertise in various evolutionary optimization techniques and process modeling. He has published 100+ research articles in reputed journals, book chapters, and conference proceedings with a combined impact factor of 358.0 and has an h-index of 23 (Scopus, Citations: 1700+) and 25 (Google Scholar, Citations: 2100+). Among these publications, 60 are Q1 and high IF journals. He is an editorial board member in 10 renowned journals and a peer-review member for more than 93 reputed journals and peer-reviewed more than 400+ manuscripts. He is recipient of Publons Peer Reviewer Award as top 1% of global peer reviewers for Environment & Ecology and Crossfield categories for the year 2019. He is also delegating as an advisory board member for many international conferences. He held a position as Editor-in-Chief

(2019–2021) in the International Journal of Chemoinformatics and Chemical Engineering, IGI Global, USA. He is also an Associate Editor in Scientific Reports, Nature Group & International Journal of Energy and Water Resources (IJEWR), Springer Inc. He is also a Managing Guest Editor for Spl. Issues: 1) “Magnetic nanocomposites and emerging applications”, in Journal of Environmental Chemical Engineering (IF: 5.909), 2) “Novel CoronaVirus (COVID-19) in Environmental Engineering Perspective”, in Journal of Environmental Science and Pollution Research (IF: 4.223), Springer. and 3) “Nanocomposites for the Sustainable Environment”, in Applied Sciences Journal (IF: 2.679), MDPI. He along with his mentor, Prof. Venkateswarlu, has authored an Elsevier book, “Optimal state estimation for process monitoring, diagnosis and control”. He is also Co-Editor and Managing Editor for 10 Elsevier, 1 Springer, and 1 CRC edited books. Recently, he has been listed in the 2021 world 2% scientists report compiled by Stanford University Researchers.

Prof. Dr. Mohammad Hadi Dehghani is a Full Professor at the Tehran University of Medical Sciences (TUMS), School of Public Health, Department of Environmental Health Engineering, Tehran, Islamic Republic Of Iran. His scientific research interests include the Environmental Science. He is the author of various research studies published at national and international journals, conference proceedings, and Head of several research projects at the TUMS. He has authored 12 books and more than 200 full papers published in peer-reviewed journals. He is an editorial board member, guest editor, and reviewer in many internal and international journals and is member of several international science committees around the world. He is supervisor and advisor for many Ph.D. and M.Sc theses at the TUMS. He is currently also a member of the Iranian Association of Environmental Health (IAEH) and member of the Institute for Environmental Research (IER) at the TUMS. He is Co-Editor for 10 Elsevier edited books. Recently, he has been listed in the 2021 world 2% scientists report compiled by Standford University Researchers.

Recent Developments in Membrane Filtration for Wastewater Treatment



Muhammad Salman, Muhammad Shakir, and Muhammad Yaseen

Abstract Freshwater resources are limited and are becoming increasingly polluted due to the rapid urbanization and industrialization. Water pollution is a preeminent pervasive problem affecting the lives of more than 785 millions people globally, both in terms of quality as well as scarcity. Due to boom in industrialization, several toxins and chemicals such as inorganic particles, harmful hydrocarbon, organic matter, and heavy metals etc. are discharged into freshwater bodies thereby making it unsuitable for domestic and drinking purposes. Therefore, it is imperative to design and perform wastewater treatment processes for the production of freshwater. Various technologies have been explored for this purpose including electrochemical oxidation, advanced oxidation process, advanced biological treatment employing algae, bacteria and fungi and membrane-based filtration techniques. Among these, membrane technology is the most suitable strategy applied for wastewater treatment and has gained considerable attention due to its exciting features such as high separation performance, smaller footprint area, cost-effectiveness, low energy requirement, convenience in operation and high efficiency. In this chapter, we will initially discuss membrane technologies applied for the treatment of wastewater. Then, we will describe various types of synthetic membranes, membrane processes and membrane modules being used in wastewater purification. Afterward, an insight into the membrane operation that includes membrane performance, membrane selectivity, separation mechanism, concentration polarization and membrane fouling will be discussed. Finally, different membrane cleaning processes such as physical, chemical, biological and physicochemical cleaning methods will be discussed.

M. Salman · M. Yaseen (✉)

Institute of Chemical Sciences, University of Peshawar, Peshawar 25120, KP, Pakistan
e-mail: myyousafzai@uop.edu.pk

M. Shakir

Institute of Space Technology, Islamabad 44000, Pakistan

1 Introduction

Freshwater is indispensable for life, food, security, public health and energy management on earth. With the increasing urbanization and boom in the human population, the demand for freshwater has excessively increased. The growing scarcity of freshwater bodies is not only alarming for the survival of human and aquatic lives but also increasing global pollution abruptly. According to a recent report, more than 785 million people are facing water scarcity, and the number is increasing gradually (Ilahi et al. 2021). Therefore, conserving the freshwater and purifying wastewater technology is the research hotspot that should be carefully managed and technically fixed in recent times.

With the rapid industrialization and increased urbanization, a large number of pollutants are directly discharged into freshwater bodies, thus making it inappropriate for drinking and domestic purposes (Mahto et al. 2021). These pollutants include harmful hydrocarbon, organic matter, inorganic particles (sand, grit, rubber residue, ceramics), heavy metals, pharmaceuticals and personal care products, pesticides and other related chemical components (Issakhov et al. 2021). Where the organic pollutants, i.e. dyes, textile and food waste, plant material, and paper fibers are among the key contributor to polluting water. These pollutants adversely affect the water quality and risk chemical oxygen demand, alter the chemical composition of water and imparts deep coloration, which ultimately increases the toxicity and decreases biodegradability of freshwater (Werber et al. 2016; Nqombolo et al. 2018; Karri et al. 2021; Dehghani et al. 2021).

To conserve the wastewater, various purification methods including advanced oxidation process, electrochemical oxidation, advanced biological treatment utilizing bacteria, algae and fungi, and membrane filtration have been used. Among these, membrane filtration-based technologies have received considerable attention attributed to their intriguing features such as smaller footprint area, high separation performance, low energy requirement, cost-effectiveness and convenience in operation (Ong et al. 2017; Noamani et al. 2019).

2 Membrane Technology

Membrane technology is a widely adopted separation and purification technique (Cui et al. 2010a). As membranes vary greatly in structure, properties and usage, an all-inclusive description that can relate all of its properties is challenging. The membrane can be defined as a synthetic film that separates two phases by restricting or allowing the passage of various components through it in a selective fashion (Singh and Hankins 2016). The movement of molecules across the membranes is the result of convective movement or diffusion of molecules. Classification of different membrane processes is primarily characterized by different propelling forces, including pressure, concentration, temperature and membrane pore size. At the same time, its

thickness ranges from several centimetres to less than 100 nm and the average pore diameter range from several micrometres to less than 0.1 nm. Membranes are largely governed by different force gradients such as osmotic pressure, concentration, applied pressure, electrical and thermal or the combination of these driving forces (Khan et al. 2021a; Lau et al. 2020). For instance, a membrane sheath can be nonporous or porous, anisotropic or isotropic and electrically charged or neutral (Strathmann 1986).

The choice of the membrane type and the process is determined by numerous factors, which include feed mixture, degree of separation projected and feed volume needed to be processed.

3 Types of Membranes

Synthetic membranes are of two types, i.e. solid or liquid. Based on the morphology, solid membranes are categorized as isotropic or anisotropic (Purkait et al. 2018). Isotropic membranes are also sometimes called symmetric membranes whose composition and physical structure are uniform all over the membrane. Isotropic membranes are further classified as microporous, nonporous, and electrically charged membranes. Isotropic microporous membranes are rigid, having highly voided structures with interconnected and randomly distributed pores that have higher permeation fluxes (Sagle and Freeman 2004). Nonporous isotropic membranes comprise a dense sheath where permeate diffuses under the effect of different propelling forces such as concentration, electric potential and pressure gradient. The separation of different mixture components and their relative transport across a membrane is reliant on their solubility and diffusibility in the membrane. These membranes have comparatively lower permeation fluxes than porous membranes, due to which their applications are limited (Obotey Ezugbe and Rathilal 2020). Electrically charged isotropic membranes are either porous or dense but are exquisitely microporous in most cases (Purkait et al. 2018). These are cationic exchange or anionic exchange membranes, whose pore walls contain fixed negative or positive charged ions, respectively. These membranes are permeable to oppositely charged ions but repel similarly charged ions (Jun et al. 2020; Jua et al. 2020). The ion charge and concentration in the solution drive the separation process. Electrodialysis reversal is the most common application of electrically charged membranes (Xu 2005). Conversely, anisotropic membranes can be asymmetric or composite membranes, which are irregular all through the membrane area and consist of multiple layers having diverse compositions and structures. These membranes are composed of a very fine selective film, which is assisted by a highly permeable and dense sheet and is specifically useful in reverse osmosis applications (Mallevalle et al. 1996).

A liquid membrane consists of a liquid phase that exists as a supported or rather unsupported form that works as a membrane fence to separate two distinct phases of a solution (Hansen et al. 2021). The supported form of the liquid membrane comprises a microporous assembly that is occupied by a liquid membrane phase. The microporous assembly and the liquid-filled pores provide the much-needed mechanical

strength and selective separation barrier, respectively. Higher porosity and smaller pore size are the key contributors to maintaining the liquid phase under hydrostatic pressure. These membranes are extensively applied both analytically and industrially for preconcentration, purification and treatment of wastewater (Parhi 2013). Conversely, an unsupported liquid membrane or emulsion liquid membrane is an emulsion-type mixture that consists of a thin liquid film and is equilibrated by the action of a surfactant. These membranes have tremendous potential for the treatment of wastewater containing heavy metals and hydrocarbons owing to their simple operation, removal and stripping in a single stage, high efficiency, superior interfacial area, and choice of continuous operation (Kumar et al. 2019; Baker 2012).

Based on membrane material, synthetic membranes are categorized as organic, inorganic, and hybrid or mixed matrix membranes (Khan et al. 2021b). Polymeric or organic membranes are synthesized from synthetic organic polymers, i.e. polytetrafluoroethylene, polyethylene, cellulose acetate and polypropylene, etc. Mostly, these polymers are utilized for the synthesis of polymeric membranes for processes that are driven by a pressure gradient, which includes ultrafiltration, microfiltration, nanofiltration, and reverse osmosis (Aliyu et al. 2018).

Inorganic membranes are synthesized from silica, ceramics, zeolites or metals. These membranes are stable in an intensive thermal and chemical environment and are extensively used for industrial applications such as ultrafiltration, microfiltration and hydrogen separation (Mallada and Menéndez 2008).

Nowadays, mixed matrix membranes or hybrid membranes have gained considerable attention. Mixed matrix membranes are considered next-generation hybrid membranes materials that combine the inherent properties of both the polymer and the fillers. The hybrid membrane overcomes limitations of the polymeric and inorganic membranes while synergizing and utilizing properties of both, i.e., easy and viable processability of the polymers and enhanced selectivity of the inorganic fillers. The polymeric material is utilized as a continuous phase in which various fillers are dispersed (Qadir et al. 2017).

4 Membranes Processes

The movement of the material through the membrane is the result of various driving forces, including pressure difference, concentration, electrical potential and temperature gradient or a combination of these processes (Jhaveri and Murthy 2016).

4.1 Pressure Difference-Based Membrane Processes

Pressure difference-based membrane processes have been the most extensively applied practices for the purification of wastewater. These practices are applied from pretreatment to posttreatment of wastewater. Two factors are responsible for

Table 1 Main characteristics of pressure difference-based membrane processes

Process	Pore size (μm)	Pressure range (bar)	MWCT* (kilo Dalton)	Average permeability ($\text{L}/\text{m}^2 \text{ h bar}$)	Solutions retained
Microfiltration	0.05–10	1–2	100–500	500	Bacteria, fat, oil, organics, colloids, microparticles
Ultrafiltration	0.001–0.05	2–5	20–150	150	Proteins, oils, pigments, organics, microplastics
Nanofiltration	<0.002	5–15	2–20	10–20	Pigments, divalent anions, cations, sulfates, lactose, sucrose, sodium chloride
Reverse osmosis	~0.0006	15–100	0.2–2	5–10	All impurities containing monovalent ions

* MCWO = molecular weight cut off

separation processes, i.e. the transmembrane pressure and the decreasing membrane pore size (Chollom 2014). These processes are grouped into four types based on transmembrane pressure and membrane pore size, i.e. microfiltration, nanofiltration, ultrafiltration, and reverse osmosis. Table 1. provides the principal characteristics of these processes.

4.1.1 Microfiltration

In microfiltration, the pressure gradient drives the membrane separation process. The pore size of the microfiltration membrane and the pressure lie in the range from 0.05–10 μm and from 1–2 bar, respectively. Microfiltration is widely used for the elimination of microbes, particulates, and turbidity and is often used as a preprocessing step to different pressure-related membrane processes (membrane distillation, ultrafiltration and reverse osmosis) (Singh 2006). Urban wastewater and drinking water production are two main applications of MF. Also, it is used for the cleansing of wastewater from the oil industry, heavy metal wastewater and paint industry (Obotey Ezugbe and Rathilal 2020).

4.1.2 Ultrafiltration

Ultrafiltration is a pressure-gradient centered membrane operation that has a pore size ranging from 0.001 to 0.05 μm and a pressure range from 2–5 bar. Ultrafiltration

eliminates macromolecular solutes, viruses, suspension, fine colloids, organic material, and other contaminations from water. It is used in the treatment of industrial wastewater (textile, oil, and pulp industry), electrophoresis coating wastewater, and wastewater having heavy metals, enzymes, and starch (Peters 2010).

Microfiltration and ultrafiltration membranes are usually made by phase inversion method and have comparatively wider pore distribution, due to which it offers certain disadvantages, including higher sensitivity to fouling and are susceptibility to pore blocking. A larger pore also lets certain species pass, which is to be retained (Obotey Ezugbe and Rathilal 2020).

4.1.3 Nanofiltration (NF)

NF is an advanced molecular level membrane process prompted by the difference in transmembrane pressure through the membrane. NF falls in the middle of ultrafiltration and reverse osmosis (RO). It can also be termed as loose RO or low-pressure RO. It separates molecules using a nano-porous permselective membrane having a pore size of less than $0.002\ \mu\text{m}$ corresponding to molecular weight cut off ranging from 200–2000 g/mol and involving the pressure of 5–15 bar, nearly at an ambient operational temperature. These membranes are capable of the exclusion of inorganic salts and minute organic molecules. The distinctive features of NF membranes are a lower and higher rejection of monovalent and divalent ions, respectively, and greater fluxes in comparison to RO membranes. These features qualify NF membranes for widespread applications, including food engineering, pharmaceutical, biotechnology, and especially for wastewater treatment, i.e., natural organic removal, water softening, pretreatment to remove scale former in thermal desalination and plays the same role prior to reverse osmosis to increase the saltwater RO (SWRO) recovery (Fane et al. 2015).

4.1.4 RO

RO is the most sophisticated pressure-related membrane purification technology (Joo and Tansel 2015). The membrane pore size is approximately in the range of $0.0006\ \mu\text{m}$, thus preventing all the dissolved solids, sediments, colloidal particles and microorganisms. In osmosis, water usually moves towards the salty concentrated solution, however, in RO the water from the concentrated side infiltrates through the semipermeable membrane in the presence of an external applied hydraulic pressure which is about 15–100 bar in range (Macedonio and Drioli 2010). RO eliminates particles in the molecular weight cut-off range greater than 50 Daltons which include suspended solids, dissolved salts and matter, colloids, organic matter, bacteria, viruses, trihalomethanes and volatile organic compounds (Abd El-Salam and Caballero 2003). RO has widespread applications including brackish water desalination and treatment of emissions from chemical, pharmaceutical, textile and

other industrial processes. The major disadvantages of RO during wastewater treatment are membrane damage due to the presence of strong bases, acids, free chlorine, and membrane fouling because of concentration polarization by inorganic, organic, metal oxides, and biological matter. RO membrane eliminates all the contaminants in a solitary step and offers an ideal and economical water cleansing process (Bartels et al. 2005).

4.2 Concentration Gradient Based Membrane Processes

4.2.1 Forward Osmosis (FO)

FO is an osmosis driven membrane-based process wherein water molecules are forced to permeate through a semipermeable membrane from a feed solution (FS) to a draw solution (DS) as a consequence of concentration difference, which offers the much-needed difference in osmotic pressure as shown in Fig. 1a. Unlike, RO which exploits the hydraulic pressure differential, FO employs the osmotic pressure differential ($\Delta\pi$) as a propelling force across the membrane. Subsequently, in FO, the diluted feed or introductory solution becomes concentrated while the highly concentrated draw solution is diluted as a result of water transport from FS to DS. FO continues until potential chemical equilibrium is established (Suwaileh et al. 2018). Except for applications, where the drawn water becomes part of the draw solution, a recovery unit is always needed that continuously extracts pure water and restores the concentration of the draw solution. In the course of FO process, the draw solution generates the driving force on the membrane permeate side. The foremost criteria for selecting a draw solution is that its osmotic pressure must be greater than the feed solution. FO is surely the most proficient membrane-based purification process in the treatment of industrial wastewater (Haupt and Lerch 2018).

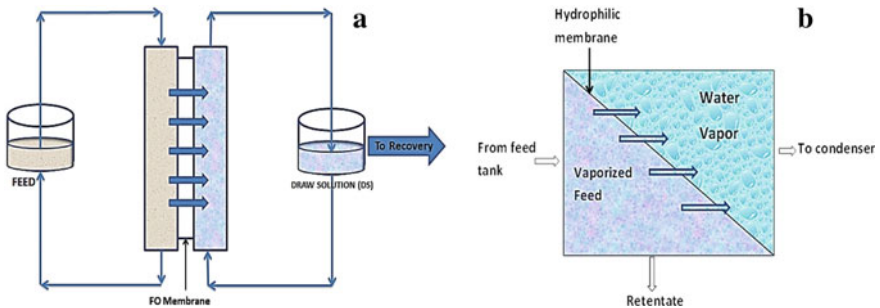


Fig. 1 Schematic illustration of forwarding osmosis **a** and pervaporation **b** (Obotey Ezugbe and Rathilal 2020)

4.2.2 Pervaporation

Pervaporation is a membrane-centered separation practice that couples evaporation with membrane permeation for the preferential purification of liquid mixtures, as shown in Fig. 1b. The feed stream, which usually contains two or more components, interacts with one side of the membrane while the membrane permeate side is conditioned with vacuum or sweeping gas. Different components in the liquid stream are sorbed onto the membrane upstream to generate vapor permeate downstream, and a liquid reject. The feed stream is processed at a temperature and pressure of about 100 °C and 1 atm respectively, however, maintaining a vacuum at the membrane permeate side. The infiltrate vaporizes as the infiltrating components pass through the membrane. The most commonly used membrane for PV is hydrophilic asymmetric composite membranes, including polyvinyl alcohol/polysulfone or PVA/polyacrylonitrile composite membranes (Kesting and Fritzsche 1993). Also, thin layer PDMS/PAN membranes were found effective for the separation of polar and nonpolar compounds. Frequently used membrane modules are spiral wound and flat sheet modules. PV is employed for the treatment of wastewater for micro-irrigation, removal of organic solvents from aqueous solution, removal of alcohols from fermentation broth and also for recovering isopropanol from water with 99% purity (Singh 2014).

The structure and chemical nature of the pervaporation membrane has a consequential function in the separation process. Therefore, these membranes are specifically devised to achieve maximum affinities for intended applications (Basile et al. 2015). Other key features that affect the pervaporation process include partial pressure, feed concentration, temperature, and feed flow rate (Gongping et al. 2011). Unlike conventional separation processes, pervaporation is environmentally friendly and energy-saving technology. However, due to sensitive operational parameters, its industrial utilization is still not achieved (Huang and Meagher 2001).

4.3 *Electric Potential Gradient-Based Membrane Processes*

4.3.1 Electrodialysis and Electrodialysis Reversal

In electrodialysis, ions are directed across an electrically charged membrane due to differences in electric potential. The electrodialysis cell consists of alternating cationic and anionic exchange membranes that are positioned in between the vicinity of two electrodes, as shown in Fig. 2. The feed solution drifts through each membrane pair in the cell. On the application of an electric potential gradient across the system, cations and anions travel through charged membranes towards their respective electrodes, i.e. cations approaching cathode and anions approaching anode. The cation exchange membrane permits cations to pass through, but anions are rejected, and the anion exchange membrane lets anion flow through but rejects cation permeability.

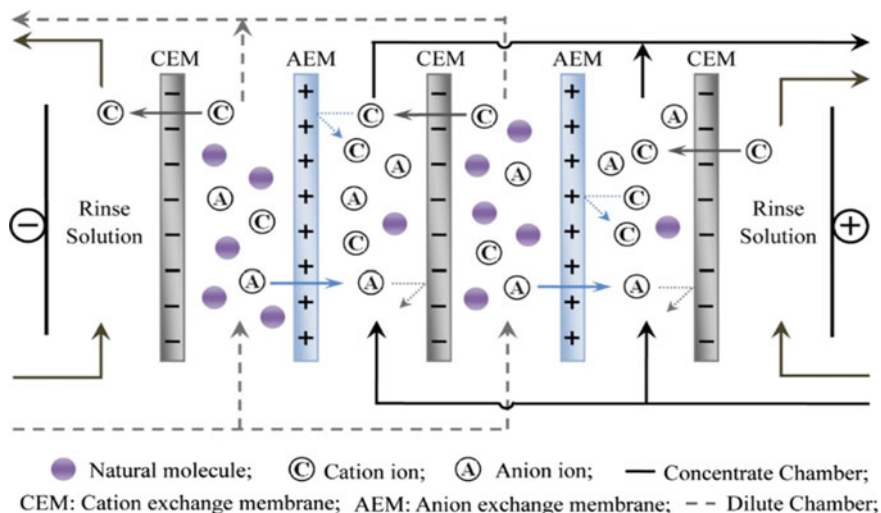


Fig. 2 Schematic representation of ion exchange membranes (Ran et al. 2017)

The arrangement of electrically charged membranes is such that there is an alternation of chambers having greater ion concentration and chambers with a very trivial ion concentration. The high concentrated ion solution is called the concentrate, while the dilute solution almost free of ions is called the diluate, which is the product of water (Baker and Wilson 2000).

In electro dialysis reversal (EDR), the movement of ions across the membranes is reversed by the periodic reversal of the electrodes. As a result, the concentrated solution becomes dilute, and the dilute solution becomes concentrated, which acts as a self-cleaning feature, thus decreasing fouling and extending membrane life (Obotey Ezugbe and Rathilal 2020).

Electro dialysis and electro dialysis reversal have immense applications in treating wastewater, especially for the elimination of total dissolved solids and ionizing species in water. ED and EDR have several important features, which include a high recovery rate of water, slight pretreatment of feed water and reduced membrane fouling because of process reversal. However, ED is ineffective in the desalination of highly saline water since the energy required for desalination is directly proportional to the removal of ions. Also, it cannot remove unionized compounds and harmful substances such as bacteria and viruses, and hence posttreatment will be required, which elevates the process cost. Moreover, chlorine formation at anode results in corrosion (Obotey Ezugbe and Rathilal 2020; Chao and Liang 2008).

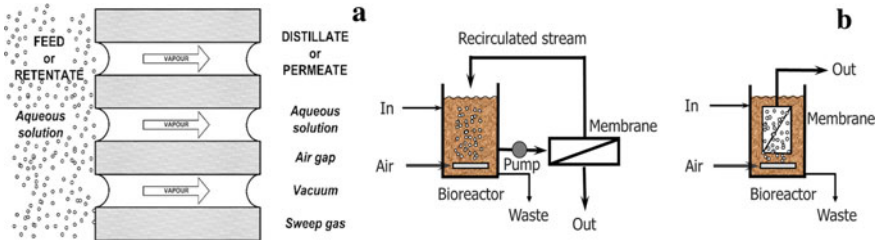


Fig. 3 Schematic representation of membrane distillation **a** (Curcio and Drioli 2005) and Membrane bioreactor **b** (Judd 2008)

4.4 Hybrid Membrane Processes

4.4.1 Membrane Distillation (Temperature Gradient-Based Membrane Processes)

Membrane distillation, a hybrid membrane purification method that integrates membrane technology with thermal distillation, as shown in Fig. 3a (Belessiotis et al. 2016). Two liquids are separated due to differences in partial pressure and temperature across the membrane. The feed is charged at a temperature of up to 100° C while the permeate is cooled down by applying distilled water. The difference in temperature via membrane creates a difference in vapor pressure that drives the H₂O vapor molecules or volatile constituents from hot feed solution through a nonporous hydrophobic membrane. Separation comes about by vaporization followed by vapor passage across the membrane pore opening and membrane network. The difference in vapor pressure is proportional to the water vapor flux. The increase in temperature difference across the membrane causes an exponential increase in the vapor pressure, which accelerates the flux substantially. Salinity in the feed stream reduces the driving force, i.e. vapor pressure, however, this effect is negligible unless salinity is too high (Mulder and Mulder 1996).

MD is an effective process in the purification of highly saline water (seawaters) and rejects brine concentrates of RO as high osmotic pressure cannot affect the process. However, several factors negatively affect the process performance, such as pore wetting, fouling, poor heat transfer, heat loss, low mass transfer due to air entrapment in the membrane pores, and high energy consumption (Gongping et al. 2011).

4.4.2 Membrane Bioreactor (MBR)

In MBRs (Fig. 3b), biological wastewater purification routes such as activated sludge processes are coupled with membrane practices including MF, UF, and NF that are extensively applied in municipal and industrial wastewater processing. MBRs are increasingly being applied in wastewater treatment due to several advantages such as

increased pollutant removal, low footprint required, and a reduced amount of sludge yield. In membrane filtration, microbes are entrapped in the biological reactor, which affords superior regulation over the biological reactions and modifiable parameters of microbes in the ventilated chamber. Thus providing an increased accumulation of mixed liquor suspended solids (MLSS) and prolonging solid retention time (SRT) (Stephenson et al. 2000). Generally, MBRs are categorized into three kinds based on operational mechanisms: rejection MBR, diffusive MBR, and extractive MBR. MBR procedures are effectively implemented in the treatment of small-scale industrial wastewater purification plants and large-scale wastewater purification plants. Mostly two types of configuration are used in MBR; (1) side stream MBR and; (2) immersed MBR. The membranes in sidestream MBR are installed externally to a bioreactor which needs a pumping system for transporting biomass for the filtration process and residue back to the reactor from the filtration unit. The advantage of this setup is that cleaning of an externally installed membrane can be done easily. However, side stream MBR has limited application due to higher energy and pressure requirements. In immersed MBR, the membrane module is immersed in a bioreactor wherein effluents are forced across the membrane. However, the sludge is stuck in the membrane. Air is usually supplied for sustaining aerobic settings and cleaning and scrubbing the exterior and surface of the membrane, respectively. Immersed MBR is used more commonly as compared to side stream MBR due to its simple operation and low energy consumption, however, cleaning the membrane module is difficult as it is submerged in the bioreactor. MBR based process has several benefits in comparison to conventional treatment processes that include production of high quality clarified water, smaller footprint, better regulation of solid and hydraulic retention time, and provides a fence to chlorine-resistant pathogens due to effective membrane pore size less than 0.1 μm . Moreover, designing long sludge age MBR can achieve low production of low excess sludge, thus endorsing the enrichment of nitrifying bacteria, which in turn increases the removal of nitrogen (Wen et al. 2010).

5 Membrane Module

The membrane module is how single operation units are designed and engineered into devices and hardware to attain the anticipated separation performance. It is composed of a membrane, feed inlet and outlet points, permeate draw-off points and pressure support structures (Obotey Ezugbe and Rathilal 2020). So far, four kinds of membrane modules are in use in the industry, which is briefly discussed:

- i. Tubular modules
- ii. Hollow fiber modules
- iii. Flat sheet modules
- iv. Spiral wound modules

5.1 Tubular Modules

The tubular module is composed of an outer covering called a shell which is tube-like in nature, as demonstrated in Fig. 4a. The tube-shaped shell is composed of a permselective membrane implanted inside porous fiberglass or stainless steel. It contains about 30 porous tubes having a diameter ranging from 0.5 to 1.0 cm. The feed to be processed is passed through the tubes by applying pressure, and the infiltrate is concentrated via infiltrating opening on the shell side. Tubular modules have some distinctive features: (1) these are adapted for feed streams with bigger particle sizes because of their large inner diameters. Additionally, their chemical or mechanical cleaning is easy; (2) they usually have a turbulent flow condition with Reynolds number $>10,000$ and need huge pumping capacity; (3) their surface area to volume ratio is the smallest among all the membranes modules and consequently

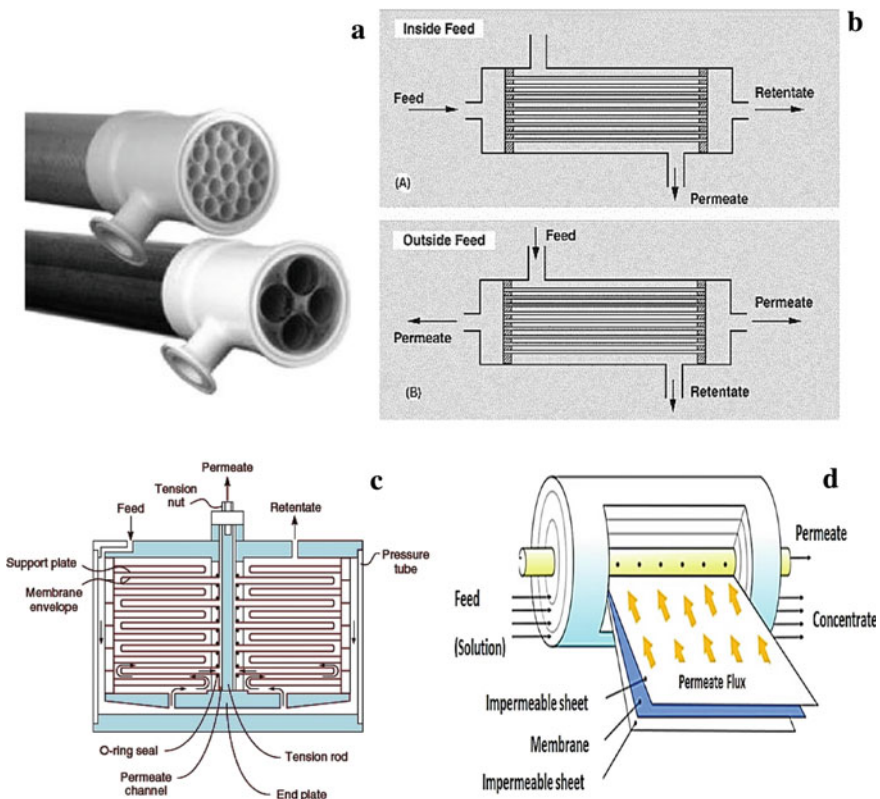


Fig. 4 Schematic representation of tubular **a** (Berk and Berk 2009), hollow fibre **b** (Bruggen et al. 2015; Bruggen et al. 2015; Heidelberg. 2015), flat sheet **c** (Baker 2012) spiral wound modules (Obotey Ezugbe and Rathilal 2020)

have high hold up a volume that necessitate huge flooring space to function (Cui et al. 2010b).

5.2 *Hollow Fiber Modules*

Hollow fiber modules (Fig. 4b), in principle, are analogous to tubular modules arrangement. As the name indicates, hollow fibers consist of thin tubes, the diameters of which range from 1 nm to capillary size fibers. These fibers, being self-supported, have a high backflushing capacity. It contains about 50–3000 hollow fibers, which are connected to porous end plates, and the intact package is inserted into a jacket or vessel. They may have outside in or inside-out flow direction (Cui et al. 2010b). Their key distinctive features, which are different from tubular modules, are: (1) mostly they have laminar flow characteristics which correspond to a Reynolds number of 500–3000. Also, their pressure domain is low, around 2.5 bar at maximum; (2) they are very economical concerning energy consumption because of low pressure and crossflow rate; (3) among all the membrane modules, hollow fibers modules possess the highest ratio of surface area to volume and have low holdup volume; (4) due to their self-sustaining characteristic, they have improved backflushing capability and are cleaned easily; (5) one characteristic shortcoming of hollow fiber module is their liability to get clogged by large size particles during the inside-out operational mode, thus it requires pretreatment to decrease the particle size to 100 μm (Singh and Hankins 2016).

5.3 *Flat Sheet Module*

The flat sheet module (Fig. 4c) is composed of an upper selective horizontal membrane sheet and bottom flat plate. A mesh-like material in between the upper sheet and the bottom plate is placed for removal of permeate, and across the flat plate, an additional membrane sheet and mesh-like material is positioned in the mirror, which forms a sandwich resembling module. The channel gaps and length in these modules range from 0.5 to 10 mm and 10 to 60 cm, respectively. Their Reynolds number corresponds to laminar flow characteristics, however, screening the feed channel results in better mixing. The pretreatment required to decrease the particle size up to 120 μm is recommended. The advantage of flat sheet modules is that they can be cleaned easily by taking out the membrane, and thus fouling can be controlled, however, they are less efficient due to their low packing density. In terms of energy requirement, cost, and packing density, these modules lie in between spiral wounds and tubular modules (Zirehpour and Rahimpour 2016).

5.4 *Spiral Wound Modules*

Spiral wound membrane modules (Fig. 4d) show resemblance to flat sheet membrane modules. These membrane modules are composed of large membranes which are wrapped around a central perforated collection tube. A mesh-like permeable plate or is inserted between two membrane sheets, the active membrane sides of which are facing away with the supporting side facing the feed distributor directly. The feed stream runs aligned to the central collection pipe wherein the permeate falls perpendicular to the feed stream flowing through the permeate spacer. On an industrial level, a tubular pressure vessel contains around six spiral wound modules which are 40 inches long having a diameter of around 8 inches. Spiral wound modules have several important features: (1) the modules flow characteristics is turbulent due to the existence of feed spacers; (2) these modules have relatively high pressure drop due to the surplus drag caused by the presence of feed spacers; (3) the surface to volume ratio is relatively high and are economical among all the membrane modules; (4) the feed stream may contain suspended particles which can block the mesh-like spacer which in turn can partly block the flow of feed channel. Hence pretreatment is required to remove the suspended particles as spiral wound modules require comparatively clear feed having a lesser amount of suspended particles (Cui et al. 2010a).

6 **Operation of Membrane**

6.1 *Membrane Performance*

The performance of a membrane depends on the permeate flow and the retainment of dispersed, suspended and dissolved solids by the membrane. Transport characteristics of different solute materials through a membrane rely on two factors, i.e. permeability of the membrane and driving force. Usually, the main driving force is a gradient in concentration, pressure and electric potential past the membrane. Membrane transport performance can also be altered by flow factors like solvent longitudinal convection, axial solute diffusion, and flow prompted solute particle drag on the surface of the membrane. The potential difference past the membrane regulates the amplitude of the driving forces while the transfer of mass from feed to infiltrate side of a solution is controlled by a membrane. The lack of external forces turns the potential difference into zero across the membrane, which develops equilibrium in the system. Membrane processes are not equilibrium processes like evaporation, distillation and crystallization but are kinetic processes, and under constant driving force and steady-state conditions, there is a constant flux through the membrane (Zirehpour and Rahimpour 2016). The correlation between flux and driving force is:

$$J = K \times X \quad (1)$$

where J represents flux or permeate flow, K demonstrates proportionality constant, and X shows the potential gradient/membrane thickness, respectively (Singh 2014).

Numerous semiempirical models like Ohm's law, Fick's and Hagen Poisseuille's have been utilized to describe the mass transport across the membrane. For processes that are driven by the pressure difference (RO, UF, NF and MF), the flux correlation follows as:

$$J = K \times \Delta P/t \quad (2)$$

where J , K , ΔP and t corresponds to transmembrane flux, permeability constant, pressure difference and membrane thickness, respectively (Zirehpour and Rahimpour 2016).

The efficacy of a liquid separation practice can be assessed from the conversion or recovery of the process, which is the combination of total membrane area and flux. The conversion percentage is the percent conversion of feed into the product stream. % recovery is given by

$$R(\%) = \frac{\text{Permeate flow}}{\text{Feed flow}} \times 100$$

6.2 Membrane Selectivity

Membrane material physical and chemical nature is responsible for the membrane separation. The difference in various features of different substances, including shape, aperture, chemical, and electrical charge, are responsible for the separation across the membrane. In porous membranes, the particles are fairly small to permeate through membrane apertures by convective flow, while in nonporous membranes, transport occurs by sorption or diffusion through the membrane (Singh 2014). The selectivity of the membrane is quantifiable vis-à-vis rejection. The rejection coefficient (R) is a dependable criterion for estimating the membrane separation performance of a process

$$\% \text{Rejection (R)} = \frac{\text{feed} \div \text{bulk solute concentration} - \text{product solute concentration}}{\text{feed} \div \text{bulk solute concentration}} \times 100$$

The value of $R = 100$ for an ideally selective membrane. Membrane selectivity of some routes, i.e. MF and UF, are well explained by the retention coefficient because the solute transport across the membrane is affected by concentration polarization or gel layer formation. % retention is given by

$$\% \text{Retention} = \frac{\text{solute concentration of membrane surface} - \text{permeate solute concentration}}{\text{solute concentration of membrane surface}} \times 100$$

The tradeoff between membrane permeability and selectivity affects membrane performance. Membrane selectivity is related to the permeation of different components through the membrane, i.e. ($\alpha = A/B$), where A represents the permeability coefficient of water and B represents the permeability coefficient of solute (pollute) (Singh 2006).

6.3 Mechanism of Separation Through the Membrane

Membrane separation underlines the ability of membranes to regulate the infiltration of various components or species. Generally, membrane separation mechanisms are of two kinds, i.e., molecular filtration and solution diffusion. In microporous membranes, molecular filtration drives the separation process while dense membranes separation follows the solution diffusion model where the mobility and diffusion of different species in the membrane drive the separation process (Zirehpour and Rahimpour 2016).

In molecular sieving membranes, the separation of feed into different components is brought about by pressure-driven drift through fixed-sized small pores. Different components are separated based on the difference in their sizes. Conversely, the membrane material of solution diffusion membranes is composed of a dense layer of polymer that contains no pores or apertures. The permeants first dissolve in the membrane material and then diffuse across the membrane due to concentration gradient.

The difference in solubility and diffusion rates is responsible for the separation of various components in these membranes. The difference in mechanism of solution diffusion and molecular sieve membranes is due to variance in size and lifespan of membrane pores.

6.4 Concentration Polarization (CP)

CP is actually the growth of the rejected components on or close to the surface of the membrane. It is shared by all the membrane separation processes in which a layer of solute particle mounts up on the membrane periphery as the feed infiltrates through the membrane. During all membrane processes, the passage of feed components towards the surface of the membrane is governed by convection which upsurges as the infiltration across the membrane accelerates. The less permeable components hold back because of membrane selectivity and are conveyed back to the bulk feed at a steady rate (Zirehpour and Rahimpour 2016). The modeling of the membrane module is complicated by CP due to the dissimilarity that exists amidst the wall concentration of solute and the concentration of the bulk feed. The wall concentration of solute is difficult to determine, and a boundary layer film model is applied to define this singularity. The convective drift of solute particles to the membrane periphery

and the infiltration of solute particles through the membrane deduct are equal under steady-state conditions with solute particles diffusion back to the bulk feed solution.

$$J.C = J.C_p - D_{ij} \frac{dC}{dz} \quad (3)$$

Equation (3) integration having boundary conditions, i.e. $z = 0, C = C_m, z = l_{bl},$ and $C = C_b$ will give the following equation

$$J = \left(\frac{D_{ij}}{l_{bl}} \right) \ln \frac{C_m - C_p}{C_b - C_p} \quad (4)$$

Equation (4) that develops the film theory model can be applied to find the solute concentration close to the membrane periphery.

Readjusting Eq. 4 will give:

$$C_m = (C_b - C_p) \exp\left(\frac{J.l_{bl}}{D_{ij}}\right) \quad (6)$$

The solute concentration close to the periphery of the membrane is very crucial for different models of membrane transport. The ratio D_{ij}/l_b can be described as mass transport coefficient and could be found from conventional chemical engineering, i.e. Reynolds number (Re), Sherwood number (Sh), Schmidt number (Sc) and Peclet number (Pe). The permeate concentration and bulk concentration could be obtained by employing analytical instruments.

The membrane filtration unit performance may be adversely affected by CP, which include a reduction in rejection of undesirable solute and water flux, precipitation caused by increased surface concentration beyond the solubility limit, altering the separation characteristics of the membrane, and increase in colloidal and particulate matter that leads to fouling which blocks the membrane surface. Therefore, designing appropriate membrane modules and suitable operating conditions are crucial to anticipate and inhibit the influence of concentration polarization (Ang et al. 2015).

6.5 Membrane Fouling

Membrane fouling can be described as a phenomenon in which dissolved or suspended particles, microbes and organic materials deposit on the periphery of the membrane material or the internal pores of the membrane material, reducing the performance of the membrane. Membrane fouling is categorized into two groups, i.e. reversible or irreversible fouling which depends on the deposition of rejected solutes on the membrane periphery of internal pores of the membrane, respectively (Speth et al. 1998).

Fouling phenomena affects the functional membrane area causing a flux drop below the theoretical capability of the membrane. Subsequently, higher pressure is required for the passage of permeate through the membrane. Membrane fouling adversely affects the overall membrane performance. These include reduction in the functional membrane area, requires more downtime, and increased energy consumption (Kucera 2015).

Different types of membrane fouling depend on and are named on the type of foulant materials such as colloidal, bio, organic, and inorganic fouling (Amy 2008). Colloidal fouling results from the deposition of biological trash, microorganism, lipoproteins, polysaccharides, proteins, clay, silt, manganese oxides, iron and oil, etc. These constituents amass and deposit on the membrane material in due course (Burn and Gray 2016). Biofouling occurs as a consequence of the growth and deposition of organized and coordinated communities of microbes called biofilms on the membrane material. These biofilms contain extracellular polymeric substances (EPS) and microorganisms which results from the adhesion of microorganisms to wet surfaces. These microorganisms nourish from the nutrients in the system and reproduce, which subsequently block the membrane apertures and thus hamper the infiltrate flow (Matin et al. 2011).

Inorganic fouling can be described as the buildup of inorganic salts on the surface of the membrane material. These inorganic salts contain CaSO_4 , SiO_2 and CaCO_3 , and some other salts (Lisdonk et al. 2000). The less soluble salts in the feed solution precipitate out and stick to the membrane surface during the formation of scales (Shirazi et al. 2010). Organic fouling is the accumulation and deposition of organic compounds onto the membrane surface. These compounds exist in natural organic material, which reduces the permeate passage through the membrane material (Amy 2008).

Several factors are responsible for membrane fouling, such as:

- Feed characteristics, i.e., ionic strength and pH.
- Membrane features such as membrane material and surface properties, distribution of pore size, roughness, hydrophobicity and hydrophilicity.
- Various process factors comprise the transmembrane pressure, time, crossflow velocity and temperature.

All these factors are crucial for determining membrane performance in comparison to membrane fouling (Cui et al. 2010a).

7 Membrane Cleaning: Control of Fouling

Membrane separation processes are principally size segregation-based mechanisms. In general, the excluded solutes cause the membrane fouling and is thus inexorable. Numerous approaches have been suggested for controlling membrane fouling. The significance of these methods relies upon the distinctive characteristic of the nature of the membrane material and the bulk feed solution. These methods comprise turbulent

inducers, improvement of membrane material, boundary layer velocity control, and the practice of exterior fields (Jagannadh and Muralidhara 1996). Similarly, pretreatment of feed, rotating membranes, flow handling, and gas sparging and have also been proposed by some researchers (Williams and Wakeman 2000).

Membrane cleaning is aimed at restoring the lost permeability and permeation flux of the membrane as a consequence of membrane fouling. It encompasses the elimination of the amassed material from the membrane periphery to ensure permeability. Cleaning methods for membranes can be classified into physical, biological, chemical, and physicochemical cleaning methods. Additionally, cleaning can be described as ex-situ or in-situ whether the membrane module is washed outside or inside the reactor, respectively (Wang et al. 2014).

7.1 Physical Cleaning

Physical cleaning encompasses the treatment of the membrane module mechanically to eradicate the accumulated material that adheres to the membrane surface. These are of different types, which include periodic backflushing, backwashing, pneumatic cleaning, ultrasonic cleaning, and sponge cleaning (Zhao et al. 2000).

7.1.1 Periodic Backflushing

Periodic backflushing is the backward movement of permeate by applying pressure from permeate side. This backflushing causes the accumulated materials to be detached from the surface of the membrane. The applied pressure required for backwashing should be greater than the filtration pressure (Yigit et al. 2010). Backwashing is the most widely applied industrial method for foulants removal and can successfully redeem the lost flux caused by reversible fouling because of the accumulation of material to the periphery of the membrane material. However, it is ineffective for reversing the irreversible fouling that results from clogging or deposition of suspended or dissolved compounds in the membrane pores (Yigit et al. 2010).

7.1.2 Pneumatic Cleaning

Pneumatic cleaning involves the use of air under pressure for cleaning membrane, usually by airlifting, air sparging, and air scouring. The air causing a shear force destabilizes and removes foulants material from the membrane surface. The method is advantageous because it does not involve the use of chemicals, however, the use of pumping air is expensive to comply with (An et al. 2010).

7.1.3 Ultrasonic Cleaning

In ultrasonic cleaning, ultrasound waves are utilized to generate disturbance in the liquid medium. The generation of vapor bubbles and their exploding as a result of cavitation transfer energy to the membrane periphery in agitation form, consequently eliminating the accumulated materials from the surface of the membrane material. The procedure relies on numerous aspects that include ultrasonic power, temperature, crossflow velocity, and pulse duration. Ultrasonic waves are functional at a molecular level and are very effective in cleaning membranes (Kyllönen et al. 2005; Wan et al. 2013).

7.1.4 Sponge Ball Cleaning

In sponge ball cleaning, sponge balls are inserted into the reactor, and it moves through the permeate, causing the foulants to dislodge off the membrane surface. Sponge balls are prepared of materials like polyurethane and are used in membrane module units having large diameters such as tubular membrane modules (Obotey Ezugbe and Rathilal 2020).

7.2 Chemical Cleaning

Chemical cleaning techniques are utilized for irreversible membrane fouling, which is impossible to remove with physical methods. The successful application of chemical methods involves the selection of cleaning chemicals and understanding the interactions among the membrane material, foulant and cleaning chemicals (Liu et al. 2001). Chemical cleaning has a few key characteristics: (1) loose and dislodge the foulant off the membrane material; (2) retain the foulant in solution; (3) should not cause any new type of fouling; (4) and also should not deteriorate the material of the membrane.

Chemical cleaning is a cleaning in place (CIP) strategy wherein cleaning chemical is charged in the retentate channel where cleaning chemical break the bonds of the foulant material which are removed normally by the crossflow. Different chemicals are utilized for cleaning irreversible fouling, which can be classified as acids, basis/alkalis, surfactants, enzymes, chelating agents and disinfectants, etc., which are aimed at removing different kinds of fouling. For instance, various acids like phosphoric acid (H_3PO_4), hydrochloric acid (HCl) and nitric acid (HNO_3), etc. (Lin et al. 2010) are used for removal of inorganic fouling while bases/alkalis such as sodium hydroxide (NaOH), carbonates, and phosphates which are normally operated at pH 11–12 or less are employed for removing organic fouling (Obotey Ezugbe and Rathilal 2020).

7.3 *Biological /biochemical Cleaning*

Biological cleaning employs active biological agents like enzymes (both in single or mixture form) for membrane cleaning. Contrary to other methods, which require intensive physical and chemical environments and larger footprint areas, biological methods are sustainable and require a low footprint membrane area. Mostly applied cleaning techniques are energy uncoupling, enzymatic cleaning, and quorum quenching in membrane bioreactors for the cleaning of membranes which are employed in the cleaning of wastewater from abattoir (Maartens et al. 1996).

7.4 *Physico-Chemical Cleaning Methods*

In physicochemical approaches, exclusion of foulants from the membrane can be done collectively by chemical and physical methods. The combined approach increases the overall efficiency of the process, which otherwise would have been less. This includes the addition of a certain chemical to the physical process. The most typical example of the physicochemical method is chemically enhanced backwashing. Other examples include chemical cleaning assisted by ultrasonic waves, which could increase flux recoveries up to 95% (Obotey Ezugbe and Rathilal 2020; Maskooki et al. 2010).

References

- Abd El-Salam MH (2003) Membrane techniques | applications of reverse osmosis. In: Caballero B (ed) *Encyclopedia of Food Sciences and Nutrition* (Second Edition). Academic Press, Oxford, pp 3833–3837
- Aliyu UM, Rathilal S, Isa YM (2018) Membrane desalination technologies in water treatment: a review. *Water Pract Technol* 13(4):738–752
- Amy G (2008) Fundamental understanding of organic matter fouling of membranes. *Desalination* 231(1–3):44–51
- An Y, Wu B, Wong FS, Yang F (2010) Post-treatment of upflow anaerobic sludge blanket effluent by combining the membrane filtration process: fouling control by intermittent permeation and air sparging. *Water Environ J* 24(1):32–38
- Ang WL, Mohammad AW (2015) 12—Mathematical modeling of membrane operations for water treatment. In: Basile A, Cassano A, Rastogi NK (eds) *Advances in Membrane Technologies for Water Treatment*. Woodhead Publishing, Oxford, pp 379–407
- Baker RW (2000) Membrane separation. In: Wilson ID (ed) *Encyclopedia of Separation Science*. Academic Press, Oxford, pp 189–210
- Baker RW (2012) *Membrane technology and applications*. Wiley
- Bartels CR, Wilf M, Andes K, Iong J (2005) Design considerations for wastewater treatment by reverse osmosis. *Water Sci Technol* 51(6–7):473–482
- Basile A, Figoli A, Khayet M (2015) *Pervaporation, vapour permeation and membrane distillation: principles and applications*. Elsevier

- Bruggen Van der B, Isotherm F (2015) In *Encyclopedia of membranes*. Drioli E, Giorno L (eds) Springer, Berlin, Heidelberg
- Belessiotis V, Kalogirou S, Delyannis E (2016) Chapter four—membrane distillation, in thermal solar desalination, Belessiotis V, Kalogirou S, Delyannis E (eds), Academic Press, pp 191–251
- Berk Z (2009) Chapter 10—Membrane processes. In: Berk Z (ed) *Food Process Engineering and Technology*. Academic Press, San Diego, pp 233–257
- Burn S, Gray S (2016) *Efficient desalination by reverse osmosis: a guide to RO practice*. IWA publishing London, UK
- Chao Y-M, Liang T (2008) A feasibility study of industrial wastewater recovery using electro dialysis reversal. *Desalination* 221(1–3):433–439
- Chollom MN (2014) Treatment and reuse of reactive dye effluent from textile industry using membrane technology
- Cui Z, Jiang Y, Field R (2010a) Fundamentals of pressure-driven membrane separation processes. *Membrane technology*. Elsevier, pp 1–18
- Cui ZF, Jiang Y, Field RW (2010b) Chapter 1—fundamentals of pressure-driven membrane separation processes. In: Cui ZF, Muralidhara HS (eds) *Membrane Technology*. Butterworth-Heinemann, Oxford, pp 1–18
- Curcio E, Drioli E (2005) Membrane distillation and related operations—a review. *Sep Purif Rev* 34(1):35–86. <https://doi.org/10.1081/SPM-200054951>
- Dehghani MH, Omrani GA, Karri RR (2021) Solid waste—sources, toxicity, and their consequences to human health. *Soft Computing Techniques in Solid Waste and Wastewater Management*. Elsevier, pp 205–213
- Fane AG, Wang R, Hu MX (2015) Synthetic membranes for water purification: status and future. *Angew Chem Int Ed* 54(11):3368–3386
- Gongping L, Dan H, Wang W, Xiangli F, Wanqin J (2011) Pervaporation separation of butanol-water mixtures using polydimethylsiloxane/ceramic composite membrane. *Chin J Chem Eng* 19(1):40–44
- Hansen FA, Santigosa-Murillo E, Ramos-Payán M, Muñoz M, Øiestad EL, Pedersen-Bjergaard SJACA (2021) Electromembrane extraction using deep eutectic solvents as the liquid membrane 1143:109–116
- Haupt A, Lerch A (2018) Forward osmosis application in manufacturing industries: a short review. *Membranes* 8(3):47
- Huang J, Meagher M (2001) Pervaporative recovery of n-butanol from aqueous solutions and ABE fermentation broth using thin-film silicalite-filled silicone composite membranes. *J Membr Sci* 192(1–2):231–242
- Ilahi H, Adnan M, ur Rehman F, Hidayat K, Amin I, Ullah A, Subhan G, Hussain I, Rehman MU, Ullah AJJPAB (2021) Waste water application: an alternative way to reduce water scarcity problem in vegetables: a review 9(1):240–248
- Issakhov A, Alimbek A, Zhandaulet YJJOC (2021) The assessment of water pollution by chemical reaction products from the activities of industrial facilities: numerical study 282:125239
- Jagannadh SN, Muralidhara H (1996) Electrokinetics methods to control membrane fouling. *Ind Eng Chem Res* 35(4):1133–1140
- Jhaveri JH, Murthy Z (2016) A comprehensive review on anti-fouling nanocomposite membranes for pressure driven membrane separation processes. *Desalination* 379:137–154
- Joo SH, Tansel B (2015) Novel technologies for reverse osmosis concentrate treatment: a review. *J Environ Manage* 150:322–335
- Jua LY, Karri RR, Mubarak NM, Yon LS, Bing CH, Khalid M, Jagadish P, Abdullah EC (2020) Modeling of methylene blue adsorption using functionalized Buckypaper/Polyvinyl alcohol membrane via ant colony optimization. *Environ Pollut*, 259. <https://doi.org/10.1016/j.envpol.2020.113940>
- Judd S (2008) The status of membrane bioreactor technology. *Trends Biotechnol* 26(2):109–116. <https://doi.org/10.1016/j.tibtech.2007.11.005>

- Jun LY, Karri RR, Yon LS, Mubarak NM, Bing CH, Mohammad K, Jagadish P, Abdullah EC (2020) Modeling and optimization by particle swarm embedded neural network for adsorption of methylene blue by jicama peroxidase immobilized on buckypaper/polyvinyl alcohol membrane. *Environ Res*, 183. <https://doi.org/10.1016/j.envres.2020.109158>
- Karri RR, Ravindran G, Dehghani MH (2021) Wastewater—sources, toxicity, and their consequences to human health. *Soft Computing Techniques in Solid Waste and Wastewater Management*. Elsevier, pp 3–33
- Kesting RE, Fritzsche A (1993) *Polymeric gas separation membranes*. Wiley-Interscience
- Khan FSA, Mubarak NM, Khalid M, Tan YH, Abdullah EC, Rahman ME, Karri RR (2021a) A comprehensive review on micropollutants removal using carbon nanotubes-based adsorbents and membranes. *J Environ Chem Eng* 9(6). <https://doi.org/10.1016/j.jece.2021a.106647>
- Khan FSA, Mubarak NM, Khalid M, Khan MM, Tan YH, Walvekar R, Abdullah EC, Karri RR, Rahman ME (2021b) Comprehensive review on carbon nanotubes embedded in different metal and polymer matrix: fabrications and applications. *Critical Rev Solid State Mater Sci*. <https://doi.org/10.1080/10408436.2021b.1935713>
- Kucera J (2015) *Reverse osmosis: industrial processes and applications*. Wiley
- Kumar A, Thakur A, Panesar PS (2019) A review on emulsion liquid membrane (ELM) for the treatment of various industrial effluent streams. *Rev Environ Sci Bio/Technology* 18(1):153–182
- Kyllönen H, Pirkonen P, Nyström M (2005) Membrane filtration enhanced by ultrasound: a review. *Desalination* 181(1–3):319–335
- Lau YJ, Karri RR, Mubarak NM, Lau SY, Chua HB, Khalid M, Jagadish P, Abdullah EC (2020) Removal of dye using peroxidase-immobilized Buckypaper/polyvinyl alcohol membrane in a multi-stage filtration column via RSM and ANFIS. *Environ Sci Pollut Res* 27(32):40121–40134. <https://doi.org/10.1007/s11356-020-10045-2>
- Lin JC-T, Lee D-J, Huang C (2010) Membrane fouling mitigation: membrane cleaning. *Sep Sci Technol* 45(7):858–872
- Liu C, Caothien S, Hayes J, Caothuy T, Otoyoto T, Ogawa T (2001) *Membrane chemical cleaning: from art to science*. Pall Corporation, Port Washington, NY, p 11050
- Maartens A, Swart P, Jacobs E (1996) An enzymatic approach to the cleaning of ultrafiltration membranes fouled in abattoir effluent. *J Membr Sci* 119(1):9–16
- Macedonio F, Drioli E (2010) 4.09—membrane systems for seawater and brackish water desalination. In: Drioli E, Giorno L (eds) *Comprehensive Membrane science and engineering*, Elsevier: Oxford. pp 241–257
- Mahto A, Aruchamy K, Meena R, Kamali M, Nataraj SK, Aminabhavi TM (2021) Forward osmosis for industrial effluents treatment—sustainability considerations. *Separation Purification Technol* 254:117568
- Mallada R, Menéndez M (2008) *Inorganic membranes: synthesis, characterization and applications*. Elsevier
- Mallevalle J, Odendaal PE, Wiesner MR (1996) *Water treatment membrane processes*. Amer Water Works Assoc
- Maskooki A, Mortazavi SA, Maskooki A (2010) Cleaning of spiralwound ultrafiltration membranes using ultrasound and alkaline solution of EDTA. *Desalination* 264(1–2):63–69
- Matin A, Khan Z, Zaidi S, Boyce M (2011) Biofouling in reverse osmosis membranes for seawater desalination: phenomena and prevention. *Desalination* 281:1–16
- Mulder M, Mulder J (1996) *Basic principles of membrane technology*. Springer Science & Business Media
- Noamani S, Niroomand S, Rastgar M, Sadrzadeh M (2019) Carbon-based polymer nanocomposite membranes for oily wastewater treatment. *NPJ Clean Water* 2(1):1–14
- Nqombolo A, Mpupa A, Moutloali RM, Nomngongo PN (2018) Wastewater treatment using membrane technology. *Wastewater Water Qual* 29
- Obotey Ezugbe E, Rathilal S (2020) Membrane technologies in wastewater treatment: a review. *Membranes* 10(5):89

- Ong CS, Al-Anzi B, Lau WJ, Goh PS, Lai GS, Ismail AF, Ong YS (2017) Anti-fouling double-skinned forward osmosis membrane with zwitterionic brush for oily wastewater treatment. *Sci Rep* 7(1):1–11
- Parhi P (2013) Supported liquid membrane principle and its practices: a short review. *J Chem*
- Peters T (2010) Membrane technology for water treatment. *Chem Eng Technol* 33(8):1233–1240
- Purkait MK, Sinha MK, Mondal P, Singh R (2018) Introduction to membranes. *Interface science and technology*. Elsevier, pp 1–37
- Qadir D, Mukhtar H, Keong LK (2017) Mixed matrix membranes for water purification applications. *Sep Purif Rev* 46(1):62–80
- Ran J, Wu L, He Y, Yang Z, Wang Y, Jiang C, Ge L, Bakangura E, Xu T (2017) Ion exchange membranes: new developments and applications. *J Membr Sci* 522:267–291. <https://doi.org/10.1016/j.memsci.2016.09.033>
- Sagle A, Freeman B (2004) Fundamentals of membranes for water treatment. *Future Desalination Texas* 2(363):137
- Shirazi S, Lin C-J, Chen D (2010) Inorganic fouling of pressure-driven membrane processes—a critical review. *Desalination* 250(1):236–248
- Singh R (2006) Hybrid membrane systems for water purification: technology, systems design and operations. Elsevier
- Singh R (2014) Membrane technology and engineering for water purification: application, systems design and operation. Butterworth-Heinemann
- Singh R, Hankins NP (2016) Introduction to membrane processes for water treatment. *Emerg Memb Technol Sustain Water Treatment*, 15–52
- Speth TF, Summers RS, Gusses AM (1998) Nanofiltration foulants from a treated surface water. *Environ Sci Technol* 32(22):3612–3617
- Stephenson T, Brindle K, Judd S, Jefferson B (2000) Membrane bioreactors for wastewater treatment. IWA Publishing
- Strathmann H (1986) Synthetic membranes and their preparation. *Synthetic Membranes: Science, Engineering and Applications*. Springer, pp 1–37
- Suwaileh WA, Johnson DJ, Sarp S, Hilal N (2018) Advances in forward osmosis membranes: altering the sub-layer structure via recent fabrication and chemical modification approaches. *Desalination* 436:176–201
- Van de Lisdonk C, Van Paassen J, Schippers J (2000) Monitoring scaling in nanofiltration and reverse osmosis membrane systems. *Desalination* 132(1–3):101–108
- Wan M-W, Reguyal F, Futralan C, Yang H-L, Kan C-C (2013) Ultrasound irradiation combined with hydraulic cleaning on fouled polyethersulfone and polyvinylidene fluoride membranes. *Environ Technol* 34(21):2929–2937
- Wang Z, Ma J, Tang CY, Kimura K, Wang Q, Han X (2014) Membrane cleaning in membrane bioreactors: a review. *J Membr Sci* 468:276–307
- Wen G, Ma J, Zhang L, Yu G (2010) 4.07—Membrane Bioreactor in water treatment, in comprehensive membrane science and engineering, Drioli E, Giorno L, (eds), Elsevier: Oxford. pp 195–209
- Werber JR, Osuji CO, Elimelech M (2016) Materials for next-generation desalination and water purification membranes. *Nat Rev Mater* 1(5):1–15
- Williams C, Wakeman R (2000) Membrane fouling and alternative techniques for its alleviation. *Membr Technol* 2000(124):4–10
- Xu T (2005) Ion exchange membranes: state of their development and perspective. *J Membr Sci* 263(1–2):1–29
- Yigit N, Civelekoglu G, Harman I, Koseoglu H, Kitis M (2010) Effects of various backwash scenarios on membrane fouling in a membrane bioreactor. *Survival and Sustainability*. Springer, pp 917–929

Zhao Y-J, Wu K-F, Wang Z-J, Zhao L, Li S-S (2000) Fouling and cleaning of membrane-a literature review. *J Environ Sci Beijing* 12(2):241–251

Zirehpour A, Rahimpour A (2016) Membranes for wastewater treatment. Nanostructured polymer membranes. Wiley, London, UK, 2, pp 159–207

Spent Filter Backwash Water Treatment by Coagulation Followed by Ultrafiltration



K. Sukanya, N. Sivarajasekar, and K. Saranya

Abstract Water is required for sustaining life. It is also used in anthropogenic activities such as agriculture, washing, and industries. Emerging technologies to decontaminate wastewater spent filter backwash water (SFBW) and waste sludge have been widely investigated in wastewater treatment plants. Most of the industries produce spent filter backwash water (SFBW). SFBW utilization is important due to the feasible heavy metals recycle, microorganisms and predecessor for disinfection outcomes. Modernization in coagulation and membrane techniques, particularly in Ultrafiltration and micro- treatment, provides an appropriate method for SFBW to assure the water quality needed for reuse. The main advantages of Ultrafiltration (UF) are less land consumption and reliable water quality. It can remove microorganisms from the water completely, improving the biological quality of water. The suspended particles, viruses and colloidal substances in water are purified using this method. As the primary purification technology of urban drinking water, Ultrafiltration is an alternative to recycling industrial wastewater and sewage drains. Compared with the conventional water treatment process, the EC and UF process has higher efficiency, better effects of treatment and low energy consumption. It is important to further investigate ultrafiltration technology to improve the quality of water, protect water resources, and balance the ecological environment.

Keywords Spent filter backwash water treatment · Coagulation · Ultrafiltration · Chemical disinfection · Water reuse

1 Introduction

Due to urbanisation, industrialisation and household consumption, a huge amount of wastewater is being generated across the globe. Nevertheless, this unsustainable growth releases toxic chemicals into the air, water, and land and thus contaminating

K. Sukanya (✉) · N. Sivarajasekar
Department of Biotechnology, Kumaraguru College of Technology, Coimbatore, India

K. Saranya
Coimbatore Institute of Technology, Coimbatore, India

them to an unprecedented scale. Among the pollutants released into water bodies, several were found to be causing serious issues to human health, and analyzing the release mechanism, degradation process, implementing their removal process before discharging into natural water bodies are needed (Karri et al. 2021; Dehghani et al. 2021).

In the traditional water treatment processes, to remove pollutants, protozoa, consisting of organic/inorganic particles, viruses and bacteria, from the coagulation basin effluents, sand filters are used (Adin et al. 2002). They are regularly backwashed to restore the quantity and the SFBW resultant, including the pollutants sedimented in the sand filter (Bourgeois et al. 2004). During backwashing of filter, SFBW consisting of the organism, colloidal materials and inorganic metals are produced by dislodging impurities (Cornwell and Macphee 2001) from the filter. SFBW is reversed to the top of the Water Treatment Plant (WTP) to redeem waste streams (Cornwell and Lee 1994).

SFBW has a negative effect on the finished quality of water if directly recycled (Arora et al. 2001a, b) and endanger the safety of drinking because pathogens, *Cryptosporidium* and *Giardia* or Disinfection outcomes might be sedimented in wastewater treatment (Nasser et al. 2002). Among all the approaches for water treating, membrane filtration has the best performance. (LeGouellec et al. 2004) indicates that gradual reduction of DBP, particles and microbes SFBW elements is obtained by separating a membrane known as Ultrafiltration (UF) (Reissmann and Uhl 2006).

SFBW restoring by filtration using a membrane (Walsh et al. 2008), fouling of membrane and clogging of pores due to organic or colloidal particles reduces the membrane flux and the recovery rate next to backwashing (Guigui et al. 2002). A hybrid technique is employed to enhance the flux in the membrane (Howe et al. 2006). Pre-coagulation in combination with separation of the membrane is used to form higher and porous floc on the membrane plane (Chen et al. 2007), deducing the fouling of membrane and clogging, in turn, increases the flux in the membrane (Lin et al. 2008).

Pre-treatment coagulation constraints like dosage of Alum coagulants and pH significantly affects the properties of flocs, that affects the separation of subsequent solid-liquid (Walsh et al. 2008), comprising specific resistance and reduced water ability of coagulated element that controls the efficiency of consequent filtration (Song et al. 2001). The coagulation filtration using membrane facilitates the value of water purified, SFBW with running (Lee et al. 2000), and quality cost at certain conditions near the existing water treatment process.

Recently, the water reuse of SFBW has gained importance in many countries due to water scarcity. SFBW serves as a forever source for the working of WTP (Raj et al. 2008). During the water treatment process, SFBW generated is about 2–10% of total production in the plant. Backwashing using a filter is performed to detach all the sedimented elements using the bed at filtration. There are constraints (Walsh et al. 2008) regarding its reuse due to a higher percentage of metals, organic elements, microbes, heavy metals, and colloidal elements.

Exposure to heavy metals routes consists of absorption, ingestion and inhalation. Insertion through the raw water is significant for exposure to heavy metals. Major

health issues like breathing shortness, mutagenic, neurotoxic effects with various cancers are caused by heavy metal contamination in drinking water (Chowdhury et al. 2016). SFBW restoration endangers the superiority of the water processed due to the contaminants with more concentration percentage (Ang et al. 2015). SFBW is conducted using various methods.

Filtration using membranes such as MF and UF effectively removes colloids, particulates and pathogens. It requires a lower footprint, low consumption of energy and quality water production. Fouling is the major issue in the membrane process, particularly for SFBW processes. UF membrane processes have proven capabilities to reject turbidity and suspended solids (Zhang et al. 2008). With proper pre-treatment, such as coagulation-flocculation-sedimentation (CFS), UF membranes can also remove viruses, bacteria, and pathogens (Gao and Yue 2005).

The required treatment for SFBW prior to restoration at the plant differs between sites provided by the purpose of the treatment (Zhao et al. 2008). A conventional approach is needed to minimize the SFBW reusing effect on raw water quality (Lai et al. 2015). SFBW has to be processed previous to its reuse (Yu et al. 2013). The choice for disposal includes discharge to a receiving stream or a sewer (Chen et al. 2014). SFBW contains heavy metals and disinfectants that are harmful to the biological life of the stream, discharging directly to streams is usually restricted (Peter et al. 2011). Discharge to the drain has to be controlled depending on the ingredients and SFBW's total amount (Wang et al. 2016). For most water processing plants, particularly in water scarce areas or arid, SFBW recycling holds to be a feasible option (Wang et al. 2014).

To control this problem, membrane elements combined with a process like coagulation pre-treatment, sedimentation and Ultrafiltration are applied (Huang et al. 2011). Coagulation is the essential technique to reduce the particulate elements, colloids, suspended solid elements, organic and dissolved elements (Yu et al. 2013) prior to the process in the membrane. The biopolymer (Uday Kumar et al. 2021) and biopolymer composites easily fit into different parts of the treatment process by acting as filtration media, adsorbents, coagulants and as flocculants. Upon increasing the aggregation of flocs (Thirugnanasambandham et al. 2021), most flocs settle down, thus improving removal efficiencies during the coagulation process.

UF is an efficient method to reduce microbes, colloids and suspended elements. Application of UF membrane (Li et al. 2012) for treatment of backwash water aids in addressing the issues of fouling and (Raj et al. 2008) the quality of treated water for drinking and other application. Many investigators have identified EC as a promising water purification method (Song et al. 2017) for potable water and wastewater. Compared to other processes, EC (Das and Nandi 2021) shows several enticing advantages like minimal expenses, ease of install, no requirement of chemicals, and lower treatment time.

2 Spent Filter Backwash Water Treatment Methods

2.1 Determination of Optimum Coagulant Dose Using Jar Test

Jar tests are the experimental way to find the optimum coagulant dosage for the SFBW treatment. The test is performed in a jar-test apparatus (Fig. 1), consisting of six beakers at room temperature with one litre volume. The test comprises three subsequent steps: rapid mixing takes place initially at 200 rpm for about 1 min, after that, mixing is done at 30 rpm for 20 min. Stirring is then stopped for the sludge to sediment. Once the sedimentation is done, the residue liquid is drawn from a zone about 2 cm beneath the liquid level of the beaker to obtain the turbidity of the SFBW treatment using a turbidimeter. pH test to observe the pH value for the water using pH electrodes, pH meters and PerpHect Ag/AgCl Gel triode. Total dissolved solids (TDS) are calculated using the Conductivity Meter equipment.

Electrical conductivity (EC) is measured to indicate changes in water composition by conductivity equipment. Chlorine test to show the amount of chlorine residue in wastewater, evaluated by Stable neutral Orth tolidine method, at a range of 625 nm with neutral Orth tolidine reagent, Buffer—stable reagent. A spectrophotometer does detection of aluminium in wastewater at 553 nm with Eriochrome cyanine R stock solution, dye solution, Sulfuric acid and Ascorbic acid. Determination of the sulphate concentration using a spectrophotometer at 420 nm with conditioning reagent, BaCl₂—crystals (20–30 mash).

To measure the Fe II, Fe III content in water, a spectrophotometer at 510 nm with Hydrochloric acid, Hydroxylamine chloride, Ammonium acetate, Sodium acetate, Phenanthroline are used. The total alkalinity test indicates the amount of carbonates, bicarbonates, and hydroxides in the water. It is noticed by titration of a sample electrometric aliquot with a standard strong acid solution (H₂SO₄), the result is identified by pH meter.

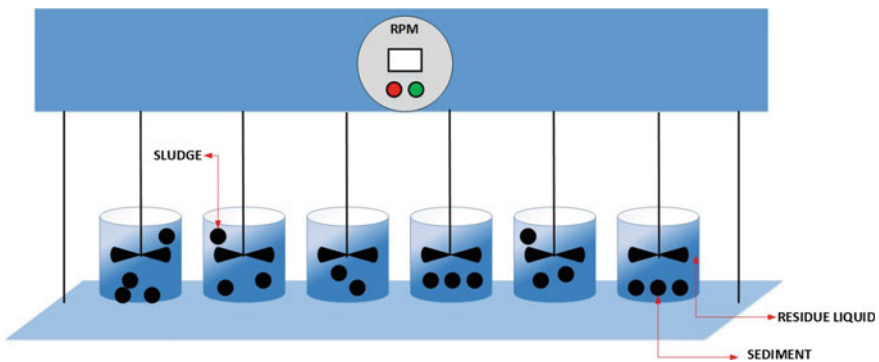


Fig. 1 Conventional jar-test apparatus

To improve filtration performance, the SFBW is to be pre-treated by two levels: sedimentation elements and coagulation. Large particles are preferably removed through pre-settling, and solid particles from supernatants become low, improving the flux in the membrane during filtration. SFBW is allowed to settle at various time durations prior to the filtration. After allowing to settle for 15 min, the supernatant liquid is used as the pre-settled SFBW for microfiltration.

2.2 Spent Filter Backwash Water Treatment by Chemical Disinfection

Chemical disinfection is an alternative technique for SFBW treatment before recycling the water for further process. (Arora et al. 2001a, b) Determination of disinfectant for the treatment is essential to measure the demand of oxygen obtained by various elements in SFBWs. Filtration techniques in wastewater treatment discharge wash water consisting of suspended solids with minimum concentration varying in the range 30 to 400 mg/l, based on precipitations of raw water treated and the amount of backwash water recycled. About 2–3% of the flow in treatment is the filter backwash water. SFBW contains 10–20% total elements, both organic elements and microbes, as the effect of microbial growth in the filters. While recycling the SFBW, there is an increase in concentrations of *Cryptosporidium* and *Giardia* in the wastewater, resulting in unwanted growth of the microorganisms into the water supply (DiGiovanni et al. 1999). Particles in SFBW affect disinfection's efficiency due to their mechanism involved in particle-less wastewaters. In the process, Potassium permanganate and Chlorine dioxide are utilized for demand in oxidant and measurement of disinfection since it does not produce Tri Halo Methane (THM) outcomes. For each sample of SFBW, oxidant demands are obtained. Particle-less samples are measured by slow centrifugation for about 10 min along with filtration using a 0.22 μm filter (bottle top). Elements containing particles are extracted utilizing a 0.22 μm filter (syringe) by a prior filtration before oxygen demand, measurements of glass-fibre residue are done. For the deactivation of *Cryptosporidium*, various SFBW elements are utilized.

Cell culture–quantitative sequence detection method (CC–QSD) is considered to find the disinfection mechanism of *Cryptosporidium*. Treated *Cryptosporidium* oocysts are obtained. In every oxidant sample, dosages are implemented for oxygen demand in SFBW samples, considering with and without elements. SFBW elements mixed with *Cryptosporidium* oocysts are processed for 10 min by KMnO_4 and ClO_2 . After the designated contact time, samples are evaluated by CC–QSD technique for *Cryptosporidium* invasion. Since the pre-settling removes large particles, the sub micrometre elements are left in the residue liquid, the initial flux is lowered by the sub micrometre elements that are lower compared to the pore of the membrane. Due to the filtration of SFBW, sludge obtained from large particles removes a particular range of submicrometric elements before passing the surface of the primary zone.

The amount of solid in SFBW improves microbial removal in the pilot run. Polymer treatment for SFBW (cationic and anion) results in an efficient deduction of total solids along with microbes in the treated wastewater.

2.3 Spent Filter Backwash Water Treatment by Coagulation

This process includes primary deposit, coagulation, thickening and Ultrafiltration using membranes for SFBW treatment. Conventional poly aluminium chloride (PACl) is generally used as a coagulant. In the pilot unit for all stages, except UF, the rate of flow to be maintained is about 10 L/h. Hydraulic retention time (HRT) in this stage is to be maintained approximately at 60, 6, 48, and 192-min (Mahdavi et al. 2016). Figure 2 represents the experimental setup used in the coagulation experiment. Coagulation is performed at standard pH (8.3) and estimated PAFCl amount (15 mg/L) with FeCl_3 amount (40 mg/L) being regularly added into the agitating zone (with HRT for 6 min, at 80 rpm speed). Next, the coagulated effluent passes through two tanks for flocculation, with a 40-rpm agitating intensity. The SFBW is pre-treated with PACl prior to the filtration using a membrane. A specific percentage of coagulant is mixed with SFBW sample at a maintained pH 7, then by fast agitation for 1 min, 20 min of slow mix and the end settling for about 20 min. Pre-treatment before coagulation depicts the decline in membrane flux and the effect of coagulation efficiency.

The coagulated sample is utilized as the feed in the membrane UF module. To identify the optimum dose, selection has been done for both coagulants for 4 days separately and continuously (Fig. 2). The optimum dose is determined to produce the reliable water quality depending on precipitation and percentage of colour. Elements are then evaluated after the second clarification of two HRT. Then about 1,000 L of SFBW is processed separately by coagulants. Next, 800 L volume processed water by PAFCl coagulant, and 800 L volume of processed water by FeCl_3 coagulant enters through UF membrane. Various parameters, like colour, turbidity, TC, FC and pH, are observed about ten times at pilot scale measurement, while the concentration of heavy metals is observed three times for optimum dose and processed water quality.

Electrocoagulation (EC) has been considered a more efficient process for removing multiple water contaminants simultaneously from contaminated water in recent years as an alternative to other conventional techniques. The main advantage of the EC process is low investment cost, no addition of chemical requirement, easy to operate and most importantly, very low production of sludge (Thakur and Mondal

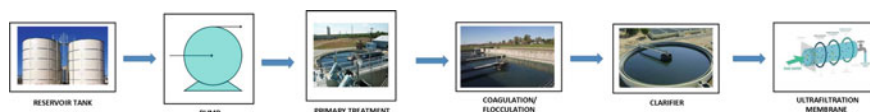


Fig. 2 Spent filter backwash water treatment by coagulation and ultrafiltration

2017). The electrocoagulation process works on the principle of a standard electrochemical cell. The sacrificial metal anode dissolves in the aqueous medium and generates hydrolysis product (hydroxo-metal species) which adequately destabilizes the contaminant particles and structures coagulants. Electrolysis gases (H_2 and O_2) produced due to electrochemical reduction (Das and Nandi 2019) of water in the cathode initiates soft turbulence in the aqueous medium and works in combination to enhance the flocculate of the coagulant materials.

2.4 Water Treatment Using Ultrafiltration Membranes

The ultrafiltration membrane extracts effluents of SFBW is a purified flow of water called permeate and a concentrated flow of water known as concentrate or retentate (Mulder et al. 1997). Membranes generally comprise a supportive porous layer (100 μm) and a thin upper layer of about 0.1 to 1.0 μm (Aptel et al. 1996). Most of the fibre utilized in the SFBW process are made of aromatic polyamides, PPL, thin-film composite (TFC) or cellulose acetate. Inorganic fibres contain extra zirconium oxide (ZrO_2) and aluminium oxide (Al_2O_3). The membrane module describes a unit including membranes, feed inlet, pressure support structure, effluent outlet and overall structure. Various membrane modules utilized in wastewater treatment are as follows:

- Tubular type has a diameter of more than 3 mm fibre inside a bundled module;
- Capillary or spiral type fiber membranes have internal diameter lower than 3 mm, inside a bundled module with 100's–1000's of particles of fibre;
- Round wound type membranes are generally flat membranes that are captured inside a spacer;
- Plate type and frame type membranes consist of flat sheets connected in series as membrane and its support sheets.

The course of flow in tube type and swirl fibre type are either interior-out or exterior-in. For the interior-out mode, the flow of influent is from the interior side of the swirl tube to the external side of the membrane, later purified water (known as permeate) is obtained. The exterior-in mode depicts flow in the opposite course.

UF membrane comprises polypropylene fibre, porous, with a range of about 0.01–0.2 μm . The area of the total UF membrane is around 0.1 m^2/module . In this module, the membrane is run in end mode using filtration at a constant rate of about 8 $\text{L}/\text{m}^2 \text{h}^1$ at the pressure of 300 Pa inside the membrane. It is processed in a duration of 60 min for filtration and SFBW for 1 min in a combination of permeate in the opposite direction.

As indicated in Table 1 (Mahdavi et al. 2018), turbidity of the residue and the color obtained after coagulation and ultrafiltration process shows major reduction (Berthon et al. 2002). The filtration's measured parameter level is comparatively very low and complies with the EPA drinking water standard. Variables in SFBW restored samples are the concentration of heavy metals that has major health effects on the environment

Table 1 Characteristics of SFBW

Parameter	SFBW	EPA standard	After Coagulation—UF treatment
Turbidity (NTU)	7.7	>5 NTU	0.1
Colour (Co. units)	4.2	15 colour units	0
pH	8.3	6.5	7.5
Iron (mg/L)	4	0.3	0.08
Aluminium (mg/L)	0.4	0.05–0.2	0.02
Lead ($\mu\text{g/L}$)	217	10	0
Arsenic ($\mu\text{g/L}$)	2.3	10	0
Cadmium ($\mu\text{g/L}$)	4	5	0.3

and humankind. It is observed that most of the heavy metals and metals are reduced by coagulation in treated SFBW. It is inferred that a major percentage of metal content is connected by elements related to clay, biological content, silt or particles while at the process of effluent treatment. Along with reducing suspended elements of solids during coagulation technique, colloids and particles, a major percentage of the heavy metals are removed efficiently.

3 Recent Developments and Research

3.1 Limiting Microbial Quality

The outcome of different doses of about 5 to 60 mg/L of FeCl_3 and PAFCl is to identify the optimum dose. It is inferred that the optimum dosage level for FeCl_3 and PAFCl is about 15 and 40 mg/L. In this dose level, the removal percentage of turbidity is 99.6 and 99.4%. In each level of dose, precipitation level is determined after HRT. While the PAFCl removal efficiency of precipitation level is enhanced to 15 mg/L. Beyond this limit, balancing of coagulant and a subsequent enhancement in precipitation occurs.

UF membrane process, the input water quality is considered important due to fouling problems. Utilizing optimum doses of FeCl_3 and PAFCl , turbidity of water treated levels up to 2.4 and 3.9 Nephelometric Turbidity Units (NTU). Next, SFBW is passed through the UF process, and the value of processed wastewater microbes are evaluated. Due to coagulation and flocculation, most microorganisms like particles refer to bacteria and protozoans, and virus refers to organic elements. Turbidity reduction is indirectly related to the reduction of microbial content in SFBW. In this process, both the coagulants depicted an influence on microbe reduction (Sutherland et al. 2003).

3.2 Minimizing Metals and Heavy Metal

It is observed that the coagulants had better efficiency for removing heavy metals (Appel et al. 2002). However, heavy metal removal by PAFCl is comparatively better than FeCl_3 . Figure 3 depicts the Concentration of heavy metals in SFBW processed with PAFCl have been resulting in the sequence: Aluminium > Iron > Cadmium > Arsenic and Lead. After coagulation by FeCl_3 , the sequence is Iron > Aluminium > Cadmium > Arsenic and Lead. Next, the PAFCl-UF process sequence of heavy metals is Aluminium > Cadmium > Iron, Arsenic and Lead. consequently, sequence for FeCl_3 with UF are Iron > Aluminium > Cadmium > Arsenic and Lead.

It is noticed, the coagulation process has deduced the majority of the percentage of the heavy metal in SFBW treatment. Clay and soil possess great properties in heavy metal adsorption like Lead are obtained from fractionation column. Heavy metals can be captured using the Fe-oxide fraction (Orrono and Lavado 2009).

Coagulation combined with FeCl_3 , experimented under high coagulant concentration of about 40 mg/L, from the flocculation process, by entrapment of organic matter and particles in the flocs that are formed, all the connected heavy metals and metals are removed consequently (Ebrahimi et al. 2015). A hydrolysed coagulant PAFCl has more positive ions than traditional coagulants. It contains Fe and Al ions. The characteristics of $\text{Al}(\text{OH})_3$ and $\text{Fe}(\text{OH})_3$ elements are utilized. Positive ions of PAFCl adsorb negatively charged colloids, particles, and organic matter attracts heavy metals. Coagulation combined with PAFCl happens under low coagulant concentration comprises adsorption kinetics. It is observed that the adsorption kinetics for heavy metals removal is better compared to PAFCl.

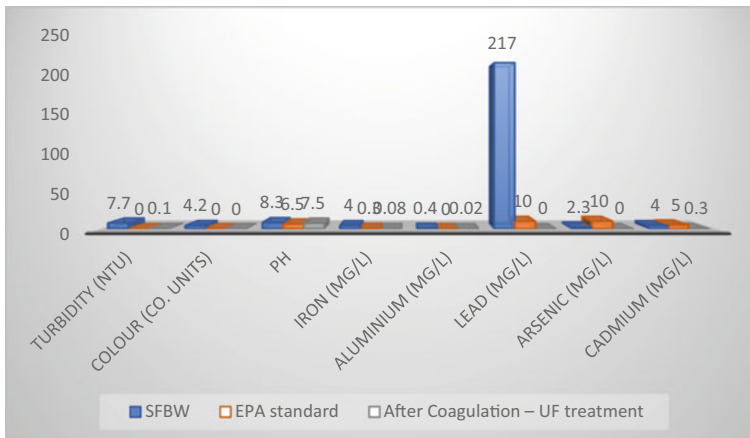


Fig. 3 The concentration of heavy metals in SFBW, EPA standard and coagulation—UF treatment

4 Future Research Perspective

Major operational challenges such as control of membrane fouling and the optimization of system recovery still exist for many surface water treatment plants (Gao et al. 2011; Huang et al. 2009). As a result, public water systems are motivated to mitigate membrane fouling while simultaneously reducing their residual streams in a cost-efficient manner. However, fouling causes loss of membrane permeability, considered a drawback to the universal application of membrane processes in the wastewater treatment industry. Fouling control is a major focus of water treatment research (Gao et al. 2011). Membrane fouling occurs during filtration as constituents accumulate on or adsorb to the surface of the membrane. Fouling causes loss of membrane permeability and continuous permeability decline (Jacangelo et al. 1989) that is often considered the largest barrier to membrane adoption in the water treatment industry. These goals must be met while continuing to meet existing and emerging regulations. As a result, research needs to explore issues related to membrane fouling and operational efficiency (Jermann et al. 2007). Recent studies have examined the long-term fouling behaviour of membrane systems used in water treatment, addressing strategies to reduce fouling through operational changes and new pre-treatment applications. Specifically, four concepts are explored in this method:

- (1) Long-term fouling behaviour of ultrafiltration membrane studied at the pilot-scale, revealing that commonly used surrogate water quality measures did not correlate well with chemically irreversible fouling.
- (2) Pre-oxidation with ozone as pre-treatment to decrease fouling rate at the pilot scale.

Membrane fouling from Organic Matter (OM) occurs as organic content sedimented as a deposit and forms a sludge or adsorbs to the surface of a membrane directly (Susanto et al. 2007; Zularisam et al. 2006). Fouling is often modelled as resistance-in series (Boyd et al. 2013; Huang et al. 2008; Nguyen et al. 2011) are characterized based on fouling through cleaning. Organic fouling leads to decreased permeability and is oftentimes difficult to reverse through cleaning (Lehman et al. 2009). Therefore, considerable research has been published on pre-treatment strategies that remove or destroy organic foulants to reduce the irreversible fraction of fouling. Previous bench-scale work has identified pre-oxidation with ozone (preozonation) as a treatment strategy to reduce the organic fouling of membranes.

Ozone is a powerful oxidant that can break down or destroy complex organic compounds known to cause fouling of polymeric membranes (Gao et al. 2011; Van Geluwe et al. 2011). Previous research has generally focused on applications of pre-ozonation with ceramic ozone-resistant membranes (Lee et al. 2013; Sartor et al. 2008). Furthermore, most studies have investigated the use of ozone in direct-filtration applications, while other studies, independently, have considered the use of preozonation as a coagulant aid (Bose et al. 2007; Schneider and Tobiasson 2000; Singer et al. 2003). However, very few studies have evaluated the integration of

ozone, coagulation, and membrane filtration. Specifically, there is a lack of knowledge regarding the downstream impact of ozone-coagulation treatment on membrane fouling.

- (3) The effect of ozone on organic matter in water investigated at the bench scale.
- (4) The impact of recycling of membrane backwash water on system performance.

The most commonly recycled waste for conventional treatment plants with traditional media filters is spent filter backwash water (Arora et al. 2001a, b). Spent filter backwash water contains concentrated levels of the constituents found in raw water, including *Cryptosporidium*. In lieu of conventional filters, water plants utilize ultrafiltration membranes instead produce membrane backwash water (MBWW). Most plants choose to recycle a portion of their MBWW in order to improve their system recovery. MBWW is concentrated with constituents retained by an ultrafiltration membrane and may contain membrane cleaning chemicals.

As demonstrated by (Boyd et al. 2012), if recycled within a treatment plant, these constituents may impact UF process performance. Given that fouling of UF membranes remains a major challenge for public water systems, there is a need to better understand the impacts of MBWW recycling, the fouling characteristics of these waste streams, and the necessary treatment to mitigate fouling.

5 Conclusion

For recycling of SFBW, presetting prior to filtration using membrane worsens separation efficiency using a membrane. The pre-treatment by coagulation improves the characteristics of UF membrane operation by enhancing flux by a reduction in the pore blockage. It is observed that pre-treatment by coagulation along with charge neutralization at the optimum dosage, the better performance of consequent filtration using membrane for restoring SFBW is obtained. Coagulation, before membrane ultrafiltration, improves permeate quality and reduces the UF membrane fouling while increasing the effectiveness and efficiency of the ultrafiltration process, i.e., elimination of the hydraulic efficiency and the organic substances. The obtained water is disinfected and particle-free, possess sufficient quality for domestic use or after treatment.

Continuous processing of pilot-plant investigation is expected for evaluation of the efficiency and to optimize the process control. Traditional treatment depicts that the polymeric treatment (anionic or cationic) efficiently calculates microorganisms and solids. Treatment with cationic polymer and chemicals like FeCl_3 infers an effective deduction of DOC (70%). In treated SFBW, all heavy metals and metals concentrations comply with the potable water guidelines published by EPA with both processes. Removal percentage is better with PAFCl than FeCl_3 in the coagulation process. Minimizing raw water demand as well as preventing the natural stream from high sedimentation by decreasing the level of pollution. Spent filter backwash water recycling accounts for water resources conservation.

References

- Adin A, Dean L, Bonner F, Nasser A, Huberman Z (2002) Characterization and destabilization of spent filter backwash water particles. *Water Supply* 2(2):115–122
- Ang WL, Mohammad AW, Hilal N, Leo CP (2015) A review on the applicability of integrated/hybrid membrane processes in water treatment and desalination plants. *Desalination* 363:2–18
- Appel C, Ma L (2002) Concentration, pH, and surface charge effects on cadmium and lead sorption in three tropical soils. *J Environ Qual* 31:581–589
- Apfel P, Buckley CA (1996) Categories of membrane operations (Ch. 2). In: Mallevalle J, Odendaal PE, Wiesner MR (eds) *Water treatment membrane processes*. McGraw-Hill, New York
- Arora H, Di Giovanni G, Lechevallier M (2001a) Spent filter backwash water contaminants and treatment strategies. *J Am Water Works Assoc* 93(5):100–112
- Arora H, Di-Giovanni G, LeChevallier M (2001b) Spent filter backwash water contaminants and treatment strategies. *J. AWWA* 93:100–112
- Berthon G (2002) Aluminium speciation in relation to aluminium bioavailability, metabolism and toxicity. *Coord Chem Rev* 228:319–341
- Bose P, Reckhow DA (2007) The effect of ozonation on natural organic matter removal by alum coagulation. *Water Res* 41(7):1516–1524
- Bourgeois JC, Walsh ME, Gagnon GA (2004) Comparison of process options for treatment of water treatment residual streams. *J Environ Eng Sci* 3(6):477–484
- Boyd CC, Duranceau SJ (2013) Evaluation of ultrafiltration process fouling using a novel transmembrane pressure (TMP) balance approach. *J Membr Sci* 446:456–464
- Boyd CC, Duranceau SJ, Tharamapalan J (2012) Impact of carboxylic acid ultrafiltration recycle streams on coagulation. *J Water Supply Res Technol AQUA* 61(5):306–318
- Chen F, Peldszus S, Peiris RH, Ruhl AS, Mehrez R, Jekel M, Legge RL, Huck PM (2014) Pilot-scale investigation of drinking water ultrafiltration membrane fouling rates using advanced data analysis techniques. *Water Res* 48:508–518
- Chen Y, Dong BZ, Gao NY, Fan JC (2007) Effect of coagulation pretreatment on fouling of an ultrafiltration membrane. *Desalination* 204(1–3):181–188
- Chowdhury S, Mazumder MAJ, Al-Attas O, Husain T (2016) Heavy metals in drinking water: occurrences, implications, and future needs in developing countries. *Sci Total Environ* 569:476–488
- Cornwell DA, Lee RG (1994) Waste stream recycling-its effect on water-quality. *J AWWA* 86:50–63
- Cornwell DA, Macphee MJ (2001) Effects of spent filter backwash recycle on Cryptosporidium removal. *J AWWA* 93(4):153–162
- Das D, Nandi BK (2019) Defluoridization of drinking water by electrocoagulation (EC): process optimization and kinetic study. *J Dispersion Sci Technol* 40(8):1136–1146
- Das D, Nandi BK (2021) Arsenic removal from tap water by electrocoagulation: investigation of process parameters, kinetic analysis, and operating cost. *J Dispersion Sci Technol* 42(3):328–337
- Dehghani MH, Omrani GA, Karri RR (2021) Solid waste—sources, toxicity, and their consequences to human health. In: *Soft computing techniques in solid waste and wastewater management* (Elsevier)
- Di Giovanni G et al (1999) Quantitation of intact and infectious cryptosporidium parvum oocysts using quantitative sequence detection. *Proc 1996 AWWA WQTC*, Tampa, Fla
- Ebrahimi A, Taheri E, Pashae A, Mahdavi M (2015) The effectiveness of polyaluminum ferric chloride (PAFCI) for turbidity and color removal from Isfahan raw water. *Desalin Water Treat* 55:1966–1972
- Gao B, Yue Q (2005) Effect of ratio and OH⁻/Al³⁺ value on the characterization of coagulant poly-aluminum-chloride-sulfate (PACS) and its coagulation performance in water treatment. *Chemosphere* 61:579–584
- Gao W, Liang H, Ma J, Han M, Chen Z-L, Han Z-S, Li G-B (2011) Membrane fouling control in ultrafiltration technology for drinking water production: a review. *Desalination* 272(1–3):1–8

- Guigui C, Rouch JC, Durand-Bourlier L, Bonnelye V, Aptel P (2002) Impact of coagulation conditions on the in-line coagulation/UF process for drinking water production. *Desalination* 147(1–3):95–100
- Howe KJ, Marwah A, Chiu KP, Adham SS (2006) Effect of coagulation on the size of MF and UF membrane foulants. *Environ Sci Technol* 40(24):7908–7913
- Huang C, Lin J-L, Lee W-S, Pan JR, Zhao B (2011) Effect of coagulation mechanism on membrane permeability in coagulation-assisted microfiltration for spent filter backwash water recycling. *Colloids Surf, A* 378:72–78
- Huang H, Schwab K, Jacangelo JG (2009) Pretreatment for low pressure membranes in water treatment: a review. *Environ Sci Technol* 43(9):3011–3019
- Huang H, Young TA, Jacangelo JG (2008) Unified membrane fouling index for low pressure membrane filtration of natural waters: principles and methodology. *Environ Sci Technol* 42(3):714–720
- Jacangelo JG, Aieta EM, Carns KE, Cummings EW, Mallevalle J (1989) Assessing Hollow-Fiber Ultrafiltration for Particulate Removal. *Journal (Amer Water Works Assoc)* 81(11):68–75
- Jermann D, Pronk W, Meylan S, Bollor M (2007) Interplay of different NOM fouling mechanisms during Ultrafiltration for drinking water production. *Water Res* 41(8):1713–1722
- Karri RR, Ravindran G, Dehghani MH (2021) Wastewater—sources, toxicity, and their consequences to human health. In: *Soft computing techniques in solid waste and wastewater management*. Elsevier, pp. 3–33
- Lai C-H, Chou Y-C, Yeh H-H (2015) Assessing the interaction effects of coagulation pretreatment and membrane material on UF fouling control using HPSEC combined with peak-fitting. *J Membr Sci* 474:207–214
- Lee JD, Lee SH, Jo MH, Park PK, Lee CH, Kwak JW (2000) Effect of coagulation conditions on membrane filtration characteristics in coagulation-microfiltration process for water treatment. *Environ Sci Technol* 34(17):3780–3788
- Lee W, Lee H-W, Choi J-S, Oh HJ (2013) Effects of transmembrane pressure and ozonation on the reduction of ceramic membrane fouling during water reclamation. *Desalin Water Treat* 52(4–6):612–617
- LeGouellec YA, Cornwell DA, MacPhee MJ (2004) Treating Microfiltration Backwash. *J AWWA* 96(1):72–83
- Lehman SG, Liu L (2009) Application of ceramic membranes with pre-ozonation for treatment of secondary wastewater effluent. *Water Res* 43(7):2020–2028
- Li S, Heijman SGJ, Verberk J, Verliefe ARD, Amy GL, Van Dijk JC (2012) Removal of different fractions of NOM foulants during demineralized water backwashing. *Sep Purif Technol* 98:186–192
- Lin JL, Huang CP, Pan JR, Wang DS (2008) Effect of Al (III) speciation on coagulation of highly turbid water. *Chemosphere* 72:189–196
- Mahdavi M, Amin MM, Hajizadeh Y, Farrokhzadeh H, Ebrahimi A (2016) Removal of different NOM fractions from spent filter backwash water by polyaluminum ferric chloride and ferric chloride. *Arabian J Sci Eng*, 1–8
- Mahdavi M, Amin MM, Mahvi AH, Pourzamani H, Ebrahimi A (2018) Metals, heavy metals and microorganism removal from spent filter backwash water by hybrid coagulation-UF processes. *J Water Reuse Desalination* 8(2):225–233
- Mulder M (1997) *Basic principles of membrane technology* (2nd edition, corrected). Kluwer Academic Publishers, Dordrecht
- Nasser A, Huberman Z, Dean L, Bonner F, Adin A (2002) Coagulation as a pretreatment of SFBW for membrane filtration. *Water Supply* 2(5–6):301–306
- Nguyen AH, Tobiason JE, Howe KJ (2011) Fouling indices for low pressure hollow fiber membrane performance assessment. *Water Res* 45(8):2627–2637
- Orrono DI, Lavado RS (2009) Distribution of extractable heavy metals in different soil fractions. *Chem Speciat Bioavailab* 21:193–198

- Peter-Varbanets M, Margot J, Traber J, Pronk W (2011) Mechanisms of membrane fouling during ultra-low pressure ultrafiltration. *J Membr Sci* 377:42–53
- Raj CBC, Kwong TE, Cheng WW, Fong LM, Tiong SH, Klose PS (2008) Wash water in waterworks: contaminants and process options for reclamation. *J Environ Sci* 20:1300–1305
- Reissmann FG, Uhl W (2006) Ultrafiltration for the reuse of spent filter backwash water from drinking water treatment. *Desalination* 198(1–3):225–235
- Sartor M, Schlichter B, Gatjal H, Mavrov V (2008) Demonstration of a new hybrid process for the decentralized drinking and service water production from surface water in Thailand. *Desalination* 222(1–3):528–540
- Schneider OD, Tobiason JE (2000) Preozonation effects on coagulation. *Journal (Amer Water Works Assoc)* 92(10):74–87
- Singer PC, Arlotta C, Snider-Sajdak N, Miltner R (2003) Effectiveness of preand intermediate ozonation on the enhanced coagulation of disinfection byproduct precursors in drinking water. *Ozone Sci Eng* 25(6):453–471
- Song H, Fan X, Zhang Y, Wang T, Feng Y (2001) Application of microfiltration for reuse of backwash water in a conventional water treatment plant—a case study. *Water Supply* 1(5–6):199–206
- Song P, Yang Z, Zeng G, Yang X, Xu H, Wang L, Xu R, Xiong W, Ahmad K (2017) Electrocoagulation treatment of arsenic in wastewater: a comprehensive review. *Chem Eng J* 317:707–725
- Susanto H (2007) Fouling study in ultrafiltration-mechanism and control via membrane surface modification, Universität Duisburg-Essen, Fakultät für Chemie» Technische Chemie
- Sutherland RA (2003) Lead in grain size fractions of road-deposited sediment. *Environ Pollut* 121:229–237
- Thakur LS, Mondal P (2017) Simultaneous Arsenic and fluoride removal from synthetic and real groundwater by electrocoagulation process: parametric and cost evaluation. *J Environ Manag* 190:102–112
- Thirugnanasambandham K, Karri RR (2021) Preparation and characterization of *Azadirachta indica* A. Juss. plant based natural coagulant for the application of urban sewage treatment: modelling and cost assessment. *Environ Technol Innov* 23:101733
- Udayakumar GP, Muthusamy S, Selvaganesh B, Sivarajasekar N, Rambabu K, Sivamani S, Hosseini-Bandegharai A (2021) Ecofriendly biopolymers and composites: preparation and their applications in water-treatment. *Biotechnol Adv*, 107815
- Van Geluwe S, Braeken L, Van der Bruggen B (2011) Ozone oxidation for the alleviation of membrane fouling by natural organic matter: a review. *Water Res* 45(12):3551–3570
- Walsh ME, Gagnon GA, Alam Z, Andrews RC (2008) Biostability and disinfectant by-product formation in drinking water blended with UF-treated filter backwash water. *Water Res* 42(8–9):2135–2145
- Wang H, Qu F, Ding A, Liang H, Jia R, Li K, Bai L, Chang H, Li G (2016) Combined effects of PAC adsorption and in situ chlorination on membrane fouling in a pilot-scale coagulation and ultrafiltration process. *Chem Eng J* 283:1374–1383
- Wang Z, Teychene BT, Chalew TEA, Ajmani GS, Zhou T, Huang H, Wu X (2014) Aluminum-humic colloid formation during pre-coagulation for membrane water treatment: mechanisms and impacts. *Water Res* 61:171–180
- Yu W-Z, Graham N, Liu H-J, Qu J-H (2013) Comparison of $FeCl_3$ and alum pre-treatment on UF membrane fouling. *Chem Eng J* 234:158–165
- Zhang L-L, Yang D, Zhong Z-J, Gu P (2008) Application of hybrid coagulation-microfiltration process for treatment of membrane backwash water from waterworks. *Sep Purif Technol* 62:415–422
- Zhao H, Hu C, Liu H, Zhao X, Qu J (2008) Role of aluminum speciation in the removal of disinfection byproduct precursors by a coagulation process. *Environ Sci Technol* 42:5752–5758
- Zularisam AW, Ismail AF, Salim R (2006) Behaviours of natural organic matter in membrane filtration for surface water treatment—a review. *Desalination* 194(1–3):211–231

Ultrafiltration Integrated Photocatalytic Treatment Systems for Water and Wastewater



C. Nirmala Rani and S. Karthikeyan

Abstract Advanced wastewater treatment and reclamation is a sustainable strategy to address the issues related to emerging contaminants (ECs) present in aqueous solutions. Conventional treatment methods are found to remove ECs only partially. Low-pressure membrane separation processes have received extensive attention from researchers worldwide due to their simplicity, eco-friendliness, continuous separation, easy scaling up, the possibility of hybrid processing, low fabrication, and operating costs. However, these processes are limited due to low membrane lifetime, low selectivity, flux decline, linear up-scaling, and fouling. Heterogeneous photocatalytic systems using TiO_2 photocatalyst had been intensively investigated and found to be efficient, economical and environmentally friendly, and sustainable for the degradation of ECs from aqueous solutions owing to the various advantages it possesses including (i) an increase in photocatalytic potential, (ii) stability (chemical and thermal), (iii) energy efficiency, (iv) cost-effectiveness, and (v) non-toxicity. However, these systems have the drawbacks of catalyst separation after treatment and incomplete mineralization. Photocatalysis (PCO) has been integrated with low-pressure membrane systems to address this issue. This chapter provides an overview of ultrafiltration (UF) integrated photocatalytic oxidation (PCO) systems in aqueous solutions, especially for the removal of emerging contaminants (ECs). The mechanisms, merits, and demerits of UF separation, PCO process, and integrated ultrafiltration-photocatalytic oxidation (UF-PCO) processes are discussed in detail. The key influencing factors/operating variables on the performance of UF-PCO systems such as; photocatalyst loading, structure, and properties of photocatalyst, light wavelength, light intensity, initial concentration of pollutant, pH of feed-water, temperature, aeration, inorganic ions, membrane material, membrane pore size, transmembrane pressure (TMP), membrane packing density, and cross-flow velocity (CFV) are discussed elaborately. Furthermore, the removal of ECs had been

C. N. Rani (✉)

Department of Civil Engineering, Jerusalem College of Engineering, Pallikaranai, Chennai 600100, India

S. Karthikeyan

Centre for Environmental Studies, Department of Civil Engineering, CEG Campus, Anna University, Chennai-600025, India

explored with respect to its characteristics and the same of the membrane. A discussion on the economic aspects of UF-PCO systems in water and wastewater treatment is also included.

Keywords Ultrafiltration · Photocatalytic oxidation · Permeate flux · Membrane fouling · Emerging contaminants

1 Introduction

Emerging contaminants (ECs) are chemicals, including pharmaceuticals, personal care products, hormones, pesticides, persistent organic pollutants (POPs), disinfection by-products, etc., that impact humans or ecology. The occurrence of ECs may be from anthropogenic and natural substances, and their concentrations in water generally range from nanograms to micrograms per litre (Luo et al. 2014). ECs in surface water would be a serious concern while using the ECs contaminated surface water for drinking purposes (Riva et al. 2018).

Membrane separation (MS) processes have become a new innovative emerging technology in treating aqueous solutions (Lau et al. 2020, Khan et al. 2021). During MS, the membrane identifies and recovers particles from aqueous solutions (Sirkar 2008). The pressure-driven (PD) membrane processes are more popular and extensively used than non-pressure-driven (NPD) processes. Microfiltration (MF), ultrafiltration (UF), nanofiltration (NF), and reverse osmosis (RO) is novel, attractive, and alternative methods to conventional treatment for treating both water and wastewater (Baker 1991; Ahmad 2005) due to their various advantages viz., (i) high-quality permeate, (ii) could be operated under moderate temperatures, (iii) low energy requirements, (iv) non-necessity of adding chemicals, (v) reusability of water, (vi) some valuable waste constituents, and (vii) could be easily coupled with other processes. During the MS process, depending upon the membrane's pore size, the contaminants/pollutants are removed, and water passes through the membrane. However, the main drawback in these systems is membrane fouling (Wiesner and Apel 1996; Scholz and Lucas 2003; Padaki et al. 2015) which leads to flux decline that can be reversible or irreversible.

UF membranes with an operating pressure of 2–8 bars can remove macromolecules with a molecular weight (MW) ranging from 1000–100,000 Da, bacteria, and viruses and fail to remove soluble and low MW compounds. However, UF membranes have successfully been applied for drinking water treatment over the past 15 years in the recently upgraded treatment plants (Huang et al. 2009).

The Photocatalytic oxidation (PCO) method is one of the advanced oxidation processes (AOPs) in which various light sources such as; ultraviolet (UV), visible (VIS), and infrared (IR) radiations are used to produce an oxidizing/reducing species (OH^{\bullet} and $\text{O}_2^{\bullet-}$) (Palmisano et al. 2007; Molinari et al. 2017, 2021). In this PCO system, hydroxyl radicals (reactive species) mineralize the hazardous, toxic organic compounds into simpler, harmless end products (Damodar et al. 2009; Rani and

Karthikeyan 2021). Heterogeneous photocatalysis has become more popular among the AOPs and found successful for the treatment of degrading hazardous pollutants due to; (i) the usage of safer and greener catalysts (particularly TiO_2), in contrast to the thermally induced catalysis that occurs in heavy metal catalysts (Guo et al. 2019; Riaz and Park 2020), (ii) mineralization of non-biodegradable organic compounds into non-toxic by-products with the help of molecular oxygen, (iii) high versatility due to its applicability in all three phases including liquid, solid and gaseous, (iv) usage of renewable solar energy and (v) could be coupled easily with other technologies (Tufail et al. 2020; Molinari et al. 2021). Despite its various advantages, the application of PCO processes in the treatment of both municipal and industrial wastewater is limited owing to; (i) the cost-related to the recovery and reuse of heterogeneous photocatalyst and (ii) poor process selectivity (Loddo et al. 2009; Molinari et al. 2017, 2021). To overcome these limitations, PCO processes are coupled with MS processes.

Coupling membrane filtration with advanced oxidation processes is an effective technique because of the technical feasibility of MS processes (Ganiyu et al. 2015). Combining classical photoreactors with membrane processes is a helpful method to meet green technology's environmental and economic benefits (Molinari et al. 2017).

Many of the organic compounds present in the water/wastewater are recalcitrant, endocrine-disrupting, and genotoxic. They directly impact ecosystems and will be a serious concern for both humans and the environment even though they are much lower in concentration up to ng/L. Recent research focused more on integrated UF-PCO systems, and the same was implemented in water and wastewater treatment (Mozia 2010). UF-PCO systems are found to be highly effective for the removal of organic compounds (Molinari et al. 2008; Sarasidis et al. 2014) due to the various advantages viz., (i) ambient temperature operation, (ii) no change in phase, and (iii) up to 90% removal of organic compounds (Rani et al. 2021).

Therefore this book chapter explores the applicability of UF-PCO systems in wastewater treatment. UF and PCO processes are overviewed separately regarding their features, mechanisms, and applications. The operating parameters that affect the integrated UF-PCO processes have been discussed elaborately. The types of UF-PCO systems and their operational limitations, such as membrane fouling and its control measures, are discussed in detail. In addition, the removal of emerging contaminants that are of great environmental concern has been discussed in detail with respect to the characteristics of ECs and membrane properties.

2 UF Membrane Process

2.1 An Overview

Ultrafiltration (UF) is a type of most widely used low pressure-driven membrane process in which molecular weight cut-off (MWCO) is used as an important tool to characterize the membrane. High molecular weight (HMW) compounds are retained

by the UF membrane, while low molecular weight compounds (LMW) are less retained/rejected or pass through the membrane (Mozia and Morawski 2009; Rani et al. 2021). The application of UF membranes is not only limited to treating industrial wastewaters, including wastewaters from food, dairy, beverage, and pharmaceutical industries, but also as an advanced method in treating municipal water and wastewater. Recovery, purification, and concentration of products are the added advantages of providing UF membranes in wastewater treatment. UF membrane was also employed in oily wastewater treatment due to: (i) the non-necessity of chemical additives and (ii) low energy cost (He and Jiang 2008). In oily wastewaters, heavy metals such as Cu and Zn have been removed up to 95% (Bilstad and Espedal 1996; Padaki et al. 2015), while benzene, toluene, and xylene (BTX) removal was only 54% (Bilstad and Espedal 1996) using UF membranes.

2.2 Membrane Materials

Membranes that treat aqueous solutions may be polymeric and inorganic (ceramic). Researchers in exploring new membrane materials have made intensive efforts.

2.2.1 Polymeric Membranes

The polymeric membrane materials could be cellulose acetate (CA), polypropylene (PP), polyacrylonitrile (PAN), polyethersulfone (PSU) and polysulfone (PSU), polytetrafluoroethylene (PTFE), and polyvinylidene fluoride (PVDF) (Ochoa et al. 2003; Rahimpour and Madaeni 2007; Mansourizadeh and Azad 2014) among which polyethersulfone (PSU) and polysulfone (PSU) are low UV resistant owing to the presence of sulfone groups. Similarly, polypropylene (PP), polyacrylonitrile (PAN), and cellulose acetate (CA) had also shown less resistance due to the breakage of chemical bonds of the methyl group (-CH-) when exposed to UV light. Meanwhile, polyvinylidene fluoride (PVDF) and polytetrafluoroethylene (PTFE) exhibited good UV resistance.

When polymeric membranes are applied in slurry UF-PCO systems, the membranes have the limitations such as; (i) low UV light resistance (Lee et al. 2001; Chin et al. 2006), (ii) damage in the structure of the membrane due to the generation of hydroxyl radicals (Chin et al. 2006; Mozia 2010) (Chin et al. 2006; Mozia 2010) and (iii) stability to resist the penetration of photocatalyst particles (Mozia et al. 2014, 2015). Photocatalytic membranes have direct exposure to the light source and get irradiated. The exposure of UV light for 10 days of 200 Mm H₂O₂ condition cracked the membrane surface. After 30_{days} of UV exposure and 3 wt% of TiO₂ nanoparticles, TiO₂/PVDF dual-layer membrane revealed a decrease in tensile strength from 28–23 MPa owing to the cracks formed on the surface of the membrane (Dzinun et al. 2017). However, UV light resistance of the membrane is based upon both the source materials and formulation of polymer (Chin et al.

2006). Hence the polymeric membranes were chosen for the water, and wastewater treatment should be better UV resistant.

2.2.2 Ceramic Membranes

A better substitute for polymeric membranes is ceramic membranes due to; (i) the high-water recovery rate, (ii) extended backwash intervals, (iii) less damage of membrane structure (Azrague et al. 2007), (iv) chemical resistance, (v) thermal stability, (vi) superior physical integrity, (vii) less chemical need, (viii) less membrane cleaning frequency, and (ix) longer membrane lifetime. In addition, the application of advanced oxidation processes could significantly reduce membrane fouling by organic compounds as a pre-treatment step, which improves the quality of water and reduces the operating costs. Ceramic membranes can withstand high backwash pressure and provide excellent backwash efficiency (Reguero et al. 2013).

Ceramic membranes are more advantageous than polymeric membranes due to; (i) great affinity between the membrane and photocatalyst, (ii) sustainability at elevated temperatures, and (iii) feasibility for transforming amorphous TiO_2 precursor to the photocatalytically active phase (e.g. anatase).

3 Photocatalyst

For photocatalytic processes, the light sources may be artificial lamps or solar irradiation (Alfano et al. 2000). The redox potential of an efficient semiconductor photocatalyst must lie within its bandgap (Li et al. 2005). Semiconductors such as; Fe_2O_3 , GaP, and GaAs have narrow bandgaps of 2.3 eV, 2.23 eV, and 1.4 eV, respectively, and can absorb visible light. TiO_2 has been widely used among semiconductor photocatalysts due to its chemical stability, low cost, and harmless nature (Fujishima et al. 2000), even though it has a broad bandgap of 3.2 eV. TiO_2 photocatalyst is not driven by visible light (Miyachi et al. 2002) and can only be activated upon irradiation in the UV domain ($\lambda \leq 387$ nm for anatase) (Irie et al. 2003; Pelaez et al. 2012). Since 5% of the solar spectrum is occupied with UV and 95% of UV are in the UV-A range, researchers had focussed their work on the preparation of novel photocatalysts that can be activated upon the solar spectrum of the visible range (Rehman et al. 2009). In the recently developed UF-PCO systems, visible-light photocatalysts (Gao et al. 2014; Athanasekou et al. 2014) had been applied. To lower the bandgap of TiO_2 and to increase the photocatalytic activity visible light active solar spectrum, photocatalysts have been modified by composite photocatalysis with carbon nanotubes (Yu et al. 2005; Ahmed et al. 2021) noble metals or metal ions (Ni et al. 2007), dye sensitizers (Tabei et al. 2012), and non-metal doping (Fujishima et al. 2008). The graphical representations of bandgaps of photocatalyst subjected to UV and visible light are graphically illustrated in Fig. 1a. Chong et al. (2010) and Malato et al. (2009) had discussed the same in detail in their studies. Modification of photocatalyst with

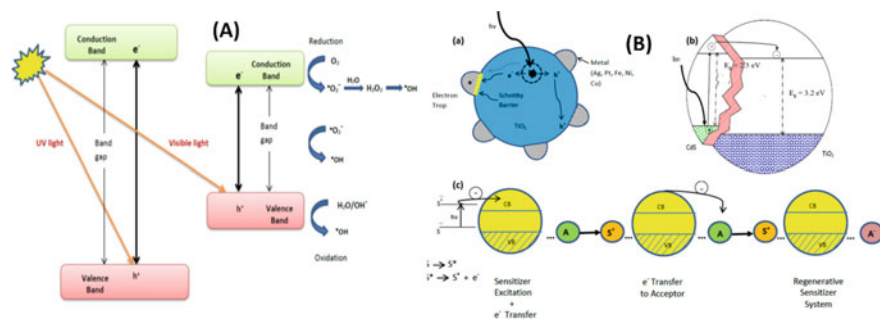


Fig. 1 A Graphical illustration of bandgaps of photocatalyst subjected to UV and visible light; **B a** Modified metal photocatalyst, **b** TiO_2 coupled semiconductor, **c** Dye sensitizer—excitation steps (Rani et al. 2021)

metal, coupling TiO_2 with semiconductor, and the excitation steps of a dye sensitizer are graphically illustrated in Fig. 1b. Even though visible light active photocatalysts are cost-effective, for the practical applicability of the process, the process should promote extensive usage of photons and high quantum efficiency (Argurio et al. 2018).

4 UF Membranes Integrated PCO (UF-PCO) Systems

The schematic diagram of a UF-PCO system is graphically illustrated in Fig. 2. The configurations of UF-PCO systems could be of two types, namely; (i) systems with immobilized photocatalyst (photocatalyst is supported on a carrier material) and (ii) systems with suspended photocatalyst (photocatalytic particles remain in suspension). Immobilized UF-PCO systems could be further divided into three types, namely; (i) membrane surface coated with photocatalyst, (ii) membrane with photocatalyst blended, and (iii) stand-alone photocatalytic membrane. In the first two types of Immobilized UF-PCO systems, photocatalysts are initially manufactured and then coated/blended with the membrane, while in the third type of system, the membrane itself is fabricated with a photocatalyst in pure form. Based upon the position of the PCO unit and UF module, UF-PCO systems with photocatalyst in suspension were further divided into two types as (i) split type and (ii) integrative type. In integrative type UF-PCO systems, the UF module and PCO unit are merged in one apparatus, and both UF separation and PCO processes occur simultaneously in the same reactor vessel, while in the split type UF-PCO systems, two processes occur separately in two different apparatuses. The merits and demerits of both types of UF-PCO systems are represented in Tables 1 and 2.

Integrated UF and PCO technology has attracted many recent researchers and has been declared an effective method of treating both water and wastewater. PCO units may be employed pre-or post-treatment with UF systems. While degrading

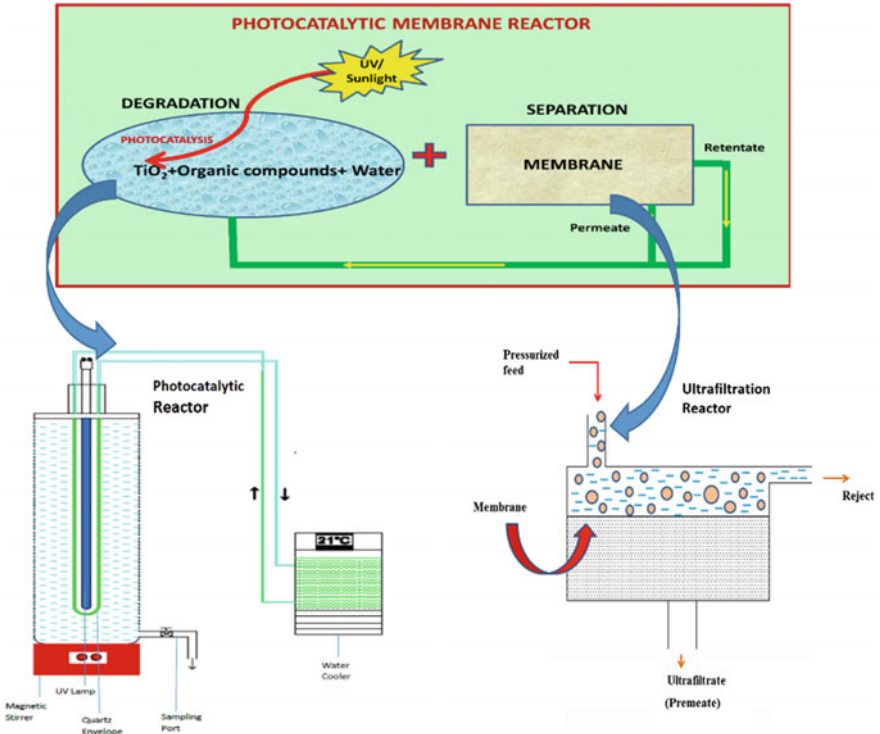


Fig. 2 A typical integrated UF-PCO system

Table 1 The characteristics of UF membrane

Type of membrane material	polymeric, metallic, ceramic
membrane pores	1 to 100 nm
Type of driving force applied	Pressure (1 to 10 bar)
Mechanism of transport	Flow through pores
Mechanism of separation	Size exclusion or sieving
Permeate flux	50 to 1000 L/m ² h
Energy requirement	10 to 150 W/m ³

organic compounds, the PCO system could be used as a pre-treatment system in the feedwater. In contrast, in the integrated UF-PCO system, PCO could be used as a post-treatment system during the mineralisation of contaminants in permeate and retentate. (Rani et al. 2021) (Fig. 3).

The application PCO unit with the UF system may be either as a (i) pre-treatment system or as a (ii) post-treatment system. During degradation of organic compounds in the feed water, the UF-PCO system could be used as a pre-treatment system. In contrast, the integrated system could be used as a post-treatment system during the

Table 2 Merits and demerits of UF-PCO systems with photocatalysts in suspension and immobilized

	UF-PCO systems with photocatalysts in suspension	UF-PCO systems with immobilized photocatalyst
Advantages	<ol style="list-style-type: none"> 1. Due to more active surface area for adsorption, high photocatalytic activity, and degradation efficiency 2. Photocatalyst loadings can be easily varied to the required value 3. Destruction of membrane structure due to UV light and hydroxyl radicals could be avoided 4. Exhausted catalysts can be replaced without replacing the membrane 	<ol style="list-style-type: none"> 1. Non-necessity of photocatalyst separation after treatment 2. Degradation of compounds occurs in both the feed and permeate sides 3. Less membrane fouling owing to the increase in hydrophilicity and degradation of organic compounds 4. Catalyst separation and recycling are not needed
Disadvantages	<ol style="list-style-type: none"> 1. Due to the presence of suspended photocatalyst nanoparticles, a light scattering effect is observed 2. Membrane fouling is caused by photocatalysts and pollutants, which leads to permeate flux decline 3. Higher operating cost 4. An additional process is needed to separate photocatalyst particles from the treated solution 	<ol style="list-style-type: none"> 1. Due to the less surface area available for photodegradation, photocatalytic efficiency is less 2. According to the wastewater composition, photocatalyst concentration cannot be adjusted 3. Destruction of polymeric membrane structure by UV light and the reactive species (hydroxyl radicals) 4. The membrane has to be exchanged when the photocatalyst loses its activity

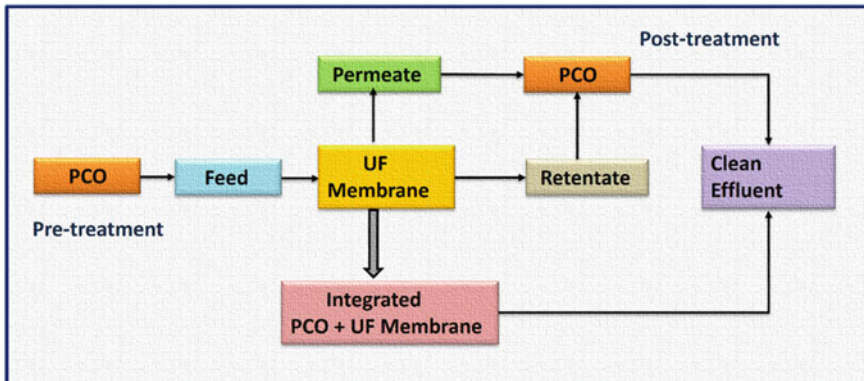


Fig. 3 The graphical illustration of the scheme UF process with PCO used for wastewater treatment (Rani et al. 2021)

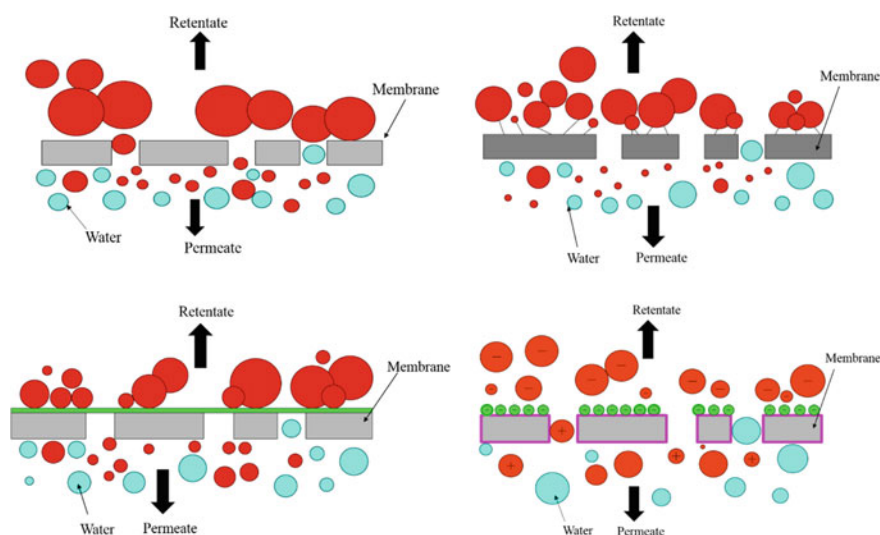


Fig. 4 ECs removal mechanisms through membrane separation; **a** size exclusion, **b** hydrophobic interactions, **c** adsorption, and **d** electrostatic interactions (Rani et al. 2021)

mineralisation of contaminants in permeate and retentate. (Rani et al. 2021). The flow diagram illustrating the scheme of the UF process with PCO used for wastewater treatment is illustrated in Fig. 4.

Even though many literature studies on UF integrated PCO processes are available with different configurations (Fernandez et al. 2014; Sarasidis et al. 2014; Rani and Karthikeyan 2018) and all cannot be discussed in order to get a complete understanding of the configurations, a thorough reading of each literature is needed.

5 Operating Variables of Integrated UF-PCO Systems and Their Effect on Degradation

While fabricating the economically viable and technically feasible UF-PCO system, selecting appropriate operating parameters is vital. The parameters that affect the UF-PCO systems are; (i) structure, properties, and loading of photocatalyst, (ii) light wavelength and intensity, (iii) initial concentration of pollutant (iv) feedwater pH (v) temperature, (vi) inorganic ions, (vii) aeration, (viii) membrane material, (ix) membrane pore size, (x) aeration, (xi) transmembrane pressure (TMP), and (xii) membrane module packing density.

5.1 Effect of Photocatalyst Loading on Pollutant Degradation

In slurry UF-PCO systems, the increase in photocatalyst loading results in increased surface area for catalyst adsorption and photodegradation up to a certain extent and a further increase in the concentration of photocatalyst reduced the degradation rate. It hence decreased the removal efficiency (Gaya and Abdullah 2008). The decrease in removal efficiency may be due to excess photocatalyst concentration, which leads to higher solution opacity, increased solution turbidity, and reduced photons' penetration through the reaction mixture. In addition, the agglomeration of photocatalyst also reduces the total surface area of photocatalyst (Mozia 2010; Zhang et al. 2016) and hence reduces the photocatalytic activity in UF-PCO systems.

In immobilized UF-PCO systems, photocatalyst concentration increases the photodegradation rate. Excessive addition of photocatalyst would diminish the photocatalytic activity of photocatalyst at the bottom layer through absorption, light scattering, reflection, and blockage of UV light. In addition, adding more amounts of photocatalyst will also decrease the membrane pores and porosity (Xiao et al. 2010). Furthermore, an optical thickness that considers both geometrical thicknesses of the photoreactor and photocatalysts concentration is identified as one of the elemental parameters of a photocatalytic reactor (Zheng et al. 2017).

5.2 Effect of Properties and Structure of Photocatalyst on Pollutant Degradation

The properties and structure of photocatalysts that include bandgap energy, active surface area, crystal composition, and particle size have a greater impact on its efficiency (Zheng et al. 2017). The bandgap is an important property that must be considered while selecting a photocatalyst. The photocatalyst can achieve visible light response when it has lower bandgap energy, due to which it needs less energy for the excitation of electrons from the valence band (VB) to the conduction band (CB). Due to more photocatalytic activity, less toxicity, and chemical stability, TiO₂ based photocatalysts have become more popular. However, photocatalysts with a greater bandgap could be modified in order to make them responsive to visible light.

5.3 Effect of Light Wavelength on Pollutant Degradation

The UV electromagnetic spectrum can be divided into three types namely; UV-A ($\lambda_{\text{max}} = 315\text{--}400\text{ nm}$) (3.10 eV to 3.94 eV), UV-B ($\lambda_{\text{max}} = 280\text{--}315\text{ nm}$) (3.94 eV to 4.43 eV) and UV-C ($\lambda_{\text{max}} = 100\text{--}280\text{ nm}$) (4.43 eV to 12.4 eV) (Chong et al. 2010; Zheng et al. 2017). The UV flux near the earth's surface is 20–30 W/m². This range of UV flux corresponds to 0.2–0.3 mol photons/m²h (300–400 nm) provided

by the sun is more efficient for the degradation of pollutants in the aqueous phase. Both UV-A and UV-C lamps are widely used due to their ability to obtain higher photon fluxes. An increase in light wavelength decreased photocatalytic degradation (Zhang et al. 2008). Shorter wavelengths caused higher energy illumination (Zertal et al. 2001; Han et al. 2004). However, the utilization of solar lights is limited during cloudy days. Hence recent studies have been focused on modifying photocatalysts to the visible solar range of the spectrum (Rehman et al. 2009). A UF-PCO system was evaluated by Kertész et al. (2014) for the removal of Acid Red 1 employing 365 nm and 254 nm irradiation intensities and reported that the degradation rate was rapid and greater at 254 nm.

5.4 Effect of Light Intensity on Pollutant Degradation

The effect of light intensity on pollutant removal could be divided into three stages (Mozia et al. 2010; Zhang et al. 2013) as (i) low intensities in the range of 0–20 mW/cm²; Due to negligible electron–hole recombination, the degradation rate of pollutant increases linearly with the intensity of light (Wang et al. 2013), (ii) High light intensities of >25 mW/cm²; Since electron–hole pair separation competes with recombination, the degradation rate of pollutant is related to the intensity of light, (iii) High light intensities of >25 mW/cm²; degradation rate of pollutant is independent of light intensity (Argurio et al. 2018). Increasing the light intensity increases the volumetric reaction rate until the mass transfer limit is obtained (Ollis et al. 1991). When the irradiation intensity of light is high, there is a transfer of electrons from the photocatalyst to oxygen in water, forming O₂^{•-}. This limits the degradation rate when the size of the photocatalyst particles is more or when it agglomerates (Doll and Frimmel 2005).

5.5 Effect of Initial Pollutant Concentration on Pollutant Degradation

The initial concentration of compound/pollutant is a key parameter that affects the performance of UF-PCO systems. An increase in the pollutant concentration imparts a negative impact on degradation efficiency due to the loss of solution opacity, less transmission of UV light, and occupation of active sites of photocatalyst by the pollutants (Damodar et al. 2010; Kertész et al. 2014). In addition, at high initial pollutant concentration, a thick fouling layer was observed on the surface of the membrane, which severely affected the compound degradation rate due to the availability of a lesser surface area. At lower initial concentrations, the degradation was more (Ong et al. 2014).

5.6 *Effect of Feedwater pH on Pollutant Degradation*

The feed solution pH significantly impacts degradation, and it is very complex. The impact of variations in feedwater pH on the photocatalytic degradation of organic compounds in aqueous solution depends upon (i) the ionization state of photocatalyst surface, (ii) generation of hydroxyl radicals, (iii) agglomeration of photocatalyst particles, (iv) position of valence and conduction band of photocatalyst, and (iv) hydroxyl radical generation.

For the membrane separation process, the difference in pH leads to a change in zeta potential values of photocatalyst particles. The change in pH will increase the particle size of the photocatalyst due to the photocatalyst particles' dispersion and agglomeration and has a significant impact on membrane permeate flux (Huang et al. 2007). In addition, electrostatic attraction between pollutants and the photocatalytic layer on the membrane surface varies at different pH conditions (Ma et al. 2009) and influences the adsorption of pollutant molecules on the membrane surface.

Wang et al. (2013) investigated the degradation of carbamazepine (CBZ) using C-N-S doped TiO₂ and reported that the degradation of CBZ was maximum at alkaline pH. This result contradicts the results obtained by Fu et al. (2006) (for fulvic acid degradation) and Chin et al. (2007b) (for Bisphenol A degradation), in which the authors reported the maximum degradation at acidic pH. Khan et al. (2015) reported that HA degradation was twice more at low pH than at high pH. Since contradictory results are available, more research needs to focus on the effect of pH on photocatalytic degradation.

5.7 *Effect of Temperature*

The ideal temperature for photodegradation studies falls between 20 °C and 80 °C (Herrmann 1995, 2005; Gogate and Pandit 2004). At low temperature (below 0 °C) there is an increase in apparent activation energy due to which the degradation products desorb from the catalyst surface, and hence the process emerges as a rate-limiting step (Chong et al. 2010). At high temperatures >80 °C, electron-hole recombination is enhanced that diminishes photodegradation and hence low degradation efficiency. For the temperature range of 20 °C–60 °C, an increase in the photodecomposition rate was observed (Mozia et al. 2005; Thiruvenkatachari et al. 2008).

In UF-PCO systems, the temperature substantially influences solution viscosity and affects the permeate flux of the membrane. At high temperatures, feed solution viscosity decreases, and induced turbulence disperses the fouling cake and concentration polarization layers on the membrane surface. This increases the permeate flux of the membrane.

5.8 Effect of Inorganic Ions

The impacts of the presence of inorganic salts such as NaHCO_3 , Na_2HPO_4 , and Na_2SO_4 in the feed solution on fouling and stability of UF membranes applied in the UF-PCO system was investigated by Darowna et al. (2014). The authors observed a remarkable decrease in membrane flux when salt content was high. Severe permeate flux decrease was noticed when HCO_3^- ions were present, which may be owing to increased pH and a dense fouling layer formed on the membrane surface. It was also observed that the maximum permeate flux (even greater than the permeate flux obtained in UF-PCO systems with fresh photocatalyst) was observed when SO_4^{2-} ions were present. The increased permeate flux was owing to the repulsion of TiO_2 photocatalyst particles over the membrane surface and produced lower fouling layer thickness.

5.9 Effect of Aeration

In PCO-UF systems, aeration serves three important purposes; (i) enhances photo-oxidation of organic molecules by providing dissolved oxygen (DO) for suppressing electron-hole recombination reactions (Asha and Kumar 2015), (ii) facilitates homogeneous mixing and fluidize the system, and (iii) induces turbulence in submerged membrane systems and reduces membrane fouling. An increase in aeration rates generates more shear rates, keeps the photocatalyst particles in suspension, and prevents agglomeration. Lesser the agglomeration, the greater the degradation rate of the compounds due to the availability of more surface area (Chin et al. 2007a). However, excessive aeration prevents the adsorption of pollutants onto the photocatalytic surface and decreases the removal efficiency. Aeration provided in the form of the coarse bubble (Huang et al. 2009) or bubbly flow (Du et al. 2017) generated turbulent flow, induced shearing effect, removed fouling layer, and concentration polarization onto membrane surface (Zheng et al. 2017).

5.9.1 Effect of Membrane Material

The membrane material is an important parameter that affects pollutant removal efficiency. UV light greatly influences polymeric membranes, and UV light exposure could damage the membrane material (Chin et al. 2006). The breakage of the chemical bonds of the methyl group (-CH-) was found to be responsible for membrane damage in PAN, polypropylene (PP) and, cellulose acetate (CA) membranes, while the presence of sulfone groups in polyethersulfone (PES) and polysulfone (PSU) membranes caused for the damage in membrane structure. However, PTFE and PVDF membranes are the least affected polymeric membranes by UV light. In addition to

this, it was also observed that ceramic and metallic membranes exhibited higher resistance to UV lights. Though ceramic membranes consist of different materials such as; TiO_2 , Al_2O_3 , and ZrO_2 , TiO_2 membranes are mostly employed in ultrafiltration (UF) systems since they possess excellent hydrophilic properties and better fouling resistance (Wang et al. 2007). Due to chemical stability and increased mechanical strength, ceramic membranes were the best suitable for UF-PCO systems (Zhang et al. 2016; Horovitz et al. 2019).

5.9.2 Effect of Membrane Pore Size on Compound Removal

The chosen pore size of the selected membrane must exhibit (i) a high retention rate for the target pollutants, (ii) high photocatalytic separation efficiency (Zheng et al. 2017) and greater membrane permeate flux (Xiao et al. 2010). For the efficient applications of UF membranes in UF-PCO systems, the membrane pores' size is greater to reduce membrane resistance and increase the permeate flux (Xiao et al. 2010). Low-pressure UF membranes can retain particles over 10 nm and hence could be able to separate the photocatalyst more efficiently. However, it is to be noted that when high-quality permeate is required, high-pressure membranes are of good choice. High-pressure membranes exhibit high separation efficiency, retain pollutants and their intermediates for further treatment, and promote removal efficiency.

5.9.3 Effect of Transmembrane Pressure (TMP) and Cross Flow Velocity (CFV) on Compound Removal

Choo et al. (2008) observed a reduction in permeability while CFV decreases from 1.45 to 0.19 m/s. Without backwashing, higher TMP and lower CFV intensified the deposition of TiO_2 particles on the membrane surface, which resulted in membrane fouling and a decrease in compound removal efficiency (Wang and Lim 2012). The cake resistance decreased with an increase in CFV. Higher values of CFV and shear rates could dislodge the photocatalyst particles on the membrane surface, lessen the cake layer thickness and reduce membrane fouling (Wang 2016). When TMP is increased, the permeation rate of the reaction mixture is accelerated. This increases cake and fouling resistances and may cause less membrane life (Zhang et al. 2007). In general, to achieve guaranteed flux, the TMP should be kept as low as possible.

5.9.4 Effect of Membrane Packing Density on Compound Removal

The voids in the fibers not only allow water to flow through but also promote mass transfer between the feedwater and the surface of the membrane (Yeo et al. 2006; Günther et al. 2010; Ren et al. 2013). Small diameter hollow fibers with high packing density contribute to more filtration area and promote profound inter-fiber fouling within the fibers (Yoon et al. 2004; Günther et al. 2010; Ong et al. 2015). Membrane

with high fiber packing density caused the foulant to accumulate inside the fiber module and adversely affected photoactivity. This observation was in line with the observations made by Günther et al. (2010). In this study, the author noticed an increase in permeate flux by 25% when fiber packing density decreased from 80 to 40%. An increase in packing density decreased the mass transfer coefficient up to 50% of the total volume fraction, and a further packing density increased the mass transfer coefficient (Wu and Chen 2000).

6 Recovery and Reuse of Photocatalyst Particles in UF-PCO Systems

The major advantage of integrating membrane processes with photocatalysis is the recovery of photocatalyst particles from the treated solution and the reuse of recovered photocatalyst particles. All types of pressure-driven membrane processes, including MF processes even with the pore sizes of 0.1 μm (Huang et al. 2007; Choo et al. 2008) and 0.4 μm (Meng et al. 2005) were found to be very effective in retaining photocatalyst particles.

By synergistically coupling MS with PCO systems and continuously operating the reactor, the photocatalyst particles were effectively recovered and reused (Jiang et al. 2010; Rani and Karthikeyan 2018; Espindola et al. 2019), which was confirmed by the low turbidity detected in the permeate. Jiang et al. (2010) reported the permeate turbidity <0.3 NTU after continuously recirculating the solution and operating the UF-PCO system for 120 min. Rani and Karthikeyan (2018) utilized the same slurry for the seven cycles and found that the degradation and mineralization efficiencies remained almost the same after running the reactor for seventh cycles when the photocatalyst was fresh and used. Due to the deposition of photocatalyst particles over the membrane surface, a small drop in removal efficiencies was noticed during the second cycle.

UF membranes were proved to be highly effective in dislodging photocatalyst particles and removing the dense cake layer formed on the membrane surface (dynamic membrane). TiO_2 photocatalyst particles are nm in size (the size lesser than the pore size of UF membrane) and hence could not be rejected by UF membranes. However, when they are dispersed into the feedwater solution, the size of the photocatalyst particles increases from nm to μm due to agglomeration and hence easily retained by low-pressure UF membranes.

Sopajaree et al. (1999) employed a UF-PCO system with a TiO_2 concentration of 1 g/L and reported the permeate turbidity of 0.22–0.45 NTU while the feedwater turbidity measured during this study was 5200 NTU. Similarly, the studies conducted by Mozia and coworkers on UF-PCO systems with TiO_2 concentrations of 0.1–0.5 g/L reported a significant reduction in permeate turbidity. The permeate turbidity ranged 0.07–0.08 NTU TiO_2 concentrations of 0.1–0.5 g/L confirms the effective separation efficiency of the UF membrane (Mozia et al. 2006, 2009). During their

study, Espindola et al. (2019) noticed that the UF-PCO system was highly efficient in separating photocatalyst particles from the treated water. The permeate turbidity noticed was 4100 times lower than feedwater turbidity, having a value of <0.1 NTU. The results obtained from the studies conducted on UF-PCO systems demonstrated the excellent separating efficiency of UF membranes.

7 Membrane Fouling and Its Control Measures in UF-PCO Systems

Modern UF-PCO systems and their applications have spanned various water and wastewater treatment fields. However, fouling on the membrane surface is a major drawback that reduces the potential of this technology. Due to high energy demand, membrane fouling may increase operational costs, additional labour needed for maintenance, the cost of chemicals needed for membrane cleaning, and reduced membrane life. More challenging and effective methods had been developed and found successful in controlling and minimizing fouling. Membrane fouling could be prevented by various methods such as; feedwater pre-treatment, surface modification of membrane, aeration, UV irradiation, optimization of operational conditions, and periodic membrane cleaning (Williams and Wakeman 2000; Hilal et al. 2005; Rani et al. 2021).

7.1 Membrane Cleaning

Among the membrane cleaning methods, periodical membrane cleaning is one of the methods applied for cleaning the membrane and reducing membrane fouling (D'Souza and Mawson 2005). The membrane could be cleaned by means of washing it with pure water or with chemicals. The chemicals used for membrane cleaning may be NaClO, NaOH, or HCl (Huang et al. 2007; Yue et al. 2021). Automatic periodic backwashing effectively controlled fouling (Molinari et al. 2000; Sarasidis et al. 2014). Backwashing displaces the photocatalyst particles from the membrane pores and loosens filtration cakes (Gao et al. 2011). The working flux required for backwashing is at least two times greater than the normal filtration flux. In UF-PCO systems, the fouling observed was reversible since even 2 min of distilled water backwashing at a flow rate of $150 \text{ cm}^3/\text{h}$ (Damszel et al. 2009) and after 15 min filtration with moderate permeate flux and 1 min of backwashing dislodged (Patsios et al. 2013) photocatalyst particles on the membrane surface and mitigated membrane fouling.

Furthermore, the membrane could be washed with either water or chemicals. If we compare both types of washing while washing the membrane with chemicals, the flux recovery rate was high. While washing plain PVDF membrane and modified

PVDF membrane with nano $\text{TiO}_2/\text{Al}_2\text{O}_3$ with pure water, the flux recovery rates were 88% and 94%, respectively, for which the flux recovery rates were 95% and 100% when washed with NaClO solution (Yi et al. 2011).

7.2 Aeration

In slurry PCO-UF systems, photocatalyst particles remained in suspension by providing aeration due to the turbulence created. Air sparging is one method that could enhance membrane flux and control membrane fouling (Cui and Taha 2003). This method could also reduce concentration polarization and perform as a good control for colloidal settlements (Laborie et al. 1997; Cabassud et al. 1997). Coarse bubble aeration was found to be a more efficient technique than fine bubble aeration, maintained the photocatalyst particles in suspension, and prevented catalyst entrapment over the membrane surface (Huang et al. 2007) in slurry UF-PCO systems.

Cleaning the membrane by the method of air sparging after 5 days of operation sustained the permeability of the membrane up to 50% of the original initial value, which was almost 30% more than that obtained by conventional backwashing. In addition, no flux decline was observed when sequentially applying air sparging along with backwashing at low TMP (Psoch and Schiewer 2006). However, the air sparging method of membrane cleaning may be applied only to the cross-flow mode of UF filtration and not to the dead-end mode (Guigui et al. 2003). In order to supply oxygen and to keep the photocatalyst particles in suspension to prevent membrane fouling during batch operations, an air blower was also provided beneath the membrane module during batch operations in UF systems (Choi et al. 2006). Continuous air bubbly flow was also proved to be an advantageous method to prevent fouling on the membrane surface. Du et al. (2017) reported that with an increase in aeration, there is a decrease in fouling rate ($\frac{dTMP}{dt}$) from 0.0908 to 0.0069 kPa/min. In addition, there is also an increase in the mean shear stress from 0.505–2.111 Pa while increasing the airflow rate from 0–3.2 L/min (Du et al. 2017).

7.3 UV Light Irradiation

Irradiation of UV light source could effectively control fouling and increase permeates flux in UF-PCO systems (Shon et al. 2005; Ma et al. 2009; Ganiyu et al. 2015; Peyravi et al. 2017). Others observed similar results in UF-PCO systems. Compared with the flux in the dark, a remarkable increase in the flux of 71.7% was observed after the illumination of UV light for an hour (Ma et al. 2009). After irradiating the PVDF-PEG- TiO_2 membrane with UV light, a decline in permeate flux from 56% to 28% was noticed while filtration duration was 100 min (Song et al. 2014). The authors also reported the flux decline of 66 and 48% on PVDF-LiCl- TiO_2 membrane

without and with UV irradiation, respectively. In UF-PCO systems, the PVDF-LiCl-TiO₂ membranes effectively decreased flux decline during the cross-flow mode of filtration.

In the WO₃-1% membrane, the fouling ratio was 53.6% and 92.4% with or without UV irradiation, respectively, and this significant difference in fouling ratio may be due to pore blocking by WO₃ photocatalyst particles on the membrane surface, which led to the reduction in pore size and hence higher rejection than fresh membrane (Peyravi et al. 2017). The study conducted by Yu et al. (2016) revealed that for a permeate flux of 20 L/m²h, the pulsed UV of 1 min with 31 min cycle at 3.17×10^{-2} W/cm² effectively prevented TMP increase over a period of 32 days. However, there was a fourfold increase in TMP for the conventional UF system without UV.

7.4 Surface Modification of Membrane

Membranes are modified via five methods in order to increase their hydrophilicity and mitigate fouling. They are; (i) plasma treatment, (ii) physical coating/adsorption, (iii) photo-assisted and miscellaneous grafting, (iv) by means of a chemical reaction, and (v) via impregnation of nanoparticles (Bet-moushoul et al. 2016). Among these methods, developing new polymeric membranes using TiO₂ nanoparticles had attracted many recent researchers, and impregnation of nanoparticles on the membrane surface could be developed through; (i) the addition of nanoparticles into casting solution (phase inversion method) (Zhao et al. 2011) and (ii) immersion of the porous membrane into nanoparticles suspension (Xu et al. 2013). The phase inversion method was used to prepare the asymmetric polymeric UF membrane (Rahimpour et al. 2011; Gao et al. 2018).

While adding TiO₂ nanoparticles into the casting solution, there was an increase in hydrophilicity and a decrease in contact angle and the coated membrane (Rahimpour et al. 2008; Song et al. 2012; You et al. 2012). Increasing the hydrophilicity of the membrane will result in an increase in fouling resistance and enhancement in flux (Madaeni et al. 2011; Song et al. 2012). PES UF membranes modified with nanoparticles improved permeate flux from 60–84% at 2 wt% loadings of TiO₂ (Razmjou et al. 2011). Studies also revealed that nano-sized TiO₂/Al₂O₃ modified PVDF membrane imparted better antifouling properties than the unmodified membrane with the same operational conditions (Yi et al. 2011).

7.5 Pre-Treatment of Feed Water

Treating feed water before it reaches the membrane is one of the fouling control strategies adopted for UF-PCO systems. Coagulation as a pre-treatment removed hydrophobic organics and increased permeate flux. Coagulated flocs efficiently absorb hydrophilic neutral organic compounds and improve flux (Chen et al. 2007).

Controlling the feedwater pH and application of aluminium chloride coagulant reduce fouling and enhance membrane permeate flux (Erdei et al. 2008; Gerrity et al. 2009). However, the application of coagulation as a pre-treatment for UF-PCO systems is restricted due to the requirement of post-treatment needed to remove foulants after the process, which may lead to an increase in the operational cost.

Employing magnetic ion exchange resin (MIEX) as a pre-treatment is another method to reduce membrane fouling (Gilbert et al. 2016; Chen et al. 2019). Chen et al. (2019) reported that even though MIEX had limitations of non-removal of suspended particles and creating secondary pollution due to the presence of some quantity of resin beads (Kabsch-Korbutowicz et al. 2018), MIEX was potentially effective in membrane fouling control.

7.6 Non-Conventional Methods of Fouling Control

The methods adopted to control membrane fouling other than non-conventional methods are ultrasonic and electrical cleaning. During the ultrasonic method, high-frequency sound waves are introduced to act on the foulant, and the aqueous solution is agitated (Shi et al. 2014). It is demonstrated that during the ultrasonic cleaning method, the filtration process is continuous while backwashing with water or chemical needs a break during operation. The ultrasonic method is also more advantageous due to; (i) the non-usage of chemicals and water for backwashing and (ii) preventing the problems pertaining to the disposal of waste and environmental concerns. For the dairy whey solutions fouled PS membranes, ultrasound had increased the cleaning efficiency by 5–10%. Optimum cleaning results were obtained at 10 min sonication period (Muthukumaran et al. 2005), and intermittent operation was carried out instead of continuous operation. Furthermore, the addition of surfactants during ultrasonic cleaning can significantly improve the flux recovery rate (Muthukumaran et al. 2004).

The transverse vibration produces shear and secondary flows and mitigates membrane fouling in the reactors. The low displacements of <5 mm and frequencies of <21 Hz contributed significantly to fouling reduction (Kola et al. 2012). An intermittent vibration with a 120 s non-vibration time interval was found to be sufficient to mitigate irreversible membrane fouling (Bilad et al. 2012). An electric field created across the membrane by placing two electrodes on either side of the membrane during electrical cleaning increase permeate flux and mitigates fouling in UF membranes (Rioss et al. 1988). The deposits on the membrane surface were lifted and carried away by electrostatic force (Saxena et al. 2009). The remarkable drawback of this method is the necessity of high energy needed for the continuous application of electric field, which may be 10 kWh/m³ of permeate (Bowen et al. 1989). The energy requirement could be reduced by introducing intermittent (pulsed) operation that can make the process more effective and reduce the energy requirement <1 kWh/m³ (Liu et al. 2012).

8 Removal of Emerging Contaminants (ECs) in UF-PCO Systems

The removal of ECs in UF-PCO systems depend upon (i) the kind of membrane process, (ii) characteristics (physico-chemical) of compounds, (iii) operational conditions, (iv) properties of membrane materials, and (iv) membrane fouling (Kumari et al. 2020; Vander Bruggen and Manttari 2008). Various ECs, including pharmaceutical compounds, diclofenac (DCF) and oxytetracycline (OTC), were found to be effectively degraded in UF-PCO systems (Reguero et al. 2013; Sarasidis et al. 2014; Asha et al. 2018; Espindola et al. 2019). Fernandez et al. (2014) explored the removal of 33 trace organic compounds (TrOCs) (drugs, analgesics, antibiotics surfactants) and reported that after 1 h reaction, 18 compounds of hydrophilic nature were completely degraded while hydrophobic tris (2-chloroethyl) phosphate (TCEP) was not degraded. Reguero et al. reported 86% trihalomethanes (THMs) removal in UF-PCO systems. Sarasidis et al. (2014) reported >96% diclofenac (DCF) degradation in the integrated UF photocatalytic systems. However, the studies also reveal that 100% degradation of oxytetracycline was obtained in UF-PCO systems in 5 h of reaction (Espindola et al. 2019).

8.1 Characteristics of ECs and Their Impacts

The characteristics of ECs have a significant impact on their removal efficiencies. The key characteristics such as; molecular weight (MW), size (length and width), acid dissociation constant (pK_a), diffusion coefficient (D_p), octanol-water partition coefficient ($\log K_{ow}$) that determines hydrophobicity/hydrophilicity, chemical structure, and charge characteristics (i.e. electron-donating or withdrawing functional group) were revealed to have a remarkable impact on ECs rejection during membrane separation process (Nghiem and Hawkes 2007; Tadkaew et al. 2011; Chon et al. 2012). The mechanisms for the removal of ECs during the UF membrane separation may be; (i) size-exclusion mechanism, (ii) adsorption phenomenon, (iii) hydrophobic interactions, and (iv) electrostatic interactions (Schafer et al. 2011). The mechanisms for ECs removal have been graphically depicted in Fig. 4.

Adsorption is one of the removal mechanisms that contribute more to the removal of ECs, while other mechanisms contribute a bit (Fernandez et al. 2014). The adsorption mechanism is responsible for the removal of ECs initially till the equilibrium is attained, and later the other mechanisms contribute. Hydrophobicity of the membrane determined the adsorption of ECs on the membrane surface (Schafer et al. 2011) and hydrophobicity depended upon its $\log K_{ow}$ value (Fernandez et al. 2014; Ojajun et al. 2015). ECs with $\log K_{ow} > 2.5$ are hydrophobic and tend to adsorb more onto the hydrophobic membrane surface (Xu et al. 2006; Hajibabania et al. 2011), while hydrophobic adsorption causes for retaining ECs. These results are in converse with the observations made by other researchers (Yoon et al. 2007; Camerton et al. 2007;

Khanzada et al. 2020), in which the authors reported that the ECs with $\log K_{ow} < 3$ (hydrophilic) were adsorbed more while ECs with $\log K_{ow} > 3$ (hydrophobic) had reflected the opposite behaviour during the UF process. Since contradictory results are available in the literature explaining the mechanisms of ECs removal, further investigations are needed in this aspect.

The removal of 33 TrOCs in a UF-PCO system was investigated by Fernandez et al. (2014). The studies revealed that the $\log K_{ow} > 4$ (hydrophobic) compounds were more adsorbed and highly retained on the membrane surface, while the hydrophilic compounds were less adsorbed and, hence, less retained. Secondes et al. (2014) investigated the pharmaceutical compounds and reported that the retention characteristics were due to $\log K_{ow}$ values. The authors also observed that diclofenac (DIC) was the highly retained compound among the three investigated pharmaceutical compounds, and the next was carbamazepine (CBZ). Amoxicillin (AMX) was the least of all.

The charge of ECs also affects the adsorption process due to electrostatic interactions. The compounds with charges as negative, similar values of $\log K_{ow}$ and MWCO were less adsorbed because of electrostatic repulsion with the negatively charged membrane. However, while computing percentage adsorption, along with feed and permeate concentrations, the amount of time taken to attain the equilibrium must also be duly considered (Fernandez et al. 2014).

The size of the ECs depends upon their molecular weight, length, and width (Tadkaew et al. 2011; Chon et al. 2012), which was more observed in the uncharged ECs (Ozaki and Li 2002). Even though Log D, molecular weight (MW), and charge-neutral pH are important variables during UF membrane separation, there was no well-defined relationship between the ECs removal by the UF membrane and their specified properties (Chon et al. 2012).

8.2 Membrane Properties and Their Effects

The membrane characteristics, such as; membrane pore size, MWCO of UF membrane, contact angle, zeta potential, and membrane surface roughness, contribute significantly to the removal of ECs (Evans et al. 2008; Wray et al. 2014). Due to the large pore size of UF membranes (10-100 kDa) relative to the size of many ECs (<1 kDa), the retention is reported to be less than 30% (Jermann et al. 2009; Schafer et al. 2011). Pharmaceutical compounds such as triclosan, oxybenzene, estrone, progesterone, and erythromycin having $\log K_{ow} > 3$ were less retained by UF membrane with a retention percentage of <30% (Yoon et al. 2007).

UF membrane separation processes have been commonly utilized for the removal of ECs. Most of the ECs have MW < 1 kDa, and their MW is at least an order of magnitude lesser than the MWCO of membranes (10–100 kDa) (Yoon et al. 2006; Dharupaneedi et al. 2019) and hence size-exclusion mechanism does not contribute for ECs removal. However, adsorption is the major mechanism for ECs removal.

Adsorption occurs both on the membrane surface and the pore structure of the membrane, while pore structure depends upon pore radius (Camerton et al. 2007). More porous the membrane, more ECs removal efficiency since more compounds are adsorbed within the membrane's pores. If we compare UF membranes with the tight NF/RO membranes, the pores are more in UF, and more ECs are adsorbed on both the surface of the membrane and its pores (Khazada et al. 2020). The removal efficiencies of perfluorooctanoic acid, perfluorooctane sulfonate, and dissolved organic compound (DOC) of $\approx 45\%$, $\approx 28\%$ and, 36% , respectively, were obtained using PVDF hollow fiber UF membranes (Kim et al. 2018). The lower removals were owing to the greater pore size of the UF membrane failed to act as a barrier for the retention of ECs (Kim et al. 2018). After the UF process, ECs having the concentration of 1000 ng/L showed $<5\%$ retention owing to adsorption alone. Size exclusion will not be responsible for its removal since the MW/size of the compounds ($MW < 300$ g/mol) was lesser than the size of membrane pores which is $0.04 \mu\text{m}$ (Pramanik et al. 2017).

During UF membrane filtration, the initial adsorption resulted in the retention of ECs, and after equilibrium is attained, the size exclusion mechanism contributes to its removal. The studies conducted by the researchers reveal that adsorption could not alone be the mechanism for ECs removal. Hydrophobic adsorption, size exclusion, and electrostatic repulsion are also mechanisms for ECs removal. The removal depends upon feedwater characteristics (Nghiem et al. 2005; Camerton et al. 2007; Jin et al. 2007).

Zeta potential is another important parameter that contributes to the retention of ECs during the UF process. Lower the zeta potential value, the greater the removal efficiencies. Bellona et al. (2004) investigated the removal of nitrate ions employing two membranes with different MWCO and zeta potentials; MWCO 350 Da (-24.1 mV) and MWCO 1000 Da (-20.4 mV). The studies revealed that the nitrate ions removal efficiency for the membrane with MWCO 350 Da was 8% lower than that of the membrane with MWCO 1000 Da.

The contact angle of the membrane is an index that determines the hydrophilicity/hydrophobicity of a membrane surface. The contact angle $< 90^\circ$ indicates the hydrophilic nature, and the contact angle $> 90^\circ$ indicates the hydrophobic nature of the membrane surface. The greater the contact angle, the more hydrophilic is the membrane surface (Camerton et al. 2007).

UF membranes with 1–3 kDa have almost the same separation efficiency as NF membranes with MWCO 350–400 kDa. The separation efficiency of UF membranes with 1–3 kDa is almost similar to the separation efficiency of NF membranes with MWCO 350–400 kDa. Low molecular weights (1–3 kDa) UF membranes were very effective in separating low MW proteins, sugars, and peptides in the range of NF membranes (Rohricht et al. 2009). Even though the MWCO of the membrane is greater than the MW of target pharmaceutical compounds, the UF membrane was having MWCO 8000 Da showed a greater removal of 25–95% pharmaceutical compounds (Ibuprofen) with an MW of 206 g/mol (Park et al. 2004). UF membranes

effectively eliminate high molecular weight NOM. However, the size/MW of most of the pharmaceutical compounds are smaller than the MWCO of UF membranes, and hence UF was employed as a pre-treatment system for NF/RO (Huang et al. 2011; Jarusutthirak et al. 2002). In addition, the adsorption capacity of hydrophobic UF membranes is in the range of hundreds of mg/m³ membranes (Galanakis 2015).

In UF-PCO systems, low MW compounds with MW < 360 Da were not retained by the UF membrane. The compounds detected in permeate confirm their passage through the membrane (Rajca et al. 2016). Despite the passage of low MW compounds through the membrane, the lower compound removal efficiency was observed owing to the partial adsorption of low MW compounds on the membrane surface (Choi et al. 2007; Rajca 2016). There is no catalyst loss in this UF-PCO system, and it could also be used for disinfection purposes.

9 Economic Aspects of Integrated UF-PCO Systems

While upscaling UF with PCO systems, the economic and costs of the system should be an important aspect that has to be given due consideration since the cost of the membrane seems to be high. The technical realization of the integrated system has to be rigorously considered.

The applied pressures have an influence on the operational costs. Lower pressure systems are more cost advantages than high-pressure systems. Based on the practical experiences in UF-PCO systems, the rough costs for permeate fluxes have to be identified before the systems will be designed for realization. Membrane fouling reduces the permeate flux. Better fouling control strategies need to be adopted to improve the permeate flux. A good UF-PCO system will have better fouling control and constant flux throughout the reactor run.

The operational cost of photocatalysts is primarily based on the cost of energy which is mainly obtained from the light source. The economic and feasibility of the process seems to be better for immobilized photocatalytic reactors than slurry reactors due to the energy costs needed for the dispersion of photocatalyst and transmission of UV light (Dostanić et al. 2013).

Even though many UF-PCO systems had been developed and evaluated by many researchers technically, only a few studies demonstrated the economic aspects and feasibility of UF-PCO systems. The energy consumption of slurry UF-PCO systems was evaluated by Eq. (1).

$$\text{Energy Consumption} = \text{EC(kWh/I)} = \frac{w \times \text{HRT}}{v} \quad (1)$$

In which EC—energy consumption, W—output energy of the light source, HRT—hydraulic retention time, and V—reactor volume (Damodar et al. 2010; Laohaprapanon et al. 2015).

Laohaprapanon et al. (2015) computed the cost of electricity to remove the colour from wastewater in a photocatalytic membrane reactor equipped with a PVDF membrane (pore size 0.45 μm). During this study, the electrical cost was calculated as approximately 0.15 USD/g (30 W UV light, time of exposure = 4 h, $[\text{RB}_5] = 75 \text{ mg/L}$, colour removal = 95% and energy consumption = 0.12 kWh/l or 1.62 kWh/g). The cost for membrane filtration was excluded since the reactor was run with a low TMP, and no significant fouling was observed on the membrane surface during 110 h. However, utilizing higher concentrations of the catalyst may increase TMP and decrease permeate flux, leading to an increase in treatment cost. This reveals that the operating variables have to be optimized to reduce the operating cost.

In the very few recent studies, the cost estimation was carried out separately for the photocatalytic and membrane parts (Dostanic et al. 2013; Samhaber and Nguyen 2014; Rani and Karthikeyan 2021). Rani and Karthikeyan (2021) estimated the operating cost for a UF-PCO system by considering the UF unit and PCO system separately. In this study, the authors estimated the treatment cost to treat 1 m^3 of effluent, and the cost was ranged from \$10.4 to \$13.6 or ₹728 to ₹952. In this integrated UF-PCO system, the area required for the installation was only 16.5 m^2 which is almost doubled when UF was used as a pre or post-treatment system. Despite the higher treatment cost of the integrated UF-PCO systems than the systems with the individual processes (UF system and PCO system), the synergies of the integrated systems will ascertain the significance of the process.

10 Conclusions and Future Scope

The studies on UF-PCO systems have made significant progress over the last twenty years of research. Among the two types of UF-PCO (slurry and immobilized systems), slurry systems are more advantageous owing to the larger surface area for the adsorption of photocatalyst and reaction. Split-type UF-PCO systems are more suitable for large-scale applications since both processes could be independently optimized. Though many types of research are available on the utilization of UV light, visible light active solar-driven photocatalytic conversion with the modified photocatalysts has become more attractive due to adsorption of visible light enhanced degradation and mineralization of compounds in UF-PCO systems.

The UV light exposure for 10 days with 200 μm H_2O_2 damaged the membrane structure (Chin et al. 2006) and 30 days with 3 wt% of TiO_2 cracked the polymeric membrane surface (decreased the tensile strength from 28 to 23 MPa) (Dzinum et al. 2017). Therefore, various challenges, including long-term stability and anti-fouling property of membrane, need to be focused on further research. Furthermore, real wastewater as feedwater, removal mechanisms of ECs, and degradation of intermediate products in UF-PCO systems need further investigation. However, applying real wastewater as a feed to the membrane reduced the membrane flux from 247 $\text{L/m}^2\text{h}$ to 82 $\text{L/m}^2\text{h}$, indicating the fouling of the membrane by the feed constituents (Vatanpour et al. 2020). Hence while using real wastewater as feedwater, care should

be taken to address the influence of wastewater constituents. Though many UF-PCO systems were developed on a lab-scale so as to successfully scale up and implement the integrated system, more studies at the pilot scale are needed.

References

- Ahmad AL, Sarif M, Ismail S (2005) Development of an integrally skinned ultrafiltration membrane for wastewater treatment: effect of different formulations of PSf/NMP/PVP on flux and rejection. *Desalination* 179:257–263
- Ahmed S, Khan FSA, Mubarak NM, Khalid M, Tan YH, Mazari SA, Karri RR, Abdullah EC (2021) Emerging pollutants and their removal using visible-light responsive photocatalysis—A comprehensive review. *J Environ Chem Eng* 9(6)
- Alfano OM, Bahnemann D, Cassano AE, Dillert R, Goslich R (2000) Photocatalysis in water environments using artificial and solar light. *Catal Today* 58(2):199–230
- Argurio P, Fontananova E, Molinari R, Drioli E (2018) Photocatalytic membranes in photocatalytic membrane reactors. *Processes* 6(162):1–27
- Asha RC, Kumar M (2015) Sulfamethoxazole in poultry wastewater: Identification, treatability and degradation pathway determination in a membrane photocatalytic slurry reactor. *J Environ Sci Health Part A* 50:1011–1019
- Asha RC, Priyanka Y, Kumar M (2018) Sulfamethoxazole removal in membrane-photocatalytic reactor system-experimentation and modelling. *Environ Technol* 42(1):1–8
- Athanasekou CP, Morales-Torres S, Likodimos V, Ramanos GE, Pastrana-Martinez LM, Falaras P, Dionysiou DD, Farria JL, Figueiredo JL, Silva AMT (2014) Prototype composite membranes of partially reduced grapheneoxide/TiO₂ for photocatalytic ultrafiltration water treatment under visible light. *Appl Catal b: Environ* 158–159:361–372
- Azrague K, Aimar P, Benoit-Marquie F, Maurette MT (2007) A new combination of a membrane and photocatalytic reactor for the depollution of turbid water. *Appl Catal B* 72:197–205
- Baker RW (1991) Membrane separation systems—Recent development. Noyes Data Corporation, New York, Future direction
- Bellona C, Drewes JE, Xu P (2004) Factors affecting the rejection of organic solutes during NF/RO treatment—a literature review. *Water Res* 38(12):2795–2809
- Bet-moushoul E, Mansourpanah Y, Farhadi KH, Tabatabaei M (2016) TiO₂ nanocomposite based polymeric membranes: a review on performance improvement for various applications in chemical engineering processes. *Chem Eng J* 283:29–46
- Bilad MR, Mezohegyi G, Declerck P, Vankelecom IFJ (2012) Novel magnetically induced membrane vibration (MMV) for fouling control in membrane bioreactors. *Water Res* 46(1):63–72
- Bilstad T, Espedal E (1996) Membrane separation of produced water. *Water Sci Technol* 34:239–246
- Bowen W, Kingdon RS, Aabuni HA (1989) Electrically enhanced separation processes: the basis of in situ intermittent electrolytic membrane restoration (IEMR). *J Membr Sci* 40:219–229
- Cabassud C, Laborie S, Lain J (1997) How slug flow can improve ultrafiltration flux in organic hollow fibres. *J Membr Sci* 128:93–101
- Camerton AM, Andrews RC, Bagley DM, Yang P (2007) Membrane adsorption of endocrine disrupting compounds and pharmaceutically active compounds. *J Membr Sci* 303:267–277
- Chen Y, Dong BZ, Gao N-Y, Fan JC (2007) Effect of coagulation pre-treatment on fouling of an ultrafiltration membrane. *Desalination* 204(1):181–188
- Chen Y, Xu W, Zhu D, Wei F, He D, Wang B, Du Q (2019) Effect of turbidity in micropollutant removal and membrane fouling by MIEEX ultrafiltration hybrid process. *Chemosphere* 216:488–498
- Chin SS, Chiang K, Fane AG (2006) The stability of polymeric membranes in a TiO₂ photocatalysis process. *J Membr Sci* 275:202–211

- Chin SS, Lim TM, Chiang K, Fane AG (2007a) Factors affecting the performance of a low-pressure submerged membrane photocatalytic reactor. *Chem Eng J* 130:53–63
- Chin SS, Lim TM, Chiang K, Fane AG (2007b) Hybrid low-pressure membrane photoreactor for the removal of bisphenol A. *Desalination* 202:253–261
- Choi H, Sofranco A, Dionysiou DD (2006) Nanocrystalline TiO₂ photocatalytic membranes with a hierarchical mesoporous multilayer structure: synthesis, characterization and multifunction. *Adv Func Mater* 16(8):1067–1074
- Choi H, Stathatos E, Dionysiou DD (2007) Photocatalytic TiO₂ films and membranes for the development of efficient wastewater treatment and reuse systems. *Desalination* 202(1–3):199–206
- Chon K, KyongShon H, Cho J (2012) Membrane bioreactor and nanofiltration hybrid system for reclamation of municipal wastewater: removal of nutrients, organic matter and micropollutants. *Bioresour Technol* 122:181–188
- Chong MN, Jin B, Chow CWK, Saint C (2010) Recent developments in photocatalytic water treatment technology: a review. *Water Res* 44:2997–3027
- Choo KH, Chang DI, Park KW, Kim MH (2008) Use of an integrated photocatalysis/hollow fiber microfiltration system for the removal of trichloroethylene in water. *J Hazard Mater* 152:183–190
- Cui Z, Taha T (2003) Enhancement of ultrafiltration using gas sparging: a comparison of different membrane modules. *J Chem Technol Biotechnol* 78:249–253
- D'Souza NM, Mawson AJ (2005) Membrane cleaning in the dairy industry: a review. *Crit Rev Food Sci Nutr* 45:125–134
- Damodar RA, You SJ, Chou HH (2009) Study the self-cleaning anti-bacterial and photocatalytic properties of TiO₂ entrapped PVDF membranes. *J Hazard Mater* 172:1321–1328
- Damodar RA, You S-J, Qu SH (2010) Coupling of membrane separation with photocatalytic slurry reactor for advanced dye wastewater treatment. *Sep Purif Technol* 76(1):64–71
- Damszel JG, Tomaszewska M, Morawski A (2009) Integration of photocatalysis with membrane processes for purification of water contaminated with organic dyes. *Desalination* 241:118–126
- Darowna D, Grondzewska S, Morawski AW, Mozia S (2014) Removal of non-steroidal anti-inflammatory drugs from primary and secondary effluents in a photocatalytic membrane reactor. *J Chem Technol Biotechnol* 89(8):1265–1273
- Dharupaneedi SP, Nataraj SK, Nadagouda M, Reddy KR, Shukla SS, Aminabhavi TM (2019) Membrane-based separation of potential emerging pollutants. *Sep Purif Technol* 210:850–866
- Doll TE, Frimmel FH (2005) Cross-flow microfiltration with periodical back-washing for photocatalytic degradation of pharmaceutical and diagnostic residues-evaluation of the long-term stability of the photocatalytic activity of TiO₂. *Water Res* 39(5):847–854
- Dostanić J, Lončarević L, Rožić S, Mijin PD, D, Jovanović DM, (2013) Photocatalytic degradation of azo pyridone dye: optimization using response surface methodology. *Desal Water Treat* 51:802–2812
- Du X, Qu FS, Liang H, Li K, Bai L-M, Li G-B (2017) Control of submerged hollow fiber membrane fouling caused by fine particles in photocatalytic membrane reactors using bubbly flow: shear stress and particle forces analysis. *Sep Purif Technol* 172:130–139
- Dzinun H, Othman MHD, Ismail AF, Puteh MH, Rahman MA, Jaafar J (2017) Stability study of PVDF/TiO₂ dual layer hollow fibre membranes under long-term UV irradiation exposure. *J Water Process Eng* 15:78–82
- Erdei L, Arecrachakul N, Vigneswaran S (2008) A combined photocatalytic slurry reactor-immersed membrane module system for advanced wastewater treatment. *Sep Purif Technol* 62:382–388
- Espindola C, Szymanski K, Cristoavao RO, Mendes A, Vilar VJP, Mozia S (2019) Performance of hybrid systems coupling advanced oxidation processes and ultrafiltration for oxytetracycline removal. *Catal Today* 328:274–280
- Evans PJ, Bird MR, Pihlajamaki A, Nystrom M (2008) The influence of hydrophobicity, roughness and charge upon ultrafiltration membranes for black tea liquor clarification. *J Membr Sci* 313:250–262

- Fernandez RL, McDonald JA, Khan SJ, Clech PL (2014) Removal of pharmaceuticals and endocrine disrupting chemicals by a submerged membrane photocatalysis reactor (MPR). *Sep Purif Technol* 127:131–139
- Fu J, Wang Z, Jin L, An D (2006) A new submerged photocatalysis reactor (SMPR) for fulvic acid removal using a nano-structured photocatalyst. *J Hazard Mater* 131(1–3):238–242
- Fujishima A, Rao TN, Tryk DA (2000) Titanium dioxide photocatalysis. *J Photochem Photobiol C: Photochem Rev* 1:1–21
- Fujishima A, Zhang X, Tryk DA (2008) TiO₂ photocatalysis and related surface phenomena. *Surf Sci Rep* 63:515–582
- Galanakis CM (2015) Separation of functional macromolecules and micromolecules: from ultrafiltration to the border to nanofiltration. *Trends Food Sci Technol* 42:44–63
- Ganiyu SO, Hullebusch ED, Cretin M, Esposito G, Oturan MA (2015) Coupling of membrane filtration and advanced oxidation processes for removal of pharmaceutical residues: a critical review. *Sep Purif Technol* 156(3):891–914
- Gao B, Chen W, Liu J, An J, Wang L, Zhu Y, Sillanpaa M (2018) Continuous removal of tetracycline in a photocatalytic membrane reactor (PMR) with ZnIn₂S₄ as adsorption and photocatalytic coating layer on PVDF membrane. *J Photochem Photobiol a: Chem* 364:732–739
- Gao W, Liang H, Ma J, Han M, Lin Z, Chen Z (2011) Membrane fouling control in ultrafiltration technology for drinking water production: a review. *Desalination* 272:1–8
- Gao Y, Hu M, Mi B (2014) Membrane surface modification with TiO₂-graphene oxide for enhanced photocatalytic performance. *J Membr Sci* 455:349–356
- Gaya UI, Abdullah AH (2008) Heterogeneous photocatalytic degradation of organic contaminants over titanium dioxide: a review of fundamentals, progress and problems. *J Photochem Photobiol c: Photochem Rev* 9(1):1–12
- Gerrity D, Mayer B, Ryu H, Crittenden J, Abbaszadegan M (2009) A comparison of pilot-scale photocatalysis and enhanced coagulation for disinfection by-product mitigation. *Water Res* 43(6):1597–1610
- Gilbert O, Pages N, Bernat X, Cortina JL (2016) Removal of dissolved organic carbon and bromide by a hybrid miex-ultrafiltration system: insight into the behaviour of organic fractions. *Chem Eng J* 312:59–67
- Gogate PR, Pandit AB (2004) A review of imperative technologies for wastewater treatment 1: oxidation technologies at ambient conditions. *Adv Environ Res* 8(3–4):501–551
- Guigui C, Mougenot M, Cabassud C (2003) Air sparging backwash in ultrafiltration hollow fibres for drinking water production. *Water Sci Technol Water Supply* 3:415–422
- Günther J, Schmitz P, Albasi C, Lafforgue C (2010) A numerical approach to study the impact of packing density on fluid flow distribution in hollow fiber module. *J Membr Sci* 348(1–2):277–286
- Guo Q, Zhou CY, Ma ZB, Yang XM (2019) Fundamentals of TiO₂ photocatalysis: concepts, mechanisms and challenges. *Adv Mater* 31:1901997
- Hajibabania S, Verliefe A, McDonald JA, Khan SJ, Le-Clech P (2011) Fate of trace organic compounds during treatment by nanofiltration. *J Membr Sci* 373(1–2):130–139
- Han WY, Zhu WP, Zhang PY, Zhang Y, Li LS (2004) Photocatalytic of phenols in aqueous solution under irradiation of 254 and 185 nm UV light. *Catal Today* 90:319–324
- He Y, Jiang ZW (2008) Technology review: treating oil field wastewater. *Filtr Sep* 45:14–16
- Herrmann JM (1995) Heterogeneous photocatalysis: fundamentals and applications to the removal of various types of aqueous pollutants. *Catal Today* 53(1):115–129
- Herrmann JM (2005) Heterogeneous photocatalysis: state of the art and present applications. *Topics in Catal* 34(1–4):49–65
- Hilal N, Ogunbiyi OO, Miles NJ, Nigmatullin R (2005) Methods employed for control of fouling in MF and UF membranes: a comprehensive review. *Sep Sci Technol* 40:1957–2005
- Horovitz I, Gitis V, Avisar D, Mamane H (2019) Ceramic-based photocatalytic membrane reactors for water treatment—where to next? *Rev Chem Eng* 36(5):593–622

- Huang H, Cho H, Schwab K, Jacangelo JG (2011) Effects of feedwater pretreatment on the removal of organic microconstituents by a low fouling reverse osmosis membrane. *Desalination* 281:446–454
- Huang H, Schwab K, Jacangeio J (2009) Pretreatment for low pressure membranes in water treatment: a review. *Environ Sci Technol* 43(9):3011–3019
- Huang X, Meng XY, Liang P, Qian Y (2007) Operational conditions of a membrane filtration reactor coupled with photocatalytic oxidation. *Sep Purif Technol* 55:165–172
- Irie H, Watanabe Y, Hashimoto K (2003) Carbon-doped anatase TiO₂ powders as a visible-light sensitive photocatalyst. *Chem Lett* 32(8):772–773
- Jarusuthirak C, Amy G, Croue J-P (2002) Fouling characteristics of wastewater effluent organic matter (Efom) isolates on NF and UF membranes. *Desalination* 145:247–255
- Jermann D, Pronk W, Boller M, Schafer AL (2009) The role of NOM fouling for the retention of estradiol and ibuprofen during ultrafiltration. *J Membr Sci* 329:75–84
- Jiang H, Zhang G, Huang T, Chen J, Wang Q, Meng Q (2010) Photocatalytic membrane reactor for degradation of acid red B wastewater. *Chem Eng J* 156:571–577
- Jin X, Hu J, Ong SL (2007) Influence of dissolved organic matter on estrone removal by NF membranes and the role of their structures. *Water Res* 41:3077–3088
- Kabsch-Korbutowicz M, Majewska-Nowak K, Winnicki T (2008) Water treatment using MIEX® DOC/ultrafiltration process. *Desalination* 221:338–344
- Kertész S, Cakl J, Jiráňková H (2014) Submerged hollow fiber microfiltration as a part of hybrid photocatalytic process for dye wastewater treatment. *Desalination* 343:106–112
- Khan S, Kim J, Sotto A, Bruggen BV (2015) Humic acid fouling in a submerged photocatalytic membrane reactor with binary TiO₂-ZrO₂ particles. *J Ind Eng Chem* 21:779–786
- Khan FSA, Mubarak NM, Khalid M, Tan YH, Abdullah EC, Rahman ME, Karri RR (2021) A comprehensive review on micropollutants removal using carbon nanotubes-based adsorbents and membranes. *J Environ Chem Eng* 9(6)
- Khanzada NK, Farid MU, Kharraz JA, Choi J, Tang CY, Nghiem LD, Jang A, An AK (2020) Removal of organic micropollutants using advanced membrane-based water and wastewater treatment: a review. *J Membr Sci* 598:117672
- Kim S, Chu KH, Al-Hamadani YAJ, Park CM, Jang M, Kim DH, Yu M, Heo J, Yoon Y (2018) Removal of contaminants of emerging concern by membranes in water and wastewater: a review. *Chem Eng J* 335:896–914
- Kola A, Ye Y, Ho A, Le-Clech P, Chen V (2012) Application of low frequency transverse vibration on fouling limitation in submerged hollow fiber membranes. *J Membr Sci* 409–410:54–65
- Kumari P, Bahadu N, Dumeé LF (2020) Photocatalytic membrane for the remediation of persistent organic pollutants—a review. *Sep Purif Technol* 230:115878–115894
- Laborie S, Cabassud C, Durand-Bourlier L, Lain J (1997) Flux enhancement by a continuous tangential gas flow in ultrafiltration hollow fibres for drinking water production: Effects of slug flow on cake structure. *Filtr Sep* 34:887–891
- Laohaprapanon A, Matahumb J, Tayob L, Youa S (2015) Photodegradation of reactive black 5 in a ZnO/UV slurry membrane reactor. *J Taiwan Inst Chem Eng* 49(1):136–141
- Lau YJ, Karri RR, Mubarak NM, Lau SY, Chua HB, Khalid M, Jagadish P, Abdullah EC (2020) Removal of dye using peroxidase-immobilized Buckypaper/polyvinyl alcohol membrane in a multi-stage filtration column via RSM and ANFIS. *Environ Sci Pollut Res* 27(32):40121–40134
- Lee SA, Choo KH, Lee CH, Lee HL, Hyeon T, Choi W, Kwon HH (2001) Use of ultrafiltration membranes for the separation of TiO₂ photocatalysis in drinking water treatment. *Ind Eng Chem Res* 40:1712–1719
- Li D, Haneda H, Labhsetwar NK, Hishita S, Ohashi N (2005) Visible-light-driven photocatalysis on fluorine-doped TiO₂ powders by the creation of surface oxygen vacancies. *Chem Phys Lett* 401:579–584
- Liu L, Liu J, Gao B, Yang F (2012) Minute electric field reduced membrane fouling and improved performance of membrane bioreactor. *Sep Purif Technol* 86:106–112

- Loddo V, Augugliaro V, Palmisano L (2009) Photocatalytic membrane reactors: case studies and perspectives. *Asia Pac J Chem Eng* 4:380–384
- Luo Y, Guo W, Ngo H, Nghiem L, Hai F, Zhang J, Liang S, Wang X (2014) A review on the occurrence of micropollutants in the aquatic environment and their fate and removal during wastewater treatment. *Sci Total Environ* 473–474:619–641
- Ma N, Quan X, Zhang Y, Chen S, Zhao H (2009) Integration of separation and photocatalysis using an inorganic membrane modified with Si doped TiO₂ for water purification. *Membr Sci* 335(2009):58–67
- Madaeni SS, Ghaemi N, Alizadeh A, Joshaghani M (2011) Influence of photo-induced superhydrophilicity of titanium dioxide nanoparticles on the anti-fouling performance of ultrafiltration membranes. *Appl Surf Sci* 257:6175–6180
- Malato S, Fernandez-Ibanez P, Maldonado MI, Blanco J, Gernjak W (2009) Decontamination and disinfection of water by solar photocatalysis: recent overview and trends. *Catal Today* 147(1):1–59
- Mansourizadeh A, Azad AJ (2014) Preparation of blend polyethersulfone/cellulose acetate/polyethylene glycol asymmetric membranes for oil-water separation. *J Polym Res* 21:1–9
- Meng Y, Huang X, Yang Q, Qian Y, Kubota N, Fukunaga S (2005) Treatment of polluted river water with a photocatalytic slurry reactor using low-pressure mercury lamps coupled with a membrane. *Desalination* 181(1):21–133
- Miyauchi M, Nakajima A, Watanabe T, Hashimoto K (2002) Photocatalysis and photoinduced hydrophilicity of various metal oxide thin films. *Chem Mater* 14:812–2816
- Molinari R, Caruso A, Argurio P, Poerio T (2008) Degradation of the drugs Gemfibrozil and Tamoxifen in pressurized and de-pressurized membrane photoreactors using suspended polycrystalline TiO₂ as catalyst. *J Membr Sci* 319:54–63
- Molinari R, Lavorato C, Argurio P (2017) Recent progress of photocatalytic membrane reactors in water treatment and in synthesis of organic compounds: a review. *Catal Today* 281:144–164
- Molinari R, Lavorato C, Argurio P (2021) Photocatalytic membrane reactors over the last 20 years: a state of the art perspective. *Catalysts* 11:775
- Molinari R, Mungari M, Drioli E, Di Paola A, Loddo V, Palmisano L, Schiavello M (2000) Study on a photocatalytic membrane reactor for water purification. *Catal Today* 55:71–78
- Mozia S (2010) Photocatalytic membrane reactors (PMR) in water and wastewater treatment. *Sep Purif Technol* 73:71–91
- Mozia S, Darowna D, Orecki A, Wrobel R, Wilpiszewska K, Morawski AW (2014) Microscopic studies on TiO₂ fouling of MF/UF polyethersulfone membranes in photocatalytic membrane reactor. *J Membr Sci* 470:356–368
- Mozia S, Darowna D, Wrobel R, Morawski AW (2015) A study on the stability of polyethersulfone ultrafiltration membranes in a photocatalytic membrane reactor. *J Membr Sci* 495:176–186
- Mozia S, Morawski AW (2009) Integration of photocatalysis with ultrafiltration or Membrane Distillation for removal of azo dye direct green 99 from water. *J Adv Oxidation Technol* 12:111–121
- Mozia S, Tomaszewska M, Morawski AW (2005) Photocatalytic degradation of azo-dye Acid-Red18. *Desalination* 185:449–456
- Mozia S, Tomaszewska M, Morawski AW (2006) Removal of azo-dye Acid Red 18 in two hybrid membrane systems employing a photodegradation process. *Desalination* 198:183–190
- Muthukumar S, Kentish S, Lalchandani S, Ashokkumar M, Mawson R, Stevens GW, Grieser F (2005) The optimization of ultra-sonic cleaning procedures for dairy fouled ultrafiltration membranes. *Ultrason Sonochem* 12:29–35
- Muthukumar S, Yang K, Seuren A, Kentish S, Ashokkumar M, Stevens G, Grieser F (2004) The use of ultrasonic cleaning for ultrafiltration membranes in the dairy industry. *Sep Purif Technol* 39:99–107
- Nghiem LD, Hawkes S (2007) Effects of membrane fouling on the nanofiltration of pharmaceutically active compounds (PhACs): mechanisms and role of membrane pore size. *Sep Purif Technol* 57:176–184

- Nghiem LD, Schafer AI, Elimelech M (2005) Pharmaceutical retention mechanisms by nanofiltration membranes. *Environ Sci Technol* 39:7698–7705
- Ni M, Leung MKH, Leung DYC, Sumathy K (2007) A review and recent developments in photocatalytic water-splitting using TiO_2 for hydrogen production. *Renew Sust Energy Rev* 11:401–425
- Ochoa A, Masuelli M, Marchese J (2003) Effect of hydrophilicity on fouling of an emulsified oil wastewater with PVDF/PMMA membranes. *J Membr Sci* 226:203–211
- Ojajuni O, Saroj D, Cavalli G (2015) Removal of organic micropollutants using membrane assisted processes: a review of recent progress. *Environ Technol Rev* 4:17–37
- Ollis DF, Pelizzetti E, Serpone N (1991) Photocatalyzed destruction of water contaminants. *Environ Sci Technol* 25(9):1522–1529
- Ong CS, Lau WJ, Goh PS, Ng BC, Ismail AF (2014) Investigation of submerged membrane photocatalytic reactor (SPMR) operating parameters during oily wastewater treatment process. *Desalination* 353:48–56
- Ong CS, Lau WJ, Goh PS, Ng BC, Ismail AF, Choo CM (2015) The impacts of various operating conditions on submerged membrane photocatalytic reactors (SMPR) for organic pollutant separation and degradation: A review. *RSC Adv* 5(118):97335–97348
- Ozaki H, Li H (2002) Rejection of organic compounds by ultra-low-pressure reverse osmosis membrane. *Water Res* 36:123–130
- Padaki M, Murali S, Abdullah MS, Misdan N, Moslehyani A, Kassim MA (2015) Membrane technology enhancement in oil-water separation—a review. *Desalination* 357:197–207
- Palmisano G, Augugliaro V, Pagliaro M, Palmisano L (2007) Photocatalysis: a promising route for 21st century organic chemistry. *Chem Commun* 33:3425–3437
- Park G-Y, Lee JH, Kim IS, Cho J (2004) Pharmaceutical rejection by membranes for wastewater reclamation and reuse. *Water Sci Technol* 50(2):239–244
- Patsios SSI, Sarasidis VC, Karabelas AJ (2013) A hybrid photocatalysis-ultrafiltration continuous process for humic acids degradation. *Sep Purif Technol* 104:334–341
- Pelaez M, Nicholas T, Nolan NT, Pillai SC, Seeryc MK, Falaras P, Kontosd AG (2012) A review on the visible light active titanium dioxide photocatalysts for environmental applications. *Appl Catal B: Environ* 125:331–349
- Peyravi M, Jahanshahi M, Khalili S (2017) Fouling of WO_3 nanoparticle-incorporated PSf membranes in ultrafiltration of landfill leachate and dairy a combined wastewaters: an investigation using model. *Chin J Chem Eng* 25:741–751
- Pramanik BK, Pramanik SK, Sarker DC, Suja F (2017) Removal of emerging perfluorooctanoic acid and perfluorooctane sulfonate contaminants from lake water. *Environ Technol* 38:1937–1942
- Psoch C, Schiewer S (2006) Critical flux aspect of air sparging and backflushing on membrane bioreactors. *Desalination* 175:61–71
- Rahimpour A, Jahanshahi M, Rajaeian B, Rahimnejad M (2011) TiO_2 entrapped nano-composite PVDF/SPES membranes: preparation, characterization, antifouling and antibacterial properties. *Desalination* 278(1–3):343–353
- Rahimpour A, Madaeni SS (2007) Polyethersulfone (PES)/cellulose acetate phthalate (CAP) blend ultrafiltration membranes: preparation, morphology, performance and antifouling properties. *J Membr Sci* 305:299–312
- Rahimpour A, Madaeni SS, Taheri AH, Mansourpanah Y (2008) Coupling TiO_2 nanoparticles with UV irradiation for modification of polyethersulfone ultrafiltration membranes. *J Membr Sci* 313(1–2):158–169
- Rajca M (2016) The effectiveness of removal of nom from natural water using photocatalytic membrane reactors in PMR-UF and PMR-MF modes. *Chem Eng J* 305:169–175
- Rani CN, Karthikeyan S (2018) Performance of indigenous integrated slurry photocatalytic membrane reactor (PMR) on the removal of aqueous phenanthrene. *Water Sci Technol* 77(11):2642–2656

- Rani CN, Karthikeyan S (2021) Synergic effects on degradation of a mixture of polycyclic aromatic hydrocarbons in a UV slurry photocatalytic membrane reactor and its cost estimation. *Chem Eng Process* 159:108179
- Rani CN, Karthikeyan S, Doss SPA (2021) Photocatalytic ultrafiltration membrane reactors in water and wastewater treatment—a review. *Chem Eng Process* 165:108445
- Razmjou A, Mansour J, Chen V (2011) The effects of mechanical and chemical modification of TiO₂ nanoparticles on the surface chemistry, structure and fouling performance of PES ultrafiltration membranes. *J Membr Sci* 378:73–84
- Reguero V, Lopez-Fernandez R, Feroso J, Pocostales O, Gonzalez R, Irusta R, Villayerde S (2013) Comparison of conventional technologies and a Submerged Membrane Photocatalytic Reactor (SMPR) for removing trihalomethanes (THM) precursors in drinking water treatment plants. *Desalination* 330:28–34
- Rehman S, Ullah R, Butt AM, Gohar ND (2009) Strategies of making TiO₂ and ZnO visible light active. *J Hazard Mater* 170(2–3):560–569
- Ren Z, Yang Y, Zhang W, Liu J, Wang H (2013) Modelling study on the mass transfer of hollow fiber renewal liquid membrane: Effect of the hollow fiber module scale. *J Membr Sci* 439:28–35
- Riaz S, Park SJ (2020) An overview of TiO₂-based photocatalytic membrane reactors for water and wastewater treatments. *J Ind Eng Chem* 84:23–41
- Rios G, Rakotoarisoa H, de la Fuente BT (1988) Basic transport mechanisms of ultrafiltration in the presence of an electric field. *J Membr Sci* 38:147–159
- Riva F, Castiglioni S, Fattore E, Manenti A, Davoli E, Zuccato E (2018) Monitoring emerging contaminants in the drinking water of Milan and assessment of the human risk. *Int J Hygiene Environ Health* 221:451–457
- Rohrlich M, Krisam J, Weise U, Kraus UR, Rolf A (2009) Elimination of carbamazepine, diclofenac and naproxen from treated wastewater by nanofiltration. *CLEAN-Soil Air Water* 37:638–641
- Saxena A, Tripathi BP, Kumar M, Shahi VK (2009) Membrane-based techniques for the separation and purification of proteins: an overview. *Adv Colloid Interface Sci* 145:1–22
- Samhaber WM, Nguyen MT (2014) Applicability and costs of nanofiltration in combination with photocatalysis for the treatment of dye house effluents. *Beilstein J Nanotechnol* 5:476–484
- Sarasidis VC, Plakas KV, Patsios SI, Karabelas AJ (2014) Investigation of diclofenac degradation in a continuous photocatalytic membrane reactor: Influence of operating parameters. *Chem Eng J* 239:299–311
- Schafer A, Akanyeti I, Semiao AJ (2011) Micropollutant sorption to membrane polymers: a review of mechanisms for estrogens. *Adv Colloid Interface Sci* 164:100–117
- Scholz M, Lucas M (2003) Techno-economic evaluation of membrane filtration for the recovery and re-use of tanning chemicals. *Water Res* 37:1859–1867
- Secundes MFN, Naddeo V, Belgiorno V, Ballesteros F (2014) Removal of emerging contaminants by simultaneous application of membrane ultrafiltration, activated carbon adsorption, and ultrasound irradiation. *J Hazard Mater* 264:342–349
- Shi X, Tal G, Hankins NP, Gitis V (2014) Fouling and cleaning of ultrafiltration membranes: a review. *J Water Process Eng* 1:121–138
- Shon HK, Vigneswaran S, Ngo HH, Kim JH (2005) Chemical coupling of photocatalysis with flocculation and adsorption in the removal of organic matter. *Water Res* 39(12):2549–2558
- Sirkar KK (2008) Membranes, phase interfaces and separations: Novel techniques and membranes—an overview. *Ind Eng Chem Res* 47:5250–5266
- Song H, Shao J, He Y, Liu B, Zhong X (2012) Natural organic matter removal and flux decline with PEG-TiO₂ doped PVDF membranes by integration of ultrafiltration with photocatalysis. *J Membr Sci* 405–406:48–56
- Song H, Shao J, Wang J, Zhong X (2014) The removal of natural organic matter with LiCl-TiO₂-doped PVDF membranes by integration of ultrafiltration with photocatalysis. *Desalination* 344:412–421

- Sopajaree K, Qasim SA, Basak S, Rajeshwar K (1999) An integrated flow reactor membrane filtration system for heterogeneous photocatalysis. Part I: experiments and modelling of a batch-recirculated photoreactor. *J Appl Electrochem* 29:533–539
- Tabei HSM, Kazemeini M, Fattahi M (2012) Preparation and characterization of visible light sensitive nano titanium dioxide photocatalyst. *Scientia Iranica C* 19(6):1626–1631
- Tadkaew N, Hai FI, McDonald JA, Khan SJ, Nghiem LD, (2011) Removal of trace organics by MBR treatment: the role of molecular properties. *Water Res* 45:2439–2451
- Thiruvenkatachari R, Vigneswaran S, Moon IS (2008) A review on UV/TiO₂ photocatalytic oxidation process. *Korean J Chem Eng* 25(1):64–72
- Tufail A, Price WE, Hai FI (2020) A critical review on advanced oxidation processes for the removal of trace organic contaminants: a voyage from individual to integrated processes. *Chemosphere* 260:127460
- Vander Bruggen B, Manttari M, Nystrom M (2008) Drawbacks of applying nanofiltration and how to avoid them: a review. *Sep Purif Technol* 63:251–263
- Vatanpour V, Darrudi N, Sheydaei M (2020) A comprehensive investigation of effective parameters in continuous submerged photocatalytic membrane reactors by RSM. *Chem Eng Process* 157:106144
- Wang P (2016) Membrane photoreactors (MPRs) for photocatalysts separation and pollutants removal: Recent overview and new perspectives. *Sep Sci Technol* 51(1):147–167
- Wang P, Fane AG, Lim TT (2013) Evaluation of a submerged membrane vis-LED photoreactor (SMPR) for carbamazepine degradation and TiO₂ separation. *Chem Eng J* 215–216:240–251
- Wang P, Lim TT (2012) Membrane vis-LED photoreactor for simultaneous penicillin G degradation and TiO₂ separation. *Water Res* 46(6):1825–1837
- Wang YH, Liu XQ, Meng GY (2007) Preparation of asymmetric pure titania ceramic membranes with dual functions. *Mater Sci Eng A* 445–446:611–619
- Wiesner MR, Aptel P (1996) Mass transport and permeate flux and fouling in pressure-driven processes. In: Mallevalle J, Odendaal PE, Wiesner M.R (Eds.) *Water treatment membrane processes*, McGraw-Hill, New York (Chapter 4)
- Williams C, Wakeman R (2000) Membrane fouling and alternative techniques for its alleviation. *Membr Technol* 124:4–10
- Wray HE, Andrews RC, Beube PR (2014) Surface shear stress and retention of emerging contaminants during ultrafiltration for drinking water treatment. *Sep Purif Technol* 122:183–191
- Wu J, Chen V (2000) Shell-side mass transfer performance of randomly packed hollow fiber modules. *J Membr Sci* 172(1–2):59–74
- Xiao YT, Xu SS, Li ZH, An H, Zhou L, Zhang YL, Fu QS (2010) Progress of applied research on TiO₂ photocatalysis-membrane separation coupling technology in water and wastewater treatments. *Environ Sci Technol* 55(4):1345–1353
- Xu C, Dong D, Meng X, Su X, Zheng X, Li Y (2013) Photolysis of polycyclic aromatic hydrocarbons on soil surfaces under UV irradiation. *J Environ Sci* 25(3):569–5750
- Xu P, Drewes JE, Kim TU, Bellona C, Amy G (2006) Effect of membrane fouling on transport of organic contaminants in NF/RO membrane applications. *J Membr Sci* 279:165–175
- Yeo APS, Law AWK, Fane AG (2006) Factors affecting the performance of submerged hollow fiber bundle. *J Membr Sci* 280(1):969–982
- Yi X, Yu S, Shi W, Sun N, Jin L, Wang S, Zhang B, Ma C, Sun L (2011) The influence of important factors on ultrafiltration of oil/water emulsion using PVDF membrane modified by nano-sized Al₂O₃. *Desalination* 281:179–184
- Yoon Y, Westerhoff P, Snyder SA, Wert EC (2006) Nanofiltration and ultrafiltration of endocrine disrupting compounds, pharmaceuticals and personal care products. *J Membr Sci* 270:88–100
- Yoon Y, Westerhoff P, Syder SA, Wert EC, Yoon J (2007) Removal of endocrine disrupting compounds and pharmaceuticals by nanofiltration and ultrafiltration membranes. *Desalination* 202:16–23
- Yoon Y, Westerhoff P, Yoon J, Snyder SA (2004) Removal of 17β Estradiol and Fluoranthene by nanofiltration and ultrafiltration. *J Environ Eng* 130:1460–1467

- You S-J, Semblante GU, Liu SC, Damodar RA, Wei TC (2012) Evaluation of the antifouling and photocatalytic properties of poly(vinylidene fluoride) plasma-grafted poly(acrylic acid) membrane with self-assembled TiO₂. *J Hazard Mater* 237–238:10–19
- Yu Y, Yu JC, Yu JG, Kwok YC, Che YK, Zhao JC, Ding L, Ge WK, Wong PK (2005) Enhancement of photocatalytic activity of mesoporous TiO₂ by using carbon nanotubes. *Appl Catal A: Gen* 289:186–196
- Yu JH, Park JY, Kim J (2016) Roles of ultrafiltration, photo-oxidation and adsorption in hybrid water treatment process of tubular alumina UF and photocatalyst coated PP beads with air back flushing. *Desal Water Treat* 57(17):1–12
- Yue C, Dong H, Chen Y, Shang B, Wang Y, Wang S, Zhu Z (2021) Direct purification of digestate using ultrafiltration membranes: Influence of pore size on filtration behaviour and fouling characteristics. *Membranes* 11:171
- Zertal A, Sehili T, Boule P (2001) Photochemical behaviour of 4-chloro-2-methylphenoxyacetic acid. Influence of pH and irradiation wavelength. *J Photochem Photobiol A: Chem.* 146(1–2):37–48
- Zhang J, Wang L, Wang L, Zhang G, Wang Z, Xu L, Fan Z (2013) Influence of azo dye-TiO₂ interactions on the filtration performance in a hybrid photocatalysis/ultrafiltration process. *J Colloid Interface Sci* 389:273–283
- Zhang W, Ding L, Luo J, Jaffrin MY, Tang B (2016) Membrane fouling in photocatalytic membrane reactors (PMRs) for water and wastewater treatment: a critical review. *Chem Eng J* 302:446–458
- Zhang X, Du AJ, Lee P, Sun DD, Leckie JO (2008) TiO₂ nanowire membrane for concurrent filtration and photocatalytic oxidation of humic acid in water. *J Membr Sci* 313:44–51
- Zhang X, Li G, Wang Y (2007) Microwave assisted photocatalytic degradation of high concentration azo dye Reactive Brilliant Red X-3B with microwave electrode less lamp as a light source. *Dyes Pigments* 74(3):536–544
- Zhao W, Huang J, Fang B, Nie S, Yi N, Su B, Li H, Zhao C (2011) Modification of polyethersulfone membrane by blending semi-interpenetrating network polymeric nanoparticles. *J Membr Sci* 369:258–266
- Zheng X, Shen ZP, Shi L, Cheng R, Yaun DH (2017) Photocatalytic membrane reactors (PMRs) in water treatment: configurations and influencing factors. *Catalysts* 7(8):224–254

Application of Electrospun Polymeric Nanofibrous Membranes for Water Treatment



Sankha Chakraborty, Jayato Nayak, and Prasenjit Chakraborty

Abstract Nanofibrous membranes created by electrospinning are nanotechnology-based technologies for developing new separating membranes, electrospun nanofibrous membranes (ENM). These can be used because of their particular characteristics to make multifunctional water treatment materials. On the other hand, its extremely porous construction with large pores reduces the capacity of NaCl to desalinate dissolved salts. As a result, it is only suited as a prefilter before delicate reverse osmosis operations to separate large/microparticles from MF applications. These membranes can be enlarged to provide water treatment by changing them to take out more intricate colloidal solutions, including oil/water suspensions, requiring an organic solution to be rejected. When an ENM surface has been changed and crosslinked with thin, selective coating layers, a combination membrane with smaller pores can be produced that can be used in UF separation. A nonporous composite membrane can be generated by adding an interfacial polymerizing layer which can be employed for nanofiltration and reverse osmosis applications. The current research on electrospun polymer membranes is covered in this chapter, emphasising progress, issues and prospective improvements in water treatment applications.

S. Chakraborty (✉)

School of Chemical Technology, KIIT Deemed To Be University, Bhubaneswar 751024, Odisha, India

e-mail: sankha.chakraborty@kiitbiotech.ac.in

J. Nayak

Department of Chemical Engineering, Kalasalingam Academy of Research and Education, Srivilliputhur 626126, Tamil Nadu, India

P. Chakraborty

Department of Chemistry, The University of Burdwan, Burdwan 713104, West Bengal, India

1 Introduction

The scarcity of clean drinking water is currently the world's most significant issue (Ramakrishna and Shirazi 2015). Every year, water pollution and other water-related issues kill millions (Montgomery and Elimelech 2007; Warsinger et al. 2018). As the world's population grows, so do concerns about water availability, particularly in arid regions like Africa and the Middle East. With rising population and consequent industrialization, water-related issues are expected to worsen alarmingly in the coming years. These factors highlight the need for extensive research into energy-efficient and cost-effective beneficial water treatment methods (Warsinger et al. 2018).

A recent study suggests that nanotechnology could help develop the next generation of water treatment systems. Experiments with engineered nanomaterials are increasingly being conducted (Warsinger et al. 2018; Daer et al. 2015; Bethi et al. 2016). Water supply and quality can be improved through the use of nanotechnology. Aquatic treatment necessitates the development of novel membranes, particularly nanoengineered membranes such as RO and NF (Fane 2018).

Because it is a separation barrier, it allows for lower working pressures. 2–100 nm membranes can remove colloids and macromolecules (Anand et al. 2018; Yang et al. 2018; Gao et al. 2011). Modern membrane-based liquid filtration technology. Used to eliminate microparticles and germs for years. As a good particle separator, MF operates at low pressures due to the significantly larger pore width of the MF membrane, which typically ranges between 0.1 and 10 m (Rayess et al. 2011; Badruzzaman et al. 2019).

NF membranes are less expensive than RO membranes for water purification. From groundwater and surface sources, they can remove a wide range of minerals, salts, cations, and pathogens (fungi, viruses and bacteria) (Mohammad et al. 2015). Aside from the benefits mentioned above, traditional membrane techniques have several drawbacks. Traditional membranes are restricted by osmotic pressure, fouling, scaling and low porosity (80%). The flaws derive from the production methods employed by conventional membranes. It is worth noting. For MF and UF membranes, the inverting phase method works well. This is a common technique for pore membranes. This method has two main flaws: the limited size of cheap pores and contamination by solvents. The only commercially viable method to produce NF membranes is interfacial polymerization. The top selective layer's thickness can be modified, albeit not well. MF membranes can employ depth-and-trace methods similar to MD. Pore distributions and pores can vary in size (Warsinger et al. 2018; Fane 2018; Yang et al. 2018; Mohammad et al. 2015; Ang et al. 2015; Ray et al. 2016). Development and track membranes are mechanically variable. Sedimentation, flocculation, coagulation, and carbon active adsorption have proven ineffectual, making membrane technology vital in international health standards (Ang et al. 2015). Therefore, a new generation of membranes is necessary, which can transcend these limits. "Electrospun nanofibrous membranes" (ENM) have aided recent developments in water treatment.

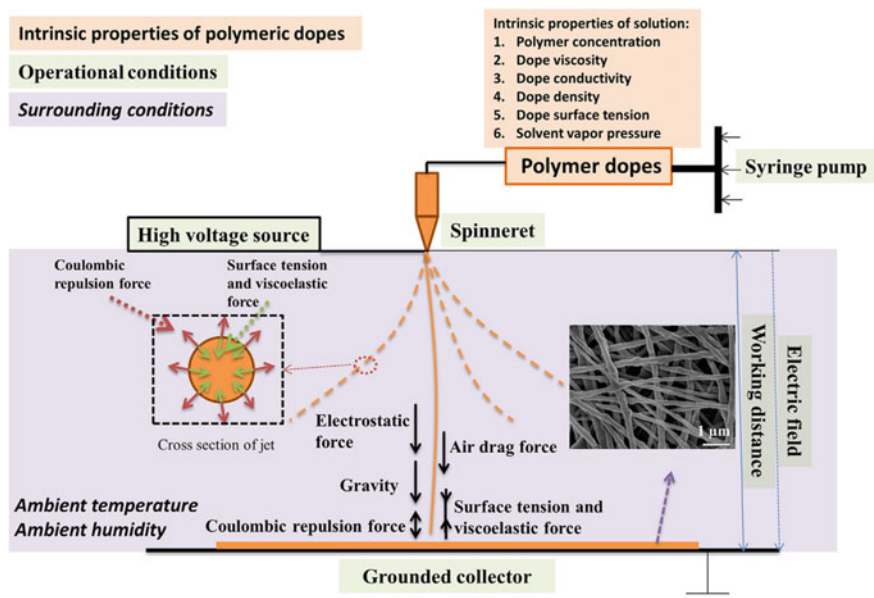


Fig. 1 Scheme of electrospinning plausible nanofibers formation (Reproduced with permission from Yang et al. (2018). Copyright 2018, Elsevier Science Ltd.)

Nanofibric nonwovens originating from basic nanofibers are created by electrospinning. Nanofibers can be produced from laboratory to pilot and industrial levels. Electrospinning has brought new possibilities in four critical areas (Ray et al. 2016; Persano et al. 2013). Some instances of energy, catalysts and health (Ray et al. 2016; Persano et al. 2013). The primary uses of electrospun nanofibers are shown in Fig. 1. Other uses for electric nanofibers include electrode materials, batteries (Jung et al. 2016) and solar power devices (Hou et al. 2019). Tissue, food and agriculture technology are useful as well. This broadens the scope of electrospun nanofiber uses. Electrospinning is the most promising and adaptable approach for producing nanofibers today.

TFC 4921 (Fluid Systems), TFC 4820-ULPT (Fluid Systems), AG 4040 (DESAL), 4040LSA-CPA2 (Hydranautics), DK2540F (DESAL), Osmonic cell unit (SEPA CF II, General electrics -USA) (Jang et al. 2020; Brandhuber and Amy 1998, 2001; Amy et al. nd) etc. membranes have been widely used for the conventional water treatment researches. But, such membranes come with fixed structured modules and tailor-making is not allowed. Nanofibrous membranes are frequently prepared by adopting methodologies involving sintering, stretching, track-etching, template leaching and phase inversion, where the electrospinning method is quite recently developed. The electrospinning methodology delivers the salient advantages of the high level of versatility to tailor-make the pore radius, nanopore structure, porosity (>90%) and ease of incorporation of additive materials (Teychene et al. 2013). Nano-metric polymer fibres are undeniably more important than in other applications as

filter media. They have distinct characteristics of liquid and air filtration. The adjustment of the operating variables and dope solution content (Ahmed et al. 2015) allows the manufacture of nanofibrous structured membranes. Electrospun membranes can efficiently remove contaminants into water and wastewater treatment with their small pore size and their narrow distribution (Khulbe and Matsuura 2019). Nanofibrous membranes can absorb heavy metals and other pollutants better due to their large surface area (Huang et al. 2014; Sarbatly et al. 2016). Electrospinning has recently seen a significant increase in use for fabricating filtration membranes, which is a significant advancement. Nanofibrous membranes' properties, structures, and functions have been gradually improved for filtration applications, allowing for new applications. New materials and functionalization methods have increased interest in electrospinning for membrane fabrication, as have advanced characterization techniques (Bassyouni et al. 2019).

This article gives an overview of recent developments in water treatment electrospun polymer nanofibrous membranes. The different modification strategies are discussed and illustrated concerning multifunctional nanofibrous composite membranes. The next section discusses the specific applications for the water treatment of these compositional nanofibrous membranes, emphasizing their past achievements in developing electrospun membranes. This paper closes with a short perspective on the role of electrospun nanofibrous membranes in future research on water treatment. The application documents for water treatment are explained in detail in this paper to encourage readers to look for new and more effective water treatment applications electrospun nanofibrous membranes through the detailed description.

2 Details of Electrospinning Process and Its Parameters for Nanofibrous Membranes Synthesis

Nanotechnology experienced a tremendous rise in the mid-1990s due to advancements in electrospinning and nanofibre formation, which promoted modern analytical methods (Formhals 1934; Morton 1902). Electrospinning of membranes has opened up several avenues for their use, including the creation of membranes and the application of biotechnology. One major advantage of electrospinning over competing nanofibers, like gas jet technology and melting fibrillation, is that the latter two have lower and higher values (Iwamoto et al. 2007; Liao et al. 2018a). Details about the different parameters in the electrospinning process are discussed here. These extrinsic properties, operational parameters, and environmental conditions affect the ENMs' properties.

2.1 *Electrospinning Process*

As demonstrated in Fig. 1, an electrospinning setup must include four components: a high voltage, a system (typically a syringe pump) that drives the dope, a spinneret, and a base metal collector. A technique called electrospinning is used to create polymer nanofibers from a liquid throttle. The charged fluid Jet is subject to various types of force, such as surface tension, Coulombic repulsion force, and electrostatic force, as shown in Fig. 1 (Liao et al. 2018a). The thinner nanofibers and increased production rate can be achieved in coaxial spinners through the air drag force applied on the outer channel (Zhmayev et al. 2010). According to the general rules, the electric spinning process follows these three phases: (1) development of rectilinear jets and spiralling trajectories, followed by bending distortion with solvent evaporation; and (2) formation of nanofibers from the nanofibers (Reneker and Fong nd).

An electric potential difference is applied primarily on a floor collector before the electrospinning process. The droplet's shape is changed to a cone-shaped Taylor Cone under the impact of applied tension. A fluid jet comes from this conical form. This cone-form structure may be maintained as long as there are sufficient solutions and each droplet is replaced during the electrospinning process. Nanofibers are not formed if the dope solution has more surface tension than the fibre voltage. All of the variables that affect nanofiber creation are the range of spinneret, the distance of the tip of a Spinneret from the grounded collection and the doping concentration.

For a predetermined distance after the start of the process of electrospinning, the polymer solution jet travels almost straight away from the orifice. The density and current of the liquid passing through the jet are inversely proportional to the distance. Electrical forces can be used to extend the jet beyond the right segment.

Rotating bending spools with increasing radius (Taylor 1969; He et al. 2005; Reneker et al. 2000) develop as a result. To reduce the jet diameter from microns to nanometers, the electrically driven non-axisymmetric bending of the jet is required (Yarin et al. 2001; Shin et al. 2001a, b; Fong et al. 1999a). While the nanofibers are being stretched and tiled, the solvents are also expelled, solidifying the nanofibers. A grounded apparatus will be used to collect nanofibers and them be analyzed and characterized once they have been bent and the solvent has been evaporated. The collection devices and design choices are important in shaping the morphologies and structures of the nanofibers (Huebner and Chu 1971; Park et al. 2007).

2.2 *Operating Conditions Required in the Electrospinning Process*

Electrospinning can create polymeric and inorganic nanofibrous membranes. This method can produce membranes quickly and cheaply using a wide range of materials. Define pore size, fibre diameter, and layout precisely with this method. The electrospinning process considerably impacts fibre morphologies, topography, and

structure. Overall, electrospinning parameters can be categorized into three types (Kenry 2017; Haider et al. 2018).

- Process variables
- Dope (polymer–solvent solution) variables
- Environmental variables

2.2.1 Process Variables

Nanofibrous membranes can be developed utilizing polymeric as well as inorganic electrospinning technologies. With this quick and cost-effective process, you can use many membrane synthesizing materials. This approach also allows the careful regulation of pore dimensions, fibre diameter and fibre characteristics. The conditions under which they have spun can have a major impact on the results of fibre morphology, topography and microstructure. In general, operating parameters may be divided into three categories for electrospinning (Kenry 2017; Deitzel et al. 2001).

2.2.2 Dope (Polymer–solvent Solution) Variables

Using nanotechnology and membrane science to develop membrane-based technologies and reduce energy costs is a good strategy. MF, UF, RDO, and Membrane Distillation (MD). As RO is the most often used press-driven strategy, membrane distillation is the preferred thermal processing method (MD). Since both RO and MD systems have been extensively investigated, they are the most widely employed approaches. Nano-liters are used to reduce salt content (20–80% NaCl) and remove brackish water (Elimelech and Phillip 2011; Essalhi and Khayet 2013; Khayet et al. 2018; Lee et al. 2011). Desalination's viability and affordability have improved over the previous decade, as has research into membrane-based desalination systems. The membrane's permeability (water permeability) is vital (selectivity or salt rejection). Membranes consume less energy than thermal processes due to ongoing improvements in membrane characteristics. Electrospinning has recently been used to create nano-branches for diaper membrane manufacture (ENMs). ENMs are distinct due to their multifunctionality as water purification products. The porous architecture contains big pores (micron-sized pores), limiting its ability to reject salt-bound water. In these cases, only coarse particles or liquids with large/microparticles can be employed in MF separation or as prefilters before delicate RO processes.

Membranes can purify water by removing colloidal solutions like oil/water suspensions. An ENM membrane crosslinked with selective coating layers can separate UF. PTFE coatings can be employed on both NF and RO composite membranes. Interfacial polymerization allows for separating an ultra-lamine surface layer by RO and MD. Adding nanoparticles (NPs) to the TFNC-membrane coated layer increases permeability and salt repulsion (NPs). Desalination (hence ux and salt efficiency) can be improved by adding NPs to ENMs, making nanotechnologies more suitable for existing desalination systems.

2.2.3 Environmental Variables

The effect on the morphology of nanofibres was proven to be ambient variables such as temperature and humidity (Vrieze et al. 2009; Hardick et al. 2011). The high temperatures can be used to manufacture thinner fibres according to the literature, which is determined to be possible. Low humidity can also speed the evaporation of solvents, whereas high moisture can lead to the development of larger fibers (Hardick et al. 2011; Pelipenko et al. 2013). As previously noted, environmental variables might affect the performance of the nanofibrous membrane resulting as well as the morphology of nanofibers (Pelipenko et al. 2013). For example, if you use a high-humidity environment, it can operate as a polystyrene fibre that is a helpful strategy for producing pores. In this scenario, the use of nanofibers for the filtration of oil spillage (Hajra et al. 2003; Kim et al. 2005) offers an important benefit.

3 Applications of ENMs in Different Pressure Driven Membrane Systems for Water Treatment

The pressure applied to the feed side of the MF, UF, NF, and RO separates water into two streams: permeate and the retentate. In many cases, permeate is used as the return solution, while retentate is thrown away and concentrated. This section studies the current state of research into electrochemically induced membrane (ENM) pressurized membrane processes.

3.1 Applications of ENMs in Microfiltration System

The nanospinning-prepared membranes of nanofibrous membranes have higher porosities than the membranes of other methods and can be qualitatively improved from submicron levels to several micrometres in size (Gopal et al. 2006). As a result, both the typical MF and cartridge MF (Wang et al. 2012) are good candidates. Electrospun nanofibrous mats were used in liquid separation and particle removal as described in Gopal et al. In a similar fashion, PVDC nanofibrous membranes performed the same way as PVDM nanofibrous membranes, rejecting 1, 5, and 10 micron polystyrene particles of liquids with greater than 90% effectiveness. Nanofibrous PAN, PSU, PES and nylon-6 membranes were made to better understand the effects on membrane performance of the electrospun nanofibrous structure (Barhate et al. 2006; Gopal et al. 2007; Aussawasathien et al. 2008; Homaeigohar et al. 2010; Yoon et al. 2009a). Its performance has been investigated with different diameters of nanofibers and membrane thicknesses. The results showed that the filtration properties are affected by ENM structures.

A chemical change can also improve the characteristics of ENM. For instance, PES nanofibrous membranes became more hydrophilic and wettable immediately (Liao et al. 2013) due to a short-term oxidation treatment. Pure water flows improved with modified PES ENMs. Nanofibrous membranes outperform typical MF membranes due to their high porosity, interconnected pores, small holes, and wettability. The nanofibric membrane rejects microparticles well (Homaeigohar et al. 2010). However, the structure of electrospun membranes can create fouling. Nanofibers can be washed away under high flux and pressure, producing mechanical failure. So, before large-scale ENM uses in water, nanofibers must be mechanically strengthened and physically integrated. Heat treatment, inter-nanofibril bonding with induced solvents and crosslinking agents were all used to knit nanofibers into mats (Homaeigohar et al. 2012; Homaeigohar and Elbahri 2012). Individual reinforcement of nanofibers also enhances compact pressure resistance. For example, zirconia nanofibers have increased filtration efficiency in PES NPs compared with neat PES NPs.

3.2 Applications of ENMs in Ultrafiltration System

Ultrafiltration is the name given to the membrane filtration technology that uses hydrostatic pressure. It is necessary to pump liquid through the membrane and feed it into the membrane with a length range between 0.01 and 0.1 μm (10–100 nm) (Fig. 2) to complete the procedure. While the UF travels across the membrane, it traps both water and low-molecular solutes. The University of Florida is a vital component in water and wastewater, which is utilized to remove bacteria, colloids, and viruses from the water. Water treatment before RO desalination, treatment to recover and MBR, and post-treatment following RO desalination are all examples of applications.

The present application of the reversal stage is in the production of traditional polymer UF membrane, with low to moderate flow and significant fouling rates. Pore distribution seems to be inherent in the inversion stage. Partial retention is worsened because of the numerous pores in the distribution network, making the dispersion less effective. A major focus in UF membrane development is the development of surface pores isoporosity and high porosity. Thin, selective layers can be built from assembling itself or through a phase reversal. In the meantime, nanofibrous fabrics are required for use as hydrophilic and highly porous substrates. Increasing flux and maintaining a strong rejection, nanofibrous UF-composite membranes have outperformed conventional flux-restricted membranes for filtration of oil-fired wastewater.

Cover materials like PVA and chitosan were employed to create surface barrier layers on ENMs, giving them nanofibrous UF composite membranes. For an oil-in-water emulsion, splitting the emulsion into two phases revealed a very high refuse-efficiency (>99.5%) for the composite nanofibrous membrane while simultaneously permitting high wastewater flows (>130 L/m²h). Chitosan is a common coating substance due to its hydrophilicity. A hydrophobic PVDF membrane with a chitosan

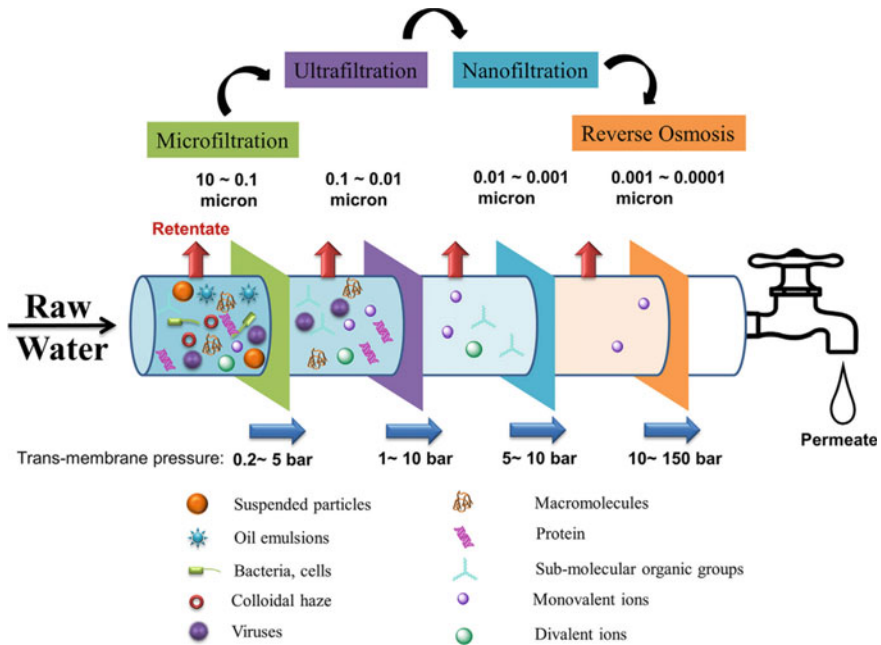


Fig. 2 Schematics of membrane water treatment system (Reproduced with permission from Yang et al. (2018). Copyright 2018, Elsevier Science Ltd.)

ultrathin selective layer was successfully tested. This composite membrane has a flow rate of 70.5 L/m²h and a BSA rejection of roughly 98.8% at 0.2 MPa after adding surface modified glutaraldehyde (GA) and terephthaloyl chloride (TPC). The membrane also shown good antifouling properties over 24 h. Finally, the adaptable electrospun was employed as a porous base material for both hydrophobic and hydrophilic polymers. Hydrophilic substrates assist resist fouling in many applications. More study is needed to maximize the network’s water permeability, hydrophilicity, and antifouling qualities.

3.3 Applications of ENMs in Nanofiltration System

The gap between Uf and the reverse (RO) (Sutherland 2008) is filled by nanofiltration (NF). (Sutherland 2008). Based on the molecular weight reduction, conventional FM-separation sizes are 100 to 1000D (MWCO). It softens, disinfects and eliminates organic pollutants and divalent ions, and NF may be widely used to clean water. NF. High transmembrane pressure causes steric and electrostatic effects of Donnan, which result in separation. While both NF and RO can reject monovalent ions like sodium chloride, NF maintains multivalent salts like sodium sulphates better.

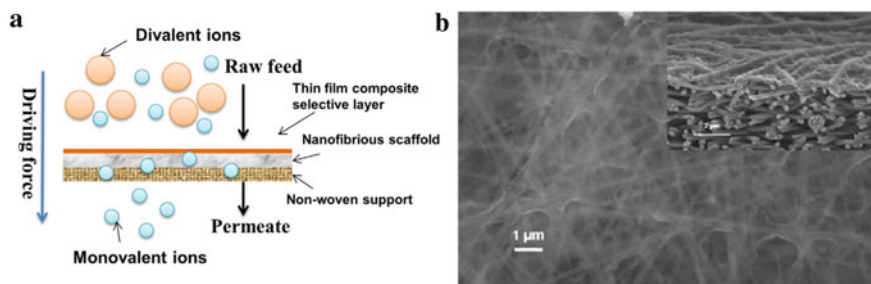


Fig. 3 **a** Schematic of nanofiltration (NF) with a thin film nanofibrous composite (TFNC) membrane; **b** Typical surface and cross-section (inserted images) morphologies of a TFNC membrane (Reproduced with permission from Yang et al. (2018). Copyright 2018, Elsevier Science Ltd.)

The most widely utilized TFC membranes are non-ionizing fluid membranes made of ultrapine skin layer IP on a porous substrate. The high surface and interior porosity of nanofibrous scaffolds make the construction of TFC membranes appealing to many researchers. It is especially true in NF due to the low pressure and compressive force. Contrast this with a laboratory-made TFC membrane's 2.4-fold higher permeate flux and near-identical rejection rate (98%). Higher TFNC membrane flux (due to increased pore and porosity of the substrate) is attained as the nanofibre pore diameter increases (Fig. 3). The nanofibrous membrane could not sustain the barrier layer due to increased surface diagram and nanofiber holes. Researchers revealed that nanofibres can reduce rejection while improving penetration. However, reducing the nanofibrous membrane thickness reduces its hydraulic resistance.

Electrospinning is a method that provides high surface porosity and linked pores in a pressured membrane process. Because electrospinning cannot manufacture dense membranes with nanometer-length pores in a single step, research focused on developing TFNC membranes. The long-term sustainability of these water treatment microorganisms was hampered by their under-pressure stability, antifouling capabilities, and mass replication. The substrate is required for high-level TFC membrane development because it defines the flow channel across the membrane.

4 Applications of ENMs for Wastewater Treatment

4.1 Applications of ENMs for Heavy Metal Removal from Contaminated Water

As mineral adsorbents and inorganic ion fixators, hydroxyapatite NPs (HAp nPs) have been shown to accommodate a wide variety of cationic and anionic replacements. Heavy metal extraction from wastewater has recently become a focus of research.

Heavy metal ions from water can be bound by HAp (Subramanian and Seeram 2013). Recently, HAp-based composite materials have gotten a lot of buzzes. A modification in humic acid HAp NPs improves Cu (II) adsorption significantly. Comparing bare HAp to ion exchange mechanisms with Ca (II) ions showed it to be greatly enhanced. A solution that adsorbs Co was found in the HAp/Zeolite composite (II). This compound (63%) outperformed HAp (58%) and zeolite (63%). (47%). It was used to calculate the Pb (II) rejection effectiveness from watery solutions using C-HAp and granular activated carbon (Fernando et al. 2015). Aqueous solutions were tested for their ability to exclude Pb (II) ions by using HAp NPs synthesized with granular activated carbon. According to the researchers, the adsorption potency of the HAp NPs was 138–83 mg/g, whereas C-HAp adsorption was 9–14 mg/g. The researchers claim that a polymeric Hap Nanocrystal and polymer composite can assist offset lower yields and longer manufacturing times for HAp NPs, respectively. Conclusions (Aliabadi et al. 2014) Plum, copper, and nickel ions are removed by a chitosan/HAp composite nanofiber. This increased the membrane's prospects for industrial application after five desorption-absorption cycles. In wastewater treatment, it is a powerful adsorbent for heavy metals like lead, mercury, and cadmium. For example, increased porosity and gas permeability.

Toxic heavy metals can be removed efficiently by electrospinning nano fibres with a high volume to the aspect ratio, specific surface area (10–100 m²/g), and porosity (80–85%) (Aadil et al. 2018). That's because they have a lot of porosity and a lot of volume-to-aspect ratios. Less need to filter wastewater after adsorption reduces costs and reduces contaminants. Adsorbent polymer (cellulose) is produced by plant cells. Dense adsorbents have been used for pollution management for decades, but little is known about their economic application. Producing submicron cellulose fibre is difficult because cellulose does not dissolve in conventional solvents. Promotes cellulose ester production (cellulose acetate) (CA). Other uses for textiles are cigarette filters, floor coverings, inks, and film. In its major application, Ca is utilized to make membrane bi-products. Non-pole solvents are easy to dissolve and treat, and they are good for electrospinning due to their strength retention when made in membranes, as shown. Making ultrafine CA porous fibres and testing their adsorption capabilities on Cu²⁺ were both successful.

By contrast, the greatest removal effectiveness of Cu²⁺ from porous ultrafine fibres was 88.6%. For CA polymer backbones without reactive function groups, the absence of reactive functional groups reduces the membranes' separation performance. Adsorbent separation using affinity principles is not suggested for this polymer. These acetyl derivatives might be employed to treat acidic chloride solutions as adsorbents, with a maximum capacity of 110 mg/g for the selective recovery of Au, to determine the optimal cellulose to acetyl derivative conversion process (III). Auxiliary metal ions, such as Pd (IV) and Pt (Pt), can also be rejected by the CA fibre (II). Filters such as silica can improve the material's chemical and physical properties while adding new and interesting capabilities. This is done by mixing inorganic fillers. CA is an inorganic filler matrix. One investigation reported an 81.1% efficacy rate for a 0.78 nm pore-sized chitosan/CA formulation in conventional wastewater treatment plants. The use of a cellulosic polymer, such as a composite material with

HAP, can assist in the purification of the environment of harmful bisphenols as the technique allows for the manufacture of ultra-thin particles with a diameter of 92 nm or less. A new method for detecting Bisphenol A in infant food samples is patentable due to new chromatography technologies being developed. It is difficult to make hybrid nanocomposites because the ceramic powder does not dissolve well in the CA. Electrospinning hybride nanofiber composites can increase the extraordinary adsorption characteristics of heavy metals due to the affinity and/or electrostatic contact between functional groups.

According to a recent study, composite CA/HAP nanofibers with a composite of 3% (wt%) CA/HAP are highly effective in repulsion of heavy metal ions from wastewater. In this composite show, one element outperforms the other. Different factors for finding the ideal conditions for ion separation of plumes (II) and iron (III) have been optimized. The ideal conditions for wastewater are pH 6, room temperature and 0.1 g V. 0.1 grammes V, pH 6, ambient temperature and lead (II) 35 min (99.7 and 95.47%). The pseudo-kinetic model and Freundlich isotherm best illustrate this process. For example, M10(XO4)6Y2 indicates a bivalent cation, while PO_4^{3-} represents XO4 and OOH. HAp, for instance, Due to its wide spectrum of anions and cations interactions in an adsorption/ion exchange process, this anion exchanger (HAp) was intensively studied for a long period, leading to the discovery of several water pollutants. Due to their similar radii and the distance between the calcium ion (0,99) and both radii, Pb (1,19) and Fe (0,645) are projected to fit into the HAp grid. If the cations do not enter the apatite structure correctly, hydroxyl, phosphate, or calcium groups must be substituted. Electrodeposited Microcapsules (tortiline nickel) made of polyester/gelatin (vinyl alcohol). However, electrocatalytic activity was more influenced by nanofibers than NPs. However, when compared to NPs of the same composition, nanofibers outperform them. Contrast this with NPs or a catalyst that was initially clean and later impregnated with W, and you get a 28% increase in current density. In the metals, tungsten presence affects electrocatalytic activity dramatically. The best performance was achieved with nanofibers electrospun from tungsten precursor solution (35% wt). There is evidence that calcines temperature affects yield. There were no differences between 1000 and 700 °C in these investigations.

4.2 Applications of ENMs for Oil Spill Removal from Contaminated Water

Much emphasis has been paid to the separation and recycling of oil/water streams utilizing energy-efficient and environmentally acceptable technology. Demulsification of oil/water emulsions can be accomplished via coalescence filtration. The coalescence filter separates emulsions into three basic phases, as shown in Fig. 4a. The filter medium removes solid particles from the fluid stream first. Second, droplets are captured by the fibrous bed, which then agglomerate within the fibrous network.

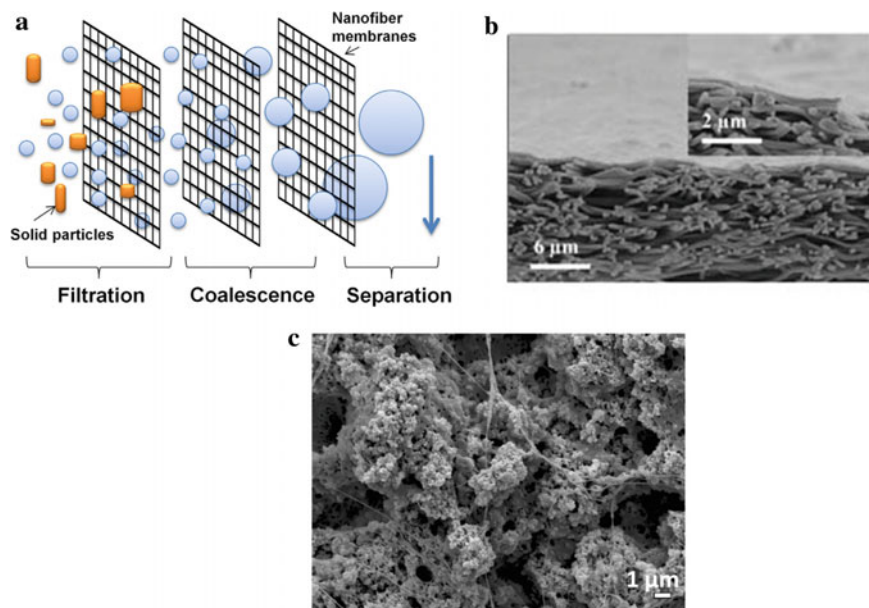


Fig. 4 **a** Filtration scheme for coalescence; **b** Transverse view of the TFNC membrane based on cellulose and **c** Superwetting membrane surface morphology fabricated for separation of water/oil. (Reproduced with permission from Yang et al. (2018). Copyright 2018, Elsevier Science Ltd.)

The coalescence system combines small oil/water droplets into larger ones by passing through numerous filter layers. Finally, gravity separates the stream into oil and water layers. When water-in-oil emulsions are handled, big water droplets sink, and giant oil droplets rise to the surface. All influences the performance of the coalescence by flow, depth of the bed, surface characteristics and droplet size. Glass nanofibre-coated fibres have been found to work well with separation between oil and water (Shin and Chase 2006, 2004; Ma et al. 2010). It was discovered that even a few nanofibers increased the filter media's capture effectiveness. It did, however, exacerbate the pressure decrease (Shin and Chase 2006). The diameter and wettability of the nanofibers were also shown to influence the performance of coalescing filter medium. By reducing nanofibers, the total efficiency of the separation was increased. Materials with better wetting enabled the coalescence of water in oils. In the investigation, the filter's performance was improved by the electrospinning nylon 6 nanofibers, which measured 250 nm in diameter on the surface of the glass filter. Furthermore, micro-sized glass fiber-coated nanofibers with a diameter of 150 nm increased separation efficiency from 71 to 80% (Shin and Chase 2004).

In the context of mineral adsorbents and inorganic ion fixators, it has been established that hydroxyapatite NPs (HAP nPs) can accept a wide range of cationic and anionic replacements in their structural composition and function. Over the last few years, researchers have concentrated their efforts on using HAP NPs to remove heavy metals from wastewater. The ability of HAP to bind heavy metal ions from water

has been proven in studies. The utilization of HAp-based composite materials has recently attracted a significant deal of attention. Increased adsorption of Cu (II) ions occurs due to the modification of humic acid HAp NPs. Comparing bare HAp to ion exchange processes with Ca (II) ions was demonstrated to be greatly improved. One of the HAp/Zeolite composite components that has been found is a solution that adsorbs Co. (II). They wanted to see if this composite (63%), HAp (58%), and zeolite would outperform HAp in terms of aiding in the elimination of toxins (47%). To calculate the Pb (II) rejection efficiency from watery solutions (Fernando et al. 2015), C-HAp has been produced in the presence of granular activated carbon. A prior study had used granular activated carbon to synthesize HAp NPs, which were then used to create C-HAp, which was used to evaluate the efficiency of aqueous solutions at excluding Pb (II). Their research revealed that, when using HAp NPs, they could increase the amount of C-HAp that could be adsorbed at the same time by a factor of 138 to 83. They also observed that the C-HAp potency could be increased by a factor of 9 to 14 mg/g. According to the researchers, a polymeric Hap Nanocrystal and polymer composite can be used to compensate for lower yields and longer manufacturing periods associated with HAp NPs. Findings from the study (Aliabadi et al. 2014) The development of a chitosan/HAp composite nanofiber to remove Plum, copper, and nickel ions has been accomplished. The membrane's chances for use in the industry significantly increased after five consecutive desorption-absorption cycles. Adsorption of poisonous pigments and heavy metals such as lead, mercury, and cadmium from wastewater is made possible by using this adsorbent. Reasons for this assumption include the permeability of gases and a material surface area with a larger porosity.

The high volume to the aspect ratio, the high specific area (10–100 m²/g), and the high porosity (up to 80%) (Aadil et al. 2018) of electrospun nanofibers (Reneker and Yarin 2008) all contribute to its excellent adsorption capacity for removing toxic heavy metals, and electrospinning for nanofiber synthesis has attracted a great deal of interest. With a standard sample volume of around 10–100 m², this is due to a high volume-to-aspect ratio, resulting in a high specific area and high porosity. Aside from economic savings from not having to filter wastewater after adsorption, other advantages of nanofibre membranes include reducing contaminants that could have been present in the wastewater. Cells extract cellulose from plants, which is a natural polymer adsorbent. Despite this, there is a continual interest in learning more about the practical application of these adsorbents in pollution control to progress the field of pollution control research. Cellulose submicron fibre production is complex because cellulose does not dissolve in conventional solvents. Acetate, for example, aids in the production of cellulose ester compounds (CA). Aside from textiles, cigarette filters, surface coatings, inks, and motion picture film, other applications include microfilm, audiotape, microfiche, ink, and optical disc media, to name a few examples. In the manufacturing of membrane bi-products, which is the primary application for calcium, it is the most often used element globally.

With regard to non-pole solvents, it has been established that they are simple to dissolve and process, and they are particularly well suited for electrospinning due to their ability to maintain strength even when made in membranes. Preparation

and analysis of Cu^{2+} adsorption qualities were effective in fabricating ultrafine CA porous fibres while researching the adsorption properties of Cu^{2+} . According to Kusworo et al. (2014), the maximal Cu^{2+} removal efficiency of ultrafine fibres and porous ultrafine fibres was 19.1, 70.8, and 88.6%, respectively.

A fundamental disadvantage of CA polymer backbones is that they lack reactive function groups, resulting in the membranes' separation performance being severely hampered. In addition, it should be highlighted that this polymer is not well suited for adsorbent separation based on the affinity principle [particularly, adsorbent separation based on affinity principles] and is therefore not suggested for this application. As part of their efforts to determine the most efficient method of converting wood pulp into acetyl derivatives, the researchers investigated whether the acetyl derivatives produced by cellulose synthesizers could be used to treat acidic chloride solutions as adsorbents, with a maximum capability of 110 mg/g for the selective recovery of gold. They found that they could (III). Thus, the CA fibre (AU(III) rejection efficiency) is active in the rejection of other metal ions, such as the metal ions Pd(IV) and Pt, which are present in the environment (II). Different inorganic fillers, such as silica, can be used to improve the chemical and physical properties of the material while also providing new and different functionalities to the end product. CA fibre connections are maintained by using a variety of inorganic fillers. A soft matrix for inorganic fillers, CA, is utilized as a binder for the fillers. One such formulation, with pores of 0.78 microns in size, was evaluated in conventional wastewater treatment plants and found to be 81.1% efficient at a pressure of 506.5 kilopascals (kPa). A cellulosic polymer, such as a composite material with HAP, can be used to clear the environment of hazardous bisphenol. There has been an interaction between hap and cellulosic polymers, and the technology now allows for the production of exceedingly thin particles with a diameter of 92 nm or smaller. A new approach for identifying Bisphenol A in baby food samples has been created due to the development of new chromatography methods. This method has been granted patent protection. The poor dispersion of ceramic powder in the CA, which occurs when the polymer matrix that holds the ceramic powder together is created, is a significant problem in the creation of hybrid nanocomposites. The amazing adsorption characteristics of heavy metals can be enhanced by using electrospinning to generate hybride nanofiber composites, which is a result of the affinity and/or electrostatic contact between the various functional groups.

It has recently been demonstrated that the use of CA/HAP composite nanofibers with 3% CA/HAP composite (wt%) as an exceptionally low-cost adsorbent, which is exceptionally effective at repelling heavy metal ions from wastewater, is extremely effective at repelling heavy metal ions from wastewater. The study involved participants from various universities and community organizations throughout the United States. The performance of this composite show outperforms the performance of either of the individual components or the combined show. Following considerable evaluation of numerous parameters, the optimal conditions for lead (II) and iron (III) ion separation in wastewater were discovered. Specifically, pH 6 wastewater, room temperature, and 0.1 grammes of V are the most favourable circumstances for this procedure. For the separation of lead (II) and iron (III), these conditions must be

established in less than 35 and 40 min, respectively. They must be achieved under pH 6, at room temperature, with 0.1 grammes of V. These conditions must be established in less than 35 and 40 min, respectively. They must be achieved under pH 6, at room temperature, with 0.1 grammes of V. (99.7 and 95.47%) (Although it has been demonstrated that this technique is capable of conducting rejection using two models, the pseudo-kinetic second-order model and the Freundlich isotherm model are the most accurate representations of the process.) The general formula $M_{10}(XO_4)_6Y_2$ denotes a bivalent cation, whereas the compound PO_4^{3-} denotes XO_4 and OOH .

In contrast, HAp denotes a bivalent cation, and the compound PO_4^{3-} denotes XO_4 and OOH . Consider HAp as an illustration: Since it interacted in an adsorption/ion exchange process with a wide range of anions and cations for a while, this particular anion exchanger (HAp) was extensively studied for a while; as a result, it was discovered that numerous water contaminants had a connection to this chemical. Due to their similar radii and the approximate distance between the calcium ion (0.99) and both radii, it is expected that Pb (1.19) and Fe (0.645) will fit into the HAp grid. If the cations are not effectively incorporated into the apatite structure, the addition of substitute hydroxyl, phosphate, or calcium groups may be necessary.

Nitric acid, tungsten chloride, and microcapsules (tortiline nickel) made from a polymer combination of polyester and gelatin are used in this process (vinyl alcohol). When NPs and nanofibrous materials were compared, it was discovered that the latter had a stronger impact on electrocatalytic activity. When the nanofibers are combined with NPs of the same composition, which was made by calcining a solution containing 10% WCl_2 in weight at 850 °C, the efficiency of the nanofibers improves. Compared with NPs, the nanofibrous morphology resulted in an increase in current density from 11.5 to 16 mA/cm² (a 28% increase) and a 42% increase in current density from 22 to 37.75 mA/cm² (a 42% increase), with the improvement in performance being realized in comparison to both a catalyst that started as pristine and then was further impregnated with W. A considerable impact on electrocatalytic activity was found to be caused by altering the tungsten content of the metals. Nanofibers displayed the highest performance when electrospun from a precursor tungsten solution containing 35 weight percent of the metal. According to the findings of several prior research, the temperature of the calcine has an impact on yield. 1000 degrees Celsius was shown to be the optimal temperature in these experiments, with 700 and 850 degrees Celsius equivalent.

5 Applications of Electrospun Nanofibrous Membranes for Desalination

Seawater desalination is a widely mentioned issue. While alternative technology research is early, seawater treatment has better reliability. Desalination can be performed on inland bodies of water where it is more difficult to treat brackish water than seawater.

Desalination is the process of removing salt, minerals, and other pollutants from seawater to create freshwater that can be used for drinking and other purposes. Seawater has a high concentration of salt, making desalination costly and impractical. Salinity in saltwater is primarily dependent on the percentage of salt in the water: 3.5% (or 35 g/L) NaCl equivalent to 3500 ppm. One would like to keep NaCl (sodium chloride) levels under 280 ppm in drinking water (Feng et al. 2008; Elimelech and Phillip 2011). To desalinate seawater, we can use several different processes that utilize both kinetic and thermodynamic energy and mechanical, electrical, and chemical. The multiple-stage effect, MSF, a distillation of multi-effects, MED, mechanical vapour pressure, MVC, diaphragm distillation, MD, RO, electrodialysis, and nanofiltration are a few of the technologies for desalination (NF). Second-generation membrane-based technologies utilize thermal-based technology, the former generation of which has a thermal base. Nanotechnology and membrane science are cost-efficient approaches for improving membrane technology and reducing energy expenses due to lower energy usage. Ultrafiltration (UF), Distillate Recirculation (RDO) and Distillation of the Membrane (MD). The RO process is the most frequently used press-driven approach, and the process of membrane distillation is the most sought in thermal treatment (MD). RO and MD water processes have been thoroughly explored, which means that the most common techniques are RO and MD systems. Nano-liters (Elimelech and Phillip 2011; Essalhi and Khayet 2013; Khayet et al. 2018; Lee et al. 2011) often involve additional procedures of decreasing the salt content to 20%–80% NaCl and removing brackish water.

The viability and cost of desalination and research into membrane-based desalination systems have progressively increased in the recent decade. Durability (water permeability) is an important attribute of the membrane (selectivity or salt rejection). Due to ongoing membrane characteristics advances, membranes utilize less energy than processes that are heat propelled. Electrospinning is used to produce nanotech-enabled diaper membranes in a recent application (ENMs). ENMs have unique qualities since water purification solutions might have multifunctionality. The porous architecture includes relatively big pores (micron-sized pores), limiting the capacity of poring water to reject salt-like chloride, for example. In certain cases, in the MF separation or prefilters before sensitive RO procedures, only coarse particles and liquids with large/microparticles can be employed that are suspended in them.

Diversified membranes may be used to remove colloidal solutions, such as suspensions of water and oil, for water treatment. For UF separation, the membrane that consists of an ENM and is connected to selective coating layers can be used. In the manufacture of the NF and RO composite membranes, PTFE or polytetrafluoroethylene (PTFE) coatings may be employed. The RO and MD separation of an ultra-selective ultra-lamine surface layer are feasible through interfacial polymerization. By integrating NPs in the TFNC membrane coated layer, the durability and repellence of salt can be further enhanced by (NPs). Adding NPs to ENMs can improve desalination (and, in turn, salt and ux-efficiency) and boost the application of nanotechnology to existing desalination systems.

6 Application of ENMs for Dye Removal

With their large surface area, electrospun nanofibers can remove greater amounts of dye from wastewater by surface adsorption. Xu et al. (2012) investigated the adsorption capacity of vinyl-modified mesoporous poly(acrylic acid)/SiO₂ composite nanofiber membranes for the adsorption of malachite green, a triarylmethane dye used in the production of silk, leather, and paper, according to the results of their research. The removal of cetyltrimethylammonium bromide (CTAB) from the electrospun fibres results in the formation of pores in the material. The fibrous membrane has an adsorption capacity of 240.49 mg/g and a satisfactory clearance rate for the first three regeneration cycles after being degraded. Nonetheless, after six regeneration cycles, the clearance rate was lowered to approximately 44% (Green Processing and Synthesis nd). In another study, Polyethylenimine (m-PEI) and polyvinyl chloride (PVDF) blend (m-PEI/PVDF) adsorption efficiency for anionic dyes was investigated by Ma et al. (2016) utilizing methyl orange (MO) as the model dye in their study.

In neutral pH, a nanofibrous mix comprising 49.5% m-PEI had a maximum adsorption capacity of 633.3 mg/g, significantly higher than previously reported adsorbents, according to the research (Xu et al. 2012). Using electrospun nylon-6 (PA-6) membranes, Yu et al. (2018) demonstrated that the membranes could remove indigo dye solution without the need for any other alterations to their chemistry. Although 10 layers of the produced membranes were hot-pressed together for filtration, this was not sufficient to completely remove the dye. An electrospun membrane with a single layer had a thickness of around 0.03 mm, while ten layers of hot-pressed membrane had a thickness of approximately 0.12. It was discovered that cake had formed on the membrane's upper surface after being subjected to dead-end filtering. Due to the solute concentration on the membrane surface being greater than its saturation solubility, a cake formed, resulting in the precipitation of the dye on the membrane surface. Despite the fact that the membrane's pores were not entirely blocked, the flow declined dramatically in the first 200 min and stabilized at greater than 15 L m² h⁻¹ after 500 min of experimentation (Ma et al. nd). Recently, Jang et al. (2020) investigated the dye adsorption capability of exfoliated graphene oxide (GO) fibres loaded with cetyltrimethylammonium chloride (CTAC) modified exfoliated graphene oxide (GO) in an aqueous system. The dyes tested were methylene blue (MB) and methyl red (MR). When combined with its different oxygenated functional groups and phenyl backbone, GO can induce attractive forces between MB and MR dye molecules, leading to an improvement in adsorption effectiveness for both dyes at higher concentrations of the compound. By employing CTAC to modify the surface of GO, researchers were able to boost the loading capacity of PAN solution from less than 10 weight percent to more than 30 weight percent of GO without affecting the electrospinning or fibre formation processes. Because the electrospun PAN membrane loaded with 30 wt% cGO was excessively brittle, 20 weight percent cGO was employed in place of the 30 weight percent cGO in the original experiment. With respect to adsorption efficiencies, the electrospun PAN/cGO membrane

displayed good performance for both MB and MR dyes, with the MR dyes exhibiting the highest efficiency. According to the researchers, this is because the MR dye has a more compatible polarity with membranes and because its molecular size is smaller, which allows for greater diffusion of the solution into the depths of the electrospun membrane (Yu et al. nd).

7 Conclusion

Electrospinning nanofibers are now standard. They are ideal for encapsulating a wide range of functional nanomaterials. Even on a large scale, basic understanding and modelling of the complex spinning process have improved. As a result, the production of novel water treatment membranes has benefited. These studies have been examined and categorized. Water treatment with nanofibrous composite membranes. Developing ultrafine nanofiber membranes with high porosity is now a priority. Most unaltered ENMs feature 1 μ m surface pores and 100 nm nanofibers. Micro- to submicron membrane surface pores and nanofiber diameters of 100 nm to several nanometers must be optimized. Because nanofibric substrates are porous, highly fine nanofibrous membranes may efficiently filter particles. Fine nanofibers can successfully sustain grafted or polymerized cutaneous layers and prevent obtrusive substrata. Dope conductivity, voltage, and viscosity control Micron-sized nanofibers are still challenging to mass manufacture. Improved membrane substrates improve selective layer adhesion. The impacts on substrate surface roughness, surface porosity, and charges require more research. In membrane operations, membrane fouling reduces flow capacity. Electrified antifouling membranes fascinate me. Deterring membrane fouling requires more coating methods. Oriented and sized nanotubes are now possible.

Electrospinning has become a widely accepted, simple process for creating nanofibers in the last few decades. Nanofibers have unique properties for academic and industrial use such as a large specific surface area, high porosity (up to 90%), one-dimensional arrangement, easy inclusion of functional nanomaterials, and a wide range of architectural styles. Because of the high porosity of nanofibrous substrates, the filtration effectiveness of smaller particles can be improved by utilizing ultrafine nanofibrous membranes. TFNC membrane applications in high-pressure processes are made easier by ultrafine nanofibers, which efficiently support grafted or polymerized skin layers and reduce their penetration into substrates even at high pressure. The ultrafine nanofibers can be made by manipulating the dope's conductivity, surface tension, and viscosity. Even still, mass production of nanofibers smaller than 100 nm is difficult at this point. Despite these efforts, more research is needed on nanofibrous membrane optimization, the development of robust and ultrathin selective layers on nanofibrous substrates, the fabrication of complicated and multifunctional nanostructures, and the mass production of these advanced technologies nanofibrous membranes. Optimized membrane substrates not only support surface coating layers but also reduce the amount of intrusion they cause. They also improve adhesion

between specific layers and substrates. Researchers aim to carry out more research on how the properties of the nanofibrous substrates interact with other properties like substrate material and roughness, surface porosity, and charge to better understand how the two materials link together. Membrane processes also face the difficulty of reducing flux below the theoretical capacity due to membrane fouling, which is a significant challenge. It's intriguing to think of electrospinning and additional modification as a way to create antifouling membranes. To prevent the formation of fouling layers on membrane surfaces, further coating techniques should be investigated.

Commercializing electrospinning technology requires more research. Besides water treatment, new ENM should be investigated. A multifunctional membrane that can disinfect, decontaminate and separate water may be developed with ENMs. The development of electrospun nanofiber membranes for water purification. Research on electrospun membrane water treatment has advanced significantly in recent years. These issues will require more effort for new electrospun membranes.

References

- Aadil KR, Mussatto SI, Jha H (2018) Synthesis and characterization of silver nanoparticles loaded poly (vinyl alcohol)-lignin electrospun nanofibers and their antimicrobial activity. *Int J Biol Macromol* 120:763–767
- Ahmed FE, Lalia BS, Hashaikeh R (2015) A review on electrospinning for membrane fabrication: challenges and applications. *Desalination* 356:15–30
- Aliabadi M, Irani M, Ismaeili J, Najafzadeh S (2014) Design and evaluation of chitosan/hydroxyapatite composite nanofiber membrane for the removal of heavy metal ions from aqueous solution. *J Taiwan Inst Chem Eng* 45:518–526
- Amy GL, Edwards M, Benjamin M, Carlson K, Chwirka J, Brandhuber P, McNeill L, Vagliasindi F (1998) Draft Report, AWWARF
- Anand A, Unnikrishnan B, Mao JY, Lin HJ, Huang CC (2018) Graphene-based nanofiltration membranes for improving salt rejection, water flux and antifouling—a review. *Desalination* 429:119–133
- Ang WL, Mohammad AW, Hilal N, Leo CP (2015) A review on the applicability of integrated/hybrid membrane processes in water treatment and desalination plants. *Desalination* 363:2–18
- Aussawasathien D, Teerawattananon C, Vongachariya A (2008) Separation of micron to sub-micron particles from water: electrospun nylon-6 nanofibrous membranes as pre-filters. *J Membr Sci* 315:11–19
- Azzaoui K, Lamhamdi A, Mejdoubi E, Berrabah M, Hammouti B, Elidrissi A, Fouda M, Al-Deyab S (2014) Synthesis and characterization of composite based on cellulose acetate and hydroxyapatite application to the absorption of harmful substances. *Carbohydr Polym* 111:41–46
- Badruzzaman M, Voutchkov N, Weinrich L, Jacangelo JG (2019) Selection of pretreatment technologies for seawater reverse osmosis plants: a review. *Desalination* 449:78–91
- Barhate RS, Loong CK, Ramakrishna S (2006) Preparation and characterization of nanofibrous filtering media. *J Membr Sci* 283:209–218
- Bassyouni M, Abdel-Aziz MH, Zoromba MS, Abdel-Hamid SMS, Drioli E (2019) A review of polymeric nanocomposite membranes for water purification. *J Ind Eng Chem* 73:19–46
- Beachley V, Wen X (2009) Effect of electrospinning parameters on the nanofiber diameter and length. *Mater Sci Eng C* 29:663–668
- Bethi B, Sonawane SH, Bhanvase BA, Gumfekar SP (2016) Nanomaterials-based advanced oxidation processes for wastewater treatment: a review. *Chem Eng Process* 109:178–189

- Brandhuber P, Amy G (1998) Alternative methods for membrane filtration of arsenic from drinking water. *Desalination* 117:1–10
- Brandhuber P, Amy G (2001) Arsenic removal by a charged ultrafiltration membrane influences of membrane operating conditions and water quality on arsenic rejection. *Desalination* 140:1–14
- Buchko CJ, Chen LC, Shen Y, Martin DC (1999) Processing and microstructural characterization of porous biocompatible protein polymer thin films. *Polymer* 40:7397–7407
- Buchko CJ, Kozloff KM, Martin DC (2001) Surface characterization of porous, biocompatible protein polymer thin films. *Biomaterials* 22:1289–1300
- Candido RG, Godoy GG, Goncalves AR (2017) Characterization and application of cellulose acetate synthesized from sugarcane bagasse. *Carbohydr Polym* 167:280–289
- Che H, Huo M, Peng L, Fang T, Liu N, Feng L et al (2015) CO₂-Responsive nanofibrous membranes with switchable oil/water wettability. *Angew Chem Int Ed* 54:8934–8938
- Choong LT, Lin YM, Rutledge GC (2015) Separation of oil-in-water emulsions using electrospun fiber membranes and modeling of the fouling mechanism. *J Membr Sci* 486:229–238
- Daer S, Kharraz J, Giwa A, Hasan SW (2015) Recent applications of nanomaterials in water desalination: a critical review and future opportunities. *Desalination* 367:37–48
- De Vrieze S, Van Camp T, Velvig A, Hagstrom B, Westbroek P, De Clerck K (2009) The effect of temperature and humidity on electrospinning. *J Mater Sci* 44:1357–1362
- Deitzel JM, Kleinmeyer J, Harris D, Beck Tan NC (2001) The effect of processing variables on the morphology of electrospun nanofibers and textiles. *Polymer* 42:261–272
- Drew C, Wang X, Samuelson LA, Kumar J (2003) The effect of viscosity and filler on electrospun fiber morphology. *J Macromol Sci Part A Pure Appl Chem* 40:1415–1422
- El Rayess Y, Albasi C, Bacchin P, Taillandier P, Raynal J, Miettton-Peuchot M et al (2011) Cross-flow microfiltration applied to oenology: a review. *J Membr Sci* 382:1–19
- Elimelech M, Phillip, WA (2011) The future of seawater desalination: energy, technology, and the environment. *science*, 333(6043), pp 712–717.
- Elkady M, Shokry H, Hamad H (2016) Effect of superparamagnetic nanoparticles on the physico-chemical properties of nano hydroxyapatite for ground water treatment: adsorption mechanism of Fe (II) and Mn (II). *RSC Adv* 6:82244–82259
- Elkady M, Shokry H, Hamad H (2018) Microwave-assisted synthesis of magnetic hydroxyapatite for removal of heavy metals from groundwater. *Chem Eng Technol* 41:553–562
- Essalhi M, Khayet M (2013) Self-sustained webs of polyvinylidene fluoride electrospun nanofibers at different electrospinning times: 1. Desalination by direct contact membrane distillation. *J Membr Sci*, 433:167–179
- Fane AG, Wang R, Hu MX (2015) Synthetic membranes for water purification: status and future. *Angew Chem Int Ed* 54:3368–86
- Fan L, Xu Y, Zhou X, Chen F, Fu Q (2018) Effect of salt concentration in spinning solution on fiber diameter and mechanical property of electrospun styrene-butadiene-styrene tri-block 29 Electrospun Nanofibrous Membranes for Water Treatment <https://doi.org/10.5772/intechopen.87948> copolymer membrane. *Polymer* 153:61–69
- Fane AG (2018) A grand challenge for membrane desalination: more water, less carbon. *Desalination* 426:155–163
- Fashandi H, Karimi M (2012) Pore formation in polystyrene fiber by superimposing temperature and relative humidity of electrospinning atmosphere. *Polymer* 53:5832–5849
- Feng C, Khulbe KC, Matsuura T, Gopal R, Kaur S, Ramakrishna S, Khayet M (2008) *J Membr Sci* 311:1–6
- Fernando MS, Silva RM, Silva KM (2015) Synthesis, characterization, and application of nano hydroxyapatite and nanocomposite of hydroxyapatite with granular activated carbon for the removal of Pb²⁺ from aqueous solutions. *Appl Surf Sci* 351:95–103
- Fong H (ed) (2006) *Polymeric nanofibers*. American Chemical Society, Washington, DC, pp 1–6
- Fong H, Reneker DH (2000) Electrospinning and the formation of nanofibers. In: Salem D (ed) *Structure formation in polymeric fibers*. Hanser Publishing, Cincinnati, Ohio, pp 269–288

- Fong H, Chun I, Reneker DH (1999) Beaded nanofibers formed during electrospinning. *Polymer* 40:4585–4592
- Formhals A (1934) Process and apparatus for preparing artificial threads. US 1975504
- Gao W, Liang H, Ma J, Han M, Chen ZL, Han ZS et al (2011) Membrane fouling control in ultrafiltration technology for drinking water production: a review. *Desalination* 272:1–8
- Ghaee A, Shariaty-Niassar M, Barzin J, Matsuura T, Ismail AF (2016) Preparation of chitosan/cellulose acetate composite nanofiltration membrane for wastewater treatment. *Desalin Water Treat* 57:14453–14460
- Gopal R, Kaur S, Ma Z, Chan C, Ramakrishna S, Matsuura T (2006) Electrospun nanofibrous filtration membrane. *J Membr Sci* 281:581–586
- Gopal R, Kaur S, Feng CY, Chan C, Ramakrishna S, Tabe S et al (2007) Electrospun nanofibrous polysulfone membranes as pre-filters: particulate removal. *J Membr Sci* 289:210–219
- Gugliuzza A, Drioli E (2013) A review on membrane engineering for innovation in wearable fabrics and protective textiles. *J Membr Sci* 446:350–375
- Gupta N, Kushwaha AK, Chattopadhyaya MC (2011) Adsorption of cobalt (II) from aqueous solution onto hydroxyapatite/zeolite composite. *Adv Mater Lett* 2:309–312
- Hamad AA, Hassouna MS, Shalaby TI, Elkady MF, Abd Elkawi MA, Hamad HA (2020) Electrospun cellulose acetate nanofiber incorporated with hydroxyapatite for removal of heavy metals. *Int J Biol Macromolecules* 151:1299–1313
- Haider A, Haider S, Kang IK (2018) A comprehensive review summarizing the effect of electrospinning parameters and potential applications of nanofibers in biomedical and biotechnology. *Arab J Chem* 11:1165–1188
- Hajra MG, Mehta K, Chase GG (2003) Effects of humidity, temperature, and nanofibers on drop coalescence in glass fiber media. *Sep Purif Technol* 30:79–88
- Hardick O, Stevens B, Bracewell DG (2011) Nanofibre fabrication in a temperature and humidity controlled environment for improved fibre consistency. *J Mater Sci* 46:3890–3898
- He JH, Wu Y, Zuo WW (2005) Critical length of straight jet in electrospinning. *Polymer* 46:12637–12640
- He JH, Wan YQ, Yu JY (2008) Effect of concentration on electrospun polyacrylonitrile (PAN) nanofibers. *Fibers and Polymers*. 9:140–142
- Homaieghar SS, Elbahri M (2012) Novel compaction resistant and ductile nanocomposite nanofibrous microfiltration membranes. *J Colloid Interface Sci* 372:6–15
- Homaieghar SS, Buhr K, Ebert K (2010) Polyethersulfone electrospun nanofibrous composite membrane for liquid filtration. *J Membr Sci* 365:68–77
- Homaieghar S, Koll J, Lilleodden ET, Elbahri M (2012) The solvent induced interfiber adhesion and its influence on the mechanical and filtration properties of polyethersulfone electrospun nanofibrous microfiltration membranes. *Sep Purif Technol* 98:456–463
- Homaieghar S, Zillohu AU, Abdelaziz R, Hedayati MK, Elbahri M (2016) A novel nanohybrid nanofibrous adsorbent for water purification from dye pollutants. *Materials* 9:848
- Homayoni H, Hosseini Ravandi SA, Valizadeh M (2009) Electrospinning of chitosan nanofibers: Processing optimization. *Carbohydr Polym* 77:656–661
- Hou W, Xiao Y, Han G, Lin JY (2019) The applications of polymers in solar cells: a review. *Polymers* 11:143–189
- Huang Y, Miao YE, Liu T (2014) Electrospun fibrous membranes for efficient heavy metal removal. *J Appl Polym Sci* 131:40864–40876
- Huebner AL, Chu HN (1971) Instability and breakup of charged liquid jets. *J Fluid Mech* 49:361–372
- Iwamoto S, Nakagaito AN, Yano H (2007) Nano-fibrillation of pulp fibers for the processing of transparent nanocomposites. *Appl Phys A* 89:461–466
- Jang W, Yun J, Seo Y, Byun H, Hou J, Kim JH (2020) Mixed dye removal efficiency of Electrospun Polyacrylonitrile-graphene oxide composite membranes. *Polymers (Basel)*. 12(9):. Open Access
- Jarusuwannapoom T, Hongrojjanawiwat W, Jitjaicham S, Wannatong L, Nithitanakul M, Pattamaprom C et al (2005) Effect of solvents on electro-spinnability of polystyrene solutions and morphological appearance of resulting electrospun polystyrene fibers. *Eur Polymer J* 41:409–421

- Jia L, Qin XH (2013) The effect of different surfactants on the electrospinning poly(vinyl alcohol) (PVA) nanofibers. *J Therm Anal Calorim* 112:595–605
- Jiang S, Chen Y, Duan G, Mei C, Greiner A, Agarwal S (2018) Electrospun nanofiber reinforced composites: a 26, advances in membrane technologies review. *Polym Chem* 9:2685–2720
- Jung JW, Lee CL, Yu S, Kim ID (2016) Electrospun nanofibers as a platform for advanced secondary batteries: a comprehensive review. *J Mater Chem A* 4:703–750
- Kaur S, Sundarrajan S, Rana D, Matsuura T, Ramakrishna S (2012) Influence of electrospun fiber size on the separation efficiency of thin film nanofiltration composite membrane. *J Membr Sci* 392–393:101–111
- Kenry LCT (2017) Nanofiber technology: Current status and emerging developments. *Prog Polym Sci* 70:1–17
- Khayet M, Garc'ia-Payo MC, Garc'ia-Fernandez L, Contreras-Mart'inez J (2018) Desalination 426:174–184
- Khulbe KC, Matsuura T (2019) Art to use electrospun nanofiber/nanofiber based membrane in waste water treatment, chiral separation and desalination. *J Membr Sci Res* 5:100–125
- Kim GT, Lee JS, Shin JH, Ahn YC, Hwang YJ, Shin HS et al (2005) Investigation of pore formation for polystyrene electrospun fiber: Effect of relative humidity. *Korean J Chem Eng* 22:783–788
- Koski A, Shivkumar YS (2004) Effect of molecular weight on fibrous PVA produced by electrospinning. *Mater Lett* 58:493–497
- Kusworo TD, Wibowo AI, Harjanto GD, Yudisthira AD, Iswanto FB (2014) Cellulose acetate membrane with improved perm-selectivity through modification dope composition and solvent evaporation for water softening. *Res J App Sci Eng Techn* 7:3852–3859
- Lee KP, Arnot, TC, Mattia D (2011) A review of reverse osmosis membrane materials for desalination—Development to date and future potential. *J Membr Sci* 370(1–2), pp 1–22.
- Liao Y, Wang R, Tian M, Qiu C, Fane AG (2013) Fabrication of polyvinylidene fluoride (PVDF) nanofiber membranes by electrospinning for direct contact membrane distillation. *J Membr Sci* 425–426:30–39
- Liao Y, Tian M, Wang R (2017) A high-performance and robust membrane with switchable super-wettability for oil/water separation under ultralow pressure. *J Membr Sci* 543:123–132
- Liao Y, Loh C-H, Tian M, Wang R, Fane AG (2018a) Progress in electrospun polymeric nanofibrous membranes for water treatment: fabrication, modification and applications. *Prog Polym Sci* 77:69–94
- Liao Y, Loh C-H, Tian M, Wang R, Fane AG (2018b) Progress in electrospun polymeric nanofibrous membranes for water treatment: Fabrication, modification and applications. *Prog Polym Sci* 77:69–94
- Liu Y, He JH, Yu JY, Zeng HM (2008) Controlling numbers and sizes of beads in electrospun nanofibers. *Polym Int* 57:632–636
- Liu RL, Tang CY, Zhao JY, Liu HQ (2015) Electrospun membranes of nanoporous structure cellulose acetate and its adsorptive behaviors using copper (II) as models. *Desalin Water Treat* 56:1768–1775
- Ma H, Yoon K, Rong L, Mao Y, Mo Z, Fang D et al (2010) High-flux thin-film nanofibrous composite ultrafiltration membranes containing cellulose barrier layer. *J Mater Chem* 20:4692–4704
- Ma Y, Zhang B, Ma H, Yu M, Li L, Li J (2016) Polyethylenimine nanofibrous adsorbent for highly effective removal of anionic dyes from aqueous solution. *Sci China Mater* 59:38. Open Access
- Macossay J, Marruffo A, Rincon R, Eubanks T, Kuang A (2007) Effect of needle diameter on nanofiber diameter and thermal properties of electrospun poly (methyl methacrylate). *Polym Adv Technol* 18:180–183
- Mit-uppatham C, Nithitanakul M, Supaphol P (2004) Ultrafine electrospun polyamide-6 fibers: Effect of solution conditions on morphology and average fiber diameter. *Macromol Chem Phys* 205:2327–2338

- Mo XM, Xu CY, Kotaki M, Ramakrishna S (2004) Electrospun P(LLA-CL) nanofiber: a biomimetic extracellular matrix for smooth muscle cell and endothelial cell proliferation. *Biomaterials* 25:1883–1890
- Mohammad AW, Teow YH, Ang WL, Chung YT, Oatley-Radcliffe DL, Hilal N (2015) Nanofiltration membranes review: recent advances and future prospects. *Desalination* 356:226–254
- Montgomery MA, Elimelech M (2007) Water and sanitation in developing countries including health in the equation. *Environ Sci Technol* 41:17–24
- Morton WJ (1902) Method of dispersing fluids. US 706691
- Noruzi M (2016) Electrospun nanofibers in agriculture and the food industry: a review. *J Sci Food Agr* 96:4663–4678
- Obaid M, Tolba GMK, Motlak M, Fadali OA, Khalil KA, Almajid AA et al (2015) Effective polysulfone-amorphous SiO₂ NPs electrospun nanofiber membrane for high flux oil/water separation. *Chem Eng J* 279:631–638
- Park S, Park K, Yoon H, Son J, Min T, Kim G (2007) Apparatus for preparing electrospun nanofibers: designing an electrospinning process for nanofiber fabrication. *Polym Int* 56:1361–1366
- Pelipenko J, Kristl J, Jankovic B, Baumgartner S, Kocbek P (2013) The impact of relative humidity during electrospinning on the morphology and mechanical properties of nanofibers. *Int J Pharm* 456:125–134
- Persano L, Camposeo A, Tekmen C, Pisignano D (2013) Industrial upscaling of electrospinning and applications of polymer nanofibers: a review. *Macromol Mater Eng* 298:504–520
- Qin XH, Yang EL, Li N, Wang SY (2007) Effect of different salts on electrospinning of polyacrylonitrile (PAN) polymer solution. *J Appl Polym Sci* 103:3865–3870
- Ramakrishna S, Shirazi MMA (2015) Electrospun membranes: next generation membranes for desalination and water/wastewater treatment. *J Membr Sci Res* 1:46–47
- Ray SS, Chen SS, Li CW, Nguyen NC, Nguyen HT (2016) A comprehensive review: Electrospinning technique for fabrication and surface modification of membranes for water treatment application. *RSC Adv* 6:85495–85514
- Reneker DH, Yarin AL (2008) Electrospinning jets and polymer nanofibers. *Polymer* 49:2387–2425
- Reneker DH, Yarin AL, Fong H, Koombhongse S (2000) Bending instability of electrically charged liquid jets of polymer solutions in electrospinning. *J Appl Phys* 87:4531–4547
- Reneker DH, Kataphinan W, Theron A, Zussman E, Yarin AL (2002) Nanofiber garlands of polycaprolactone by electrospinning. *Polymer* 43:6785–6794
- Reneker DH, Fong H (2006) Polymeric nanofibers: Introduction. in ACS Symposium Series; American Chemical Society: Washington, DC
- Sainudeen SS, Asok LB, Varghese A, Sreekumaran Nair A, Krishnan G (2017) Surfactant-driven direct synthesis of a hierarchical hollow MgO nanofibernanoparticle composite by electrospinning. *RSC Adv* 7:35160–35168
- Sarbatly R, Krishnaiah D, Kamin Z (2016) A review of polymer nanofibers by electrospinning and their application in oil-water separation for cleaning up marine oil spills. *Mar Pollut Bull* 106:8–16
- Shang Y, Si Y, Raza A, Yang L, Mao X, Ding B et al (2012) An in situ polymerization approach for the synthesis of superhydrophobic and superoleophilic nanofibrous membranes for oil-water separation. *Nanoscale* 4:7847–7854
- Shawon J, Sung C (2004) Electrospinning of polycarbonate nanofibers with solvent mixtures THF and DMF. *J Mater Sci* 39:4605–4613
- Shin C, Chase GG (2004) Water-in-oil coalescence in micro-nanofiber composite filters. *AIChE J* 50:343–350
- Shin C, Chase GG (2006) Separation of water-in-oil emulsions using glass fiber media augmented with polymer nanofibers. *J Disper Sci Technol* 27:517–522
- Shin YM, Hohman MM, Brenner MP, Rutledge GC (2001a) Experimental characterization of electrospinning: the electrically forced jet and instabilities. *Polymer* 42:09955–09967

- Shin YM, Hohman MM, Brenner MP, Rutledge GC (2001b) Electrospinning: a whipping fluid jet generates submicron polymer fibers. *Appl Phys Lett* 78:1149–1151
- Shin C, Chase GG, Reneker DH (2005) The effect of nanofibers on liquid–liquid coalescence filter performance. *AIChE J* 51:3109–3113
- Son WK, Youk JH, Lee TS, Park WH (2004) The effects of solution properties and polyelectrolyte on electrospinning of ultrafine poly(ethylene oxide) fibers. *Polymer* 45:2959–2966
- Subramanian S, Seeram R (2013) New directions in nanofiltration applications—are nanofibers the right materials as membranes in desalination?. *Desalination*, 308, pp198–208.
- Sutherland K (2008) Developments in filtration: what is nanofiltration. *Filtr Separat* 45:32–35
- Tan SH, Inai R, Kotaki M, Ramakrishna S (2005) Systematic parameter study for ultra-fine fiber fabrication via electrospinning process. *Polymer* 46:6128–6134
- Tang Z, Wei J, Yung L, Ji B, Ma H, Qiu C et al (2009) UV-cured poly(vinyl alcohol) ultrafiltration nanofibrous membrane based on electrospun nanofiber scaffolds. *J Membr Sci* 328:1–5
- Taylor G (1964) Disintegration of water drops in an electric field. *Proc R Soc Lond Ser A* 280:383–397
- Taylor G (1969) Electrically driven jets. *Proc R Soc Lond Ser A* 313:453–475
- Teychene B, Collet G, Gallard H, Croue JP (2013) A comparative study of boron and arsenic (III) rejection from brackish water by reverse osmosis membranes. *Desalination* 310:109–114
- Thom NT, Thanh DTM, Nam PT, Phuong NT, Buess-Herman C, Adsorption behavior of Cd²⁺ ions using hydroxyapatite (HAP) powder. *Green Process Synthesis*. <https://doi.org/10.1515/gps-2018-0031>
- Uyar T, Besenbacher F (2008) Electrospinning of uniform polystyrene fibers: the effect of solvent conductivity. *Polymer* 49:5336–5343
- Wang XL, Zhang C, Ouyang P (2002) The possibility of separating saccharides from a NaCl solution by using nanofiltration in diafiltration mode. *J Membr Sci* 204:271–281
- Wang X, Fang D, Yoon K, Hsiao BS, Chu B (2006) High performance ultrafiltration composite membranes based on poly(vinyl alcohol) hydrogel coating on crosslinked nanofibrous poly(vinyl alcohol) scaffold. *J Membr Sci* 278:261–268
- Wang R, Liu Y, Li B, Hsiao BS, Chu B (2012) Electrospun nanofibrous membranes for high flux microfiltration. *J Membr Sci* 392–393:167–174
- Wannatong L, Sirivat A, Supaphol P (2004) Effects of solvents on electrospun polymeric fibers: preliminary study on polystyrene. *Polym Int* 53:1851–1859
- Warsinger DM, Chakraborty S, Tow EM, Plumlee MH, Bellona C, Loutatidou S et al (2018) A review of polymeric membranes and processes for potable water reuse. *Prog Polym Sci* 81:209–237
- Xu R, Jia M, Zhang Y, Li F (2012) Sorption of malachite green on vinyl-modified mesoporous poly(acrylic acid)/SiO₂ composite nanofiber membranes. *Microporous Mesoporous Mater* 149:111
- Yang J, Kubota F, Baba Y, Kamiya N, Goto M (2014) Application of cellulose acetate to the selective adsorption and recovery of Au (III). *Carbohydr Polym* 111:768–774
- Yang L, Wei Z, Zhong W, Cui J, Wei W (2016) Modifying hydroxyapatite nanoparticles with humic acid for highly efficient removal of Cu (II) from aqueous solution. *Colloids Surf A* 490:9–21
- Yang Z, Ma XH, Tang CY (2018) Recent development of novel membranes for desalination. *Desalination* 434:37–59
- Yarin AL, Koombhongse S, Reneker DH (2001) Bending instability in electrospinning of nanofibers. *J Appl Phys* 89:3018–3026
- Yoon K, Kim K, Wang X, Fang D, Hsiao BS, Chu B (2006) High flux ultrafiltration membranes based on electrospun nanofibrous PAN scaffolds and chitosan coating. *Polymer* 47:2434–2441
- Yoon K, Hsiao BS, Chu B (2009a) Formation of functional polyethersulfone electrospun membrane for water purification by mixed solvent and oxidation processes. *Polymer* 50:2893–2899
- Yoon K, Hsiao BS, Chu B (2009b) High flux nanofiltration membranes based on interfacially polymerized polyamide barrier layer on polyacrylonitrile nanofibrous scaffolds. *J Membr Sci* 326:484–492

- Yoon K, Hsiao BS, Chu B (2009c) High flux ultrafiltration nanofibrous membranes based on polyacrylonitrile electrospun scaffolds and crosslinked polyvinyl alcohol coating. *J Membr Sci* 338:145–152
- Yordem OS, Papila M, Menceloglu YZ (2008) Effects of electrospinning parameters on polyacrylonitrile nanofiber diameter: An investigation by response surface methodology. *Mater Des* 29:34–44
- Yu Y, Ma R, Yan S, Fang J (2018) Preparation of multi-layer nylon-6 nanofibrous membranes by electrospinning and hot pressing methods for dye filtration. *RSC Adv* 8:12173. Open Access
- Zaher A, El Rouby WMA, Barakat NAM (2020) Influences of tungsten incorporation, morphology and calcination temperature on the electrocatalytic activity of Ni/C nanostructures toward urea elimination from wastewaters. *Int J Hydrogen Energy* 45(15):8082–8093
- Zargham S, Bazgir S, Tavakoli A, Rashidi AS, Damerchely R (2012) The effect of flow rate on morphology and deposition area of electrospun nylon 6 nanofiber. *J Eng Fibers Fabr* 7:42–49
- Zhang C, Yuan X, Wu L, Han Y, Sheng J (2005) Study on morphology of electrospun poly(vinyl alcohol) mats. *Eur Polymer J* 41:423–432
- Zhang S, Shim WS, Kim J (2009) Design of ultra-fine nonwovens via electrospinning of nylon 6: Spinning parameters and filtration efficiency. *28 Adv Membr Technol Mater Design* 30:3659–3666
- Zhao G, Zhang X, Lu TJ, Xu F (2015) Recent advances in electrospun nanofibrous scaffolds for cardiac tissue engineering. *Adv Func Mater* 25:5726–5738
- Zhmayev E, Cho D, Joo YL (2010) Nanofibers from gas-assisted polymer melt electrospinning. *Polymer* 51:4140–4144
- Zhou W, He J, Cui S, Gao W (2011) Preparation of electrospun silk fibroin/cellulose acetate blend nanofibers and their applications to heavy metal ions adsorption. *Fibers Polym.* 12:431–437

Biosorbents in Industrial Wastewater Treatment



Ali Nematollahzadeh and Zahra Vaseghi

Abstract Pollution resulting from industrial wastewater imposes a significant threat to human life and the environment. Adsorption is recognized as a suitable tool to overcome the water contamination problem of industrial origin. Nevertheless, high costs of commercial adsorbents like activated carbon led to eco-friendly low-cost natural biosorbents such as plants, microbes (e.g. bacteria, fungi, microalgae), biomaterials (e.g. chitosan, chitin), agricultural wastes, etc. The present chapter covers biosorption as a useful technique for industrial wastewater treatment. Different types of biosorbents and mechanisms of the biosorption process are initially explained. Afterwards, regeneration of biosorbent achieved by desorption is explained, followed by a cost estimation of biosorbents for wastewater treatment. Finally, probable challenges for industrial implementation of biosorption for wastewater treatment and prospects are explained.

1 Introduction

Developments in technology and industrialization have revolutionized the world toward an easier lifestyle but have caused various environmental problems instead. Modernization cannot occur without direct/indirect influence on the environment (Esmaeili et al. 2015; Gonçalves et al. 2017; Kunjirama et al. 2017). The foremost issue drawing the attention of researchers in the 21 century is the water contamination caused by the disposal of industrial effluents into water bodies. Textile industries, Tannery, dye industries, fertilizer industries, pharmaceutical industries, mining industries, etc., are among the important industries reported to produce a huge amount of wastewater. Industrial effluents are mainly composed of a huge amount of hazardous compounds like toxic metals (Pb, Zn, Cd, Co, Cu, As, Hg, etc.), organic contaminants, and microbial contaminants. Also, the presence of dyes and their intermediates, various salts, nitrogen, and phosphorous is confirmed in some types of industrial effluents (Sörme and Lagerkvist 2002; Sun et al. 2020).

A. Nematollahzadeh (✉) · Z. Vaseghi
Department of Chemical Engineering, University of Mohaghegh Ardabili, 179 Ardabil, Iran
e-mail: nematollahzadeha@uma.ac.ir

The United States Environmental Protection Agency (US EPA) has listed the chemicals from different industries which might threaten both humans and the environment. For example, effluents of the oil industry contain considerable amounts of phenol and cobalt (Khraisheh et al. 2020). Hexavalent chromium is applied in industries such as electroplating, stainless steel, dyes, and leather tanneries is also introduced by the US EPA as one of the seventeen chemicals threatening humans (Jobby et al. 2018). Several standards have been applied to solve the problems raised by the excessive amount of water pollutants that endanger human health. For instance, in the case of heavy metals, the World Health Organization (WHO) has specified guideline values as well as the maximum permitted level of these substances in the European Union (EU) and the USA (US EPA) (Table 1).

Disposal of industrial wastewater into water bodies without undergoing proper treatment is dangerous for human health and the whole ecosystem. It may cause several deficiencies in the human body, such as carcinogenic properties, skin irritation, poor eyesight, neurotoxicity, genotoxicity, breathing difficulty, etc., for human beings and lead to degradation of the ecosystem (Saha et al. 2019). Therefore, industrial wastewater treatment containing compounds with complicated and complex

Table 1 Sources of heavy metals and their drinking water standard levels (Calderón et al. 2020)

Heavy metal	Anthropogenic sources	WHO guidelines ($\mu\text{g/L}^{-1}$)	Maximum permitted level for drinking water ($\mu\text{g/L}^{-1}$)	
			EC	USEPA
Arsenic	Glass and electronics production	10	10	10
Cadmium	Batteries and paints, steel and plastic industries, metal refineries, corroded galvanized pipes	3	5	5
Chromium	Steel and pulp mills, tanneries	50	50	100
Copper	Corroded interior copper plumbing systems	2000	2000	1300
Lead	Lead-acid batteries, solder, alloys, corroded plumbing systems	10	10	15
Mercury	Refineries and factories, runoff from landfills and agriculture, electrical appliances	6	1	2
Nickel	Stainless steel and nickel alloys production	70	20	–
Selenium	Mines and petroleum refineries	40	10	50

structures is substantially urgent (Li et al. 2020; Karri et al. 2021; Dehghani et al. 2021).

Currently, complete treatment of wastewater is done using physical (ion exchange, membrane separation, adsorption, etc.), chemical (chemical oxidation, coagulation/flocculation, etc.), and biological (aerobic/anaerobic reactors, phytoremediation, mycoremediation) processes (Crini and Lichtfouse 2019; Sarode et al. 2019). Although the mentioned methods are useful in treating wastewater, they have their limitations. The common problems with these methods are the persistence of the applied chemicals in the treated water and the feasibility of reaction between the added chemicals leading to the generation of secondary products with unknown influence on human beings (Bhattacharjee et al. 2020). For example, oxidants such as O_3 , Cl_2 , ClO_2 , H_2O_2 , and $KMnO_4$ are used in chemical oxidation. Although this method is advantageous in terms of integration of physicochemical processes, being facile, efficient, and on-site formation of ozone, it has some drawbacks like requirement of chemicals, problems associated with oxidants (e.g. production, transport, and management), necessity for pretreatment, and dependence of process efficiency on the type of oxidant applied. Moreover, involvement of non-reusable chemicals such as coagulants, flocculants, etc. in the coagulation/flocculation method is considered as the main disadvantage of this method (Crini and Lichtfouse 2019). Adsorption is the increasingly being used technique for the treatment of wastewater owing to low cost, high removal efficiency, manageability, ability to remove different types of contaminants, and ease of regeneration (Yusof et al. 2020; Koduru et al. 2019; Putro et al. 2017; Mehmood et al. 2021; Khan et al. 2021; Ahmed et al. 2021). Activated carbon is a famous adsorbent used to remove toxic compounds from wastewater in the adsorption process (Saha et al. 2019). Due to its porous structure, high surface area, easy operation, sensitivity to toxic compounds, and high efficiency, activated carbon was selected as the first-choice adsorbent in adsorption researches for wastewater treatment (Saraswat et al. 2020; Dehghani et al. 2021; Karri and Sahu 2018). Nevertheless, the drawbacks such as high costs and limited reusability have persuaded the researchers to work on other adsorbents, which are more environmentally friendly and cost efficient (Saraswat et al. 2020; Saha et al. 2019).

Limitations with activated carbon and environmental considerations led to the development of alternative treatment approaches based on green chemistry principles, emphasising minimizing contamination by maximizing the use of biodegradable and naturally available resources. The use of such approaches in wastewater treatment is in good compliance with sustainability. Biosorption has come into existence for sustainable wastewater treatment by using different types of biomass (Bhattacharjee, Dutta, and Saxena 2020). Dead or alive microorganisms and biological substances have been used since 1980 for the treatment of wastewater contaminated by heavy metals and dyes (Atar et al. 2008; Çolak et al. 2009). Biosorption can be applied for heavy metals removal (Papirio et al. 2017), dyes (Mishra et al. 2020), pesticides (ul Haq et al. 2021), phenolic compounds (Mallek et al. 2018), etc., from wastewater. Up to the present, various agro-industrial and food wastes (chitosan, sugarcane bagasse, cocoa shell, sawdust, mungbean husk, rice husk, straw, coconut waste, coffee waste,

etc.), plant materials, and microbes (algae, fungi, bacteria) have been utilized successfully as biosorbents for the treatment of wastewater (Mella et al. 2017; Nazir et al. 2019; Sahu et al. 2019).

The chapter covers biosorbents in industrial wastewater treatment. It aims at providing a good understanding of the mechanism of wastewater treatment using different types of naturally occurring biosorbents. Also, the regeneration of biosorbents, which is the foremost challenge of a good treatment procedure, is discussed in detail. To continue, costs of the treatment process needed to determine the economic feasibility of the operation were evaluated. Finally, challenges to perform the projects related to the use of biosorbents in wastewater treatment on an industrial scale were explained and discussed, while the outlook for the future of this approach was clarified.

2 Biosorption

Biosorption is defined as the capability of biological substances to accumulate toxic materials from wastewater (Fard et al. 2011). Biosorption is a physicochemical process that occurs in natural biomasses, leading to the passive binding of cellular constituents with the contaminants through biological, physical, and chemical mechanisms resulting in industrial wastewater treatment. The process has long been recognized but has appeared as an inexpensive, environmentally safe method for wastewater treatment during recent decades (Ubando et al. 2021; Eletta and Ighalo 2019; Jobby et al. 2018).

2.1 *Biosorption History*

The ability to live microorganisms for metal uptake from aqueous solutions was known during the eighteenth and nineteenth centuries. But it was only during the twentieth century that the ability of some living/non-living microorganisms for metal removal leading to the elimination of pollutants and their subsequent regeneration was studied by different researchers (Modak and Natarajan 1995). However, the use of dead or live microorganisms is mechanistically different. The term bioaccumulation is usually used for the live biomass, while adsorption by dead microorganisms is typically called biosorption (de Freitas et al. 2019).

Wutrich was the first one who carried out a well-organized study in 1892 reporting the interaction between fungal spores and metals. Later in 1902, the first research study on the biosorption of metals was published (Muraleedharan et al. 1991). Sewage and wastewater treatment were among the earliest technological applications of the biosorption process (Ullrich and Smith 1951). The first patent (specification number GB 1,324,358) was granted in 1973 to Mills and Sanderson for the biosorption apparatus they have designed and used for the treatment of sewage (de Freitas et al.

2019). Since then, scientists and researchers worldwide have shown different attitudes toward the biosorption process. For example, regarding heavy metals, scientists of the life sciences have studied the toxicological effects of different concentrations of heavy metals on microorganisms; while, environmental engineers and scientists used this capability of microorganisms to monitor the pollution of water by heavy metals, removal of heavy metals from the wastewaters and their subsequent recovery/regeneration (Muraleedharan et al. 1991).

2.2 *Biosorption in Industrial Wastewater Treatment*

Industrial wastewater should go through a chain of treatment steps before being discharged into water bodies so that the concentration of its pollutants reaches acceptable standards (Shafiq et al. 2018). Since industrial wastewater contains pollutants with various concentrations, its treatment is a rather complex task. Thus, selective removal of specific pollutants from industrial wastewater with high efficiency is challenging. Due to different affinities of the contaminants toward the adsorbent's active sites, which rises from different electronegativity, different ionic strength, etc., various adsorptive behaviors of pollutants may be observed.

Although biosorption could be used for different purposes, its usage is strongly recommended for industrial wastewater treatment based on multitudes of reports regarding the decisive role of this technique in removing pollutants like heavy metals and some organic materials from industrial wastewater (Crini 2006). For example, in the research conducted by Adenuga et al. (2019), simultaneous removal of metal ions including Pb(II), Cd(II), and Zn(II) from industrial wastewater using the Spent Seed-cake of *Calophyllum inophyllum* as a sustainable and low-cost biosorbent was investigated. The adsorption capability of the biosorbent was evaluated using the batch adsorption process. Also, carbonization and microwaving the biosorbent resulted in optimum operation at solution pH of 9, dosage of 10 g/L, temperature of 30 °C, and equilibrium time of 60 min. Maximum adsorption capacity for Pb(II), Cd(II) and Zn(II) was calculated as 52.63, 51.28, and 17.99 mg/g, respectively. Real industrial wastewater was tested for the effectiveness of the biosorbent, and it was found that the metal removal percentage was between 55 and 71%. In another study, removal of BOD, COD, Oil & Grease was considered in the derivatives of oil and soap in the effluents of industrial wastewater using a cost-effective environmentally benign biosorbent, namely *Phragmites australis*. Their results demonstrated that biosorption capacity for BOD, COD, and Oil & Grease was maximized at neutral pH. SEM image clarified that the surface texture of the plant converted from being smooth and entire into coarse and irregular after the biosorption process (Fig. 1). Furthermore, *P. australis* exhibited good performance in removing organic pollutants such as BOD, COD, Oil & Grease from the industrial wastewater samples (El Shahawy and Heikal 2018).

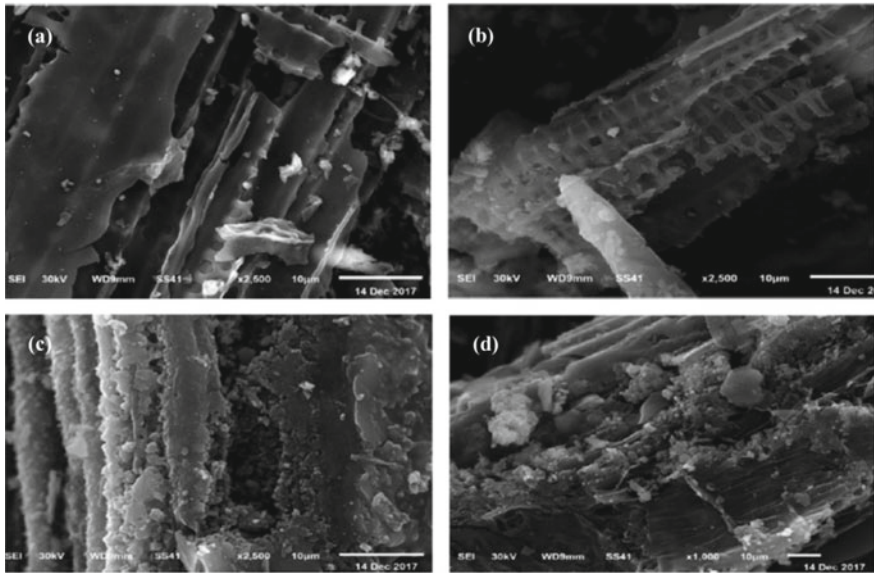


Fig. 1 **a** and **b** SEM images of raw dried *P. australis* (magnification power 2500 ×), **c** and **d** SEM images of dried *P. australis* biomass after adsorption (magnification power 2500 × and 1000 ×) (El Shahawy and Heikal 2018)

3 Types of Biosorbents for Industrial Wastewater Treatment

Adsorbents with biological origins are called biosorbents. Biosorbents usually belong to the family of bacteria, fungi, algae, plant wastes, fruits, active sludge, and biopolymers such as chitosan. Some of the main features of commercial biosorbents include high biosorption capacity, good adsorption kinetics, proper physical properties (size, shape, etc.), cost-effectiveness and availability of biosorbents, facile separation of the biosorbents from the solution, good thermal stability and chemical resistance, strong mechanical properties, and regeneration and reusability of biosorbents (Beni and Esmaeili 2020). Following, different types of biosorbents are classified and explained by giving useful examples.

3.1 Use of Plants as Biosorbents

Biomass obtained from plants is frequently used for decontaminating synthetic and industrial effluents. The cellulosic content of plants has made them strong biosorbents for removing wastewater contaminants. So far, different plant organs like seed, leaf,

root, bark, and peel are used as biosorbents in removing pollutants from wastewater (Jain et al. 2016).

3.1.1 Plant Leaves

Plant leaves are excellent biosorbents as they are cheap, biodegradable, non-toxic, and highly efficient in wastewater treatment (Anastopoulos et al. 2019; Kyzas and Kostoglou 2014). Thus, lots of research was devoted to exploring the role of this organ of plants in removing contaminants from wastewater bodies through the last two decades. Before being utilized as biosorbents, most of the leaves go through some preparation steps, including cleaning, drying, grinding, and sieving. Chemical modification may also be needed in some cases. Modification is usually done by soaking the plant leaves in acid (nitric acid, sulphuric acid, hydrochloric acid, and formic acid) or alkali (sodium hydroxide) for a specific time (often several hours) under stirring. For some plant species, chemical activation and carbonization are done instead of chemical modification to produce activated carbon out of plant leaves. Activation is achieved by chemicals such as zinc chloride, sulphuric acid, and phosphoric acid in a period ranging between 1 and 24 h.

Lots of plant species have been used as biosorbents to decontaminant wastewater from heavy metals, dyes, etc. The removal efficiency of plant leaves to remove heavy metals such as chromium, lead, cadmium, zinc, nickel, and copper was greater than 90%. For example, alkali-modified spent tea leaves were used as cost-effective biosorbents to remove Cu(II) from its containing solution. The pseudo-second-order model well represented adsorption kinetics, and equilibrium data followed Langmuir adsorption isotherm. The maximum removal efficiency was calculated as 96.12% (Ghosh et al. 2015). Removal of other pollutants like dyes, especially methylene blue, was done with approximately 80% efficiency by most leaves obtained from different plant species.

Furthermore, a high adsorption capacity was achieved using plant leaves as biosorbents. Das et al. (2020) used *Butea monosperma* leaf powder to remove methylene blue dye from an aqueous solution. Maximum adsorption (98.70%) was achieved at the adsorbent dosage of 0.5 g L⁻¹, pH value of 8, and contact time of 120 min. In another study, *Ficus palmate* leaves were used as effective plant adsorbents to remove methylene blue. Operating conditions, including initial dye concentration of 15 mg L⁻¹, the adsorbent dosage of 0.45 g, contact time of 80 min, the temperature of 318 K, and neutral pH, led to maximum removal efficiency of 98% (Fiaz et al. 2019).

3.1.2 Plant Seed

Plant seeds have been reported for their ability in serving as potential biosorbents for contaminants elimination from wastewater. The textile industry is a typical example for which the seeds of plants have been used as biosorbents for their treatment. For

example, sunflower seed hull previously treated with alkali was used in the research performed by Oguntimein (2015) for dye removal from the effluent of textile factory (decolorization of the effluent). The Pseudo-second order model conformed well to the kinetic data at all tested dye concentrations. Activation parameters between the sunflower seed hull and the textile dye such as activation energy (8.79 kJ/mol), enthalpy (8.79 kJ/mol), the entropy change (-39.57 kJ/mol/K), and Gibbs free energy (6.27–8.11 kJ/mol) were calculated. In another research, biosorption of cadmium was studied using the seeds of *Alhaji Maurorum*. The seeds went through some preparation steps before being used as adsorbents. They were thoroughly washed with distilled water followed by drying at ambient temperature for 48 h. A grinder then powdered the seeds and sieved to reach the desired particle size. Maximum removal of cadmium (85.5%) occurred at pH 6, adsorption dosage of 20 g/L, and duration of 45 min. Also, the mean adsorption energy determined from the Dubinin-Radushkevitch isotherm algorithm confirmed the physical nature of the biosorption process (Ebrahimi et al. 2015).

Powdered seeds of *Annona crassiflora* (araticum fruit) were used as efficient biosorbents for the adsorption of crystal violet dye as well as simulated textile wastewater. Characterization of biosorbent showed that seeds of araticum had an amorphous nature with irregular and heterogeneous shapes. Maximum removal of crystal violet occurred at pH 7.5 and araticum seed powder dosage of 0.7 g L⁻¹. A maximum biosorption capacity of 300.96 mg g⁻¹ was achieved at 328 K. Also, the efficiency of the biosorbent was confirmed by the 87.8% removal of the dye from simulated textile wastewater (Franco et al. 2020).

Brazilian berry seeds (*Eugenia uniflora*) were also used as cost-effective and eco-friendly biosorbents to effectively treat textile effluents containing methylene blue. For lower methylene blue concentrations, equilibrium reached after 20 min, while 120 min were required to reach the higher concentrations. Meanwhile, kinetic data were well presented by the general and pseudo-second-order models. The biosorbents were also successful in treating two different simulated textile effluent (92.2 and 88.7% removal). The Brazilian berry seeds also served as packing in a fixed-bed column reaching to biosorption capacity of 88.7 mg g⁻¹ within 840 min (Georgin et al. 2020). *Allium Cepa* seed biomass (ASCB) was prepared and used as an effective biosorbent for biosorption of Cr(VI), Cd(II), Cu(II), Zn(II), Pb(II) from aqueous media. Before being applied as biosorbent, the biomass went through some preparation steps such as cleaning (in a granular bed with the flow of deionized water), drying (under natural convection mode for 10 days followed by oven drying for 1 h at 100 °C), and grinding process. FTIR spectrum revealed the hydroxyl group as the source of metal uptake. Maximum adsorption of metal ions was obtained at 4 gL⁻¹ of ASCB, 50 mgL⁻¹ adsorbates, and neutral pH. Maximum removal efficiency under these conditions was determined as high as 99% for Pb(II), Cu(II), while rather lower removal efficiencies were obtained for Zn(II) and Cr(VI) (Fig. 2) (Sheikh et al. 2021).

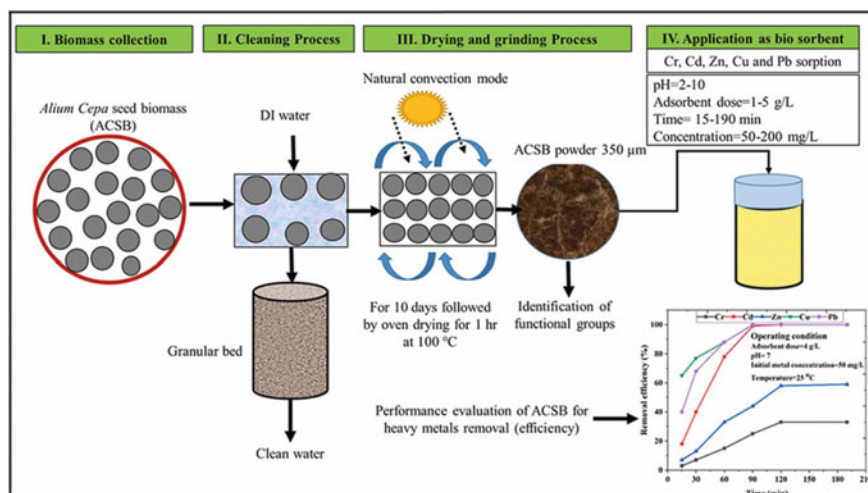


Fig. 2 Schematic of whole biosorption process including biomass preparation and the diagram of removal efficiency for the removal of Cr(VI), Cd(II), Cu(II), Zn(II), Pb(II) using *Allium Cepa* seed biomass (ACSB) (Sheikh et al. 2021)

3.1.3 Plant Root

Plant roots have been used as biosorbents to remove heavy metals, dyes, salinity, etc., from the wastewater. For example, water hyacinth (*Eichhornia crassipes*) roots were used as biosorbents to remove BF-4B red reactive dye from the aqueous solution. Dye removal was conducted with 95% efficiency until the equilibrium time of 110 min was reached. The biosorption kinetic data conformed well to the Pseudo-second order and Elovich models. A maximum biosorption capacity of 43.28 mg g^{-1} was obtained with the biosorption process tending to the Langmuir model (Rigueto et al. 2020). In another study, biosorption of fluoride from water using coconut tree (*Cocos Nucifera* Linn.) was investigated. Equilibrium studies disclosed that the biosorption capacity of coconut roots for fluoride was significantly high and linearly increased with the enhancement of the initial concentration of adsorbate. Kinetic data fitted well to the Pseudo-second order model signifying the chemical nature of the adsorption process. Also, the thermodynamic study confirmed the endothermic and spontaneous nature of the biosorption process ($\Delta H = 12.728 \text{ kJ} \cdot \text{mol}$) (George and Temburkar 2019).

The roots of plants also adsorb heavy metals as biosorbents. Heavy metals including Pb, Cu, Zn, and Cd were removed by the root powder of Long-root *Eichhornia crassipes* from the aqueous media. Analysis of the energy spectrum revealed that the mentioned heavy metals were adsorbed on the biosorbent after their adsorption. The adsorption of metals was investigated in the single-metal and multi-metal systems (competitive adsorption). It was found that in the competitive adsorption, an increase in the concentration of metals led to a significant decline in the adsorption of Zn, Pb, and Cd. Also, the adsorption of every two metals on the plant powder

showed that the involvement of either Cu or Pb in the binary metal group masters the adsorption proficiency of Cd and Zn (Li et al. 2016).

3.1.4 Plant Bark

Plant bark has an excellent absorption capacity for pollutants such as heavy metals, salts, pharmaceuticals, pesticides, etc. However, about two-thirds of the literature regarding biosorption using this plant organ is devoted to heavy metals. Based on the preparation technique, plant barks are subdivided into unmodified biosorbents, pre-modified biosorbents, chemically modified biosorbents, physically modified biosorbents, and bio-based activated carbon. The latter is obtained when the biomaterials (plant barks) are sent into a furnace to go through the carbonization process.

Heavy metals like Cd, Cr, Ni, Pb, and Cu are mostly studied in plant barks' biosorption. The adsorption capacity of plant barks for heavy metals depends upon several factors, including the type of the biomaterial (plant), the method used to modify the biosorbent, type of the heavy metal, temperature, and pH. Dyes studied as pollutants include methylene blue, methyl orange, methyl red, congo red, solar blue, and remazol. Also, pharmaceutical compounds such as ibuprofen, amoxicillin, naproxen, ketoprofen, and diclofenac were among pharmaceutical pollutants being removed so far with certain efficiencies using plant barks. Sorption of plant bark usually fits Langmuir isotherm. Also, the kinetic data generally obeys the Pseudo-second order model. Search into the thermodynamics of the biosorption process utilizing plant barks showed that the process is spontaneous, having a physical nature. Regeneration studies show good potential for these biosorbents, making them excellent biosorbents for industrial applications (Ighalo and Adeniyi 2020).

3.1.5 Plant Peel

In recent years, fruit peel has been investigated for its adsorption ability to eliminate pollutants like heavy metals, dyes, and organic pollutants from industrial wastewater. The most studied fruit peels are orange and banana peels, while Pb and methylene blue biosorption is done with greater removal efficiencies than the rest of the pollutants. Adsorption isotherms usually obey the Langmuir and Freundlich, isotherm models. Like most biosorbents, kinetic data are well represented by the Pseudo-second order model. Thermodynamic studies usually reveal the exothermic nature of the biosorption process using fruit peels which is consistent with the nature of the adsorption process.

Citrullus colocynthis peels were used as adsorbents to remove methylene blue dye from an aqueous solution. Langmuir isotherm followed by Temkin isotherm best fitted to equilibrium data. Maximum adsorption capacity and removal efficiency were found to be 4.48 mg g^{-1} and 91.43%, respectively (Alghamdi and El Mannoubi 2021). In another study, the peels of *Artocarpus Nobilis* exhibited good adsorption ability toward Ni(II) ions. Air-dried particles led to 50% removal when the reaction

mixture was kept at both static and dynamic conditions. After optimizing shaking time, settling time, and process temperature, the removal efficiency increased 71%. Also, it was found that linearized Langmuir isotherm better described equilibrium data compared to the Freundlich model. Further enhancement of removal efficiency up to 93% was achieved at dynamic mode by optimising the packing bed's height and flow rate (Priyantha and Kotabewatta 2019).

Pretreatment of fruit peels enhances their adsorption capacity but influences the total cost of the process, which is definitely of great importance for the scale-up of the process. The use of fruit peels as biosorbents has not been commercialized yet and remains in batch mode. Surface characteristics of fruit peels as natural biomaterials depend on several factors, including location and geological conditions of the source fruit, season, ripening state of the fruit, and its quality. These properties directly affect the biosorption capability of fruit peels, which makes comparisons between similar fruit peels of different origins difficult (Pathak et al. 2015).

3.2 Use of Microbes as Biosorbents

Microbial biosorbents fall into the following category: Bacterial biosorbents, fungal biosorbents, and microalgal biosorbents. Biosorption of pollutants with microbial biosorbents offers some advantages compared to the rest of biosorbents. In the case of metal removal, due to their selectivity in binding to specific metal ions, they possess high metal removal efficiency. Besides, the small size of microorganisms provides a large surface area per volume ratio, which favors the adsorption process. Other advantages include low cost and environmental friendliness of the microbial biosorbent and the feasibility of using dead or live biomass in the biosorption of pollutants from the wastewater (Yu et al. 2020; Vijayaraghavan and Yun 2008).

3.2.1 Bacterial Biosorbents

Bacteria, which are single-cell microbes, are the most abundant microorganisms. Bacterial cells lack membrane-bound organelles and nuclei. Therefore, the cell structure is simpler compared to other organisms. Bacteria can grow under severe conditions. Thus, bacterial biomass is abundantly available. Due to bacterial biomass's distinctive properties like high efficiency and low cost, they can serve as suitable adsorbents. For example, biosorption of heavy metals from wastewater capabilities of bacterial biomass in binding to metals through its functional groups and high biosorption capacity have made them excellent adsorbents. In addition, the reusability of bacterial biomass aids in the cost-effectiveness of the process and minimises the remaining wastes (Priyadarshane and Das 2020). Bacterial biosorbents are mostly used in treating metal/dye-containing wastewaters. Metal removal is extensively done using bacterial biosorbents such as *Bacillus* sp., *Pseudomonas* sp., *Sphaerotilus* sp., *Thiobacillus* sp., *Staphylococcus* sp., *Streptomyces* sp., *Desulfovibrio* sp., and

Corynebacterium sp.; while bacterial species such as *Corynebacterium glutamicum*, *Streptomyces rimosus*, *Bacillus catenulatus*, and *Acidithiobacillus thiooxidans* were mostly involved in the biosorption of dyes (Vijayaraghavan and Yun 2008; Kim et al. 2015; Nguyen et al. 2016).

In bacteria, the sorption ability of biomass could be enhanced by modification methods through enhancement or activation of the binding sites on the surface of bacterial biomass (Suazo-Madrid et al. 2011). The typical pretreatment methods recommended for bacterial biomass are physical, chemical, and biological pretreatment methods.

3.2.2 Fungal Biosorbents

Fungal biosorption is defined as the ability of fungal biomass, especially its cell wall, to accumulate dangerous wastes (pharmaceuticals, heavy metals, and dyes). Fungi offer several advantages in the treatment of wastewater, including being facile, inexpensive, high efficient, and flexible in operation (Legorreta-Castañeda et al. 2020). These groups of microbes are formed as unicellular and multicellular organisms. The latter shows quite different development mechanisms compared to plants and animals due to the formation of long filaments called hyphae (Riquelme et al. 2018). The filaments are like eukaryotic cells and are surrounded by a cell wall composed mainly of glycoproteins, chitin, and glycans. Also, the functional groups responsible for the biosorption process, including carboxyl, amine, and hydroxyl, are present in great amounts in the cell wall (Lo et al. 2014). It is worthy to note that most fungi used in the biosorption process to remove pollutants are non-pathogenic, so they can be used without safety recommendations. Fungal biomass is accessible in great amounts, yielding an abundance of functional groups that can bind to metals, thereby preparing a strong biosorptive agent (Ayele et al. 2021).

Filamentous fungi biomass being recognized as a valuable source for the adsorption of heavy metals greatly threatens human health and the ecosystem. Fungal biomass should satisfy some requirements before being applied as heavy metal biosorbents. For instance, factors such as bioavailability, cost-effectiveness, reusability, and high adsorption capacity are necessary for an efficient biosorption process using these biosorbents with microbial origin. In this sense, effluents from large-scale bioprocess industries such as antibiotic industries, which contain a great amount of filamentous biomass, maybe a great help. Various heavy metals have been removed by fungal biosorbents mainly from the fungal strains of *Aspergillus carbonarius*, *Aspergillus lentulus*, *Aspergillus flavus*, *Aspergillus niger*, *Aspergillus fumigatus*, *Funalia trogii*, *Aspergillus japonicus*, *Lentinus edodes*, *Penicillium chrysogenum*, *Phanerochaete chrysosporium*, *Pleurotus ostreatus*, *Rhizopus arrhizus*, *Rhizopus nigricans*, *Rhizopus oryzae*, and *Trametes versicolor*.

Fungal biosorbents have been applied extensively for the removal of dyes. High resistance and survival under extreme conditions of highly toxic dye contaminants and reusability of the fungal biosorbent after several treatment cycles have made these biosorbents an attractive choice for dye removal. Fungal species such as *Aspergillus*

sp., *Penicillium* sp., *Trametes versicolor*, *Phanerochaete chrysosporium*, and *Funalia trogii* have been used for the removal of a variety of dyes from dye-contaminated effluents.

Phenolic compounds such as phenol, 2-chlorophenol, pentachlorophenol, bisphenol A, benzophenone, 1-naphthalenamine, naphthol, etc., were successfully removed by the adsorption capability of some fungi such as *Anthraco-phyllum discolor*, *Funalia trogii*, *Penicillium oxalicum*, *Phanerochaete chrysosporium*, *Phanerochaete chrysosporium*, and *Trametes versicolor*. However, the biosorption capacity of fungi for phenolic compounds is lower than that of dyes mainly due to the greater molecular weight of dyes than phenolic compounds, as adsorption is directly calculated based on the molecular weight of the adsorbate. Another reason for better adsorption of dye may be high values for solubility and pK_a of phenolic compounds; since enhancement in these factors leads to a significant decline in the adsorption ability of the adsorbate. Other pollutants yet to be removed by fungal biosorbents are known as organic compounds, such as pesticides, humic substances, and pharmaceuticals (Legorreta-Castañeda et al. 2020).

3.2.3 Microalgal Biosorbents

Microalgae are known as photosynthetic microorganisms with the ability to change solar energy into biomass. Microalgae use sunlight as a source of energy to fix CO_2 and produce different biomaterials in turn. The selection of suitable microalgae strain is vital to use these biofactories' capability for wastewater treatment. Those microalgae species able to undergo mixotrophic or chemoheterotrophic metabolism satisfy the requirements for wastewater treatment (Ubando et al. 2021). The metal-binding sites of a microalgae cell are depicted in Fig. 3. When metal accumulates inside the cell, the metal ions are instantly placed in specific organelles and attach to metal-binding ligands like phytochelatin and metallothioneins. Although microalgae are less used to remove contaminants from wastewater than other microbes such as bacteria and fungi, interest in this field has been increasing in the recent decade.

The cell wall in microalgae is usually composed of polysaccharides, glycoproteins, and an external layer composed mainly of chitin in some species. The functional groups present in the microalgae cell wall are responsible for binding to contaminants, especially metals existing in the wastewater. Different laboratory conditions lead to the production of microalgae with various functional groups, which can be utilized for the biosorption of various contaminating agents in wastewater (Escudero et al. 2019). Wastewater treatment using microalgae is preferred over seaweeds. The reason lies in the potential of cultivating microalgae on a large scale and thus reaching a tremendous amount of biomass. Furthermore, wastewater treatment using microalgae can be done simultaneously with other value-added operations like the production of biofuels (Chu and Phang 2019).

Microalgae have been successfully utilized in the biosorption of heavy metals and dyes from wastewater. In the case of heavy metals, *Chlorella*, *chlamydomonas* and

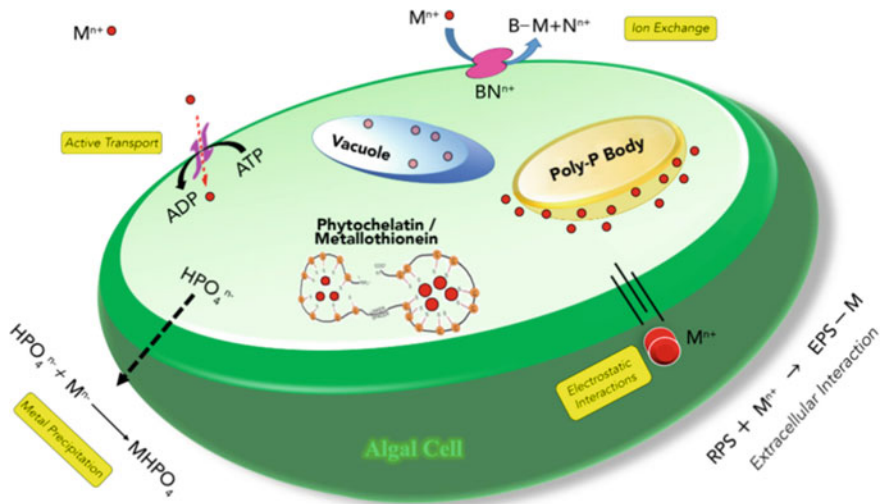


Fig. 3 Binding site of metals in microalgae cell (Chai et al. 2020)

Desmodesmus (green algae), *Phaeodactylum*, *Cyclotella* and *Aulosira* (diatoms), *Spirulina*, *Oscillatoria*, and *Phormidium* (cyanobacteria) have been evaluated for their ability in the adsorption of heavy metals. *Chlorella vulgaris* is the most researched species used as non-living, living, free, or immobilized cells (Kumar et al. 2015). It is worthy to note that various pretreatments (physical or chemical) on microalgae before being used as biosorbents favor the sorption capacity of microalgae by improving cell wall features. Different dyes, especially malachite green and methylene blue, are reported to be removed with the biosorptive performance of various types of microalgae. Studies mostly involve non-living algal biomass with a synthetic dye solution. Nevertheless, some of the reports focus on using living microalgae and cyanobacteria (Chu and Phang 2019).

3.3 Use of Agricultural Wastes as Biosorbents

Agricultural wastes, especially cellulosic materials, show outstanding capacity for biosorption of pollutants from wastewater. Agricultural wastes are mainly composed of hemicellulose, lignin, lipids, proteins, a simple sugar, starch, hydrocarbons, and water. Most agricultural wastes contain various functional groups such as aldehyde, amine, keto groups, etc. Due to their distinct chemical composition, cost-effectiveness, high removal efficiency, availability, simple operation, and regeneration, agricultural wastes are suitable options for wastewater treatment. The use of agricultural wastes as biosorbents may be helpful in two ways: first, it can help solve

environmental issues concerning the use of chemical adsorbents; second, it can help reduce the operation costs (Mo et al. 2018).

3.3.1 Rice Waste

Rice is the seed of the grass species *Oryza sativa* grown extensively worldwide. Owing to millions of tones of rice world production industry, numerous by-products of rice like rice husk, rice hull, and rice bran are produced. Bažant and Estenssoro (1979) have used alkali-modified rice husk to eliminate copper from its containing solution. Experimental results showed that approximately 90–98% copper was removed using the modified rice husk. In another study, the ability of rice straw, rice husk, and rice bran was evaluated in the biosorption of Pb(II) ions both from its containing solution and wastewater produced from the battery industry. The Pseudo-second order model well represented kinetic data. However, rice husk was an exception that was best fitted to the intraparticle diffusion model. Biosorption capacity for rice straw, rice bran, and rice husk were calculated as 24.17, 20.54, and 21.38 mg g⁻¹, respectively (Singha and Das 2012).

Dyes are other pollutants to be adsorbed onto rice wastes. For instance, several studies have studied the biosorption of methylene blue using rice husk. Ahmad et al. (2019) studied the influence of sorption parameters, including initial dye concentration (10–50 mg L⁻¹), contact time (10–120 min), pH (2–10), and adsorbate dosage (0.05–0.25 g) on the removal efficiency of methylene blue. Acid Yellow 17 dye left from the textile and paper industries is toxic to human health and the environment. This dye was removed by the biosorption ability of rice husk with the removal efficiency of 97.97% at the optimum operating conditions when 0.7 g of biosorbent was present (Patil et al. 2015). Other compounds removed by rice wastes include herbicides, phenolic (mono aromatic), and poly aromatic compounds. As expected, pretreatments (chemical, physical, and biological) positively impact the biosorption ability of rice waste (Shamsollahi and Partovinia 2019).

3.3.2 Tea and Coffee Waste

Coffee and tea are the most popular beverages in the world. Tea and coffee wastes are the product of their manufacturing companies and cafeterias. Cellulose, hemicellulose, lignin, condensed tannins, and functional groups including carboxylate, aromatic carboxylate, phenolic, hydroxyl, and oxyl groups make the chemical composition of tea leaves. Generally, removal of contaminants present in the wastewater is done with the mentioned functional groups (Amarasinghe and Williams 2007). Çelebi et al. (2020) examined the adsorption ability of tea wastes in the removal of lead (II), cadmium (II), nickel (II), and zinc (II). Study of the parameters such as pH (2.0–6.0), adsorbent amount (0.1–5.0 g), and contact time (1–150 min) revealed that the removal efficiency of heavy metals was inversely affected by pH; while increase in other parameters resulted in linear enhancement of removal efficiency. Maximum

adsorption capacity for Pb, Zn, Ni, and Cd at the optimum pH value (between 4.0 and 5.0) was found to be 1.20, 1.46, 1.16, and 2.47 mg g⁻¹. In another study, tea waste was utilized for methylene blue dye removal from its containing solution. The adsorption process is composed of two stages. The first stage included adsorption with a fast trend, while a rather slow adsorption process was in progress throughout the second stage. Based on Langmuir isotherm, the maximum adsorption capacity of the tea waste was found to be 113.15 mg g⁻¹ (Liu et al. 2018).

The coffee tree belongs to the family Rubiaceae. Two plant species, namely *Coffea Arabica* (Arabica) and *Coffea canephora* (Robusta), supply 75 and 25% of the world's total coffee production. The main by-products from the coffee industry include spent coffee grounds, the coffee silverskin, and the coffee husks. Microscopic tests confirm the presence of fibrous tissues in the surface layer of the coffee wastes. These fibrous tissues are mainly composed of cellulose and hemicellulose. Glucose has the greatest amount among the monosaccharides present in the coffee wastes. Proteins and extractives also constitute a major part of coffee wastes (Anastopoulos et al. 2017). The Biosorption ability of different types of coffee wastes is proved in literature. For example, coffee husk biomass was used for heavy metal removal from wastewater. Coffee waste was used to produce biochar, which was modified with sodium hydroxide after that to create functional groups on the surface of the biosorbent and enhance the specific surface area. The maximum adsorption capacity for Cd and Pd was 116.3 and 139.5 mg g⁻¹, respectively. The produced biochar removed 89.6% of Pb (II) and 81.5% of Cd (II) from wastewater (thi Quyen et al. 2021). Ahsan et al. (2018) primarily used a facile method for the synthesis of sulfonated coffee waste and then utilized the produced biosorbent for the adsorption of bisphenol A (endocrine-disrupting chemical) and sulfamethoxazole (antibiotic) from the solution. Biosorption capacity for bisphenol A and sulfamethoxazole biosorption was calculated as 271 and 256 mg g⁻¹. Efficient biosorption of both contaminants is provided by the formation of π - π interaction and electrostatic interaction between sulfonated coffee waste and the contaminants.

3.3.3 Sawdust

Sawdust is a waste mainly produced in the paper, carpentry, and furniture industries (Dolatabadi et al. 2018). Wood is generally composed of hemicellulose (20–30%), lignin (20–30%), and extractives (1–5.5%). However, the exact composition strongly depends on the specific tree species from which the wood is obtained. Different bonding exists among hemicellulose, cellulose, and lignin. The three compounds are bound with hydrogen bonding primarily, while a chemical bonding exists between hemicellulose and lignin. This bonding results in the involvement of a small number of carbohydrates in the lignin structure. Various functional groups, including hydroxyl, carboxyl, amid, and phenolic groups, are present in the chemical structure of sawdust. These functional groups pose the adsorptive ability to sawdust

and provide binding to pollutants, especially heavy metals (Ouafi et al. 2017). Typically, sawdust treatment with acid or alkali is carried out to enhance its adsorption capacity.

During the last decades, sawdust has been utilized as an efficient precursor to produce activated carbon with improved characteristics compared to the typical activated carbon, such as higher porosity, larger surface area, and more functional groups. The produced activated carbon is used for various applications like heavy metal removal, dye removal, etc. Various types of water-soluble dyes, such as methylene blue, methyl violet, congo red, malachite green, etc., are reported to be removed by the sawdust-derived activated carbon. Akhouairi et al. (2019) used the sawdust-derived activated carbon as a natural, widespread, and low-cost biosorbent for Eriochrome Black T (EBT) adsorption from aqueous media its adsorption onto sawdust. A maximum adsorption capacity of 40.96 mg g^{-1} corresponding to 80% removal was obtained at pH 4. In another study, sulfonic acid incorporated pine sawdust (APSD) was used as a cost-efficient adsorbent for the batch removal of Maxilon Red GRL (MR GRL) from a synthetic dye solution. Under the optimal conditions (pH value in the range between 5.7 and 6.0, the temperature of 298 K, dye concentration of 250 mg L^{-1} , and adsorbent dosage of 8 g L^{-1} maximum MR GRL removal of 99.35% was obtained within 180 min (Şentürk and Yıldız 2020).

Sawdust was also applied for the uptake and removal of heavy metal ions. Literature on the adsorption ability of sawdust is available in great number. For example, Alhumaimess et al. (2019) firstly enhanced the uptake capacity of metal ions by sawdust through grafting phosphorus oxychloride over the surface of raw sawdust. The resulting biosorbent was used to remove Cd(II), Cr(III), and Pb(II) metal ions from an aqueous medium with a maximum adsorption capacity of 244.3, 325, and 217 mg g^{-1} . Sawdust-derived biochar was used for the treatment of gold tailings wastewater. Using the biosorbent, concentration of CN^- , Cr^{3+} , Fe^{3+} , Zn^{2+} , Ni^{3+} , Pb^{2+} , Mn^{2+} , and Cu^{2+} was reduced to 0.76, 0.74, 0.75, 0.83, 0.85 and 0.87, respectively. While the reduced concentrations for Cr^{3+} , Fe^{2+} , Zn^{2+} , Mn^{2+} , and Cu^{2+} met the WHO guidelines, More retention time and biochar dosage were needed to satisfy WHO guidelines of CN^- , Ni^{3+} , and Pb^{2+} (Manyuchi et al. 2021).

3.3.4 Sugarcane Bagasse

Ease of access and availability are important factors that determine whether an agro-based waste product is suitable to be used as a biosorbent or not. Sugarcane bagasse, the main agro-waste from the sugar industry being utilized worldwide, seems reasonably eligible for this purpose. Sugarcane bagasse was found to be capable of adsorption of heavy metals in wastewater treatment. Improvement of biosorption ability of this agro-waste for heavy metal removal could be achieved considerably by its binding into functional groups such as carboxylic, amin, etc., or by removing soluble organic compounds (Pereira et al. 2010; Martín-Lara et al. 2010; Karri et al. 2020; Lingamdinne et al. 2020; Kaur et al. 2020). Removal of dyes was also conducted using sugarcane bagasse. In research performed by Gusmão et al. (2012), removal

of methylene blue as the most common dye in the textile and paper industries was achieved utilizing succinylated sugarcane bagasse. The negative charge of carboxylate function in the chemical structure of sugarcane bagasse interacts with cationic dyes. In this sense, succinic anhydride and sodium bicarbonate solutions could be used to improve the functionality. FTIR spectroscopy revealed that carboxylate group and symmetric stretching of ester group were responsible for dye biosorption.

The Biosorption ability of sugarcane bagasse is also observed in removing petroleum, phenolic compounds, and organic nutrients. Like other agro-waste products, modification of sugarcane bagasse conducted by different methods (mechanical, chemical, magnetic, immobilization), enhances its biosorption capacity noticeably (Sarker et al. 2017). Kamel et al. (2012) modified sugarcane bagasse by different methods (chemical bleaching, acrylonitrile grafting, and thermal charring) to remove phenol. They found that the maximum potential of each of these methods for modifying bagasse (186.50, 160.64, and 195.00 mg L⁻¹) is achieved when the initial concentration of adsorbate is high (500 ppm).

3.4 Use of Other Biomaterials as Biosorbents

3.4.1 Chitin and Chitosan

Chitin, chitosan, and their derivatives are natural, low-cost biopolymers available in abundance. During recent years, these biopolymers have been used extensively to eliminate toxic contaminants from wastewater due to their nontoxicity, biodegradability, biocompatibility, and bioactivity (Xiong Chang et al. 2021; Dehghani et al. 2020a, b). In addition, the excellent physical and chemical performance of chitin and chitosan has made them excellent candidates to serve as metal chelating agents for the biosorption of toxic metals present in the wastewaters (Sarode et al. 2019; Saha et al. 2019).

By boiling chitin in potassium hydroxide, acid-soluble chitosan would be synthesized. Chitin, the second most plentiful polysaccharide worldwide, is usually extracted from the exoskeleton of aquatic organisms like lobster, crayfish, prawns, shrimp, and crab. The chemical composition of chitin and chitosan is demonstrated in Fig. 4. Chitosan is not soluble in water, alkaline solutions, and organic solvents due to hydrogen bonding among its molecules. This biopolymer is soluble in acidic solutions due to the protonation of its amine functional groups. Due to having various functional groups (e.g. dihydroxyl and amino groups), chitosan has a high affinity toward the biosorption of pollutants like heavy metals and dyes. Cationization of amino groups in chitosan enriches its affinity to adsorb anionic dyes through electrostatic attraction in acidic solutions. Furthermore, the sensitivity of chitosan to pH has made it feasible to form either gel or solution based on the pH of the solution.

However, the use of these biomaterials has some drawbacks as well. For instance, low mechanical resistance, solubility in acidic medium, and low surface area have

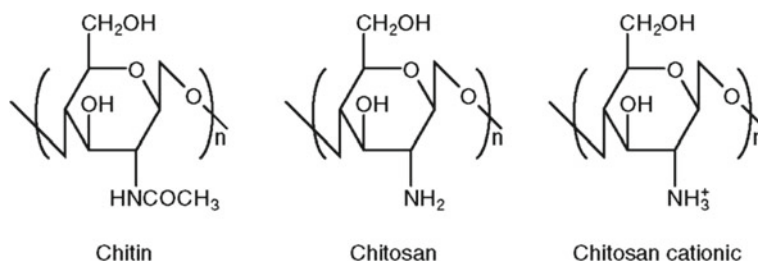


Fig. 4 Chemical structures of chitin and chitosan (free base and cationic form) (Fini and Orienti 2003)

limited the performance of chitosan as an efficient biosorbent. Therefore, modification of this biomaterial is needed to reach the standard requirements for proper biosorption performance (Sheth et al. 2021; Knidri et al. 2018).

4 Mechanism of Biosorption

Biosorption is generally defined based on the interaction between a sorbate (i.e. atom, ion, or molecule) and a biosorbent (with biological origin), resulting in biosorption and accumulation of the sorbate in the sorbate-biosorbent interface. This phenomenon usually leads to a considerable decline in the sorbate concentration inside the primary solution (Gadd 2009). Due to the lack of precise scientific evidence, the exact mechanism of the biosorption process remains unknown. The mechanisms proposed by the scientists so far are mostly based on presumptions and experimental results (Saha et al. 2019). Four primary mechanisms, namely chemisorption, physisorption, precipitation, and oxidation/reduction, comprise the biosorption mechanism. However, the complex process of biosorption sometimes necessitates more than one mechanism.

4.1 Biosorption of Metals

Due to the diversity of biosorbent material and contaminants present in wastewater. Complexation, chelation, reduction, precipitation, and ion exchange are the most common mechanisms, especially for the adsorption of heavy metals (Tsezos et al. 2006). Feasible mechanisms for decontaminating wastewater via the biosorption process are schematically represented in Fig. 5.

Functional groups involved in the adsorption of metal ions include carboxyl, hydroxyl, sulfate, phosphoryl, and amino groups. Therefore, pH has a key role in metals biosorption by influencing the charge of the mentioned functional groups, which directly affects the amount of metals biosorbed by the biomass. Since most of

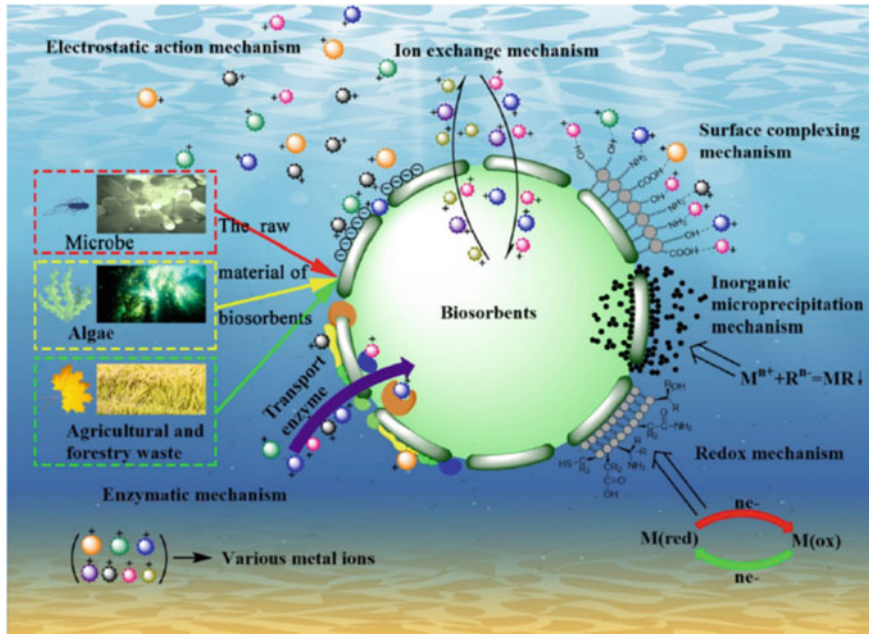


Fig. 5 Schematic diagram of prevalent adsorption mechanisms (Huang et al. 2020)

the metals present in the wastewater are in their cationic form, the intense negative charge of the biosorbent results in better biosorption of the metal ion. Thus, pH in the range between 7.0 and 8.0 is recognized as the most suitable pH for the adsorption of heavy metals. At lower pH values, there is competition between hydrogen ions and metal ions for binding sites of the adsorbent, while at higher pH values, metal ions are precipitated in the form of hydroxides, resulting in the reduction of biosorbed metal ions. However, for metals, which are predominantly in their anionic form, acidic pH values in the range between 2.0 and 4.0 represent the best pH range for the biosorption process. Anions are attracted onto the biomass with more positively charged functional groups at acidic pHs more easily.

Temperature is another important factor, which greatly affects the rate of reaction. Generally, the rate of biosorption increases at higher temperatures by enhancing surface activity and kinetic energy of adsorbate. An increase in temperature usually increases the maximum amount of metals biosorbed by the adsorbent. This happens when the process is endothermic. In the case of the exothermic process, an increase in temperature has a negative effect on biosorption capacity, which is most probably a result of the damage imposed to the surface of the biosorbent. This effect of temperature is more considerable in living biomass compared to dead biomass. Finally, enhancement of ionic strength negatively affects the biosorption capacity as a result of competition between other cations for the binding sites of the functional

groups. This is a crucial problem in real wastewater solutions where great amounts of various cations are involved in the solution (Torres 2020).

4.2 *Biosorption of Organic Compounds*

Many organic compounds, such as antibiotics, dyes, phenolic compounds, etc., have adverse effects on human health and the ecosystem. Some of the persistent organic pollutants (POPs), such as pesticides, organochlorines, insecticides, herbicides, etc., have been developed and known for a long time; while a group of these compounds are created due to the advances in analytical methods and are called emerging organic contaminants (EOCs). Even at low temperatures, such compounds should be eliminated from wastewaters because of their toxicity. The biosorption process for eliminating these contaminants is similar to the metal biosorption process, and the factors influencing the biosorption capacity are identical. However, the response to the changes in these factors may be different, which necessitates a thorough study of each case.

The complex composition of organic compounds, unlike metals, shows that they have different functional groups with different charges and degrees of ionization based on the solution pH. Thus, optimization of pH is very important in these compounds. Hydrophobicity is another important factor that should be considered in the case of organic pollutants. Hydrophobic materials can interact with the biosorbent via hydrophobic interactions. They can even go through the cell membrane when the biosorbent is a living organism. Therefore, this property of organic pollutants contributes to their efficient removal through biosorption.

The effect of temperature on biosorption of organic pollutants is the same as metals, meaning that for endothermic biosorption, an increase in temperature enhances the adsorption effectiveness, while the opposite result is obtained when the process is exothermic. Although the effect of ionic strength on the biosorption capacity is less studied compared to metals, it is known that a high concentration of salts is required in the solution so that the biosorption of organic compounds is decreased considerably (Torres 2020).

5 **Desorption and Regeneration of Biosorbents**

Reusability of the biosorbent means the removal of adsorbate from the biosorbent surface after usage and its return to its primary state, especially in terms of morphology and efficiency. Recovery of biosorbent after usage is one of the key issues in selecting suitable biosorbents. In other words, the reusability of biosorbent is as important as its good biosorption performance. Thus, desorption and regeneration of biosorbents are two fundamental processes that should be checked, so that effectiveness of a biosorbent is confirmed.

Several methods have been proposed for the regeneration of biosorbents, among which the use of eluents is the most promising method. The selection of appropriate eluents, which is based on the composition of biosorbent, adsorbate, and the mechanism of biosorption, is of great importance. A good eluent does not vary or harm the structure of biosorbent, is environmentally friendly, inexpensive, has a high affinity toward the particular adsorbate, and easily separates from the adsorbate. Mineral acids (HCl, H₂SO₄, and HNO₃), organic acids (citric, acetic, and lactic acids), and complexing agents (EDTA, thiosulphate, etc.) are some examples of eluents used in recent years for the regeneration of biosorbents.

It is feasible to perform desorption in batch or column. However, the packed column system provides an easier mode for this process, especially when the biosorption process is performed in the column as well. Desorption efficiency is defined by the S/L ratio, where S represents solid (biosorbent), and L represents liquid (eluent volume). It is worthy of mentioning that a high S/L ratio favors the desorption process (Adewuyi 2020; Kanamarlapudi et al. 2018). Table 2 summarizes information on the reusability potential of some plant leaves as an example of biosorbents used in many kinds of research for wastewater treatment. To examine this, biosorbents obtained from plant leaves go through some adsorption/desorption cycles until lost most of their adsorption capacity. It can be inferred from the information given in Table 1 that except for some rare cases, most of the plants maintained their removal efficiency up to the fifth cycle. After 5 cycles, the removal efficiency reduced by 5–15% in most species. These findings indicate that plant leaves are interestingly efficient in removing pollutants from wastewater (Adeniyi and Ighalo 2019).

6 Cost Estimation of Biosorbents for Wastewater Treatment

Evaluating the cost of the biosorption process is not a simple task since it relies on several factors such as required pretreatments on biosorbent, transportation, maintenance, energy consumption, regeneration, desorption, etc. The nature of wastewater to be treated by biosorption and the operational volume are other key factors to be considered. However, the type and size of the treatment plant specify capital costs. To minimize process costs, it is recommended to use waste materials such as agro-industrial wastes as biosorbents (see Sect. 3).

The dependence of cost estimation on numerous factors discussed earlier makes it hard to generalise and reach a specified relation. The composition of biosorbent has a major effect on the cost of the biosorption process. Pretreatment of biosorbent before use increases operational costs. To minimize cost, it is better to place a pretreatment facility close to where the waste is kept. Energy consumption is another important factor influencing process cost related to the biosorbent used and its biosorption capacity. For example, less energy is consumed with a fast biosorbent capable of completing the biosorption process within a short time. In other words,

Table 2 Reusability potential of some plant leaves

Leaves	Pollutants	No. of cycles	Adsorbed (%)	Decreased (%)	References
Aloe Vera ash (magnetic modified)	Pb ²⁺	5	71.64	26.86	Abedi et al. (2016)
	Cu ²⁺	5	88.15	11.85	
	Zn ²⁺	5	86.67	12.45	
	Cr ³⁺	5	92.08	7.92	
Teak	Zn ²⁺	5	91.6	7.40	Ajmal et al. (2011)
Bael	Pb ²⁺	2	80	19	Chakravarty et al. (2010)
Sesame	Cd ²⁺	4	72.41	–	Cheraghi et al. (2015)
<i>L. speciosa</i>	Pd ²⁺	10	>90	<9	Choudhary et al. (2017)
Oil palm (functionalised)	Cr ⁶⁺	5	90	9	El-Sayed and Nada (2017)
	Pb ²⁺	5	80	11	
Maple	Pb ²⁺	5	>94	<4.5	Hossain et al. (2014)
Dragon tree	Cd ²⁺	3	100	0	Mahmoud et al. (2016)
<i>R. communis</i> AC	Ni ²⁺	2	43.44	<46.54	Makeswari and Santhi (2013)
Bamboo (SDS modified)	Hg ²⁺	2	–	3	Mondal et al. (2013)
Rubber	Cr ⁶⁺	3	79.4	17.6	Nag et al. (2016)
Rubber	Cu ²⁺	3	72.3	5	Ngah and Hanafiah (2009)
<i>P. orientalis</i>	Methylene blue	5	24	51	Peydayesh and Rahbar-Kelishami (2015)
Moringa	Pb ²⁺ (10 mg/L)	5	95.45	3.89	Reddy et al. (2010)
<i>U. carpinifolia</i> <i>F. excelsior</i>	Pb ²⁺ , Cd ²⁺ , Cu ²⁺	3	–	5	Sangi et al. (2008)
	Pb ²⁺ , Cd ²⁺ , Cu ²⁺	3	–	5	
<i>R. communis</i> AC	Cr ⁶⁺	2	35.14	23.83	Makeswari and Santhi (2014)
Mistletoe	Pb ²⁺	3	96.47	3.34	Van Suc and Son (2016)
	Cd ²⁺	3	96.21	3.53	
Tarap	Rhodamine B	4	–	11	Zaidi et al. (2018)
Lemongrass	Crystal violet	2	61.79	23.72	Putri et al. (2021)
	Methylene blue		60.62	25.47	

(continued)

Table 2 (continued)

Leaves	Pollutants	No. of cycles	Adsorbed (%)	Decreased (%)	References
<i>Eichhornia crassipes</i>	Acid red 27	7	100	0	Ramírez-Rodríguez et al. (2018)
<i>Dimorcarpus longan</i> ssp. malesianus var. Malesianus (Mata Kuching)	Crystal violet	5	>96	<4	Priyanthaa et al. (2021)
<i>Forsythia suspense</i> (magnetic modified)	Cr ⁶⁺	5	>50	>10	Geng and Chang (2020)
	Congo red		>80	>10	
	Rhodamine B		146.66	20	

more energy consumption equals to high biosorption cost. Disposal of biosorbent, which is inevitable after several cycles and its replacement by new biosorbent, also increases process costs (Adewuyi 2020).

Overall, compared to other methods for wastewater treatment like ion exchange, adsorption, membrane separation, chemical oxidation, coagulation/flocculation, process cost is much less in the case of the biosorption process. The reason mainly lies in eliminating chemicals and the use of microorganisms or agricultural/food wastes instead.

7 Challenges for Industrial Implementation

Typically, all the biosorbents show promising results in terms of their adsorption capacity for particular contaminants at laboratory and pilot scales. However, few reports are available on the feasibility of their application at an industrial scale. Industrial application of biosorption process is faced by several challenges as follows:

- Since wastewater from some industries like electroplating contains heavy metals with different pHs, it is impossible to use biofilters that require stable conditions for their growth and maintenance at an industrial scale.
- Unlike the lab scale in which an increase in agitation rate enhances the biosorption capacity due to providing additional turbulence in the solution, industrial-scale biosorption is not affected by this parameter due to the process's rapid rate and surface saturation.
- Lab-scale studies reveal that increase in contact time results in enhancement of pollutant removal through active sites till saturation is reached with an increase in time. On the industrial scale, the contact time is much less, with millions of tons of pollutants normally present in industrial wastewaters, resulting in less pollutant biosorption.

Therefore, it is reasonably rejected to directly transfer information and practices on a laboratory scale into an industrial scale. Further efforts are needed to commercialize and scale the technology on a lab scale (Singh et al. 2020).

8 Prospects

Removing contaminants like toxic industrial compounds, heavy metals, dyes, hydrocarbons, pesticides, drugs, etc., from wastewater requires methods with high efficiency, low operational costs, high selectivity, and simplicity. Biosorption satisfies these requirements in its best condition. Although a lot of research has been done regarding using several biosorbents for wastewater treatment, commercialization has not been done yet. Commercialization of the biosorption process will not occur unless important factors such as industrial requirements, problems raised in the scale-up of the process, and the operational costs are managed technically and scientifically. Biosorbents such as agro-industrial wastes, plant/fruit wastes, and microorganisms (bacteria, fungi, and algae) are highly efficient in removing different pollutants from the wastewater by their functional groups and characteristics such as high pore volume and large surface area. Several pretreatments may be done on the biosorbents to enhance their biosorption capacity. In addition to this, researchers are seeking new materials to increase the efficiency of the typical biosorbents and design hybrid biosorption systems such as nano biocomposites through which biosorption of pollutants from wastewaters would be feasible with high efficiency. Future will witness biosorbents at domestic and industrial scales as an efficient and eco-friendly method for wastewater treatment.

References

- Abedi S, Mousavi HZ, Asghari A (2016) Investigation of heavy metal ions adsorption by magnetically modified aloe vera leaves ash based on equilibrium, kinetic and thermodynamic studies. *Desalin Water Treat* 57:13747–13759
- Adeniyi, George A, Ighalo JO (2019) Biosorption of pollutants by plant leaves: an empirical review. *J Environ Chem Eng* 7:103100
- Adenuga, Abiodun A, Amos OD, Oyekunle JAO, Umukoro EH (2019) Adsorption performance and mechanism of a low-cost biosorbent from spent seedcake of *Calophyllum inophyllum* in simultaneous cleanup of potentially toxic metals from industrial wastewater. *J Environ Chem Eng* 7:103317
- Adewuyi A (2020) Chemically modified biosorbents and their role in the removal of emerging pharmaceutical waste in the water system. *Water* 12:1551
- Ahmad LN, Zakariyya UZ, Garba Zaharaddeen N (2019) Rice husk as Biosorbent for the adsorption of methylene blue. *Sci World J* 14:66–70
- Ahmed S, Khan FSA, Mubarak NM, Khalid M, Tan YH, Mazari SA, Karri RR, Abdullah EC (2021) Emerging pollutants and their removal using visible-light responsive photocatalysis—a comprehensive review. *J Environ Chem Eng* 9

- Ahsan MA, Islam MT, Imam MA, Hyder AG, Jabbari V, Dominguez N, Noveron JC (2018) Biosorption of bisphenol A and sulfamethoxazole from water using sulfonated coffee waste: Isotherm, kinetic and thermodynamic studies. *J Environ Chem Eng* 6:6602–6611
- Ajmal M, Rao RAK, Ahmad R (2011) Adsorption studies of heavy metals on *Tectona grandis*: removal and recovery of Zn (II) from electroplating wastes. *J Dispersion Sci Technol* 32:851–856
- Akhouairi S, Ouachtak H, Addi AA, Jada A, Douch J (2019) Natural sawdust as adsorbent for the eriochrome black T dye removal from aqueous solution. *Water Air Soil Pollut* 230:1–15
- Alghamdi WM, El Mannoubi I (2021) Investigation of seeds and peels of *Citrullus Colocynthis* as efficient natural adsorbent for Methylene Blue Dye. *Processes* 9:1279
- Alhumaimes MS, Alsohaimi IH, Alqadami AA, Kamel MM, Naushad Mu, Ahamad T, Alshammari H (2019) Synthesis of phosphorylated raw sawdust for the removal of toxic metal ions from aqueous medium: adsorption mechanism for clean approach. *J Sol-Gel Sci Technol* 89:602–615
- Amarasinghe BMWPK, Williams RA (2007) Tea waste as a low cost adsorbent for the removal of Cu and Pb from wastewater. *Chem Eng J* 132:299–309
- Anastopoulos I, Karamesouti M, Mitropoulos AC, Kyzas GZ (2017) A review for coffee adsorbents. *J Mol Liq* 229:555–565
- Anastopoulos I, Robalds A, Tran HN, Mitrogiannis D, Giannakoudakis DA, Hosseini-Bandegharaei A, Dotto GL (2019) Removal of heavy metals by leaves-derived biosorbents. *Environ Chem Lett* 17:755–766
- Atar N, Olgun ASİM, Çolak F (2008) Thermodynamic, equilibrium and kinetic study of the biosorption of basic blue 41 using *Bacillus macerans*. *Eng Life Sci* 8:499–506
- Ayele A, Haile S, Alemu D, Tesfaye T, Kamaraj M (2021) Mycoremediation: fungal-based technology for biosorption of heavy metals—a review. *Strat Tools Pollut Mitigat: Avenues Clean Environ* 355
- Bažant ZP, Estensoro LF (1979) Surface singularity and crack propagation. *Int J Solids Struct* 15:405–426
- Beni AA, Esmaeili A (2020) Biosorption, an efficient method for removing heavy metals from industrial effluents: a review. *Environ Technol Innov* 17:100503
- Bhattacharjee C, Dutta S, Saxena VK (2020) A review on biosorptive removal of dyes and heavy metals from wastewater using watermelon rind as biosorbent. *Environ Adv* 2:100007
- Calderón OA, Ramírez OM, Abdeldayem AP, Rene ER (2020) Current updates and perspectives of biosorption technology: an alternative for the removal of heavy metals from wastewater. *Curr Pollut Rep* 6:8–27
- Çelebi H, Gök G, Gök O (2020) Adsorption capability of brewed tea waste in waters containing toxic lead (II), cadmium (II), nickel (II), and zinc (II) heavy metal ions. *Sci Rep* 10:1–12
- Chai WS, Tan WG, Munawaroh HSH, Gupta VK, Ho S-H, Show PL (2020) Multifaceted roles of microalgae in the application of wastewater biotreatment: a review. *Environ Pollut* 116236
- Chakravarty S, Ashok Mohanty T, Nag Sudha AK, Upadhyay JK, Sircar JK, Madhukar A, Gupta KK (2010) Removal of Pb (II) ions from aqueous solution by adsorption using bael leaves (*Aegle marmelos*). *J Hazard Mater* 173:502–509
- Cheraghi E, Ameri E, Moheb A (2015) Adsorption of cadmium ions from aqueous solutions using sesame as a low-cost biosorbent: kinetics and equilibrium studies. *Int J Environ Sci Technol* 12:2579–2592
- Choudhary BC, Paul D, Borse AU, Garole DJ (2017) Recovery of palladium from secondary waste using soluble tannins cross-linked *Lagerstroemia speciosa* leaves powder. *J Chem Technol Biotechnol* 92:1667–1677
- Chu W-L, Phang S-M (2019) Biosorption of heavy metals and dyes from industrial effluents by microalgae. In: *Microalgae biotechnology for development of biofuel and wastewater treatment*. Springer
- Çolak F, Atar N, Olgun A (2009) Biosorption of acidic dyes from aqueous solution by *Paenibacillus macerans*: kinetic, thermodynamic and equilibrium studies. *Chem Eng J* 150:122–130
- Crini G (2006) Non-conventional low-cost adsorbents for dye removal: a review. *Biores Technol* 97:1061–1085

- Crini G, Lichtfouse E (2019) Advantages and disadvantages of techniques used for wastewater treatment. *Environ Chem Lett* 17:145–155
- Das M, Samal AK, Mehar N (2020) Butea monosperma leaf as an adsorbent of methylene blue: recovery of the dye and reuse of the adsorbent. *Int J Environ Sci Technol* 17:2105–2112
- de Freitas G, Rocha MG, da Silva C, Vieira MGA (2019) Biosorption technology for removal of toxic metals: a review of commercial biosorbents and patents. *Environ Sci Pollut Res* 26:19097–19118
- Dehghani MH, Karri RR, Alimohammadi M, Nazmara S, Zarei A, Saedi Z (2020a) Insights into endocrine-disrupting Bisphenol-A adsorption from pharmaceutical effluent by chitosan immobilized nanoscale zero-valent iron nanoparticles. *J Mol Liq* 311
- Dehghani MH, Karri RR, Yeganeh ZT, Mahvi AH, Nourmoradi H, Salari M, Zarei A, Sillanpää M (2020b) Statistical modelling of endocrine disrupting compounds adsorption onto activated carbon prepared from wood using CCD-RSM and DE hybrid evolutionary optimization framework: comparison of linear vs non-linear isotherm and kinetic parameters. *J Mol Liq* 302:112526
- Dehghani MH, Omrani GA, Karri RR (2021) Solid waste—sources, toxicity, and their consequences to human health. In: *Soft computing techniques in solid waste and wastewater management*. Elsevier
- Dolatabadi M, Mehrabpour M, Esfandyari M, Alidadi H, Davoudi M (2018) Modeling of simultaneous adsorption of dye and metal ion by sawdust from aqueous solution using of ANN and ANFIS. *Chemom Intell Lab Syst* 181:72–78
- Ebrahimi A, Ehteshami M, Dahrzama B (2015) Isotherm and kinetic studies for the biosorption of cadmium from aqueous solution by Alhaji maurorum seed. *Process Saf Environ Prot* 98:374–382
- Eletta OAA, Ighalo JO (2019) A review of fish scales as a source of biosorbent for the removal of pollutants from industrial effluents. *J Res Inf Civ Eng* 16:2479–2510
- El Shahawy A, Heikal G (2018) Organic pollutants removal from oily wastewater using clean technology economically, friendly biosorbent (*Phragmites australis*). *Ecol Eng* 122:207–218
- El-Sayed M, Nada AA (2017) Polyethylenimine—functionalized amorphous carbon fabricated from oil palm leaves as a novel adsorbent for Cr (VI) and Pb (II) from aqueous solution. *J Water Process Eng* 16:296–308
- Escudero LB, Quintas PY, Wuilloud RG, Dotto GL (2019) Recent advances on elemental biosorption. *Environ Chem Lett* 17:409–427
- Esmaili A, Saremnia B, Kalantari M (2015) Removal of mercury (II) from aqueous solutions by biosorption on the biomass of *Sargassum glaucescens* and *Gracilaria corticata*. *Arab J Chem* 8:506–511
- Fard RF, Azimi AA, Nabi Bidhendi GR (2011) Batch kinetics and isotherms for biosorption of cadmium onto biosolids. *Desalination Water Treat* 28:69–74
- Fiaz R, Hafeez M, Mahmood R (2019) *Ficus palmata* leaves as a low-cost biosorbent for methylene blue: Thermodynamic and kinetic studies. *Water Environ Res* 91:689–699
- Fini A, Orienti I (2003) The role of chitosan in drug delivery. *Am J Drug Deliv* 1:43–59
- Franco DSP, Georgin J, Drumm FC, Netto MS, Allasia D, Oliveira MLS, Dotto GL (2020) *Araticum* (*Annona crassiflora*) seed powder (ASP) for the treatment of colored effluents by biosorption. *Environ Sci Pollut Res* 27:11184–11194
- Gadd G (2009) Heavy metal pollutants: environmental and biotechnological aspects. In: *Encyclopedia of microbiology*. Elsevier
- Geng J, Chang J (2020) Synthesis of magnetic *Forsythia suspensa* leaf powders for removal of metal ions and dyes from wastewater. *J Environ Chem Eng* 8:104224
- George AM, Tembhurkar AR (2019) Analysis of equilibrium, kinetic, and thermodynamic parameters for biosorption of fluoride from water onto coconut (*Cocos nucifera* Linn.) root developed adsorbent. *Chin J Chem Eng* 27:92–99
- Georgin J, Franco DSP, Netto MS, Allasia D, Oliveira MLS, Dotto GL (2020) Treatment of water containing methylene by biosorption using Brazilian berry seeds (*Eugenia uniflora*). *Environ Sci Pollut Res* 27:20831–20843

- Ghosh A, Das P, Sinha K (2015) Modeling of biosorption of Cu (II) by alkali-modified spent tea leaves using response surface methodology (RSM) and artificial neural network (ANN). *Appl Water Sci* 5:191–199
- Gonçalves AL, Pires JCM, Simões M (2017) A review on the use of microalgal consortia for wastewater treatment. *Algal Res* 24:403–415
- Gusmão KA, Guimarães LV, Gurgel A, Melo TMS, Gil LF (2012) Application of succinylated sugarcane bagasse as adsorbent to remove methylene blue and gentian violet from aqueous solutions—kinetic and equilibrium studies. *Dyes Pigm* 92:967–974
- Hossain MA, Ngo HH, Guo W, Zhang J, Liang S (2014) A laboratory study using maple leaves as a biosorbent for lead removal from aqueous solutions. *Water Qual Res J Can* 49:195–209
- Huang D, Li B, Ou J, Xue W, Li J, Li Z, Li T, Chen S, Deng R, Guo X (2020) Megamerger of biosorbents and catalytic technologies for the removal of heavy metals from wastewater: preparation, final disposal, mechanism and influencing factors. *J Environ Manag* 261:109879
- Ighalo JO, Adeniyi AG (2020) Adsorption of pollutants by plant bark derived adsorbents: an empirical review. *J Water Process Eng* 35:101228
- Jain CK, Malik DS, Yadav AK (2016) Applicability of plant based biosorbents in the removal of heavy metals: a review. *Environmental Processes* 3:495–523
- Jobby R, Jha P, Yadav AK, Desai N (2018) Biosorption and biotransformation of hexavalent chromium [Cr (VI)]: a comprehensive review. *Chemosphere* 207:255–266
- Kamel S, Abou-Yousef H, Yousef M, El-Sakhawy M (2012) Potential use of bagasse and modified bagasse for removing of iron and phenol from water. *Carbohydr Polym* 88:250–256
- Kanamarlapudi SLRK, Chintalputi VK, Muddada S (2018) Application of biosorption for removal of heavy metals from wastewater. *Biosorption* 18:69
- Karri RR, Sahu JN, Meikap BC (2020) Improving efficacy of Cr (VI) adsorption process on sustainable adsorbent derived from waste biomass (sugarcane bagasse) with help of ant colony optimization. *Indus Crops Prod* 143:111927
- Karri RR, Ravindran G, Dehghani MH (2021) Wastewater—sources, toxicity, and their consequences to human health. In: *Soft computing techniques in solid waste and wastewater management*. Elsevier
- Karri RR, Sahu JN (2018) Process optimization and adsorption modeling using activated carbon derived from palm oil kernel shell for Zn (II) disposal from the aqueous environment using differential evolution embedded neural network. *J Mol Liq* 265:592–602
- Kaur M, Mubarak NM, Chin BLF, Khalid M, Karri RR, Walvekar R, Abdullah EC, Tanjung FA (2020) Extraction of reinforced epoxy nanocomposite using agricultural waste biomass. In: *IOP conference series: materials science and engineering*
- Khan FSA, Mubarak NM, Tan YH, Khalid M, Karri RR, Walvekar R, Abdullah EC, Nizamuddin S, Mazari SA (2021) A comprehensive review on magnetic carbon nanotubes and carbon nanotube-based buckypaper for removal of heavy metals and dyes. *J Hazard Mater* 413
- Khraisheh M, Al-Ghouti MA, AlMomeni F (2020) *P. putida* as biosorbent for the remediation of cobalt and phenol from industrial waste wastewaters. *Environ Technol Innov* 20:101148
- Kim SY, Jin MR, Chung CH, Yun Y-S, Jahng KY, Yu K-Y (2015) Biosorption of cationic basic dye and cadmium by the novel biosorbent *Bacillus catenulatus* JB-022 strain. *J Biosci Bioeng* 119:433–439
- Knidri El, Hakima RB, Addaou A, Laajeb A, Lahsini A (2018) Extraction, chemical modification and characterization of chitin and chitosan. *Int J Biol Macromol* 120:1181–1189
- Koduru JR, Karri RR, Mubarak NM (2019) Smart materials, magnetic graphene oxide-based nanocomposites for sustainable water purification. *Sustain Polym Comp Nanocomp* 759–781
- Kumar KS, Dahms H-U, Won E-J, Lee J-S, Shin K-H (2015) Microalgae—a promising tool for heavy metal remediation. *Ecotoxicol Environ Saf* 113:329–352
- Kunjirama M, Saman N, Johari K, Song S-T, Kong H, Cheu S-C, Lye JWP, Mat H (2017) Adsorption affinity and selectivity of 3-ureidopropyltriethoxysilane grafted oil palm empty fruit bunches towards mercury ions. *Environ Sci Pollut Res* 24:15167–15181

- Kyzas GZ, Kostoglou M (2014) Green adsorbents for wastewaters: a critical review. *Materials* 7:333–364
- Legorreta-Castañeda AJ, Lucho-Constantino CA, Beltrán-Hernández RI, Coronel-Olivares C, Vázquez-Rodríguez GA (2020) Biosorption of water pollutants by fungal pellets. *Water* 12:1155
- Li Q, Chen Bo, Lin P, Zhou J, Zhan J, Shen Q, Pan X (2016) Adsorption of heavy metal from aqueous solution by dehydrated root powder of long-root *Eichhornia crassipes*. *Int J Phytorem* 18:103–109
- Li J, Ninh Pham A, Dai R, Wang Z, David Waite T (2020) Recent advances in Cu-Fenton systems for the treatment of industrial wastewaters: role of Cu complexes and Cu composites. *J Hazard Mater* 392:122261
- Lingamdinne LP, Vemula KR, Chang Y-Y, Yang J-K, Karri RR, Koduru JR (2020) Process optimization and modeling of lead removal using iron oxide nanocomposites generated from bio-waste mass. *Chemosphere* 243:125257
- Liu Li, Fan S, Li Y (2018) Removal behavior of methylene blue from aqueous solution by tea waste: kinetics, isotherms and mechanism. *Int J Environ Res Pub Health* 15:1321
- Lo Y-C, Cheng C-L, Han Y-L, Chen B-Y, Chang J-S (2014) Recovery of high-value metals from geothermal sites by biosorption and bioaccumulation. *Biores Technol* 160:182–190
- Mahmoud AE, Din MF, Radwan A (2016) Optimization of Cadmium (CD^{2+}) removal from aqueous solutions by novel biosorbent. *Int J Phytorem* 18:619–625
- Makeswari M, Santhi T (2013) Optimization of preparation of activated carbon from *Ricinus communis* leaves by microwave-assisted zinc chloride chemical activation: competitive adsorption of Ni^{2+} ions from aqueous solution. *J Chem* 2013:314790
- Makeswari M, Santhi T (2014) Adsorption of Cr (VI) from aqueous solutions by using activated carbons prepared from *ricinus communis* leaves: Binary and ternary systems. *Arab J Chem* 57:57–69
- Mallek M, Chtourou M, Portillo M, Monclús H, Walha K, Salah A, Salvadó V (2018) Granulated cork as biosorbent for the removal of phenol derivatives and emerging contaminants. *J Environ Manag* 223:576–585
- Manyuchi MM, Sukdeo N, Stinner W, Mutusva TN (2021) Influence of sawdust based biochar on gold tailings wastewater heavy metal contaminants removal. *S Afr J Chem Eng* 37:81–91
- Martín-Lara M Á, Rico ILR, de la Caridad Alomá Vicente I, García GB, de Hoces MC (2010) Modification of the sorptive characteristics of sugarcane bagasse for removing lead from aqueous solutions. *Desalination* 256:58–63
- Mehmood A, Khan FSA, Mubarak NM, Tan YH, Karri RR, Khalid M, Walvekar R, Abdullah EC, Nizamuddin S, Mazari SA (2021) Magnetic nanocomposites for sustainable water purification—a comprehensive review. *Environ Sci Pollut Res* 28:19563–19588
- Mella B, Puchana-Rosero MJ, Costa DES, Gutterres M (2017) Utilization of tannery solid waste as an alternative biosorbent for acid dyes in wastewater treatment. *J Mol Liq* 242:137–145
- Mishra S, Cheng L, Maiti A (2020) The utilization of agro-biomass/byproducts for effective bio-removal of dyes from dyeing wastewater: a comprehensive review. *J Environ Chem Eng* 10:4901
- Mo J, Yang Q, Zhang N, Zhang W, Zheng Y, Zhang Z (2018) A review on agro-industrial waste (AIW) derived adsorbents for water and wastewater treatment. *J Environ Manag* 227:395–405
- Modak JM, Natarajan KA (1995) Biosorption of metals using nonliving biomass—a review. *Min Metall Explor* 12:189–196
- Mondal DK, Nandi BK, Purkait MK (2013) Removal of mercury (II) from aqueous solution using bamboo leaf powder: equilibrium, thermodynamic and kinetic studies. *J Environ Chem Eng* 1:891–898
- Muraleedharan TR, Iyengar L, Venkobachar C (1991) Biosorption: an attractive alternative for metal removal and recovery. *Curr Sci* 61:379–385
- Nag S, Mondal A, Mishra U, Bar N, Das SK (2016) Removal of chromium (VI) from aqueous solutions using rubber leaf powder: batch and column studies. *Desalin Water Treat* 57:16927–16942

- Nazir H, Salman M, Athar M, Farooq U, Wahab A, Akram M (2019) Citric acid functionalized *Bougainvillea spectabilis*: a novel, sustainable, and cost-effective biosorbent for removal of heavy metal (Pb^{2+}) from waste water. *Water Air Soil Pollut* 230:1–16
- Ngh WSW, Hanafiah MAKM (2009) Surface modification of rubber (*Hevea brasiliensis*) leaves for the adsorption of copper ions: kinetic, thermodynamic and binding mechanisms. *J Chem Technol Biotechnol: Int Res Process Environ Clean Technol* 84:192–201
- Nguyen TA, Chun-Chieh Fu, Juang R-S (2016) Biosorption and biodegradation of a sulfur dye in high-strength dyeing wastewater by *Acidithiobacillus thiooxidans*. *J Environ Manage* 182:265–271
- Oguntimein GB (2015) Biosorption of dye from textile wastewater effluent onto alkali treated dried sunflower seed hull and design of a batch adsorber. *J Environ Chem Eng* 3:2647–2661
- Ouafi R, Rais Z, Taleb M, Benabbou M, Asri M (2017) Sawdust in the treatment of heavy metals-contaminated wastewater. *Environ Res J* 11
- Papirio S, Frunzo L, Mattei MR, Ferraro A, Race M, D'Acunto B, Pirozzi F, Esposito G (2017) Heavy metal removal from wastewaters by biosorption: mechanisms and modeling. In: Sustainable heavy metal remediation. Springer
- Pathak PD, Mandavgane SA, Kulkarni BD (2015) Fruit peel waste as a novel low-cost bio adsorbent. *Rev Chem Eng* 31:361–381
- Patil C, Ratnamala GM, Channamallayya ST (2015) Adsorption studies for removal of acid yellow 17 using activated rice husk. *Int Res J Eng Technol* 2:769
- Pereira FV, Gurgel LVA, Gil LF (2010) Removal of Zn^{2+} from aqueous single metal solutions and electroplating wastewater with wood sawdust and sugarcane bagasse modified with EDTA dianhydride (EDTAD). *J Hazard Mater* 176:856–863
- Peydayesh M, Rahbar-Kelishami A (2015) Adsorption of methylene blue onto *Platanus orientalis* leaf powder: kinetic, equilibrium and thermodynamic studies. *J Ind Eng Chem* 21:1014–1019
- Priyadarshane M, Das S (2020) Biosorption and removal of toxic heavy metals by metal tolerating bacteria for bioremediation of metal contamination: a comprehensive review. *J Environ Chem Eng* 104686
- Priyantha N, Kotabewatta PA (2019) Biosorption of heavy metal ions on peel of *Artocarpus nobilis* fruit: 1—Ni (II) sorption under static and dynamic conditions. *Appl Water Sci* 9:1–10
- Priyanthaa N, Romzib AA, Chanb CM, Limb LBL (2021) Enhancing adsorption of crystal violet dye through simple base modification of leaf adsorbent: isotherm, kinetics, and regeneration. *Desalination Water Treat* 215:194–208
- Putri KN, Atika SK, Keereerak A, Chinpa W (2021) Facile green preparation of Lignocellulosic Biosorbent from Lemongrass Leaf for Cationic Dye Adsorption. *J Polym Environ* 29:1681–1693
- Putro JN, Kurniawan A, Ismadji S, Yi-Hsu J (2017) Nanocellulose based biosorbents for wastewater treatment: study of isotherm, kinetic, thermodynamic and reusability. *Environ Nanotechnol Monitori Manag* 8:134–149
- Ramírez-Rodríguez AE, Reyes-Ledezma JL, Chávez-Camarillo GM, Cristiani-Urbina E, Morales-Barrera L (2018) Cyclic biosorption and desorption of acid red 27 onto *Eichhornia crassipes* leaves. *Revista Mexicana De Ingeniería Química* 17:1121–1134
- Reddy DH, Kumar YH, Seshiah K, Reddy AVR (2010) Biosorption of Pb (II) from aqueous solutions using chemically modified *Moringa oleifera* tree leaves. *Chem Eng J* 162:626–634
- Rigueto CVT, Piccin JS, Dettmer A, Rosseto M, Dotto GL, de Oliveira Schmitz AP, Perondi D, de Freitas TSM, Loss RA, Geraldi CAQ (2020) Water hyacinth (*Eichhornia crassipes*) roots, an amazon natural waste, as an alternative biosorbent to uptake a reactive textile dye from aqueous solutions. *Ecol Eng* 150:105817
- Riquelme M, Aguirre J, Bartnicki-García S, Braus GH, Feldbrügge M, Fleig U, Hansberg W, Herrera-Estrella A, Kämper J, Kück U (2018) Fungal morphogenesis, from the polarized growth of hyphae to complex reproduction and infection structures. *Microbiol Mol Biol Rev* 82:e00068-e117
- Saha S, Muhammad Zubair MA, Khosa SS, Ullah A (2019) Keratin and chitosan biosorbents for wastewater treatment: a review. *J Polym Environ* 27:1389–1403

- Sahu JN, Karri RR, Zabed HM, Shams S, Qi X (2019) Current perspectives and future prospects of nano-biotechnology in wastewater treatment. *Separat Purificat Rev* 1–20
- Sangi MR, Shahmoradi A, Zolgharnein J, Azimi GH, Ghorbandoost M (2008) Removal and recovery of heavy metals from aqueous solution using *Ulmus carpinifolia* and *Fraxinus excelsior* tree leaves. *J Hazard Mater* 155:513–522
- Saraswat SK, Demir M, Gosu V (2020) Adsorptive removal of heavy metals from industrial effluents using cow dung as the biosorbent: kinetic and isotherm modeling. *Environ Qual Manage* 30:51–60
- Sarker TC, Md Golam Gousul Azam S, El-Gawad AMA, Gaglione SA, Bonanomi G (2017) Sugar-cane bagasse: a potential low-cost biosorbent for the removal of hazardous materials. *Clean Technol Environ Policy* 19:2343–2362
- Sarode S, Punita Upadhyay MA, Khosa TM, Shakir A, Song S, Ullah A (2019) Overview of wastewater treatment methods with special focus on biopolymer chitin-chitosan. *Int J Biol Macromol* 121:1086–1100
- Şentürk İ, Yıldız MR (2020) Highly efficient removal from aqueous solution by adsorption of Maxilon Red GRL dye using activated pine sawdust. *Korean J Chem Eng* 37:985–999
- Shafiq M, Alazba AA, Amin MT (2018) Removal of heavy metals from wastewater using date palm as a biosorbent: a comparative review. *Sains Malaysiana* 47:35–49
- Shamsollahi Z, Partovinia A (2019) Recent advances on pollutants removal by rice husk as a bio-based adsorbent: a critical review. *J Environ Manage* 246:314–323
- Sheikh Z, Amin M, Khan N, Khan MN, Sami SK, Khan SB, Hafeez I, Khan SA, Bakhsh EM, Cheng CK (2021) Potential application of *Allium Cepa* seeds as a novel biosorbent for efficient biosorption of heavy metals ions from aqueous solution. *Chemosphere* 279:130545
- Sheth Y, Dharaskar S, Khalid M, Sonawane S (2021) An environment friendly approach for heavy metal removal from industrial wastewater using chitosan based biosorbent: a review. *Sustain Energy Technol Assess* 43:100951
- Singh S, Kumar V, Datta S, Dhanjal DS, Sharma K, Samuel J, Singh J (2020) Current advancement and future prospect of biosorbents for bioremediation. *Sci Total Environ* 709:135895
- Singha B, Das SK (2012) Removal of Pb (II) ions from aqueous solution and industrial effluent using natural biosorbents. *Environ Sci Pollut Res* 19:2212–2226
- Sörme L, Lagerkvist R (2002) Sources of heavy metals in urban wastewater in Stockholm. *Sci Total Environ* 298:131–145
- Suazo-Madrid A, Morales-Barrera L, Aranda-García E, Cristiani-Urbina E (2011) Nickel (II) biosorption by *Rhodotorula glutinis*. *J Ind Microbiol Biotechnol* 38:51–64
- Sun Y, Zhou S, Sun W, Zhu S, Zheng H (2020) Flocculation activity and evaluation of chitosan-based flocculant CMCTS-gP (AM-CA) for heavy metal removal. *Separat Purificat Technol* 241:116737
- thi Quyen V, Pham T-H, Kim J, Thanh DM, Thang PQ, Le QV, Jung JSH, Kim T (2021) Biosorbent derived from coffee husk for efficient removal of toxic heavy metals from wastewater. *Chemosphere* 131312
- Torres E (2020) Biosorption: a review of the latest advances. *Processes* 8:1584
- Tsezos M, Remoundaki E, Hatzikioseyan A (2006) Biosorption-principles and applications for metal immobilization from waste-water streams. In: *Proceedings of EU-Asia workshop on clean production and nanotechnologies*, Seoul, pp 23–33
- Ubando AT, Africa ADM, Maniquiz-Redillas MC, Culaba AB, Chen W-H, Chang J-S (2021) Microalgal biosorption of heavy metals: a comprehensive bibliometric review. *J Hazard Mater* 402:123431
- ul Haq A, Saeed M, Usman M, Zahoor AF, Anjum MN, Maqbool T, Naheed S, Kashif M (2021) Mechanisms of halosulfuron methyl pesticide biosorption onto neem seeds powder. *Sci Re* 11:1–13
- Ullrich AH, Smith MW (1951) The biosorption process of sewage and waste treatment. *Sewage Indus Wastes* 1248–1253
- Van Suc N, Son LN (2016) Mistletoe leaves as a biosorbent for removal of Pb (II) and Cd (II) from aqueous solution. *Desalinat Water Treat* 57:3606–3618

- Vijayaraghavan K, Yun Y-S (2008) Bacterial biosorbents and biosorption. *Biotechnol Adv* 26:266–291
- Xiong Chang X, Mujawar Mubarak N, Ali Mazari S, Sattar Jatoi A, Ahmad A, Khalid M, Walvekar R, Abdullah EC, Karri RR, Siddiqui MTH, Nizamuddin S (2021) A review on the properties and applications of chitosan, cellulose and deep eutectic solvent in green chemistry. *J Ind Eng Chem* 104:362–380
- Yu Z, Han H, Feng P, Zhao S, Zhou T, Kakade A, Kulshrestha S, Majeed S, Li X (2020) Recent advances in the recovery of metals from waste through biological processes. *Bioresour Technol* 297:122416
- Yusof NH, Foo KY, Hameed BH, Hazwan Hussin M, Lee HK, Sabar S (2020) One-step synthesis of chitosan-polyethyleneimine with calcium chloride as effective adsorbent for Acid Red 88 removal. *Int J Biol Macromol* 157:648–658
- Zaidi M, Hazirah NA, Lim LBL, Priyantha N, Usman A (2018) *Artocarpus odoratissimus* leaves as an eco-friendly adsorbent for the removal of toxic Rhodamine B Dye in aqueous solution: equilibrium isotherm, kinetics, thermodynamics and regeneration studies. *Arab J Sci Eng (Springer Science & Business Media BV)* 43

Nanoparticles in Industrial Wastewater Treatment: An Overview



Rekha Pachaiappan, Saravanan Rajendran, and Lorena Cornejo Ponce

Abstract The elixir of life is water which drives the entire natural process that occurs on our planet. Such an exotic gift by nature undergoes severe damage due to reckless activity by a human. Majorly water sources got polluted by ejection of industrial contaminated wastewater, domestic household wastewater and sewage wastes. Industrial wastewater is introduced in large volumes into the water sources, in turn producing intense health hazards on living beings and the environment. The contaminants from industries include toxic chemicals, heavy metals, metal dust, dyes, radioactive substances etc. At present, people across the globe are so much concerned about protecting and restoring water sources. Conventional industrial wastewater treatments like filtration, adsorption, flotation, ion exchange, coagulation and chemical precipitation are effectively adopted to remove the pollutants. However, these techniques are not sufficient in the case of the removal of hazardous heavy metals and microorganisms. In this scenario, advancement in nanoscience and nanotechnology has opened a new avenue to remove these toxic chemicals from waste water has gained importance and drawn attention with an eagle eye among researchers. Nanomaterials have been attracted due to their excellent physicochemical and flexible characteristics providing significant results with 100% efficiency. Nanomaterials in the form of nano-photocatalyst, nano adsorbents and nano membranes are widely committed. Nano metals, nano metallic oxides, nano metal sulfides, hybrid nanostructures (metal & metal oxides), magnetic nanoparticles, carbon nanotubes, graphene oxide, silica, nano polymers etc., have been utilized for removing contaminants in wastewater. This chapter expresses in detail the capacity of these nanoparticles to provide a sustainable approach in the industrial wastewater treatment process.

Keywords Wastewater treatment · Nanoadsorbents · Nanomembranes · Nano photocatalysts · Carbon based nanomaterials

R. Pachaiappan (✉) · S. Rajendran · L. C. Ponce
Facultad de Ingeniería, Departamento de Ingeniería Mecánica, Universidad de Tarapacá,
Avda.General Velasquez, 1775 Arica, Chile
e-mail: rekha.ap@gmail.com

1 Introduction

All living creatures require water for their survival on our planet. Humans need potable water to continue with healthy and hygienic life. As per United Nations (UN) words in 2010, every human has the right to get safe water for their daily usage. World health organization has released a report which concludes 785 million people around the world suffer from a lack of basic potable water. Drinking water sources are mainly contaminated by the development of urban areas with heavy populations and the ejection of harmful polluted water from industrial and agricultural activities. Globally, 829 million peoples' lives are ended up consuming contaminated drinking water through disease diarrhoea. By 2025, the main estimation was given, which concludes that half of the world population suffers from water scarcity (<https://www.who.int/news-room/fact-sheets/detail/drinking-water>). The evolution of various industries such as textile, chemical, leather, paper, pharmaceutical industry etc., has ejected harmful pollutants into the environment. Due to these contaminants, water sources are severely damaged, losing their characteristics and causing diseases in living organisms. The contaminants identified are organic chemicals, heavy inorganic metals, and microbes that are poisonous to creatures (El-Sayed 2020; Karri et al. 2021; Dehghani et al. 2021; World Health Organization 2012). More than 120 organic chemicals (pesticides, dyes, phenols etc.) are recognized for producing toxicity towards organisms. Inorganic heavy metals like arsenic, chromium, lead, cadmium and mercury are important in producing toxicity and chronic diseases (Dinka et al. 2018). Disease causing microbes include some bacteria, viruses, fungi, algae and protozoa (Ashbolt 2015). It is inevitable to carry out different strategies to eliminate the pollutants from contaminated water sources in this scenario. Water purification was done by boiling, sedimentation, coagulation/flocculation, filtration, irradiation, long storage, solar radiation, and chlorination (Odugbemi and Ogunsola 2002). Contaminants present in waste water are complex natured with different physicochemical properties. Also, existing traditional or conventional water purification processes display several limitations like a high cost for installation, high power consumption, the low removal rate of contaminants (~50%), maintenance cost, and the chance of secondary pollutants (Odugbemi & Ogunsola 2002). Considering these limitations, the research community developed advanced water treatment methods to complete water purification by eradicating entire contaminants. Nanofiltration, reverse osmosis, advanced oxidation process, ozonation, and activated carbon methods have produced a high removal rate (~90%) of contaminants from wastewater (https://apps.who.int/iris/bitstream/handle/10665/44630/9789241502085_eng.pdf). Nanoscience and nanotechnology have gained paramount importance in the production of nanomaterials with remarkable properties such as nanosize, high stability, sensitivity, low concentration, high specific surface area, surface plasmon resonance, high adsorption capacity, facile synthesis, ease in functionalization and ecofriendly (Ge et al. 2019). These nanomaterials are expanded into different substances such as nanoadsorbents, nanomembranes and nano photocatalysts. These nanomaterials have shown their remarkable role in waste water

treatment as an emerging substance. Unique characteristics of nanomaterials allow them to perform a major role in removing organic chemicals, heavy inorganic metals and biological contaminants from wastewater, which were the main cause of health hazards in organisms. Considering the global scenario of potable water requirement by living organisms, nanofabricated materials in industrial wastewater treatment are valuable topics to analyse. The synthesis of nanomaterials involves physical, chemical and biological methods. The physical type of fabrication techniques includes mechanical milling, melt mixing, pyrolysis (laser & flash spray), electro-spraying, inert gas condensation, and pulse vapour deposition. Whereas chemical vapour synthesis, plasma enhanced chemical vapour deposition, sol-gel technique, hydrothermal, polyol and microemulsion methods come under chemical methods. In the case of biological nanomaterial preparation, the plant extracts, microorganisms and bio templates are involved in obtaining nanomaterials. A plethora of research works are reported on metals (silver, zinc, iron etc.), metal oxides (zinc oxide, titanium dioxide, iron oxide, etc.), carbon based nanomaterials (carbon nanotube, graphene oxide, etc.), polymers etc., and their nanocomposites with excellent results in the eradication of above said contaminants from wastewater. Recently, Sikder et al. (2020) have fabricated the antibacterial biomaterial with a silver (3 wt %) doped magnesium phosphate, which showed 100% efficiency in the degradation of *Escherichia coli*. Another wonderful work on silver nanoparticle heavily loaded on magnetic graphene oxide functionalized by tannic acid and Fe^{3+} ions have exhibited 100% killing of *Escherichia coli* bacteria and ultimate recyclable rate (Yang et al. 2021). Aspherical covalent organic framework loaded with silver nanoparticles had proved its significant result in the continuous reduction of 4-nitrophenol (Wang et al. 2021). Nanocomposite developed with the combination of N doped titanium dioxide in graphene oxide acts an effective nanoadsorbents (chemisorption) by adsorbing hydrogen sulfide and 30–60% reduction in adsorption after two repetitions of experiment cycle (Daraee et al. 2020). Zinc oxide-based nanocomposite/nanoparticle acted as an effective photocatalyst in hydroxyl radical production degrading organic pollutants and other contaminants (Jain et al. 2020; Sultana et al. 2020). Leachate treatment was proposed by utilizing natural iron oxide as an adsorbent. The iron oxide nanoparticle had adsorbed the color, nitrogen ammonia and chemical oxygen demand at the rate of 97%, 43.8% and 75.9%, respectively (Shadi et al. 2020). Very recent accurate solute-solute separation was carried out by employing polyamide nanofiltration membrane with uniform pore size engineered using surfactant assembly regulated interfacial polymerization technique (SARIP) (Liang et al. 2020). Nano filters fabricated with polypiperazine-amide have shown a sodium sulfate rejection rate of 97.7% (Huang et al. 2020). This chapter starts with the elucidation of traditional wastewater treatment methodologies, followed by advancements in nanotechnology supporting obtaining better wastewater purification with enhanced nanomaterials. The main content describes the research works with nanoadsorbents, nanomembranes and nano photocatalysts to efficiently remove industrial water pollutants.

2 Traditional Methods for the Wastewater Treatment Process

2.1 Water Treatment

Water treatment is necessary to make the water eligible for consumption by a human without any health risk. Surface water purification consists of raw water treated with coagulant materials followed by flocculation. Then the sedimentation of contaminations takes place to which disinfectant was mixed. Disinfectant treated water led to a filtration unit to further remove contaminants, and clean water was sent to water tank storage (https://www.cdc.gov/healthywater/drinking/public/water_treatment.html). Currently, water sources are polluted heavily by the contaminants such as physical, chemical, microbes and radioactive substances. Mainly, the wastewater produced by the industry plays a key role in polluting water resources. Hence, it is necessary to conduct wastewater treatment plants or strategies to make contaminant water into potable ones and avoid disease outbreaks. The traditional water treatment process was done to treat industrial effluents through effluent treatment plants (ETP). This process has treatment steps: physical removal method, chemical process, biological water treatment, and sludge process (Poerio et al. 2019; <https://eponline.com/articles/2018/02/08/four-effective-processes-to-treat-wastewater.aspx>) (Figs. 1 and 2) (Table 1).

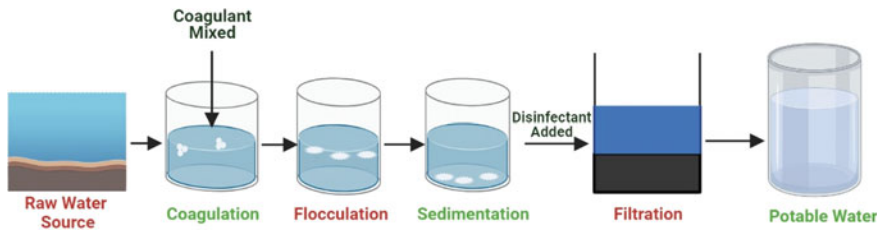


Fig. 1 Traditional water treatment process converting raw water source into potable water

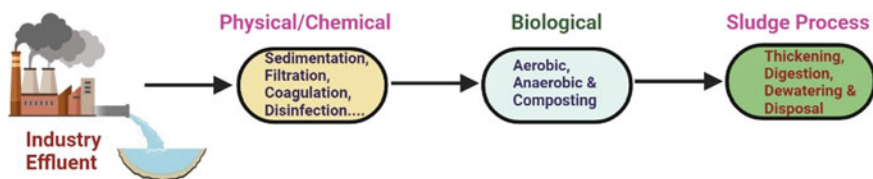


Fig. 2 Schematic illustration of physical, chemical, biological and sludge process to acquire organic and inorganic contaminants from industrial wastewater

Table 1 Merits and demerits of physical, chemical, biological and sludge process engaged in the wastewater treatment (Nur Hazirah et al. 2014; Samer 2015)

Wastewater treatment process	Technique employed	Merits	Demerits
Physical and chemical process	Adsorption on activated carbon	Effective and high capacity	Expensive regeneration process, loss of adsorbent and ineffective against dispersing and vat dyes
	Coagulant/flocculants	Simple process and economically feasible	High quantity chemicals are needed for pH adjustment. More amount of sludge is produced
	Electrolysis	Varying degree of success in colour removal	By products generation and not evaluated for full scale operations
	Fenton reagents	Effective decolourization for soluble and insoluble dyes	Sludge generation
	Ion exchange	Operative with no loss of regeneration	No significant results for disperse dyes. Expensive regeneration process
	Membrane Separation	All types of chemical class dyes can be decolorized	Due to sludge production not employable for large scale water treatment, expensive and high pressure
	Oxidation	Rapid and proficient technique	Generation of by products, high energy cost and chemicals required
	Ozonation	Applied in gaseous state and no toxic metabolites complete chemical oxygen demand (COD)	Short half-life, stability affected by auxiliary chemicals expensive

(continued)

Table 1 (continued)

Wastewater treatment process	Technique employed	Merits	Demerits
	Photochemical	No sludge and foul odours are produced	The emergence of secondary pollutants
Biological process	Anaerobic treatment	<ul style="list-style-type: none"> • Low operational cost • Sludge production is low and highly stabilized • No odour or aerosols were observed at the closed reactor • Methane is the end product • Low nutrient enough due to lower growth rate of anaerobes 	<ul style="list-style-type: none"> • High investment • Heating • Retention time >24 h. Not efficient towards pathogen destroy • Malodorous and corrosive compounds are produced • Production of hydrogen sulphide • Additional alkalinity
Sludge process	Activated sludge	<ul style="list-style-type: none"> • High flexibility in operating conditions such as pH, temperature and organic variations • Nitrogen removal is under control • Small installation area • Odours are the least 	<ul style="list-style-type: none"> • Skilled professionals are needed • Low pathogen removal • Uninterrupted power and air supply • Expensive

2.1.1 Physical Removal Method

Physical wastewater treatment consists of a combination of sedimentation, coagulation, filtration, screening and skimming processes. Sedimentation is the major method of removing insoluble large solid, dense particles by gravity. These particles might be large microbes, sand, silts, grit and other types of solids. Domestically, sedimentation is done by storing water in pots, buckets and available vessels.

Mostly two containers were used to carry out sedimentation. One container for settling down the particles and another container to collect the supernatant water. Commercially, large storage systems like reservoirs, settling tanks, basins and cisterns are used for sedimentation. Individual or dispersed small microbes are difficult to remove with gravitational effect. It was done by the microbes' aggregation with larger particles and eliminated by another method of coagulation and flocculation. In the coagulation method, chemicals/coagulants with a positive charge are added to the wastewater. When these chemicals react with the negative charge of small particles (aggregates) in water, they start to thicken or bind together as flocs.

These flocs and suspended products produce larger aggregated particles settling down at the bottom of the container. In this method, iron or aluminium salts such as ferric chloride, ferric sulphate, aluminium sulphate salts are used as coagulants.

Next is the filtration process, in which the water with particulate matter is allowed to pass through the porous media to remove the contaminants. Various filters are used depending upon the size and distribution of the particulates and microbial contaminants. Slow sand, roughing, cistern, bucket, drum filters, diatomaceous filters, porous ceramic filters, fiber, fabric and membrane filters are used to eradicate the granular substances present in water. Bucket and drum filters are effectively employed at the household level of water filtration. In filter media, slow sand and fiber fabric and membrane filters reduce microbe at household or point usage levels. Also, porous ceramic filters are simple and elegant to use, care should be given to the quality of porous ceramic substances used. Diatomaceous filters are efficient in removing waterborne pathogens. The screening process eliminates water heavy solids like metals, plastic, and paper. Freely floating oil substances like oil, grease, fats etc., on the surface of the oil is removed by skimming technique.

2.1.2 Chemical Process

In the chemical process, oxidizing chemical compounds such as chlorine and ozone are employed for water disinfections. These chemicals react with the microbes present in water and avoid the decomposition of water by stopping the reproduction of microbes. In water, neutral pH 7 is maintained by neutralisation methods and adding suitable acid or alkali to water. Worldwide, chlorine is used as a disinfectant in wastewater or water purification. Every disinfectant releases its products after its usage. For a long time, chlorine was employed as a principal disinfectant, and deep knowledge exists on its byproducts release. Hence, chlorine is widely applied as a disinfectant not to risk health effects among people. Also, this is one of the precautions taken to avoid the spread of infectious diseases like diarrhea and improve people's lifetime.

2.1.3 Biological Water Treatment

Organic substances present in water as the contaminant can be broken into small particles by the microorganisms. Bacteria can metabolize organic contaminants like food, oil, human waste, soaps etc. Since the living organism is engaged, this process is known as biological water treatment. The biological water treatment was categorized into aerobic, anaerobic and composting processes. Aerobic and anaerobic processes are carried out by decomposing organic matter in the presence and absence of oxygen. In the aerobic process, carbon dioxide was released and used by the plants for photosynthesis. The anaerobic process is done by the fermentation of organic contaminants in the absence of oxygen at a specific temperature. Composting is the

aerobic process in which carbon sources and sawdust are added to the wastewater to treat the contaminants.

2.1.4 Sludge Process

In the sludge process, liquid and solid are separated from each other. Major steps involved in this process are thickening, digestion, dewatering and disposal. The first step, thickening, is done by gravity thickener or dissolved air floatation methods. The overall volume of the sludge got decreased in gravity thickening and was removed easily. Air bubbles enable the solid sludge to float on the top of wastewater for easy removal in air floatation. Digestion is the process involved in decomposing organic solid wastes present in sludge into small water-soluble substances. This process was done by heating the sludge in the tank and anaerobic digestion by bacteria. Lipids and proteins are converted into small substances, further converted into methane and carbon dioxide gases. These gases are used as energy products upon requirement. The third step involves the dewatering of sludge. By centrifugation, drying beds, belt filter and drum vacuum filter are used to remove the water from sludge. Centrifugation includes easy handling, short duration with low investment and is mostly considered for dewatering the sludge. Drying beds find their possibility at rural or semiurban areas for the large land requirement. After the process mentioned above, the disposal of the remaining was done. The disposal residue might be used as fertilizer for crops by considering its chemical composition. Otherwise, incineration of the sludge was done, turned into ash and buried.

3 Emergence of Nanotechnology in Wastewater Purification

In wastewater treatment, existing conventional techniques have shown some falls to be progressed like investment cost, usage of chemical agents (chlorine, ozone) for disinfection, formation of byproducts, lack in complete removal of contaminants, fouling and time consumption (Crini and Lichtfouse 2019). Developments in nanotechnology have paved a path for emerging out with nanomaterials of different sizes and shapes at atomic and molecular level changes. Thus, formed nanomaterials exhibit better conductive, electronic, optical, magnetic and mechanical properties for achieving significant results in wastewater treatment. Nanomaterials with specific surface area, nano-size, high sensitivity, adsorption capacity and simple functionalization made them readily available to remove contaminants from wastewater. Nanotechnology has given out a variety of nanomaterials in the form of nanoadsorbents, nano-filters, nanomembranes, nano photocatalysts, nano antimicrobial agents and nano-sensors to perform corresponding operations regarding wastewater treatment technology. These materials had shown significant results in removing industrial

contaminants such as dyes, heavy metals, and pathogens in wastewater (Kumar et al. 2014; Khan et al. 2021a, b; Mehmood et al. 2021a, b; Mehmood et al. 2021a, b). Considering the past fifteen years of nanomaterials for wastewater treatment research works was drastically elevated from 5 to 80% (Yaqoob et al. 2014). Nanoadsorbents were constructed from metal and carbon as a base to remove dyes and heavy metal ions present in industrial wastewater (Sadegh et al. 2017). Different synthesis techniques are reported to craft the required nanoadsorbents. These new nanoadsorbents depend upon the pH, dose of adsorbent, exposure time and temperature to produce an effective removal of contaminants even at low concentrations ($\mu\text{g/L}$) (Basheer 2018). Nanotechnology has developed nanomembranes to replace the regular membrane of reverse osmosis used to carry out desalination, oil/water separation and wastewater treatment for reuse. Nanomembranes engineered from inorganic substances possessed high thermal and structural stability without any external triggering to do the process. Carbon based nanomembranes like graphene oxide and carbon nanotubes have shown higher water flux than conventional membranes.

On the other hand, zeolite coated nanomembranes exhibit good mechanical, thermal and chemical stabilities like conventional membranes. Hence, nanomembranes are used for advanced wastewater filtration processes (Singha et al. 2020). Another important in nanotechnology is the production of nano photocatalysts. Multiple applications such as dye removal, heavy metal capture, and antimicrobial activity are made with nano photocatalyst. Results obtained from nano photocatalyst are so efficient in the removal of contaminants. Research works were proposed in the synthesis of nano photocatalysts which were active or harvest solar energy, abundance, less or non-toxic nature and eco-friendly by solving wastewater purification at low investment.

Further, photocatalysts are expected to have the qualities such as enhanced light harvesting, especially solar harvesting, charge carrier generation, transfer and increased separation rate of charge carriers. While considering nano photocatalyst, metal, metal oxide, carbon, polymer and metal organic framework based photocatalyst are reported to eliminate contaminants in water.

Ahmed et al. (2021). Plethoras of appreciable results were demonstrated with titanium dioxide and zinc oxide semiconductors based nano photocatalyst. Other oxides include silver, iron, and copper oxide for effective dye removal and antimicrobial activity (Naseem et al. 2021). Carbon based nano photocatalysts such as carbon nanotubes, graphene-based nanomaterial and graphitic carbon nitride are employed effectively to decompose contaminants present in wastewater (Madima et al. 2020). Wonderful results with nano photocatalysts are due to the ejection of reactive oxygen species and their reaction. Hence, nanomaterials that emerged from the improvement of nanotechnology have paved a new way to remove organic and inorganic pollutants in all possible ways.

4 Application of Nanomaterials in Industrial Wastewater Technologies

In the past decade, advancements in nanotechnology resulted in the development of nanomaterials or nanosystems showing the capacity for efficient removal of pollutants from water. The pollutants present in wastewater from industries are organic and inorganic chemicals (dyes, phenols, oils, pharmaceutical chemicals etc.,) and heavy metals. Various dyes and heavy metals are the major pollutants or contaminants released to the water sources by industrial wastewater. Research works are reported with the nanoadsorbents, nanomembranes and nano photocatalysts to remove these contaminants in wastewater to restore the quality of water sources.

4.1 Nanoadsorbents for Removal of Water Pollutants

4.1.1 Adsorption

In 1881, Heinrich Kayser, a German scientist, introduced adsorption to accumulate materials on the surface (Roque-Malherbe and del Rio 2019). Adsorption is defined as the surface phenomenon in which the solid adsorbent with a porous layer adsorbs the adsorbate in the form of solid, liquid or gaseous ions or molecules. Due to the existence of attractive interaction between the adsorbent and adsorbate produce more adsorbate settle on the top layer surface of the adsorbent.

4.1.2 Adsorption Types

Adsorption is majorly classified into two types, depending upon the surface interaction of adsorbent towards adsorbate, physical adsorption and chemisorption. In physical adsorption, Vander Waals forces (weak force) hold the liquid or gas molecules. No transfer or sharing of electrons happens in physical adsorption, and it's a reversible process. Chemisorption happens by the force of interaction between the adsorbent surface and adsorbate. This process is irreversible, as it is difficult to pull out the molecules (adsorbate) settle on the adsorbent. Depending upon the need, adsorbent condition allows both physical and chemical adsorptions to be carried out simultaneously to remove contaminants (Patterson 2009). In addition, exchange adsorption can occur by exchanging charges between the adsorbent and adsorbate.

4.1.3 Nanoadsorbents

Hazardous pollutants are added to the water sources through the mixing of industrial wastewater without any treatment. The pollutants from industrial wastewater

contaminate water sources heavily. These pollutants are removed effectively by the nanoadsorbents with several qualities. It includes non-toxicity, selectivity, low dosage, greater affinity, easy removal, adaptability and eco-friendly. Majorly, nanoadsorbents are expected to be active with less concentration and remove even trace amounts of pollutants in water or wastewater from industrial effluents. Nanoadsorbents are synthesized using physical, chemical, biological and hybrid approaches. Nanoadsorbents with definite shape and size are possible with physical and chemical synthesis (Rashed et al. 2017; Alhan et al. 2019). The chemical ingredients are hazardous to the environment and found to be toxic. Hence, researchers are interested in proceeding with the biological synthesis of nanomaterials to be employed in contaminant removal (Kazemi et al. 2020). In the biological method, plant extract, microbes (bacteria & fungi) and algae are used to form the nanomaterials (Masoudi et al. 2018; Sebeia et al. 2019). Enzymes and proteins released by these biological species play as a reducing and capping agent towards metal ions and control nanomaterials' size (1–100 nm) and structure. Nanoadsorbents have tunable pore size, high active surface area, facile synthesis, modification at low temperature and low intraparticle diffusion distance (Sarma et al. 2019). Several merits over conventional methods are bio-based low-cost synthesis, regenerative, no secondary pollutant and recovery of adsorbed pollutant.

Nanoadsorbents for the wastewater treatment are expected to satisfy the below three conditions,

1. Nanoadsorbent should not possess any toxicity.
2. Nanoadsorbent should have the capability to adsorb even trace amounts of contaminants.
3. Highly active and reactivation of surface area.

Mostly, nanoadsorbents are engineered from metal, carbon, zeolite, polymer and other hybrids.

Metal Based Nanoadsorbents

Amidst metal based nanoadsorbents, zinc oxide, titanium dioxide, iron oxide and silver oxide are largely employed to remove the heavy metals and adsorb the dye present in the waste water. Adsorption data of the prepared nanoadsorbents was correlated with several isotherm models (Langmuir, Freundlich etc..) to determine the correlation coefficient and used for fabrication purposes. Pseudo first and second order kinetic models were used to decide the sorption kinetics of the nanoadsorbents in the removal of pollutants. Madan et al. (2019) have improved the surface of the zeolite by using zinc oxide nanoflakes to perform better adsorption of Congo red dye (Fig. 3). Adsorption kinetics of the prepared nanocomposite was studied with various concentrations and time, which appeared to follow the pseudo second order kinetics and Langmuir isotherm model. This zinc oxide-based nanocomposite had adsorbed the Congo red dye homogeneously on its surface (161.3 mg/g). Even after five cycles of experiments, the adsorption capacity was found to be 90%.

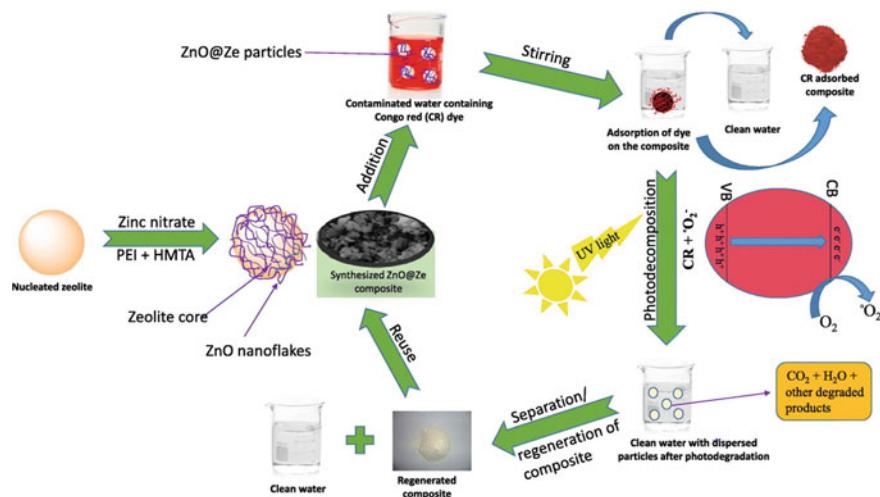


Fig. 3 Zeolite nanocore functionalized with zinc oxide nanoflakes applied in the adsorption and complete photodegradation of Congo red dye and separated nanocomposite for repeating the experiment up to five cycles in acquiring pure water (adopted from Madan et al. 2019)

Similarly, methylene blue dye was adsorbed in the other work by employing zinc oxide combined with cellulose from sawdust. In this process, the pseudo second order kinetic and Langmuir isotherm model was followed in the adsorption of methylene blue dye with adsorption measurement recorded as 64.93 mg/g. Enhanced interaction of nanocomposite with the dye and maximum adsorption was due to the electrostatic interaction between the opposite charges of the dye and nanocomposite, hydrogen bonding and π - π interaction. Maximum removal of dye (90%) was observed at pH 4.0 (Oyewo et al. 2020).

Recently, Sharma et al. (2021) reported heavy metal ion adsorption and methylene blue dye degradation by in situ zinc oxide@graphitic carbon nitride preparation. Lead, cadmium and chromium metal ions were adsorbed at the rate of 48.144, 48.883 and 40.108 mg/g. The result was better from pure graphitic carbon nitride and zinc oxide@graphitic carbon nitride. Recent works with titanium dioxide-based nanocomposite were proposed to remove lead, arsenic and copper ions from water. Pomegranate peel fixed with titanium dioxide nanoparticles was used to remove arsenic from water (Poudel et al. 2020). Batch experiments were carried out to know the better adsorption for pH values, concentration, time and adsorption isotherm and kinetics. In the existence of anions, the prepared nanocomposite worked effectively with the adsorption of 76.92 mg/g and dissociation coefficient $K_D \sim 10^3$ mL/g. Adsorption kinetic mechanism found to follow the pseudo second order and effective at neutral pH.

Similarly, mesoporous titanium dioxide was used to adsorption lead ions (Xu et al. 2020). Fluorination with hydrofluoric acid has improved the surface area to a higher value of 102.4 m²/g and spatial charge separation. These properties had

shown the adsorption of lead to be 31%. Manganese ferrite oxide coupled with titanium dioxide and reduced graphene oxide was used to remove copper ions and ciprofloxacin from water (Chang et al. 2021). Even though six cycles of experiments have not reduced the adsorption capacity of the nanocomposite. The adsorption capacity of nanocomposite towards copper ion and ciprofloxacin were 118.45 and 76.56 mg/g, respectively. The adsorption mechanism was appeared to be endothermic chemisorption and spontaneous fixed to Langmuir isotherm and Pseudo second order kinetics. Appreciable adsorption was due to the surface negative charge and oxygen groups (hydroxyl and carboxyl) of the nanoadsorbent.

Carbon Based Nanoadsorbents

Carbon Nanotubes

Jauris et al. (2016) have developed the ab initio simulation based on density functional theory to analyze the interaction between the dyes (methylene blue and acridine orange) and single walled carbon nanotubes. In this study, four different configurations were studied. Dyes with pristine single walled carbon nanotubes of (5,5), (8,0), (16,0) and (25,0) are used with and without vacancy. The average binding energy was 0.75 eV for the proposed configurations. Nanotubes with vacancy have shown lower binding energies when interacting with dyes than the nanotubes without vacancy. But in the case of methylene, blue interacts over nanotubes with vacancy exhibited charge donor characteristics whereas charge accepting nature for nanotubes without vacancy. This might be due to the presence of electrostatic interaction. In addition, nanotubes have exhibited enhancement in adsorption with an increase in their diameter.

Further, when the dyes arranged in parallel or planar to nanotubes have formed stabilized configuration due to the presence of π - π interaction. Thus, various features like charge transfer, size and arrangement of dyes concerning nanotubes determine the dye adsorption rate by single walled carbon nanotubes. Similar work was reported on simultaneous theoretical and experimental analysis on evaluating the efficiency of single and multi walled carbon nanotubes in alizarin red S (ARS) dye adsorption. Adsorption efficiency was calculated for both the carbon nanotubes, considering pH, contact time, and temperature. It was found that pH at 2.0 and temperature 318 K with contact time 65 and 100 min have produced a maximum adsorption rate of 312.5 and 135.2 mg/g for single and multi walled carbon nanotubes, respectively. For both the types of nanotubes with alizarin red S dye, values of electrostatic interaction and enthalpy remains in coordination with one another. The change in enthalpy was recorded as -22.45 kJ/mol (single wall) and -24.09 kJ/mol (multi walled) and consistent for the electrostatic attraction of carbon nanotubes and dye. Other thermodynamic quantities Gibbs free energy and change in entropies were also recorded. Adsorption kinetics was the best fit with the general order equations than pseudo first and second order kinetics equation. Amidst Freundlich, Langmuir, and Liu Isotherm models, the Liu model has provided the best fit for the obtained equilibrium data.

At temperature 318 K, the maximum sorption capacity of single and multi walled carbon nanotubes was 312.5 ± 0.48 mg/g and 135.2 ± 0.38 mg/g, respectively. The experimental and theoretical data were very well correlated. This study also confirms that the diameter of nanotubes and dye arrangement with nanotubes were responsible for the adsorption capacity (Machado et al. 2016). Recently, another work was demonstrated by Balarak et al. (2021) to show the efficiency of adsorbent single walled carbon nanotubes in the adsorption of acid blue 92 (AB92) dye. Gibbs free energy lies in the range—12.73 to -16.08 kJ/mol, change in entropy of 0.055 kJ/mol K and change in enthalpy of 2.51 kJ/mol. Maximum dye sorption efficiency of 99.4% (pH 3% & 75 min). Mechanisms responsible for the maximum dye uptake are π - π and London dispersion interactions, hydrogen and dipole bonds and hydrophobic effect. This study reveals the capability of single walled carbon nanotubes in the consumption of AB92 dye from industrial wastewater.

Multiwalled carbon nanotubes functionalized with water soluble hyperbranched polyamine to enhance the adsorption of organic dyes from industrial wastewater. The addition of polyamine has provided better water dispersion along with readily available amine and hydroxyl groups. These properties support the adsorbent to acquire adsorbate proficiently from wastewater. The nanocomposite has exhibited the adsorption capacity of 800.0, 840.3 and 970.9 mg/g of methylene blue, malachite green and methyl violet, respectively. The thermodynamic mechanism had shown the adsorption process to be spontaneous and exothermic by the existence of π - π interaction, hydrogen bonding and electrostatic force (Hu et al. 2017). In another study, magnetic multiwalled carbon nanotubes were synthesized by following the chemical co-precipitation method to capture methyl violet. The central composite design was adopted for experiments to find the optimal value of pH, contact time, adsorbent dosage, and ionic strength. Methyl violet was adsorbed at the rate of 101.19% for pH 4.92, contact time of 40.98 min for 0.99 g/L adsorbent dosage and 0.04 mol/L of ionic strength. The Langmuir isotherm equation had given the correlation coefficient 0.9968 better fits than Freundlich (0.9940) and Tempkin (0.9904) models. Experimental result shows that 99.51% of methyl violet was uptaken by these magnetic multiwalled carbon nanotubes (Ehyaee et al. 2017). Magnetic cobalt fixed multiwalled carbon nanotubes in the adsorption of methylene blue. Adsorption kinetics had followed the pseudo second order model. Thermodynamic parameters had shown the process to be endothermic with a maximum adsorption capacity of 324.34 mg/g. Hydroxyl radicals had played a major role in removing dye with the magnetic cobalt-based carbon nanotubes followed ultrasonication. The correlation coefficient was higher in Langmuir fit to be 0.9912, attaining equilibrium and no dye capture afterwards (Çalimli 2021).

Oligosaccharide β -Cyclodextrin and glycine were combined with multiwalled carbon nanotubes to produce organic dye adsorption. This nanocomposite has exhibited strong adsorption due to hydroxyl groups and hydrophobic cavity forming complexes with organic dyes. Maximum sorption capacities for methylene blue, methyl orange, acid blue 113 (AB113), and disperse red 1 (DR1) were 90.90, 96.15, 172.41 and 500 mg/g, respectively. The kinetic adsorption mechanism had shown the

system follows the pseudo second order and Langmuir isotherm model for significant dye adsorption (Mohammadi et al. 2018). A combination of carbon nanotubes, chitosan and octa-amino polyhedral oligomeric silsesquioxanes had shown its potential in adsorption of Congo red (314.97 mg/g) and methyl orange (63.23 mg/g) dyes (Zhao et al. 2020).

Graphene Oxide

Activated graphene oxide was synthesized in the presence of potassium hydroxide using a solid state reaction at high temperatures (Guo et al. 2016). The external surface of activated graphene oxide possesses fewer functional groups of oxygen than graphene oxide synthesized from Hummer's method. This was the main reason for the excellent attraction of anionic orange IV dye. The adsorption mechanism best fit the Langmuir isotherm model and pseudo second order adsorption kinetic equations. The maximum adsorption capacity of 606.1 mg/g was possible with a large surface area (672.5 m²/g) of activated graphene oxide. Composite prepared from graphene oxide, magnetic nanoparticles, and β -Cyclodextrin had efficient adsorption of methylene blue. The nanocomposite possesses excellent superparamagnetic nature, which showed remarkable dye adsorption at high pH values. After five cycles of experiments, the attraction of dye by nanocomposite decreased to 126.4 mg/g (Initial adsorption 196.2 mg/g) with 64.4% of adsorption efficiency (Cao et al. 2016). Similar work on magnetic graphene oxide for methylene blue adsorption by utilizing reversible addition fragmentation chain transfer polymerization followed epoxide ring opening reactions. Magnetic hysteresis loop had shown the prepared composite adapts ferromagnetic property with very low remanence and coercivity values. The Langmuir isotherm model, the adsorption of 153.85 mg/g with 75.3% of removal efficiency (Le et al. 2017).

Very recent, Rebekah et al. (2020) have proposed the adsorption of phenolic compound 2-naphthol by using magnetic graphene fixed with chitosan nanoparticles. The nanocomposite had shown low coercivity (50 Oe) and high saturation magnetization value (46.5 emu/g). Hence, maximum adsorption of 2-naphthol 169.49 mg/g with an efficiency rate of 99.8% (pH 2). Another work on magnetic particles decorated on reduced graphene oxide sheets was employed to remove crystal violet. This nanocomposite too possessed superparamagnetic nature with a saturation magnetization value of 42 emu/g. Further, the pseudo second order kinetics of chemisorption and Freundlich isotherm equations have described the adsorption mechanism. The adsorption capacity of nanocomposite was recorded to be 62 mg/g with a correlation coefficient r^2 of 0.9989 (Kahsay et al. 2020). Congo red dye adsorptions with graphene oxide nano-adsorbent sheets were demonstrated by Zhang et al. (2020a) and Yokwana et al. (2018). Nitrogen doped graphene oxide sheets contain negative (oxygen) and positive (nitrogen) charged groups which interact with positive (linkages of azo) and negative (sulfonic group) of Congo red dye. Hence, congo red capture was more with an adsorption rate of 99% under electrostatic interaction (Yokwana et al. 2018). Nano-adsorbent sheets prepared with graphene oxide and silica possessed a multipore structure with a large surface area of 345.7176 m²/g. At

room temperature, the adsorption capacity was 416.6667 mg/g (Zhang et al. 2020a). These works followed Langmuir isotherm and pseudo second order kinetics.

Ou et al. (2019) have successfully demonstrated the good separation rate of oil and dye adsorption with graphene oxide nanomembranes coupled with dopamine modified chitin nanocrystals. Membrane possessed a very good hydrophilic and oleophobic nature favouring dye removal (Congo red—98.3% and Methylene blue—99.3%) and oil separation (97.5%). Similarly, with good efficiency, dye removal was reported with three-dimensional graphene oxide combined graphitic carbon nitride and titanium dioxide with melamine foam (Zhan et al. 2021). The nanocomposite had done selective removal of organic dyes by adsorbing cationic dyes alone. Further, for all emulsions with a stabilized surfactant, the separation ability was at a higher rate of 99.9% due to the high viscosity of oil blocking the foam. Rhodamine dye adsorption was appreciably performed by metal organic framework (MOF-5) combined graphene oxide nanocomposite prepared using the grinding method (Kumar and Masram 2010). Adsorption kinetic mechanism with correlation coefficients was documented as 0.9703 (Langmuir isotherm) and 0.9908 (Pseudo second order kinetics). This MOF based graphene oxide had shown better stability and reusability. Maximum adsorption of 151.62 mg/g with a removal efficiency rate of 60.64% was produced.

4.2 *Nanomembranes for the Filtration Process*

4.2.1 **Nanofiltration Membrane Technology**

Cadotte was the pioneer in the employment of nanofiltration membranes for a wide range of applications, including water purification (Cadotte et al. 1988). In detail, nanofiltration membrane technology works under pressure and crossflow mechanism. In the pressure that has driven the nanofiltration membrane, the applied pressure was greater than the system's osmotic pressure, than the reverse flow of solvent takes place at the semipermeable membrane. The filtration process proceeds with a degree of permeability and the reversed flow. Solutes of large size were rejected and remained in the high concentration region of a semipermeable membrane. The acceptable solutes and pure water were allowed to pass into the low concentration region of the membrane. The solute settled on the semipermeable membrane to be removed to avoid any fouling and done by crossflow mechanism. Pressurized water flow was fed in crossflow, which transversely moves away from the solute (impurities) present in the higher concentration side of the membrane while pushing low concentration water (pure) to the other side of the membrane.

A higher rejection rate was observed for multivalent ions, proteins, molecules of less weight (>200 g/mol), sugar, microbes and organic substances. The membrane's pore size lies in 0.5–2 nm and 400–500 Da of molecular weight cut-off (Giorno et al. 2015). Water and some salts are allowed to pass through these nanomembranes, i.e., hydrophilic by nature. Further, nanomembrane works under charge and size of the

solute component under analysis. Temperature, pressure, feedwater concentration, pH and surface charge are important operating parameters of the nanomembrane (Figoli et al. 2010). Contaminant removal and antifouling characteristics of nanofiltration membrane were improved with the fabrication of super hydrophilicity three dimensional hyperbranched glycerol on polyamide thin film nanocomposite (Liu et al. 2017; An et al. 2020).

Nanomembranes find their place in industrial wastewater treatment (removal of organic and inorganic contaminants) and dairy (demineralization) applications (Pal 2017). Nanofiltration membrane had gained more attraction in the wastewater treatment process, whose characteristics lie between ultrafiltration and reverse osmosis methods. Nanofiltration membrane properties, experimental operating conditions, and feed characteristics determine nanofiltration membrane performance (Mulyanti et al. 2018). Nanofiltration membranes are of two types organic and inorganic membranes. An organic membrane includes polyethylene, polypropylene, polyimide, polysulfone, polyethersulfone, polytetrafluoroethylene, cellulose acetate, and polyacrylonitrile (Aliyu et al. 2018). Inorganic membranes widely used for water purification are carbon-based membranes, ceramic, silica, zeolite, liquid and dynamic membranes. The remarkable merits of inorganic nanomembrane are that no external chemical agent initiate the filtration process, high thermal and structural stability to withstand high temperature and corrosive environments (Kayvani Fard et al. 2018). The suitable membrane for the filtration process got selected by its pore size, very low or no fouling and high flux (Obotey Ezugbe et al. 2020).

4.2.2 Carbon Based Nanomembranes

The carbon based nanomembranes are used in oil/water separation due to their high mechanical and chemical stability. Gu et al. (2016) have formed multifunctional carbon nanotubes-based membranes embedded with polyacrylic acid brushes then loaded with silver nanoparticles. The formed hybrid membrane had shown superoleophobic and superhydrophilic under water and oil, respectively. Flux of 2930 ± 448 , 3220 ± 434 and 3480 ± 555 L/m²·h·bar were recorded for water in toluene, chloroform and hexane respectively. Silver nanoparticles acted as a good antimicrobial agent by destroying the DNA replication and cell membrane rupture of the microbes in water. Thus, carbon nanotubes combined with polyacrylic acid and silver nanoparticles membranes had shown its multicapacity in water treatment. Another work shows the coal-based carbon nanomembranes under the influence of electric field has produced enhanced removal efficiency of oil from wastewater and permeate flux. The wonderful separation efficiency was appeared by anodic oxidation by the electric field. Here the optimum level for the study was observed to be electric field strength of 0.31 V/cm, rotation speed of peristaltic pump of 7.5 r/min and electrolytic concentration of 5 g/L (Li et al. 2016).

Carbon hybrid membrane was yielded with ceramic combination for oil eradication (Fard et al. 2018). The membrane is formed by the congress of activated carbon and alumina of high surface area. The contact angle of the membrane was

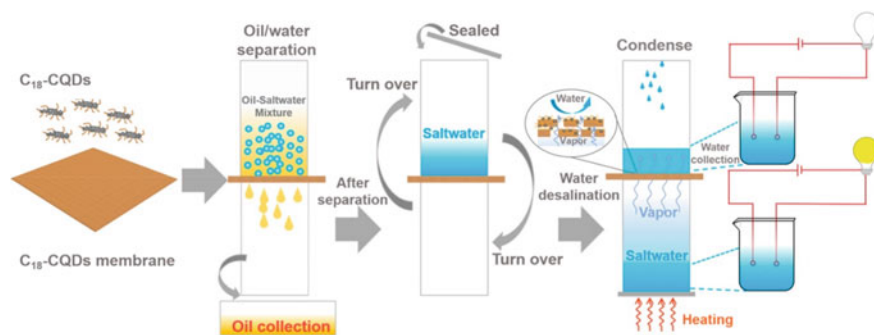


Fig. 4 Cotton textile modified with octadecylamine carbon quantum dots to form nanofiltration membrane for its dual role in oil–water separation and saltwater desalination (adopted from Lei et al. 2019)

zero, enhanced porosity and pored with superhydrophilic properties. Hence, 99% oil removal from oil–water emulsion was carried out on the formation of constant surfactant. Zhu et al. (2018) have proposed the preparation of carbon nanotubes as ultrafiltration membranes as a surfactant in treating oil–water with ionic strength of 100 mM. When the membrane changes to anodic or cathodic, it resists the surfactant molecules or elevates the surfactant concentration, respectively. Hence, the property finds its place in heavy salinity conditions separating oil from water. Further, the surfactant molecule mechanism decreases the oil merging and reduces the fouling effect. Similarly, single hydrophobic carbon-based membranes were prepared for the dual role to separate oil/water and desalination of saltwater. An octadecylamine carbon quantum dots with cotton textile in the presence of tolylene-2,4-diisocyanate by cross linking technique. The membranes showed an appreciable oil–water separation of 99% with excellent permeability irrespective of pH (acid or base) and temperature (low or high). It is worth noting that the liquid water is not allowed to pass through these membranes whereas permeable for water vapour (Fig. 4). Water permeability was given $>145 \text{ kg/m}^2 \cdot \text{h}$ and for oil $>600 \text{ L/m}^2 \cdot \text{min}$. Also, the desalination method had given salinity rejection of 99% for DI water (methyl blue dye added) and different salinity of 3.5, 35, and 300 g/L sodium chloride included brackish, seawater and saline water (Lei et al. 2019).

In the other work, Wu et al. (2020) have fabricated a carbon nanofiber membrane with titanium dioxide nanorods arrays. Carbon nanofiber membrane was developed from polyacrylonitrile and other substances by electrospinning followed by hydrothermal process. The then formed membrane was treated with titanium butoxide for the final nanofiber membrane for the oil–water separation process. The titanium dioxide of the rutile phase has shown better chemical stability, recyclability along withstanding high temperature and corrosion. Due to the membrane's enhanced hydrophilicity and high specific surface area had given out oil–water separation of $1108.8 \text{ L/m}^2 \cdot \text{h}$.

Using a hydrothermal approach, ternary carbon-based nanomembrane of a hydrophilic nature was developed for dye and oil–water separation (Venkateshab et al. 2020). Polyvinylidene difluoride was modified by a hybrid nanocomposite mixture of graphitic carbon nitride, reduced graphene oxide and titanium dioxide by probing the electrospun technique. The membrane showed a high separation efficiency of 95.4 ± 0.1 and $94.2 \pm 0.5\%$ for different oils and methylene blue dye. The pure water flux of the formed membrane was $1261.2 \pm 2 \text{ L/m}^2 \cdot \text{h}$. Recently, Sun et al. (2021) reported synthesizing carbon fiber membrane with a high surface area for oil–water separation. Inside these membranes, pores are developed using zinc acetate, which exhibited superhydrophobicity. Oil flux recorded with the membrane was $3590 \text{ L/m}^2 \cdot \text{h}$ and contact angle of 155.9° . The separation efficiency of emulsified and non emulsified oil in water appeared in the order of 98%. These carbon membranes show good thermal, chemical stabilities, which work under different pH and temperatures.

4.2.3 Ceramic Based Nanomembrane

Alumina

Ma et al. (2019) have engineered a nanofiltration membrane made of amorphous silica doped into alumina (5 mol%) for tertiary treatments, which include removal of coloured organic substance, micropollutants and metal ions. Aluminium isopropoxide and tetraethyl orthosilicate as alumina and silica precursors along with Cetyltrimethylammonium bromide used to produce the highly homogenous nanomembrane using sol–gel technique. Thus, nanomembranes have shown high water permeability, salt rejection values, and organic pollutants. Surfactant concentrations (S/O) of 0.5 and 2.0 have produced high rejection value and high water permeability of $2.3 \text{ L/m}^2 \cdot \text{h} \cdot \text{bar}$. The same group has tested the nanomembrane for filtering neonicotinoid pesticides (cetamidrid, thiacloprid and imidacloprid). The result was 56–85% rejection against the pesticides with a diffusion flux of $14.2 \text{ L/m}^2 \cdot \text{h}$ for a transmembrane at 5 bar pressure (Ma et al. 2020). Very recent, Sherugar et al. (2021) have developed the alumina-based nano matrix membrane for heavy metal removal and improved antifouling characteristics. Zinc was doped into alumina by utilizing the combustion method, followed by polysulfone. The membrane holds a high surface area of $261.44 \text{ m}^2/\text{g}$ with increased porosity, surface charge and hydrophilicity. The presence of bovine serum albumin in feed solution had produced a 98.4% flux recovery ratio to reuse the nanomembrane with the antifouling property. Arsenic and lead were removed at the rate of 87% and 98%, respectively. Alumina with natural polymer chitosan with hydroxypropyl methylcellulose was employed to perform both adsorptions of dye and fluorine removal from groundwater (Barik et al. 2020). It was obtained that 0.1 g of nanocomposite has exhibited adsorption capacity of 125.1 mg/g with 96 and 82.7% removal efficiency of fluorine from groundwater and fluoride solution of concentration $\geq 100 \text{ mg/L}$, respectively. Methyl orange dye adsorption rate occurred as 498 mg/gm. A higher adsorption rate was

due to hydrogen bonding between hydroxyl groups of chitosan and hydroxypropyl methylcellulose and electrostatic interaction aroused from amine groups of chitosan. This nanocomposite had shown good stability with positive charges on the surface. Thus, an effective multipurification of water was demonstrated with alumina based nanomembrane.

Titania

Another interesting work was reported on the construction of titania (TiO_2) and graphene oxide (GO) coupled polymeric nanomembranes used in azo dye degradation (Dadvar et al. 2017). Carbonyl, Carboxyl, and epoxy groups in graphene oxide are responsible for producing hydrophilicity. Further, titania as a semiconductor material degrades the organic substances and encourage antifouling property. Hence, the membrane has shown high diffusion flux, photocatalytic degradation, antifouling effect and organic pollutant adsorption. Cobalt ion (30 mg/L of concentration) removal with this nanomembrane produced 90% efficiency in 5 min. Also, by controlling the thickness of graphene oxide-titania, the passing flow can be changed accordingly, and in turn, the required removal efficiency was obtained. Higher membrane thickness produces low pass flow and vice versa. Bergamasco et al. (2019) have developed titanium dioxide based polyamide nanomembrane for the water treatment. This nanomembrane was procured by self assembling titania on polyamide.

Hydrophilicity was improved by the presence of an OH bond in the modified nanomembrane. Degradation of dyes, organic pollutants, and phenolic compounds was effectively reduced under ultraviolet irradiation of this titanium dioxide fixed polyamide nanomembrane. Similarly, recent work on titanium dioxide nanotube incorporated with polyvinylidene fluoride and polyaniline to form nanocomposite membrane was reported. It was engaged in the degradation of pollutants released from the textile industry (Nawaz et al. 2021). After combining titanium dioxide, the water flux value increased from 312 ± 1.91 to 484.8 ± 2.9 $\text{L/m}^2 \cdot \text{h}$ of polyvinylidene fluoride. Methyl orange dye adsorption was enhanced and 90% of efficiency for pollutant removal under ultraviolet radiation. The high flux ratio of 94% greatly improved the nanocomposite membrane's self-cleaning property. Hence, this study shows that the physicochemical properties, including pore size, active area, mechanical and thermal properties, vary for the nanocomposite membrane from individual pure components. These characteristics of nanocomposite membrane greatly support water purification with multiple applications. Gelde et al. (2021) have proposed the influence of pore radii and porosity of alumina nanoporous membranes coated with titanium dioxide. Two nanomembranes of interpore radii of 10 and 13 nm were prepared and studied with bovine serum albumin as a stable substance. The electrochemical impedance spectroscopic measurements were obtained. The result shows that bovine serum albumin settles on the surface of nanomembrane with lower pore

size, whereas deposits on the pore wall with larger radii. This study proves the importance of nanomembranes' pore size's importance in effective ion transportation and fouling mechanism.

Silicon Carbide

Several groups report silicon carbide nanomembranes and their composites (Xu et al. 2021). Silicon carbide nanomembranes possess very good thermal, mechanical and chemical stability. So, find its vast role in wastewater treatment methodologies. Das et al. (2018) have proved the silicon carbide membrane synthesized to form the oxygen bonding technique holds high corrosion resistance and removal of pollutants than the liquid phase sintering technique. Here, silicon carbide produced 89–93% removal of chemical oxygen demand, 88.4–92% of kitchen wastes solids and 77–86% of oil/grease substances. The result yielded was the porosity 31–43 vol% and flexural strength of ~34–12 MPa for oxygen bonding silicon membrane.

On the other hand, liquid phase sintering silicon membrane has shown 41–51 vol% and 54–30 MPa flexural strength. Also, previously glass clubbed silicon carbide membrane covered with alumina has exhibited a very high rejection rate of 99.9% for oil with a flexural strength of ~81 MPa. The pore size of the homogenous formed membrane influences the outcome of the removal/separation of pollutants from wastewater (Kim et al. 2017). Solar light has driven sea, and domestic water filtration with silicon carbide and carbon composite was developed. The composite exhibits good structure and thermal stability photothermal evaporation of seawater under sunlight (Shi et al. 2018). Even physical cleaning of this membrane by sonication and scrubbing activity have produced no carbon loss to maintain antifouling. In the case of domestic wastewater treatment, the pollutants on the membrane got removed by annealing at 1000 °C in the presence of nitrogen. The pore size varied by controlling the deposition time during the preparation of silicon carbide fixed ultrathin alumina membrane using a chemical vapour deposition method. Chen et al. (2020a, b) have reported pore size of the membrane decrease linearly to 71–47 nm by increasing the deposition time from 0 to 120 min. A thin, dense layer resulted above 120 min of deposition time instead of the membrane with pores. The membrane has produced pure water permeance of 350 to 157 L/m² · h · bar with increased deposition time. Hydrophilic and interaction of charges of the silicon carbide membrane had given low fouling and less permeance loss when compared to that of the pristine membrane in separation oil from the oil–water emulsion. Another work reported on the synthesis of silicon carbide by dip coating technique by water dispersion of α -silicon carbide powder. In this work, they propose the influence of coating parameters (temperature, particle size, mixing ratio etc.) and to optimize for final product suspension (Eray et al. 2020). It is worth noting that flawless membranes are obtained by increasing the silicon carbide coarse powder ratio to silicon carbide fine powder. Thus, the homogeneous silicon carbide membranes without any defect (sintering temperature 100 °C and selected binder) were produced for secondary effluent removal from wastewater. The colloidal substances and suspended solids were removed at the percentage of

96%, and 99.4%, respectively and chemical oxygen demand was found to be reduced by 83%.

Zirconia

Zirconia is another substance that comes under the ceramic group. The Zirconia membrane possesses high chemical, mechanical and thermal stability with appreciable hydrophilicity. Hence, the high filtration efficiency percentage provided a significant water purification system. Yang et al. (2016) have fabricated the zirconium oxide (multiwall carbon nanotubes) based ultrafiltration membrane poly(vinylidene fluoride) with hydrophilic nature for oil/water separation. Homogenous dispersion of zirconium oxide had resulted in a final composite membrane with low contact angle, super hydrophilicity and increased pure water flux than pure poly(vinylidene fluoride) membrane. An oil rejection ratio was ~95%, leading to the antifouling property. Following, a high hydrophilic hybrid membrane was engineered by functionalizing zirconium oxide on poly(N-acryloyl morpholine) fixed poly(vinylidene fluoride) for effective oil/water segregation (Shen et al. 2017). This was carried out through the facile phase inversion method to obtain uniform nanoparticles. Protein absorbed on this hybrid membrane was very less when compared to raw polyvinylidene fluoride membrane. Feature of the membrane converts to spongy layer from finger like structure by increasing the concentration of zirconium oxide-poly(N-acryloyl morpholine) in the casting solution.

Also, the pore size and porosity got affected, and a rough surface was generated. Hence, due to the dense surface of membrane projects rejection ratio is as high as 99.9% and exhibits antifouling property. Zirconium oxide coated on stainless steel mesh was used to separate oil/water. The electrophoretic deposition technique was used for coating. Oleophobic and superoleophobic surfaces were introduced underwater. The structure formed was highly hydrophilic and had 97.5% separation efficiency for oil from water. Hence, oil is difficult to enter through the zirconium layer deposition. After thirty cycles of scrapping with sandpaper, the separation efficiency was high, and the angle contact of oil underwater reduced to 140°. Thus, the zirconium oxide coated stainless steel was the best separator of oil/water (Chen et al. 2018).

Also, defluoridation of groundwater was executed with zirconium based adsorbents. Through electrospinning technique, hydrous zirconium oxide modified by polyethylenamine (branched) fixed polyacrylonitrile nanocomposite was constructed. Fixed bed column and spectroscopic techniques were used in the confirmation of the adsorption capacity of the material. At neutral conditions, the fluoride adsorption capacity of the nanocomposite was found to be 67.51 mg/g, and 4300 kg water/kg water was treated by the composite material (Wang et al. 2019c). Recently, the inner membrane with zirconia and kaolin clay was developed for drinking water purification (Boussemghoune et al. 2020). This ceramic membrane holds all coliforms (type of bacteria) present in water with improved physicochemical quality of drinking water. External chemicals chlorine (disinfectant) and aluminium

(coagulator) usage was greatly declined or not required in the presence of zirconia membrane. Following, zirconia based ultrafiltration membrane with Moroccan clay was employed to eliminate acid orange 74 dye (AO74) (Elomari et al. 2021). Zirconia membrane on clay was carried out by depositing the zirconyl oxalate by a dip coating method. Zirconyl oxalate was synthesized from zirconium oxychloride as a precursor and oxalic acid using a sol-gel route with a pore diameter of 80 nm. Diffusion capability was recorded as $36 \text{ L/m}^2 \cdot \text{h} \cdot \text{bar}$ and dye rejection rate of $\sim 98\%$ for pressure ranging from 1 to 3 bar. Thus, the above study describes the multi applications of zirconium as dye remover, oil/water separator, and defluoridation activity.

Polymer Based Nanomembrane

Xiao et al. (2016) have designed the conducting polymer-based coaxial like cable mesh to separate oil/water mixture with 99.09% efficiency. Polyaniline/polypyrrole was combined with the stainless-steel mesh and stearyl chloride by electropolymerization and acylation to attain the superoleophilic and superhydrophobic mesh to withstand different environmental conditions. The contact angles for oil and water were found to be 0 and 154° , respectively. Even after 25 times of reuse of the mesh, the separation efficiency was $>98\%$ with ultra stability. Similarly, ultradurable superhydrophilic and underwater superoleophobic membranes were obtained by vapour nano-coating polyisocyanate (130 nm) on woollen fabrics. The membrane possesses an oil/separation capability of 99.9% with excellent durability. Recently, Wang et al. (2020) have successfully prepared the biodegradable nanofiltration membrane with supporting, connection and active layers made up of regenerative cellulose membrane by self-polymerization of dopamine. Thus, stable polyamide nanofiltration membrane with water flux in the range of $14.04\text{--}25.06 \text{ L/m}^2 \cdot \text{h}$ (78.5% enhanced) and a good rejection rate for salt solution in water purification. The rejection order as $\text{Na}_2\text{SO}_4 > \text{MgSO}_4 > \text{NaCl} > \text{MgCl}_2 > \text{CaCl}_2$.

Zeolite Based Nanomembrane

Zeolite membrane NaY was combined with alpha and gamma alumina to check for its oil/water emulsion separation. The rejection percentage of alpha and gamma alumina was found to be 84.9 and 92.2%, whereas zeolite (NaY) combined alpha and gamma alumina composites showed 98.7 and 95.7%. These results show the presence of zeolite improves the oil/water separation process. Due to its properties like porosity and tortuosity. Further, the flux 1024 and $716 \text{ L/m}^2 \cdot \text{h} \cdot \text{bar}$ was tabulated for zeolite (NaY) combined alpha and gamma alumina respectively (dos Santos Barbosa et al. 2018). Barbosa and Rodrigues (2019) have prepared the zeolite membrane MCM-22 by utilizing vapor phase transport and dip coating techniques at 150°C for oil/water emulsion separation. The permeation concentration was observed to be 3.2 and 3.9 mg/L for the membranes prepared from dip coating and vapor phase transport techniques. Following, the same group has proposed the preparation of NaA zeolite

with gamma-alumina nanomembrane for efficient oil/water separation. The removal of oil content from water for disposal 29 mg/L the permeable concentration was less than the standard allowed disposal value. The removal efficiency of oil was 97.8%. Due to the thickness of the membrane, water flow was found to be low at $150 \text{ L/m}^2 \cdot \text{h}$ (Barbosa et al. 2020).

Zeolite based thin film nanocomposite forward osmosis membrane was synthesized by incorporating zeolitic imidazolate framework (ZIF-8) coated with poly(sodium 4-styrene sulfonate) (PSS). The chemical stability of the membrane got increased by the inclusion of PSS. Pure water flux was greatly enhanced (116.2%) by the addition of an acid acceptor-triethylamine. In the absence of triethylamine, sodium chloride rejection minimally at 61.1%. This thin film nanocomposite membrane has enhanced swelling resistance in oil separation (Beh et al. 2020). Zeolite nanomembrane for pore size 28 nm ultrafiltration was developed for the oil/water nano-emulsion segregation process. These nanomembranes have a 20% increased flux than the zeolite micro membrane at 70 kPa pressure. Depending on the type of oil, the flux lies in the range of $45\text{--}70 \text{ L/m}^2 \cdot \text{h}$. Here, motor oil, xylene and crude oil mixture for 600 mg/L. Low flux was observed for motor oil due to the presence of heavy components than the other two xylene and crude oil. Further, the zeolite nanomembrane possessed super hydrophilicity in air and superoleophobicity inside the water with a 156° contact angle. For low oil content of $1.57 \pm 0.2 \text{ mg/L}$, the high oil rejection rate was 99.8% (Anis et al. 2021).

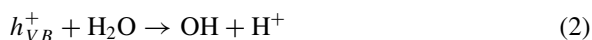
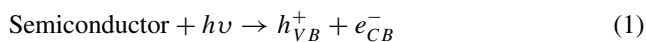
4.3 Nanophotocatalysts for the Detection and Removal of Pollutants

4.3.1 Photocatalyst and Its Mechanism

In 1972, Akira Fujishima and Kenichi Honda discovered the photocatalysis process. Photo means photons (light) and catalysis (chemical reaction). Photolysis of water occurred electrochemically between electrodes of titanium dioxide and platinum. Under ultraviolet exposure, electrons from titanium dioxide moved towards the platinum. Thus, titanium dioxide acts as an anode at which oxidation occurs, whereas platinum acts as cathode accepting electrons into it, releasing hydrogen through a reduction reaction. By definition, photocatalysis is defined as the acceleration of photogenerated electrons in the presence of photocatalyst, and photocatalyst experiences no change after reaction got over (Ganguly et al. 2019).

Photocatalyst is the material that absorbs incident light energy, generating holes and electrons at valence (lowest unoccupied molecular orbital-LUMO) and conduction bands (highest occupied molecular orbital-HOMO), respectively. Then, provide that higher energy to a reactant substance readily available for a chemical reaction (Oshida 2013).

By equation,



The energy difference between valence and conduction band decides the nature of the material and is known as a bandgap (E_g). Bandgap for metal (conductor), semiconductor and insulator were <1.0 eV, $1.5\text{--}3.0$ eV and > 5.0 eV respectively. Insulating materials have no free electrons to promote the oxidation process. Semiconductors are active towards light excitation under room temperature producing electron–hole pairs. These holes oxidize the donor molecules (oxidation), and electrons reduce the acceptor molecules (reduction) simultaneously. Hence, semiconductor-based photocatalysis has gained importance in overcoming recombination of charges and recyclability. Further, the unique characteristics of nano photocatalyst made it readily available for wastewater treatment with eco-friendly nature (Fig. 5).

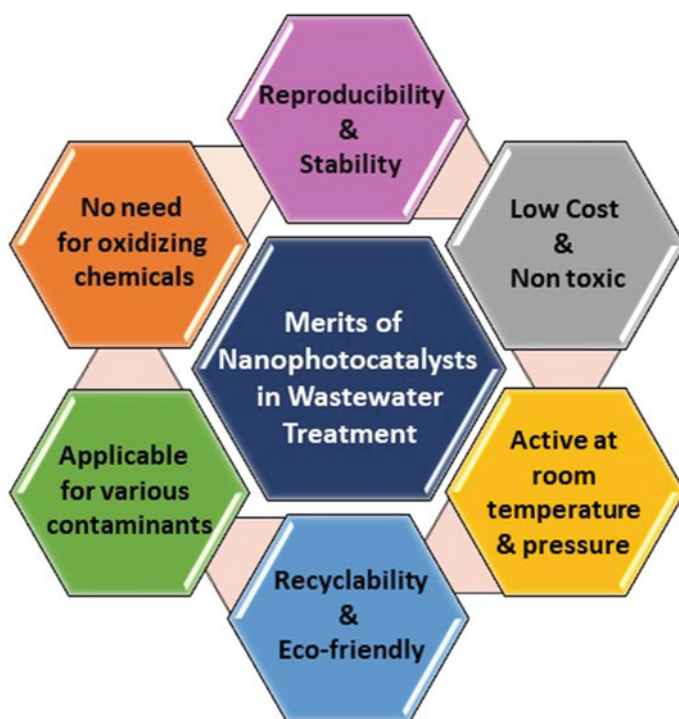


Fig. 5 Graphical representation of merits of nano photocatalysts utilized in the wastewater treatment process

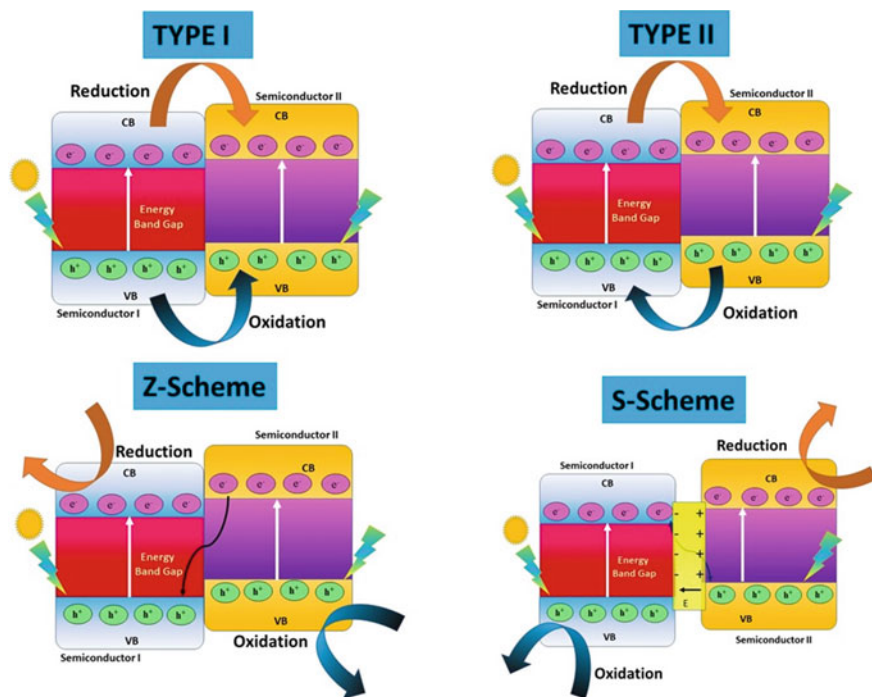


Fig. 6 Schematic diagram representing the various heterojunction photocatalysts of type I, type II, Z-scheme and S-scheme systems with respective charge carriers transformation

4.3.2 Types of Photocatalyst

Photocatalysts are divided into homogenous and heterogeneous. Homogeneous photocatalyst has semiconductors, and reactant substances are in the same phase, whereas in different phases in heterogeneous photocatalyst (Ameta et al. 2018). Further, heterogeneous photocatalysts are classified into type I, type II, Z-scheme and S-scheme, as given in the Fig. 6.

4.3.3 Operating Parameters of Photocatalyst

Important operating parameters in the photocatalytic process are pH and temperature of the solution, size, surface area and concentration of photocatalyst, intensity and exposure time of light and presence of donors and acceptors.

4.3.4 Dye Degradation by Nano Photocatalyst

Copper doped zinc oxide photocatalyst was prepared using the co-precipitation method to degrade direct blue 71 (DB 71) dye. At pH 6.8, a photocatalyst of 3 g/L had produced the entire degradation of direct blue 71 dye 0.01 g/L under visible light exposure of 120 min. Reusability tests show that 96.19% of the dye degraded proficiently even after three cycles. Due to the oxidation mechanism of photocatalyst, the degradation/detoxification of dye takes place (Thennarasu et al. 2016). Balcha et al. (2016) have reported that zinc oxide photocatalyst made out of sol-gel technique (with suitable capping ligands) appeared to be better than precipitation method to achieve the elevated photocatalytic activity. Under ultraviolet irradiation, zinc oxide photocatalyst (250 mg/L) prepared from sol-gel and precipitation had given 92.5 and 81% of degradation of methylene blue dye. The photocatalytic mechanism shows the reaction comes under pseudo first order kinetics. In this work, starch is better than polyethylene glycol due to its hydroxyl group strong binding with zinc oxide. Another work represents the formation of p-n type heterojunctions by using the p-type (copper oxide) and n-type semiconductors (zinc oxide or iron oxide) in the degradation of Congo red dye under solar light activation (Malwal et al. 2016). The role of pH was studied, point of zero charges was maximum at pH 4 and 9, which states that photocatalysts are active at acidic and alkali conditions. Here, three-dimensional p-n type of photocatalysts extends the activity by the enhanced separation rate of charge carriers. Iron oxide coupled copper oxide (94%) showed the highest degradation of dye followed by zinc oxide combined copper oxide (90%), copper oxide (74%) and copper foam (60%) under 300 min of solar excitation. The surface area of the photocatalyst remains a prominent reason for reducing industrial dyes. Tripathy et al. (2017) have fabricated zinc oxide nano nails and nanorods for comparative study of degradation of crystal violet dye underexposure of ultraviolet irradiation. The degradation analysis reported that zinc oxide nanonails with a surface area of 56.8 m²/g had degraded the crystal violet dye at the rate of ~95% within 70 min of exposure to ultraviolet radiation. But zinc oxide nanorods had provided only ~82% degradation efficiency. Successive degradation of zinc oxide nanonails was due to its more contribution of active sites, high crystalline nature and elevated level of reactive species to support the photo-degradation. Kamaraj et al. (2018) have developed a p-n heterojunctions photocatalyst out of the combination of copper oxide and lead oxide by a facile wet chemical technique. The photocatalyst degraded Rhodamine B dye at a rate constant of 0.092 per minute with a decomposition rate of ~99% under 90 min exposure of xenon lamp ($\lambda > 420$ nm). Individual copper oxide and lead oxide have produced 64 and 30% degradation percentages, respectively. The work clearly represents the significance of the combination of the p-n type of semiconductors to yield photocatalyst for dye removal from industrial wastewater.

Similarly, Nguyen et al. (2018) have reported noble metal palladium doped titanium dioxide for the degradation of methylene blue dye and methyl orange dye under an ultra violet range of excitation. The prepared photo-nano catalyst has exhibited exceptional stability. Further, the large-scale production with sol-gel technique and easy separation after dye degradation made this photocatalyst available for dye

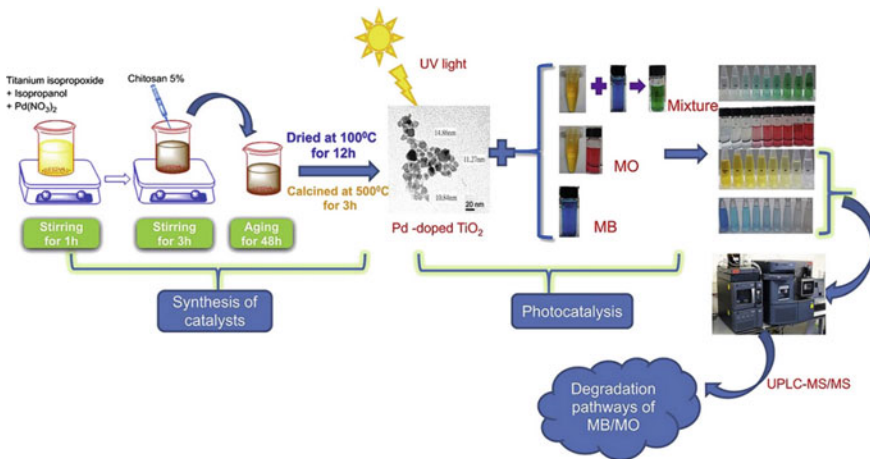


Fig. 7 Synthesis of palladium doped titanium dioxide using a simple sol–gel technique for the photocatalytic degradation of methylene blue and methyl orange dyes followed by the identification of intermediates by utilizing ultra-performance liquid chromatography in the wastewater treatment for its reuse (adopted from Nguyen et al. 2018)

degradation in water treatment (Fig. 7). Molybdenum oxide nanosheets prepared through liquid exfoliation have shown near infrared plasmonic resonance at visible light exposure. Instead of the bulk structure of molybdenum oxide, aqueous molybdenum oxide nanosheets possessed more photocatalytic activity in degrading dyes. Rhodamine B or methylene blue dyes (47.6 mg/L) of 20 mL mixed with 8 mg of molybdenum oxide for 10 min of exposure of visible light of power 150 W. Localized surface plasmon resonance absorption peaks were observed at 1160 and 954 nm. The absence of characteristic peaks of dyes in Fourier transform infrared spectroscopic analysis suggests the degradation of dyes about ~ 45–80% percentage. These results show the release of more free charge carriers to conduct the photocatalytic process (Etman et al. 2018).

Mahalingam et al. (2018) have constructed ternary hybrid nanocomposite from mixing iron oxide, nickel oxide, and reduced graphene oxide in treating the synthetic, influent, and effluent dyes present in industrial wastewater. The nanocomposite was prepared through in situ hydrothermal technique. Crystal violet and methyl red synthetic dyes are removed with 99% degradation efficiency within 15 min of exposure to photocatalyst (2 wt%) under visible light excitation. Influent and effluent dyes are removed at 87% and 97% within 300 and 60 min of visible light exposure, respectively. These efficient results are attained due to the release of more oxide and hydroxyl radicals by the interaction of functional groups of reduced graphene oxide and photoexcited electrons in the conduction band of the system.

Similarly, Shubha et al. (2021) have given out the worth of ternary nanocomposite forming heterostructure in the deradation of methylene blue dye. Oxides of zinc, europium and nickel are combined through one pot combustion process to form

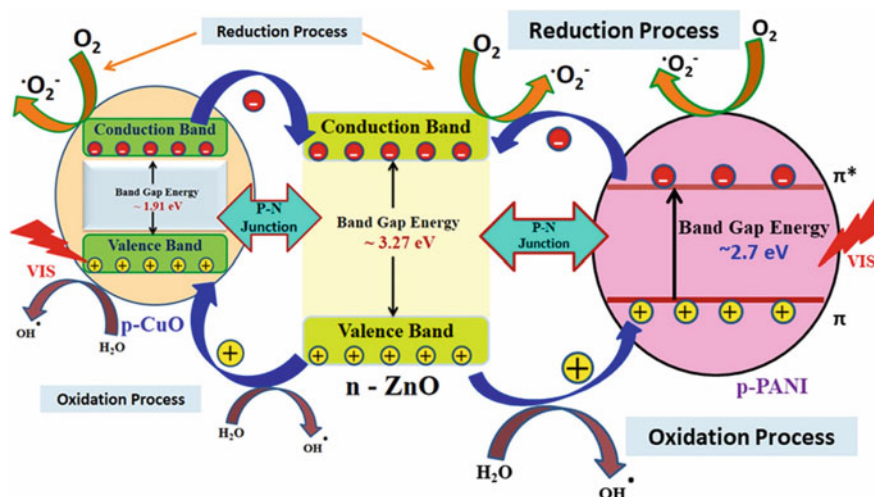


Fig. 8 Schematic illustration of nano photocatalyst of p-n-p type (here CuO–ZnO–polyaniline) engaged in the degradation of 4-chlorophenol, one of the hazardous contaminants of polluted water under visible light excitation (Rajendran et al. 2021)

the final nano photocatalyst. This heterostructured nanocomposite was found to be very active in the degradation of methylene blue dye at the exposure of visible light and pH dependent. Recently, another natural nano photocatalyst film came out of a combination of chlorophyll, polyvinyl alcohol, zinc oxide and silver iodide for a dual role in removing pollutants and antimicrobial activity (Soltaninejad et al. 2021). Methylene blue degraded with 95.5% efficiency in 60 min, whereas Congo red and 4-chlorophenol decomposed at the rate of 92 and 88% for 150 and 270 min, respectively. Another work on the degradation of 4-chlorophenol with copper oxide (p-type), zinc oxide (n-type) and polyaniline (p-type)- the p-n-p combination was employed (Rajendran et al. 2021) (Fig. 8). Conducting polymer polyaniline led to one more channel along with p–n junction, which absorbs more photons and is highly stable to induce photocatalytic activity in the degradation of 4-chlorophenol (88%).

Wang et al. (2019d) proposed the ternary magnetic-based nanocomposite rose out of silver carbonate, bismuth oxyiodide and cobalt ferrite nanoparticles by utilizing deposition and precipitation. Combining the bandgap of three components suitably to obtain the p-np model had produced an increase in the absorption of a photon to produce dense charge carriers for an efficient photocatalytic activity. The nanocomposite of p-n-p type was noticed for its wonderful role in removing the elemental mercury (HgO) in the wet flue gas from jet bubble type reactor. The main reactive component involved ineffective removal of elemental mercury (98%) was superoxide anion radical. O₂^{•-}. Carbonate ions and sulphur dioxide occurred as an important constraint in removing mercury. Table 2 provides various nano photocatalysts in the treatment of industrial wastewater.

Table 2. Summarization of nano photocatalyst engaged in the removal of heavy metal ions, degradation of pharmaceuticals and microbes present in industrial wastewater

Photocatalyst	Target	Source of light	Initial concentration	pH & Time	Degradation efficiency (%)	Dose of photocatalyst	References
PVA/ZnO polymer	Arsenic	–	30 mg/L	9 & 38 s	97	0.01 mg	Sargazi et al. (2019)
ZnO–TiO ₂	Arsenic	UV & visible	0.1 ppm	– 120 min	>70	–	Arabnezhad et al. (2019)
ZnO	Arsenic & lead	UV source	5 mg/L	8 & 60 min	98.3 & 99.8	250 mg/L	Moafi et al. (2021)
Curcumin/ZnO	Arsenic	Xenon (100 W)	903 µg/L	– 30 min	93.6	31.5 mg/g	Moussawi et al. (2016)
ZnFe	Arsenic	Xenon (500 W)	1000 µg/L	6 & 30 min	90.8	0.2 g/L	Di et al. (2017)
Ag/TiO ₂ /Fe ₃ O ₄ @GO	Arsenic (III & V)	–	24 & 17 ppm	5 & 90 min 3 & 30 min	91 & 87	20 & 11 mg	Miranzadeh et al. (2020)
Eosin Y-sensitized TiO ₂	Cadmium	Xenon (100 W)	20–100 ppm	7 & 3 h	37–100	~42 ppm	Chowdhury et al. (2017)
TiO ₂ /ASS	Cadmium	–	30 mg/L	7 & 5 h	>90	100 mg	Rashed et al. (2017)
EDTA/Chitosan/TiO ₂	Cadmium	UV-A lamp (365 nm)	100 mg/L	5 & 120 min	82	1 g/L	Alizadeh et al. (2018)
RS-TONR/TiNT	cadmium	Xenon (420 nm)	50 ppm	–	–	–	Kim et al. (2018)
ZnO@activated carbon (3:7)	Cadmium	–	100 ppm	2–7 & 90 s	86.4	1 mg/ml	Alhan et al. (2019)

(continued)

Table 2 (continued)

Photocatalyst	Target	Source of light	Initial concentration	pH & Time	Degradation efficiency (%)	Dose of photocatalyst	References
NiFe ₂ O ₄ -Pd	Cadmium & lead	Xenon (300 W)	-	-	97 & 98	-	Thomas et al. (2020)
TiO ₂ @rGO	Chromium and lead	Mercury lamp (300 W & 400 nm)	50 mg/L	2 & 5.5 & 150 min	91 & 89.2	0.4 g/L	Al-Qahtani et al. (2020)
g-C ₃ N ₄ /MIL-53(Fe)	Chromium	Xe lamp (500 W)	10 ppm	-	~ >95	20 mg	Huang et al. (2017)
Mn ion doped ZnO	Chromium	Non-halogen lamps (250 W, 24 V)	40-80 ppm	180 min	72	40-60 mg L ⁻¹	Kumar et al. (2017)
MoS ₂ /CPVA	Chromium	Xenon (300 W)	25-75 ppm	-	96	5-15 mg/L	Wang et al. (2019a)
CD/SnS ₂	Chromium	Xenon (250 W)	50 ppm	-	77.34	50 mg	Han et al. (2019)
ZnO	Lead	UV	150 ppm	-	-	-	Park et al. (2020)
TiO ₂	Lead	UV lamps	1.25-10 ppm	2.5 min	82.53	-	Sethy et al. (2020a, b)
N-doped TiO ₂	Lead	Wolfram lamps philip 20 W	15 mg/L	7.6-7.8 & 12 h	98%	15 mg	Wahyuni et al. (2021)
Cu-TiO ₂ Nanotubes	Lead	Germicidal light (UV light 120 W)	100 ppm	11 & 5	79.5 & 56.3	-	Sreekantan et al. (2014)

(continued)

Table 2 (continued)

Photocatalyst	Target	Source of light	Initial concentration	pH & Time	Degradation efficiency (%)	Dose of photocatalyst	References
SrWO ₄	Lead	Halogen lamp (Okano 1000 W)	8.40 ppm	4.5	–	0.30 g	Sharma et al. (2013)
TiO ₂ -PVA-alginate beads	Lead	Sunlight	25 mg/L	7 & 150 min	99.1	50 mg/L	Idris et al. (2016)
MnO ₂ /TiO ₂	Lead	UV lamp (6 W)	500 ppm	4.9	–	0.1 g	Kobayashi et al. (2017)
TiO ₂ -Citric acid complex	Cu(II), Ni(II), Pb(II) and Zn(II)	Solar energy	20 mg/L	6.5–8 & 9–17 h	97, 36.4, 41.4 and 22.2	2 g/L	Kabra et al. (2008)
La ₂ O ₃ -modified CeO ₂	Lead	Hg-Xe lamp (200 W)	1000 mg/L	5–6	56	50 mg	Ayawanna et al. (2019)
WO ₃ /TiO ₂	Lead	UV light (254 nm)	10–25 mg/L	6	74.7	22–26 mg/g	Mirghani et al. (2015)
CdO/ZnO	Mercury	Visible light	–	–	100	–	Mohamed et al. (2021a, b)
g-C ₃ N ₄ /Bi ₅ O ₇ I	Mercury	LED (9 W)	60 µg/m ³	–	80.3	–	Zhou et al. (2020)
SrRuO ₃ /C ₃ N ₄	Mercury	Visible light	–	50 min	100	–	Albukhari et al. (2021)
Bi ₂ O ₃ /MIL-53(Fe)	Mercury	Visible light	–	–	74.19	–	Guo et al. (2021)

(continued)

Table 2 (continued)

Photocatalyst	Target	Source of light	Initial concentration	pH & Time	Degradation efficiency (%)	Dose of photocatalyst	References
TiO ₂ /Fe ₃ O ₄	Uranium	Mercury lamp (100 W)	0.1 mM	8.3 & 30 min	36.4	0.38 g/L	Li et al. (2017)
mesoporous CuO/ZnO	Mercury	Visible light	–	60 min	100	–	Mohamed et al. (2021a, b)
Palygorskite (Pal) AgBr–TiO ₂	Tetracycline hydrochloride	Xenon lamp (300 W)	10 mg/L	9	90	0.5 g/L	Shi et al. (2020)
WO ₂ -7ZnIn ₂ S ₄ hybrid	Tetracycline hydrochloride	Xenon lamp (300 W)	30 mL	60 min	97.3	30 mg	Chen et al. (2020a, b)
CoO/CuFe ₂ O ₄	Tetracycline	Sun light	20 mg/L	6 & 60 min	52–93	50 mg	Ifebajo et al. (2019)
Au/Pu/g-C ₃ N ₄	Tetracycline hydrochloride	Xenon lamp (500 W)	20 mg/L	3 h	93	100 mg	Xue et al. (2015)
CdS/Nitrogen-Doped-Carbon	Tetracycline	Visible light	–	1 h	83	–	Cao et al. (2019a, b)
Bi/BiOBr	TC (tetracycline hydrochloride), CIP (ciprofloxacin) and DOX (doxycycline)	Xenon lamp (300 W)	75 mL	30 min	100	60 mg	Cao et al. (2019a, b)
CoFe ₂ O ₄ @CuS	Penicillin G	UV light	0.2 g/L	5 & 120 min	70.7	10 mg/L	Kamranifar et al. (2019)

(continued)

Table 2 (continued)

Photocatalyst	Target	Source of light	Initial concentration	pH & Time	Degradation efficiency (%)	Dose of photocatalyst	References
C ₃ PbBr ₃ /CN	7-aminocephalosporanic acid	UV light (300 W Xe lamp)	10 mg mL	140 min	92.79	100 mg	Zhao et al. (2019)
SnO ₂ /BiOI	Oxytetracycline hydrochloride	Xenon lamp (300 W)	50 mg	5.49 & 90 min	94	50 mL, 10 mg/L	Wen et al. (2017)
				140 min	80.9	10 mg/mL	Ji et al. (2018)
ZnO@ ZnS	Tetracycline hydrochloride	Xenon lamp (500 W)	–	2 h	94.39	15 mg/mL	Boxi and Paria (2014)
Ag@TiO ₂ , CdS, & ZnS	Metronidazole	Mercury vapor lamp (125 W)	0.5 g/L		95.11		
					94.9		
					96.15		
Ag/Bi ₁₂ O ₁₇ Cl ₂	Sulfamethazine	Xenon lamp (300 W)	10 mg/L	30 min	86	50 mg	Zhou et al. (2018)
Ag-bridged 2D/2D Bi ₅ FeTi ₃ O ₁₅ /ultrathin g-C ₃ N ₄	Tetracycline	300 W Xe lamp	20 mg/L	20 min	60–72	0.05 g	Wang et al. (2019b)
CdS@AC	Tetracycline	Visible light	–	1 h	72.5	–	Yu et al. (2018)
RGO/g-C ₃ N ₄ /BiVO ₄	Tetracycline hydrochloride	Tungsten light lamp (500 W)	40 mL	150 min	91.5	40 mg	Jiang et al. (2017)
				30 min	–	50 mg	Yan et al. (2016)
(NGQDs)-BiVO ₄ /g-C ₃ N ₄	Tetracycline (TC), oxytetracycline (OTC) and ciprofloxacin (CIP)	Xenon lamp (250 W)	100 mL	30 min			

(continued)

Table 2 (continued)

Photocatalyst	Target	Source of light	Initial concentration	pH & Time	Degradation efficiency (%)	Dose of photocatalyst	References
Ag/BiVO ₄	Tetracycline	Xenon lamp (300 W, $\lambda = 420$ nm)	20 mg/L	120 min	75.43	0.03 g	Chen et al. (2016)
Bi ₃ TaO ₇ QDs and g-C ₃ N ₄ NSs	Ciprofloxacin	Blue LED lamp ($\lambda = 420$ nm, 86 W) ^a	10 mg/L	2 h	91	0.05 g	Wang et al. (2017)
GCN/NiFe ₂ O ₄	Oxytetracycline	Solar light	50 mL	10 h	97	0.50 g/100 ml	Sudhaik et al. (2018)
Cu ₂ O/rGO on Vietnamese traditional paper	Ciprofloxacin	Solar light	10 mg/L	1.5 h	80	0.02 g	Uyen et al. (2020)
RGO-CdS/ZnS	Tetracycline	Xenon lamp (300 W, $\lambda = 420$ nm)	15 mg/L	60 min	90	0.05 g	Tang et al. (2015)
UV/ZnO	Penicillin G	UV	10 mg/L	5 & 180 min	74.65	0.1 g/L	Chavoshan et al. (2020)
ZnO/N,S-CQDs	Ciprofloxacin	Stimulated (Xenon 300 W) & natural sunlight	25 mL (2 × 10 ⁻⁵ M)	20 min & 50 min	92.9 85.8	10 mg	Qu et al. (2020)
p-CaFe ₂ O ₄ @n-ZnFe ₂ O ₄	Tetracycline and ciprofloxacin	125 W, mercury lamp	100 mL	60 min	89.5 and 78%	100 mg	Behera et al. (2019)
CdS-CaFe ₂ O ₄ -clinoptilolite	Cefazoline	Visible light	15 mg L ⁻¹	7 & 90 min	86	0.6 g L ⁻¹	Ataai et al. (2021)

(continued)

Table 2 (continued)

Nanophotocatalyst	Microbes	Incubation	Antimicrobial test	Minimum inhibitory concentration	Zone of inhibition (mm)	Dose of nanophotocatalyst	References																																					
Ag@g-C ₃ N ₄	Escherichia coli, Staphylococcus aureus, and Pseudomonas aeruginosa	24 h incubation@ 37 °C; 150 rpm	Agar disk-diffusion method	37.5 µg/mL	-	10 µg/mL	Khan et al. (2018)																																					
								γ-Bi ₂ M ₂ O ₆	Escherichia coli, Staphylococcus aureus, Aspergillus niger	-	Agar-well diffusion method	-	10	10 mg/ml	Lavakusa et al. (2020)	10	18	Ag-ZnO-Fe ₃ O ₄ n	MRSA, Listeria monocytogenes, Candida albicans, Staphylococcus epidermidis, Staphylococcus aureus, Escherichia coli, Acinetobacter baumannii	37 °C for 24 h under LED light	Well diffusion assay	50 mg/ml	21	-	Abutaha et al. (2020)	23	24	26	20	24	17													
													γ-Bi ₂ M ₂ O ₆			Escherichia coli, Staphylococcus aureus, Aspergillus niger	-						Agar-well diffusion method			-	10	10 mg/ml	Lavakusa et al. (2020)	10	18	Ag-ZnO-Fe ₃ O ₄ n	MRSA, Listeria monocytogenes, Candida albicans, Staphylococcus epidermidis, Staphylococcus aureus, Escherichia coli, Acinetobacter baumannii	37 °C for 24 h under LED light	Well diffusion assay	50 mg/ml	21	-	Abutaha et al. (2020)	23	24	26	20	24
γ-Bi ₂ M ₂ O ₆	Escherichia coli, Staphylococcus aureus, Aspergillus niger	-	Agar-well diffusion method	-	10	10 mg/ml	Lavakusa et al. (2020)																				10			18	Ag-ZnO-Fe ₃ O ₄ n						MRSA, Listeria monocytogenes, Candida albicans, Staphylococcus epidermidis, Staphylococcus aureus, Escherichia coli, Acinetobacter baumannii			37 °C for 24 h under LED light	Well diffusion assay	50 mg/ml	21	-
					γ-Bi ₂ M ₂ O ₆			Escherichia coli, Staphylococcus aureus, Aspergillus niger	-	Agar-well diffusion method	-	10		10 mg/ml	Lavakusa et al. (2020)																													
												10																																
18																																												
Ag-ZnO-Fe ₃ O ₄ n	MRSA, Listeria monocytogenes, Candida albicans, Staphylococcus epidermidis, Staphylococcus aureus, Escherichia coli, Acinetobacter baumannii	37 °C for 24 h under LED light	Well diffusion assay	50 mg/ml	21	-	Abutaha et al. (2020)																																					
					23																																							
					24																																							
					26																																							
					20																																							
					24																																							
					17																																							

(continued)

Table 2 (continued)

Nanophotocatalyst	Microbes	Incubation	Antimicrobial test	Minimum inhibitory concentration	Zone of inhibition (mm)	Dose of nanophotocatalyst	References
Thorn-like TiO ₂ nanoarrays	Escherichia coli, Staphylococcus aureus, MS2 coliphage	UV illumination (a black light blue (BLB) lamp (4-W, $\lambda = 350\text{--}400\text{ nm}$)), 48 h incubation	Drop test method	–	~ >95% inactivation efficiency	–	Kim et al. (2019)
10% CdS-Ag ₂ S	Pseudomonas aeruginosa, Staphylococcus aureus and Escherichia coli	Incubation 37 °C for 24 h	Well diffusion method	87 μm	35.88	150 μL	Iqbal et al. (2019)
				565 μm	30.23		
				169 μm	39.24		
PEI-ZnO/GQD	Escherichia coli	Incubation 37 °C for 24 h	–	2 mg/ml	–	0.5 mL	Liu et al. (2019)
MnNPs	Escherichia coli Staphylococcus aureus	Incubation 37 °C for 24 h	Disc diffusion method	–	22 \pm 0.25 24.5 \pm 0.55	1 mg/mL	Kamran et al. (2019)
Cu-Doped TiO ₂	Escherichia coli Staphylococcus aureus	Incubation 37 °C for 24 h	Agar-well diffusion method	1 g/L	100% removal	1 g/L	Mathew et al. (2018)
SnO ₂ /TiO ₂ /RGO	Escherichia coli	Tungsten halogen lamp, Incubation 37 °C	Agar-well diffusion method	1 mg mL	–	–	Yao et al. (2019)
GO/g-C ₃ N ₄	Escherichia coli	300 W xenon lamp; 2 h	Plate count	–	97.9%	100 $\mu\text{g/mL}$	Sun et al. (2017)

(continued)

Table 2 (continued)

Nanophotocatalyst	Microbes	Incubation	Antimicrobial test	Minimum inhibitory concentration	Zone of inhibition (mm)	Dose of nanophotocatalyst	References
GO-Ag-TiO ₂ @ZnO	Staphylococcus aureus	Incubation 37 °C for 24 h	Disc-diffusion method	–	–	0.005 g/10 ml	El-Shafai et al. (2019)
	Bacillus anthracoides Escherichia coli Pasteurella multocida						
rGO-WO ₃	Bacillus subtilis Pseudomonas aeruginosa	Incubation 37 °C for 24 h	Agar-disc-diffusion method	–	–	100 µg/ml	Ahmed et al. (2018)
Ag/Ag ₂ S/rGO s	Escherichia coli	Incubator at 37 °C for 24 h	Agar-disc-diffusion method	–	97.76%	0.034 g/L	Huo et al. (2018)
g-C ₃ N ₄ /PVA	Pseudomonas aeruginosa	Incubation for 30 min at 37 °C; visible light exposure	Agar well diffusion	–	39.4% (planktonic cells) 80.3% (biofilm)	2.5 mL	Thurston et al. (2020)
Ag NPs-PANI/MWCNTS	Escherichia coli Staphylococcus aureus	Incubator at 37 °C for 24 h	Disc diffusion method	20	–	20 µg/mL	Deshmukh et al. (2019)
				19			
AgNPs-loaded ACFs	Escherichia coli Staphylococcus aureus	Incubator at 37 °C for 24 h	Disk diffusion method	20.5	98.03%	12 mm	Tang et al. (2014)
				20.0	96.88%		

(continued)

Table 2 (continued)

Nanophotocatalyst	Microbes	Incubation	Antimicrobial test	Minimum inhibitory concentration	Zone of inhibition (mm)	Dose of nanophotocatalyst	References
Ag zeolite/silicone	<i>Escherichia coli</i> and <i>Staphylococcus epidermidis</i>	Incubator at 37 °C for 24 h; 150 rpm	Agar plate	–	<10 CFU mL	–	Belkhair et al. (2015)
WO ₃ -GO	<i>Escherichia coli</i> <i>Bacillus subtilis</i>	Incubator at 37 °C for 20 h	Well diffusion method	2.5–5 mg/mL	–	139.6 µg/mL	Jeevitha et al. (2018)
NiFe/Si/Au	<i>Klebsiella pneumoniae</i> <i>Proteus mirabilis</i> <i>Escherichia coli</i> <i>Pseudomonas aeruginosa</i> <i>Staphylococcus aureus</i> <i>Enterococcus faecalis</i> <i>Acinetobacter baumannii</i>	Incubator at 37°C for 20 h	Agar diffusion method	2.5 mg/ml	–	100 µl (10 mg/mL)	Shirzadi-Ahodashi et al. (2020)
				1.25 mg/ml			
				5 mg/ml			
				5 mg/ml			
				2.5 mg/ml			
				5 mg/ml			
2 mg/ml							
GO–Ag ₃ PO ₄	<i>Escherichia coli</i>	Incubator at 37 °C for 24 h; visible light	Agar disc diffusion method	–	100%	20 mg L ⁻¹	Liu et al. (2012)

(continued)

Table 2 (continued)

Nanophotocatalyst	Microbes	Incubation	Antimicrobial test	Minimum inhibitory concentration	Zone of inhibition (mm)	Dose of nanophotocatalyst	References
P25/Ag ₃ PO ₄ /GO	Escherichia coli Staphylococcus aureus Salmonella typhi Pseudomonas aeruginosa Bacillus subtilis Bacillus pumilus	Incubation 35 °C for 48 h; high pressure mercury lamp	Agar well diffusion method	<100 ppm	99%	–	Yang et al. (2015)
Ag/AgCl/G-ZnFe ₂ O ₄	Staphylococcus aureus and Escherichia coli	Incubation 37 °C; visible light, Xe Lamp 300 W	Agar plate	13 and 22 mm	–	0.05 g	Zhang et al. (2020b)
Date pulp ZnO	Streptococcus pyogenes Staphylococcus aureus Pseudomonas aeruginosa Proteus mirabilis	Incubator at 37 °C for 24 h	In-vitro disc diffusion technique	14.5 15.9 18.4 18.7	–	25, 50 and 100 µg/mL	Rambabu et al. (2021)

ASS—sewage sludge-based activated carbon; RS-TONR/TINT—rhodium and antimony doped nanorod titanate nanotube; CPVA—conjugated polyvinyl alcohol; CD—Carbon dot; AC—activated carbon; NGQDs—nitrogen-doped graphene quantum dots; NSs—nanosheets; PEI—polyethyleneimine

5 Conclusion and Future Outlook

Water is one of the essential substances which makes our planet unique filled with living creatures. Water obtained from several resources is insufficient to meet the basic need of people. Hence, research communities are extensively showing their concern towards safeguarding the water resources by removing hazardous contaminants. Wastewater from industries is the major cause of water resource pollution. Due to challenges in the conventional water treatment process gives rise to an alternate approach. Progress in nanotechnology opened a new avenue in industrial wastewater treatment. Nanomaterials such as nanoadsorbents, nanomembrane and nano photocatalyst were observed to be efficient and reusable. Challenges like toxicity, expensive, recovery of nanomaterial, antifouling, no secondary pollutant, chemical, thermal and mechanical stabilities are to be addressed. Effective approaches could result in multirole nanocomposites and be designed according to the pollutant and its environment. Carbon based nanomaterials, metal organic frameworks and zeolites could be explored and combined for improved nanocomposite. Magnetic based nanomaterials are easy to remove with the external field, no corrosion & adaptability in zeolites and reduced toxicity of graphene. Further, appropriate functionalization, combination and experimental parameters with optimized values could produce the nanomaterials/nanocomposites for real time applications on a large scale. In future, excellent nanomaterials will be available for regular utilization to reach the ultimate target by removing the various pollutants under a single approach in industrial wastewater treatment.

References

- Abutaha N, Hezam A, Almekhlafi FA, Saeed AM, Namratha K, Byrappa K (2020) Rational design of Ag-ZnO-Fe₃O₄ nanocomposite with promising antimicrobial activity under LED light illumination. *Appl Surf Sci* 15(527):146893. <https://doi.org/10.1016/j.apsusc.2020.146893>
- Ahmed B, Ojha AK, Singh A, Hirsch F, Fischer I, Patrice D, Materny A (2018) Well-controlled in-situ growth of 2D WO₃ rectangular sheets on reduced graphene oxide with strong photocatalytic and antibacterial properties. *J Hazard Mater* 347:266–278. <https://doi.org/10.1016/j.jhazmat.2017.12.069>
- Ahmed S, Khan FSA, Mubarak NM, Khalid M, Tan YH, Mazari SA, Karri RR, Abdullah EC (2021) Emerging pollutants and their removal using visible-light responsive photocatalysis—a comprehensive review. *J Environ Chem Eng* 9(6). <https://doi.org/10.1016/j.jece.2021.106643>
- Albukhari SM, Alshaikh H, Mahmoud MH, Ismail AA (2021) Intense visible-light absorption in SrRuO₃/C₃N₄ heterostructures for the highly efficient reduction of Hg (II). *ACS Omega*. <https://doi.org/10.1021/acsomega.1c01969>
- Alhan S, Nehra M, Dilbaghi N, Singhal NK, Kim KH, Kumar S (2019) Potential use of ZnO@activated carbon nanocomposites for the adsorptive removal of Cd²⁺ ions in aqueous solutions. *Environ Res* 173:411–418. <https://doi.org/10.1016/j.envres.2019.03.061>
- Aliyu UM, Rathilal S, Isa YM (2018) Membrane desalination technologies in water treatment: a review. *Water Pract Technol* 13(4):738–752. <https://doi.org/10.2166/wpt.2018.084>

- Alizadeh B, Delnavaz M, Shakeri A (2018) Removal of Cd (II) and phenol using novel cross-linked magnetic EDTA/chitosan/TiO₂ nanocomposite. *Carbohydr Polym* 181:675–683. <https://doi.org/10.1016/j.carbpol.2017.11.095>
- Al-Qahtani KM, Ali MH, Al-Afify AG (2020) Synthesis and use of TiO₂@ rGo nanocomposites in photocatalytic removal of chromium and lead ions from wastewater. *J Elementol* 25(1). <https://doi.org/10.5601/jelem.2019.24.2.1862>
- Ameta R, Solanki MS, Benjamin S, Ameta SC (2018) Chapter 6—photocatalysis. In: Ameta SC, Ameta R (eds) *Advanced oxidation processes for waste water treatment*. Academic Press, pp 135–175, ISBN 9780128104996. <https://doi.org/10.1016/B978-0-12-810499-6.00006-1>
- An X, Zhang K, Wang Z, Ly QV, Hu Y, Liu C (2020) Improving the water permeability and antifouling property of the nanofiltration membrane grafted with hyperbranched polyglycerol. *J Membr Sci* 612:118417. <https://doi.org/10.1016/j.memsci.2020.118417>
- Anis SF, Lalia BS, Lesimple A, Hashaikheh R, Hilal N (2021) Superhydrophilic and underwater superoleophobic nano zeolite membranes for efficient oil-in-water nanoemulsion separation. *J Water Process Eng* 40:101802. <https://doi.org/10.1016/j.jwpe.2020.101802>
- Arabnezhad M, Afarani MS, Jafari A (2019) Co-precipitation synthesis of ZnO–TiO₂ nanostructure composites for arsenic photodegradation from industrial wastewater. *Int J Environ Sci Technol* 16(1):463–468. <https://doi.org/10.1007/s13762-017-1585-7>
- Ashbolt NJ (2015) Microbial contamination of drinking water and human health from community water systems. *Curr Environ Health Rep* 2(1):95–106. <https://doi.org/10.1007/s40572-014-0037-5>
- Ataei A, Mehrizad A, Zare K (2021) Photocatalytic degradation of cefazoline antibiotic using zeolite-supported CdS/CaFe₂O₄ Z-scheme photocatalyst: Optimization and modeling of process by RSM and ANN. *J Mol Liq* 328:115476. <https://doi.org/10.1016/j.molliq.2021.115476>
- Ayawanna J, Sato K (2019) Photoelectrodeposition effect of lanthanum oxide-modified ceria particles on the removal of lead (II) ions from water. *Catal Today* 321:128–134. <https://doi.org/10.1016/j.cattod.2017.11.010>
- Balarak D, Zafariyan M, Igwegbe CA, Onyechi KK, Ighalo JO (2021) Adsorption of acid blue 92 dye from aqueous solutions by single-walled carbon nanotubes: isothermal, kinetic, and thermodynamic studies. *Environ Process* 8(2):869–888. <https://doi.org/10.1007/s40710-021-00505-3>
- Balcha A, Yadav OP, Dey T (2016) Photocatalytic degradation of methylene blue dye by zinc oxide nanoparticles obtained from precipitation and sol-gel methods. *Environ Sci Pollut Res* 23(24):25485–25493. <https://doi.org/10.1007/s11356-016-7750-6>
- Barbosa AS, Rodrigues MG (2019) Influence of the methodology on the formation of zeolite membranes MCM-22 for the oil/water emulsion separation. *Cerâmica* 65(376):531–540. <https://doi.org/10.1590/0366-69132019653762676>
- Barbosa TL, Silva FM, Barbosa AS, Lima EG, Rodrigues MG (2020) Synthesis and application of a composite NaA zeolite/gamma-alumina membrane for oil-water separation process. *Cerâmica* 66(378):137–144. <https://doi.org/10.1590/0366-69132020663782820>
- Barik B, Nayak PS, Achary LS, Kumar A, Dash P (2020) Synthesis of alumina-based cross-linked chitosan–HPMC biocomposite film: an efficient and user-friendly adsorbent for multipurpose water purification. *New J Chem* 44(2):322–337. <https://doi.org/10.1039/C9NJ03945G>
- Basheer AA (2018) New generation nano-adsorbents for the removal of emerging contaminants in water. *J Mol Liq* 261:583–593, ISSN 0167–7322, <https://doi.org/10.1016/j.molliq.2018.04.021>
- Beh JJ, Ooi BS, Lim JK, Ng EP, Mustapa H (2020) Development of high water permeability and chemically stable thin film nanocomposite (TFN) forward osmosis (FO) membrane with poly (sodium 4-styrenesulfonate) (PSS)-coated zeolitic imidazolate framework-8 (ZIF-8) for produced water treatment. *J Water Process Eng* 33:101031. <https://doi.org/10.1016/j.jwpe.2019.101031>
- Behera A, Kandi D, Martha S, Parida K (2019) Constructive interfacial charge carrier separation of a p-CaFe₂O₄@ n-ZnFe₂O₄ heterojunction architect photocatalyst toward photodegradation of antibiotics. *Inorg Chem* 58(24):16592–16608. <https://doi.org/10.1021/acs.inorgchem.9b02610>

- Belkhair S, Kinninmonth M, Fisher L, Gasharova B, Liauw CM, Verran J, Mihailova B, Tosheva L (2015) Silver zeolite-loaded silicone elastomers: a multidisciplinary approach to synthesis and antimicrobial assessment. *RSC Adv* 5(51):40932–40939. <https://doi.org/10.1039/C5RA03856A>
- Bergamasco R, Coldebella PF, Camacho FP, Rezende D, Yamaguchi NU, Klen MR, Tavares CJ, Amorim MT (2019) Self-assembly modification of polyamide membrane by coating titanium dioxide nanoparticles for water treatment applications. *Revista Ambiente & Água* 14. <https://doi.org/10.4136/ambi-agua.2297>
- Bousseghoune M, Chikhi M, Balaska F, Ozay Y, Dizge N, Kebabi B (2020) Preparation of a zirconia-based ceramic membrane and its application for drinking water treatment. *Symmetry* 12(6):933. <https://doi.org/10.3390/sym12060933>
- Boxi SS, Paria S (2014) Effect of silver doping on TiO₂, CdS, and ZnS nanoparticles for the photocatalytic degradation of metronidazole under visible light. *RSC Adv* 4(71):37752–37760. <https://doi.org/10.1039/C4RA06192F>
- Britannica. <https://www.britannica.com/technology/wastewater-treatment/Dewatering>
- Cadotte J, Forester R, Kim M, Petersen R, Stocker T (1988) Nanofiltration membranes broaden the use of membrane separation technology. *Desalination* 70(1–3):77–88. [https://doi.org/10.1016/0011-9164\(88\)85045-8](https://doi.org/10.1016/0011-9164(88)85045-8)
- Çalimli MH (2021) Magnetic nanocomposite cobalt-multiwalled carbon nanotube and adsorption kinetics of methylene blue using an ultrasonic batch. *Int J Environ Sci Technol* 18(3):723–740. <https://doi.org/10.1007/s13762-020-02855-1>
- Cao HL, Cai FY, Yu K, Zhang YQ, Lü J, Cao R (2019a) Photocatalytic degradation of tetracycline antibiotics over CdS/nitrogen-doped-carbon composites derived from in situ carbonization of metal-organic frameworks. *ACS Sustain Chem Eng* 7(12):10847–10854. <https://doi.org/10.1021/acssuschemeng.9b01685>
- Cao XT, Showkat AM, Kang I, Gal YS, Lim KT (2016) β -Cyclodextrin multi-conjugated magnetic graphene oxide as a nano-adsorbent for methylene blue removal. *J Nanosci Nanotechnol* 16(2):1521–1525. <https://doi.org/10.1166/jnn.2016.11987>
- Cao F, Wang J, Wang Y, Zhou J, Li S, Qin G, Fan W (2019b) An in situ Bi-decorated BiOBr photocatalyst for synchronously treating multiple antibiotics in water. *Nanoscale Adv* 1:1124–1129. <https://doi.org/10.1039/C8NA00197A>
- Centers for disease control and prevention, Drinking water. https://www.cdc.gov/healthywater/drinking/public/water_treatment.html, 26 July 2021
- Chang L, Pu Y, Jing P, Cui Y, Zhang G, Xu S, Cao B, Guo J, Chen F, Qiao C (2021) Magnetic core-shell MnFe₂O₄@ TiO₂ nanoparticles decorated on reduced graphene oxide as a novel adsorbent for the removal of ciprofloxacin and Cu (II) from water. *Appl Surf Sci* 541:148400. <https://doi.org/10.1016/j.apsusc.2020.148400>
- Chavoshan S, Khodadadi M, Nasseh N (2020) Photocatalytic degradation of penicillin G from simulated wastewater using the UV/ZnO process: isotherm and kinetic study. *J Environ Health Sci Eng* 18(1):107. <https://doi.org/10.1007/s40201-020-00442-7>
- Chen F, Yang Q, Sun J, Yao F, Wang S, Wang Y, Wang X, Li X, Niu C, Wang D, Zeng G (2016) Enhanced photocatalytic degradation of tetracycline by AgI/BiVO₄ heterojunction under visible-light irradiation: mineralization efficiency and mechanism. *ACS Appl Mater Interf* 8(48):32887–32900. <https://doi.org/10.1021/acsmi.6b12278>
- Chen M, Shang R, Sberna PM, Luiten-Olieman MW, Rietveld LC, Heijman SG (2020a) Highly permeable silicon carbide-alumina ultrafiltration membranes for oil-in-water filtration produced with low-pressure chemical vapor deposition. *Sep Purif Technol* 253:117496. <https://doi.org/10.1016/j.seppur.2020.117496>
- Chen W, Chang L, Ren SB, He ZC, Huang GB, Liu XH (2020b) Direct Z-scheme 1D/2D WO₂.72/ZnIn₂S₄ hybrid photocatalysts with highly-efficient visible-light-driven photodegradation towards tetracycline hydrochloride removal. *J Hazard Mater* 384:121308. <https://doi.org/10.1016/j.jhazmat.2019.121308>

- Chen Z, Zhou C, Lin J, Zhu Z, Feng J, Fang L, Cheng J (2018) ZrO₂-coated stainless steel mesh with underwater superoleophobicity by electrophoretic deposition for durable oil/water separation. *J Sol-Gel Sci Technol* 85(1):23–30. <https://doi.org/10.1007/s10971-017-4518-5>
- Chowdhury P, Athapaththu S, Elkamel A, Ray AK (2017) Visible-solar-light-driven photo-reduction and removal of cadmium ion with Eosin Y-sensitized TiO₂ in aqueous solution of triethanolamine. *Sep Purif Technol* 174:109–115. <https://doi.org/10.1016/j.seppur.2016.10.011>
- Crini G, Lichtfouse E (2019) Advantages and disadvantages of techniques used for wastewater treatment. *Environ Chem Lett* 17(1):145–155. <https://doi.org/10.1007/s10311-018-0785-9>
- Dadvar E, Kalantary RR, Ahmad Panahi H, Peyravi M (2017) Efficiency of polymeric membrane graphene oxide-TiO₂ for removal of azo dye. *J Chem*. <https://doi.org/10.1155/2017/6217987>
- Daraee M, Ghasemy E, Rashidi A (2020) Effective adsorption of hydrogen sulfide by intercalation of TiO₂ and N-doped TiO₂ in graphene oxide. *J Environ Chem Eng* 8(4):103836. <https://doi.org/10.1016/j.jece.2020.103836>
- Das D, Baitalik S, Halder B, Saha R, Kayal N (2018) Preparation and characterization of macroporous SiC ceramic membrane for treatment of waste water. *J Porous Mater* 25(4):1183–1193. <https://doi.org/10.1007/s10934-017-0528-5>
- Dehghani, Hadi M, Omrani GA, Karri RR (2021) Solid waste—sources, toxicity, and their consequences to human health. In: *Soft computing techniques in solid waste and wastewater management*. Elsevier. <https://doi.org/10.1016/B978-0-12-824463-0.00013-6>
- Deshmukh SP, Dhodamani AG, Patil SM, Mullani SB, More KV, Delekar SD (2019) Interfacially interactive ternary silver-supported polyaniline/multiwalled carbon nanotube nanocomposites for catalytic and antibacterial activity. *ACS Omega* 5(1):219–227. <https://doi.org/10.1021/acsomega.9b02526>
- Di G, Zhu Z, Zhang H, Zhu J, Lu H, Zhang W, Qiu Y, Zhu L, Küppers S (2017) Simultaneous removal of several pharmaceuticals and arsenic on Zn–Fe mixed metal oxides: combination of photocatalysis and adsorption. *Chem Eng J* 328:141–151. <https://doi.org/10.1016/j.cej.2017.06.112>
- Dinka MO (2018) Safe drinking water: concepts, benefits, principles and standards. *Water challenges of an urbanizing world*. IntechOpen, London, pp 163–81. <https://doi.org/10.5772/intechopen.71352>
- dos Santos Barbosa A, dos Santos Barbosa A, Barbosa TL, Rodrigues MG (2018) Synthesis of zeolite membrane (NaY/alumina): effect of precursor of ceramic support and its application in the process of oil–water separation. *Sep Purif Technol* 12(200):141–154. <https://doi.org/10.1016/j.seppur.2018.02.001>
- Ehyaee M, Safa F, Shariati S (2017) Magnetic nanocomposite of multi-walled carbon nanotube as effective adsorbent for methyl violet removal from aqueous solutions: response surface modeling and kinetic study. *Korean J Chem Eng* 34(4):1051–1061. <https://doi.org/10.1007/s11814-016-0353-6>
- Elomari H, Achiou B, Beqqour D, Khaless K, Beniazza R, Ouammou M, Aaddane A, Younsi SA, Benhida R (2021) Preparation and characterization of low-cost zirconia/clay membrane for removal of acid orange 74 dye. *Mater Today: Proc*. <https://doi.org/10.1016/j.matpr.2021.03.674>
- El-Sayed ME (2020) Nano-adsorbents for water and wastewater remediation. *Sci Total Environ* 739:139903. <https://doi.org/10.1016/j.scitotenv.2020.139903>
- El-Shafai N, El-Khouly ME, El-Kemary M, Ramadan M, Eldesoukey I, Masoud M (2019) Graphene oxide decorated with zinc oxide nanoflower, silver and titanium dioxide nanoparticles: fabrication, characterization, DNA interaction, and antibacterial activity. *RSC Adv* 9(7):3704–3714. <https://doi.org/10.1039/C8RA09788G>
- Environmental Protection. <https://eponline.com/articles/2018/02/08/four-effective-processes-to-treat-wastewater.aspx>, 26 July 2021
- Eray E, Boffa V, Jørgensen MK, Magnacca G, Candelario VM (2020) Enhanced fabrication of silicon carbide membranes for wastewater treatment: from laboratory to industrial scale. *J Membr Sci* 606:118080. <https://doi.org/10.1016/j.memsci.2020.118080>

- Etman AS, Abdelhamid HN, Yuan Y, Wang L, Zou X, Sun J (2018) Facile water-based strategy for synthesizing MoO_3-x nanosheets: efficient visible light photocatalysts for dye degradation. *ACS Omega* 3(2):2193–2201. <https://doi.org/10.1021/acsomega.8b00012>
- Fard AK, Bukenhoudt A, Jacobs M, McKay G, Atieh MA (2018) Novel hybrid ceramic/carbon membrane for oil removal. *J Membr Sci* 559:42–53. <https://doi.org/10.1016/j.memsci.2018.05.003>
- Feng J, Sun M, Ye Y (2017) Ultradurable underwater superoleophobic surfaces obtained by vapor-synthesized layered polymer nanocoatings for highly efficient oil–water separation. *J Mater Chem A* 5(29):14990–14995. <https://doi.org/10.1039/C7TA03297H>
- Figoli A, Cassano A, Criscuoli A, Mozumder MS, Uddin MT, Islam MA, Drioli E (2010) Influence of operating parameters on the arsenic removal by nanofiltration. *Water Res* 44(1):97–104. <https://doi.org/10.1016/j.watres.2009.09.007>
- Ganguly P, Panneri S, Hareesh US, Breen A, Pillai SC (2019) Recent advances in photocatalytic detoxification of water. *Nanoscale Mater Water Purificat.* 653–688. <https://doi.org/10.1016/B978-0-12-813926-4.00029-X>
- Ge J, Zhang Y, Heo YJ, Park S (2019) Advanced design and synthesis of composite photocatalysts for the remediation of wastewater: a review. *Catalysts* 9(2):122. <https://doi.org/10.3390/catal9020122>
- Gelde L, Cuevas AL, Benavente J (2021) Influence of pore-size/porosity on ion transport and static BSA fouling for TiO_2 -covered nanoporous alumina membranes. *Appl Sci* 11(12):5687. <https://doi.org/10.3390/app11125687>
- Giorno L, Drioli E, Strathmann H (2015) The principle of nanofiltration (NF). In: Drioli E, Giorno L (eds) *Encyclopedia of membranes*. Springer, Berlin, Heidelberg. https://doi.org/10.1007/978-3-642-40872-4_2234-1
- Gu J, Xiao P, Zhang L, Lu W, Zhang G, Huang Y, Zhang J, Chen T (2016) Construction of super-hydrophilic and under-water superoleophobic carbon-based membranes for water purification. *RSC Adv* 6(77):73399–73403. <https://doi.org/10.1039/C6RA14310E>
- Guo J, Wu J, Guan Y, Wang J, Liu Q, Mao X, Qi X, He P, Wang H (2021) Fabrication of a Z-scheme heterojunction polyhedral-shaped $\text{BiOIO}_3/\text{MIL-53 (Fe)}$ photocatalyst for enhancing gaseous HgO removal. *Energy Fuels* 35(4):3252–3265. <https://doi.org/10.1021/acs.energyfuels.0c03376>
- Guo Y, Deng J, Zhu J, Zhou C, Zhou C, Zhou X, Bai R (2016) Removal of anionic azo dye from water with activated graphene oxide: kinetic, equilibrium and thermodynamic modeling. *RSC Adv* 6(46):39762–39773. <https://doi.org/10.1039/C6RA03423C>
- Patterson HBW (2009) Chapter 2—Adsorption. In: Gary R (ed) *List, bleaching and purifying fats and oils*, 2nd edn. AOCs Press, pp 53–67, ISBN 9781893997912, <https://doi.org/10.1016/B978-1-893997-91-2.50008-0>
- Han L, Zhong YL, Lei K, Mao D, Dong YZ, Hong G, Zhou YT, Fang D (2019) Carbon dot– SnS_2 heterojunction photocatalyst for photoreduction of Cr (VI) under visible light: a combined experimental and first-principles DFT study. *J Phys Chem C* 123(4):2398–2409. <https://doi.org/10.1021/acs.jpcc.8b10059>
- Hu L, Yang Z, Wang Y, Li Y, Fan D, Wu D, Wei Q, Du B (2017) Facile preparation of water-soluble hyperbranched polyamine functionalized multiwalled carbon nanotubes for high-efficiency organic dye removal from aqueous solution. *Sci Rep* 7(1):1–3. <https://doi.org/10.1038/s41598-017-03490-6>
- Huang BQ, Tang YJ, Zeng ZX, Xu ZL (2020) Microwave heating assistant preparation of high permselectivity polypiperazine-amide nanofiltration membrane during the interfacial polymerization process with low monomer concentration. *J Membr Sci* 596:117718. <https://doi.org/10.1016/j.memsci.2019.117718>
- Huang W, Liu N, Zhang X, Wu M, Tang L (2017) Metal organic framework $g\text{-C}_3\text{N}_4/\text{MIL-53 (Fe)}$ heterojunctions with enhanced photocatalytic activity for Cr (VI) reduction under visible light. *Appl Surf Sci* 425:107–116. <https://doi.org/10.1016/j.apsusc.2017.07.050>

- Huo P, Liu C, Wu D, Guan J, Li J, Wang H, Tang Q, Li X, Yan Y, Yuan S (2018) Fabricated Ag/Ag₂S/reduced graphene oxide composite photocatalysts for enhancing visible light photocatalytic and antibacterial activity. *J Ind Eng Chem* 57:125–133. <https://doi.org/10.1016/j.jiec.2017.08.015>
- Idris A, Majidnia Z, Nor Kamarudin KS (2016) Photocatalyst treatment for lead (II) using titanium oxide nanoparticles embedded in PVA-alginate beads. *Desalin Water Treat* 57(11):5035–5044. <https://doi.org/10.1080/19443994.2015.1006256>
- Ifebajo AO, Oladipo AA, Gazi M (2019) Efficient removal of tetracycline by CoO/CuFe₂O₄ derived from layered double hydroxides. *Environ Chem Lett* 17(1):487–494. <https://doi.org/10.1007/s10311-018-0781-0>
- Iqbal T, Ali F, Khalid NR, Tahir MB, Ijaz M (2019) Facile synthesis and antimicrobial activity of CdS-Ag₂S nanocomposites. *Bioorg Chem* 90:103064. <https://doi.org/10.1016/j.bioorg.2019.103064>
- Jain B, Hashmi A, Sanwaria S, Singh AK, Susan MA, Singh A (2020) Zinc oxide nanoparticle incorporated on graphene oxide: an efficient and stable photocatalyst for water treatment through the Fenton process. *Adv Compos Hybrid Mater* 3:231–242. <https://doi.org/10.1007/s42114-020-00153-5>
- Jauris IM, Fagan SB, Adebayo MA, Machado FM (2016) Adsorption of acridine orange and methylene blue synthetic dyes and anthracene on single wall carbon nanotubes: a first principle approach. *Comput Theor Chem* 1076:42–50. <https://doi.org/10.1016/j.comptc.2015.11.021>
- Jeevitha G, Abhinayaa R, Mangalaraj D, Ponpandian N (2018) Tungsten oxide-graphene oxide (WO₃-GO) nanocomposite as an efficient photocatalyst, antibacterial and anticancer agent. *J Phys Chem Solids* 116:137–147. <https://doi.org/10.1016/j.jpics.2018.01.021>
- Ji B, Zhang J, Zhang C, Li N, Zhao T, Chen F, Hu L, Zhang S, Wang Z (2018) Vertically aligned ZnO@ZnS nanorod chip with improved photocatalytic activity for antibiotics degradation. *ACS Appl Nano Mater* 1(2):793–799. <https://doi.org/10.1021/acsnm.7b00242>
- Jiang D, Xiao P, Shao L, Li D, Chen M (2017) RGO-promoted all-solid-state g-C₃N₄/BiVO₄ Z-scheme heterostructure with enhanced photocatalytic activity toward the degradation of antibiotics. *Ind Eng Chem Res* 56(31):8823–8832. <https://doi.org/10.1021/acs.iecr.7b01840>
- Kabra K, Chaudhary R, Sawhney RL (2008) Solar photocatalytic removal of Cu (II), Ni (II), Zn (II) and Pb (II): speciation modeling of metal–citric acid complexes. *J Hazard Mater* 155(3):424–432. <https://doi.org/10.1016/j.jhazmat.2007.11.083>
- Kahsay MH, Belachew N, Tadesse A, Basavaiah K (2020) Magnetite nanoparticle decorated reduced graphene oxide for adsorptive removal of crystal violet and antifungal activities. *RSC Adv* 10(57):34916–34927. <https://doi.org/10.1039/d0ra07061k>
- Kamaraj E, Somasundaram S, Balasubramani K, Eswaran MP, Muthuramalingam R, Park S (2018) Facile fabrication of CuO-Pb₂O₃ nanophotocatalyst for efficient degradation of Rose Bengal dye under visible light irradiation. *Appl Surf Sci* 433:206–212. <https://doi.org/10.1016/j.apsusc.2017.09.139>
- Kamran U, Bhatti HN, Iqbal M, Jamil S, Zahid M (2019) Biogenic synthesis, characterization and investigation of photocatalytic and antimicrobial activity of manganese nanoparticles synthesized from Cinnamomum verum bark extract. *J Mol Struct* 1179:532–539. <https://doi.org/10.1016/j.molstruc.2018.11.006>
- Kamranifar M, Allahresani A, Naghizadeh A (2019) Synthesis and characterizations of a novel CoFe₂O₄@CuS magnetic nanocomposite and investigation of its efficiency for photocatalytic degradation of penicillin G antibiotic in simulated wastewater. *J Hazard Mater* 366:545–555. <https://doi.org/10.1016/j.jhazmat.2018.12.046>
- Karri RR, Ravindran G, Dehghani MH (2021) Wastewater—sources, toxicity, and their consequences to human health. In: Soft computing techniques in solid waste and wastewater management. Elsevier. <https://doi.org/10.1016/B978-0-12-824463-0.00001-X>
- Kayvani Fard A, McKay G, Buekenhoudt A, Al Sulaiti H, Motmans F, Khraisheh M, Atieh M (2018) Inorganic membranes: preparation and application for water treatment and desalination. *Materials* 11(1):74. <https://doi.org/10.3390/ma11010074>

- Kazemi MS, Rasaeinezhad S, Es' hagh Z (2020) Evaluation of flutamide loading capacity of biosynthesis of plant-mediated glutathione-modified gold nanoparticles by *Dracocephalum Kotschy* Boiss extract. *Chem Pap* 1–8. <https://doi.org/10.1007/s11696-019-01048-6>
- Khan ME, Han TH, Khan MM, Karim MR, Cho MH (2018) Environmentally sustainable fabrication of Ag@ g-C₃N₄ nanostructures and their multifunctional efficacy as antibacterial agents and photocatalysts. *ACS Appl Nano Mater* 1(6):2912–2922. <https://doi.org/10.1021/acsnm.8b00548>
- Khan FSA, Mubarak NM, Khalid M, Tan YH, Abdullah EC, Rahman ME, Karri RR (2021a) A comprehensive review on micropollutants removal using carbon nanotubes-based adsorbents and membranes. *J Environ Chem Eng* 9(6). <https://doi.org/10.1016/j.jece.2021.106647>
- Khan, F. S. A., N. M. Mubarak, Y. H. Tan, M. Khalid, R. R. Karri, R. Walvekar, E. C. Abdullah, S. Nizamuddin and S. A. Mazari (2021b). A comprehensive review on magnetic carbon nanotubes and carbon nanotube-based buckypaper for removal of heavy metals and dyes. *Journal of Hazardous Materials* 413. <https://doi.org/10.1016/j.jhazmat.2021.125375>
- Kim EJ, Choi M, Park HY, Hwang JY, Kim HE, Hong SW, Lee J, Yong K, Kim W (2019) Thorn-like TiO₂ nanoarrays with broad spectrum antimicrobial activity through physical puncture and photocatalytic action. *Sci Rep* 9(1):1–2. <https://doi.org/10.1038/s41598-019-50116-0>
- Kim SC, Yeom HJ, Kim YW, Song IH, Ha JH (2017) Processing of alumina-coated glass-bonded silicon carbide membranes for oily wastewater treatment. *Int J Appl Ceram Technol* 14(4):692–702. <https://doi.org/10.1111/ijac.12693>
- Kim SG, Dhandole LK, Lim JM, Chae WS, Chung HS, Oh BT, Jang JS (2018) Facile synthesis of ternary TiO₂ NP/Rh & Sb-codoped TiO₂ NR/titanate NT composites photocatalyst: Simultaneous removals of Cd²⁺ ions and Orange (II) dye under visible light irradiation ($\lambda \geq 420$ nm). *Appl Catal B* 224:791–803. <https://doi.org/10.1016/j.apcatb.2017.11.013>
- Kobayashi Y, Kanasaki R, Nozaki T, Shoji R, Sato K (2017) Improving effect of MnO₂ addition on TiO₂-photocatalytic removal of lead ion from water. *J Water Environ Technol* 15(2):35–42. <https://doi.org/10.2965/jwet.16-021>
- Kumar G, Masram DT (2010) Sustainable synthesis of MOF-5@ GO nanocomposites for efficient removal of Rhodamine B from water. *ACS Omega* 6(14):9587–9599. <https://doi.org/10.1021/acs.omega.1c00143>
- Kumar KA, Amanchi SR, Sreedhar B, Ghosal P, Subrahmanyam C (2017) Phenol and Cr (VI) degradation with Mn ion doped ZnO under visible light photocatalysis. *RSC Adv* 7(68):43030–43039. <https://doi.org/10.1039/C7RA08172C>
- Kumar S, Ahlawat W, Bhanjana G, Heydarifard S, Nazhad MM, Dilbaghi N (2014) Nanotechnology-based water treatment strategies. *J Nanosci Nanotechnol* 14:1838–1858. <https://doi.org/10.1166/jnn.2014.9050>
- Lavakusa B, Devi DR, Belachew N, Basavaiah K (2020) Selective synthesis of visible light active γ -bismuth molybdate nanoparticles for efficient photocatalytic degradation of methylene blue, reduction of 4-nitrophenol, and antimicrobial activity. *RSC Adv* 10(60):36636–36643. <https://doi.org/10.1039/D0RA07459D>
- Le MQ, Cao XT, Lee WK, Hong SS, Lim KT (2017) Fabrication and adsorption properties of novel magnetic graphene oxide composites for removal of methylene blue. *Mol Cryst Liq Cryst* 644(1):160–167. <https://doi.org/10.1080/15421406.2016.1277467>
- Lei S, Zeng M, Huang D, Wang L, Zhang L, Xi B, Ma W, Chen G, Cheng Z (2019) Synergistic high-flux oil-saltwater separation and membrane desalination with carbon quantum dots functionalized membrane. *ACS Sustain Chem Eng* 7(16):13708–13716. <https://doi.org/10.1021/acssuschemeng.9b01073>
- Li C, Song C, Tao P, Sun M, Pan Z, Wang T, Shao M (2016) Enhanced separation performance of coal-based carbon membranes coupled with an electric field for oily wastewater treatment. *Separat Purificat Technol* 47–56. <https://doi.org/10.1016/j.seppur.2016.05.020>
- Li ZJ, Huang ZW, Guo WL, Wang L, Zheng LR, Chai ZF, Shi WQ (2017) Enhanced photocatalytic removal of uranium (VI) from aqueous solution by magnetic TiO₂/Fe₃O₄ and its graphene composite. *Environ Sci Technol* 51(10):5666–5674. <https://doi.org/10.1021/acs.est.6b05313>

- Liang Y, Zhu Y, Liu C, Lee KR, Hung WS, Wang Z, Li Y, Elimelech M, Jin J, Lin S (2020) Polyamide nanofiltration membrane with highly uniform sub-nanometre pores for sub-1 Å precision separation. *Nat Commun* 11(1):1–9. <https://doi.org/10.1038/s41467-020-15771-2>
- Liu J, Shao J, Wang Y, Li J, Liu H, Wang A, Hui A, Chen S (2019) Antimicrobial activity of zinc oxide–graphene quantum dot nanocomposites: enhanced adsorption on bacterial cells by cationic capping polymers. *ACS Sustain Chem Eng* 7(19):16264–16273. <https://doi.org/10.1021/acssuschemeng.9b03292>
- Liu L, Liu J, Sun DD (2012) Graphene oxide enwrapped Ag₃PO₄ composite: towards a highly efficient and stable visible-light-induced photocatalyst for water purification. *Catal Sci Technol* 2(12):2525–2532. <https://doi.org/10.1039/C2CY20483E>
- Liu Z, An X, Dong C, Zheng S, Mi B, Hu Y (2017) Modification of thin film composite polyamide membranes with 3D hyperbranched polyglycerol for simultaneous improvement in their filtration performance and antifouling properties. *J Mater Chem A* 5(44):23190–23197. <https://doi.org/10.1039/C7TA07335F>
- Ma X, Janowska K, Boffa V, Fabbri D, Magnacca G, Calza P, Yue Y (2019) Surfactant-assisted fabrication of alumina-doped amorphous silica nanofiltration membranes with enhanced water purification performances. *Nanomaterials* 9(10):1368. <https://doi.org/10.3390/nano9101368>
- Ma X, Quist-Jensen CA, Ali A, Boffa V (2020) Desalination of groundwater from a well in Puglia Region (Italy) by Al₂O₃-doped silica and polymeric nanofiltration membranes. *Nanomaterials* 10(9):1738. <https://doi.org/10.3390/nano10091738>
- Machado FM, Carmalin SA, Lima EC, Dias SL, Prola LD, Saucier C, Jauris IM, Zanella I, Fagan SB (2016) Adsorption of alizarin red S dye by carbon nanotubes: an experimental and theoretical investigation. *J Phys Chem C* 120(32):18296–18306. <https://doi.org/10.1021/acs.jpcc.6b03884>
- Madan S, Shaw R, Tiwari S, Tiwari SK (2019) Adsorption dynamics of Congo red dye removal using ZnO functionalized high silica zeolitic particles. *Appl Surf Sci* 487:907–917. <https://doi.org/10.1016/j.apsusc.2019.04.273>
- Madima N, Mishra SB, Inamuddin I, Mishra AK (2020) Carbon-based nanomaterials for remediation of organic and inorganic pollutants from wastewater: a review. *Environ Chem Lett* 18(4):1169–1191. <https://doi.org/10.1007/s10311-020-01001-0>
- Mahalingam S, Ahn YH (2018) Improved visible light photocatalytic activity of rGO–Fe₃O₄–NiO hybrid nanocomposites synthesized by in situ facile method for industrial wastewater treatment applications. *New J Chem* 42(6):4372–4383. <https://doi.org/10.1039/C8NJ00013A>
- Malwal D, Gopinath P (2016) Enhanced photocatalytic activity of hierarchical three dimensional metal oxide@ CuO nanostructures towards the degradation of Congo red dye under solar radiation. *Catal Sci Technol* 6(12):4458–4472. <https://doi.org/10.1039/C6CY00128A>
- Masoudi R, Moghimi H, Azin E, Taheri RA (2018) Adsorption of cadmium from aqueous solutions by novel Fe₃O₄-newly isolated Actinomucor sp. bio-nano-adsorbent: functional group study. *Artif Cells Nanomed Biotechnol* 46(Suppl 3):S1092–S1101. <https://doi.org/10.1080/21691401.2018.1533841>
- Mathew S, Ganguly P, Rhatigan S, Kumaravel V, Byrne C, Hinder SJ, Bartlett J, Nolan M, Pillai SC (2018) Cu-doped TiO₂: visible light assisted photocatalytic antimicrobial activity. *Appl Sci* 8(11):2067. <https://doi.org/10.3390/app8112067>
- Mehmood A, Khan FSA, Mubarak NM, Mazari SA, Jatoi AS, Khalid M, Tan YH, Karri RR, Walvekar R, Abdullah EC, Nizamuddin S (2021a) Carbon and polymer-based magnetic nanocomposites for oil-spill remediation—a comprehensive review. *Environ Sci Pollut Res* 28(39):54477–54496. <https://doi.org/10.1007/s11356-021-16045-0>
- Mehmood A, Khan FSA, Mubarak NM, Tan YH, Karri RR, Khalid M, Walvekar R, Abdullah EC, Nizamuddin S, Mazari SA (2021b) Magnetic nanocomposites for sustainable water purification—a comprehensive review. *Environ Sci Pollut Res* 28(16):19563–19588. <https://doi.org/10.1007/s11356-021-12589-3>
- Miranzadeh M, Afshari F, Khataei B, Kassaei MZ (2020) Adsorption and photocatalytic removal of arsenic from water by a porous and magnetic nanocomposite: Ag/TiO₂/Fe₃O₄@ GO. *Adv J Chem-Sect A* 3(4):408–421. <https://doi.org/10.33945/SAMI/AJCA.2020.4.3>

- Mirghani M, Al-Mubaiyedh UA, Nasser MS, Shawabkeh R (2015) Experimental study and modeling of photocatalytic reduction of Pb^{2+} by WO_3/TiO_2 nanoparticles. *Sep Purif Technol* 41:285–293. <https://doi.org/10.1016/j.seppur.2014.12.006>
- Moafi MH, Ardestani M, Mehrdadi N (2021) Use of zinc oxide nano-photocatalyst as a recyclable catalyst for removal of arsenic and lead ions from polluted water. *J Health* 12(1):130–143. <http://healthjournal.arums.ac.ir/article-1-2374-en.html>
- Mohamed RM, Ismail AA (2021a) Photocatalytic reduction and removal of mercury ions over mesoporous CuO/ZnO S-scheme heterojunction photocatalyst. *Ceram Int* 47(7):9659–9667. <https://doi.org/10.1016/j.ceramint.2020.12.105>
- Mohamed RM, Ismail AA (2021b) Doping cadmium oxide into mesoporous zinc oxide matrix for enhanced removal/reduction of $Hg(II)$ Ions. *Ceram Int* 47(7):9896–9906. <https://doi.org/10.1016/j.ceramint.2020.12.134>
- Mohammadi A, Veisi P (2018) High adsorption performance of β -cyclodextrin-functionalized multi-walled carbon nanotubes for the removal of organic dyes from water and industrial wastewater. *J Environ Chem Eng* 6(4):4634–4643. <https://doi.org/10.1016/j.jece.2018.07.002>
- Moussawi RN, Patra D (2016) Modification of nanostructured ZnO surfaces with curcumin: fluorescence-based sensing for arsenic and improving arsenic removal by ZnO . *RSC Adv* 6(21):17256–17268. <https://doi.org/10.1039/c5ra20221c>
- Mulyanti R, Susanto H (2018) Wastewater treatment by nanofiltration membranes. In: IOP conference series: earth and environmental science, vol 142, no 1. IOP Publishing, p 012017. <https://doi.org/10.1088/1755-1315/142/1/012017>
- Naseem T, Durrani T (2021) The role of some important metal oxide nanoparticles for wastewater and antibacterial applications: a review. *Environ Chem Ecotoxicol*. <https://doi.org/10.1016/j.eco.2020.12.001>
- Nawaz H, Umar M, Nawaz I, Zia Q, Tabassum M, Razzaq H, Gong H, Zhao X, Liu X (2021) Photodegradation of textile pollutants by nanocomposite membranes of polyvinylidene fluoride integrated with polyaniline–titanium dioxide nanotubes. *Chem Eng J* 419:129542. <https://doi.org/10.1016/j.cej.2021.129542>
- Nguyen CH, Fu CC, Juang RS (2018) Degradation of methylene blue and methyl orange by palladium-doped TiO_2 photocatalysis for water reuse: efficiency and degradation pathways. *J Clean Prod* 202:413–427. <https://doi.org/10.1016/j.jclepro.2018.08.110>
- Nur Hazirah R, Nurhaslina CR, Ku Halim KH (2014) Enhancement of biological approach and potential of *Lactobacillus delbrueckii* in decolorization of textile wastewater—a review. *IOSR. J Environ Sci Toxicol Food Technol* 8:6–10. <https://doi.org/10.9790/2402-081120610>
- Obotey Ezugbe E (2020) Rathilal S (2020) Membrane technologies in wastewater treatment: a review. *Membranes* 10(5):89. <https://doi.org/10.3390/membranes10050089>
- Odugbemi TI, Ogunisola FT (2002) An assessment of existing common traditional methods of water purification. *Afric J Clin Exp Microbiol* 3(1):41–44. <https://doi.org/10.4314/ajcem.v3i1.7351>
- Oshida Y (2013) 4-Oxidation and oxides. In: Oshida Y (ed) *Bioscience and bioengineering of titanium materials*, 2nd edn. Elsevier, pp 87–115, ISBN 9780444626257, <https://doi.org/10.1016/B978-0-444-62625-7.00004-2>
- Ou X, Yang X, Zheng J, Liu M (2019) Free-standing graphene oxide–chitin nanocrystal composite membrane for dye adsorption and oil/water separation. *ACS Sustain Chem Eng* 7(15):13379–13390. <https://doi.org/10.1021/acssuschemeng.9b02619>
- Oyewo OA, Adeniyi A, Sithole BB, Onyango MS (2020) Sawdust-based cellulose nanocrystals incorporated with ZnO nanoparticles as efficient adsorption media in the removal of methylene blue dye. *ACS Omega* 5(30):18798–18807. <https://doi.org/10.1021/acsomega.0c01924>
- Pal P (2017) Chapter 5—Water treatment by membrane-separation technology. In: Pal P (ed) *Industrial water treatment process technology*. Butterworth-Heinemann, pp 173–242, ISBN 9780128103913, <https://doi.org/10.1016/B978-0-12-810391-3.00005-9>
- Park S, Park G, Byun K, Lee SH, Han MJ (2020) Utilization of zinc oxide nanopowder for photocatalytic removal of Pb^{++} Ions from Aqueous wastewater. *J Nanosci Nanotechnol* 20(11):6831–6834. <https://doi.org/10.1166/jnn.2020.18780>

- Poerio T, Piacentini E, Mazzei R (2019) Membrane processes for microplastic removal. *Molecules* 24(22):4148. <https://doi.org/10.3390/molecules24224148>
- Poudel BR, Aryal RL, Bhattarai S, Koirala AR, Gautam SK, Ghimire KN, Pant B, Park M, Paudyal H, Pokhrel MR (2020) Agro-waste derived biomass impregnated with TiO₂ as a potential adsorbent for removal of as (III) from water. *Catalysts* 10(10):1125. <https://doi.org/10.3390/catal10101125>
- Qu Y, Xu X, Huang R, Qi W, Su R, He Z (2020) Enhanced photocatalytic degradation of antibiotics in water over functionalized N, S-doped carbon quantum dots embedded ZnO nanoflowers under sunlight irradiation. *Chem Eng J* 382:123016. <https://doi.org/10.1016/j.cej.2019.123016>
- Rajendran S, Pachiappan R, Hoang TK, Karthikeyan S, Gnanasekaran L, Vadivel S, Soto-Moscoso M, Gracia-Pinilla MA (2021) CuO-ZnO-PANI a lethal pnp combination in degradation of 4-chlorophenol under visible light. *J Hazard Mater* 416:125989. <https://doi.org/10.1016/j.jhazmat.2021.125989>
- Rambabu K, Bharath G, Banat F, Show PL (2021) Green synthesis of zinc oxide nanoparticles using Phoenix dactylifera waste as bioreductant for effective dye degradation and antibacterial performance in wastewater treatment. *J Hazard Mater* 402:123560. <https://doi.org/10.1016/j.jhazmat.2020.123560>
- Rashed MN, Eltahir MA, Abdou AN (2017) Adsorption and photocatalysis for methyl orange and Cd removal from wastewater using TiO₂/sewage sludge-based activated carbon nanocomposites. *Royal Soc Open Sci* 4(12):170834. <https://doi.org/10.1098/rsos.170834>
- Rebekah A, Bharath G, Naushad M, Viswanathan C, Ponpandian N (2020) Magnetic graphene/chitosan nanocomposite: a promising nano-adsorbent for the removal of 2-naphthol from aqueous solution and their kinetic studies. *Int J Biol Macromol* 159:530–538. <https://doi.org/10.1016/j.ijbiomac.2020.05.113>
- Roque-Malherbe R, del Rio CD (2019) Synthesis, characterization, and adsorption properties of nanoporous materials. In: *Appl Surf Sci. IntechOpen*. <https://doi.org/10.5772/intechopen.83355>
- Sadegh H, Ali GA, Gupta VK, Makhlof AS, Shahryari-Ghoshekandi R, Nadagouda MN, Sillanpää M, Megiel E (2017) The role of nanomaterials as effective adsorbents and their applications in wastewater treatment. *J Nanostruct Chem* 7(1):1–4. <https://doi.org/10.1007/s40097-017-0219-4>
- Samer M (2015) Biological and chemical wastewater treatment processes. *Wastewater Treat Eng* 150. <https://doi.org/10.5772/61250>
- Sargazi G, Ebrahimi AK, Afzali D, Badoei-dalfard A, Malekabadi S, Karami Z (2019) Fabrication of PVA/ZnO fibrous composite polymer as a novel sorbent for arsenic removal: design and a systematic study. *Polym Bull* 76(11):5661–5682. <https://doi.org/10.1007/s00289-019-02677-3>
- Sarma GK, Sen Gupta S, Bhattacharyya KG (2019) Nanomaterials as versatile adsorbents for heavy metal ions in water: a review. *Environ Sci Pollut Res* 26:6245–6278. <https://doi.org/10.1007/s11356-018-04093-y>
- Sebeia N, Jabli M, Ghith A (2019) Biological synthesis of copper nanoparticles, using Nerium oleander leaves extract: characterization and study of their interaction with organic dyes. *Inorg Chem Commun* 105:36–46. <https://doi.org/10.1016/j.inoche.2019.04.023>
- Sethy NK, Arif Z, Mishra PK, Kumar P (2020a) Green synthesis of TiO₂ nanoparticles from Syzygium cumini extract for photo-catalytic removal of lead (Pb) in explosive industrial wastewater. *Green Process Synth* 9(1):171–181. <https://doi.org/10.1515/gps-2020-0018>
- Sethy PK, Shivapriya PM, Banerjee S, Sahoo AK, Samanta SK (2020b) Biogenic fabrication of iron nanoadsorbents from mixed waste biomass for aqueous phase removal of alizarin red S and tartrazine: kinetics, isotherm, and thermodynamic investigation. *Environ Prog Sustain Energy* 39(2):e13326. <https://doi.org/10.1002/ep.13326>
- Shadi AM, Kamaruddin MA, Niza NM, Emmanuel MI, Hossain MS, Ismail N (2020) Efficient treatment of raw leachate using magnetic ore iron oxide nanoparticles Fe₂O₃ as nanoadsorbents. *J Water Process Eng* 38:101637. <https://doi.org/10.1016/j.jwpe.2020.101637>
- Sharma D, Saini A, Choudhary D, Kumari M, Chaudhary A, Dhayal V (2021) In-situ synthesis of ZnO modified g-C₃N₄ composite: a potential photocatalyst and adsorbent for waste water remediation. *Mater Res Innov* 1. <https://doi.org/10.1080/14328917.2021.1901424>

- Sharma JC, Vijay A, Bhardwaj S (2013) Photocatalytic activity of a novel compound SrWO₄: removal of toxic metal lead (II) from water. *World Appl Sci J* 23:208–212. <https://doi.org/10.5829/idosi.wasj.2013.23.02.639>
- Shen X, Xie T, Wang J, Liu P, Wang F (2017) An anti-fouling poly (vinylidene fluoride) hybrid membrane blended with functionalized ZrO₂ nanoparticles for efficient oil/water separation. *RSC Adv* 7(9):5262–5271. <https://doi.org/10.1039/C6RA26651G>
- Sherugar P, Naik NS, Padaki M, Nayak V, Gangadharan A, Nadig AR, Déon S (2021) Fabrication of zinc doped aluminium oxide/polysulfone mixed matrix membranes for enhanced antifouling property and heavy metal removal. *Chemosphere* 275:130024. <https://doi.org/10.1016/j.chemosphere.2021.130024>
- Shi L, Shi Y, Li R, Chang J, Zaouri N, Ahmed E, Jin Y, Zhang C, Zhuo S, Wang P (2018) SiC–C composite as a highly stable and easily regenerable photothermal material for practical water evaporation. *ACS Sustain Chem Eng* 6(7):8192–8200. <https://doi.org/10.1021/acssuschemeng.7b04695>
- Shi Y, Yan Z, Xu Y, Tian T, Zhang J, Pang J, Peng X, Zhang Q, Shao M, Tan W, Li H (2020) Visible-light-driven AgBr–TiO₂-Palygorskite photocatalyst with excellent photocatalytic activity for tetracycline hydrochloride. *J Clean Prod* 277:124021. <https://doi.org/10.1016/j.jclepro.2020.124021>
- Shirzadi-Ahodashi M, Ebrahimzadeh MA, Amiri O, Naghizadeh A, Mortazavi-Derazkola S (2020) Novel NiFe/Si/Au magnetic nanocatalyst: Biogenic synthesis, efficient and reusable catalyst with enhanced visible light photocatalytic degradation and antibacterial activity. *Appl Organomet Chem* 34(4):e5467. <https://doi.org/10.1002/aoc.5467>
- Shubha JP, Adil SF, Khan M, Hatshan MR, Khan A (2021) Facile Fabrication of a ZnO/Eu₂O₃/NiO-based ternary heterostructure nanophotocatalyst and its application for the degradation of methylene blue. *ACS Omega* 6(5):3866–3874. <https://doi.org/10.1021/acsomega.0c05670>
- Sikder P, Bhaduri SB, Ong JL, Guda T (2020) Silver (Ag) doped magnesium phosphate microplatelets as next-generation antibacterial orthopedic biomaterials. *J Biomed Mater Res B Appl Biomater* 108(3):976–989. <https://doi.org/10.1002/jbm.b.34450>
- Singha I, Mishrab PK (2020) Nano-membrane filtration a novel application of nanotechnology for waste water treatment. *Mater Today: Proc* 29:327–332. <https://doi.org/10.1016/j.matpr.2020.07.284>
- Soltaninejad V, Ahghari MR, Taheri-Ledari R, Maleki A (2021) Bifunctional PVA/ZnO/AgI/Chlorophyll nanocomposite film: enhanced photocatalytic activity for degradation of pollutants and antimicrobial property under visible-light irradiation. *Langmuir* 37(15):4700–4713. <https://doi.org/10.1021/acs.langmuir.1c00501>
- Sreekantan S, Lai CW, Mohd Zaki S (2014) The influence of lead concentration on photocatalytic reduction of Pb (II) ions assisted by Cu–TiO₂ nanotubes. *Int J Photoenergy*, Article ID 839106. <https://doi.org/10.1155/2014/839106>
- Sudhaik A, Raizada P, Shandilya P, Singh P (2018) Magnetically recoverable graphitic carbon nitride and NiFe₂O₄ based magnetic photocatalyst for degradation of oxytetracycline antibiotic in simulated wastewater under solar light. *J Environ Chem Eng* 6(4):3874–3883. <https://doi.org/10.1016/j.jece.2018.05.039>
- Sultana KA, Islam MT, Silva JA, Turley RS, Hernandez-Viezcas JA, Gardea-Torresdey JL, Noveron JC (2020) Sustainable synthesis of zinc oxide nanoparticles for photocatalytic degradation of organic pollutant and generation of hydroxyl radical. *J Mol Liq* 307:112931. <https://doi.org/10.1016/j.molliq.2020.112931>
- Sun L, Du T, Hu C, Chen J, Lu J, Lu Z, Han H (2017) Antibacterial activity of graphene oxide/g-C₃N₄ composite through photocatalytic disinfection under visible light. *ACS Sustain Chem Eng* 5(10):8693–8701. <https://doi.org/10.1021/acssuschemeng.7b01431>
- Sun X, Bai L, Li J, Huang L, Sun H, Gao X (2021) Robust preparation of flexibly super-hydrophobic carbon fiber membrane by electrospinning for efficient oil-water separation in harsh environments. *Carbon*. <https://doi.org/10.1016/j.carbon.2021.05.047>

- Tang C, Sun W, Yan W (2014) Green and facile fabrication of silver nanoparticles loaded activated carbon fibers with long-lasting antibacterial activity. *RSC Adv* 4(2):523–530. <https://doi.org/10.1039/C3RA44799E>
- Tang Y, Liu X, Ma C, Zhou M, Huo P, Yu L, Pan J, Shi W, Yan Y (2015) Enhanced photocatalytic degradation of tetracycline antibiotics by reduced graphene oxide–CdS/ZnS heterostructure photocatalysts. *New J Chem* 39(7):5150–5160. <https://doi.org/10.1039/C5NJ00681C>
- Thennarasu G, Sivasamy A (2016) Enhanced visible photocatalytic activity of cotton ball like nano structured Cu doped ZnO for the degradation of organic pollutant. *Ecotoxicol Environ Saf* 134:412–420. <https://doi.org/10.1016/j.ecoenv.2015.10.030>
- Thomas B, Alexander LK (2020) Removal of Pb²⁺ and Cd²⁺ toxic heavy metal ions driven by Fermi level modification in NiFe₂O₄–Pd nano hybrids. *J Solid State Chem* 288:121417. <https://doi.org/10.1016/j.jssc.2020.121417>
- Thurston JH, Clifford AJ, Henderson BS, Smith TR, Quintana D, Cudworth KF, Lujan TJ, Cornell KA (2020) Development of photoactive g-C₃N₄/poly (vinyl alcohol) composite hydrogel films with antimicrobial and antibiofilm activity. *ACS Appl Bio Mater* 3(3):1681–1689. <https://doi.org/10.1021/acsabm.9b01240>
- Tripathy N, Ahmad R, Song JE, Park H, Khang G (2017) ZnO nanonails for photocatalytic degradation of crystal violet dye under UV irradiation. *AIMS Mater Sci* 4(1):267–276. <https://doi.org/10.3934/matserci.2017.1.267>
- Uyen DM, Nguyen MH, Thu VT, Khieu DQ (2020) Facile fabrication of highly flexible and floatable Cu₂O/rGO on Vietnamese traditional paper toward high-performance solar-light-driven photocatalytic degradation of ciprofloxacin antibiotic. *RSC Adv* 10(28):16330–16338. <https://doi.org/10.1039/D0RA01854F>
- Venkateshab K, Arthanareeswaran G, Boseb AC, Kumar PS (2020) Hydrophilic hierarchical carbon with TiO₂ nanofiber membrane for high separation efficiency of oil in water emulsion and dye. *Sep Purif Technol* 241:116709. <https://doi.org/10.1016/j.seppur.2020.116709>
- Wahyuni ET, Rahmaniati T, Hafidzah AR, Suherman S, Suratman A (2021) Photocatalysis over N-Doped TiO₂ Driven by Visible Light for Pb (II) Removal from Aqueous Media. *Catalysts* 11(8):945. <https://doi.org/10.3390/catal11080945>
- Wang K, Zhang G, Li J, Li Y, Wu X (2017) 0D/2D Z-scheme heterojunctions of bismuth tantalate quantum dots/ultrathin g-C₃N₄ nanosheets for highly efficient visible light photocatalytic degradation of antibiotics. *ACS Appl Mater Interf* 9(50):43704–43715. <https://doi.org/10.1021/acsami.7b14275>
- Wang D, Yuan H, Chen Y et al (2020) A cellulose-based nanofiltration membrane with a stable three-layer structure for the treatment of drinking water. *Cellulose* 27:8237–8253. <https://doi.org/10.1007/s10570-020-03325-0>
- Wang K, Chen P, Nie W, Xu Y, Zhou Y (2019a) Improved photocatalytic reduction of Cr (VI) by molybdenum disulfide modified with conjugated polyvinyl alcohol. *Chem Eng J* 359:1205–1214. <https://doi.org/10.1016/j.cej.2018.11.057>
- Wang K, Li J, Zhang G (2019b) Ag-bridged Z-scheme 2D/2D Bi₅FeTi₃O₁₅/g-C₃N₄ heterojunction for enhanced photocatalysis: mediator-induced interfacial charge transfer and mechanism insights. *ACS Appl Mater Interf* 11(31):27686–27696. <https://doi.org/10.1021/acsami.9b05074>
- Wang X, Pan S, Zhang M, Qi J, Sun X, Gu C, Wang L, Li J (2019c) Modified hydrous zirconium oxide/PAN nanofibers for efficient defluoridation from groundwater. *Sci Total Environ* 685:401–409. <https://doi.org/10.1016/j.scitotenv.2019.05.380>
- Wang Y, Zhang A, Zhang D, Zhou P, Wang R, Xiang J, Zhang X, Su S (2019d) Ag₂CO₃ anchored on BiOI/CoFe₂O₄ composites with pnp heterojunctions: highly enhanced activity for photocatalytic oxidation of HgO under fluorescent light irradiation. *Colloids Surf, A* 579:123654. <https://doi.org/10.1016/j.colsurfa.2019.123654>
- Wang N, Wang F, Pan F, Yu S, Pan D (2021) Highly efficient silver catalyst supported by a spherical covalent organic framework for the continuous reduction of 4-Nitrophenol. *ACS Appl Mater Interf* 13(2):3209–3220. <https://doi.org/10.1021/acsami.0c20444>

- Wen XJ, Niu CG, Zhang L, Zeng GM (2017) Fabrication of SnO₂ nanoparticles/BiOI n–p heterostructure for wider spectrum visible-light photocatalytic degradation of antibiotic oxytetracycline hydrochloride. *ACS Sustain Chem Eng* 5(6):5134–5147. <https://doi.org/10.1021/acssuschemeng.7b00501>
- World Health Organization. <https://www.who.int/news-room/fact-sheets/detail/drinking-water>
- World Health Organization. https://www.who.int/water_sanitation_health/hygiene/emergencies/fs2_10.pdf
- World Health Organization (2012) Pharmaceuticals in drinking-water. https://apps.who.int/iris/bitstream/handle/10665/44630/9789241502085_eng.pdf
- Wu X, Luo Z, Lei Y, Wen B, Yang D (2020) Hierarchical TiO₂ nanorod arrays/carbon nanofiber membranes for oil-in-water emulsion separation. *Ind Eng Chem Res* 59(48):21097–21105. <https://doi.org/10.1021/acs.iecr.0c04831>
- Xiao C, Si L, Liu Y, Guan G, Wu D, Wang Z, Hao X (2016) Ultrastable coaxial cable-like superhydrophobic mesh with self-adaption effect: facile synthesis and oil/water separation application. *J Mater Chem A* 4(21):8080–8090. <https://doi.org/10.1039/C6TA01621A>
- Xu M, Girish YR, Rakesh KP, Wu P, Marichannegowda MH, Byrappa SM, Byrappa K (2021) Recent advances and challenges in silicon carbide (SiC) Ceramic nanoarchitectures and their applications. *Mater Today Commun* 102533. <https://doi.org/10.1016/j.mtcomm.2021.102533>
- Xu Y, Tay TF, Cui L, Fan J, Niu C, Chen D, Guo ZX, Sun C, Zhang XL, Caruso RA (2020) Trace-level fluorination of mesoporous TiO₂ improves photocatalytic and Pb (II) adsorbent performances. *Inorg Chem* 59(23):17631–17637. <https://doi.org/10.1021/acs.inorgchem.0c02869>
- Xue J, Ma S, Zhou Y, Zhang Z, He M (2015) Facile photochemical synthesis of Au/Pt/g-C₃N₄ with plasmon-enhanced photocatalytic activity for antibiotic degradation. *ACS Appl Mater Interf* 7(18):9630–9637. <https://doi.org/10.1021/acsami.5b01212>
- Yan M, Zhu F, Gu W, Sun L, Shi W, Hua Y (2016) Construction of nitrogen-doped graphene quantum dots-BiVO₄/g-C₃N₄ Z-scheme photocatalyst and enhanced photocatalytic degradation of antibiotics under visible light. *RSC Adv* 6(66):61162–61174. <https://doi.org/10.1039/C6RA07589D>
- Yang W, Hu W, Zhang J, Wang W, Cai R, Pan M, Huang C, Chen X, Yan B, Zeng H (2021) Tannic acid/Fe³⁺ functionalized magnetic graphene oxide nanocomposite with high loading of silver nanoparticles as ultra-efficient catalyst and disinfectant for wastewater treatment. *Chem Eng J* 405:126629. <https://doi.org/10.1016/j.cej.2020.126629>
- Yang X, He Y, Zeng G, Zhan Y, Pan Y, Shi H, Chen Q (2016) Novel hydrophilic PVDF ultrafiltration membranes based on a ZrO₂–multiwalled carbon nanotube hybrid for oil/water separation. *J Mater Sci* 51(19):8965–8976. <https://doi.org/10.1007/s10853-016-0147-6>
- Yang X, Qin J, Jiang Y, Chen K, Yan X, Zhang D, Li R, Tang H (2015) Fabrication of P25/Ag₃PO₄/graphene oxide heterostructures for enhanced solar photocatalytic degradation of organic pollutants and bacteria. *Appl Catal B* 166:231–240. <https://doi.org/10.1016/j.apcatb.2014.11.028>
- Yao S, Zhou S, Wang J, Li W, Li Z (2019) Optimizing the synthesis of SnO₂/TiO₂/RGO nanocomposites with excellent visible light photocatalytic and antibacterial activities. *Photochem Photobiol Sci* 18(12):2989–2999. <https://doi.org/10.1039/C9PP00242A>
- Yaqoob AA, Parveen T, Umar K, Mohamad Ibrahim MN (2014) Role of nanomaterials in the treatment of wastewater: A review. *Water* 12(2):495. <https://doi.org/10.3390/w12020495>
- Yokwana K, Kuvarega AT, Mhlanga SD, Nxumalo EN (2018) Mechanistic aspects for the removal of Congo red dye from aqueous media. *Phys Chem Earth, Parts A/B/C* 107:58–70. <https://doi.org/10.1016/j.pce.2018.08.001>
- Yu JY, Chen ZJ, Zeng XY, Liu C, Cai FY, Cao HL, Lü J (2018) Morphological control of CdS@ AC nanocomposites for enhanced photocatalytic degradation of tetracycline antibiotics under visible irradiation. *Inorg Chem Commun* 95:134–138. <https://doi.org/10.1016/j.inoche.2018.07.024>
- Zhan B, Liu Y, Zhou WT, Li SY, Chen ZB, Stegmaier T, Aliabadi M, Han ZW, Ren LQ (2021) Multifunctional 3D GO/g-C₃N₄/TiO₂ foam for oil-water separation and dye adsorption. *Appl Surf Sci* 541:148638. <https://doi.org/10.1016/j.apsusc.2020.148638>

- Zhang C, Gu Y, Teng G, Wang L, Jin X, Qiang Z, Ma W (2020a) Fabrication of a double-shell Ag/AgCl/G-ZnFe₂O₄ nanocube with enhanced light absorption and superior photocatalytic antibacterial activity. *ACS Appl Mater Interf* 12(26):29883–29898. <https://doi.org/10.1021/acsami.0c01476>
- Zhang L, Song F, Wang S, Wang H, Yang W, Li Y (2020b) Efficient removal of hexavalent chromium and congo red by graphene oxide/silica nanosheets with multistage pores. *J Chem Eng Data* 65(9):4354–4368. <https://doi.org/10.1021/acs.jced.0c00006>
- Zhao H, Wang R, Deng H, Zhang L, Gao L, Zhang L, Jiao T (2020) Facile preparation of self-assembled chitosan-based POSS-CNTs-CS composite as highly efficient dye absorbent for wastewater treatment. *ACS Omega* 6(1):294–300. <https://doi.org/10.1021/acsomega.0c04565>
- Zhao Y, Wang Y, Liang X, Shi H, Wang C, Fan J, Hu X, Liu E (2019) Enhanced photocatalytic activity of Ag-CsPbBr₃/CN composite for broad spectrum photocatalytic degradation of cephalosporin antibiotics 7-ACA. *Appl Catal B* 247:57–69. <https://doi.org/10.1016/j.apcatb.2019.01.090>
- Zhou C, Lai C, Xu P, Zeng G, Huang D, Zhang C, Cheng M, Hu L, Wan J, Liu Y, Xiong W (2018) In situ grown AgI/Bi₁₂O₁₇Cl₂ heterojunction photocatalysts for visible light degradation of sulfamethazine: efficiency, pathway, and mechanism. *ACS Sustain Chem Eng* 6(3):4174–4184. <https://doi.org/10.1021/acssuschemeng.7b04584>
- Zhou M, Wu J, Wang H, Guan D, Dong X, Wang J, Jia T, Liu Q (2020) Fabrication of Z-scheme heterojunction g-C₃N₄/Yb³⁺-Bi₅O₇I photocatalysts with enhanced photocatalytic performance under visible irradiation for HgO removal. *Energy Fuels* 34(12):16445–16455. <https://doi.org/10.1088/1755-1315/512/1/012045>
- Zhu X, Dudchenko AV, Khor CM, He X, Ramon GZ, Jassby D (2018) Field-induced redistribution of surfactants at the oil/water interface reduces membrane fouling on electrically conducting carbon nanotube UF membranes. *Environ Sci Technol* 52(20):11591–11600. <https://doi.org/10.1021/acs.est.8b02578>

Green Magnetic Nanoparticles in Industrial Wastewater Treatment: An Overview



**Laiza Bergamasco Beltran, Anna Carla Ribeiro,
Elizabeth da Costa Neves Fernandes de Almeida Duarte,
Rosângela Bergamasco, and Angélica Marquetotti Salcedo Vieira**

Abstract Overcoming the present global water quality and safety concern is a real challenge for the actual and future generations, and the green synthesis of nanomaterials has become a rising investigation point to support this goal due to its non-toxic and cost-effective aspects when compared with the conventional synthesised nanomaterials techniques, namely physical and chemical method. The nanomaterials green synthesis approach is classified as a bottom-top methodology. The nanoparticle formation occurs through a bio reduction mechanism of biological materials in the atoms/molecules level to nuclei and after towards a nanoscale particle ranging between (1–100 nm). The secondary metabolites present in leaf, peel and fruit extracts are responsible for the presence of bioactive compounds (alkaloids, lipids, terpenes, phenolic compounds), which have strong antioxidant activity and act as stabilising agents, being able to reduce metal ions. The application of metallic green nanoparticles (silver, gold, iron, copper) has been reported to efficiently remove emerging pollutants (heavy metals, dyes, etc.) from industrial wastewater by adsorption and photocatalytic treatment technologies. The great prospect of plant-mediated nanoparticles has been extensively explored; however, the scientific community should keep addressing all the efforts to guarantee the safety criteria for human health and ecosystems focusing on a sustainable decision.

L. B. Beltran (✉)

Post-Graduate Program in Food Sciences, State University of Maringá, Maringá, Paraná, Brazil

A. C. Ribeiro

Department of Environmental Biotechnology, State University of Maringá, Maringá, Paraná, Brazil

E. da Costa Neves Fernandes de Almeida Duarte

Linking Landscape, Environment, Agriculture and Food, Higher, Institute of Agronomy - University of Lisbon, Lisbon, Portugal

R. Bergamasco · A. Marquetotti Salcedo Vieira

Department of Chemical Engineering, State University of Maringá, Maringá, Paraná, Brazil

1 Introduction

The actual technology rhythm of the global society is very ambiguous in terms of advantages and disadvantages to the environment. As industrialisation can provide incredible progress, it also promotes an irrational use of natural resources to large-scale consumption goods production. Consequently, a huge amount of toxic and dangerous substances is released into nature without any treatment, which contributes to raising the negative pressure under the water bodies and compromises the access right to clean and safe water to every citizen. In some localities globally, the situation is even worse because the sanitation feature is absent, which is a very precise parameter to measure society's poor development and living inequality (Palani et al. 2021).

Industrial wastewaters are generated from many sectors, including agriculture, industries, and urban activities, and their composition is intrinsically linked to the source of origin. In general, it can contain organic and inorganic matter, pesticides, dyes, pharmaceuticals, heavy metals, metal ions, microorganisms, and others (Dehghani et al. 2021; Karri et al. 2021). Table 1 shows some industry types and the wastewater features generated by them (Abdelbasir and Shalam 2019).

As the industrial wastewater is particular to the industrial processing structure, its treatment is also specifically engineered to reach the removal efficiency to the specific pollutant target in question. Conventional water treatment plants are inefficient in treating such wastewater properly to eliminate such emerging pollutant particles (Goutam et al. 2020).

The need to ensure good water quality for present and future generations aroused the academic community's interest in refining available treatment technologies and their parameters to optimise the removal efficiency of emerging contaminants (Ahmed et al. 2021). Adsorption has emerged as an excellent option due to its applicability and cost-effective implementation. Adsorption has been recognised as a great option due to its applicability and low-cost implementation (Khan et al. 2021;

Table 1 Industry types its respective industrial wastewater feature (Abdelbasir and Shalan 2019; Palani et al. 2021)

Industry type	Industrial wastewater composition
Mining industries	Metals, acids and salts
Metal working and electroplating industries	Heavy metals and derivatives
Photo processing workshops and printing plants	Dyes, inks and Ag compounds
Paper and cellulose industries	Dioxins and chloride compounds
Petrochemicals industry	Oils and phenols compounds
Food industries	Suspended solids and organic matters

Mehmood et al. 2021; Lingamdinne et al. 2022). Moreover, the vast range of adsorbent materials is quite valuable in the field, as the researchers are also betting on the most greener source materials, as wastes from the industrial activity or urban residues, to re-signifying their destination and reintegrating them into the treatment process, applying the circular economy concept (Bolade et al. 2020).

For this purpose, nanotechnology has become a promising pathway in the wastewater purification sphere. The nanoscale dimension (10–100 μm) provides special physical and chemical properties to the materials, making them suitable for the pollutant's removal through main adsorption and photocatalytic processes. The high surface-to-volume ratio has a key role in their degree of functionalisation and high reactivity (Goutam et al. 2020; Palani et al. 2021).

Different nanoparticles have been successfully reported in the literature to treat industrial wastewater, such as carbon nanotubes (CNTs), zeolites, graphene-based nanomaterials, dendrimers, zero-valent metals (iron, gold, silver, and zinc), and metals oxide (iron oxide, silver oxide, titanium dioxide, zinc oxide, manganese oxide) nanoparticles. The wastewater treatment is categorised into three material classes: nano-adsorbents, nanomembranes, and nano-catalysts (Abdelbasir and Shalam 2019; Goutam et al. 2020; Palani et al. 2021).

Besides the great prospects of nanotechnology applied to wastewater, it also presents associated risks that must be considered in a global ecotoxicological assessment. The behavior of chemically synthesised nanomaterials, which are released into the environment, requires deep engagement from science to prevent environmental pollution and human health hazards (Goutam et al. 2020). Thus, overcoming the present global water quality and safety concern is a real challenge for the actual and future generations, and the green synthesis of nanoparticles has become a rising investigation point to support this goal due to its non-toxic and cost-effective aspects when compared with the conventional synthesised nanomaterials techniques, namely physical and chemical method.

The nanomaterials green synthesis approach is classified as a bottom-top methodology. The nanoparticle formation occurs through a bioreduction mechanism of biological materials in the atoms/molecules level to nuclei and towards a nanoscale particle ranging between (1–100 nm). The secondary metabolites present in leaf plant extracts, seeds, and peel extracts, named phytochemical compounds (alkaloids, lipids, terpenes, phenolic compounds), exhibit strong antioxidant activity and stabilise and reduce metal ions agents (Salem and Fouda 2020). The great benefit of such the green synthesis approach is its eco-friendly, non-toxic nature, and low production costs characteristics, which highlights its practical application and surpasses potential risks (Goutam et al. 2020).

This chapter will briefly approach the green synthesis of metallic nanoparticles (silver, gold, iron, copper) and their application in industrial wastewater treatment in recent literature. The challenges of the process will also be discussed.

2 Metallic Nanoparticles Synthesis Approaches

Recently, the use of metallic nanoparticles has been a widespread trend topic in the nanotechnology area due to the incredible characteristics of such materials. As its biotechnology applications are expanding in different areas (biomedicals, electronic and magnetic devices, electrocatalysts process), your synthesis methodology is also running to a more sustainable orientation (Salem and Fouda 2020).

The refined techniques that have been developed allow control of the synthesis methods to produce specific sizes, shapes, and chemical compositions of such nanoparticles. Furthermore, the nanoparticles can be classified according to some parameters, such as functionalisation degree (coated, bare NPs), chemical nature (organic or inorganic), surface morphology (high or low aspect ratio), physico-chemical properties (polymeric, metallic, carbon-based, lipid-based, semiconductor, ceramic), dimension (zero, one or two dimensional), crystallinity (amorphous, crystalline or polycrystalline), origin or source (natural or anthropogenic) and magnetic properties (paramagnetic or diamagnetic) (Goutam et al. 2020; Naseem and Durrani 2021; Salem and Fouda 2020).

The synthesis methodology has two different start pointing approaches: top-down and bottom-up. The first involves breaking a particle's bulk through a crystallographic injury on the particle surface to obtain smaller particles, which can be considered a negative impact on the formed nanostructure. The second, in its turn, is about a formation that starts at atomic or molecular levels and provides uniform structures and distributions when compared to the top-down approach (Goutam et al. 2020).

2.1 Conventional Methods

The nanoparticles can be synthesised by physical process (top-down approach). They can be categorised into two groups: mechanical methods, which involves milling, crushing, pulse wire discharge, lithography, and vapor methods through physical vapor deposition that consist in the incidence of a focused beam of electrons in a specific material to produce nanostructures at the gas phase. Besides the physical vapor deposition occurring without any catalytic interaction or chemical reactions, it can also be realised based on three different techniques: sputtering, laser ablation, and laser pyrolysis. On the other hand, the chemical method is considered a bottom-up approach, and the most used techniques are microwave, sol-gel, microemulsion, chemical vapor deposition, sonochemical, colloidal method, photochemical, solvothermal, coprecipitation, electrochemical, pyrolysis, chemical reduction (Goutam et al. 2020; Salem and Fouda 2020).

The conventional nanoparticles synthesis approach mentioned above has many limitations associated with utilising huge toxic chemical compounds, which will negatively impact the environment. Besides that, the cost of the whole process is

high due to the energy demand to keep all the variables working (pH, temperature, and pressure) (Goutam et al. 2020; Salem and Fouda 2020).

2.2 *Green Synthesis Methods*

As an alternative to the environmental risks associated with the conventional nanoparticles synthesis approaches, the green synthesis has demonstrated a great potential to overcome such drawbacks and keep a high pollutant removal performance. The use of the green synthesised nanoparticles also highlights effluents zero charge solution in low-economy countries considering its low-cost characteristics due to the catalytic reactions occurring in standard temperature and pressure, meaning an energy reduction, eco-friendly and non-toxic in terms of the materials origin, and suitable for scale-up implementation (Xiong Chang et al. 2021). Thus, in the present, the sustainable management of the use of nanotechnology applied to industrial wastewater treatment is urgently recommended, and it has captured substantial attention (Goutam et al. 2020; Salem and Fouda 2020; Vijayaraghavan and Ashokkumar 2017).

The green synthesis method is classified as a bottom-up approach and consists of applying biological systems to produce metallic nanoparticles without using hazardous reducing, capping, or stabilising chemical compounds in the process. Indeed, the premise of such a procedure is to apply the natural process pattern of bioleaching and bioaccumulation in the plant's cells into a systematised methodology that can be controlled and fitted according to the environmental issues needed (Goutam et al. 2020; Vijayaraghavan and Ashokkumar 2017).

Different biomaterials can be used as a basis for the green metallic nanoparticle's synthesis, namely: microalgae, fungi, bacteria, yeast, virus, and plant biomass/extract (Sahu et al. 2019a, b). The biochemical mechanism routes of the interaction of the metallic ions that end in nanoparticle synthesis are particular to each microorganism and require a deeper knowledge about the process (Goutam et al. 2020; Salem and Fouda 2020; Vijayaraghavan and Ashokkumar 2017). Thus, nanoparticles produced by the same microorganism type can vary in their characteristics (size, morphology, and shape) due to different environmental conditions (pH and temperature) (Makarov et al. 2014). Table 2 shows some examples of such biomaterials and their nanoparticles.

The fungi and bacterial cells frequently have been studied as biofactories for metallic nanoparticles synthesis through their cultivation in disinfected distilled water with some specific metallic salt under stirring and dark ambience. The microbes can synthesise the metallic nanoparticles from two routes: intracellularly and extracellularly by utilising secreted materials in the culture medium. This approach eventually presents some inconveniences related to microorganisms' growth rate, potential culture contamination, maintenance of optimal culture conditions of the process, which require constant assistance, difficulty on the standardisation of the inoculum size and less control about the nanoparticle size (Ahmad et al. 2019; Srikar et al. 2016; Vanlalveni et al. 2021).

Table 2 Examples bacteria, fungi and algae used in metallic nanoparticles green synthesis method (Salem and Fouda 2020)

	NPs	Synthesised by	Size (nm)
Bacteria	Au	<i>Pseudomonas aeruginosa</i>	15–30
		<i>Thermomonospora sp</i>	8–12
		<i>Pseudomonas aeruginosa</i>	10–20
		<i>Salmonella enterica</i>	42
		<i>Bacillus subtilis</i>	20–25
	Ag	<i>Bacillus sp.</i>	42–92
		<i>Bacillus licheniformis</i>	50
		<i>Pseudomonas</i>	20–70
TiO ₂	<i>Bacillus amyloliquefaciens</i>	15–87	
Fungi	Ag	<i>Beauveria bassiana</i>	10–50
		<i>Duddingtonia flagrans</i>	11.38
		<i>An amorphous Bjerkandera sp. R1</i>	10–100
		<i>Rhizopus stolonifer</i>	9.47
		<i>Cladosporium cladosporioides</i>	100
	Au	<i>Cladosporium oxysporum</i>	21–72
		<i>Fusarium oxysporum</i>	22–30
	Se	<i>Mariannaea sp.</i>	45–212
Algae	Ag	<i>Portieria hornemannii</i>	70–75
		<i>Botryococcus braunii</i>	88.87
	Au	<i>Egria sp.</i>	50
		<i>Chlorella sorokiniana</i>	5–15
		<i>Chlorella vulgaris</i>	5–9
	ZnO	<i>Sargassum muticum</i>	30–57

In fact, besides the microorganism's availability, the angiosperms plants species have been extensively used biomaterial to the metallic nanoparticle's green synthesis in comparison with other sources due to their practical methodological aspect and better reduction and stabilisation power (Ahamed et al. 2019; Srikar et al. 2016; Vijayaraghavan and Ashokkumar 2017).

Plant-mediated biomaterials have been investigated successfully for their effectiveness and potential viability for nanoparticle synthesis. This is because its attributes contemplate their vast abundance in nature conjugated with an enormous variety of metabolites in their chemical composition that may act in the reduction processes producing stable and presented metallic nanoparticles features with controlled size and shape (Thirugnanasambandham and Karri 2021). Furthermore, the green synthesis methodology is quite safe to handle, and it is based on a simple one-step process. Their rapid rate synthesis is also of great usefulness to enable large-scale

production in real industrial wastewater treatment plants (Salem and Fouda 2020; Vijayaraghavan and Ashokkumar 2017).

Briefly, the nanoparticles are formed by reducing metal ions by biomolecules present in plants such as terpenoids, enzymes, flavonoids, alkaloids, phenolic and carbonyl compounds, proteins, sugars, amine and amide groups, and other reducing agents. In a practical scenario, different plants have their own specific composition, and the mechanisms of biosynthesis should be analysed in each case. This is because several factors can affect the synthesis of these compounds due to the conditions the plant is exposed to, such as weather conditions, cultivation, age and other factors which directly affect the synthesis of bioactive compounds formed by the plant, which in turn has a direct impact on the synthesis of nanoparticles (Salem and Fouda 2020; Vijayaraghavan and Ashokkumar 2017).

Different parts of the plants (leaves, flower, fruit, seed, seed coat, roots, fruits, rhizomes) or whole plants can be used as biomass. After collecting the fresh plant and excluding any foulness, it will be washed with distilled water and cut into pieces, or if they are used in powder form, they will be properly dried and grounded. The biomass will be put in solution (deionised water or alcohol) and will be submitted to heating at a temperature below 60 °C, which is very important to keep the process performance since the target phytochemicals can decompose at high temperature. In short, plant-mediated metallic nanoparticles green synthesis involves mixing such prepared biomass with a metal salt solution of different concentrations, acting as the metal precursor, with a pH range previously defined at room temperature submitted or not to the agitation. The centrifuge separates the nanoparticles from the solution, and proper solvents are needed to wash them. The final step is to dry them in the oven, always taking care and avoiding high temperatures (Vanlalveni et al. 2021; Vijayaraghavan and Ashokkumar 2017).

After the reaction is complete, the formation of the nanoparticles can be detected through visual changes in solution color or using UV–Visible spectrophotometry to analyse the wavelength of the specific metal of interest. Beyond that, other characterisation techniques should be performed to confirm the nanoparticle's features, like Fourier transform infrared (FTIR) spectroscopy that is responsible for detecting the surface functional groups; Scanning Electron Microscopy (SEM) for topography and morphology visualisation; Transmission electron microscopy (TEM) for nanoparticle shape assessment and surface morphology and X-ray diffraction (XRD) that provides details about the crystalline structure. Figure 1 shows an experimental protocol of the process (Vijayaraghavan and Ashokkumar 2017).

As important as size and shape, the nanoparticle's real stability deserves attention once this parameter can create an aggregation tendency and lead to nanoparticle precipitation interfering in their pollutant's removal performance (Vanlalveni et al. 2021).

Therefore, it is essential to keep in mind that the formation process NPs is a compiled result of all the methodological variables that influence the reaction and consequently will determine its morphological and magnetic properties, such as pH, reaction contact time, concentration dosage, incubation temperature, types of the

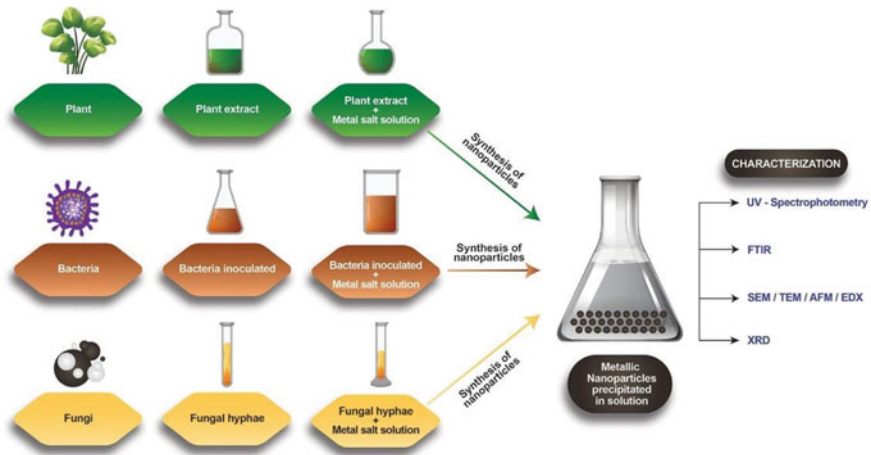


Fig. 1 Experimental protocol summary for plant-bacterial-fungal mediated biosynthesis of nanoparticles. *Source* Gupta et al. (2020)

chosen plant or part of them, or even the type of microorganisms to be used for the green synthesis.

Several works are found using the application of nanomaterials in the removal of industrial effluents such as removal of heavy metals, personal care and pharmaceutical products, halogenated compounds, toxic dyes and pesticides (Saleem and Zaidi 2020).

In this way, different plant species have been used in the green synthesis of metal and metal oxide nanoparticles in order to explore their potential in treating contaminated industrial wastewater containing recalcitrant pollutants. Several studies in the literature have demonstrated the green synthesis of such nanoparticles: Ag, CuO, Cu, Au, Ni, FeO, TiO₂, ZrO₂ (Peralta-Videa et al. 2016; Yadi et al. 2018; Salem and Fouda 2020).

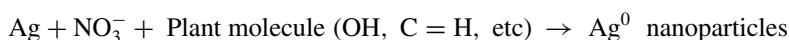
This section will summarise some plants used on the green synthesis of four noble metals emerging in the nanotechnology field, namely: Silver, Gold, Iron, and Copper nanoparticles and recent reports about their application in industrial wastewater treatment.

2.2.1 Silver Nanoparticles

The oldest human civilisation well knows the use of silver as Egyptians, Persians, Greeks, and Romans as a great metallic element to be used for food products storage, as a constituent for eating utensils and used as an antimicrobial agent until the antibiotic's discovery in the last century. Recently, silver nanoparticles have drawn a lot of attention due to their wide scope of properties, namely: antibacterial, anti-viral, anti-inflammatory, anti-parasitic, anti-fungal and anti-fouling, which can be applied

in diverse areas like biomedical, drug delivery, water treatment and agriculture (Ahamed et al. 2019; Srikar et al. 2016).

Compared with the routes of green synthesis, the plant-mediated method has been a great option for silver nanoparticle production. The material requirement base for the process is a silver metal ion solution, which can be prepared with different water-soluble silver salts and a reducing biological agent, which can be obtained from the biomass or extracts of various plants. When put together, the formation of the silver nanoparticles is visually detected by the brownish yellow color aspect and occurs according to the following reaction (Srikar et al. 2016; Vijayaraghavan and Ashokkumar 2017):



Different plants have been related to successfully producing silver nanoparticles such as fruit extract of tomato plant (*Solanum Lycopersicum*), *Abelmoschus esculentus* juice, *Hevea brasiliensis* latex and bark extracts of *Ficus benghalensis*, *Azadirachta indica*, lemongrass, red apple; Table 3 presents some suitable plants for this application and the respective silver nanoparticle size (Ahmad et al. 2019; Vijayaraghavan and Ashokkumar 2017).

The Ag NPs size has been reported to influence its disinfection power, meaning that the smaller sizes magnify the bactericidal effect since a greater superficial surface is available. The mechanisms that culminate in the bacterial, fungal and viral cell death is in the open debate yet, but the proposed studies indicate that the high Ag NP toxicity affects the cell membrane permeability, which will lead to structural alterations that may reach the DNA and hence, destroy it. The Ag^+ ions released into the cells also can cause many disturbs in different essential enzymes, cell replication and respiration, which are crucial for cell survival (Abdelbasir and Shalam 2019; Vanlalveni et al. 2021).

Table 3 Examples of plants used in the green synthesis of silver nanoparticles (Goutam et al. 2020; Salem and Fouda 2020; Vijayaraghavan and Ashokkumar 2017)

Plant	Ag NPs size (nm)
<i>Ziziphora tenuior</i> leaf extract	8–40
<i>Ficus carica</i> leaf extract	13
<i>Cymbopogon citratus</i> leaf extract	32
<i>Premna herbacea</i> leaf extract	10–30
<i>Alternanthera dentata</i> leaf extract	50–100
<i>Piper nigrum</i> leaf extract	4–50
<i>Piper nigrum</i> stem extract	9–30
<i>Cinnamomum camphora</i> leaf extract	55–80
<i>Pelargonium graveolens</i> leaf extract	16–40
<i>Podophyllum hexandrum</i> leaf extract	12–40
<i>Ocimum sanctum</i> extract	1.5–10

Ag NPs Applications in the Industrial Wastewater Field

Water purification is necessary due to the high load of microorganisms that can be contained in the hydraulic installations that bring water to the tap in homes and industries. Therefore, tap water must undergo a disinfection process to avoid bacterial incrustations, being very useful in the food industry. Ag NPs have controlled the release of silver ions, playing an efficient role in water disinfection and related disinfection applications (Mauter et al. 2018).

Among the vast applications and the great development of nanotechnology recently, silver nanoparticles have been extensively pointed as an important antimicrobial resource to water treatment and industrial wastewater sanitisation. In order to overcome the possibility of the Ag NPs agglomeration in solution, the use of sheet filters impregnated with such materials demonstrates a great potential to eliminate *Enterococcus faecalis*, *Escherichia coli* during water disinfection. Moreover, Ag NPs can improve the biofouling reduction of the filters, optimising the efficiency of the operation (Abdelbasir and Shalam 2019; Dankovich and Gray 2011; Mikelonis et al. 2016).

The oxide nanoparticles (Ag₂O) produced by the green synthesis method also has been reported as an efficient growth inhibitor of gram-negative bacteria (*Escherichia coli*, *Enterococcus faecalis*, *Proteus mirabilis*, and *Pseudomonas aeruginosa*), a great photocatalytic degradation agent for different dyes (acid orange 8 and methyl orange dye) and malachite green dye adsorbent from wastewater (Naseem and Durrani 2021).

Kumari and Tripathi (2020) described the bacteria *Bacillus cereus* cell extract utilisation for Au NPs production and its posterior addition in alumina support to the nanocomposite formation. The authors confirmed the great nano adsorbent performance of 98.43% chrome (Cr) removal and 99.4% lead (Pb) removal from pharmaceutical effluents collected from Lucknow city located in India.

The success removal of heavy metals (copper, iron, magnesium and lead) by Ag NPs originated from *Piliostigma thonningii* leaf extracts from synthetic wastewater was reported in the literature, as well as dye degradation (safranin orange, methyl red and methylene blue) for Ag NPs obtained by green synthesis through *Zingiber officinale rhizome* extract (Ganguly et al. 2021).

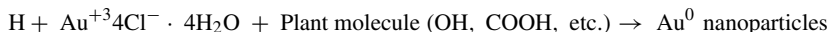
Indeed, the Ag NPs obtained from the green synthesis approach can be associated to support materials to form nanocomposites that will potentialise their pollutants removal efficiency from industrial wastewater, avoid eventual nanoparticles aggregation and enhance its reusability chances. Here are some examples: mixed composites of silver and cellulose for dyes removal (methyl orange, rhodamine B and congo red) from industrial, laboratory and household contaminated wastewater; mixed composites-based coconut shell activated carbon impregnated with Ag NPs to remove Cr (VI) from effluents. Effectively, the Ag NPs can be combined with chitosan, alginate, bimetallic nanoparticles, magnetic and other polymers to form different kinds of nanocomposites (Ganguly et al. 2021).

2.2.2 Gold Nanoparticles

Beyond this precious metal's ornamental and financial value, the gold possesses an interesting nature that includes monodispersity, large surface area, and availability for functionalisation with other particles, allowing different uses. Thus, nano-sized gold particles have captured substantial interest in scientific research due to their great application potential in many fields of knowledge, such as biomedical, electronics and catalytic processes (Choudhary et al. 2017; Vijayaraghavan and Ashokkumar 2017).

In the water and wastewater treatment domain, the Au NPs catalytic properties, which are derived from your negative redox potential, are extremely valuable. The Au NPs high optical absorption under ultraviolet (UV) and visible light irradiation has been investigated in photocatalytic reduction of contaminants through its electrons exchange with the reductor agente. Then, Au NPs is considered a great alternative to overcoming the limitation of the most used photocatalytic, namely TiO₂, which requires preferably UV light. In addition, the antimicrobial capacity is also detected in the Au NPs (Choudhary et al. 2017).

In this regard, the Au NPs green synthesis occurs by reducing the chloroaurate ions and capping through phytochemicals compounds. Several plants have been used for this function, and the Au NPs formation can be recognised when the solution has a ruby colored appearance. The process follows the reaction described below (Vijayaraghavan and Ashokkumar 2017):



The examples of plants that have been employed in the Au NPs are *Pelargonium graveolens* (geranium) leaves, *Azadirachta indica* leaf extract, black tea leaf extract, *Garcinia cambogia* fruit, *Pistacia integerrima* leaf galls extract, lemongrass plant extract, *Sphaeranthus indicus* fresh leaves, *Syzygium aromaticum*, *Cassia auriculata*, *Sesbania grandiflora*, *Allium cepa* cell extract and *Ficus racemosa* extract. Cumin seed powder, mango peel extract, and rose petals are also rich in sugars and protein compounds suitable for Au NPs biosynthesis (Choudhary et al. 2017; Yadi et al. 2018) (Table 4).

Au NPs Applications in the Industrial Wastewater Field

The evaluation of Au NPs in organic dyes removal has been reported with satisfactory results. The photocatalytic properties of the Au NPs enable them a great performance concerning reaction rate, which implies a reduction in the operation time (Choudhary et al. 2017; Salem and Fouda, 2020; Ahmed et al. 2021).

Adenigba et al. (2020) reported heavy metal removal, namely, lead (Pb) and zinc (Zn), from pharmaceutical wastewater by Au NPs produced from green synthesis of two types of microalgae as bioagents: *Chlorella vulgaris* and *Nannochloropsis* sp.

Table 4 Examples of plants used in the green synthesis of gold nanoparticles (Goutam et al. 2020; Vijayaraghavan and Ashokkumar 2017; Yadi et al. 2018)

Plant	Au NPs size (nm)
<i>Magnolia kobus</i> and <i>Diospyros kaki</i> leaf extracts	5–300
Pear fruit extract	200–500
Ethanolic extract <i>Mentha arvensis</i> leaves	15–39
<i>Digitaria radicata</i> leaves extract	90
<i>Diospyros paniculata</i> root extract	14–28
<i>Emblica Officinalis</i> fruit	10–70
<i>Dioscorea alata</i> extract	10–20
<i>Pelargonium graveolens</i> extract	20–40
<i>Trigonella foenum-graecum</i> extract	15–25

Regarding the Au NPs derived from *Nannochloropsis* sp, the results showed 60.32% Zn removal and 66.53% Pb removal. On the other hand, *Chlorella vulgaris* presented 66.83% of Zn removal and 57.41% removal of Pb. This study certainly highlights the great prospect of this application in industrial wastewater with such characteristics.

The efforts to degrade non-biodegradable dyes of industrial effluents has been the focus of numerous reports nowadays since almost 15% of them are released during the process in textile industries. On this matter, Bonigala et al. (2018) synthesised Au NPs from *Stemona tuberosa* Lour plant extract to degrade methyl orange, methyl red and methylene blue through catalytic activity, methyl orange, methyl red and methylene blue in the presence of sodium borohydride (NaBH₄). The study also includes the removal of a phenolic compound: 4-nitrophenol. The results obtained showed that the Au NPs were efficient in the proposed toxic chemicals removal.

In the same perspective, Teimouri et al. (2018) reviewed the 4-nitrophenol compound degradation in industrial wastewater by Au NPs originated from different botanical sources and reported the great potential of such application. The insecticidal effect of Au NPs over some mosquito species, which are disease vectors, were also discussed and presented promising highlights. However, it requires deep research to guarantee no harmful effects on non-target species.

2.2.3 Iron Oxide Nanoparticles

The use of iron nanoparticles (Fe NPs) has been studied due to their advantages over other nanoscale materials used to treat industrial effluents. They have a high surface area and good adsorption capacity due to their ferromagnetic property. In addition to being low-cost, it is economically viable. It is efficient as a photocatalyst in metal degradation reactions, organic pollutants, as well as in the inactivation of viruses in aquatic environments, showing the potential of this material (Ahmed et al. 2014; Mohammed et al. 2017).

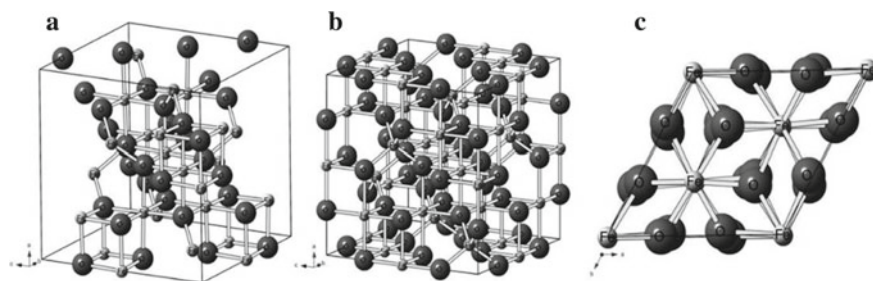


Fig. 2 Morphological dimensions and chemical structures of different iron oxide nanoparticles: crystal structure of magnetite **a** the crystal structure of maghemite **b** and crystal structure of hematite **c** Oliveira et al. (2013)

The green synthesis of Fe NP is carried out from biodegradable organic matter as it is carried out by the process in which extracts from plants and microorganisms are responsible for its production. The synthesis carried out by these extracts is advantageous due to the reaction time in which it occurs, as well as the stability of the cellular structure of the material is maintained all the process (Devatha et al. 2016).

Iron oxides have anionic arrangements, generally hexagonal or cubic shapes, in relation to their empirical form. The properties of iron oxides are directly related to the dimensions and morphology of their structures. Therefore, iron oxide nanoparticles have different properties when compared to materials in a massive state (Silva et al. 2015). The researchers used iron oxide nano adsorbents such as magnetite (Fe₃O₄) (Fig. 1a), maghemite (γ-Fe₂O₃) (Fig. 1b) and hematite (α-Fe₂O₃) (Fig. 1c) to remove industrial effluents from the aqueous medium (Zargoosh et al. 2013) (Fig. 2).

Iron nanoparticles synthesised by plant extracts are increasingly used due to their environmental and economic potential (Devatha et al. 2016; Bolade et al. 2020). The green synthesis of Fe NP is done from biodegradable organic matter as it is carried out by the process in which extracts from plants and microorganisms are responsible for the production. The synthesis carried out by these extracts is advantageous as the reaction time in which it takes place, as well as the stability of the cell structure of the material, is maintained throughout the process (Devatha et al. 2016).

This technique is based on the metabolites obtained during the bioprocess. Therefore, compounds such as flavonoids, phenols, tannin, and others are used as reducing agents in the production of nanoparticles, replacing methods that use chemical products that are toxic to the environment (Abdullah et al. 2020). Table 5 shows some plants used to synthesise Fe nanoparticles and the size of the synthesised nanoparticles.

He attributes his redox potential and propensity for ion exchange with various pollutants to the use of iron-based nanomaterials as adsorbents (Kebede et al. 2020). The mechanism of pollutant removal may be achieved by different functional groups simultaneously due to surface properties and characteristics, and there may be a combination of methods such as adsorption-disinfection (Mashkoo and Nasar 2020).

Table 5 Examples of plants used in the green synthesis of iron nanoparticles

Plant	Fe NPs size (nm)	References
<i>Green tea</i> leaf extract	40–60	Mareedu et al. (2021)
<i>Tree leaf</i> extracts	10–30	Machado et al. (2013)
<i>Terminalia chebula</i> fruit extract	80	Mohan Kumar et al. (2013)
<i>Colocasia esculenta</i> leaves extract	10–25	Thakur and Karak (2014)
<i>Sorghum bran</i> extract	50	Njagi et al. (2011)
<i>eucalyptus</i> leaf extract	20–80	Wang et al. (2014)
<i>Tridax procumbens</i> leaf extract	80–100	Senthil and Ramesh (2012)
<i>Camellia sinensis</i> leaf extract	10–30	Gottimukkala et al. (2017)

Fe NPs Applications in the Industrial Wastewater Field

The reduction, oxidation, adsorption and conversion methods have been successfully obtained to eliminate many industrial contaminants, including heavy metals, organic compounds, dyes, and others (Abdelbasir and Shalan 2019).

Bibi et al. (2019) had carried out the green synthesis of Fe₂O₃ NPs using *Punica granatum* extract to remove the reactive blue dye 4 using the ultraviolet irradiation technique. The Fe₂O₃ exhibited promising photocatalytic activity as 95.08% of the dye degradation was degraded in 56 min of ultraviolet irradiation.

To evaluate the removal of acid black dye, Wang et al. (2014) had developed iron polyphenol nanoparticles (Fe–P NPs) from extracts of *E. tereticornis*, *M. nesophila* and *R. officinalis* plants. The authors reported that about 100% removal of acid black dye was achieved. Of the extracts studied, the extract from the *E. Tereticornis* plant showed better activity against dye degradation than the other extracts.

In their study, Huang et al. (2014) prepared Fe NPs from green tea leaf extract and evaluated the following parameters: solution pH, temperature and extract volume to determine the best condition for malachite green dye removal from an aqueous medium. It was reported that increasing the pH of the solution and volume of extract negatively lead to dye removal. Therefore, increasing the temperature improved the interaction/reactivity of the nanoparticles. The removal of malachite green dye from Fe nanoparticles prepared using green tea leaves was 90.56%.

The adsorption capacity of an adsorbent is one of the most important parameters, as it directly affects its removal efficiency. Heavy metals are harmful to health, and their disposal without proper treatment can be extremely harmful. In their study, Zargoosh et al. (2013) evaluated the ability of Fe₃O₄ nanoparticles to remove heavy metals Co²⁺, Cu²⁺, Zn²⁺, Cd²⁺ and Pb²⁺ from an aqueous medium. The capacity of adsorption and removal of metals was reported to be 27.7, 76.9, 51.3, 107.5 and 188.7, respectively. Therefore, the authors concluded that Fe₃O₄ nanoparticles are easy to synthesise, have a high capacity to remove heavy metals from industrial residues, and be reused, making the process economically viable.

Table 6 Examples of plants used in the green synthesis of copper nanoparticles

Plant	Cu NPs size (nm)	References
<i>Celastrus paniculatus</i> Willd. leaf extract	2–10	Mali et al. (2020)
<i>Aloe Vera</i> leaf extract	20	Biftu et al. (2020)
<i>Azadirachta indica</i> leaves extract	48	Nagar and Devra (2018)
<i>M. oleifera</i> leaves extract	35–49	Das et al. (2020)
<i>Calotropis gigantea</i> leaf extract	20–30	Sharma et al. (2015)
<i>Tecoma castanifolia</i> leaf extract	100	Sharmila et al. (2016)
<i>Piper retrofractum</i> Vahl fruit extract	2–10	Amaliyah et al. (2020)

2.2.4 Copper Nanoparticles

Green synthesis in the production of copper nanoparticles (Cu NPs) and copper oxide (CuO NPs) turns out to be the most feasible and economical method at present, as plants and microorganisms can produce it. Since plants have biologically active compounds, they are responsible for the process of synthesis of nanoparticles. All parts of plants can be used, such as leaves, flowers, and fruits (Murthy et al. 2020). Table 6 shows some examples of common plants in the synthesis of Cu NPs and the size of nanoparticles.

The applications of copper (Cu) and Cu-based nanoparticles based on copper, an abundant and inexpensive metal on Earth, have attracted great interest in recent years. Cu-based materials can promote and perform a variety of reactions due to the wide range of accessible oxidation states of Cu (Cu0, CuI, CuII, and CuIII), which enable reactivity via both one- and two-electron pathways. Due to their unique features and properties, Cu-based nanoparticles are widely used to decontaminate industrial water (Gawande et al. 2016).

Cu NPs Applications in the Industrial Wastewater Field

In recent years, various methods have been developed to remove industrial contaminants, such as reverse osmosis, ion exchange, coagulation, adsorption, flocculation, and others. Adsorption has gained popularity as it is a highly efficient process for removing various impurities and is also economically viable. Copper and copper oxide nanoparticles (Cu/CuO NPs) are widely used as adsorbents due to their large surface area and small size (Rather and Sundarapandian 2021).

To evaluate the removal of the dye rhodamine-b, Rather and Sundarapandian (2021) carried out the synthesis of copper oxide nanoparticles (CuO NPs) using the leaf extract *Wedelia urticifolia*. It was found that the dye adsorption increased with the volume of adsorbent and contact time, and removal of more than 99% was achieved. Therefore, they concluded that nanoparticles are commonly synthesised as an alternative adsorbent and are economically viable as they can be reused in future processes.

Dyes have high toxicity to the environment and animals. Several researchers have made efforts to find adsorbents/bioadsorbents that can remove them (Safavi and Momeni 2012). Given this, Vidovix et al. (2019) synthesised copper oxide nanoparticles (CuO NPs) using *Punica granatum* leaf extract to study the removal of methylene blue dye from the aqueous medium. The material used as an adsorbent showed high removal of 96.91% of methylene blue dye, which shows that its application in contaminated wastewater is feasible.

To evaluate the removal of crystal violet dye, Khani et al. (2018) synthesised copper nanoparticles using *Z. Spina-Christi* fruit extract as adsorbent. Using a small amount of adsorbent (80 mg), 95% removal was observed in 7.5 min. This shows the efficiency in the removal of crystal violet dye.

Prakash et al. (2018) used a *Cordia sebestena* bloom to synthesise copper oxide particles (CuO NPs). The catalytic efficiency of hydrogen peroxide from nanoparticles was evaluated to degrade bromothymol blue (BTB). The authors reported 100% efficiency in removing the dye after 3 h of sun exposure. The extract is also antibacterial, showing efficacy against gram-positive bacteria (*S. aureus*) and gram-negative bacteria (*E. coli*, *K. Pneumonia*, and *B. subtilis*), proving that it has potential for environmental and antimicrobial applications.

3 Physico-Chemical Parameters Influencing in Metallic Nanoparticles Green Synthesis

The metallic nanoparticle's green synthesis is influenced by the physico-chemical parameters that control the bioreduction reaction. In the plant-mediated green synthesis approach, the electrical charges of phytochemical compounds and their capping and stabilising nature are affected by the pH of the solution. The nanoparticles' speed formation and their size, shape, and agglomeration tendency are regulated according to pH conditions: acid, neutral or basic (Vijayaraghavan and Ashokkumar 2017).

In acid conditions, the formation of large-sized nanoparticles is more likely to occur due to the low rate of metal ion nucleation, leading to agglomeration. Whereas in basic conditions, the homogeneous distribution and the increasing metal nucleation rate propitiates the reduction of metallic ions to spherical and decahedral small-size metallic nanoparticles. In high pH values, the functional group's availability degree

of the biomolecules presents in the plant extract is crucial to provide binding places to the metallic nanoparticles (Goutam et al. 2020; Vanlalveni et al. 2021).

Likewise, the reaction temperature directly impacts the biosynthesis rate, meaning that the increase of it causes the increase in the nucleation centers, which is favorable to the formation of metallic nanoparticles. In terms of the energetic demand and operation costs, the ideal situation would be expected that the green synthesis would be conducted under room temperature, considering that the spherical shape would probably be obtained. However, specific applications can require proper shapes, such as cubic, pentagonal, hexagonal or triangular, and the process should be regulated to favorable conditions for them (Vanlalveni et al. 2021; Vijayaraghavan and Ashokkumar 2017).

The reaction time is also an important parameter to consider in the nanoparticles green synthesis, and it has been reported as a great gain of the plant-mediated synthesis over the microorganisms-mediated synthesis since the last ones necessitate more time to grow. However, many authors in the literature have demonstrated that the yield rate is also improved as long as the reaction time is prolonged (Vijayaraghavan and Ashokkumar 2017).

Other factors like the chemical composition of the chosen plant determine the presence of specific biomolecules and which kind of solvent (level of solubility) and reaction time and temperature should be addressed to extract them during the plant extract preparation. Other factors, like the plant extract concentration plus the metal salt concentration, should be adjusted to the optimal conditions (Vanlalveni et al. 2021).

4 Conclusion and Future Perspectives

The metallic nanoparticles green synthesis, especially the plant-mediated approach, has shown effective contaminants removal results, namely heavy metals, organic pollutants (essential dyes), besides the antimicrobial properties and disinfection power in contaminated wastewaters.

These findings highlight the expansion of its applicability in industrial wastewater treatment plants, as the urgency to recover the quality of the effluent before its release in water bodies should be considered an environmental priority nowadays.

The green synthesis approach has opened the pathway to sustainable use of metallic nanoparticles in wastewater remediation, nano-photocatalysis materials, nanomembranes, and nano sorbents, due to its non-toxic and eco-friendly characteristics. However, deeper studies should focus on this research line to overview all the secondary effects that can bring to the ecosystem and the society. The whole understanding of the mechanisms of action of such nanoparticles in the environment could be investigated by toxicity studies which will investigate the pose effect over the target (algae, crustaceans, bacteria) and non-target species (mammalian cells). Moreover, the evaluation of dissolution rate, size, and toxicity levels is imprescriptible for the material's rational utilisation. The scientific proposal should aim to construct

a detailed risk assessment for nanoparticles, including their proper waste disposal through official regulations.

The recovery, through the separation process and reusability of metallic nanoparticles from aqueous solutions, is a remarkable matter to guarantee its implementation for commercial use and clearly demands intensive research community efforts.

Acknowledgements The authors thank the Conselho Nacional de Desenvolvimento Científico e Tecnológico (CNPq, Brasília, Brazil) and Coordenação de Aperfeiçoamento de Pessoal de Nível Superior (CAPES, Brasília, Brazil) by the financial support for this research (financing code 001).

Conflict of Interest The authors declare that they have no conflicts of interest.

References

- Abdelbasir S, Shalan A (2019) An overview of nanomaterials for industrial wastewater treatment. *Korean J Chem Eng* 36:1209–1225
- Abdullah JAA, Salah Eddine E, Abderrhmane B, Alonso-González M, Guerrero A, Romero A (2020) Green synthesis and characterisation of iron oxide nanoparticles by *Phoenix dactylifera* leaf extract and evaluation of their antioxidant activity. *Sustain Chem Pharm* 17:100280
- Adenigba VO, Omomowo IO, Oloke JK et al (2020). Evaluation of microalgal-based nanoparticles in the adsorption of heavy metals from wastewater. In: IOP Conference series: materials science and engineering, vol 805, no 1, pp 012030
- Ahmad S, Munir S, Zeb N et al (2019) Green nanotechnology: a review on green synthesis of silver nanoparticles—An ecofriendly approach. *Int J Nanomed* 14:5087
- Ahmed T, Imdad S, Yaldran K et al (2014) Emerging nanotechnology-based methods for water purification: a review. *Desalin Water Treat* 52:4089–4101
- Ahmed S, Khan FSA, Mubarak NM, Khalid M, Tan YH, Mazari SA, Karri RR, Abdullah EC (2021). Emerging pollutants and their removal using visible-light responsive photocatalysis – A comprehensive review. *J Environ Chem Eng* 9(6)
- Amaliyah S, Pangesti DP, Masruri M, Sabarudin A, Sumitro SB (2020) Green synthesis and characterization of copper nanoparticles using Piper retrofractum Vahl extract as bioreductor and capping agent. *Heliyon* 6(8):e04636. <https://doi.org/10.1016/j.heliyon.2020.e04636>
- Bibi I, Nazar N, Ata S, Sultan M, Ali A, Abbas A (2019) Green synthesis of iron oxide nanoparticles using pomegranate seeds extract and photocatalytic activity evaluation for the degradation of textile dye. *Integr Med Res* 8:6115–6124
- Biftu WK, Ravindhranath K, Ramamoorthy M (2020) New research trends in the processing and applications of iron-based nanoparticles as adsorbents in water remediation methods. *Nanotechnol Environ Eng* 5(2). <https://doi.org/10.1007/s41204-020-00076-y>
- Bolade OP, Williams AB, Benson NU (2020) Green synthesis of iron-based nanomaterials for environmental remediation: A review *Environ. Nanotechnol Monit Manag* 13:100279
- Bonigala B, Kasukurthi B, Konduri VV et al (2018) Green synthesis of silver and gold nanoparticles using *Stemona tuberosa* Lour and screening for their catalytic activity in the degradation of toxic chemicals. *Environ Sci Pollut Res* 25(32):32540–32548
- Choudhary BC, Paul D, Gupta T et al (2017) Photocatalytic reduction of organic pollutant under visible light by green route synthesised gold nanoparticles. *J Environ Sci* 55:236–246
- Dankovich TA, Gray DG (2011) Bactericidal paper impregnated with silver nanoparticles for point-of-use water treatment. *Environ Sci Technol* 45(5):1992–1998
- Das PE, Abu-Yousef IA, Majdalawieh AF, Narasimhan S, Poltronieri P (2020) Green synthesis of encapsulated copper nanoparticles using a hydroalcoholic extract of *Moringa oleifera* leaves and

- assessment of their antioxidant and antimicrobial activities. *Molecules* 25(3):555. <https://doi.org/10.3390/molecules25030555>
- Dehghani MH, Omrani GA, Karri RR (2021) Solid waste—sources, toxicity, and their consequences to human health. *Soft computing techniques in solid waste and wastewater management*. Elsevier, pp 205–213. <https://doi.org/10.1016/B978-0-12-824463-0.00013-6>
- Devatha CP, Thalla AK, Katte SY (2016) Green synthesis of iron nanoparticles using different leaf extracts for treatment of domestic waste water. *J Clean Prod* 139:1425–1435
- Ganguly K, Dutta SD, Patel DK et al (2021). Silver nanoparticles for wastewater treatment. In: *Aquananotechnology*. Elsevier, pp 375–391
- Gawande MB, Goswami A, Felpin FX (2016) Cu and Cu-based nanoparticles: synthesis and applications in catalysis. *Chem Rev* 116(6):3722–3811
- Gottimukkala KSV, Harika RP, Deeveka Z (2017) Green synthesis of iron nanoparticles using green tea leaves extract. *J Nanomedicine Biotherapeutic Discov* 7:1–4
- Goutam SP, Saxena G, Roy D et al (2020) Green synthesis of nanoparticles and their applications in water and wastewater treatment. *Bioremediation of industrial waste for environmental safety*. Springer, Singapore, pp 349–379
- Gupta A, Tandon M, Kaur A (2020) Role of metallic nanoparticles in water remediation with special emphasis on sustainable synthesis: a review. *Nanotechnol Environ Eng* 5(3):1–13
- Huang L, Weng X, Chen Z, Megharaj M, Naidu R (2014) Spectrochimica acta part a: molecular and biomolecular spectroscopy synthesis of iron-based nanoparticles using oolong tea extract for the degradation of malachite green. *Spectrochim Acta Part A Mol Biomol Spectrosc* 117:801–804
- Karri RR, Ravindran G, Dehghani MH (2021). Wastewater—sources, toxicity, and their consequences to human health. *Soft computing techniques in solid waste and wastewater management*. Elsevier, pp 3–33. <https://doi.org/10.1016/B978-0-12-824463-0.00001-X>
- Kebede W, Ravindhranath BK, Ramamoorthy M (2020) New research trends in the processing and applications of iron-based nanoparticles as adsorbents in water remediation methods. *Nanotechnol Environ Eng* 5(2):1–12
- Khan FSA, Mubarak NM, Khalid M, Walvekar R, Abdullah EC, Ahmad A, Karri RR, Pakalapati H (2021). Functionalized multi-walled carbon nanotubes and hydroxyapatite nanorods reinforced with polypropylene for biomedical application. *Sci Rep* 11(1)
- Khani R, Roostaei B, Bagherzade G et al (2018) Green synthesis of copper nanoparticles by fruit extract of *Ziziphus spina-christi* (L.) Willd.: application for adsorption of triphenylmethane dye and antibacterial assay. *J Mol Liq* 255:541–549
- Kumari V, Tripathi AK (2020) Remediation of heavy metals in pharmaceutical effluent with the help of *Bacillus cereus*-based green-synthesised silver nanoparticles supported on alumina. *Appl Nanosci* 10(6):1709–1719
- Lingamdinne LP, Choi JS, Angaru GKR, Karri RR, Yang JK, Chang YY, Koduru JR (2022) Magnetic-watermelon rinds biochar for uranium-contaminated water treatment using an electromagnetic semi-batch column with removal mechanistic investigations. *Chemosphere* 286
- Machado S, Pinto SL, Grosso JP, Nouws HPA, Albergaria JT (2013) Science of the Total Environment Green production of zero-valent iron nanoparticles using tree leaf extracts. *Sci Total Environ* 445–446:1–8
- Makarov VV, Love J, Sinityna OV et al (2014) Green nanotechnologies: synthesis of metal nanoparticles using plants. *Acta Naturae* 6(1):35–44
- Mali SC, Dhaka A, Githala CK, Trivedi R (2020) Green synthesis of copper nanoparticles using *Celastrus paniculatus* Willd. leaf extract and their photocatalytic and antifungal properties. *Biotechnol Rep* 27:e00518. <https://doi.org/10.1016/j.btre.2020.e00518>
- Mareedu T, Poiba VR, Vangalapati M (2021) Green synthesis of iron nanoparticles by green tea and black tea leaves extract. *Mater Today Proc* 42:1498–1501. <https://doi.org/10.1016/j.matpr.2021.01.444>
- Mashkoor F, Nasar A (2020) Magsorbents: Potential candidates in wastewater treatment technology—a review on the removal of methylene blue dye. *J Magn Magn Mater* 500:166408.

- Mauter MS, Zucker I, Perreault F, Werber JR, Kim J-H, Elimelech M (2018) The role of nanotechnology in tackling global water challenges. *Nat Sustain* 1(4):166–175. <https://doi.org/10.1038/s41893-018-0046-8>
- Mehmood A, Khan FSA, Mubarak NM, Tan YH, Karri RR, Khalid M, Walvekar R, Abdullah EC, Nizamuddin S, Mazari SA (2021) Magnetic nanocomposites for sustainable water purification—a comprehensive review. *Environ Sci Pollut Res* 28(16):19563–19588
- Mikelonis AM, Youn S, Lawler DF (2016) DLVO approximation methods for predicting the attachment of silver nanoparticles to ceramic membranes. *Langmuir* 32(7):1723–1731
- Mohammed L, Gomaa HG, Ragab D et al (2017) Magnetic nanoparticles for environmental and biomedical applications: a review. *Particuology* 30:1–14
- Mohan Kumar K, Mandal BK, Siva Kumar K, Sreedhara Reddy P, Sreedhar B (2013) Biobased green method to synthesise palladium and iron nanoparticles using *Terminalia chebula* aqueous extract. *Spectrochim Acta A Mol Biomol Spectrosc* 102:128–133
- Murthy HCA, Desalegn T, Kassa M, Abebe B, Assefa, T (2020) Synthesis of green copper nanoparticles using medicinal plant *hagenia abyssinica* (Brace) JF. Gmel. leaf extract: antimicrobial properties. *J Nanomater* 1–12
- Nagar N, Devra V (2018) Green synthesis and characterization of copper nanoparticles using *Azadirachta indica* leaves. *Mater Chem Phys* 213:44–51 <https://doi.org/10.1016/j.matchemphys.2018.04.007>
- Naseem T, Durrani T (2021) The role of some important metal oxide nanoparticles for wastewater and antibacterial applications: a review. *Environ Chem Ecotoxicol* 3:59–75
- Njagi EC, Huang H, Stafford L, Genuino H, Galindo HM et al (2011) Biosynthesis of iron and silver nanoparticles at room temperature using aqueous sorghum bran extracts. *Langmuir* 27(1):264–271
- Oliveira LCA, Fabris JD, Pereira MC (2013) Óxidos de ferro e suas aplicações em processos catalíticos: uma revisão. *Quim Nova* 36(1):123–130
- Palani G, Arputhalatha A, Kannan K et al (2021) Current trends in the application of nanomaterials for the removal of pollutants from industrial wastewater treatment—a review. *Molecules* 26(9):2799
- Peralta-Videa JR, Huang Y, Parsons JG et al (2016) Plant-based green synthesis of metallic nanoparticles: scientific curiosity or a realistic alternative to chemical synthesis. *Nanotechnol Environ Eng* 1(1):1–29
- Prakash S, Elavarasan N, Venkatesan A et al (2018) Green synthesis of copper oxide nanoparticles and its effective applications in Biginelli reaction, BTB photodegradation and antibacterial activity. *Adv Powder Technol* 29(12):3315–3326
- Rather MY, Sundarapandian S (2021) Facile green synthesis of copper oxide nanoparticles and their Rhodamine-b dye adsorption property. *J Clust Sci* 1–9
- Safavi A, Momeni S (2012) Highly efficient degradation of azo dyes by palladium/hydroxyapatite/Fe₃O₄ nano-catalyst. *J Hazard Mater* 201:125–131
- Sahu JN, Zabed H, Karri RR, Shams S, Qi X (2019a). Applications of nano-biotechnology for sustainable water purification. *Ind Appl Nanomater* 313–340
- Sahu JN, Karri RR, Zabed HM, Shams S, Qi X (2019b). Current perspectives and future prospects of nano-biotechnology in wastewater treatment. *Sep Purif Rev* 1–20
- Salem SS, Fouda A (2020) Green synthesis of metallic nanoparticles and their prospective biotechnological applications: an overview. *Biol Trace Elem Res* 199(1):344–370
- Saleem H, Zaidi SJ (2020) Developments in the application of nanomaterials for water treatment and their impact on the environment. *Nanomaterials* 10(9):1764. <https://doi.org/10.3390/nano1091764>
- Senthil M, Ramesh C (2012) Biogenic synthesis of Fe₃O₄ nanoparticles using *tridax procumbens* leaf extract and its antibacterial activity on *pseudomonas aeruginosa*. *Dig J Nanomater Biostruct* 7:1655–1660

- Sharma JK, Akhtar MS, Ameen S, Srivastava P, Singh G (2015) Green synthesis of CuO nanoparticles with leaf extract of *Calotropis gigantea* and its dye-sensitized solar cells applications. *J Alloys Compd* 632:321–325. <https://doi.org/10.1016/j.jallcom.2015.01.172>
- Sharmila G, Thirumarimurugan M, Sivakumar VM (2016) Optical catalytic and antibacterial properties of phytofabricated CuO nanoparticles using *Tecoma castanifolia* leaf extract. *Optik* 127(19):7822–7828. <https://doi.org/10.1016/j.ijleo.2016.05.142>
- Silva MF, Pineda EAG, Bergamasco R (2015) Aplicação de óxidos de ferro nanoestruturados como adsorventes e fotocatalisadores na remoção de poluentes de águas residuais. *Quim Nova* 38:393–398
- Srikar SK, Giri DD, Pal DB et al (2016) Green synthesis of silver nanoparticles: a review. *Green Sustain Chem* 6(1):34–56
- Teimouri M, Khosravi-Nejad F, Attar F et al (2018) Gold nanoparticles fabrication by plant extracts: synthesis, characterisation, degradation of 4-nitrophenol from industrial wastewater, and insecticidal activity—a review. *J Clean Prod* 184:740–753
- Thakur S, Karak N (2014) One-step approach to prepare magnetic iron oxide/reduced graphene oxide nanohybrid for efficient organic and inorganic pollutants removal. *Mater Chem Phys* 144(3):425–432
- Thirugnanasambandham K, Karri RR (2021) Preparation and characterization of *Azadirachta indica* A. Juss. plant based natural coagulant for the application of urban sewage treatment: Modelling and cost assessment. *Environ Technol Innov* 23
- Vanlalveni C, Lallianrawna S, Biswas A et al (2021) Green synthesis of silver nanoparticles using plant extracts and their antimicrobial activities: a review of recent literature. *RSC Adv* 11(5):2804–2837
- Vidovix TB, Quesada HB, Januário EFD et al (2019) Green synthesis of copper oxide nanoparticles using *Punica granatum* leaf extract applied to the removal of methylene blue 257:126685
- Vijayaraghavan K, Ashokkumar T (2017) Plant-mediated biosynthesis of metallic nanoparticles: a review of literature, factors affecting synthesis, characterisation techniques and applications. *J Environ Chem Eng* 5(5):4866–4883
- Wang T, Jin X, Chen Z, Megharaj M, Naidu R (2014) Science of the total environment green synthesis of Fe nanoparticles using *eucalyptus* leaf extracts for treatment of eutrophic wastewater. *Sci Total Environ* 466–467:210–213
- Xiong Chang X, Mujawar Mubarak N, Ali Mazari S, Sattar Jatoti A, Ahmad A, Khalid M, Walvekar R, Abdullah EC, Karri RR, Siddiqui MTH, Nizamuddin S (2021) A review on the properties and applications of chitosan, cellulose and deep eutectic solvent in green chemistry. *J Ind Eng Chem* 104:362–380
- Yadi M, Mostafavi E, Saleh B et al (2018) Current developments in green synthesis of metallic nanoparticles using plant extracts: a review. *Artif Nanomedicine Biotechnol* 46:336–343
- Zargoosh K, Abedini H, Abdolmaleki A, Molavian MR (2013) Effective removal of heavy metal ions from industrial wastes using thiosalicylhydrazide-modified magnetic nanoparticles. *Ind Eng Chem Res* 52:14944–14954

Nanocellulose in Industrial Wastewater Treatment: An Overview



Vartika Srivastava

Abstract Over the past few decades, the urge for fresh and pure water has been rising each day. The need of the hour is to develop such viable technologies which are economical, have greater efficacy and lower carbon footprint over conventional methods. The current chapter features modern research studies related to the application of nanocellulose and its composites for the treatment of wastewater. Cellulose in the form of nanocrystal and nanofibrils are used effectively for the purpose of water purification owing to their unique properties. Nanocelluloses are bio-degradable, non-toxic materials used sustainably as nanofiller due to their remarkable mechanical properties, larger surface area, controllable surface chemistry and high aspect ratio. The chapter discusses the effectiveness of these materials for the removal of water pollutants through adsorption, catalytic degradation, photocatalysis, and flocculation. The mechanisms involved in the action of these processes are also discussed. Moreover, the limitations of these nanocellulose-based materials, along with the opportunities and the future prospects for wastewater treatment, have been discussed in detail.

1 Introduction

The evolution of Nanotechnology over the past few decades has redefined several industries and diminished the conventional scientific limitations. The objective of achieving viable development can be accomplished by substituting the non-renewable sources of energy with biodegradable and green renewable sources around the world. In the past few years, Nanotechnology has come up as a budding approach for the removal of harmful pollutants such as greenhouse gases, high molecular weight organic compounds, toxic chemicals, and various biological agents. These nanomaterials are applied in several forms and morphologies (e.g., membranes,

V. Srivastava (✉)

Department of Basic Sciences and Humanities, Rajiv Gandhi Institute of Petroleum Technology, Jais 229304, India

e-mail: pc16001@rgipt.ac.in

adsorbents or catalysts) for different functions. The high surface area of these nanomaterials imparts them higher reactivity and certain distinguished properties, which are advantageous for environmental remediation (Khin et al. 2012). Currently, most of the research work for environmental remediation and energy production is focused on carbon and metal-based nanomaterials such as metal/metal oxide nanoparticles and nanocomposites, carbon nanodots (Cringoli et al. 2017), two-dimensional carbon-based nanocomposites (Kumar et al. 2017; Chen et al. 2017; Ma et al. 2017a). Although these materials exhibit excellent efficiency for environmental remediation, the major disadvantages associated with these materials are a requirement of non renewable sources for their production, toxic by-products, and biological incompatibility. The best possible substitute for these materials could be ones that are primarily abundant in nature. Considering the abundance of available resources of plants, plant extracts are the most reliable root for the fabrication of nanomaterials (Lu and Ozcan 2015). Among the naturally available components, cellulose is the most abundantly found polymer, which has the ability to outgrow the persisting challenges related to cost, biodegradability, energy and renewability (Klemm et al. 2005). The lignocellulosic biomass is extracted from fodder, i.e., agricultural waste and forest residues. These fodder crops are available in huge quantities, are extremely low-cost, and are also nугatory for human consumption, making them an even better choice over food crops as a renewable source for the fabrication of nanomaterials (Loow et al. 2017; Bhatnagar et al. 2015; Mahfoudhi and Boufi 2017). Several articles are reported by researchers where nano cellulosic materials (CNs) have been applied for different applications such as paper making (Park et al. 2017a), energy production (Du et al. 2017), biomedical engineering (Liu et al. 2017) and wastewater treatment (Putro et al. 2017).

In this chapter, the application of nanocellulose for wastewater treatment has been discussed in detail. The two major forms of liquid waste that are most often discharged into the water bodies and causes harm to water ecology are wastewater and spilled oil. Industrial and municipal wastewater consists of an enormous amount of dissolved or suspended contaminants from different sources. Waste oil is spilled into the water bodies through different sources, including land drainage and disposal of waste. Moreover, the leakage from tank ship spills during their routine maintenance, and offshore oil production operation etc. also leads to spilling of oil in water bodies. The application of nanocellulose is highly effective for the removal of both types of liquid wastes (Mehmood et al. 2021).

In view of all aspects, the aim of the chapter is to summarize the advanced methods for the preparation of nanocellulose-based composites that can be applied as bio-based materials for the treatment of wastewater and also for remediation of wastewater. The nanocellulose-based materials are applied for wastewater treatment in the form of adsorbents, membranes, flocculants and also as catalyst carriers. Moreover, its shortcomings and perspectives on future research about further modifications in this area have been discussed.

2 Categorization of Nanocellulose

Nanocellulosic membrane can be majorly classified into two groups: (i) nano-objects and (ii) nanostructures (Kargarzadeh et al. 2017a). These two groups are further classified into subgroups. Nano-objects are comprised of cellulose microcrystal and cellulose microfibril, while nanostructures are branched into cellulose nanocrystal (CNCs) and cellulose nanofibers (CNFs). The major difference between the two main groups is the size range of nano cellululosic materials. Nano-object cellulose is in the range of 10–100 μm , while the size of nanostructured cellulose lies between 1 and 50 nm. Figure 1 illustrates the length of CNF and CNC.

2.1 Cellulose Nanofiber (CNFs)

CNFs are identified by their specific structure having elementary nanofibrils alternating with crystalline and amorphous domains of cellulose (Kargarzadeh et al. 2017a). Mechanical disintegration of the plant cell wall is done before turning the complex structure cellulose fiber into CNF. Depending on the power of disintegration, the diameter of fibers may range from 10–100 nm. Bacterial cellulose is the only type of nanocellulose fibers that are synthesized using enzymatic polymerization of organic compounds such as glycerol or sugar (Mahfoudhi and Boufi 2017; Gama et al. 2017). Bacterial cellulose has exceptional purity, water holding capacity and crystallinity as compared to other types of CNFs (Mahfoudhi and Boufi 2017).

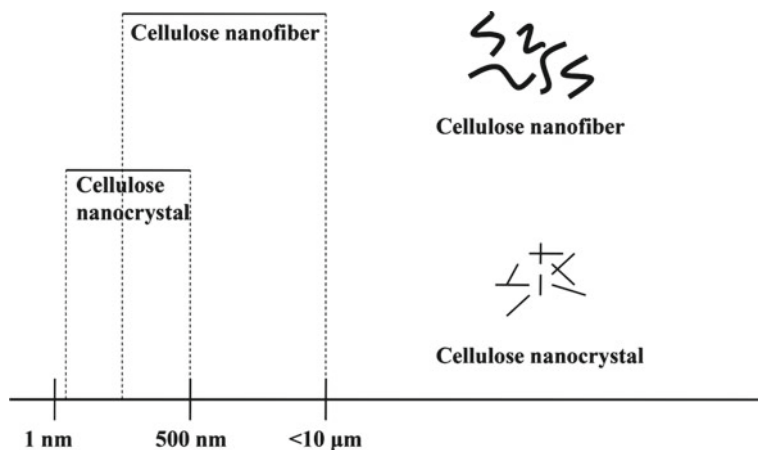


Fig. 1 Size chart of nanocellulose-based on material length

2.2 Cellulose Nanocrystal (CNC)

CNCs are identified by their rod shape composed of crystalline regions separated from CNFs (Kargarzadeh et al. 2017a). It is assembled up by a series of alternations starting with the isolation of the crystalline region by separating the amorphous region. This isolation is attained by applying acid digestion before other treatment methods. Overall, CNCs are obtained after multiple steps of purification and post treatments.

3 Sources of Cellulose

Before the production of nanocellulose, it is important to identify the sources from where cellulosic materials can be extracted. There is a wide range of sources for obtaining cellulose, including algae, bacteria, plants and tunicates. Although under certain conditions, the final properties of CNF are mildly influenced by the source of cellulose, the properties of CNCs are entirely dependent on the source (Missoum et al. 2013; Smyth et al. 2017). Thus, it is very important to select the suitable source and extraction technique for obtaining the nano cellulosic material of desired properties (García et al. 2016). Moreover, the impact of the source, extraction and processing on the environment should also be taken into consideration (Rosa et al. 2010).

3.1 Algae

The utilization of budding algal sources of green energy ensures environmental sustainability. The requirement of algae has been enhanced by executing researches on artificial photosynthesis such as CO₂ fixation and water splitting (Huang et al. 2018). Algae is vitally used for the extraction of nanocellulose, which are exploited for the fabrication of adsorbents and thin films. Different varieties of algae, such as green algae (also known as *Cladophora*), are largely being explored by researchers for the production of nanocellulose. Green algae are found to be the most effective variety of algae when compared to others owing to their ability to resolve concerns related to water pollution in coastal areas. The study of the cell wall of various algae species exhibits that the *Cladophorales* possesses a highly crystalline cell wall (Nicolai et al. 1952). As reported by Mihranyan, the higher crystallinity of the cell wall of *Cladophora* advocates its inert nature, which makes it unsusceptible to chemical treatments when compared to cellulose derived from other conventional natural sources (Mihranyan 2011). The nanocellulose derived from the plant source is used for the fabrication of membranes and adsorbents. The membranes prepared from *Cladophora* algae trap the particles of the swine influenza virus as effectively as industrial filters (Metreveli et al. 2014a). Moreover, the beads prepared from green

algal cellulose have the capacity to adsorb Pd (II) ions upto 80% within a time span of 2 h (Ruan et al. 2016). The exploitation of algae for nanocellulose extraction is not only cost-effective but also helps adsorb CO₂ gas, which reduces greenhouse gases (El-Safty et al. 2015).

3.2 Bacteria

The scope of using microbial hosts is extensively being studied owing to the multi-functional benefits derived from nanocellulose materials. Similar to algal cellulose, bacterial cellulose exhibits high purity, which is free from other polymers or functional groups except for the alcoholic group (Nechyporchuk et al. 2016; Uzyol and Saçan 2017). The smaller degree of purification, which is required, is also less energy consumption as per the research conducted by Gatenholm and Klemm (2010), the time required for the production of cellulose through bacteria is up to two weeks. Bacterial celluloses are prepared through the process of fermentation, wherein the movement of bacteria is either free in the culture medium or sometimes get attached to cellulose fiber forming swollen gel structure. These swollen balls are then purified by the death of the microorganism followed by the removal of cell waste and culture medium. The cellulose produced by bacteria is necessarily nanocellulose as fibrils can be united by bacteria only at the nanoscale. The nanocellulose is produced by different types of bacterial species such as *Acetobacter xylinum* (presently *Gluconacetobacter xylinus* or *Komagataeibacter medellinensis*) and *Gluconacetobacter medellinensis* (Gatenholm and Klemm 2010). The production of cellulose from these species occurs by polymerization of monomeric units of cellulose, i.e., glucose, into the external environment. This complex process leads to the formation of a three-dimensional network of microfibril and nanofibril. This 3D network imparts crystallinity, mechanical strength, and water retaining capacity to the nanocellulose.

3.3 Plants

The major source of nanocellulose which is studied across the board is fabrication using plants. Plant nanocellulose can be majorly categorized into two types: (i) cellulose nanofibers and (ii) cellulose nanocrystals (Kargarzadeh et al. 2017b). Plant nanocellulose can be obtained from a variety of sources (Ventura-Cruz and Tecante 2019), such as coconut husk fiber, corncob residue, barley wastes, mengkuang leaves (*Pandanus tectorius*), garlic straw residues, raw cotton linter, *Agave tequilana*, tomato peels, forest residues, *Gigantochloa scortechinni* bamboo culms, industrial waste cotton, cassava root bagasse and peelings, sugar palm fibers (*Arenga pinnata*), corn straw and sago seed shells. Plant fibers used as a source of cellulose are classified into several groups, including bast fiber, grass fiber, core fiber, reed fiber, leaf

fiber, seed fiber and other fibers. Among all these, the most frequently used plant fiber for nanocellulose production is wood pulp. Wood pulp has a relatively higher content of pure cellulose, ductility and durability when compared to other plant sources (Menon et al. 2017). Wood pulp nanocellulose has been reported to be used effectively used as a microfiltration membrane for the removal of bacteria, viruses and heavy metal ions from water bodies. In addition to the membrane, wood pulp nanocellulose has also been used to design catalysts for reducing hazardous organic compounds like 4-nitrophenol. Similarly, bleached birch fibres obtained from *Betula verrucosa* and *Betula pendula* have been used by Suopajarvi et al. (2013) for fabrication of dicarboxylic acid nanocellulose applied for the treatment of wastewater. On account of these facts, plant based nanocellulose is considered the most beneficial and environment friendly source for the production of nanocellulose.

3.4 Tunicates

Tunicates (marine invertebrate animals) are the contemporary alternative for the fabrication of nanocellulose. Cellulose composed of highly crystalline and pure triclinic (CI_{β}) allomorphs is generally being deposited on the outer issue of the tunicates (such as sea squirts) (Kargarzadeh et al. 2017a). Researchers have explored different species of sea squirts, including *Metandrocarpa ueda* (Kimura and Itoh 1996), *Halocynthia roretzi* (Elazzouzi-Hafraoui et al. 2008) and *Halocynthia papillosa* (Iwamoto et al. 2011), for the production of cellulose microfibrills. Cellulose derived from tunicates has been applied in several works for environmental remediation. A study reported by Cheng et al. (2017) discussed the synthesis of a filter membrane designed by homogenizing the nanocrystals of tunicate cellulose which are hydrophilic in nature with cholesteric liquid crystals. These filter membranes were found to be highly efficient for the separation of oil/water. Moreover, stalked sea squirts (*Styela Clava*) have also been used for the fabrication of nanocomposites. These nanocomposites have been effectively used as catalysts in the process of water treatment (Wei et al. 2014). In research carried out by Yu et al. (2016a), nanocomposites derived from stalked sea squirt were used as flocculant for flocculating and harvesting microalgae used for the production of biodiesel.

4 Methods of Preparation of Nanocellulose

4.1 Mechanical Disintegration

The most accepted method for the preparation of CNF is the mechanical disintegration used as a principal treatment to generate CNFs (Carpenter et al. 2015). In

the process of fabrication of CNFs, mechanical disintegration is executed as a post-treatment step used to serve the purpose of purification (García et al. 2016). This method is applied for breaking down the heavier chunks of cellulose pulp into smaller particles. For an efficient mechanical disintegration to take place, delamination of cellulosic nanofibrils is required instead of basic fiber shredding (Nechyporchuk et al. 2016). The mechanical disintegration of cellulose pulp, which is subjected to fiber shredding, produces nanocellulose possessing poor mechanical properties. For enhanced delamination of nanofibrils, interfibrillar hydrogen bonding needs to be loosened for inhibiting the fibril aggregation. This condition is satisfied by employing an aqueous medium during the process of mechanical disintegration. The delamination of cellulose fibers is carried out by using techniques such as homogenization (Abdul Khalil et al. 2014), refining (Sacui et al. 2014) and grinding (Nair et al. 2014; He et al. 2018). The nanocelluloses generated using mechanical disintegration methods are of larger dimensions and heavily clustered (Sacui et al. 2014). Park et al. (2017b) reported that the defibrillation efficiency of wood based CNF in wet-disk milling is influenced by its chemical composition. The defibrillation efficiency is improved in the absence of lignin and hemicelluloses in the source material. The curtailment of viscosity, crystallinity and thermal stability conveys the transition of materials from micro to nanosize. In the majority of the cases, the most prominent mechanical treatments used include blending, electrospinning, grinding, ball milling, homogenization, cryocrushing, refining, ultrasonication, steam explosion or a combination thereof.

4.2 Chemical Method

The demand for large scale production of nanocellulose can be fulfilled by applying preparation techniques that are effective and low energy consuming. The chemical treatment of cellulose has been experimented with by researchers for the generation of nanocellulose. Fan et al. (2011) reported that the defibrillation process used for the production of nanocellulose is executed effectively by involving chemical agents (variation in pH). Chemical pretreatment techniques which are widely used in the current scenario include acid hydrolysis (Vanderfleet et al. 2018), sulphonation (Rocha et al. 2018), carboxylation (Sharma et al. 2018), quaternization (Santos et al. 2018), carboxymethylation (Onyianta et al. 2018), ionic liquid (Ninomiya et al. 2018) and pretreatments assisted by solvents (Laitinen et al. 2017). The most common technique for extracting CNC from cellulose is acid hydrolysis. The technique is helpful for destroying the non-crystalline region present in the microfibril. The destruction of the amorphous region helps in keeping the crystalline portion intact. Liu et al. demonstrated the fabrication of CNC through hydrolysis of sulphuric acid (Liu et al. 2014). Other than CNC extraction, bacteria nanocrystals can also be generated from bacterial microfibrils via acid hydrolysis (Börjesson and Westman 2015). Chemical treatment is used as a pre-treatment technique before the process of mechanical disintegration for preparing nanocellulose. These techniques are used to bring in

the charge on the surface of the cellulose. The modification in the surface charge by sulphonation, carboxylation, and carboxymethylation, assists in the defibrillation of cellulose fibers (Nechyporchuk et al. 2016). Wågberg et al. (2008) prepared thin nanofibrils through carboxymethylation of CNFs. The nanofibrils fabricated with chemical pre-treatment exhibited uniform width distribution and minimum agglomeration when compared to those prepared directly through mechanical disintegration without pre-treatment.

4.3 Biological Method

The biological method is an effective method for the hydrolysis of chemical waste. Enzymatic hydrolysis is a pre-treatment step which assists in combating issues related to energy cost and environmental hazards. This pre-treatment step is applied before mechanically disintegrating cellulose to nanocellulose through methods like refining or blending. The delamination of the cell wall during the disintegration of cellulose is further enhanced by the incorporation of the endoglucanase enzyme in a homogenizer (Pääkkö et al. 2007). The average molar mass and aspect ratio of nanofibers manufactured through this treatment were found to be greater than those nanofibers which are fabricated through chemical treatment involving acid hydrolysis (Henriksson et al. 2007). Besides endoglucanase, various other enzymes such as cellulases (Beltramino et al. 2015), ligninases, xylanases (Tibolla et al. 2014), pectinases (Hideno et al. 2014) etc., have also been used for enzymatic hydrolysis of cellulose to nanocellulose.

Beltramino, along with the co-workers, synthesized CNC crystals that have superior dimensions and a lesser quantity of sulphur when compared to cotton linter (Beltramino et al. 2015). This CNC was generated using the enzyme substrate of cellulose accompanied with acetate buffer. On the contrary, banana fibers obtained through chemical treatment have higher crystallinity in comparison to those obtained through xylanase treatment. The reason for this lower crystallinity is that these enzymes are not easily soluble in hemicelluloses which make it difficult for them to penetrate the cellulosic chains to hydrolyze them. The presence of hemicelluloses in the cellulose sources clogs the separation of cellulose nanofibrils. Nechyporchuk et al. (2016) studied the rheological behavior of CNF produced with both enzymatic and chemical treatment. It was found that the flocculation capacity of CNF generated via enzymatic treatment is better than that obtained by chemical treatment. Figure 2 represents the method of preparation of nanocellulosic materials.

5 Nanocellulose Materials Used for Water Treatment

The deteriorating quality of water resources is a serious matter of concern all over the globe. The perpetually growing urbanization and industrialization have led to

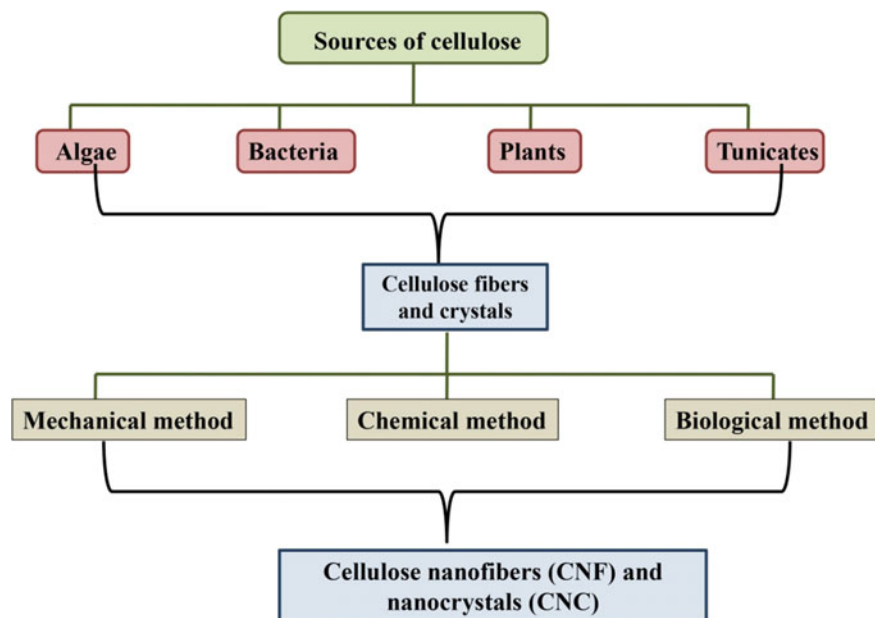


Fig. 2 Sources of cellulose and methods of preparation of CNCs and CNFs

an increase in the release of toxic substances into the water bodies. The decontamination of water bodies is an urgent need of the hour. Of lately, a lot of work is being done on utilizing environment friendly and long-lasting products derived from natural resources for their potential application in wastewater treatment. The environment friendly cellulose material in the micro and nanosize range is advantageous over conventional cellulose fibers owing to their high surface area, aspect ratio, and Young's modulus (Suopajärvi et al. 2014). These cellulose-based nanomaterials are supremely versatile and have found their applications for various purposes. In this chapter, a summary of contemporary applications of cellulose-based materials as adsorbents, photocatalysts, flocculants and membranes for wastewater treatment has been reviewed and is represented in Fig. 3.

5.1 Nanocellulose-Based Adsorbents

The purification of wastewater using adsorbents derived from nanocellulose is currently a promising method in contrast to high energy consumption and overpriced technology employing carbon-based adsorbents. Unaltered cellulose does not possess the desired adsorptive property, therefore tailoring of cellulose is needed to achieve improved interaction and a productive outcome. The vital properties acquired by cellulose are (i) its hydrophilic nature, (ii) its ability to functionalize, (iii) its

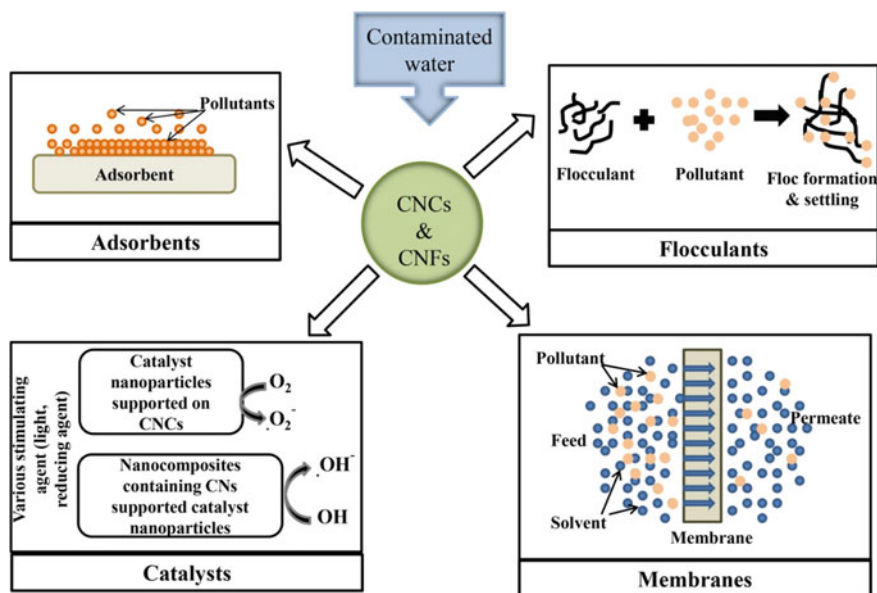


Fig. 3 Schematic diagram describing the various water/wastewater treatment processes in which CN based systems can be used

tendency to reconcile its properties such as surface area, quantum size, aspect ratio and chemical accessibility (Anirudhan and Rejeena 2012).

5.1.1 Adsorption of Heavy Metal Ions

The utilization of heavy metal ions in different industries poses a serious threat to human health. Metal ions used in industries (such as copper, silver, chromium, iron etc.) are leaked into the water bodies, including groundwater and contaminate these water sources. The intake of these ions by a human being in excess would have threatening repercussions (Bilal et al. 2013). Jalali and Aboulghazi et al. (2013) and Johari et al. (2016) used plant-derived cellulose as an adsorbent for metal ions. Cellulose-derived from sunflower stalk and coconut husk waste was used for adsorption of Cd (II) and Pb (II) metal ions and Hg (II) metal ions, respectively. In contrast to this, Bediako et al. (2016) prepared carboxymethyl cellulose using lyocell fabric via crosslinking reactions followed by carboxymethylation. The carboxymethyl cellulose was used to adsorb Cd (II) ions from their aqueous solution. The process of adsorption was found to be approximately 17 times more efficient. The efficiency of adsorption of Cd (II) using nanofiber is notable even at a lower concentration. Sun et al. (2017) prepared a cellulose adsorbent by halogenation of microcrystalline cellulose. Halogenated cellulose was then functionalized with pyridine diacid and further used for the removal of Pb (II) and Co (II). Several other chemicals have

been reported by researchers for modification of CNCs for making them an efficient adsorbent (de Castro Silva et al. 2018; Jain et al. 2017; Li et al. 2019; Madivoli et al. 2016; Mautner et al. 1861; Sun et al. 2018). Rafeian et al. (2019) made an attempt to prepare and characterize a CNC membrane containing (3-aminopropyl) triethoxysilane or APTES (MCNC) and a non-woven substrate at the bottom for removing Cu (II) ions in water. It was observed that the efficiency of removal of metal ions was enhanced using polyethersulfone (PES)/MCNC membrane. MCNC has the ability to upgrade the fouling resistance and water flux of the membrane. Similarly, Mathew and co-workers (Liu et al. 2014, 2015) studied the potential of pristine surface functionalization of CNCs for adsorption of metal ions such as Ag (I), Cu (II), and Fe (III) from water bodies. A study of both the classes of CNs, i.e. CNCs and CNFs derived from cellulose sludge, was carried out for adsorption of Ag (I) ions. CNCs were prepared by acid hydrolysis while CNFs were homogenization of cellulosic fibers. The surface area of fabricated CNCs and CNFs were found to be 138–226 m²/g and 146–219 m²/g, respectively. Adsorption experiments were carried out over a range of pH. It was found that adsorption of Ag (I) ions make the CNC suspension stable, whereas no stability was seen in Ag (I) treated CNF suspension. CNF suspensions were mostly sedimented, and well-defined layers were separated from them owing to the surface charge characteristics of CN/Ag (I) complexes. Moreover, the maximum adsorption capacity for CNCs and CNFs were calculated to be 0.32 and 0.14 mmol/g, respectively. From these observations, it can be concluded that CNCs do not settle down in solution even after treatment with Ag (I) ions and have higher adsorption capacity due to larger surface area.

5.1.2 Adsorption of Dyes

The chemical discharge from several industries, including textile, pharmaceutical, leather tanning, pulp and paper, comprises different types of dyes that pollute the water bodies and needs to be removed necessarily (Crini 2006; Rafatullah et al. 2010). Lately, several articles have been reported on the development of CNs-based adsorbents for the removal of these dyes from water bodies. CNCs obtained from acid hydrolysis were examined by Batmaz et al. (2014) for their potential to attract positively charged dye molecules such as methylene blue. The adsorption capacity was found to be good enough, which was further upgraded by modification of these CNCs by functionalization via 2, 2, 6, 6-tetramethylpiperidin-1-oxyl (TEMPO) oxidation. It was found that the adsorption capacity was improved by up to 6 times. The CNCs developed by acid hydrolysis possess a negative charge on its surface, and oxidation of its primary hydroxyl groups using TEMPO reagents introduced more negative charges. The increase in negative charge facilitated its easier interaction with positively charged dye molecules. The maximum adsorption capacity of unaltered CNCs and TEMPO-oxidized CNCs were found to be 0.37 and 2.40 mmol/g, respectively. The increase in the value of maximum adsorption capacity indicates the adsorption of positively charged dye molecules over anionic sites of adsorbent as a result of counter ion exchange.

Gholami Derami et al. (2019) used thin films composed of nanocellulose with polydopamine (PDA) for adsorbing toxic dyes such as rhodamine 6G, methylene blue and methyl orange.

Apart from targeting cationic dyes, CNCs are also modified to act as an adsorbent for anionic dyes from their aqueous solutions. Eyley and Thielemans (2011) grafted the imidazolium group over CNCs through azide-alkyne cycloaddition reaction catalyzed using a heterogeneous Cu (I). The cycloaddition of imidazolium groups imparts positive charges over grafted CNCs. These positively charged species were capable of attracting negatively charged dye molecules such as orange II. The maximum adsorption capacity of this adsorption process was found to be 0.28 mmol/g.

Apart from the grafting of these nanocellulose membranes, double-layered membranes are also being prepared by implementing a layer of some other material over the CNF membrane. It was observed that merging the CNF membrane with that of graphene oxide improves the adsorption efficiency of the membrane (Liu et al. 2019). The merged membranes produce synergistic membranes owing to the presence of inter and intramolecular hydrogen bonds forming a network (Sajab et al. 2016; Fang et al. 2016). These membranes were used for the removal of dyes such as rhodamine 6G, victoria blue and methyl violet from their aqueous solution.

5.1.3 Adsorption of Other Water Contaminants

Besides dyes, oils and heavy metal ions, there are several other substances which may contaminate water bodies. The presence of pharmaceuticals, agrochemicals, and biomolecules in municipal/industrial wastewater may create major health problems. Researchers have made attempts to evolve CN based materials to remove these contaminants. Chen et al. (2014) developed β -cyclodextrin modified $\text{CNCs}@Fe_3O_4@SiO_2$ superparamagnetic nanorods. These nanorods were applied for the adsorption of pharmaceutical wastes such as procaine hydrochloride and imipramine hydrochloride. These pharmaceutical compounds got trapped into the hydrophobic cavity of β -cyclodextrin grafted on the $\text{CNCs}@Fe_3O_4@SiO_2$ superparamagnetic nanorods. After the completion of the adsorption process, these nanoparticles could be easily recovered from the aqueous solution under the influence of a magnetic field. The maximum adsorption capacity for procaine hydrochloride and imipramine hydrochloride was found to be 0.055 and 0.052 mmol/g, respectively. In a study reported by Herrera-Morales et al. (2017), CNC composites were altered by polyethylene glycol (PEG). These composites were utilized for the separation of pharmaceutical compounds such as acetaminophen, sulfamethoxazole and N, N-diethyl-meta-toluamide (DEET) from aqueous solutions. PEG provides ease in immobilization of poorly soluble drugs in water which activates the interaction between CNCs and hydrophobic drugs. The modified composite acquired improved physical properties such as high surface area and hydrophilicity, which permitted the adsorption of pharmaceutical compounds via electrostatic interactions.

Similar to pharmaceutical compounds, insecticides such as chlorpyrifos was also targeted by Moradeeya et al. (2017) for their removal from wastewater using pristine CNCs. The maximum adsorption experiment for this adsorption experiment which takes about 60 min to reach equilibrium, was found to be 0.027 mmol/g. It was also reported by them that using an eluent solution comprising of 80% methanol and 20% water could completely separate chlorpyrifos from CNC during the cycle of adsorption–desorption. Researchers have also shown the budding approach of CN based systems for the adsorption of biomolecules. CNCs functionalized with di-aldehyde were prepared by Huang et al. (2016) for the adsorption of creatinine. Di-aldehyde groups were attached to the surface of CNCs through sodium peroxide oxidation (referred to as D-CNCs). The increase in aldehyde content increased the adsorption capacity of D-CNCs, while the reduction in the size of D-CNCs enhanced the rate of reaction. The maximum adsorption capacity of D-CNCs having the highest aldehyde content was calculated to be 0.013 mmol/g. The mechanism of adsorption of creatinine is the crosslinking reaction taking place between the aldehyde group of D-CNCs and the amino group of the creatinine molecule. Anirudhan and co-workers targeted (Anirudhan and Rejeena 2012, 2013a, b) adsorption of biomolecule known as trypsin using CNCs modified with carboxylate functionalized cation exchanger such as polyacrylic acid modified polyglycidylmethacrylate attached to CNCs. The maximum adsorption capacity for this adsorption process that attains equilibrium within 90 min was found to be 0.006 mmol/g. The adsorbent used in a cycle is 100% regenerated by using 0.1 mol/L KSCN as eluent (Anirudhan and Rejeena 2012). Besides this, a novel adsorbent for the removal of proteins such as immunoglobulin (IgG) and haemoglobin (Hb) was also developed by grafting magnetic CNC composites with poly (methacrylic acid-co-vinyl sulfonic acid). The maximum adsorption capacity for adsorption of Hb and IgG attaining equilibrium in 2 and 3 h were found to be 0.003 and 0.013 mmol/g, respectively. This novel adsorbent selectively removes the Hb or IgG from their mixture with bovine serum albumin. The adsorption takes place under the influence of a magnetic field owing to the magnetic properties of the modified CNCs associated with Fe_3O_4 . Regeneration of adsorbent is carried out using 0.01 mol/L KOH eluent without compromising on its adsorptive capacity (Anirudhan and Rejeena 2013a, b). In each of these reports, biomolecules get adsorbed via electrostatic attraction between the adsorbent possessing a negative charge and positively charged protein molecule below their isoelectric point. The detailed list of CN-based adsorbents used for heavy metal ions, insecticides, anions and proteins is given in Table 1.

5.2 Oil–Water Separation

Nanofibrillated cellulose is also used to prepare nanocomposites in the form of aerogels (Mehmood et al. 2021). These aerogels possess a structure having a strong network through interfibrillar hydrogen bonding via the freezing–thawing process. This nanofibrillated cellulose (NFC) aerogels are effectively used as oil sorbents. In

Table 1 CN-based adsorbents used for removal of water pollutants

Cellulose based adsorbent	Heavy metal ions	Maximum adsorption capacity (mmol/g)	References
Sulphonated nanofibrillar cellulose	Pb (II)	248.6	Suopajärvi et al. (2015)
Pristine CNCs	Ag (I) Cu (II) Fe (III)	0.52 0.31 0.11	Liu et al. (2015)
Succinic anhydride modified CNCs	Pb (II) Cd (II)	1.77 2.31	Yu et al. (2013)
APTES modified CNFs	Ni (II) Cu (II) Cd (II)	2.73 3.15 4.19	Hokkanen et al. (2014a)
Poly (itaconic acid)-poly (methacrylic acid)-grafted-nanocellulose/nanobentonite composite	Co (II) U (VI)	350.8 121.02	Anirudhan et al. (2016)
Pristine CNCs	Methylene blue	0.37	Batmaz et al. (2014)
Maleic anhydride grafted CNCs	Crystal violet	0.59	Qiao et al. (2015)
Imidazolium grafted CNCs	Orange II	0.28	Eyley and Thielemans (2011)
Functionalization of cellulose with hyperbranched polyethylenimine	Congo red Basic yellow 28	2100 1860	Zhu et al. (2016)
MnO ₂ coated CNFs	Methylene blue	–	Wang et al. (2014a)
Pristine CNCs	Chlorpyrifos	0.027	Moradeeya et al. (2017)
D-ialdehyde functionalized CNCs	Creatinine	0.013	Huang et al. (2016)
APTES modified CNFs Epoxy modified CNFs	Hydrogen sulphide	3.05 0.373	Hokkanen et al. (2014b)
Cationic CNFs functionalized with glycidyltrimethylammonium chloride	PO ₄ ³⁻ SO ₄ ²⁻ F ⁻ NO ₃ ⁻	55 50 10.6 44	Sehaqui et al. (2016)
Poly (methacrylic acid-co-vinyl sulfonic acid) grafted magnetic CNCs	Haemoglobin (Hb) Immunoglobulin (IgG)	0.003 0.013	Anirudhan and Rejeena (2013a, b)

Table 2 Oil/water separation using various CN based adsorbents

CNC based adsorbent	Adsorbent characteristics	Adsorption capacity	References
Cellulosic scaffolds made from acetate esterified CNCs	$\rho = 3.3$ to 7.5 kg/m^3 ; $\theta = 140^\circ$	100–200 g/g^a	Anirudhan and Deepa (2017)
CNF aerogels treated with methyltrimethoxysilane	$\rho = 5.07$ to 17.3 mg/cm^3 ; Porosity = $> 99\%$, SSA = 3 to 25 m^2/g , $\theta = 110$ to 150°	49–102 g/g^a	Zhang et al. (2014)
CNF aerogels coated with TiO_2	$\rho = 20$ to 30 mg/cm^3 ; Porosity = $> 98\%$, $\theta = > 90^\circ$	20–40 g/g^a	Korhonen et al. (2011)
Hydrazone-carboxyl ligand-linked CNC based aerogel	$\rho = 22.4$ to 23.3 mg/cm^3 ; Porosity 96.3–97.2% SSA = 195 to 303	133 g/g (for water), 99 g/g (for ethanol), 34 g/g (for toluene) 54 g/g (for dodecane)	Ma et al. (2017b)

^a Adsorption capacity for a range of organic solvents and oils, ρ -density, SSA-specific surface area, θ -contact angle

this regard, Gao et al. (2018) prepared superhydrophobic NFC aerogels by firstly coating the NFC with dopamine/octadecyl amine (ODA) accompanied by a freeze drying process. This leads to the formation of a PDA coating acting as a layer between the NFC platform and ODA. The fabricated aerogel possessed a high contact angle of 152.5° and an ultralow density of 6.04 mg/cm^3 , which provided buoyancy to these materials and aided them with exceptional oil/water absorption selectivity. Similarly, Chhajed et al. (2019) prepared NFC/PVA (polyvinyl alcohol) aerogels with the coating of stearic acid chloride (SAC). These SAC conjugated aerogels also showed superhydrophobicity and a contact angle of 0° . The capacity of adsorption is gauged by the ratio of the weight of liquid adsorbed to the dry weight of aerogel. NFC/PVA aerogels showed remarkable selectivity in the separation of oil/water mixtures along with other organic solvents. Table 2 represents the list of cellulose based adsorbents used for oil/water separation.

5.3 Nanocellulose-Based Photocatalyst

Recently, a lot of work has been done on employing several inorganic-organic hybrid based nanocomposites possessing distinct electrical, thermal and mechanical properties for photocatalysis (Yang et al. 2011). The transition from petrochemical-based feedstock to biomaterials is slowly making its way for a sustainable and cleaner ecosystem. Cellulose acts as biocompatible support due to the chirality, broad chemical variability, and hydrophilicity possessed by this material. Although cellulose alone is not a good photocatalytic agent, the incorporation of semiconductor materials into its matrix enhances its photocatalytic activity by several folds. Research

Table 3 CN-based hybrid photocatalysts for degradation of organic pollutants

Cellulose based photocatalyst	Model pollutant	Degradation efficiency (%) and reaction time (min)	References
CdS nanoparticle/bacterial cellulose nanofibers	200 mL 20 ppm methyl orange	82%, 90 min	Yang et al. (2011)
N-doped TiO ₂ nanorods in regenerated cellulose thin films	150 mL 40 mg/L methylene blue	96%, 360 min	Mohamed et al. (2015)
Graphene oxide/TiO ₂ based ultrafiltration cellulose membranes	3.40 × 10 ⁻⁵ mol/L diphenhydramine at flow rate of ≈0.25 mL/min	65%, 240 min	Pastrana-Martínez et al. (2015)
Alginate/carboxymethyl cellulose/TiO ₂ nanocomposite hydrogel	30 mL 30 mg/L Congo red	91.5%, 240 min	Thomas et al. (2016)

groups are now working on examining cellulose-based metal oxide nanomaterials for photocatalytic wastewater treatment in the form of membranes, fibers, thin films and hybrid materials under UV and visible light irradiation (Table 6). Metal oxides have the ability to adsorb cellulose on their surface, which creates additional –OH groups on their surface. In addition to the –OH group, the fibrous network also assists the adsorption of cellulose on the surface of metal oxide. Li et al. (2017) studied the incorporation of TiO₂ nanoparticles within the fibrous network matrix of bacterial cellulose via hydrogen bonds. The modified cellulose material was used for photocatalytic degradation of reactive X-3B. TiO₂ nanoparticles were bounded with cellulose chains through a covalent bond which made the polymer chains rigid. The improved rigidity of the polymer chains enhanced the stability of these chains (Mohamed et al. 2015). Similar results were obtained with CdS nanocrystals coated on cellulose derived from microbes (Yang et al. 2011). The nanocomposite catalyst showed excellent photocatalytic activity and successfully degraded 82% of dye in 90 min. of time span. These catalysts were 100% recovered after each cycle without losing their efficiency. A detailed list of cellulose-based photocatalysts is given in Table 3.

5.4 Nanocellulose-Based Catalyst Carriers

In addition to photocatalysis, fibrillated cellulose also has the potential to act as a support/ carrier for nanoparticles used as a catalyst. The porous structure and presence of a large number of functional groups on their surface make these materials an ideal catalyst carrier. An et al. (2016) studied the use of nanocellulose as support for TiO₂ nanoparticles to fabricate nano-fibrillated-TiO₂ nanoparticles nanocomposite

for hydrogen generation through photocatalysis. The capacity of hydrogen generation by nanocomposites was found to be greater than that of TiO₂ nanoparticles. However, it was found that nanocomposites photo degraded during the course of the photocatalytic reaction and hence, 100% catalyst could not be generated at the end of a cycle. Another study reported by Ren et al. (2018) discussed the preparation of metal–organic frameworks (MOFs)/cellulose aerogels used as a catalyst for the removal of organic pollutants, including rhodamine B 4-nitrophenol and tetracycline hydrochloride. The MOFs were applied for triggering peroxymonosulphate (PNP) to react with the above mentioned contaminants. After the end of the reaction, MOFs were separated from the solution by using zeolite imidazole framework (ZIF) materials (ZIF-9 and ZIF-12). Cellulose aerogels were soaked into the solution of ZIF materials to load the ZIF materials (ZIF-9 and ZIF-12) on cellulose aerogels. The degradation of PNP was then carried out. The experiments showed that a hybrid aerogel system could degrade 90% PNP in 1 h. The aerogels were also regenerated easily from the solution. The efficient degradation of PNP showed the budding prospects of applying hybrid aerogels as a catalyst in the advanced oxidation process. In another study carried out by Taranto et al. (2009), it was observed that cellulose exhibited sensitivity towards UV radiation and, therefore, is susceptible to degradation during photocatalysis. Degradation of cellulose is accompanied by degradation of other organic contaminants such as methanol producing photocatalytically active species. The degradation of cellulose might compete with organic contaminants leading to a reduction in the rate of reaction. Moreover, Puls et al. (2011) also explained that under the illumination of UV light, TiO₂ nanoparticles could create holes on the surface of cellulose acetate/cellulose pulp fibers. Therefore, to prevent UV bleaching, coating of the cellulose nanomaterials need to be done for covering the holes perfectly by inert materials capable of absorbing UV light. Table 4 represents such reports where nanocellulose has been used as a catalyst carrier.

5.5 Nanocellulose-Based Flocculants

Flocculation is a technique used for removing fine solid particles of metals, dyes and other organic compounds suspended in water bodies. The addition of flocculants accelerates the colloidal particles to collide among themselves and form bigger unstable particles. These bigger particles, known as flocs, precipitate from the solution in due course of time (Lee et al. 2014; Quinlan et al. 2015). In recent times, majorly used flocculants include inorganic, cationic and multivalent coagulants such as aluminium iron salts and synthetic polymers like polyacrylic acids and polyacrylamides derived from petroleum-based non-renewable sources are applied as flocculants in wastewater treatment (Suopajarvi et al. 2017). The use of these flocculants is hazardous to the environment. Therefore, research efforts are being made to substitute these harmful substances with biodegradable, biocompatible and long lasting flocculants based on CNs.

Table 4 Nanostructured cellulose-based materials used as a catalyst in synthetic reactions

Cellulose based catalyst	Catalytic conversion	Conversion efficiency	References
Cellulose-nano magnetite Fe ₃ O ₄ nanocomposites	Synthesis of methyl esters from oleic acid	Conversion yield of 89.21%	Anggraini (2019)
Carboxylated cellulose doped with Sn (II) ions	Transesterification and hydrolysis of soybean oil and esterification of fatty acids	Conversion yield = 55%, 93% and 95% respectively	Santos et al. (2016)
Cellulose matrix embedded copper decorated magnetic bionanocomposite	Synthesis of dihydropyridines and polyhydroquinolines	Conversion yield = More than 85%	Maleki et al. (2019)
Cellulose@hematite-zirconia nanocomposite	Production of biodiesel through the esterification of biomass-derived materials	Conversion yield = 92.5%	Helmiyati et al. (2021)
Novel magnetic biobased heteropolyacid prepared via in-situ reaction	Transesterification of tree-born oil	Conversion yield = 96.6%	Bao et al. (2021)

Presently, biopolymer-based flocculants which are mostly being used and are gaining attention include chitosan, cellulose, tannin and alginate. Biofloculant is not only beneficial for their biodegradability, but these materials have dimensions in the nanorange and also possess a high surface specific area (Haver and Nayar 2017). Natural polymer-based flocculants can be categorized into two groups: (i) grafted natural polymers to develop semi-natural flocculants, (ii) modified natural polymers to design natural flocculants (Zhu et al. 2015; Das et al. 2013). Nanocelluloses are still not much frequently used as flocculants. As discussed in the previous sections, researchers majorly use these materials either as an adsorbent or as a photocatalyst. The main issue of using CNCs as flocculants is their tendency of agglomeration because of the networks developing by the formation of hydrogen bonds between –OH groups on the surface of CNCs (Yu et al. 2016b). The adjustment in the surface –OH group changes the properties of CNC flocculants and prevents them from agglomerating. Nanocellulose obtained from the processing of pulp acquires a negative charge on its surface. As a result, anionic nanocellulose does not interact strongly with negatively charged inorganic minerals. Moreover, anionic flocculants are poorly soluble in an acidic medium and, therefore, cannot be used in these conditions (Kono 2017). The chemical pre-treatment of CNCs applying different methods such as carboxymethylation (Liimatainen et al. 2014), citric/hydrochloric acid hydrolysis (Habibi et al. 2010), periodate-chlorite oxidation (Yu et al. 2016b; Liimatainen et al. 2014), TEMPO-mediated (Suopajarvi et al. 2017) etc. is done for increasing the density of negative charge or furnishing nanocellulose with cationic

charges. Cationic counterparts of nanocellulose assist the removal of anionic dyes through electrostatic interaction of oppositely charged particles.

Currently, researchers are working on the functionalization of nanocellulose by instigating anionic, cationic or hydrophobic functional groups onto the surface of CNCs through the mechanism of charge neutralization. The presence of -OH groups on the surface of cellulose facilitates the insertion of desired functionality on their surface and thereby forms an effective flocculant (Azizi et al. 2013). The application of flocculants for wastewater treatment is presented in detail in Table 5. Suopajarvi and co-workers reported nano cellulose materials functionalized with anionic and cationic di-aldehyde as water chemicals in wastewater flocculation (Liu et al. 2012, 2015; Ma et al. 2017b). Productive results were obtained, which proved the potential of flocculants for wastewater treatment. The remodeling of CNCs was done by periodate oxidation through which the aldehyde group was introduced by oxidation of surface -OH groups and modification in the carbon network of glucopyranose ring (Wang et al. 2014b). Liimatainen et al. examined the application of both anionic and cationic di-aldehyde cellulose generated via aqueous periodate oxidation (Liimatainen et al. 2011, 2012). The study revealed that the flocculation performance of kaolin was better using anionic cellulose nanoparticles as compared to cationic ones.

Table 5 Flocculation of water contaminants using water-based flocculants

CNC based flocculant	Pollutant	Flocculant performance	References
CNCs modified with 1-(3-aminopropyl)-imidazole (APIIm)	Microalgae (<i>Chlorella vulgaris</i>)	Efficiency = 100%, Maximum adsorption capacity = 43.4 g algae/g	Ge et al. (2016)
Anionic dicarboxylic acid nanocellulose	Municipal wastewater	Turbidity reduction = 80% ^a , COD removal = 60%	Kimura and Itoh (1996)
Dicarboxylic acid CNFs	Municipal wastewater solid particles	Turbidity reduction = 40–80%, ^a COD removal = 40–60%	Suopajarvi et al. (2013)
Rod-shaped cellulose nanocrystals	Flocculation and phase separation of bacteria	Aggregation percentage = 100%	Vanderfleet et al. (2018)
Quaternized CNFs	Reactive orange 16	maximum adsorption capacity = 0.477 mmol/g for reactive orange 16	Haver and Nayar (2017)

^a COD–Chemical Oxygen Demand

5.6 Nanocellulose-Based Membranes

This section elaborates on the fabrication of nanocellulosic membranes and their role in environment remediation. Nanocellulosic membranes are constituted of both cellulose nanofibers and cellulose nanocrystals. The fabricated membranes are employed not only for wastewater treatment (Cruz-Tato et al. 2017) but also for gas separation (Ansaloni et al. 2017), dye removal (Karim et al. 2014), removal of heavy metal ions through ultrafiltration (Karim et al. 2016a, b), adsorption (Karim et al. 2017) and ion exchange process (Chitpong and Husson 2017). In this regard, Cruz-Tato et al. (2017) reported metal-based nanocellulose composites for developing a membrane capable of supporting forward osmosis for the removal of pollutants from water bodies. The change of nanocellulose was done to attach the functionalities of amino silane before the coating of platinum and silver nanoparticles. The fabricated membrane was more efficient as compared to HTI-CTA membrane (Cellulose acetate membrane from Hydration Innovation Technologies) in terms of water flux but shows the contrasting result for total organic carbon rejection. In contrast to this, a highly productive and high capacity cation exchange membrane was developed by Chitpong and Husson (2017) for the elimination of trace Cd (II) ions discharged in water bodies.

The removal of contaminants via membranes is greatly influenced by the pore size. For this reason, membranes are developed in such a way that the size of their pores excludes the contaminants allowing only purified water to pass through. Several researchers have employed nanocellulosic papers derived from plants and algae for the removal of water pollutants via size based exclusion. Bismarck and co-workers prepared nanopaper from plant sources (Mautner et al. 2014, 2015). In their work, two different types of nanopapers were prepared using CNF-0 having a fibril diameter of 5–30 nm and CNF-K of fibril diameter of 50 to 100 nm. It was observed that the permeability of nanopapers prepared using CNF-K could be regulated over a wider range owing to larger pore dimensions.

The chemical functionality of membranes also has an influence on the membrane filtration process. The membrane can be made selectively permeable for chemically mediated interactions by regulating the charge present on its surface. Mathew and co-workers used cellulose nanomembrane for charge mediated adsorption of water contaminants (Karim et al. 2014, 2016b, c).

Apart from using these techniques, individual simultaneous application of these techniques has also been reported by researchers. Researchers from Hsiao and Chu's group were successful in removing several types of water pollutants simultaneously using nanocellulose membrane by applying both the principles of size based exclusion and charge mediated adsorption in a single process (Wang et al. 2013; Ma et al. 2011, 2012). Several other membranes are listed in Table 6.

Table 6 Application of nanocellulose-based membrane in membrane technology for wastewater treatment

Cellulose type	Membrane application	Membrane performance	References
Chitosan based cellulose nanocrystal	Removal of dye	Removal percent: 69–98%	Karim et al. (2014)
TFNC membrane infused with carboxylated CNCs	Removal of bacteria (<i>E.coli</i> , <i>B.diminuta</i>), virus (Bacteriophage MS2) and organic dye (crystal violet)	Average pore size = 0.22 μm ; Porosity = 80%; Pressure drop = 3.0 kPa; Permeability = 59 $\text{Lm}^{-2} \text{h}^{-1} \text{kPa}^{-1}$; LRV = 6 for bacteria and 2 for MS2 virus; maximum adsorption capacity for crystal violet = 0.166 mmol/g	Ma et al. (2012)
PAN composite membrane blended with carboxylated CNCs	Removal of silica particles (7–40 nm), oil water emulsions	Pore size = 5–60 nm; Rejection ratio = > 99%	Cao et al. (2013)
Nanopaper made from pristine CNFs	Filtration of swine flu influenza virus (80–120 nm) and polystyrene latex beads of size(30, 100, 500 nm)	Average pore size = 19 nm; Porosity = 35%; SSA = 88 m^2/g ; Flux = 50 $\mu\text{Lh}^{-1} \text{cm}^{-2}$	Metreveli et al. (2014b)
Metalized nanocellulose composites–thin film composite membrane (MNC-TFC)	Wastewater treatment (to remove urea)	water flux (LMH/bar): 1. urea: 7.4; wastewater: 11.8 2. urea: 5.4; wastewater: 11.5 (both membranes performed better than a commercial HTI-CTA membrane)	Cruz-Tato et al. (2017)

6 Limitations and Future Prospects

Although nanocellulose has proven to be successful in addressing the concerns related to wastewater treatment, there are still several challenges and disadvantages associated with it which needs to be resolved. The commercialization of nanomaterials can be promoted only if these materials are prepared on a large scale at a low cost and generate valuable end products (Carpenter et al. 2015). Most of the works reported on the preparation of nanocellulose are at a laboratory scale. The major challenges with selecting the treatment method for fabricating nanocelluloses are the larger scale of production, lower cost and environment feasibility. In order to upscale the production, several techniques related to mechanical disintegration are applied by researchers. But the higher energy consumption is the drawback associated with these techniques. Although a lot of effort is being invested in discovering other mechanical techniques,

most of them are still at a primitive stage and are not applicable for upscaling. In contradiction to this, Arvidsson et al. (2015) reported that chemical pre-treatment is not necessarily less energy consuming for generating nanocellulose. In this study, a chemical treatment known as carboxymethylation was carried out, which exhibited that a higher energy consumption occurs in chemical pre-treatment as compared to applying only homogenization without any pre-treatment because of the high intake of chemicals such as methanol, ethanol, and isopropanol for the production of nanocellulose (Arvidsson et al. 2015). In this case, the consumption of electricity is low, but the presence of acidic and solvent waste results in a higher environmental impact (Carpenter et al. 2015). The second challenge is the production of bacterial and nanofibrillated cellulose at a large scale. The reason for this uncertainty is the dependence of production on the build up of nanofibers from low molecular weight sugars by bacteria and dissolved cellulose by electrospinning, respectively (Nechyporchuk et al. 2016). The strategies of production need strict vigilance to formulate an eco-friendly and economically viable method for the production of nanocellulose. Furthermore, the undefined toxicology of modified nanocellulose materials creates economic obstacles for its application in wastewater treatment. In general, the reduction in the size of nanoparticles increases the risk of their inhalation to cells, lymph and blood circulation and damage the potentially sensitive target area (Oberdörster et al. 2005). Although most of the research work shows that nanocellulose-based materials are non toxic (or slightly toxic) in nature, researchers have also reported that at higher concentrations, these materials have a negative impact on cell viability and proliferation (Alexandrescu et al. 2013). Moreover, prolonged inhalation of these nanofibers may have cytotoxic and inflammatory effects on human lung cells and also on the lung cells of mice, as reported by Yanamala et al. (2014).

7 Conclusion

The recognition of nanocellulosic materials may be considered a major milestone in the field of Materials Science and Engineering. A lot of attention has been grabbed by these nanocellulosic materials owing to their application in several fields such as bio-based food packaging, tissue regeneration, optoelectronics and environmental remediation, to name a few. Cellulosic nanomaterials possess properties such as large surface area, facile functionality, and eco-friendly nature (renewability and low toxicity), which makes them suitable for application in water and wastewater treatment. As discussed in the chapter, cellulosic nanomaterials effectively remove the pollutants present in water bodies through different methods such as adsorption, flocculation, membrane formation, and catalyst carrier. The challenges associated lie with the percentage yield and energy consumed during the stage of preparation and toxicity of the product obtained at the end. Both these issues were simultaneously sorted by applying an integrated method for the preparation of nanocellulose. The alteration in the structure of these nanocelluloses improved its functionality, making it even more efficient for the removal of pollutants. In spite of several advantages,

there is still a possibility to develop further improved treatment schemes for effective extraction of nanocellulose and its functionality as agents to be applied not only for wastewater treatment but also for other environmental remediation with reference to economic feasibility and its performance for wastewater treatment.

References

- Abdul Khalil HPS, Davoudpour Y, Islam MN, Mustapha A, Sudesh K, Dungani R, Jawaid M (2014) *Carbohydr Polym* 99:649–665. <https://doi.org/10.1016/j.carbpol.2013.08.069>
- Alexandrescu L, Syverud K, Gatti A, Chinga-Carrasco G (2013) *Cellulose* 20:1765–1775. <https://doi.org/10.1007/s10570-013-9948-9>
- An X, Wen Y, Almuji A, Cheng D, Li J, Jia X, Zou J, Ni Y (2016) *RSC Adv* 6:89457–89466. <https://doi.org/10.1039/C6RA21042B>
- Anggraini H (2019) *Int J Techn* 10:798–807
- Anirudhan TS, Deepa JR (2017) *J Colloid Interface Sci* 490:343–356
- Anirudhan TS, Rejeena SR (2012) *J Colloid Interface Sci* 381:125–136. <https://doi.org/10.1016/j.jcis.2012.05.024>
- Anirudhan TS, Rejeena SR (2013a) *Carbohydr Polym* 93:518–527
- Anirudhan TS, Rejeena SR (2013b) *Sep Purif Technol* 119:82–93
- Anirudhan TS, Deepa JR, Christa J (2016) *J Colloid Interface Sci* 467:307–320. <https://doi.org/10.1016/j.jcis.2016.01.023>
- Ansaloni L, Salas-Gay J, Ligi S, Baschetti MG (2017) *J Membr Sci* 522:216–225. <https://doi.org/10.1016/j.memsci.2016.09.024>
- Arvidsson R, Nguyen D, Svanström M (2015) *Environ Sci Technol* 49:6881–6890. <https://doi.org/10.1021/acs.est.5b00888>
- Azizi S, Ahmad M, Hussein M, Ibrahim N (2013) *Molecules* 18:6269–6280
- Bao S, Shen C, Wu X, Cao J, Zhao C, Wang W, Fu Y (2021) *Ind Crops Prod* 164:113342. <https://doi.org/10.1016/j.indcrop.2021.113342>
- Batmaz R, Mohammed N, Zaman M, Minhas G, Berry RM, Tam KC (2014) *Cellulose* 21:1655–1665
- Bediako JK, Wei W, Yun YSJ (2016) *Taiwan Inst Chem Eng* 63:250
- Beltramino F, Roncero MB, Vidal T, Torres AL, Valls C (2015) *Bioresour Technol* 192:574–581. <https://doi.org/10.1016/j.biortech.2015.06.007>
- Bhatnagar A, Sillanpää M, Witek-Krowiak A (2015) *Chem Eng J* 270:244–271. <https://doi.org/10.1016/j.cej.2015.01.135>
- Bilal M, Shah JA, Ashfaq T, Gardazi SMH, Tahir AA, Pervez A, Haroon H, Mahmood Q (2013) *J Hazard Dent Mater* 263(Part 2):322
- Börjesson M, Westman G (2015) Crystalline nanocellulose—preparation, modification, and properties. In: Poletto M (ed) *Cellulose—fundamental aspects and current trends*. IntechOpen. <https://doi.org/10.5772/61899>
- Cao X, Huang M, Ding B, Yu J, Sun G (2013) *Desalination* 316:120–126
- Carpenter AW, de Lannoy C-F, Wiesner MR (2015) *Environ Sci Technol* 49:5277–5287. <https://doi.org/10.1021/es506351r>
- de Castro Silva F, da Silva MMF, Lima LCB, Osajima JA, da Silva Filho EC (2018) *Int J Biol Macromol* 114:470
- Chen L, Berry RM, Tam KC (2014) *ACS Sustain Chem Eng* 2:951–958
- Chen P, Li N, Chen X, Ong WJ, Zhao X (2017) *2D Mater* 5:014002. <https://doi.org/10.1088/2053-1583/aa8d37>
- Cheng Q, Ye D, Chang C, Zhang L (2017) *J Membr Sci* 525:1–8. <https://doi.org/10.1016/j.memsci.2016.11.084>

- Chhaged M, Yadav C, Agrawal AK, Maji PK (2019) *Carbohydr Polym* 226(115286):110144–118617. <https://doi.org/10.1016/j.carbpol.2019.115286>
- Chitpong N, Husson SM (2017) *J Membr Sci* 523:418–429. <https://doi.org/10.1016/j.memsci.2016.10.020>
- Cringoli MC, Kralj S, Kurbasic M, Urban M, Marchesan S, Beilstein J (2017) *Nanotechnol* 8:1553–1562. <https://doi.org/10.3762/bjnano.8.157>
- Crini G (2006) *Bioresour Technol* 97:1061–1085
- Cruz-Tato P, Ortiz-Quiles EO, Vega-Figueroa K, Santiago-Martoral L, Flynn M, Díaz-Vázquez LM, Nicolau E (2017) *Environ Sci Technol* 51:4585–4595. <https://doi.org/10.1021/acs.est.6b05955>
- Das R, Ghorai S, Pal S (2013) *Chem Eng J* 229:144–152. <https://doi.org/10.1016/j.cej.2013.05.104>
- dos Santos DM, Leite IS, de Lacerda Bukzem A, de Oliveira Santos RP, Frollini E, Inada NM, Campana-Filho S (2018) *P. Carbohydr Polym* 186:110–121. <https://doi.org/10.1016/j.carbpol.2018.01.045>
- Du X, Zhang Z, Liu W, Deng Y (2017) *Nano Energy* 35:299–320. <https://doi.org/10.1016/j.nanoen.2017.04.001>
- Elazzouzi-Hafraoui S, Nishiyama Y, Putaux J-L, Heux L, Dubreuil F, Rochas C (2008) *Biomacromol* 9:57–65. <https://doi.org/10.1021/bm700769p>
- El-Safty SA, Shenashen MA, Sakai M, Elshehy E, Halada KJ (2015) *Visualized Exp.* e53044. <https://doi.org/10.3791/53044>
- Eyley S, Thielemans W (2011) *Chem Commun* 47:4177–4179
- Fan M, Dai D, Yang A (2011) *Int J Polym Mater* 60:1026–1040. <https://doi.org/10.1080/00914037.2010.551347>
- Fang Q, Zhou X, Deng W, Zheng Z, Liu Z (2016) *Sci Rep* 6:1
- Gama M, Gatenholm P, Klemm D (2017) *Bacterial nanocellulose: a sophisticated multifunctional material*. CRC Press, Boca Raton, Florida
- Gao R, Xiao S, Gan W, Liu Q, Amer H, Rosenau T, Li J, Lu Y (2018) *ACS Sustain Chem Eng* 6(7):9047–9055. <https://doi.org/10.1021/acssuschemeng.b01397>
- García A, Gandini A, Labidi J, Belgacem N, Bras J (2016) *Ind Crops Prod* 93:26–38. <https://doi.org/10.1016/j.indcrop.2016.06.004>
- Gatenholm P, Klemm D (2010) *MRS Bull* 35:208–213. <https://doi.org/10.1557/mrs2010.653>
- Ge S, Champagne P, Wang HD, Jessop PG, Cunningham MF (2016) *Environ Sci Technol* 50:7896–7903
- Gholami Derami H, Jiang Q, Ghim D, Cao S, Chandar YJ, Morrissey JJ, Jun S, Singamaneni YS (2019) *ACS Appl Nano Mater* 2:1092
- Habibi Y, Lucia LA, Rojas OJ (2010) *Chem Rev* 110:3479–3500. <https://doi.org/10.1021/cr900339w>
- He M, Yang G, Chen J, Ji X, Wang Q (2018) *J Wood Chem Technol* 38:149–158. <https://doi.org/10.1080/02773813.2017.1411368>
- Helmiyati H, Budiman Y, Abbas GH, Dini FW, Khalil M (2021) *Heliyon* 7(3):e06622. <https://doi.org/10.1016/j.heliyon.2021.e06622>
- Henriksson M, Henriksson G, Berglund L, Lindström T (2007) *Eur Polym J* 43:3434–3441. <https://doi.org/10.1016/j.eurpolymj.2007.05.038>
- Herrera-Morales J, Morales K, Ramos D, Ortiz-Quiles EO, Lopez-Encarnacion JM, Nicolau E (2017) *ACS Omega* 2:7714–7722
- Hideno A, Abe K, Yano H (2014) *J Food Sci* 79:N1218–N1224. <https://doi.org/10.1111/1750-3841.12471>
- Hokkanen S, Repo E, Suopajarvi T, Liimatainen H, Niinimaa J, Sillanpaa M (2014a) *Cellulose* 21:1471–1487
- Hokkanen S, Repo E, Bhatnagar A, Tang WZ, Sillanpaa M (2014b) *Environ Technol* 35:2334–2346
- Huang R, Liu Z, Sun B, Fatehi P, Can J (2016) *Chem Eng* 94:1435–1441
- Huang X, Wang J, Li T, Wang J, Xu M, Yu W, El Abed A, Zhang X, Beilstein J (2018) *Nanotechnol* 9:30–41. <https://doi.org/10.3762/bjnano.9.5>
- Iwamoto S, Isogai A, Iwata T (2011) *Biomacromol* 12:831–836. <https://doi.org/10.1021/bm101510r>

- Jain P, Varshney S, Srivastava S (2017) *IET Nanobiotechnol* 11:45
- Jalali M, Aboulghazi F (2013) *J Mater Cycles Waste Manag* 15:548
- Johari K, Saman N, Song ST, Chin CS, Kong H (2016) *Mat Int Biodeterior Biodegrad* 109:45
- Kargarzadeh H, Ioelovich M, Ahmad I, Thomas S, Dufresne A (2017a) Methods for extraction of nanocellulose from various sources. In: Kargarzadeh H, Ahmad I, Thomas S, Dufresne A (eds) *Handbook of nanocellulose and cellulose nanocomposites*. Wiley-VCH, Weinheim, Germany, pp 1–49. <https://doi.org/10.1002/9783527689972.ch1>
- Kargarzadeh H, Mariano M, Huang J, Lin N, Ahmad I, Dufresne A, Thomas S (2017b) *Polymer* 132:368–393. <https://doi.org/10.1016/j.polymer.2017.09.043>
- Karim Z, Mathew AP, Grahn M, Mouzon J, Oksman K (2014) *Carbohydr Polym* 112:668–676. <https://doi.org/10.1016/j.carbpol.2014.06.048>
- Karim Z, Claudpierre S, Grahn M, Oksman K, Mathew AP (2016a) *J Membr Sci* 514:418–428. <https://doi.org/10.1016/j.memsci.2016.05.018>
- Karim Z, Mathew AP, Kokol V, Wei J, Grahn M (2016b) *RSC Adv* 6:20644–20653. <https://doi.org/10.1039/C5RA27059F>
- Karim Z, Claudpierre S, Grahn M, Oksman K, Mathew APJ (2016c) *Memb. Sci.* 514:418–428
- Karim Z, Hakalahti M, Tammelin T, Mathew AP (2017) *RSC Adv* 7:5232–5241. <https://doi.org/10.1039/C6RA25707K>
- Khin MM, Nair AS, Babu VJ, Murugan R, Ramakrishna S (2012) *Energy Environ Sci* 5:8075–8109. <https://doi.org/10.1039/c2ee21818f>
- Kimura S, Itoh T (1996) *Protoplasma* 194:151–163. <https://doi.org/10.1007/BF01882023>
- Klemm D, Heublein B, Fink H-P et al (2005) *Angew Chem Int Ed* 44:3358–3393. <https://doi.org/10.1002/anie.200460587>
- Kono H (2017) *Resour-Effic Technol* 3:55–63. <https://doi.org/10.1016/j.refit.2016.11.015>
- Korhonen JT, Kettunen M, Ras RHA, Ikkala O (2011) *ACS Appl Mater Interfaces* 3:1813–1816
- Kumar S, Kumar A, Bahuguna A, Sharma V, Krishnan V, Beilstein J (2017) *Nanotechnol* 8:1571–1600. <https://doi.org/10.3762/bjnano.8.159>
- Laitinen O, Suopajarvi T, Österberg M, Liimatainen H (2017) *ACS Appl Mater Interfaces* 9:25029–25037. <https://doi.org/10.1021/acsami.7b06304>
- Lee CS, Robinson J, Chong MF (2014) *Process Saf Environ Prot* 92:489–508
- Li G, Nandgaonkar AG, Wang Q, Zhang J, Krause WE, Wei Q, Lucia LA (2017) *J Membr Sci* 525:89–98. <https://doi.org/10.1016/j.memsci.2016.10.033>
- Li B, Li M, Zhang J, Pan Y, Huang Z, Xiao H (2019) *Int J Biol Macromol* 122:149
- Liimatainen H, Sirviö J, Sundman O, Visanko M, Hormi O, Niinimäki J (2011) *Bioresour Technol* 102:9626–9632. <https://doi.org/10.1016/j.biortech.2011.07.099>
- Liimatainen H, Sirviö J, Sundman O, Hormi O, Niinimäki J (2012) *Water Res* 46:2159–2166. <https://doi.org/10.1016/j.watres.2012.01.035>
- Liimatainen H, Suopajarvi T, Sirviö J, Hormi O, Niinimäki J (2014) *Carbohydr Polym* 103:187–192. <https://doi.org/10.1016/j.carbpol.2013.12.042>
- Liu S, Tao D, Bai H, Liu X (2012) *J Appl Polym Sci* 126:E282–E290
- Liu P, Sehaqui H, Tingaut P, Wichser A, Oksman K, Mathew AP (2014) *Cellulose* 21:449–461. <https://doi.org/10.1007/s10570-013-0139-5>
- Liu P, Borrell PF, Božič M, Kokol V, Oksman K, Mathew AP (2015) *J Hazard Mater* 1590(294):177–185
- Liu J, Willför S, Mhraryan A (2017) *Carbohydr Polym* 172:11–19. <https://doi.org/10.1016/j.carbpol.2017.05.002>
- Liu P, Zhu C, Mathew AP (2019) *J Hazard Mater* 371:484
- Loow YL, New EK, Yang GH, Ang LY, Foo LYW, Wu TY (2017) *Cellulose* 24:3591–3618. <https://doi.org/10.1007/s10570-017-1358-y>
- Lu L, Ozcan S (2015) *Nano Today* 10:417–420. <https://doi.org/10.1016/j.nantod.2015.04.010>
- Ma H, Burger C, Hsiao BS, Chu B (2011) *Biomacromol* 12:970–976
- Ma H, Burger C, Hsiao BS, Chu B (2012) *Biomacromol* 13:180–186

- Ma T, Fan Q, Tao H, Han Z, Jia M, Gao Y, Ma W, Sun Z (2017a) *Nanotechnology* 28:472001. <https://doi.org/10.1088/1361-6528/aa8f6f>
- Ma H, Wang S, Meng F, Xu X, Huo X (2017b) *Cellulose* 24:797–809
- Madivolli E, Kareru P, Gachanja A, Mugo S, Murigi M, Kairigo P, Kipyegon C, Mutembei J, Njonge F (2016) *Int Res J Pure Appl Chem* 12:1
- Mahfoudhi N, Boufi S (2017) *Cellulose* 24:1171–1197. <https://doi.org/10.1007/s10570-017-1194-0>
- Maleki A, Eskandarpour V, Rahimi J, Hamidi N (2019) *Carbohyd Polym* 208:251–260. <https://doi.org/10.1016/j.carbpol.2018.12.069>
- Mautner A, Maples HA, Kobkeathawin T, Kokol V, Karim Z, Li K, Bismarck A (1861) *Int J Environ Sci Technol* 2016:13
- Mautner A, Lee KY, Lahtinen P, Hakalahti M, Tammelin T, Li K, Bismarck A (2014) *Chem Commun* 50:5778–5781
- Mautner A, Lee KY, Tammelin T, Mathew AP, Nedoma AJ, Li K, Bismarck A (2015) *React Funct Polym* 86:209–214
- Mehmood A, Khan FSA, Mubarak NM, Mazari SA, Jatoi AS, Khalid M, Tan YH, Karri RR, Walvekar R, Abdullah EC, Nizamuddin S (2021) Carbon and polymer-based magnetic nanocomposites for oil-spill remediation—a comprehensive review. *Environ Sci Pollut Res* 28(39):54477–54496. <https://doi.org/10.1007/s11356-021-16045-0>
- Menon MP, Selvakumar R, Kumar PS, Ramakrishna S (2017) *RSC Adv* 7:42750–42773. <https://doi.org/10.1039/C7RA06713E>
- Metreveli G, Wågberg L, Emmoth E, Belák S, Strømme M, Mihranyan A (2014a) *Adv Healthcare Mater* 3:1546–1550. <https://doi.org/10.1002/adhm.201300641>
- Metreveli G, Wågberg L, Emmoth E, Belak S, Stromme M, Mihranyan A (2014b) *Adv. Healthc. Mater.* 3:1546–1550
- Mihranyan A (2011) *J Appl Polym Sci* 119:2449–2460. <https://doi.org/10.1002/app.32959>
- Missoum K, Belgacem MN, Bras J (2013) *Materials* 6:1745–1766. <https://doi.org/10.3390/ma6051745>
- Mohamed MA, Salleh WNW, Jaafar J, Ismail AF, Abd Mutalib M, Jamil SM (2015) *Carbohyd Polym* 133:429–437. <https://doi.org/10.1016/j.carbpol.2015.07.057>
- Moradeeya PG, Kumar MA, Thorat RB, Rathod M, Khambhaty Y, Basha S (2017) *Cellulose* 24:1319–1332
- Nair SS, Zhu JY, Deng Y, Ragauskas AJ (2014) *J Nanopart Res* 16:2349. <https://doi.org/10.1007/s11051-014-2349-7>
- Nechyporchuk O, Belgacem MN, Bras J (2016) *Ind Crops Prod* 93:2–25. <https://doi.org/10.1016/j.indcrop.2016.02.016>
- Nicolai E, Preston RD (1952) *Proc R Soc Lond Ser B* 140:244–274. <https://doi.org/10.1098/rspb.1952.0061>
- Ninomiya K, Abe M, Tsukegi T, Kuroda K, Tsuge Y, Ogino C, Taki K, Taima T, Saito J, Kimizu M, Uzawa K, Takahashi K (2018) *Carbohyd Polym* 182:8–14. <https://doi.org/10.1016/j.carbpol.2017.11.003>
- Oberdörster G, Oberdörster E, Oberdörster J (2005) *Environ Health Perspect* 113:823–839. <https://doi.org/10.1289/ehp.7339>
- Onyianta AJ, Dorris M, Williams RL (2018) *Cellulose* 25:1047–1064. <https://doi.org/10.1007/s10570-017-1631-0>
- Pääkkö M, Ankerfors M, Kosonen H, Nykänen A, Ahola S, Österberg M, Ruokolainen J, Laine J, Larsson PT, Ikkala O, Lindström T (2007) *Biomacromol* 8:1934–1941. <https://doi.org/10.1021/bm061215p>
- Park N-M, Koo JB, Oh J-Y, Kim HJ, Park CW, Ahn S-D, Jung SW (2017a) *Mater Lett* 196:12–15. <https://doi.org/10.1016/j.matlet.2017.03.003>
- Park C-W, Han S-Y, Namgung H-W, Seo P-N, Lee S-Y, Lee S-H (2017b) *BioResources* 12:5031–5044. <https://doi.org/10.15376/biores.12.3.5031-5044>
- Pastrana-Martínez LM, Morales-Torres S, Figueiredo JL, Faria JL, Silva AMT (2015) *Water Res* 77:179–190. <https://doi.org/10.1016/j.watres.2015.03.014>

- Puls J, Wilson SA, Hölter D (2011) *J Polym Environ* 19:152–165. <https://doi.org/10.1007/s10924-010-0258-0>
- Putro JN, Kurniawan A, Ismadji S, Ju Y-H (2017) *Environ. Nanotechnol. Monit. Manage* 8:134–149. <https://doi.org/10.1016/j.enmm.2017.07.002>
- Qiao H, Zhou Y, Yu F, Wang E, Min Y, Huang Q, Pang L, Ma T (2015) *Chemosphere* 141:297–303
- Quinlan PJ, Tanvir A, Tam KC (2015) *Carbohydr Polym* 133:80–89
- Rafatullah M, Sulaiman O, Hashim R, Ahmad A (2010) *J Hazard Mater* 177:70–80
- Rafieian F, Jonoobi M, Yu Q (2019) *Cellulose* 26:3359
- Ren W, Gao J, Lei C, Xie Y, Cai Y, Ni Q, Yao J (2018) *Chem Eng J* 349:766–774. [10.1016/j.cej.2018.05.143](https://doi.org/10.1016/j.cej.2018.05.143)
- Rocha I, Ferraz N, Mihranyan A, Strømme M, Lindh J (2018) *Cellulose* 25:1899–1910. <https://doi.org/10.1007/s10570-018-1661-2>
- Rosa MF, Medeiros ES, Malmonge JA, Gregorski KS, Wood DF, Mattoso LHC, Glenn G, Orts WJ, Imam SH (2010) *Carbohydr Polym* 81:83–92. <https://doi.org/10.1016/j.carbpol.2010.01.059>
- Ruan C, Strømme M, Jonas L (2016) *Cellulose* 23:2627–2638. <https://doi.org/10.1007/s10570-016-0976-0>
- Sacui IA, Nieuwendaal RC, Burnett DJ, Stranick SJ, Jorfi M, Weder C, Foster EJ, Olsson RT, Gilman JW (2014) *ACS Appl Mater Interfaces* 6:6127–6138. <https://doi.org/10.1021/am500359f>
- Sajab MS, Chia CH, Chan CH, Zakaria S, Kaco H, Chook SW, Chin SX, Noor AM (2016) *RSC Adv* 6:19819
- Santos MR, Rodrigues MVR, Santos ABS et al (2016) *J. Mol. Catal. Chem.* 422:131–141
- Sehaqui H, Mautner A, Perez De Larraya U, Pfenninger N, Tingaut P, Zimmermann T (2016) *Carbohydr Polym* 135:334–340. <https://doi.org/10.1016/j.carbpol.2015.08.091>
- Sharma PR, Cattopadhyay A, Sharma SK, Geng L, Amiralian N, Martin D, Hsiao BS (2018) *ACS Sustain Chem Eng* 6:3279–3290. <https://doi.org/10.1021/acssuschemeng.7b03473>
- Smyth M, Fournier C, Driemeier C, Picart C, Foster EJ, Bras J (2017) *Biomacromol* 18:2034–2044. <https://doi.org/10.1021/acs.biomac.7b00209>
- Sun C, Ni J, Zhao C, Du J, Zhou C, Wang S, Xu C (2017) *Cellulose* 24:5615
- Sun N, Wen X, Yan C (2018) *Int J Biol Macromol* 108:1199
- Suopajarvi T, Liimatainen H, Hormi O, Niinimäki J (2013) *Chem Eng J* 231:59–67
- Suopajarvi T, Liimatainen H, Hormi O, Niinimäki J (2013) *Chem Eng J* 231:59–67. <https://doi.org/10.1016/j.cej.2013.07.010>
- Suopajarvi T, Koivuranta E, Liimatainen H, Niinimäki JJ (2014) *Environ. Chem Eng* 2:2005–2012. <https://doi.org/10.1016/j.jece.2014.08.023>
- Suopajarvi T, Liimatainen H, Karjalainen M, Upola H, Niinimäki JJ (2015) *Water Process Eng.* 5:136–142. <https://doi.org/10.1016/j.jwpe.2014.06.003>
- Suopajarvi T, Sirviö JA, Liimatainen HJ (2017) *Environ Chem Eng* 5:86–92. <https://doi.org/10.1016/j.jece.2016.11.021>
- Taranto J, Frochot D, Pichat P (2009) *Sep Purif Technol* 67:187–193. <https://doi.org/10.1016/j.seppur.2009.03.017>
- Thomas M, Naikoo GA, Sheikh MUD, Bano M, Khan FJ (2016) *Photochem Photobiol A* 327:33–43. <https://doi.org/10.1016/j.jphotochem.2016.05.005>
- Tibolla H, Pelissari FM, Menegalli FC (2014) *LWT-Food. Sci Technol* 59:1311–1318. <https://doi.org/10.1016/j.lwt.2014.04.011>
- Uzyl HK, Saçan MT (2017) *Environ Sci Pollut Res* 24:11154–11162. <https://doi.org/10.1007/s11356-016-7049-7>
- Van Haver L, Nayar S (2017) *Algal Res* 24:167–180. <https://doi.org/10.1016/j.algal.2017.03.022>
- Vanderfleet OM, Osorio DA, Cranston ED (2018) *Philos Trans R Soc A* 376:20170041. <https://doi.org/10.1098/rsta.2017.0041>
- Ventura-Cruz S, Tecante A (2019) *Carbohydr Polym* 220:53–59. <https://doi.org/10.1016/j.carbpol.2019.05.053>
- Wägberg L, Decher G, Norgren M, Lindström T, Ankerfors M, Axnäs K (2008) *Langmuir* 24:784–795. <https://doi.org/10.1021/la702481v>

- Wang R, Guan S, Sato A, Wang X, Wang Z, Yang R, Hsiao BS, Chu BJ (2013) *Memb Sci* 446:376–382
- Wang Y, Zhang X, He X, Zhang W, Zhang X, Lu C (2014a) *Carbohydr Polym* 110:302–308
- Wang MS, Jiang F, Hsieh YL, Nitin NJ (2014b) *Mater Chem B* 2:6226–6235
- Wei H, Rodriguez K, Rennecker S, Vikesland PJ (2014) *Environ. Sci. NANO* 1:302–316. <https://doi.org/10.1039/C4EN00059E>
- Yanamala N, Farcas MT, Hatfield MK, Kisin ER, Kagan VE, Geraci CL, Shvedova AA (2014) *ACS Sustain Chem Eng* 2:1691–1698. <https://doi.org/10.1021/sc500153k>
- Yang J, Yu J, Fan J, Sun D, Tang W, Yang X (2011) *J Hazard Mater* 189:377–383. <https://doi.org/10.1016/j.jhazmat.2011.02.048>
- Yu X, Tong S, Ge M, Wu L, Zuo J, Cao C, Song W (2013) *J Environ Sci* 25:933–943
- Yu SI, Min SK, Shin HS (2016a) *Sci Rep* 6(35684). <https://doi.org/10.1038/srep35684>
- Yu HY, Zhang DZ, Lu FF, Yao J (2016b) *ACS Sustain Chem Eng* 4:2632–2643. <https://doi.org/10.1021/acssuschemeng.6b00126>
- Zhang Z, Sebe G, Rentsch D, Zimmermann T, Tingaut P (2014) *Chem Mater* 26:2659–2668
- Zhu H, Zhang Y, Yang X, Liu H, Shao L, Zhang X, Yao J (2015) *J Hazard Mater* 296:1–8. <https://doi.org/10.1016/j.jhazmat.2015.04.029>
- Zhu W, Liu L, Liao Q, Chen X, Qian Z, Shen J, Liang J, Yao J (2016) *Cellulose* 23:3785–3797. <https://doi.org/10.1007/s10570-016-1045-4>

Synthesis and Applications of Polymer–Nano Clay Composites in Wastewater Treatment: A Review



Priyanka Pareek and Lalita Ledwani

Abstract Polluted water is the outcome of human deeds, which become a problem due to its toxicity and hazardous effects on aquatic life. Recent advancements in material science have developed various strategies and applications of Nanocomposites based on clay minerals and polymers in the environmental remediation of wastewater. Nanocomposites are made up of clay minerals, and polymers have shown improvement in properties of compatibility and degradability, high surface area, amplified active sites, and high clay minerals' adsorption capacity, which makes Nanocomposites very important striking. This chapter focuses on applications of different composite clay materials to eliminate wastewater pollutants. Modified polymers and clay minerals' structural and physicochemical properties have also been discussed in detail. The key direction of this chapter is the discussion of the various clay polymer composites, together with their synthesis and use in the adsorption of contaminants. The key focus of this chapter is the discussion of different synthesis methods of clay-polymer composites and their use in wastewater treatment. The discussion highlights the potential future aspects in the development of nanocomposite sound polymers.

Keywords Nanocomposites · Remediation · Wastewater treatment · Adsorption

1 Introduction

Water is a valuable natural resource; the availability and purity of water are important for the survival of living beings in the biosphere. However, fast marketing and industrialization reduce the quality of water by adding a large number of toxic pollutants into the open water body. Heavy metals, dyes and other toxic pollutants have emerged as extortion throughout the biosphere so that the elimination of those pollutants becomes a priority (Karri et al. 2021). According to the UN report (UN-Water 2015), consistent access to clean and pure water is one of the most basic goals and is an important challenge for the whole community. The essential requirements for

P. Pareek · L. Ledwani (✉)

Department of Chemistry, Manipal University Jaipur, Jaipur 302007, India

e-mail: lalita.ledwani@jaipur.manipal.edu

water decontamination are the material that suits high separation capacity, ease of availability, cheaper, broad surface area, porosity, and recyclable (Gupta et al. 2003; Carolin et al. 2017). In this regard, nanotechnology offers the prospect of creating sophisticated materials for the most effective water remediation by providing their properties such as porosity, functional groups, mechanical strength, surface improvement, and spreading (Pandey and Ramontja 2016; Karri et al. 2018; Sahu et al. 2019). Nanoparticles with a large surface area can do water remediation effectively, but their accumulation restricts their use. However, agglomeration can diminish by altering Nanomaterials into Nanocomposites. This chapter discussed different types of clay polymer composites, synthesis and their utilities. Importance is given to polymer Nano-clay composite and their use for wastewater treatment. Polymer composites with nano-clay are explained as a mixture of polymers with clay minerals to create a new material with desired properties such as low density, high specific surface area, increased functional groups, toughness, low cost, stiffness, thermal stability, chemical resistance and mechanical stability, which depends on the level of water pollution. Many polymer clay composites are prepared for significant water pollution control and detoxification, including biopolymer composites, protein composites, and clay composites. (Bitinis et al. 2011; Berber 2020). The preparation of polymer composites with nano-clay was introduced due to the need for materials with better adsorption efficiency and removal of heavy metals, dyes and other carcinogenic impurities. Clays are classified into several classes depending on their chemical structure and morphology: smectite, chlorite, kaolinite, illite, and halloysite (Zhirong et al. 2011). Due to their ease of use, relatively low cost, and low environmental impact, nano-clays have been considered and created for various applications (Zhu et al. 2016). With the rapid development of nanotechnology, clay minerals are gradually being used for much better quality nanomaterials and cheaper ones. (Sdiri et al. 2016). Nano-clays are nanoparticles of mineral layers, systematically arranged in the form of silicates with different layered structural units, forming compound clay crystallites by assembling these layers. The individual clay layer consists of octahedral and tetrahedral plates (Gupta et al. 2015; Al-Essa 2018). Octahedral sheets are composed of basic clay minerals such as aluminium or magnesium in a sixfold arrangement with oxygen in the form of a tetrahedral sheet with hydroxyl bonds. Tetrahedral sheets include a silicon-oxygen tetrahedron connected to an adjacent tetrahedron to which three corners are assigned, although the fourth corner of each tetrahedral sheet is covalently bonded to the adjacent octahedral sheet. The arrangements of these sheets influence various significant and distinctive aspects of Nano-clays. Based on their mineralogical location, about 30 different types of nano-clay determine their use for various purposes (Kausar et al. 2018).

2 Synthesis

There are several blending methods: solution-blending, melt-mixing and *in-situ* polymerization (Bitinis et al. 2011). The dispersal of nano-clay in the polymer matrix

is necessary for forming a polymer/nano-clay composite. The solution-blending process has a high mixing capacity and low viscosity, which ensures the necessary cracking of the clay layer during the polymerization process. The melt-blending process is environmentally friendly, and the manufacturing process has high business potential (El-Sheikhy and Al-Shamrani 2015). The *in-situ* polymerization process is based on a globally recognized process that ensures uniform distribution and can be modified by changing the polymerization process (El-Korashy et al. 2016). Various synthesis processes have also been adopted to form polymers/nano clay composites with exclusive characteristics (Guo et al. 2018). This chapter also discussed different synthesis methods and synthesis interactions, designs, physical and mechanical properties, and features of polymer/nano-clay composites.

2.1 Solution Blending Method

Solution- blending is a solvent driven system in which the polymer and prepolymer are soluble, and the clays are swellable (Jlassi et al. 2017). The swelled clay is converted into layered form by mixing with any polar or non-polar solvent-soluble polymer or prepolymer (El-Sheikhy and Al-Shamrani 2015). After the polymer and the exfoliated clay are mixed in the solvent, the polymer chain is interpolated and displaced between the solvent and the clay interlayer. The interpolated sheets are reunited during solvent removal by evaporation or deposition to form polymer/nano-clay composites. After removing the solvent, the interpolated system retained the nanoscale morphology. Entropy is achieved during intercalation due to the desorption of solvent particles. A three-step solvent mixing process in which clay is swallowed into the polymer. Mixing, separating the solvent, and finally pouring the composite layer. Swallowing clay is an energetic process; shaking is done by stirring, stirring with shear, and refluxing (Slavutsky et al. 2012; Bojnour and Pakizeh 2018). Ultrasonication treatment is also an effective way to increase the absorption of nano clay in a polymer blend. It breaks down nano-clay groups by creating a cavity in the mixture. The swallowing quality depends on various parameters such as the clay bed, the type of sonication, the type of solvent, and the sonication duration. Ultrasonic processing shows numerous advantages in response time, sound recording, and polymer / nano-clay composite yield. Thermostable composites are usually made by mixing solutions at the laboratory level. It has several advantages, such as ease of use, extreme particle dispersion, and coupled chemical reactions (Fig. 1).

2.2 Melt Blending Method

The polymer is mixed directly with the clay during the melt mixing process using a twisting machine (Jlassi et al. 2017). When the clay particles are well aligned with the polymer matrix, the polymer begins to pass through the clay surface, increasing the

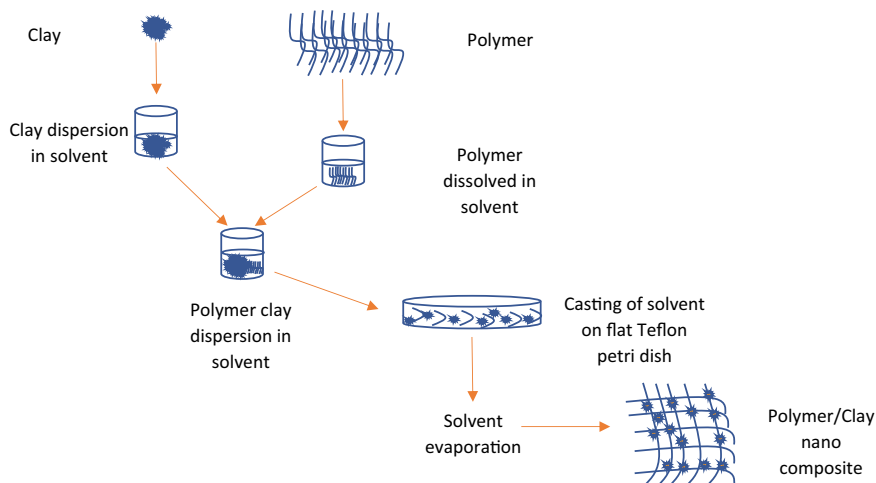


Fig. 1 Solution blending method

distance between the layers. Driving power is called shear strength, and this method is inexpensive because it does not use a solvent. This method has high efficiency and can produce the polymer, which we do not do in the other two polymerization solutions-based and in-situ intercalation methods. The melt blending process is comparatively better than the solution mixing process as it provides better mixing of the polymer and clay (El-Sheikhy and Al-Shamrani 2015). No solvent is used for melt blending, making it more compatible and environmentally friendly (Fig. 2).

Several parameters for synthesizing composites include mixing time, temperature, feed rate, material quality and filling, pressure, mixing medium, and the chemical nature of the clay and polymer components. The thermal driving force of functional macromolecules increased spacing between layers, and sufficient time to disperse centrally stacked sheets are three critical components of the fusion process. The melt mixing process is carried out in two ways: static or dynamic. These processes are carried out in a static manner (control of the melt temperature) at a pore temperature of about 50°C with a change in temperature without liquid without stirring. The active method is performed with inactive gas. The Melt mixers are divided into batch mixtures (internal) and conventional mixers (diffusers). The blending machine used provides excellent control over time, shear, pressure and temperature. This is significant when mixing heat-sensitive materials or dispersing nano clay dispersant fillers, heat sensitive materials or nano-clay. Brabender or Haake manufactures conventional laboratory-type batch mixers, and their equivalents are produced on a large scale by Banbury or Moriyama as spreading mixers (Tomaszewska and Walczak 2021). The high thermal conductivity of the mixing shaft is the main disadvantage of these mixers. Some melt blenders have recently been developed. The aim is to develop a new melt mixing process for modern thermoplastics and elastomer/nano-clay composites.

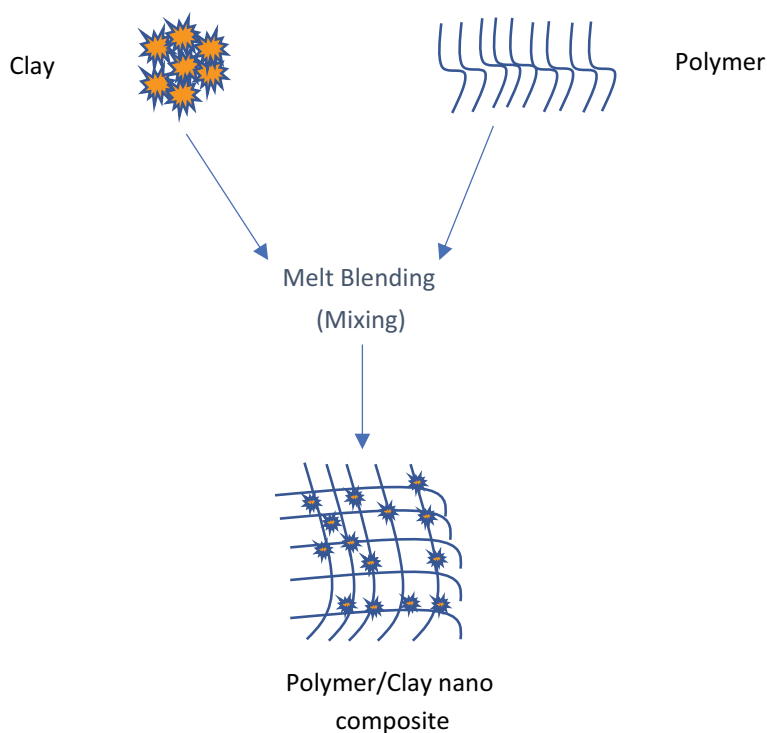


Fig. 2 Melt blending method

2.3 *In-Situ Polymerization Method*

The melt mixing process regularly results in inadequate filler dispersion, which leads to aggregation and intercalation, especially with high filler contents (Jlassi et al. 2017). *In-situ* polymerization is more efficient in forming composites and avoids the stringent thermodynamic requirements of the polymer intercalation process (El-Korashy et al. 2016). In addition, the *in-situ* polymerization allows the generation of a large number of molecular structures of the polymer matrix; it offers an effective method for the synthesis of various polymer/nano-clays composites with a wide range of properties and allows the design of the interface between nano-clays and polymers, due to which the composition and structure of the matrix can be suitably flexible (Yu et al. 2011). Several studies relate to the production of new polymer/nano-clay composites by *in-situ* polymerization and show the advantages of this method compared to other synthesis methods. The polymer and clay are introduced during this process by taking appropriate monomers and then polymerizing them in place (Carvalho et al. 2013). The polymerization process can be started either by heating or by irradiation, diffusion of an appropriate initiator or organic catalyst fixed cationically in the intermediate layer before the swelling step. The monomer is used directly

as a solubilizer to swell the phyllosilicate. After fusion of the silicate layers and the monomer, a sequential polymerization occurs, which permits the establishment of polymer chains between the encrusted layers. This method has extensively opted for thermosetting polymeric silicate nanocomposites (Delhom et al. 2010). The *in-situ* polymerization process provides clay fillers well discrete in the polymer matrix, giving the biodegradable composite superior antibacterial properties and improved modulus of elasticity (Jlassi et al. 2017) (Fig. 3).

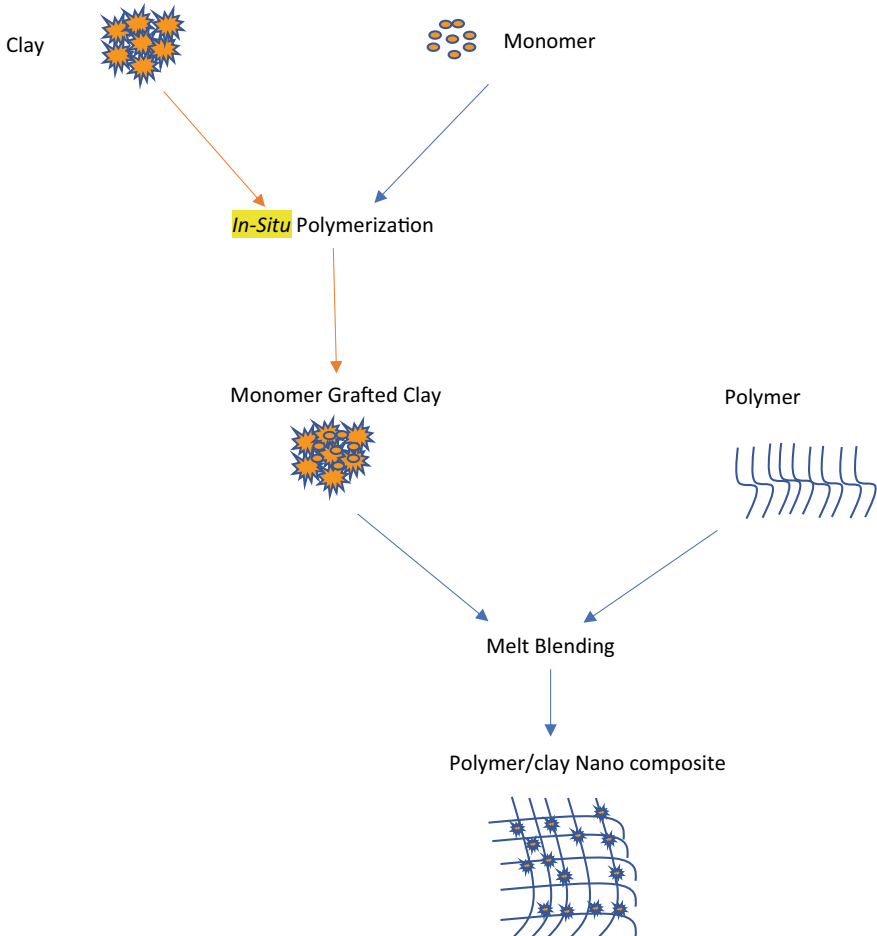


Fig. 3 *In-Situ* polymerization method

3 Characterization Techniques of Biopolymer-Clay Nanocomposites

X-ray diffraction (XRD) is a high-resolution technique used to determine the crystalline state of crystalline materials and deliver evidence about the morphology of adsorbents (Şahin et al. 2015). XRD defines the adsorbent's surface properties using the adsorbent's tuning. The increase in basal area defines the amount of puffiness of clay minerals by the overview of organic molecules. The adsorbent's surface morphology and physical properties are characterized by a scanning electron microscope (SEM) (Paulchamy et al. 2015). The SEM determines the particle shape, particle size distribution and viscosity. Fourier transform spectrophotometer (FTIR) analysis is used to perform spectroscopic characterization of compounds (Etim et al. 2016). The particle diameter of composite, clay and polymer samples is determined using a transmission electron microscope (TEM) (Gupta et al. 2015). Thermal stability and proportion of volatile components are determined by the continuous heating rate of the material by thermometric measurement analysis (TGA) (Belhouchat et al. 2017; Al-Essa 2018).

4 Applications of Polymer/Clay Nanocomposites in Wastewater Treatment

Water, the origin of life, is more important than any precious metal. Water is responsible for the social development of every community. Water is directly related to health and nutrition. Adulteration and pollution of the marine environment are one of the most important universal problems. Carbon-based and mineral waste, heavy metal ions, dyes and aromatic complexes are a high threat to water resources. Clay has a serial structure that is suitable for wastewater treatment. It can trap water among the interlayer spaces for absorption and ion exchange pollution. The following clay-based compounds are possible options for wastewater treatment using various techniques.

4.1 Poly Vinyl Imidazole (PVI)/Bentonite Nano Clay Composites

Polyvinyl imidazole (PVI) is a feeble basic polyelectrolyte. Imidazole fragments can form complexes containing divalent ions. When PVI is swollen in an acidic solvent, the imidazole moiety is protonated, and the gel acts as a polyelectrolyte. Therefore, due to its tertiary amine groups, it is pH sensitive. PVI is a polybase, and its cation density is pH-dependent. PVI is highly charged in less than pH 7, which is acidic. (Yildiz and Senkal 2016) Special attention has been paid to the characterization of the structure and properties of the polymer clay interface. Working with PVI

is interesting because it has a relatively simple synthetic adsorption property. The polyimide/bentonite-nano clay composite is created by *in-situ* polymerization (Jlassi et al. 2017). This process involves exfoliation-absorption. The bentonite is peeled off in layers. The polymer absorbs on the exfoliating layer. Evaporation of a mixture of rearranged clay layers with an absorbent polymer. Polymer-bentonite composites exhibit significant improvements in mechanical properties. Composite materials have increased mechanical strength, tensile strength, fraction and augmented modulus (Hernández-Hernández 2016). The adsorption of Remazol black B using a PVI/bentonite composite was carried out at pH 2. The adsorption process was determined using the Langmuir and Freundlich isothermal model. Langmuir's isothermal model suggests that this is single-layer adsorption and the maximum adsorption capacity was 230 mg/g using PVI-modified Na bentonite.

4.2 PANI/bentonite Nano Clay

Conventional adsorbents typically use low productivity and/or are expensive to track U (VI) in an aqueous medium. Thus, creating a competent adsorbent with outstanding adsorbing capacity is a serious technical problem in nuclear science and technology. Clay is an important component of the environment that significantly impacts the relocation of radionuclides in solution from the environment. It contains a lot of cations such as Cu^{2+} , Mg^{2+} , Na^+ , K^+ , including bentonite, which is a dioctahedral clay mineral, which is present in the structure and can be easily replaced by other ions during the adsorption process (Ramakrishna and Viraraghavan 1997). However, the lower number of efficient surface groups severely restricts the use of bentonite in practice. To additional increase the adsorption capacity of bentonite, alteration of the bentonite surface with polyaniline (PANI) to take benefit of the strong attraction of many amine and imine groups in PANI for U (VI) (Liu et al. 2017). Bentonite modified with polyaniline (PANI) (PANI/bentonite) was produced by plasma polymerization of aniline on the bentonite surface. This composite type was used to remove uranium (VI) ions from an aqueous solution (Liu et al. 2018). The periodic adsorption method was used to study the adsorption of U (VI) on bentonite and PANI/bentonite composite. The adsorption of U (VI) on the exterior of the composite depends completely on the pH of the solution, the ionic strength and the temperature of the solution. The exterior of the composite significantly raises the adsorption capacity of U (VI). Humic acid improves the adsorption of U (VI) on the composite at $\text{pH} < 6.5$. U (VI) adsorption on the PANI/bentonite surface is a completely impulsive and endothermic process (Fosso-Kankeu et al. 2016).

4.3 Thiourea-Formaldehyde/Bentonite Nano Clay

Bentonite has an efficient sorption mechanism, which is explained by the isomorphous substitution of Si (IV) and Al (III) in the silicon dioxide layer, which leads to permanent negative charges on its surface (Al-Asheh et al. 2003). Compared to activated carbon, clay minerals are not very effective in removing micropollutants from water due to their low specific surface. Thiourea formaldehyde (TUF), a chelating resin well known for recovery, selective separation and enrichment of Pd (II), Ag (III), Au (III), Hg (II), Fe (III), can be used for the separation of Co (II), Ni (II), Cu (II) and other metals ions (El-Korashy et al. 2016). TUF showed a high specific exterior area and outstanding adsorption capacity (El-Bindary et al. 2019); However, the disadvantage of TUF as a sorbent is its low thermal stability and low resistance to acids and alkalis. In recent years, various modifications of the sorption properties of bentonite have been studied. An important modification is the inclusion of sorbents such as chitosan (Kyzas and Kostoglou 2014), calcium alginate (El-Bindary et al. 2019), activated carbon (Bhatnagar and Minocha 2006), hydrocarbon, polymerized 4-vinyl pyridine and magnesite to combine them into a composite material, which is effective to remove metal ions. In addition, the number of contaminated sites of individual adsorbents can be minimized by combining them (Mukhopadhyay et al. 2020). *In-situ* polymerization of thiourea and formaldehyde on bentonite surfaces forms durable composites (El-Korashy et al. 2016). This composite was used to remove heavy metal ions such as Pb (II), Mn (II), and Cr (VI) from a virtual aqueous solution. The adsorption of metal ions depended on the pH value, the initial concentration of heavy metal ions and the adsorbent dose. The pH of the solution for the maximum adsorption of Mn (VII) and Pb (II) was 4, and for Cr (VI)–2. A pseudo-second-order reaction was found according to kinetic studies of the adsorption mechanism of Mn (VII) and Cr (VI) using a thiourea-formaldehyde/bentonite composite. The Langmuir isotherm model best described the adsorption isotherm, and the maximum adsorption capacity for Pb (II), Mn (II), and Cr (VI) was 13.38, 14.81, and 4.20 mg/g, respectively. The removal efficiency of the composite was 90% over four successive cycles.

4.4 Biopolymer/Clay Composite

Advances in nanotechnology facilitate the synthesis of bio nanocomposites from clay minerals and biopolymers. It has proven to be a promising material for removing contaminants from contaminated water (Jlassi et al. 2017). It has improved properties in terms of biocompatibility and digestibility. Biodegradation of biopolymers, large specific surface area, increased number of active sites and the excellent adsorption capacity of the clay makes them very close together. There are several types of biopolymer clay nanocomposites designed for environmental remediation.

4.4.1 Chitosan-Based Bio-Nano-Composites

Chemical flocculants are not suitable for water purification because of health and financial reasons. Biodegradable and biocompatible natural components of low toxicity and of renewable origin are suitable for the adsorption and retention of various toxins from wastewater. Chitosan (CS) is a derivative of chitin (N-deacetylated). It is hydrophilic in nature and has many hydroxyl and amino groups. It is a biodegradable and biocompatible environmental material (Dehghani et al. 2020; Chang et al. 2021). It is the least toxic and abundant in nature. Due to its high hydrophilicity and large amino and hydroxyl groups, CS combines well with clay minerals. CS is a widely known adsorbent for removing heavy metals and pigments from water. However, pure chitosan as an adsorbent has certain limitations, such as high cost due to low mechanical properties and low density. Chitosan swells and floats when dissolved in water and is poorly stable in acidic environments to overcome these drawbacks. It has been proposed to fix chitosan in inexpensive materials such as bentonite, sand and montmorillonite (Marey 2019) because clay minerals have a large surface area and surface energy. Therefore, bentonite is used for this purpose for its high adsorption capacity (Özcan and Özcan 2004). However, its surface anion and many exchanged cations lead to the formation of an upper layer of water molecules on its internal surface. The internal coating of water molecules makes bentonite a very hydrophilic material. Therefore, bentonite is not suitable for absorbing organic pollutants. To modify the hydrophilicity of the surface of the bentonite, it has been envisaged to modify the surface of the bentonite with CS or to modify the surface of the organic bentonite with organic cations such as cationic surfactants. Therefore, organically modified bentonite is much more attractive as an adsorbent for removing organic pollutants (Özcan et al. 2007). Chitosan/bentonite composite materials are obtained by mixing in solution. Chitosan is dissolved in an acidic solution. This is trailed by centrifugation to remove turbid material. The bentonite will first be foamed in distilled water. Then added to the chitosan solution and mixed. The bentonite and chitosan tablets are filtered and washed with distilled water to remove additional sodium hydroxide or hydrochloric acid. The optimal dosage of bentonite (clay) in combination with chitosan (polymer) is 5 and 1 mg/L at pH = 7.4 (Giannakas and Pissanou 2018).

4.4.2 Cellulose-Based Bio Nanocomposites:

The cellulose-montmorillonite nanocomposite was produced to remove heavy metals from wastewater (Bajpai et al. 2019). Montmorillonite was first modified with a surfactant and polymerized with a cellulose biopolymer. Bio-nanocomposites are used to absorb Cr (VI) from wastewater. Biochromatic ions appear on the surface of bio-nano-composites. The maximum adsorption capacity was 22.2 mg/g using Langmuir's thermal adsorption model (Santoso et al. 2019). Bio-nanocomposites are naturally Bulgarian and follow a sequenced kinetic reaction. This composite material can be recycled up to 10 cycles after reconstitution of sodium hydroxide.

Adsorption occurs in the column process, and the cellulose/bentonite nanocomposite is also used to remove azo dyes from wastewater (maximum single layer adsorption capacity 45.77 mg/g).

4.4.3 Starch-Based Bio Nanocomposites

Corn starch polymer has specific functional properties that have made it useful in wastewater treatment processes. The corn starch polymer's surface properties have been improved by incorporating montmorillonite clay minerals. The composite was produced by *in-situ* polymerization, and intercalated nanocomposites were obtained (Lozano-Morales et al. 2018). Na montmorillonite (Na-MMT), intercalated in polyacrylic acid and polyacrylamide, grafted onto starch hydrogel (Zarei et al. 2018). Isothermal adsorption studies and kinetic studies displayed that the adsorption of safranin dye using Na-mmt-starch composite was a pseudo-second-order reaction and followed Elovich's kinetic models. Freundlich isotherm models well described the adsorption process. This study confirms that the adsorption of dyes with mmt-starch composite was very efficient.

4.4.4 Alginate-Based Bio-Nano Composites

Alginate clay compounds have been used as adsorbents to remove heavy metal ions and organic acid ions. Calcium alginate has a spherical structure, and its composites are made using natural clays as fillers. The clay-alginate composite was obtained after the preliminary processing of clay minerals. Batch adsorption was carried out to study the effect of various reaction parameters, such as stirring rate, the contribution of polymer reaction time, etc. (Fabryanty et al. 2017). The maximum adsorption capacity of bentonite/alginate compounds of methylene blue and crystal violet dyes was 780 and 546 mg/g (Belhouchat et al. 2017). The Langmuir isotherm model estimates the best attempt, describes a monolayer and is uniform adsorption. Thus, the alginate-bentonite compound has an effective adsorption capacity to remove heavy metal ions, dyes and other organic acid ions (Aziz et al. 2020).

4.4.5 Xanthan Gum-Based Bio-Nano Composites

A pretreated xanthan gum/montmorillonite composite nano-clay was produced as an antibacterial and biodegradable composite polymer (Abu Elella et al. 2021). The maximum adsorption capacity for malachite green was recorded at 99.99% or 909.1 mg/g at 300 °C for 90 min. To remove malachite green with composites of xanthan gum and montmorillonite, various isotherms models such as Langmuir, Freundlich, Temkin, and Flory Huggins have been studied. Langmuir's isotherm model works best for all adsorption isotherm models (Fosso-Kankeu et al. 2016).

Kinetic studies have shown that the manufactured nanocomposites are an excellent antibacterial material and effectively inhibit bacterial growth by increasing the concentration of montmorillonite. Antibacterial activity increases with the increasing concentration of montmorillonite.

4.4.6 Bio-Nano Cyclodextrin Composites

Polymer cyclodextrin and polysaccharides containing cyclodextrin are promising adsorbents for removing contaminants from wastewater (Tian et al. 2021). The water-soluble nature of cyclodextrin made it unsuitable for use as an adsorbent in liquid media, so the polymerization of cyclodextrin with various crosslinking agents made it available for wastewater treatment (Qin et al. 2019). Polymerized cyclodextrin, which is used as a sorbent for some colorants. This type of composite material shows high adsorption efficiency for Congo Red and Rhodamine B. The removal efficiency is over 80%, and q_{\max} is 712 and 175 mg/g, respectively (Cova et al. 2021).

4.5 Nanocomposites Based on Polyurethane Clay

Polyurethane (PU)/clay nanocomposites were synthesized with organically modified phyllosilicates by *in-situ* polymerization, and foams were synthesized in a batch process (Cao et al. 2005). XRD and BET have been used to study the clay dispersion of polyurethane nanocomposites. Physical interactions and chemical reactions occur between the functional groups of polyurethane and organoclay. Layers of silica clay are exfoliated in a single layer in the PU matrix by adding hydroxyl and organotin functional groups to the surface of the clay. The composite formation changed the chemical and physical properties of PU: increased cell density and decreased size, improved mechanical properties, decreased compressive strength, decreased modulus. (Zizi Abdeen 2014) created a bentonite-polyurethane composite called PUN, which had a sophisticated site structure and provided adsorption sites for the Pb^{2+} ion. It was inexpensive and showed maximum adsorption capacity for Pb^{2+} ions 125 mg/L at pH 5.0; the adsorbent dose was 0.5 g/L or 142.85 mg/g. The adsorption of Pb^{2+} ions using PUN follows a pseudo-second-order kinetic pattern and depends on the adsorbent dose, pH, initial concentration of metal ions and contact time (Abdeen 2015).

5 Mechanisms of Wastewater Treatment Using Clay–Polymer Nanocomposites

5.1 Membranes

Polymer/clay composites are broadly used for wastewater treatment, gas separation and detoxification due to their improved mechanical stability, flexibility, small footprint and low manufacturing costs (Environmental Physical Chemistry Laboratory 2014; Galimberti et al. 2013; Singh et al. 2018). In addition to removing toxic metals, dyes are also treated with CPN membranes (Bojnourd and Pakizeh 2018; Lau et al. 2020; Khan et al. 2021). However, the capacities and costs of clay polymer composite mediated membranes need to be enhanced so that they can be deployed in the field or on a nanoscale in rural areas. A membrane filled with 15 g of PVC and 1.37 g of bentonite with a thickness of 100 μm at pH 9 and a transmembrane pressure of 250 kPa has the maximum permeability. The membrane is composed of montmorillonite, PVC and a copolymer of polystyrene sulfonic acid and maleic acid, which is used to dispose of pharmaceutical waste. The waste elimination rate is 98.8%, thanks to the addition of functionalized clay (Alexander et al. 2019).

5.2 Flocculation/Coagulation

Waste from various food processing industries such as wineries, piggeries, olive mills or processing soybeans and coffee releases significant amounts of organic matter and fine dust. All suspended solids (TSS) remain dispersed and are problematic to eliminate with traditional adsorbents used to remove inorganic and organic micropollutants. Therefore, pretreatment of wastewater should be necessary before it is discharged to treatment plants. TSS reduction involves three steps: coagulation, flocculation and filtration. Clay minerals are useful for wastewater pretreatment; the removal efficiency of clay minerals is increased when used in combination (Amari et al. 2021). Sepiolite modified to reduce organics in wastewater, Sepiolite composites increase the deposition of bigger particles and decrease the amount of TSS (Song et al. 2021). The results showed that 1.0 kg of organic clay could remediate up to 8,000 L of wastewater. The authors discovered that very rapid coagulation is a major advantage of nanocomposites. According to research, the best polymers for wastewater pretreatment are water-soluble polymers, biopolymers, aromatic polymers, and molecules like quaternized hydroxyethyl cellulose ethoxylate (Huang et al. 2019; Pandey et al. 2017). The possibility of CPN-based coagulation-flocculation for organic wastewater treatment requires further study.

5.3 Columns/Barriers

The use of a clay polymer nanocomposite as a column or barrier to purify water is an auspicious area of research. (Ganigar et al. 2010) uses modified montmorillonite to remove 2,4,5-trichlorophenol from water. This study showed that the organic clay composite reduced the concentration of toxic inorganic contaminants in water through the use of a column filtration process. Likewise, a vesicle-clay complex (Amari et al. 2021) was made to remove pesticides. They used the composite as a means of the pillar (Rytwo et al. 2007). A column prepared to remove organic micropollutants and ammonium ions from wastewater. The columns were fitted with side openings to allow water and blockade material selection, and oxygen sensors were also situated below the top of the barrier. Microbial inoculation of the selected barriers was performed with fresh activated sludge from a local sewage treatment plant bypassing the settled fraction through columns. A synthetically purified wastewater resolution, which consisted of two separate mixed solutions with different concentrations, was introduced into the columns. Thus, CPN adsorbents obtained from organically improved clays can be used as a filter for a wastewater treatment column (Galimberti et al. 2013). However, the use of CPN as a pillar as a low-cost water purification method should deserve more research attention.

6 Water Treatment Options by Clay–Polymer Nanocomposites

6.1 Chemisorption

The mechanism of chemisorption involves the mechanism of electrostatic interaction, the mechanism of ion exchange, the mechanism of oxidation/reduction and the mechanism of chelation (Berber 2020). All mechanisms can be used individually or in combination to remove impurities. The adsorption process depends on the functional groups present on the surface of the adsorbent (Fabryanty et al. 2017). The surface of the adsorbent contains different functional groups in different forms of protonation, which affect the adsorption process. Figure 4 shows the chemisorption mechanism. If functional groups are presented in a protonated form, they can enter a complex or chelation process with water pollutants, but if they are present in a deprotonated form, a process of an electrostatic interaction process will occur (Mallampati et al. 2015). Thermodynamic chemical adsorption is a heat-releasing process in which heat is released during the adsorption process. Adsorption is a spontaneous process; Because of this, the entropy is reduced (Banerjee and Chattopadhyaya 2017). Adsorption Isothermal chemisorption studies show a single layer

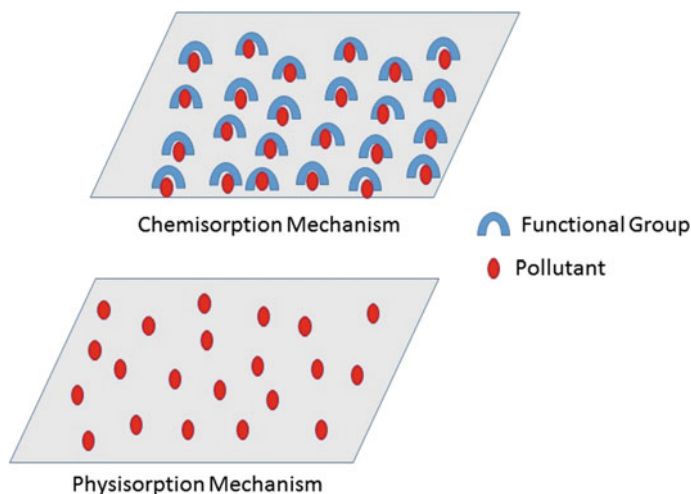


Fig. 4 Diagrammatic illustration of chemisorption and physisorption mechanism

creation of pollutants on the exterior of the adsorbent (Pandey and Ramontja 2016). The kinetic study shows that chemisorption follows a pseudo-second-order process; it defines that the adsorption process depends on both the adsorbents and the adsorbate (Ramakrishna and Viraraghavan 1997).

6.2 Physisorption

The physical adsorption mechanism occurs between the adsorbent and the adsorbates due to van der Waals forces (Taher et al. 2017). Figure 4 shows physical adsorption. The surface of the adsorbent during chemisorption contains many functional groups about physisorption. During physical adsorption, adsorbates physically adhere to the surface of the adsorbent due to weak van der Waals forces. This occurs on hard surfaces with low adhesion. Physisorption is a reversible mechanism and depends on the temperature of the environment (Gupta et al. 2003). The rate of adsorption and desorption is very high in physical adsorption. It follows pseudo-second-order kinetics; it specifies that adsorption depends on the concentration and surface structure of the adsorbents (Inyinbor et al. 2016). The best adsorbents for physical adsorption are adsorbents with high surface porosity and large specific surface area. It does not require high activation energy for the adsorption process.

7 Conclusions and Prospects

This chapter review concluded that:

- (a) Polymers integrated with other metals, clay, and other sorbents are low-cost and eco-friendly.
- (b) Additional functional groups from new functional materials can be done by designing hybrid technologies to enhance the adsorption efficiency.
- (c) Explore more natural/agro waste as adsorbents to reduce the production cost.
- (d) Reviewing the Mechanism of adsorption to improve the effect of adsorbents in different conditions.
- (e) Biomass feedstock is used after improvement and pretreatment methods.
- (f) Nanocomposite preparation reduces the operational costs for large-scale applications of the adsorbents.

In the future, the following points should be taken into account:

1. Non-toxic metals such as Cu, Zn and Fe should be approved for water treatment instead of Ti and Ag.
2. Environmentally friendly materials such as agricultural waste and plant material must be approved to manufacture polymer–clay nanocomposites.
3. Photo-catalytic polymer/clay Nanocomposites should be prepared to remove microbes from wastewater.
4. More attention is required in the regeneration of used adsorbents.
5. Awareness of Nano-composites-based water remediation must be heightened.

Acknowledgements Authors would like to thank the Department of Science and Technology, Govt. of Rajasthan and Department of Chemistry, School of Basic Sciences, Manipal University Jaipur, for supporting this review work.

References

- Abdeen Z (2015) Enhanced recovery of Pb²⁺ ions from aquatic media by using polyurethane composite as adsorbent. *Environ Process* 2:189–203. <https://doi.org/10.1007/s40710-014-0048-0>
- Abu Elella MH, Goda ES, Abdallah HM et al (2021) Innovative bactericidal adsorbents containing modified xanthan gum/montmorillonite nanocomposites for wastewater treatment. *Int J Biol Macromol* 167:1113–1125. <https://doi.org/10.1016/j.ijbiomac.2020.11.065>
- Al-Asheh S, Banat F, Abu-Aitah L (2003) The removal of Methylene Blue dye from aqueous solutions using activated and non-activated bentonites. *Adsorpt Sci Technol* 21:451–462. <https://doi.org/10.1260/026361703769645780>
- Al-Essa K (2018) Activation of jordanian bentonite by hydrochloric acid and its potential for olive mill wastewater enhanced treatment. *J Chem* <https://doi.org/10.1155/2018/8385692>
- Alexander JA, Ahmad Zaini MA, Surajudeen A et al (2019) Surface modification of low-cost bentonite adsorbents—a review. *Part Sci Technol* 37:534–545. <https://doi.org/10.1080/02726351.2018.1438548>

- Amari A, Alzahrani FM, Katubi KM et al (2021) Clay-polymer nanocomposites: preparations and utilization for pollutants removal. *Materials* 14:1–21. <https://doi.org/10.3390/ma14061365>
- Aziz F, El AM, Lissaneddine A et al (2020) Composites with alginate beads: a novel design of nano-adsorbents impregnation for large-scale continuous flow wastewater treatment pilots. *Saudi J Biol Sci* 27:2499–2508. <https://doi.org/10.1016/j.sjbs.2019.11.019>
- Bajpai A, Sharma M, Gond L (2019) Nanocomposites for environmental pollution remediation
- Banerjee S, Chattopadhyaya MC (2017) Adsorption characteristics for the removal of a toxic dye, tartrazine from aqueous solutions by a low cost agricultural by-product. *Arab J Chem* 10 <https://doi.org/10.1016/j.arabjc.2013.06.005>
- Belhouchat N, Zaghouane-Boudiaf H, Viseras C (2017) Removal of anionic and cationic dyes from aqueous solution with activated organo-bentonite/sodium alginate encapsulated beads. *Appl Clay Sci* 135 <https://doi.org/10.1016/j.clay.2016.08.031>
- Berber MR (2020) Current advances of polymer composites for water treatment and desalination. *J Chem* <https://doi.org/10.1155/2020/7608423>
- Bhatnagar A, Minocha AK (2006) Conventional and non-conventional adsorbents for removal of pollutants from water—a review. *Indian J Chem Technol* 13:203–217
- Bitinis N, Hernandez M, Verdejo R et al (2011) Recent advances in clay/polymer nanocomposites. *Adv Mater* 23:5229–5236. <https://doi.org/10.1002/adma.201101948>
- Cao X, James Lee L, Widya T, Macosko C (2005) Polyurethane/clay nanocomposites foams: processing, structure and properties. *Polymer* 46:775–783. <https://doi.org/10.1016/j.polymer.2004.11.028>
- Carolin CF, Kumar PS, Saravanan A et al (2017) Efficient techniques for the removal of toxic heavy metals from aquatic environment: a review. *J Environ Chem Eng* 5
- Carvalho HWP, Santilli CV, Brioso V, Pulcinelli SH (2013) Polymer-clay nano-composites thermal stability: experimental evidence of the radical trapping effect. *RSC Adv* 3:22830–22833. <https://doi.org/10.1039/c3ra44388d>
- Chang XX, Mujawar Mubarak N, Ali Mazari S, Sattar Jatoi A, Ahmad A, Khalid M, Walvekar R, Abdullah EC, Karri RR, Siddiqui MTH, Nizamuddin S (2021) A review on the properties and applications of chitosan, cellulose and deep eutectic solvent in green chemistry. *J Ind Eng Chem* 104:362–380
- Cova TF, Murtinho D, Aguado R et al (2021) Cyclodextrin polymers and cyclodextrin-containing polysaccharides for water remediation. *Polysaccharides* 2:16–38. <https://doi.org/10.3390/polysaccharides2010002>
- Dehghani MH, Karri RR, Alimohammadi M, Nazmara S, Zarei A, Saeedi Z (2020) Insights into endocrine-disrupting Bisphenol-A adsorption from pharmaceutical effluent by chitosan immobilized nanoscale zero-valent iron nanoparticles. *J Mol Liq* 311
- Delhom CD, White-Ghoorahoo LA, Pang SS (2010) Development and characterization of cellulose/clay nanocomposites. *Compos Part B Eng* 41:475–481. <https://doi.org/10.1016/j.compositesb.2009.10.007>
- El-Bindary AA, Kiwaan HA, Shoair AGF, Hawas AR (2019) A novel crosslinked amphoteric adsorbent thiourea formaldehyde calcium alginate: preparation, characterization and adsorption behaviors of removing color from acidic and basic dyes. *Desalin Water Treat* 151:145–160. <https://doi.org/10.5004/dwt.2019.23809>
- El-Korashy SA, Elwakeel KZ, El-Hafeiz AA (2016) Fabrication of bentonite/thiourea-formaldehyde composite material for Pb(II), Mn(VII) and Cr(VI) sorption: a combined basic study and industrial application. *J Clean Prod* 137:40–50. <https://doi.org/10.1016/j.jclepro.2016.07.073>
- El-Sheikhy R, Al-Shamrani M (2015) On the processing and properties of clay/polymer nanocomposites CPNC. *Lat Am J Solids Struct* 12:385–419. <https://doi.org/10.1590/1679-78251399>
- Environmental Physical Chemistry Laboratory (2014) Commercial application of hybrid clay polymer nanocomposites in water treatment. <https://doi.org/10.1016/i.colcom.2014.06.001>
- Etim UJ, Umoren SA, Eduok UM (2016) Coconut coir dust as a low cost adsorbent for the removal of cationic dye from aqueous solution. *J Saudi Chem Soc* 20 <https://doi.org/10.1016/j.jscs.2012.09.014>

- Fabryanty R, Valencia C, Soetaredjo FE et al (2017) Removal of crystal violet dye by adsorption using bentonite—alginate composite. *J Environ Chem Eng* 5 <https://doi.org/10.1016/j.jece.2017.10.057>
- Fosso-Kankeu E, Waanders F, Fourie CL (2016) Adsorption of congo red by surfactant-impregnated bentonite clay. *Desalin Water Treat* 57 <https://doi.org/10.1080/19443994.2016.1177599>
- Galimberti M, Cipolletti VR, Coombs M (2013) Applications of clay–polymer nanocomposites, 2nd edn. Elsevier Ltd.
- Ganigar R, Rytwo G, Gonen Y et al (2010) Polymer-clay nanocomposites for the removal of trichlorophenol and trinitrophenol from water. *Appl Clay Sci* 49:311–316. <https://doi.org/10.1016/j.clay.2010.06.015>
- Giannakas A, Pissanou M (2018) Chitosan/bentonite nanocomposites for wastewater treatment : a review. *SF J Nanochem Nanotechnol* 1:1010
- Guo F, Aryana S, Han Y, Jiao Y (2018) A review of the synthesis and applications of polymer-nanoclay composites. *Appl Sci* 8:1–29. <https://doi.org/10.3390/app8091696>
- Gupta VK, Ali I, Suhas MD (2003) Equilibrium uptake and sorption dynamics for the removal of a basic dye (basic red) using low-cost adsorbents. *J Colloid Interface Sci* 265:257–264. [https://doi.org/10.1016/S0021-9797\(03\)00467-3](https://doi.org/10.1016/S0021-9797(03)00467-3)
- Gupta VK, Sharma M, Vyas RK (2015) Hydrothermal modification and characterization of bentonite for reactive adsorption of methylene blue: an ESI-MS study. *J Environ Chem Eng* 3:2172–2179. <https://doi.org/10.1016/j.jece.2015.07.022>
- Hernández-Hernández KA, Illescas J, Díaz-Nava MDC, Muro-Urista CR, Martínez-Gallegos S, Ortega-Aguilar RE (2016) Polymer-clay nanocomposites and composites: structures, characteristics, and their applications in the removal of organic compounds of environmental interest. *Med Chem* 6:201–210. <https://doi.org/10.4172/2161-0444.1000347>
- Huang W, Wang S, Li D (2019) Polymers and polymer composites for adsorptive removal of dyes in water treatment
- Inyinbor AA, Adekola FA, Olatunji GA (2016) Kinetics, isotherms and thermodynamic modeling of liquid phase adsorption of Rhodamine B dye onto *Raphia hookeri* fruit epicarp. *Water Resour Ind* 15 <https://doi.org/10.1016/j.wri.2016.06.001>
- Jlassi K, Chehimi MM, Thomas S (2017) Clay-polymer nano-composites
- Karri RR, Shams S, Sahu JN (2018) 4—overview of potential applications of nano-biotechnology in wastewater and effluent treatment. In: *Nanotechnology in water and wastewater treatment: theory and applications*. Elsevier, pp 87–100
- Karri RR, Ravindran G, Dehghani MH (2021) Wastewater—sources, toxicity, and their consequences to human health. In: *Soft computing techniques in solid waste and wastewater management*. Elsevier, pp 3–33. <https://doi.org/10.1016/B978-0-12-824463-0.00001-X>
- Kausar A, Iqbal M, Javed A, et al (2018) Dyes adsorption using clay and modified clay: a review. *J Mol Liq* 256 <https://doi.org/10.1016/j.molliq.2018.02.034>
- Khan FSA, Mubarak NM, Khalid M, Tan YH, Abdullah EC, Rahman ME, Karri RR (2021) A comprehensive review on micropollutants removal using carbon nanotubes-based adsorbents and membranes. *J Environ Chem Eng* 9(6)
- Kyzas GZ, Kostoglou M (2014) Green adsorbents for wastewaters: a critical review. *Materials* 7:333–364. <https://doi.org/10.3390/ma7010333>
- Lau YJ, Karri RR, Mubarak NM, Lau SY, Chua HB, Khalid M, Jagadish P, Abdullah EC (2020) Removal of dye using peroxidase-immobilized Buckypaper/polyvinyl alcohol membrane in a multi-stage filtration column via RSM and ANFIS. *Environ Sci Pollut Res* 27(32):40121–40134
- Liu X, Cheng C, Xiao C et al (2017) Polyaniline (PANI) modified bentonite by plasma technique for U(VI) removal from aqueous solution. *Appl Surf Sci* 411:331–337. <https://doi.org/10.1016/j.apsusc.2017.03.095>
- Liu H, Xie S, Liao J et al (2018) Novel graphene oxide/bentonite composite for uranium(VI) adsorption from aqueous solution. *J Radioanal Nucl Chem* 317:1349–1360. <https://doi.org/10.1007/s10967-018-5992-0>

- Lozano-Morales V, Gardi I, Nir S, Undabeytia T (2018) Removal of pharmaceuticals from water by clay-cationic starch sorbents. *J Clean Prod* 190:703–711. <https://doi.org/10.1016/j.jclepro.2018.04.174>
- Mallampati R, Xuanjun L, Adin A, Valiyaveettil S (2015) Fruit peels as efficient renewable adsorbents for removal of dissolved heavy metals and dyes from water. *ACS Sustain Chem Eng* 3:1117–1124. <https://doi.org/10.1021/acssuschemeng.5b00207>
- Marey A (2019) Composite of chitosan and Bentonite as coagulant agents in removing turbidity from Ismailia canal as water treatment plant. *Rev Bionatura* 4:8–11. <https://doi.org/10.21931/RB/2019.04.03.3>
- Medhat Bojnour F, Pakizeh M (2018) Preparation and characterization of a nanoclay/PVA/PSf nanocomposite membrane for removal of pharmaceuticals from water. *Appl Clay Sci* 162:326–338. <https://doi.org/10.1016/j.clay.2018.06.029>
- Mukhopadhyay R, Bhaduri D, Sarkar B et al (2020) Clay–polymer nanocomposites: progress and challenges for use in sustainable water treatment. *J Hazard Mater* 383:121125. <https://doi.org/10.1016/j.jhazmat.2019.121125>
- Özcan AS, Özcan A (2004) Adsorption of acid dyes from aqueous solutions onto acid-activated bentonite. *J Colloid Interface Sci* 276:39–46. <https://doi.org/10.1016/j.jcis.2004.03.043>
- Özcan A, Ömeroğlu Ç, Erdoğan Y, Özcan AS (2007) Modification of bentonite with a cationic surfactant: an adsorption study of textile dye Reactive Blue 19. *J Hazard Mater* 140:173–179. <https://doi.org/10.1016/j.jhazmat.2006.06.138>
- Pandey S, Ramontja J (2016) Natural bentonite clay and its composites for dye removal: current state and future potential. *Am J Chem Appl* 3:8–19
- Pandey N, Shukla SK, Singh NB (2017) Water purification by polymer nanocomposites: an overview. *Nano-Composites* 3:47–66. <https://doi.org/10.1080/20550324.2017.1329983>
- Paulchamy B, Arthi G, Lignesh BD (2015) A simple approach to stepwise synthesis of graphene oxide nanomaterial. *J Nanomed Nanotechnol* 6:1–4. <https://doi.org/10.4172/2157-7439.1000253>
- Qin X, Bai L, Tan Y et al (2019) B-Cyclodextrin-crosslinked polymeric adsorbent for simultaneous removal and stepwise recovery of organic dyes and heavy metal ions: Fabrication, performance and mechanisms. *Chem Eng J* 372:1007–1018. <https://doi.org/10.1016/j.cej.2019.05.006>
- Ramakrishna KR, Viraraghavan T (1997) Dye removal using low cost adsorbents. *Water Sci Technol* 36:189–196. [https://doi.org/10.1016/S0273-1223\(97\)00387-9](https://doi.org/10.1016/S0273-1223(97)00387-9)
- Rytwo G, Kohavi Y, Botnick I, Gonen Y (2007) Use of CV-and TPP-montmorillonite for the removal of priority pollutants from water. *Appl Clay Sci* 36:182–190. <https://doi.org/10.1016/j.clay.2006.04.016>
- Şahin Ö, Kaya M, Saka C (2015) Plasma-surface modification on bentonite clay to improve the performance of adsorption of methylene blue. *Appl Clay Sci* 116–117:46–53. <https://doi.org/10.1016/j.clay.2015.08.015>
- Sahu JN, Zabed H, Karri RR, Shams S, Qi X (2019) Applications of nano-biotechnology for sustainable water purification. *Indus Appl Nanomater* 313–340
- Santoso SP, Kurniawan A, Soetaredjo FE et al (2019) Eco-friendly cellulose–bentonite porous composite hydrogels for adsorptive removal of azo dye and soilless culture. *Cellulose* 26:3339–3358. <https://doi.org/10.1007/s10570-019-02314-2>
- Sdiri A, Khairy M, Bouaziz S, El-Safty S (2016) A natural clayey adsorbent for selective removal of lead from aqueous solutions. *Appl Clay Sci* 126:89–97. <https://doi.org/10.1016/j.clay.2016.03.003>
- Singh NB, Nagpal G, Agrawal S (2018) Water purification by using adsorbents: a review. *Environ Technol Innov* 11
- Slavutsky AM, Bertuzzi MA, Armada M (2012) Water barrier properties of starch-clay nanocomposite films. *Brazilian J Food Technol* 15:208–218. <https://doi.org/10.1590/s1981-6723201205000014>
- Song N, Hursthouse A, McLellan I, Wang Z (2021) Treatment of environmental contamination using sepiolite: current approaches and future potential. *Environ Geochem Health* 43:2679–2697. <https://doi.org/10.1007/s10653-020-00705-0>

- Taher T, Mohadi R, Rohendi D, Lesbani A (2017) Kinetic and thermodynamic adsorption studies of congo red on bentonite. *AIP Conf Proc* 1823 <https://doi.org/10.1063/1.4978101>
- Tian B, Hua S, Tian Y, Liu J (2021) Cyclodextrin-based adsorbents for the removal of pollutants from wastewater: a review. *Environ Sci Pollut Res* 28:1317–1340. <https://doi.org/10.1007/s11356-020-11168-2>
- Tomaszewska J, Walczak D (2021) Thermal stability of nanosilica-modified poly(vinyl chloride). 2:1–18
- UN-Water (2015) Water for a sustainable world (2015 report)
- Yildiz G, Senkal BF (2016) Formation of composites between polyvinylimidazole and bentonites and their use for removal of remazol black B from water. *Sep Sci Technol* 51:2596–2603. <https://doi.org/10.1080/01496395.2016.1165707>
- Yu Y, Qi S, Zhan J et al (2011) Polyimide/sepiolite nanocomposite films: preparation, morphology and properties. *Mater Res Bull* 46:1593–1599. <https://doi.org/10.1016/j.materresbull.2011.06.009>
- Zarei S, Sadeghi M, Rezanejade Bardajee G (2018) Dye removal from aqueous solutions using novel nanocomposite hydrogel derived from sodium montmorillonite nanoclay and modified starch. *Int J Environ Sci Technol* 15:2303–2316. <https://doi.org/10.1007/s13762-017-1531-8>
- Zhirong L, Azhar Uddin M, Zhanxue S (2011) FT-IR and XRD analysis of natural Na-bentonite and Cu(II)-loaded Na-bentonite. *Spectrochim Acta Part A Mol Biomol Spectrosc* 79:1013–1016. <https://doi.org/10.1016/j.saa.2011.04.013>
- Zhu R, Chen Q, Zhou Q et al (2016) Adsorbents based on montmorillonite for contaminant removal from water: a review. *Appl Clay Sci* 123

Polymeric Composites for Industrial Water Treatment: An Overview



Jordana Bortoluz, Mário César Vebber, Nayrim Brizuela Guerra, Janaina da Silva Crespo, and Marcelo Giovanela

Abstract Several advanced techniques for water treatment depend on materials and chemicals that can pose a secondary pollution risk if not removed, such as nanoparticles, catalysts, and disinfectants. The removal of these compounds requires the use of additional unit operations, making the water treatment process more expensive or even non-scalable. Immobilizing active materials in polymeric composites is an effective way to address these concerns. Such hybrid materials possess a combination of properties that are not normally found in a single constituent, combining the thermal and chemical stabilities of inorganic materials with the processability and flexibility of organic compounds while avoiding dangerous chemicals leech into the treated water. Given that water producers are required to provide high-quality drinking water, polymeric composites have been broadly employed to abate several pollutants. In this context, several nanometric materials have been integrated into polymeric matrices to form state-of-the-art water treatment composites, finding application in microbiological treatment, adsorption and photocatalysis. Due to their chemical flexibility, high surface area, optimal mechanical properties, and cost-effectiveness, such composites have great potential in water purification. The possibilities for tuning polymeric networks are virtually endless, which allows for relatively simple control of functionality (chemical modification, surface modification) and nanomorphology (porosity, structure) of the composites, and fine-tuning of these materials for specific applications and contaminants. In this chapter, we provide an up-to-date review of the importance of polymeric composites in removing several pollutants from water. The main techniques and materials employed in preparing nanocomposites for water treatment, along with their target contaminants, will be addressed, as well as a discussion on their economic feasibility and comparison with well-established techniques.

J. Bortoluz · M. C. Vebber · N. B. Guerra · J. da Silva Crespo · M. Giovanela (✉)
Área do Conhecimento de Ciências Exatas e Engenharias, Universidade de Caxias do Sul, Rua Francisco Getúlio Vargas, 1130, Caxias do Sul, RS 95070-560, Brazil
e-mail: mgiovan1@ucs.br

M. C. Vebber
Department of Chemical and Biological Engineering, University of Ottawa, 161 Louis Pasteur, Ottawa, ON K1N 6N5, Canada

1 Introduction

The diversification and development of industrial plants and different types of products come to the diversification of pollutants that contaminate the environment, especially through wastewaters (Farré et al. 2008; Pal et al. 2014; Peña-Guzmán et al. 2019). Dyes, heavy metals, pharmaceuticals, pesticides and industrial chemicals in general are among the micropollutants often detected in the water. Additionally, the inactivation of pathogenic microbes that may be found in the water streams also needs to be carried out for their safe consumption (Geissen et al. 2015; Sauvé and Desrosiers 2014; Dong et al. 2021). While conventional water treatments (filtering, flocculation and chlorination) are suitable to eliminate common, concentrated pollutants; some compounds can go through the process virtually unchanged or as byproducts that are still dangerous, even in trace amounts, and need to be completely removed (Huerta-Fontela et al. 2011; Yang et al. 2017). This has fomented the field of modern treatment technologies, including nanoparticles, adsorption, ultrafiltration, and advanced oxidation processes (AOPs) (Fig. 1). Such treatment techniques can remove pollutants in the parts per billion range and can also be fine-tuned for specific contaminants (Papageorgiou et al. 2014; Hernández-Leal et al. 2011; Restrepo and Villa 2021; Zoschke et al. 2011; Röhricht et al. 2009; Yoon et al. 2013).

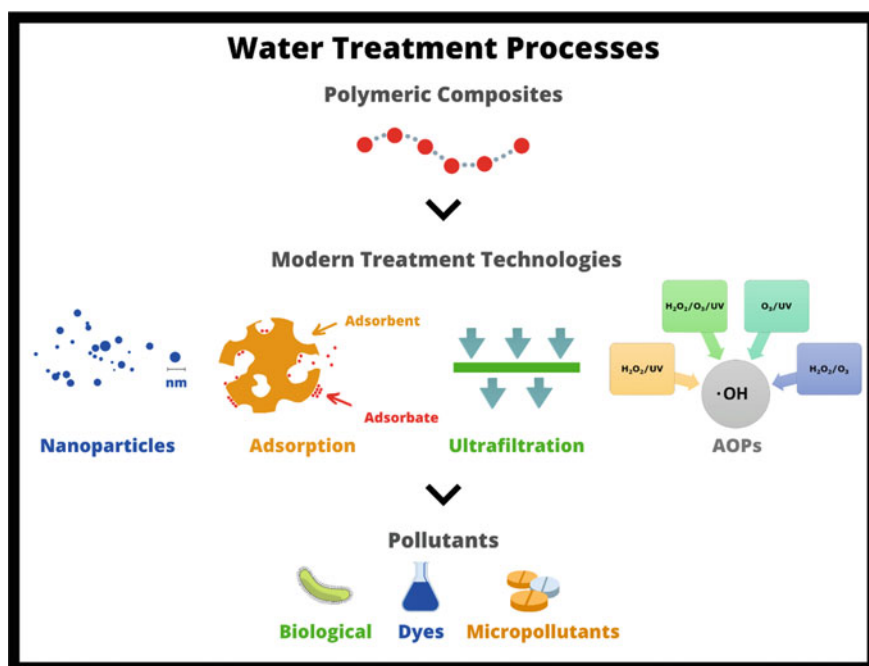


Fig. 1 Water treatment processes using polymeric composites

The main drawback of these techniques is that they often involve introducing materials in the waste stream that may also pose environmental risks. If released into nature, they can affect complex metabolic pathways of microbiomes, which are at the base of any ecosystem, while also increasing oxidative stress, as is the case for peroxides and many catalysts, or even increasing heavy metal concentrations in the case of metallic nanoparticles (Li et al. 2016; Venditti et al. 2013). While additional unit operations can be carried out to remove these materials from water, and this imposes an increase in the cost of water treatment which may not be economically feasible. Moreover, in the case of nanoparticles, complete removal from water is difficult due to their small size.

In light of these facts, the immobilization of active water treatment compounds in polymeric matrices is a promising approach, which prevents or drastically reduces the release of chemical compounds into the treated water while also allowing reutilization of such composites for several cycles (Nunes et al. 2017). A polymeric matrix is especially useful for the versatility of organic compounds, which can be functionalized for specific substrates and have their nanomorphology optimized to increase the efficiency of the final composite. Moreover, polymers have unique chemical resistance and mechanical flexibility, adjusting different types of substrates and water treatment systems (Khan et al. 2021; Yahaya et al. 2021).

In the past 20 years, we have seen a boom in research focused on composites for water treatment as complementary approaches to treatment plants already in place in cities and industries. Most of the efforts in this field involved the optimization of polymer matrixes in achieving high durability, sustainability and increased performance by functionalizing the composites to target specific contaminants. The diversifications of active nanoparticles, either metallic or ceramic, have also gathered large attention from the research community as an approach to increase the efficiency of these materials. More recently, carbon-based composites have arguably been the most extensively explored class of materials, where graphene, activated carbon and carbon nanotubes stand out as both matrix and active components in water-treatment composites (Jaspal and Malviya 2020; Berber 2020). In the following chapter, we will explore a few strategies for producing polymeric composites and their application in different types of water treatment.

2 Polymeric Composites Production Techniques

Techniques employed in the fabrication of polymeric composites should be simple and offer the possibility of tuning the surface properties of the mixture depending on the target pollutant while maintaining the chemical stability of the composite. However, choosing the correct preparation technique is a critical point in pursuing polymer composites with desirable properties (Pandey et al. 2017). Figure 2 illustrates a few of the most common techniques.

Thin films are of great interest for pollutants removal; they have exceptional surface properties and can be supported on a convenient substrate that enables their

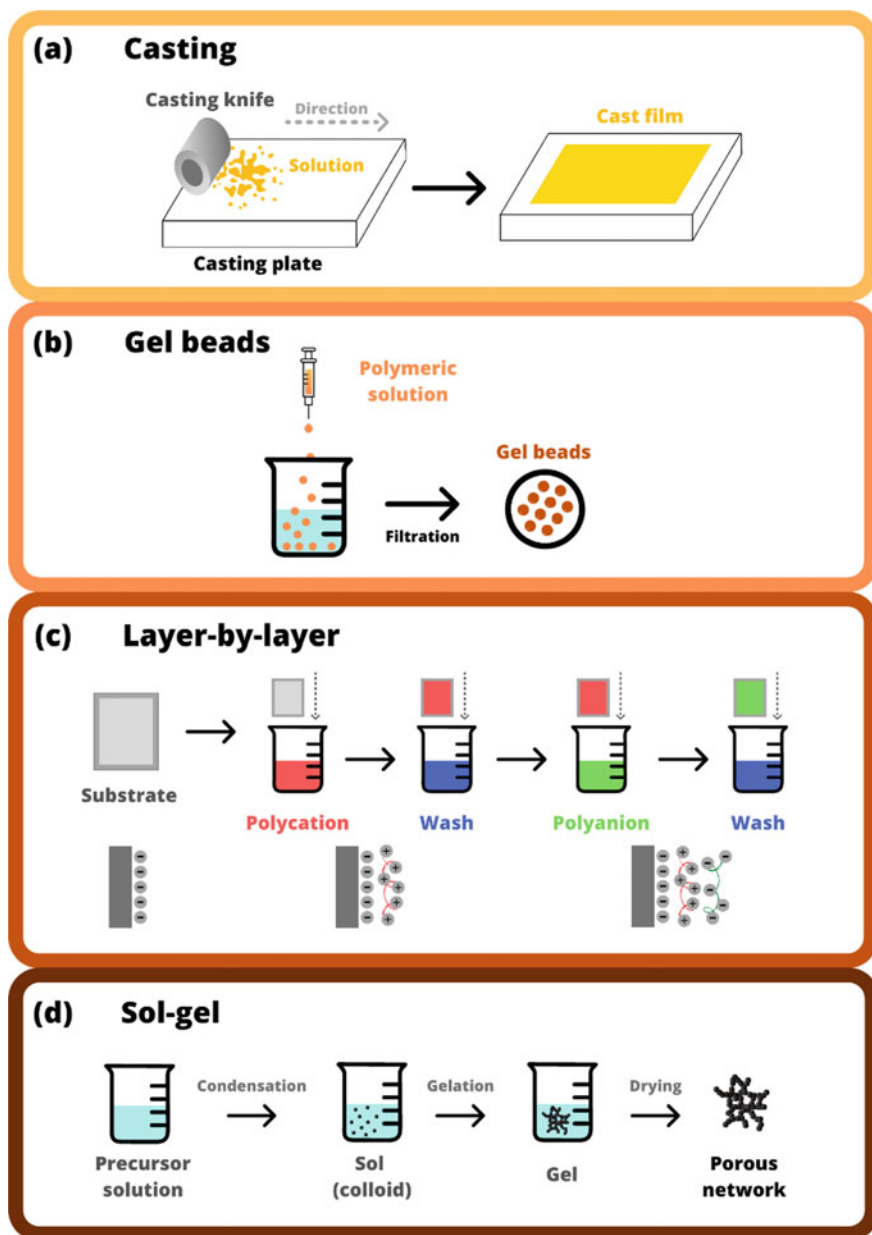


Fig. 2 Illustrative image of the techniques for the preparation of polymeric composites used in the removal of pollutants from wastewater: **a** casting, **b** gel beads, **c** layer-by-layer and **d** sol-gel

reuse. Furthermore, control of the film deposition process enables the formation of organized structures at the nanometer or micrometer level, increasing the efficiency of films (Nunes et al. 2017).

Thin films can be produced using several techniques, such as sublimation, (Liu et al. 2014) castings, (Lefatshe et al. 2017) sol–gel, (Cho et al. 2016) Langmuir–Blodgett (LB) (Dahdal et al. 2016) and layer-by-layer (LbL) (Vebber et al. 2019a). Most of these methods are robust, have experimental simplicity, allow film thickness control, and lead to homogeneous deposition on the substrate (Ferreira 2004). In this section, some techniques for the fabrication of polymer composite films used in water treatment will be discussed in more detail.

2.1 Casting

Casting is arguably the simplest technique employed in producing polymeric films, mainly membranes (Karami et al. 2020). It consists of the mechanical spreading of a forming solution to form polymeric films in a process called phase inversion (Fig. 2a). This technique usually yields thicker films (micrometer range), which rely on porosity to achieve the required properties for water treatment: ultrafiltration, catalysis, or adsorption (Khan et al. 2021; Tan and Rodrigue 2019). Additives and active materials can be incorporated in the forming solution to impart the membrane's active properties, porosity, and increased surface area. Alternatively, the self-assembly of a porous network can be achieved by choice of polymer and film formation conditions (Karami et al. 2020). The phase inversion, which is the phase separation of the components of the forming solution, can be carried out by cooling the solution or adding an anti-solvent to force the precipitation of the polymeric phase. This process is followed by washing the additive or templating phase off the films to yield a porous structure in the film with a high surface area (Tan and Rodrigue 2019). Different porous nanostructures can be achieved by manipulating the forming solution and the phase separation of its components. Traditionally, a mixture of polymers that are known to form domains of the desired pore size is employed (Tan and Rodrigue 2019).

2.2 Gel Beads

The fabrication of polymeric beads is another simple approach for immobilizing and reutilization of active water-treatment materials (Fig. 2b) (Lovatel et al. 2015). These beads are usually of millimetric size and, because of that, do not require any complex process to be recovered from the treated water. This technique is often used to immobilize metallic nanoparticles for microbiological treatment and carriers for clay particles in adsorption (Raota et al. 2019). The relatively large size of the beads tend to reduce the available surface area in contact with water and, with it,

the efficiency of these materials. Similarly to the materials discussed above, porous additives, such as clays can be incorporated to impart porosity to the beads. Nonetheless, the application of hydrophilic polymers with some degree of permeability is necessary for good results (Liu et al. 2012).

Biopolymers are the most often used to fabricate water-treatment beads due to their non-toxicity, biodegradability, permeability and hydrophilicity. In a typical procedure, a concentrated polymer solution is dropped with a syringe into an anti-solvent mixture containing metallic nanoparticles and/or clay particles (Raota et al. 2019). The polymer then immediately precipitates in the format of beads, trapping the active component in the structure. The concentration and pH of the solutions are key parameters that largely affect the final properties of the composites, especially when using the mentioned biopolymers, which contain protic groups that take part in acid–base reactions, changing their solubility, microstructure and porosity (Lovatel et al. 2015; Liu et al. 2012).

2.3 *Layer-By-Layer*

Broadly, LbL encompasses all techniques consisting of the sequential deposition of nanometric layers onto a substrate (Fig. 2c), whether this is achieved by spin-coating, dip-coating, or vapor deposition, among others (Nunes et al. 2017). In the context of water-treatment composites, the self-assembly of polymeric layers, more specifically polyelectrolytes, stands out as an efficient, high surface area template for catalysis. In this technique, polyelectrolytes of opposite charges are sequentially and alternatively deposited on a chosen substrate to form thin films that can vary from a few nanometers (20–40 nm) until a few micrometers depending on the total number of layers (Decher and Hong 1991). The charged polymers are deposited by adsorption and held together by electrostatic interactions of the second order. The concentration, salinity, and pH control the structure of the resulting film by changing the configuration of the polymer chains, which tend to be linear due to electric repulsion when the chains are mostly ionized and tangled if the ionization rate is low. Tangled chains form thicker, more porous films, suitable for water treatment (Decher 1997). With the same principle at work, other charged species can be incorporated in such films, namely functionalized metallic nanoparticles for microbial treatment and ceramic photocatalysts (Vebber et al. 2019a, b; Faria et al. 2014).

The employment of polyelectrolytes also imparts hydrophilicity and permeability to the films. It has been shown that small species can easily penetrate the film, while large molecules, such as pharmaceutical compounds, do not and tend to interact only on the surface (Eltz et al. 2020). This characteristic also allows for nanoparticles, catalysts, and other active components to be incorporated into the polymeric film in a posterior step, simplifying the manufacture of these films (Liu et al. 2016). Moreover, many environment-friendly polymers are compatible with this technique, further reducing their possible detrimental impact in the treated wastewater (Decher and Hong 1991; Decher 1997).

2.4 Sol–gel

The sol–gel method is a traditional approach to producing inorganic nanostructures of different sizes and properties and is often used to fabricate nanoporous inorganic films (Fig. 2d) (Momina 2021). Crystalline chains of oxides are grown from metal precursors, often an organic compound, utilizing acid or basic hydrolysis. While these sol–gel films generally present high surface activity, they lack important properties for their use as a recoverable material in water treatment, mechanical flexibility and adherence being the main ones (Clarke et al. 2013; Bahuguna et al. 2016). Polymeric composites address these issues, and sol–gel nanoparticles are frequently incorporated in thin films by the techniques mentioned above, although often with some reduction inefficiency (Vebber et al. 2019a, b).

To combine the efficiency of free nanoparticles with the mechanical properties of polymeric thin films, sol–gel and polymerization can be carried out simultaneously to yield a composite with a tunable nanostructure (Liaw and Chen 2007). In this approach, monomers/polymers and nanoparticle precursors react simultaneously. This technique is complex and requires the conditions in terms of solvent, pH, temperature and catalyst to be suitable for two different reactions simultaneously. Nonetheless, it allows for fine control of the nanostructure, such as reducing pore size, the increased mechanical stability of the microstructure, and good dispersion of nanoparticles in the matrix, maximizing the active surface area (Liu et al. 2021).

3 Natural and Synthetic Polymeric Composites for Water Treatment

As mentioned previously, polymer matrices are currently receiving much attention from many researchers due to their ease of surface modification, biodegradability, easy availability and low cost (Pathania and Kumari 2020; Rajeswari et al. 2021). The combination of reinforcing fillers into a polymer matrix can solve the drawbacks of polymers and nanomaterials when used separately. Due to their biphasic nature, these materials are known as polymeric composites and, depending on the origin of the polymer, they can be classified (Khodakarami and Bagheri 2021).

Natural polymers or biopolymers are so-called macromolecules because they are derived from natural sources. Some examples of them are cellulose, lignin, chitin and chitosan, pectin, alginate, gum, gelatin and starch (Fig. 3). Conversely, synthetic polymers are defined as polymers that are artificially produced in laboratories. In wastewater treatment, some of the most commonly used synthetic polymers are polyamide, polysulfone, polyethersulfone, polyvinylidene fluoride, polypropylene and polyacrylonitrile (Ahmed et al. 2014; Siti Aisyah et al. 2014) (Fig. 4).

It is also important to highlight that these materials are diverse in size and chemical structure and that these characteristics make them versatile compounds for stabilization, immobilization and the reduction of nanoparticles (Nasrollahzadeh et al. 2021).

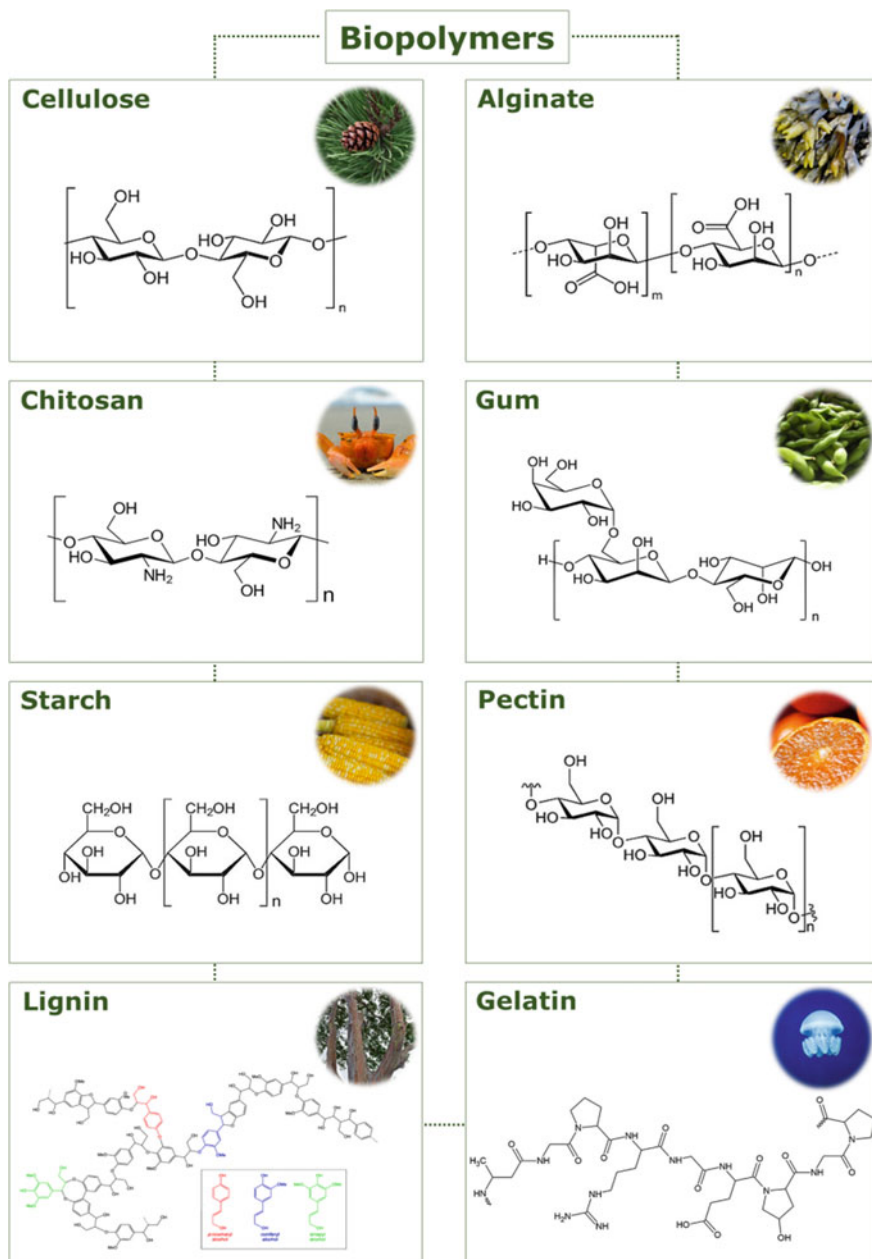


Fig. 3 Examples of natural polymers used in the pollutant's removal

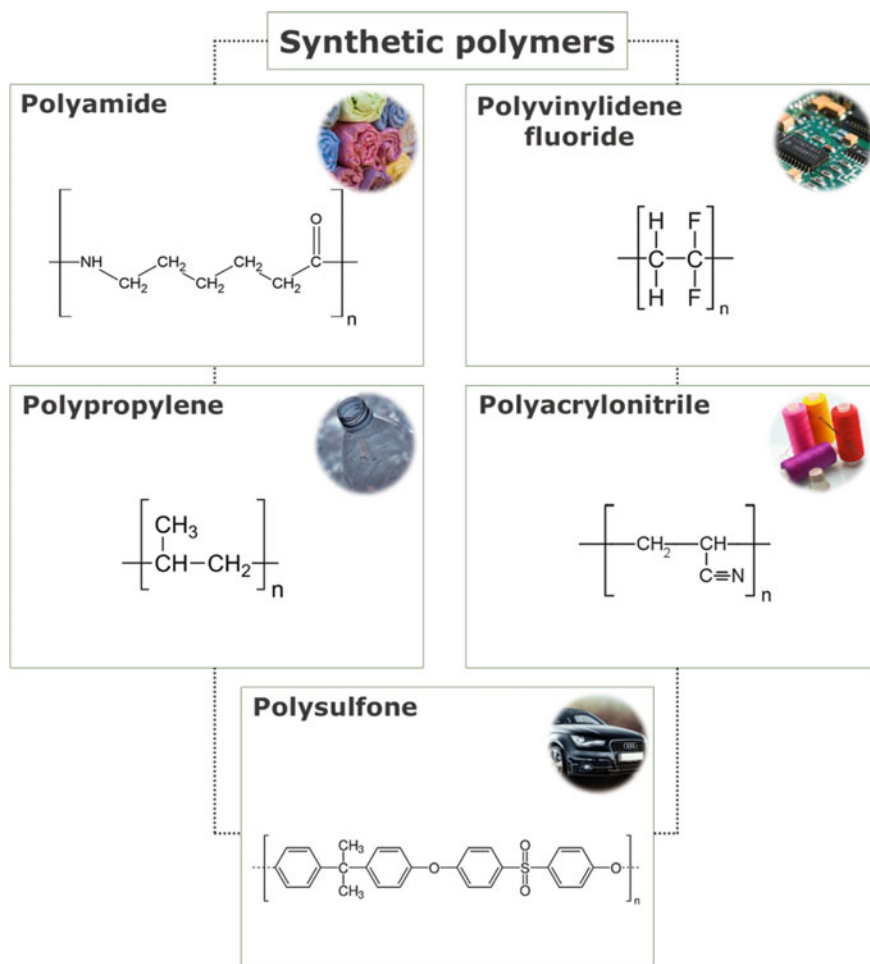


Fig. 4 Examples of synthetic polymers used in the pollutant's removal

In this sense, the investment and advances in the development of polymer composites can bring promising solutions for water treatment (Motshekga et al. 2018).

Different characteristics influence the choice of polymer composite to treat a specific pollutant, among them is the type and concentration of the contaminant present in the wastewater, pollutant removal capacity and the efficiency/cost ratio. It is also important to consider the composite's ability to regenerate and be able to be used several times without modifying or losing the material's physical–chemical properties (Unuabonah and Taubert 2014). In the next sections, we will describe three main categories of pollutants that can be removed from wastewater using natural and synthetic polymeric composites.

3.1 Biological Pollutants

Water purification is motivated by one main reason: all living beings need uncontaminated water to survive. Pure water refers to the nonexistence of heavy impurities and bacteria and microorganisms disease-causing (Chopparapu et al. 2020). It is well known that in the water, there are several microorganisms responsible for many diseases, for example, dysentery and diarrhea are caused by amoeba and *Shigella dysenteriae*, typhoid fever occurs by microorganisms such as *Salmonella paratyphi* and *Salmonella typhi*. In water, there is also *Escherichia coli*, *Giardia lamblia*, *Campylobacter* and *Vibrio cholerae*. Chlorination of water has been used for many years to eliminate biological pollutants; however, due to the formation of harmful waste (i.e., chlorophenols), this technique is rapidly losing ground (Nikolaou and Lekkas 2001). Currently, filtration is usually the most common process of getting pure water as it removes all bacteria, microorganisms and little particles based on size. Chitosan is a natural polysaccharide biopolymer that is mainly used for filtration purposes (Sharma and Kumar 2019). In this sense, attempts are made to purify water through advanced technologies that employ composite polymeric materials.

For example, Charpentier et al. (2012), prepared nanometric films of polyurethane and titanium dioxide (TiO₂). The removal of biological pollutants such as *Escherichia coli* was evaluated using solar irradiation (photocatalysis). According to these authors, in almost 1 h of treatment, they eliminated more than 99.5% of the microorganisms, or which is related to the photocatalytic effect of the TiO₂ in the polyurethane matrix. In another study, Undabeytia et al. (2014) developed N-bentonite composites with three commercial polymers for *Escherichia coli* removal. The antimicrobial effect was influenced by the charges of the monomers adsorbed on the clay, providing a high cationic density on the surface. Using sodium hypochlorite and hydrochloric acid, the clay-polymer system demonstrated total regeneration of filters loaded with microorganisms.

Zarpelon et al. (2016) fabricated thin films obtained from poly(allylamine hydrochloride) (PAH) and poly(acrylic acid) (PAA) polyelectrolytes with silver nanoparticles (AgNPs) and crosslinked with glutaraldehyde to be used as a biological agent in wastewater treatment. The total *Escherichia coli* count was reduced by 93% after 6 h. Four years later, the same authors (Eltz et al. 2020) evaluated the elimination of *Escherichia coli* from other industrial wastewater using thin films of PAH/PAA/AgNPs and copper nanoparticles (CuNPs). All films studied showed bactericidal activity against this microorganism. However, polymeric thin films with only AgNPs showed better biological results than films containing CuNPs. After 2 h of treatment, it was found that minimal amounts of copper and silver were released (0.027 and 0.0083 mg L⁻¹, respectively). Thin films with smaller nanoparticles and lower concentrations promoted a more effective interaction with microbial membranes, favoring the destruction of bacteria.

Some biopolymer nanocomposites have also been investigated for use in the removal of organic pollutants. Cellulose-based polymers have often been used for

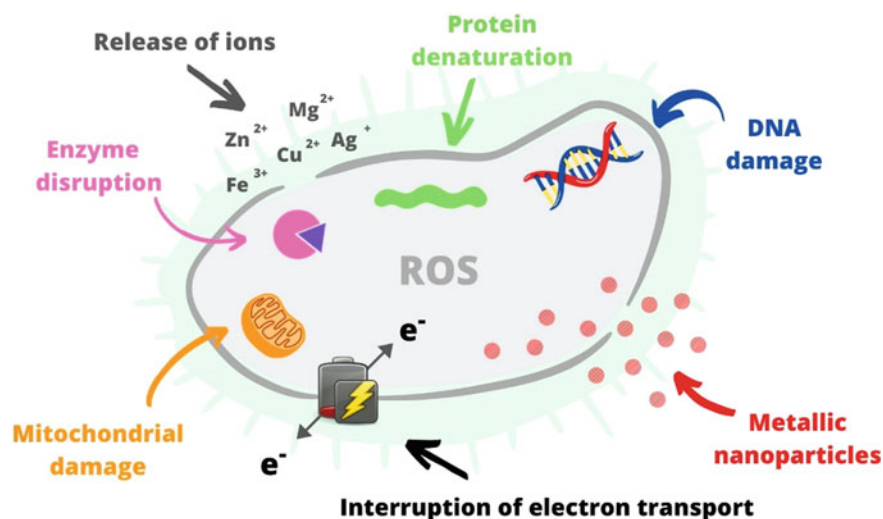


Fig. 5 Illustrative image of the antimicrobial effects of metallic nanoparticles

this purpose since they are non-toxic, biodegradable, and highly efficient in water treatment. Yoosefi Booshehri et al. (2015), for example, performed the deposition of CuNPs onto a cellulose matrix to evaluate its antibacterial activity using *Escherichia coli* and *Staphylococcus aureus*. The tests showed that the disinfection occurred after a contact time between 150 and 180 min. They explained that this result is mainly due to the CuNPs present in the cellulose matrix. The mechanisms of leaching and penetration cells were responsible for interrupting the cellular function of these microorganisms (Fig. 5). In other words, the mechanism of antibacterial activity of Cu(II) ions occurred predominantly through the formation of the copper-peptide complex that catalyzes reactive oxygen species (ROS) formation and drastically increases its production, which results in cell death. The authors also found that the composite can be reused, maintaining the same antibacterial capacity at least three times after the first use.

Lefatshe et al. (2017) used another nanoparticle with the same biopolymer-matrix. They prepared zinc oxide (ZnO)/cellulose nanocomposite with photocatalytic and antibacterial activities against *Staphylococcus aureus* and *Escherichia coli*. This study found that when the ZnO nanoparticles (ZnONPs) were introduced in the biopolymer-matrix, a good activity against both bacteria was verified, as evidenced by a large zone of inhibition (ZOI) around the material. The authors explain that the ZnONPs produces ROS, such as superoxides (O_2^-), hydroxyl radicals ($\bullet OH$) and hydrogen peroxide (H_2O_2) when coming into contact with bacteria cells. The ROS generated may promote the peroxidation of the polyunsaturated phospholipid component of the lipids in the microorganism.

Alginate-based nanocomposites have also been shown to be an effective material for water disinfection. For example, Motshekga et al. (2018) fabricated alginate beads

encapsulated with ZnONPs for bacteria disinfection from water. The antimicrobial tests were performed using surface water and synthetic water with *Staphylococcus aureus*. In the surface water samples, it was found that all bacterial activity was inactivated in less than one minute. On the other hand, when synthetic water was used, the nanocomposites showed good results after 120 min, when a low concentration of bacteria was used. Thus, these authors concluded that a small amount of zinc was leached into the aqueous medium. This was a satisfactory result since the environmental limits allowed for water treatment were not exceeded.

Baek et al. (2019) also evaluated a nanocomposite that encapsulated ZnONPs in an alginate biopolymer (ZnONPs-alginate beads). The antibacterial effects were verified with two antibiotic-resistant bacteria (*Escherichia coli* DH5- α and *Pseudomonas aeruginosa*). This study showed that the ZnONPs-alginate beads are promising for disinfection water, once presented 98 and 88% removal, respectively. The generation of ROS is the responsible mechanism of disinfection activity. Finally, the reusability tests showed that this material could be reused, even when it is used for a resistant contaminant such as *Pseudomonas aeruginosa*. Lovatel et al. (2015), in another study, prepared a nanocomposite with AgNPs onto montmorillonite and fixed it in a polymer matrix of sodium alginate. The bactericidal potential was tested using the agar diffusion method with two microorganisms (*Escherichia coli* and *Staphylococcus aureus*). From these tests, the authors were able to verify that there was a significant reduction (~98%) in the total number of coliforms on the disinfection of industrial wastewater. The authors also emphasized that this nanocomposite does not present environmental risks, as the concentration of AgNPs leached into the aqueous medium is almost insignificant (~3.0 $\mu\text{g L}^{-1}$). In addition, they considered that due to the stability of the material during the 90 min of evaluated treatment, there is a possibility of reusing this material.

Chitosan, a natural polymer that comes from crustaceans, has also been widely used to immobilize metallic nanoparticles for the microbiological treatment of water. Chatterjee et al. (2017) prepared and used chitosan beads with silver and ZnO (Ag-ZnO) to disinfect secondary treated sewage. The antimicrobial action was evaluated with and without sunlight incident on the samples to verify the influence of this external factor on water disinfection. The study showed that the nanocomposite presents good results for the inactivation of coliforms in treated sewage water, mainly under visible light irradiation. The authors explained that bacterial inactivation happens due to the associated effects of H_3O^+ , $\bullet\text{OH}$, $\text{O}_2\bullet$ and silver species. Finally, the authors also found that the chitosan/Ag-ZnO beads can be reused for at least five operation cycles.

In the same way, Raota et al. (2019) synthesized AgNPs through a green route with an extract of Ives cultivar (*Vitis labrusca*) pomace for subsequent preparation of a chitosan-based nanocomposite. The bactericidal activity of this material was evaluated using two Gram-negative (*Escherichia coli* and *Pseudomonas aeruginosa*) and two Gram-positive (*Staphylococcus aureus* and *Enterococcus faecalis*) bacteria. In this study, the authors verified that three compounds could be responsible for the bactericidal activity of the studied composite: AgNPs, chitosan and phenolic compounds from the pomace grape. AgNPs contribute by penetrating

the cell wall of microorganisms. Chitosan, in turn, acts as a binding agent to the surface of the bacteria. Phenolic compounds also contribute to damage to the cell membranes of bacteria. The authors verified that after 1 h of wastewater treatment, the nanocomposite promoted a 47% reduction in the initial counting of *Escherichia coli*.

3.2 Dyes

Nowadays, the existence of dyes in wastewater is a worrying factor for the population, as this contamination causes major problems to human health. If the dyes remain for long periods in running water, this can cause a decrease in dissolved oxygen, which slows down the expansion of aquatic biota (Gao et al. 2019). In this sense, the scientific community has dedicated a large effort to producing materials that are used to eliminate these pollutants from wastewater. Several methods have been used, such as precipitation, solvent extraction, neutralization, reverse osmosis, ion exchange, and adsorption. Among these methods, the cheapest, most efficient and easiest to implement a process for removing pollutants is adsorption, or which works even to eliminate pollutants at relatively low levels (Chung et al. 2014).

Cho et al. (2016) using a sol–gel method, synthesized inorganic–organic particles using an amphiphilic polymer functionalized with alkoxy silane bonded to silica particles (M-APAS-SiO₂) as a precursor. The adsorption essay was used to verify the possibility of M-APAS-SiO₂ particles to adsorb water-soluble dye compounds and water-insoluble dye (orange-16 and solvent blue-35; respectively). The results showed that the tested particles can work as an adsorbent in removing hydrophobic and hydrophilic pollutants. The authors investigated that the hybrid particles studied can be reused by simple pH adjustments.

Magnetite ionic polymer nanocomposites were developed by Atta et al. (2016) at room temperature and tested as methylene blue (MB) adsorbents. For this, the copolymerization of acrylonitrile (AN) and 2-acrylamido-2-methylpropane sulfonic acid (AMPS) monomers was performed and subsequently swollen in ferric chloride (FeCl₃) and potassium iodide (KI) solutions to produce magnetite nanocomposites (Fe(AN-co-AMPS)). It is known that the electrostatic attraction, chemical interactions, and ionic characteristics of dyes and ionic polymeric nanocomposites influence the adsorption process. In this study, the authors concluded that the presence of negative charges on the surface of Fe(AN-co-AMPS) was responsible for the fast diffusion of a large amount of MB dye. MB recoveries were 93.2 and 88.4% after two adsorption–desorption cycles, without loss of adsorption capacity.

El-Shamy (2020) developed inexpensive nanocomposites of polyvinyl alcohol/zinc peroxide (PVA/ZnO₂) and polyvinyl alcohol/carbon dots decorated with zinc peroxide (PVA/CZnO₂) using the casting technique. For the same filler concentration, the dye adsorption was 1972 ± 40 and 1831 ± 20 mg g⁻¹ in PVA/CZnO₂ and PVA/ZnO₂, respectively, showing the positive influence of carbon points in the adsorption process. After 1 h of study, a 98% removal of MB was obtained.

According to the recycling experiments, the PVA/CZnO₂ nanocomposites were used for five cycles maintaining high efficiency.

Malachite green (MG) is a water-soluble dye used in various industries (textile, wool, cotton, paper, leather, silk and jute). It can also be used as a fungicide and ectoparasiticide in aquaculture and fisheries (Rajabi et al. 2017). In this context, Rajabi et al. (2019) prepared poly(methylmethacrylate)/graphene oxide-Fe₃O₄ (PMMA/GOFe₃O₄) and poly(methylmethacrylate)/graphene oxide (PMMA/GO) nanocomposites to be used as adsorbents for the removal of MG dye. The highest adsorption rate was obtained for nanocomposites containing Fe₃O₄ nanoparticles. This fact was explained by the high interaction between nanoparticles and MG. The adsorption capacity was maintained for up to 35 min under experimental conditions. Different polymer composites have been used as adsorbents for MG removal, such as tetraethylenepentamine-functionalized *Rosa canina*-L fruits activated carbon, (Ghasemi et al. 2016) multi-walled carbon nanotubes (MWCNs), (Rajabi et al. 2016) melamine/maleic anhydride composites, (Rong et al. 2014) and amylopectin-poly(acrylic acid) copolymer, (Sarkar et al. 2014) among others.

Hir et al. (2017) evaluated the photodegradation of methyl orange (MO) dye using polyethersulfone films prepared with different TiO₂ levels. The greatest removal of MO was achieved under acidic conditions since the pH of the zero-point charge (pH_{ZPC}) of TiO₂ is 6.8, therefore, its surface becomes positively charged when the pH is below 6.8. The best photocatalytic activity was exhibited in acidic environments since MO is an anionic dye and easily adsorbs on TiO₂ positive surfaces. The MO photodegradation followed pseudo-first-order kinetics. The authors found that the 13% TiO₂ film can be reused for five cycles without losing efficiency.

Clays are natural materials with intercalated cationic and anionic layers and are widely used as adsorbents for various micropollutants. Montmorillonite was used as filler of a hydrogel polymer to study the removal of three dyes: methyl red (MR), crystal violet (CV) and MB from wastewater (Nakhjiri et al. 2018). Two pH were evaluated, and in the neutral environment, the removal of MR, CV and MB was 51, 80, and 89%, respectively. However, for pH ~12.0, the adsorption values obtained were 23, 86 and 93%, reporting a maximum capacity of 113, 176, and 155 mg g⁻¹ for MR, CV, and MB, respectively.

Biopolymers have also been applied as a matrix material to prepare nanocomposites to remove dyes from contaminated water. In this sense, Saber-Samandari et al. (2016) reported the direct red 80 (DR) and MB dyes adsorption process using magnetic gelatin nanocomposite beads comprising carboxylic acid-functionalized MWCNTs. The results showed that the nanocomposite can remove about 96% of the DR dye and 76% of the MB dye, respectively. The charges between the adsorbent and the adsorbate are opposite, resulting in an electrostatic interaction between them. The same did not happen for the cationic dye (MB). In this case, the MB dye ended up being partially repelled due to both material and pollutant having a positive charge. On the other hand, the carboxyl groups present in the CNTs interacted electrostatically with the cationic dye. This made the percentage of removal of this dye still quite significant.

A nanocomposite of gelatin hydrogel with copper oxide nanoparticles (GL-CuO) was developed by Ahmad et al. (2020) for the catalytic reduction of the MO and Congo red (CR) dyes. This study verified that the introduction of this nanocomposite accelerated the reaction of sodium borohydride (NaBH_4) reducing agent with the tested dyes (5 min for MO dye and 7 min for CR dye, respectively). The recyclability and activity of the GL-CuO were monitored for three successive MO reduction reactions. A chitosan–gelatin hydrogel with Zr(IV) selenophosphate nanoparticles (CH-GEL/ZSPNC) was prepared by Kaur and Jindal (2019) for the adsorption and photodegradation of MB dye. The Zr(IV) selenophosphate nanoparticles (ZSPNPs) were incorporated to make this material selective for cationic dyes. The tests showed that the higher percentage removal (~99% of MB dye) and photodegradation was observed under sunlight. The maximum adsorption capacity was equal to 10.46 mg g^{-1} , and the degradation efficiency was satisfactory during the first four cycles (82% dye removal). Even so, CH-GEL/ZSPNC can be reused.

The CuO/chitosan nanocomposite thin film was investigated by Kumar et al. (2015) in the photocatalytic degradation of rhodamine B (RhB) dye. This study revealed that this nanocomposite could degrade about 99% of the dye. The authors explained that this occurs due to the slow electron–hole pair recombination rate of nanosized CuO in the chitosan matrix, the large surface area of the nanoparticles, and the high absorption capacity associated with the biopolymer. The reusability tests showed that the decolorized percentages of RhB dye solution during five cycles of use were 98.8, 78.3, 72.8, 70.6, and 69.2%, respectively.

The utilization of di-aldehyde alginate crosslinking gelatin hydrogel decorated with AgNPs was investigated in removing MB dye from water by Abou-zeid et al. (2019). The authors performed a comparative study using a composite without AgNPs. This experiment showed that the best result was achieved when AgNPs were present on the composite surface, as they provide additional sites for electrostatic interaction with the cationic molecules of the MB dye. The maximum adsorption capacity found was equal to 625 mg g^{-1} . In the same way, a sodium alginate hydrogel with silver nanoparticles was tested by Karthiga et al. (2016) as a biosorbent for the removal of MB dye from water. The adsorption tests showed that the nanocomposite exhibited excellent adsorption property toward removing MB dye from an aqueous solution. The adsorption kinetic data follows the pseudo-first-order model, and the Elovich model confirmed the chemisorption mechanism.

Mohammed et al. (2015) produced cellulose nanocrystal–alginate hydrogel (CNC-ALG) beads to be applied to remove MB dye from water. This study showed that the adsorption process followed the Langmuir isotherm, and the maximum adsorption capacity of CNC-ALG was equal to 256.4 mg g^{-1} for MB dye. The kinetics exhibited a better correlation with the pseudo-second-order model, and the nanocomposite showed that it was reusable as it presented more than 97% dye removal during five adsorption–desorption tests.

Masilompane et al. (2018) studied the removal of brilliant black (BB) dye using a nanocomposite of lignin–chitosan–based with titania nanoparticles (TiO_2 NPs). The functional oxygen groups present in all nanocomposite components, the amine groups in chitosan, and the π -electron system in the benzene structure of the lignin

matrix make this material a potential adsorbent to be applied in the dye removal processes. The value found for k_f ($8.98 \times 10^{-5} \text{ mg g}^{-1}$) indicated that the adsorbent had a low adsorption capacity, and the magnitude of n (5.5) suggested that the adsorption process was easily achieved. The kinetics was better correlated with the pseudo-second-order model.

The gum tragacanth, the polysaccharide extracted from plants of the genus *Astragalus*, was used by Sharma et al. (2021) The authors prepared a gum tragacanth-based hydrogel nanocomposite modified with TiO_2NPs for the adsorption of MG dye from an aqueous solution. The TiO_2NPs were incorporated in this material to improve the adsorption character of the matrix. In fact, an enhancement in dye removal was observed with the increase in the amount of TiO_2NPs in the material (from 88.57 to 103.09 mg g^{-1}). The adsorption study also showed that the material presented about 99% of the dye removal under optimized conditions. The study also showed that the nanocomposite can be reused up to three times without losing significant efficiency.

Vanaamudan et al. (2018) developed a chitosan/guar gum blend with green AgNPs (from palm shell extract) to evaluate the catalytic activity degradation of an individual and binary mixture of dyes (reactive blue-21 (RB), reactive red-141 (RR), and rhodamine-6G (Rh)). The results revealed that this nanocomposite is efficient on heterogeneous catalysis. The complete degradation of the individual dyes occurred between 2 and 15 min. In the case of a mixture of dyes, a degradation of 95% to RB-Rh, 100% to RR-Rh and 90% to RB-RR mixtures was observed. The reusability test showed that after three cycles of the catalytic process, the efficiency decreased by only 2–3%, proving that this material can be reused.

Starch, a natural carbohydrate biopolymer that has low cost, biodegradability and versatility, was used as a matrix material by Gomes et al. (2015), who prepared starch/cellulose nanowhiskers hydrogel composite to remove MB dye from water. Incorporating 5 wt.% of nanoparticles in the hydrogel matrix increased the adsorption capacity from 1872.90 to 1918.81 mg g^{-1} . However, the authors highlight that the adsorption capacity decreased with the additional increase in the amount of cellulose nanowhiskers (more than 5 wt.%). It was related that in optimized experimental conditions, the maximum adsorption capacity of the nanocomposite was 2050 mg g^{-1} and about 90% removal for all tested concentrations of MB dye.

3.3 Micropollutants Removal

The production and consumption of pharmaceutical products have increased considerably in recent years. This fact has become a concern for water resources because the pharmaceutical industry produces many toxic residues for biological life. These contaminants could have an antagonistic impact on the marine ecosystem and human health through endocrine disturbance and the development of antibiotic resistant bacteria (superbugs) (Yang et al. 2017; Patel et al. 2019). The drugs most commonly found in industrial wastewater are antibiotics, anti-depressants, anti-inflammatories, lipid regulators, tranquilizers, (Gros et al. 2010; Yuan et al. 2014), and hormones

including natural estrogens and 17 β -estradiol, as well as the contraceptive 17 α -ethinylestradiol (Amouzgar et al. 2016).

In this sense, Tang et al. (2019), using a simple method, manufactured a multi-functional adsorbent composed of Zr(IV)/carboxymethyl- β -cyclodextrin (Zr/CM- β -CD) to remove female hormones from the liquid medium. The oligosaccharide CD cavities allowed encapsulating the hormone micropollutants through physical interactions between host-guest. The maximum adsorption capacity was 210.53 mg g⁻¹, achieving the best fitting with the Langmuir isothermal model. The Zr/CM- β -CD composite continued to be highly efficient after five cycles.

Bisphenol A (BPA) can cause several endocrine disorders, including female and male infertility, risk of breast and prostate cancer, etc. Here, cyclodextrin again appears as an option to degrade BPA in the aqueous medium. Zhang et al. (2012) evaluated the photocatalytic capacity of TiO₂ with cyclodextrin (TiO₂/ β -CD). TiO₂/ β -CD is an efficient catalyst of BPA. However, the evident degradation of BPA was mainly caused by O₂[•], which was generated through the charge transfer complex between cyclodextrin and TiO₂.

Two adsorbent materials, the polyaniline and MWCNT, were mixed until obtaining the composite PANI/MWCNTs, to be used to eliminate meloxicam from the liquid medium (Dutra et al. 2018). The adsorption capacity of the mixture was 221.2 mg g⁻¹, and the adsorption process presented a better fit with the theoretical pseudo-second order and Elovich models. The kinetic study indicated that adsorption was favored by the surface chemistry and the porous structure of the energetically heterogeneous composite.

The biopolymer nanocomposites have shown that they can also remove micropollutants from water. Photocatalysis was used by Sarkar et al. (2015) who immobilized TiO₂NPs with calcium alginate beads (TIAB) to degrade chlorhexidine digluconate (CHD), ibuprofen (IBP), atenolol (ATL) and carbamazepine (CBZ). The performance of the nanocomposite beads was compared with the efficiency of free TiO₂. This study showed that about 55% removal of CHD was possible using TIAB in a packed bed photoreactor (PBPR), while almost 70% removal was achieved using free TiO₂. The percentage of steady-state removal was reached 58, 85, and 80% for ATL, IBP and CBZ, respectively. These three results were lower when are compared with the free TiO₂. However, the authors emphasized that although the TIAB has lower performance, many medications can be removed with this system. The TIAB was reused without becoming ineffectiveness for five cycles in PBPR.

Using the LbL technique, Vebber et al. (2019a) prepared a nanostructured thin film of PAA, PAH and TiO₂, intending to degrade IBP in aqueous media by photocatalysis using the film and solar energy. The film achieved to degrade, after 150 min, up to 95% of IBF, as well as 50% of its aromatic centers using neutral pH. In another study carried out by these same authors, (Vebber et al. 2019b) the self-assembled thin films of PAA, PAH, TiO₂, and copper were evaluated in the photodegradation of IBP. All films showed high stability in water, releasing only 0.4 wt.% TiO₂ and the photocatalytic efficiency was demonstrated during three cycles of 150 min each. The films with copper showed greater photocatalytic degradation when compared to those without copper, indicating an IBF degradation rate of 76%. Through a

composite experimental design, Kerwald et al. (2020) evaluated the influence of different factors on the photocatalytic activity of PAA/PAH/TiO₂ thin films on the drug bezafibrate (BZF). The results exposed that the film degraded more than 80% of BZF, and the incorporation of AgNPs provided a 64% increase in the photocatalytic efficiency compared to films without AgNPs. Film reuse has been demonstrated for up to four cycles without loss of efficiency.

Attallah and Rabee (2020) investigated a nanocomposite with pectin, chitosan and zinc oxide (Pec/CS/ZnO) to remove CBZ in aqueous solutions under direct sunlight. The results showed that under optimum conditions, the degradation efficiency of CBZ was found to be 69.5%. Two main phenomena were observed: firstly, there was the adsorption of CBZ on Pec/CS/ZnO nanocomposite, and then the photodegradation of this molecule happened. When direct sunlight illuminated ZnO in Pec/CS/ZnO nanocomposite, photons were absorbed, and electron–hole (e^- – h^+) pairs and free radicals were created. Thus, the solution's adsorbed and free CBZ molecules were degraded due to those free radicals that disrupted their conjugation. The authors verified that the Pec/CS/ZnO nanocomposite did not lose significant efficiency in the degradation of the drug after three consecutive uses.

An ecofriendly and sustainable nanocomposite was fabricated by Mohamed and Mahmoud (2020) with biochar from *Pisum sativum* pods and starch hydrogel (N-PSPB/SHGL) for naproxen (NAP) removal. The results showed that this material presented an excellent adsorption capacity value (309.82 mg g⁻¹) and was confirmed to be an advantageous nano sorbent for pharmaceutical removal from aqueous solutions. The N-PSPB/SHGL showed high removal percentage value of NAP (90.07%) even after five cycles.

Hu et al. (2019) developed a bilayer amino-functionalized cellulose nanocrystals/chitosan beads nanocomposite (CNC-ED@CS-ED) for diclofenac sodium (DS) removal. The authors explain that the functionalization of adsorbent materials with amino groups become capable of forming an ionic bond with the carboxyl group of DS at suitable experimental conditions. As expected, the adsorption experiments presented good results for DS removal with an adsorption capacity equal to 444.44 mg g⁻¹. The adsorption process can be described by pseudo-second-order kinetic model and Langmuir adsorption isotherm. The reusability tests showed that even after five adsorption/desorption process cycles, the adsorption capacity of CNC-ED@CS-ED for DS was only reduced by about 10%.

Pesticides used in agriculture are another example of micropollutants that can cause serious health and environmental problem. Thus, several studies have investigated ways to remove them from the aquatic ecosystem. In this sense, TiO₂/chitosan beads (TCB) were tested by Balakrishnan et al. (2020) for photocatalytic degradation of broadleaf pesticide 2,4-dichlorophenoxyacetic acid. The TCB showed a maximum photocatalytic degradation under UV light of 92% compared to TiO₂ (53%), P25 (64%) and chitosan (39%). According to the authors, the altered bandgap of catalyst, better adsorption due to incorporating chitosan, and retarded fast e^- – h^+ pair recombination's affected by aeration were the responsible factors to the improved results beads. The reusability studies showed the nanocomposite can be reused since the degradation efficiency only decreased from 92 to 80% after 11 consecutive cycles.

In another study, Dehaghi et al. (2014) used batch adsorption experiments and fabricated chitosan-ZnO nanoparticles (CS-ZnONPs) composite beads to remove Permethrin pesticide, a neurotoxin widely used in agriculture. The experiments showed satisfactory results, removing 99% of the pesticide from an aqueous solution. The desorption experiment showed that this nanocomposite could be regenerated about 56% after three cycles. The removal of the pesticide from liquid media using a polymeric composite of mesoporous silica and polyaniline monomer (MSNPs/PANI) was studied by El-Said et al. (2018) The exclusion efficiency of the pesticide chloridazon MSNPs/PANI mesosorbent was around 96%, and the Langmuir and Freundlich models were the ones with the best fit. The ability to reuse composites over several cycles without losing or modifying their physical integrity and adsorption activity was investigated. The authors identified that MSNPs/PANI can be used up to seven cycles, performing simple washes with acetonitrile solution.

4 Applications and Comparison with Traditional Techniques

Although the use of polymeric composites in water treatment is mainly a topic of research, there are a few examples of real pilot-plant scale treatment processes that employ the materials described in this chapter. In this sense, to employ lab-scale adsorption technology in a large-scale purification system, Aziz et al. (2020) conducted experiments in a steady-flow reactor and modelled the adsorption kinetics. Activated charcoal was immobilized in alginate beads for easy recovery and employed to eliminate heavy metals from wastewater in a fixed bed column. Nearly 100% of dissolved cadmium was removed in large-scale tests, and the composite became saturated only after 25 h of treatment. Additionally, activated charcoal composites have the distinction of being used not only for targeted micropollutants but are also widely used in domestic tap water treatment due to their large absorbance capacitance and non-selectivity (Jaspal and Malviya 2020). These composites remove fine suspended particulate and microorganisms, odors, tastes and regulate the pH, which are the main contaminants of domestic waters (Siong and Atabaki 2014).

Silver nanoparticles incorporated in membranes have been employed for simultaneous filtration and disinfection of drinking water, (Ursino et al. 2018), as well as being incorporated in inorganic ceramic filters, reaching a bacteria inactivation of 97–100% (Ren and Smith 2013; Oyanedel-Craver and Smith 2008). Photocatalytic TiO₂-polyvinylidene fluoride/PMMA nanocomposites flat sheet membranes were produced by phase inversion and a modelled crossflow filtration system, aiming the removal of pollutants with contrasting chemical properties. In this study, filtration and photocatalysis processes using ultraviolet light were used simultaneously. The combination of these treatments removed nearly 100% of CR dye and over 80% of Tartrazine, with reduced fouling (Errahmani et al. 2021). In fact, when moving composites from laboratory to pilot-plant scale, especially in the form of films and

membranes, the fouling and general contamination of these selective materials can be major drawbacks. Therefore, the transfer of technologies needs to be closely controlled to ensure the composites functionality (Berber 2020; Bouziane Errahmani et al. 2021).

As the efficiency of these advanced materials improves and the regulations for wastewaters become stricter, the use of composites in water treatment is expected to keep increasing, especially to target specific pollutants than conventional treatment plants do not remove. That is supported by the numbers shown above in the pilot plant scale for adsorption, photocatalysis, and microbiological treatments using polymeric composites. While the composites could remove between 80 and 100% of the targeted micropollutants, traditional water treatment generally removes less than 50% of these emerging chemicals, often less than 20% (Huerta-Fontela et al. 2011; Huang et al. 2003). Given that health effects and ecosystem disruption can happen at concentrations of parts per billion in the case of pesticides and pharmaceuticals, less than 50% abatement is not nearly enough for safe drinking water or even wastewater (Huerta-Fontela et al. 2011; Huang et al. 2003). Alternatively, many of these advanced techniques cannot be optimally employed in the treatment of macropollutants, as they are sensitive to the aqueous environment around them, which is the case of photocatalysis that can become poisoned by excess organic matter occupying active sites, (Vebber et al. 2019a; Pettibone et al. 2008) as well as adsorbents (organic or clay), whose performance is highly sensitive to pH, which can vary greatly in a highly contaminated source (Berber 2020). Therefore, it should be clear that the techniques reviewed here function as complementary treatments that, nonetheless, are necessary due to the increasing complexity and variety of chemicals that end up in water streams (Yang et al. 2017).

5 Challenges, Perspectives and Environmental Sustainability

The mission of offering adequate treatment for different water contaminants sometimes becomes difficult and expensive. For this reason, there is currently an abundant request for cutting-edge and cheap technologies. However, as described in this chapter, several pollutants have been eliminated using polymer compounds of natural and synthetic origin, demonstrating their potential in wastewater treatment. Arguably, the use of nanostructured materials as a filling for polymeric matrices has emerged as an emerging area to increase the potential for removing aqueous contaminants. Substantial research has been devoted to achieving high adsorption performance, recyclability, selectivity of different pollutants and durability. However, despite all the efforts made, the market does not have a polymer composite that can eliminate 100% of the contaminants, which can be produced on a large scale.

Another challenging issue in selecting polymeric compounds for water treatment is preserving the environmental sustainability of the ecosystem. It is known that

the use of some chemical processes in wastewater treatment can become a possible source of environmental pollution in the long term. In this sense, the development of green composites through green approaches has gained prominence in recent years as alternatives for ecosystem security. Green compounds are eco-friendly, efficient, reliable and alternative to traditional compounds for environmental sustainability. Furthermore, using materials from natural sources can help reduce costs and facilitate large-scale applications (Mukhopadhyay et al. 2020).

In this sense, the authors identify as a possible future challenge the synthesis of compounds that present specific functional groups that increase the performance of the final composite, ensuring environmental safety. Continuing studies on possible pollutant elimination mechanisms is still a very important challenge, as we need to understand these mechanisms in greater depth, which helps to define a better choice of material. Despite the challenges to be overcome, polymer composite research opens a new route in science for a pollution-free environment.

References

- Abou-zeid RE, Awwad NS, Nabil S, Salama A, Youssef MA (2019) Oxidized alginate/gelatin decorated silver nanoparticles as new nanocomposite for dye adsorption. *Int J Biol Macromol* 141:1280–1286. <https://doi.org/10.1016/j.ijbiomac.2019.09.076>
- Ahmad S, Bahadar S, Asiri AM, Marwani HM, Kamal T (2020) Polypeptide and copper oxide nanocomposite hydrogel for toxicity elimination of wastewater. *J Sol-Gel Sci Technol* 96(2):382–394. <https://doi.org/10.1007/s10971-020-05357-1>
- Ahmed AE-SI, Moustafa HY, El-Masry AM, Hassan SA (2014) Natural and synthetic polymers for water treatment against dissolved pharmaceuticals. *J Appl Polym Sci* 131(13):40458. <https://doi.org/10.1002/app.40458>
- Aisyah SI, Norfariha MS, Azlan MAM, Norli I (2014) Comparison of synthetic and natural organic polymers as flocculant for textile wastewater treatment. *Iran J Energy Environ* 5(4):436–445. <https://doi.org/10.5829/idosi.ijee.2014.05.04.11>
- Amouzgar P, Wong MY, Horri BA, Salamatnia B (2016) Advanced material for pharmaceutical removal from wastewater. In: *Smart materials for waste water applications*. John Wiley & Sons, Inc., Hoboken, NJ, USA, pp 179–212. <https://doi.org/10.1002/9781119041214.ch7>
- Atta AM, Al-Lohedan HA, Ezzat AO, Issa ZA, Oumi AB (2016) Synthesis and application of magnetite polyacrylamide amino-amidoxime nano-composites as adsorbents for water pollutants. *J Polym Res* 23(4):69. <https://doi.org/10.1007/s10965-016-0963-z>
- Attallah OA, Rabee M (2020) A pectin/chitosan/zinc oxide nanocomposite for adsorption/photocatalytic remediation of carbamazepine in water samples. *RSC Adv* 10(67):40697–40708. <https://doi.org/10.1039/d0ra08010a>
- Aziz F, Achaby EM, Lissaneddine A, Aziz K, Ouazzani N, Mamouni R, Mandi L (2020) Composites with alginate beads: a novel design of nano-adsorbents impregnation for large-scale continuous flow wastewater treatment pilots. *Saudi J Biol Sci* 27(10):2499–2508. <https://doi.org/10.1016/j.sjbs.2019.11.019>
- Baek S, Joo SH, Toborek M (2019) Treatment of antibiotic-resistant bacteria by encapsulation of ZnO nanoparticles in an alginate biopolymer: insights into treatment mechanisms. *J Hazard Mater* 373:122–130. <https://doi.org/10.1016/j.jhazmat.2019.03.072>
- Bahuguna G, Mishra NK, Chaudhary P, Kumar A, Singh R (2016) Thin film coating through sol-gel gel technique. *Res J Chem Sci* 6(7):65–72

- Balakrishnan A, Appunni S, Gopalram K (2020) Immobilized TiO₂/chitosan beads for photocatalytic degradation of 2,4-dichlorophenoxyacetic acid. *Int J Biol Macromol* 161:282–291. <https://doi.org/10.1016/j.ijbiomac.2020.05.204>
- Berber MR (2020) Current advances of polymer composites for water treatment and desalination. *J Chem* 2020:1–19. <https://doi.org/10.1155/2020/7608423>
- Bouziane Errahmani K, Benhabiles O, Bellebia S, Bengharez Z, Goosen M, Mahmoudi H (2021) Photocatalytic nanocomposite polymer-TiO₂ membranes for pollutant removal from wastewater. *Catalysts* 11(3):402. <https://doi.org/10.3390/catal11030402>
- Charpentier PA, Burgess K, Wang L, Chowdhury RR, Lotus AF, Moula G (2012) Nano-TiO₂ /polyurethane composites for antibacterial and self-cleaning coatings. *Nanotechnology* 23(42):425606. <https://doi.org/10.1088/0957-4484/23/42/425606>
- Chatterjee P, Ghangrekar MM, Rao S (2017) Disinfection of secondary treated sewage using ZnO-Ag nanoparticles coated chitosan beads to facilitate reuse. *J Chem Technol Biotechnol* 92(9):2334–2341. <https://doi.org/10.1002/jctb.5235>
- Cho S, Kim N, Lee S, Lee H, Lee S-H, Kim J, Choi J-W (2016) Use of hybrid composite particles prepared using alkoxysilane-functionalized amphiphilic polymer precursors for simultaneous removal of various pollutants from water. *Chemosphere* 156:302–311. <https://doi.org/10.1016/j.chemosphere.2016.05.004>
- Chopparapu R, Sambattula KR, Edara DK, Dasari R, Sycam V, Srivalli G, Chennaiah MB (2020) A review article on water purification techniques by using fiber composites and biodegradable polymers. 040007. <https://doi.org/10.1063/5.0004069>
- Chung S-G, Ryu J-C, Song M-K, An B, Kim S-B, Lee S-H, Choi J-W (2014) Modified composites based on mesostructured iron oxyhydroxide and synthetic minerals: a potential material for the treatment of various toxic heavy metals and its toxicity. *J Hazard Mater* 267:161–168. <https://doi.org/10.1016/j.jhazmat.2013.12.056>
- Clarke SR, Markovic E, Nguyen KAT (2013) Sol-gel materials for WSUD water treatment applications. *ACS Symp Ser* 1154:15–32. <https://doi.org/10.1021/bk-2013-1154.ch002>
- Dahdal YN, Oren Y, Schwahn D, Pipich V, Herzberg M, Ying W, Kasher R, Rapaport H (2016) Biopolymer-induced calcium phosphate scaling in membrane-based water treatment systems: langmuir model films studies. *Coll Surf B Biointerf* 143:233–242. <https://doi.org/10.1016/j.col surfb.2016.02.047>
- Decher G (1997) Fuzzy nanoassemblies: toward layered polymeric multicomposites. *Science* 277(5330):1232–1237. <https://doi.org/10.1126/science.277.5330.1232>
- Decher G, Hong J (1991) Buildup of ultrathin multilayer films by a self-assembly process, 1 consecutive adsorption of anionic and cationic bipolar amphiphiles on charged surfaces. *Makromol Chem Macromol Symp* 46(1):321–327. <https://doi.org/10.1002/masy.19910460145>
- Dehaghi SM, Rahmanifar B, Moradi AM, Azar PA (2014) Removal of permethrin pesticide from water by chitosan-zinc oxide nanoparticles composite as an adsorbent. *J Saudi Chem Soc* 18(4):348–355. <https://doi.org/10.1016/j.jscs.2014.01.004>
- Dong H, Xu L, Mao Y, Wang Y, Duan S, Lian J, Li J, Yu J, Qiang Z (2021) Effective abatement of 29 pesticides in full-scale advanced treatment processes of drinking water: from concentration to human exposure risk. *J Hazard Mater* 2021(403):123986. <https://doi.org/10.1016/j.jhazmat.2020.123986>
- Dutra FVA, Pires BC, Nascimento TA, Borges KB (2018) Functional polyaniline/multiwalled carbon nanotube composite as an efficient adsorbent material for removing pharmaceuticals from aqueous media. *J Environ Manage* 221:28–37. <https://doi.org/10.1016/j.jenvman.2018.05.051>
- El-Said WA, El-Khouly ME, Ali MH, Rashad RT, Elshehy EA, Al-Bogami AS (2018) Synthesis of mesoporous silica-polymer composite for the chloridazon pesticide removal from aqueous media. *J Environ Chem Eng* 6(2):2214–2221. <https://doi.org/10.1016/j.jece.2018.03.027>
- El-Shamy AG (2020) An efficient removal of methylene blue dye by adsorption onto carbon dot @ zinc peroxide embedded poly vinyl alcohol (PVA/CZnO₂) nano-composite: a novel reusable adsorbent. *Polymer* 202:122565. <https://doi.org/10.1016/j.polymer.2020.122565>

- Eltz FZ, Vebber MC, Aguzzoli C, Machado G, da Silva Crespo J, Giovanela M (2020) Preparation, characterization and application of polymeric thin films containing silver and copper nanoparticles with bactericidal activity. *J Environ Chem Eng* 8(3):103745. <https://doi.org/10.1016/j.jece.2020.103745>
- Errahmani KB, Benhabiles O, Bellebia S, Bengharez Z, Goosen M, Mahmoudi H (2021) Pollutant removal from wastewater. pp 1–15
- Faria ACR, Menezes FD, Milani R, Pereira MB, Gonçalves VR, Horowitz F, Giovanela M, Machado G, Crespo JS (2014) Preparation, characterization and application of polyelectrolytes/TiO₂/CdSe self-assembled films. *Thin Solid Films* 551:79–85. <https://doi.org/10.1016/j.tsf.2013.11.116>
- Ferreira M (2004) Langmuir-blodgett films from polyaniline/ruthenium complexes as modified electrodes for detection of dopamine. *Thin Solid Films* 446(2):301–306. <https://doi.org/10.1016/j.tsf.2003.10.006>
- Gao L, Su K, Fan T, Li Z (2019) Study on the structure and properties of PPS/PCNF hybrid membranes and their applications in wastewater treatment. *Polymer* 176:274–282. <https://doi.org/10.1016/j.polymer.2019.05.021>
- Geissen V, Mol H, Klumpp E, Umlauf G, Nadal M, van der Ploeg M, van de Zee SEATM, Ritsema CJ (2015) Emerging pollutants in the environment: a challenge for water resource management. *Int. Soil Water Conserv Res* 3(1):57–65. <https://doi.org/10.1016/j.iswcr.2015.03.002>
- Ghasemi M, Mashhadi S, Asif M, Tyagi I, Agarwal S, Gupta VK (2016) Microwave-assisted synthesis of tetraethylenepentamine functionalized activated carbon with high adsorption capacity for malachite green dye. *J Mol Liq* 213:317–325. <https://doi.org/10.1016/j.molliq.2015.09.048>
- Gomes RF, de Azevedo ACN, Pereira AGB, Muniz EC, Fajardo AR, Rodrigues FHA (2015) Fast dye removal from water by starch-based nanocomposites. *J Colloid Interface Sci* 454:200–209. <https://doi.org/10.1016/j.jcis.2015.05.026>
- Gros M, Petrović M, Ginebreda A, Barceló D (2010) Removal of pharmaceuticals during wastewater treatment and environmental risk assessment using hazard indexes. *Environ Int* 36(1):15–26. <https://doi.org/10.1016/j.envint.2009.09.002>
- Hernández-Leal L, Temmink H, Zeeman G, Buisman CJN (2011) Removal of micropollutants from aerobically treated grey water via ozone and activated carbon. *Water Res* 5:1–10. <https://doi.org/10.1016/j.watres.2011.03.009>
- Hir ZAM, Moradihamedani P, Abdullah AH, Mohamed MA (2017) Immobilization of TiO₂ into polyethersulfone matrix as hybrid film photocatalyst for effective degradation of methyl orange dye. *Mater Sci Semicond Process* 57:157–165. <https://doi.org/10.1016/j.mssp.2016.10.009>
- Hu D, Jiang R, Wang N, Xu H, Wang Y (2019) Adsorption of diclofenac sodium on bilayer amino-functionalized cellulose nanocrystals/chitosan composite. *J Hazard Mater* 369:483–493. <https://doi.org/10.1016/j.jhazmat.2019.02.057>
- Huang Y, Twidwell DL, Elrod JC (2003) Occurrence and effects of endocrine disrupting chemicals in the environment. *Pract Period Hazard Toxic Radioact Waste Manag* 7:241–252. [https://doi.org/10.1061/\(ASCE\)1090-025X\(2003\)7](https://doi.org/10.1061/(ASCE)1090-025X(2003)7)
- Huerta-Fontela M, Galceran MT, Ventura F (2011) Occurrence and removal of pharmaceuticals and hormones through drinking water treatment. *Water Res* 45(3):1432–1442. <https://doi.org/10.1016/j.watres.2010.10.036>
- Jaspal D, Malviya A (2020) Composites for wastewater purification: a review. *Chemosphere* 246:125788. <https://doi.org/10.1016/j.chemosphere.2019.125788>
- Karami P, Khorshidi B, McGregor M, Peichel JT, Soares JBP, Sadrzadeh M (2020) Thermally stable thin film composite polymeric membranes for water treatment: a review. *J Clean Prod* 250. <https://doi.org/10.1016/j.jclepro.2019.119447>
- Karthiga Devi G, Senthil Kumar P, Sathish Kumar K (2016) Green synthesis of novel silver nanocomposite hydrogel based on sodium alginate as an efficient biosorbent for the dye wastewater treatment: prediction of isotherm and kinetic parameters. *Desalin Water Treat* 57(57):27686–27699. <https://doi.org/10.1080/19443994.2016.1178178>
- Kaur K, Jindal R (2019) Comparative study on the behaviour of chitosan-gelatin based hydrogel and nanocomposite ion exchanger synthesized under microwave conditions towards photocatalytic

- removal of cationic dyes. *Carbohydr Polym* 2019(207):398–410. <https://doi.org/10.1016/j.carbpol.2018.12.002>
- Kerwald J, Vebber MC, Aguzzoli C, da Silva Crespo J, Giovanela M (2020) Influence of silver nanoparticle deposition on self-assembled thin films of weak polyelectrolytes/TiO₂ for bezafibrate photodegradation through central composite experimental design. *J Environ Chem Eng* 8(1):103619. <https://doi.org/10.1016/j.jece.2019.103619>
- Khan F, Zahid M, Hanif MA, Tabasum A, Mushtaq F, Noreen S, Mansha A (2021) Photocatalytic polymeric composites for wastewater treatment. <https://doi.org/10.1016/b978-0-12-821141-0.00005-7>
- Khodakarami M, Bagheri M (2021) Recent advances in synthesis and application of polymer nanocomposites for water and wastewater treatment. *J Clean Prod* 296:126404. <https://doi.org/10.1016/j.jclepro.2021.126404>
- Kumar PS, Selvakumar M, Babu SG, Jaganathan SK, Karuthapandian S, Chattopadhyay S (2015) Novel CuO/chitosan nanocomposite thin films: facile hand picking recoverable, efficient and reusable heterogeneous photocatalyst. *RSC Adv* 5(71):57493–57501. <https://doi.org/10.1039/C5RA08783J>
- la Farré, M, Pérez S, Kantiani L, Barceló D (2008) Fate and toxicity of emerging pollutants, their metabolites and transformation products in the aquatic environment. *TrAC Trends Anal Chem* 27(11):991–1007. <https://doi.org/10.1016/j.trac.2008.09.010>
- Lefatshe K, Muiva CM, Kebaabetswe LP (2017) Extraction of nanocellulose and in-situ casting of ZnO/cellulose nanocomposite with enhanced photocatalytic and antibacterial activity. *Carbohydr Polym* 164:301–308. <https://doi.org/10.1016/j.carbpol.2017.02.020>
- Li S, Ma H, Wallis LK, Etterson MA, Riley B, Hoff DJ, Diamond SA (2016) Impact of natural organic matter on particle behavior and phototoxicity of titanium dioxide nanoparticles. *Sci Total Environ* 542:324–333. <https://doi.org/10.1016/j.scitotenv.2015.09.141>
- Liaw WC, Chen KP (2007) Preparation and characterization of poly(Imide Siloxane) (PIS)/Titania(TiO₂) hybrid nanocomposites by sol-gel processes. *Eur Polym J* 43(6):2265–2278. <https://doi.org/10.1016/j.eurpolymj.2007.01.015>
- Liu L, Wan Y, Xie Y, Zhai R, Zhang B, Liu J (2012) The removal of dye from aqueous solution using alginate-halloysite nanotube beads. *Chem Eng J* 187:210–216. <https://doi.org/10.1016/j.cej.2012.01.136>
- Liu H, Cao C-Y, Wei F-F, Huang P-P, Sun Y-B, Jiang L, Song W-G (2014) Flexible macroporous carbon nanofiber film with high oil adsorption capacity. *J Mater Chem A* 2(10):3557. <https://doi.org/10.1039/c3ta14468b>
- Liu Z, Yan Z, Bai L (2016) Layer-by-layer assembly of polyelectrolyte and gold nanoparticle for highly reproducible and stable SERS substrate. *Appl Surf Sci* 360:437–441. <https://doi.org/10.1016/j.apsusc.2015.09.151>
- Liu Y, Gao J, Ge Y, Yu S, Liu M, Gao C (2021) A combined interfacial polymerization and in-situ sol-gel strategy to construct composite nanofiltration membrane with improved pore size distribution and anti-protein-fouling property. *J Memb Sci* 2021(623):119097. <https://doi.org/10.1016/j.memsci.2021.119097>
- Lovatel RH, Neves RM, Oliveira GR, Mauler RS, Crespo JS, Carli LN, Giovanela M (2015) Disinfection of biologically treated industrial wastewater using montmorillonite/alginate/nanosilver hybrids. *J. Water Process Eng.* 7:273–279. <https://doi.org/10.1016/j.jwpe.2015.07.003>
- Masilompane TM, Chaukura N, Mishra SB, Mishra AK (2018) Chitosan-lignin-titania nanocomposites for the removal of brilliant black dye from aqueous solution. *Int J Biol Macromol* 120:1659–1666. <https://doi.org/10.1016/j.ijbiomac.2018.09.129>
- Mohamed AK, Mahmoud ME (2020) Nanoscale pisum sativum pods biochar encapsulated starch hydrogel: a novel nanosorbent for efficient chromium (VI) ions and naproxen drug removal. *Bioresour Technol* 308:123263. <https://doi.org/10.1016/j.biortech.2020.123263>
- Mohammed N, Grishkewich N, Berry RM, Chiu K (2015) Cellulose nanocrystal—alginate hydrogel beads as novel adsorbents for organic dyes in aqueous solutions. *Cellulose* 22:3725–3738. <https://doi.org/10.1007/s10570-015-0747-3>

- Momina AK (2021) Study of different polymer nanocomposites and their pollutant removal efficiency: review. *Polymer* 217:123453. <https://doi.org/10.1016/j.polymer.2021.123453>
- Motshekga SC, Ray SS, Maity A (2018) Synthesis and characterization of alginate beads encapsulated zinc oxide nanoparticles for bacteria disinfection in water. *J Colloid Interface Sci* 512:686–692. <https://doi.org/10.1016/j.jcis.2017.10.098>
- Mukhopadhyay R, Bhaduri D, Sarkar B, Rusmin R, Hou D, Khanam R, Sarkar S, Kumar Biswas J, Vithanage M, Bhatnagar A, Ok YS (2020) Clay-polymer nanocomposites: progress and challenges for use in sustainable water treatment. *J Hazard Mater* 383:121125. <https://doi.org/10.1016/j.jhazmat.2019.121125>
- Nakhjiri MT, Bagheri Marandi G, Kurdtabar M (2018) Effect of Bis[2-(Methacryloyloxy)Ethyl] phosphate as a crosslinker on poly(AAm-Co-AMPS)/Na-MMT hydrogel nanocomposite as potential adsorbent for dyes: kinetic, isotherm and thermodynamic study. *J Polym Res* 25(11):244. <https://doi.org/10.1007/s10965-018-1625-0>
- Nasrollahzadeh M, Sajjadi M, Irvani S, Varma RS (2021) Starch, cellulose, pectin, gum, alginate, chitin and chitosan derived (Nano) materials for sustainable water treatment: a review. *Carbohydr Polym* 251:116986. <https://doi.org/10.1016/j.carbpol.2020.116986>
- Nikolaou AD, Lekkas TD (2001) The role of natural organic matter during formation of chlorination by-products: a review. *Acta Hydrochim Hydrobiol* 29(2–3):63–77. [https://doi.org/10.1002/1521-401X\(200109\)29:2/3%3c63::AID-AHEH63%3e3.0.CO;2-C](https://doi.org/10.1002/1521-401X(200109)29:2/3%3c63::AID-AHEH63%3e3.0.CO;2-C)
- Nunes BN, Paula LF, Costa ÍA, Machado AEH, Paterno LG, Patrocínio AOT (2017) Layer-by-layer assembled photocatalysts for environmental remediation and solar energy conversion. *J Photochem Photobiol C Photochem Rev* 32:1–20. <https://doi.org/10.1016/j.jphotochemrev.2017.05.002>
- Oyanedel-Craver VA, Smith JA (2008) Sustainable colloidal-silver-impregnated ceramic filter for point-of-use water treatment. *Environ Sci Technol* 42(3):927–933. <https://doi.org/10.1021/es071268u>
- Pal A, He Y, Jekel M, Reinhard M, Gin KYH (2014) Emerging contaminants of public health significance as water quality indicator compounds in the urban water cycle. *Environ Int* 71:46–62. <https://doi.org/10.1016/j.envint.2014.05.025>
- Pandey N, Shukla SK, Singh NB (2017) Water purification by polymer nanocomposites: an overview. *Nanocomposites* 3(2):47–66. <https://doi.org/10.1080/20550324.2017.1329983>
- Papageorgiou A, Voutsas D, Papadakis N (2014) Science of the total environment occurrence and fate of ozonation by-products at a full-scale drinking water treatment plant. *Sci Total Environ* 481:392–400. <https://doi.org/10.1016/j.scitotenv.2014.02.069>
- Patel M, Kumar R, Kishor K, Mlsna T, Pittman CU, Mohan D (2019) Pharmaceuticals of emerging concern in aquatic systems: chemistry, occurrence, effects, and removal methods. *Chem Rev* 119(6):3510–3673. <https://doi.org/10.1021/acs.chemrev.8b00299>
- Pathania D, Kumari S (2020) Nanocomposites based on biopolymer for biomedical and antibacterial applications. In: *Adapting 2D nanomaterials for advanced applications*. American Chemical Society. <https://doi.org/10.1021/bk-2020-1353.ch015>
- Peña-Guzmán C, Ulloa-Sánchez S, Mora K, Helena-Bustos R, Lopez-Barrera E, Alvarez J, Rodríguez-Pinzón M (2019) Emerging pollutants in the urban water cycle in Latin America: a review of the current literature. *J Environ Manage* 2019(237):408–423. <https://doi.org/10.1016/j.jenvman.2019.02.100>
- Pettibone JM, Cwiertny DM, Scherer M, Grassian VH (2008) Adsorption of organic acids on TiO₂ nanoparticles: effects of pH, nanoparticle size, and nanoparticle aggregation. *Langmuir* 24(13):6659–6667. <https://doi.org/10.1021/la7039916>
- Rajabi M, Mirza B, Mahanpoor K, Mirjalili M, Najafi F, Moradi O, Sadegh H, Shahryari-ghoshekandi R, Asif M, Tyagi I, Agarwal S, Gupta VK (2016) Adsorption of malachite green from aqueous solution by carboxylate group functionalized multi-walled carbon nanotubes: determination of equilibrium and kinetics parameters. *J Ind Eng Chem* 34:130–138. <https://doi.org/10.1016/j.jiec.2015.11.001>

- Rajabi M, Mahanpoor K, Moradi O (2017) Removal of dye molecules from aqueous solution by carbon nanotubes and carbon nanotube functional groups: critical review. *RSC Adv* 7(74):47083–47090. <https://doi.org/10.1039/C7RA09377B>
- Rajabi M, Mahanpoor K, Moradi O (2019) Preparation of PMMA/GO and PMMA/GO-Fe₃O₄ nanocomposites for malachite green dye adsorption: kinetic and thermodynamic studies. *Compos Part B Eng* 167:544–555. <https://doi.org/10.1016/j.compositesb.2019.03.030>
- Rajeswari A, Christy EJS, Pius A (2021) Biopolymer blends and composites: processing technologies and their properties for industrial applications. In: *Biopolymers and their industrial applications*. Elsevier Inc., pp 105–147. <https://doi.org/10.1016/B978-0-12-819240-5.00005-5>
- Raota CS, Cerbaro AF, Delamare APL, Echeverrigaray S, Crespo JS, Silva TB, Giovanela M (2019) Green synthesis of silver nanoparticles using an extract of ives cultivar (*Vitis Labrusca*) pomace: characterization and application in wastewater disinfection. *J Environ Chem Eng* 7(5):103383. <https://doi.org/10.1016/j.jece.2019.103383>
- Ren D, Smith JA (2013) Retention and transport of silver nanoparticles in a ceramic porous medium used for point-of-use water treatment. *Environ Sci Technol* 47(8):3825–3832. <https://doi.org/10.1021/es4000752>
- Restrepo CV, Villa CC (2021) Synthesis of silver nanoparticles, influence of capping agents, and dependence on size and shape: a review. *Environ Nanotechnol Monit Manag* 15:100428. <https://doi.org/10.1016/j.enmm.2021.100428>
- Röhricht M, Krisam J, Weise U, Kraus UR, Düring R-A (2009) Elimination of carbamazepine, diclofenac and naproxen from treated wastewater by nanofiltration. *Soil Air Water* 37(8):638–641. <https://doi.org/10.1002/clen.200900040>
- Rong X, Qiu F, Qin J, Yan J, Zhao H, Yang D (2014) Removal of malachite green from the contaminated water using a water-soluble melamine/maleic anhydride sorbent. *J Ind Eng Chem* 20(5):3808–3814. <https://doi.org/10.1016/j.jiec.2013.12.083>
- Saber-Samandari S, Saber-Samandari S, Joneidi-Yekta H, Mohseni M (2016) Adsorption of anionic and cationic dyes from aqueous solution using gelatin-based magnetic nanocomposite beads comprising carboxylic acid functionalized carbon nanotube. *Chem Eng J* 308:1133–1144. <https://doi.org/10.1016/j.cej.2016.10.017>
- Sarkar AK, Pal A, Ghorai S, Mandre NR, Pal S (2014) Efficient removal of malachite green dye using biodegradable graft copolymer derived from amylopectin and poly(Acrylic Acid). *Carbohydr Polym* 111:108–115. <https://doi.org/10.1016/j.carbpol.2014.04.042>
- Sarkar S, Chakraborty S, Bhattacharjee C (2015) Photocatalytic degradation of pharmaceutical wastes by alginate supported TiO₂ nanoparticles in packed bed photo reactor (PBPR). *Ecotoxicol Environ Saf* 121:263–270. <https://doi.org/10.1016/j.ecoenv.2015.02.035>
- Sauvé S, Desrosiers M (2014) A review of what is an emerging contaminant. *Chem Cent J* 8(1):8–15. <https://doi.org/10.1186/1752-153X-8-15>
- Sharma B, Thakur S, Mamba G, Gupta RK, Gupta VK, Thakur VK (2021) Titania modified gum tragacanth based hydrogel nanocomposite for water remediation. *J Environ Chem Eng* 9(1):104608. <https://doi.org/10.1016/j.jece.2020.104608>
- Sharma R, Kumar D (2019) Chitosan-based membranes for wastewater desalination and heavy metal detoxification. In: *Nanoscale materials in water purification*. Elsevier, pp 799–814. <https://doi.org/10.1016/B978-0-12-813926-4.00037-9>
- Siong Y, Atabaki MJI (2014) Performance of activated carbon in water filters. pp 1–19
- Tan XM, Rodrigue D (2019) A review on porous polymeric membrane preparation. Part I: production techniques with polysulfone and poly(vinylidene fluoride). *Polymers* 11(8)
- Tang P, Sun Q, Zhao L, Tang Y, Liu Y, Pu H, Gan N, Liu Y, Li H (2019) A simple and green method to construct cyclodextrin polymer for the effective and simultaneous estrogen pollutant and metal removal. *Chem Eng J* 366:598–607. <https://doi.org/10.1016/j.cej.2019.02.117>
- Undabeytia T, Posada R, Nir S, Galindo I, Laiz L, Saiz-Jimenez C, Morillo E (2014) Removal of waterborne microorganisms by filtration using clay-polymer complexes. *J Hazard Mater* 279:190–196. <https://doi.org/10.1016/j.jhazmat.2014.07.006>

- Unuabonah EI, Taubert A (2014) Clay-polymer nanocomposites (CPNs): adsorbents of the future for water treatment. *Appl Clay Sci* 99:83–92. <https://doi.org/10.1016/j.clay.2014.06.016>
- Ursino C, Castro-Muñoz R, Drioli E, Gzara L, Albeirutty MH, Figoli A (2018) Progress of nanocomposite membranes for water treatment. *Membranes* 8(2):1–40. <https://doi.org/10.3390/membranes8020018>
- Vanaamudan A, Sadhu M, Pamidimukkala P (2018) Chitosan-guar gum blend silver nanoparticle bionanocomposite with potential for catalytic degradation of dyes and catalytic reduction of nitrophenol. *J Mol Liq* 271:202–208. <https://doi.org/10.1016/j.molliq.2018.08.136>
- Veber MC, da Silva Crespo J, Giovanela M (2019a) Self-assembled thin films of PAA/PAH/TiO₂ for the photooxidation of ibuprofen. Part I: optimization of photoactivity using design of experiments and surface response methodology. *Chem Eng J* 360:1447–1458. <https://doi.org/10.1016/j.cej.2018.10.189>
- Veber MC, Aguzzoli C, Beltrami LVR, Fetter G, da Silva Crespo J, Giovanela M (2019b) Self-assembled thin films of PAA/PAH/TiO₂ for the photooxidation of ibuprofen. Part II: characterization, sensitization, kinetics and reutilization. *Chem Eng J* 361:1487–1496. <https://doi.org/10.1016/j.cej.2018.10.186>
- Venditti P, Di Stefano L, Di Meo S (2013) Mitochondrial metabolism of reactive oxygen species. *Mitochondrion* 13(2):71–82. <https://doi.org/10.1016/j.mito.2013.01.008>
- Yahaya N, Zain NNM, Miskam M, Kamaruzaman S (2021) Molecularly imprinted polymer composites in wastewater treatment. <https://doi.org/10.1016/b978-0-12-819952-7.00013-5>
- Yang Y, Ok YS, Kim K, Kwon EE, Tsang YF (2017) Occurrences and removal of pharmaceuticals and personal care products (PPCPs) in drinking water and water/sewage treatment plants: a review. *Sci Total Environ* 596–597:303–320. <https://doi.org/10.1016/j.scitotenv.2017.04.102>
- Yoon TJ, Shao H, Weissleder R, Lee H (2013) Oxidation kinetics and magnetic properties of elemental iron nanoparticles. Part Part Syst Charact 30(8):667–671. <https://doi.org/10.1002/ppsc.201300013>
- Yoosefi Booshehri A, Wang R, Xu R (2015) Simple method of deposition of CuO nanoparticles on a cellulose paper and its antibacterial activity. *Chem Eng J* 262:999–1008. <https://doi.org/10.1016/j.cej.2014.09.096>
- Yuan X, Qiang Z, Ben W, Zhu B, Liu J (2014) Rapid detection of multiple class pharmaceuticals in both municipal wastewater and sludge with ultra high performance liquid chromatography tandem mass spectrometry. *J Environ Sci* 26(9):1949–1959. <https://doi.org/10.1016/j.jes.2014.06.022>
- Zarpelon F, Galiotto D, Aguzzoli C, Carli LN, Figueroa CA, Baumvol IJR, Machado G, da Sliva Crespo J, Giovanela M (2016) Removal of coliform bacteria from industrial wastewaters using polyelectrolytes/silver nanoparticles self-assembled thin films. *J Environ Chem Eng* 4(1):137–146. <https://doi.org/10.1016/j.jece.2015.11.013>
- Zhang X, Li X, Deng N (2012) Enhanced and selective degradation of pollutants over Cyclodextrin/TiO₂ under visible light irradiation. *Ind Eng Chem Res* 51(2):704–709. <https://doi.org/10.1021/ie201694v>
- Zoschke K, Engel C, Bo H, Worch E (2011) Adsorption of geosmin and 2-methylisoborneol onto powdered activated carbon at non-equilibrium conditions : influence of nom and process modelling. *Water Res* 5:0–6. <https://doi.org/10.1016/j.watres.2011.06.006>

Optimisation and Modeling Approaches for the Textile Industry Water Treatment Plants



M. Magesh Kumar

Abstract The textile industry is considered a major pollutant source among all the industrial units because this industry intensively uses a variety of chemicals for the pre-treatment and processing of fibres, wool etc. The wastewater generated from textile processing plants has a complex chemical composition and abnormally elevated physical characteristics. Various chemicals such as organic dyes, bleaching agents, fixing agents etc., are used to upgrade the characteristics of the finished textile materials. A number of methods such as adsorption, coagulation, electro-Fenton oxidation, membrane separation and biological degradation are followed to eliminate the undesirable components from the outlet stream. The success of the treatment process depends on understanding the underlying mechanism of mass transfer by diffusion, the kinetics of pollutant removal and hydrodynamics of mixing. Modeling represents a process by mathematical equations, which comprises the variables affecting the process performance. The model equation shows the relationship between the input and response variables in a process. Model of a process helps to simulate the conditions and understand the robust behavior of systems. The optimisation is a mathematical approach to identify the best condition for a process. The objective of optimisation is to minimise the operating cost or maximise process efficiency. In the wastewater treatment domain, modelling and optimisation are helpful to understand the pollutant removal rate, demarcate the major variables affecting the process efficiency and identify the range of operating conditions. Textile wastes have high salinity, prohibitive total dissolved solids and residual organic dye compounds. The important models developed for a treatment plant are the mass transfer, kinetic, adsorption, and process models. The mass transfer model gives an insight into the rate of diffusion of pollutants in an aqueous medium. A kinetic model explains the rate at which undesirable compounds are removed from wastewater and elucidates the effects of temperature on the process. The process models are used to realise the important variables affecting the process efficacy. The process model explains the interactive effect and linear effect of variables on the response variable. The modelling

M. Magesh Kumar (✉)

Department of Chemical Engineering, SRM Institute of Science and Technology, Kattankulathur 603 203, Tamil Nadu, India

e-mail: mmagesh23@gmail.com; mageshkm@srmist.edu.in

tools used in textile treatment plants are response surface method (RSM) and Artificial Neural Networking (ANN). RSM is the most widely used method to develop the model equations and optimise the process. The second order quadratic models developed by the RSM method interpret the effects of parameters on the response variables. RSM utilises the experimental design method to develop the complete model expression for the operation with the least number of experiments. Irrespective of treatment strategies for textile wastewater such as coagulation, adsorption, electrochemical oxidation, bio-degradation, ozonation, photolytic degradation and membrane filtration, the RSM is used as a versatile method for building the model and process analysis. The quality of the model equations is tested by statistical tools such as ANOVA table, fit statistics table, 2-D contour graph and 3-D response surface plot.

Keywords Response surface methodology · Kinetic model · Mass transfer model · Quadratic model · Wastewater treatment

1 Introduction

Textile industries are responsible for generating a large volume of wastewater because a sizeable quantity of fresh water is used for the dyeing of processed fibres and finished goods. Textile wastewater is characterised by high pH value, excessive suspended solids concentration, and prohibitive concentration of chlorides, nitrates, copper, chromium, and outrageous biochemical oxygen demand (BOD) and chemical oxygen demand (COD) value. The point of source for the wastewater decides the concentration level of contaminants. This industry is considered one of the highest polluting industrial units because of the volume of waste generated and its hazardous constituents. Textile wastewater shows utmost COD, BOD, pH, colour, and salinity variations. The properties of chemicals, dye compounds and organic compounds determine the characteristics of the effluent stream from the textile industry. Almost 10–50% of unfixed dye molecules are lost to the environment as pollutants in the dyeing process. The dye chemicals are less susceptible to biodegradation, and hence they persist in the effluent stream for a long period. The textile industry is associated with spinning natural and synthetic fibres into yarn, and the fabrics are produced from yarn. Various unit operations and unit processes such as carding, weaving, bleaching, drying, sizing, dyeing finishing etc., take place in processing raw fibre into useful textile products. The process of adding dye compounds to textile products is called dyeing. The bleaching process removes natural colour and odour from textile raw materials. Around 140–200 l/d of water is consumed for producing 1 kg of fabric material in a textile dyeing unit (Report on assessment of pollution 2014). Different chemicals such as strong acids, bases, colouring agents, bleaching agents, finishing chemicals, thickening agents, surfactants and dispersing agents are used in each stage of the textile industry. The aesthetic appearance of the finished goods is improved by using multi-colour dyeing compounds. A typical textile processing unit is composed of the steps elucidated in Fig. 1.

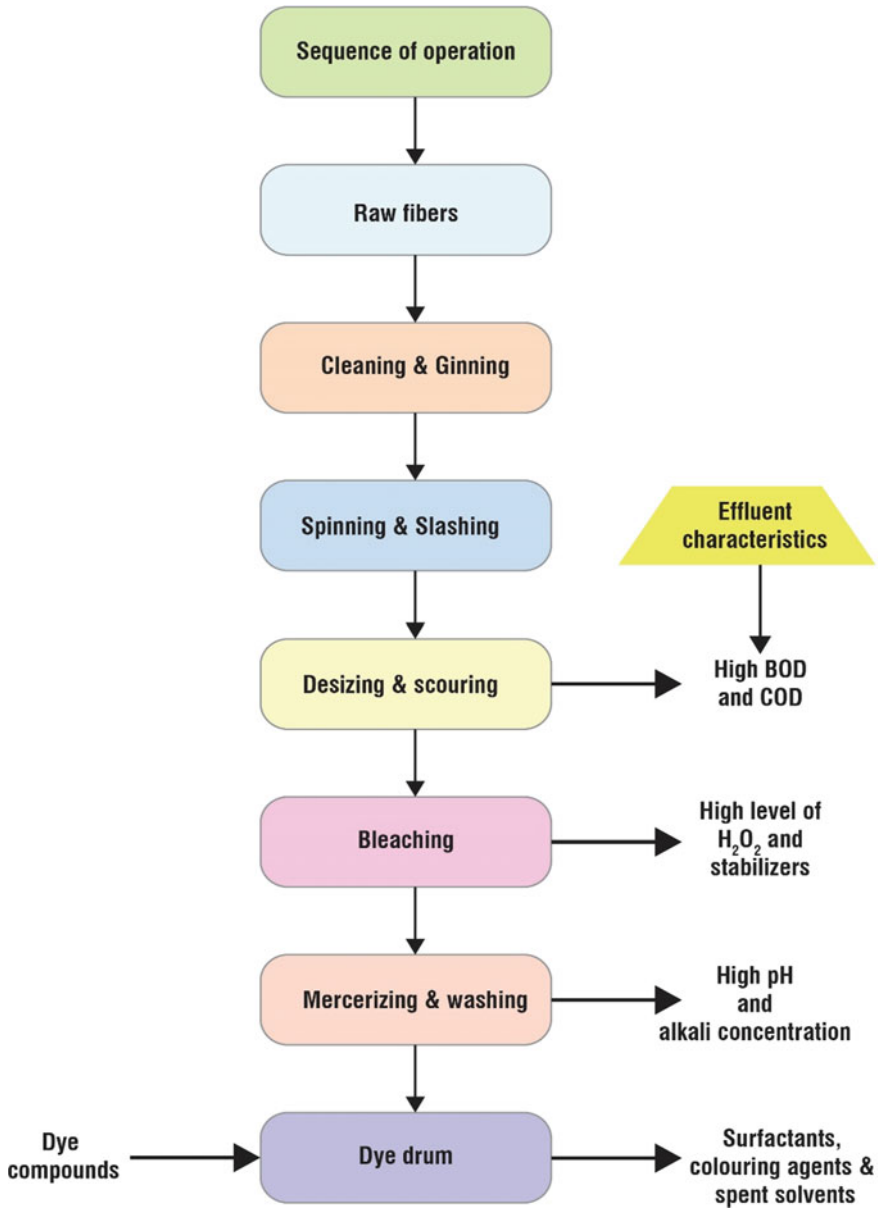


Fig. 1 Sequence of steps in a textile processing unit and characteristics of effluent generated from each process

Table 1 Physico-chemical properties of effluent streams produced from different unit operation and unit process in tannery industry

Unit operation/unit process involved	Physico-chemical characteristics of wastewater
Sizing	Outrageous values of BOD and COD
De-sizing	Outrageous values of BOD and COD; elevated dissolved solids concentration
Bleaching	High alkalinity, excessive suspended solids
Mercerizing	High pH, high dissolved solids
Dyeing	Strong colour, high BOD, dissolved solids

The effluent stream from each step has the Physico-chemical properties defined in Table 1.

Process modeling is the representation of a physical system by variables and equations. Modeling a process requires a sound knowledge of major process variables, operating conditions used and constraints applicable. The model equation explains the variation of the dependent variable as a function of independent variables. The three major components in a general model equation are the input, response, and parameter. Process models are used to calculate and interpolate the responses as well as calibrate and optimise the process variables. The average magnitude of the output variable is calculated for a specific amalgamation of the input variables. The interpolation is done to determine the new values of the response variable without conducting the experiments. Mathematical modeling has suffused all branches of engineering and science and assisted in better understanding of processes mechanism. Process industries provide the analytical basis for the design and control of equipment and process optimisation with limited effort and time. The purpose of the mathematical model is to understand the system's robustness and predict the system's future behaviour (Bravo et al. 2011). The modeling of the process can be broadly categorised into a series of activities, namely, building, studying, testing and use. The developed model equations are useful in all stages of operation in the industry. It helps screen the important process parameters and analyse the influence of various process parameters on selecting control strategies and optimisation methodology to follow. Analysis of simulated results from a model equation gives an idea about the best arrangement of process equipment to improve the yield from a process. In the wastewater treatment domain, the ordering of units determines the treatment potential of the wastewater treatment plant.

2 Textile Industry Wastewater: Source, Characteristics and Environmental Impacts

Textile industry discharges effluent stream with pollutants such as colouring agents, sizing agents, fixing salts, bleaching agents etc. The wastewater discharged from the

textile industry is a complex mixture of organic and inorganic chemicals with poor biodegradability and a high concentration of dissolved salts. Even though textile industries generate all kinds of waste, liquid effluent is a major concern because of its bulk volume and antagonistic environmental impacts. The physicochemical nature of liquid effluent generated depends on the nature of fiber being processed, type of chemical reagents used, technology adapted, operating variables etc. The pollutants from the textile industry are due to the processes such as desizing, scouring, mercerising, bleaching, neutralising, dyeing, printing and finishing. Apart from these sources, gaseous pollutants such as suspended particulate matter, sulphur oxides and nitrogen gases are produced from boilers, thermo-pack utilities and generators.

Textile industry liquid waste is characterised by high pH value, and excessive concentration suspended particles, outrageous chloride and nitrate ions. Severe environmental damages are caused by the contaminants present in wastewater emanating from the textile industry. The composition of textile wastewater changes dynamically because of the process diversity and varieties of chemicals used in each unit process (Correia et al. 1994). The different categories of chemicals used in the textile industry are detrimental to the environment and health. The stain remover can cause ozone depletion; oxalic acid is toxic to aquatic organisms, printing gums is responsible for dermatitis, liver malfunction and kidney damage, bleaching agent chlorine causes skin irritation, and azo dyes are well-known carcinogens. The organic waste present in the effluent stream consumes dissolved oxygen from receiving water bodies and destroys the aquatic biosphere. The liquid wastes have high BOD and COD concentrations because the concentration of dissolved oxygen is too low in the effluent stream. The high colour intensity of effluent reduces the sunlight penetration into receiving water bodies and decreases the oxygen solubility. Apart from other chemicals used in various processing stages, the effluents contain inflated dye concentrations. The effluent has excessive dye concentration apart from having varieties of spent chemicals used in different processing units. Various health hazards such as haemorrhage, skin dermatitis, severe ulcer of skin etc., are caused by remnant metals, namely Cr, As, Cu and Zn.

The major environmental concern associated with textile dyeing units is removing colour and dissolved salts from wastewater. Along with these pollutants, the effluents do contain trace elements such as chromium, arsenic, copper, zinc, which has the potential of causing health ailments including haemorrhage, skin rashes and cancer, dermatitis etc. Azo dyes are mainly used as a colouring agent for cotton fibers. The azo dyes are electron deficient because they have a nitrogen-nitrogen bond in the chemical structure. The waste stream containing these dye compounds can cause damage to flora and fauna in receiving water bodies. The hazardous effect of azo dye depends mainly on the duration of exposure time and exit dye concentration (Hassan and Nemr 2017). The textile wastewater is of potential environmental concern because it substantially decreases the dissolved oxygen concentration in the receiving water body due to hydrosulfides. Textile industry wastewater is one of the reasons for rapid environmental degradation and human illnesses. The quantum of degradation caused is very high compared with other process industries. The carcinogenic nature of colourants used in the textile industry is due to the presence of organic chlorine.

The normal functioning of cells is disturbed in living organisms due to this chemical pollutant which ultimately affects the physical appearance and biological mechanisms. The heavy metals are non-biodegradable and accumulate in vital organs in the body. The partially treated or untreated effluent from the textile industry is very harmful to all life forms, including aquatic and terrestrials. Many methods such as oxidation methods (cavitation, photocatalytic oxidation, ozone, hydrogen peroxide oxidation, Fenton oxidation process), physical methods (adsorption and filtration) and biological methods (fungi, algae, bacteria, microbial fuel cell) are followed to minimise the pollutant concentration in textile wastewater (Holkar et al. 2016).

3 Treatment Methods and Strategies

The textile processing unit is a water-intensive industry because it utilises a large quantum of water for washing, dyeing, and finishing operations. Hence this industry releases a huge volume of wastewater characterised by its immense colour, high level of suspended solids and dissolved solids concentration. The methods, namely biological treatment, coagulation and flocculation, adsorption, oxidation, is widely used to treat textile wastewater. The activated sludge process can reduce the COD concentration to a significant level. The treated water from this process has high ammonia content and residual colouring agents. Coagulation-flocculation is suitable to remove dissolved colour completely from wastewater, but this method suffers from the drawbacks such as unreliable performance of the plant and secondary sludge disposal problems. The physical adsorption method is most suited for the elimination of suspended as well as dissolved solids. The efficiency of this method depends on the way of regenerating the spent adsorbent and methods of handling the secondary pollutants generated. Membrane filtration is used for the post-treatment process to remove the pollutants present at the microscopic level. Membrane techniques are efficient than conventional methods, and it is very specific to handling dissolved pollutants. The processes based on membranes are used to improve the quality of wastewater which is already treated by conventional methods. This method is used to fine tune the characteristics of wastewater by removing the micro level pollutants even when they are present in very small quantities. The only problem associated with the membrane technique is the efficient management of concentrate because the concentrated stream from the membrane treatment unit is a complex mixture of varieties of contaminants.

Ozonation is employed for wastewater having oxidisable pollutants. The decomposition of ozone produces hydroxyl radicals which are highly reactive and deteriorate the pollutants present in wastewater. This method focuses mainly on colour removal and the disinfection process. This method is expensive because the operating cost is high. Photocatalysis is the acceleration of the reaction rate of a photochemical reaction in the presence of a catalyst. The pollutant reduction using the electrolysis method is a feasible approach to remove the hazardous pollutants, which is not eliminated by conventional treatment techniques. The efficacy of the electrolysis method

depends primarily on the rate of energy consumption, the lifetime of electrodes and the foaming tendency of wastewater during the treatment process.

4 Process Modeling

4.1 Mass Transfer Modeling and Kinetic Modeling

Mass transfer modeling in an aqueous effluent treatment plant is essential to understand the rate of pollutant movement, energy cost involved, and equipment design. These modeling aspects include the adsorption of pollutants, diffusion process and oxygen transfer in the oxidation process. The mechanism of the adsorption process for pollutant removal is understood by a mass balance equation of the adsorbate, rate of pollutant movement from the bulk solution to the surface of adsorbent and adsorption isotherm. An unsteady state solute balance equation in a fixed bed adsorber for an elemental section is written as,

$$\varepsilon \frac{\partial c}{\partial t} + (1 - \varepsilon) \rho_p \frac{\partial q}{\partial t} = -v \frac{\partial c}{\partial z} + \frac{\partial^2 c}{\partial z^2} \quad (1)$$

where ε is the fraction of void volume in bed, v is the superficial velocity (m/s) in vacant bed, ρ_p is particle density (kg/m^3), and D is axial dispersion coefficient (m^2/s). The leading term indicates the accumulated solute concentration in the liquid, and the second term represents the quantity of solute adsorbed in the adsorbent. The third term gives the amount of solute movement by convective (bulk) movement. The rearmost variable measures the extent of solute dispersion in the axial direction and measures the degree of mixing between the solute and solvent. The second model equation explains the kinetics of the adsorption process

$$\rho_b \frac{\partial a}{\partial t} = k_i (c - c^*) \quad (2)$$

where k_i is the mass transfer coefficient (s^{-1}), q is adsorption capacity (gm adsorbed/gm adsorbate), and C^* is the equilibrium concentration of adsorbed species. The third equation is the equilibrium isotherm which is generalized as

$$a = f(c^*) \quad (3)$$

The equilibrium concentration of solute between the liquid phase and solid phase adsorbent is defined by the Freundlich equation and Langmuir equation.

The gas–liquid mass transfer models are very important to understand the mechanism of the advanced oxidation process and ozone treatment of wastewater. Aeration is a key process for achieving the best treatment efficiency in a water treatment unit.

Various theories such as two-film theory, penetration theory and surface-renewal theory are developed to elucidate the rate and mechanism of oxygen transfer. The governing model equation for the absorption of oxygen in the liquid is defined as

$$\frac{dC}{dt} = Q_{O_2} = k_{liq} a'(C^* - C) \quad (4)$$

where Q_{O_2} is the oxygen transfer rate, a' is the gas–liquid interfacial area per unit liquid volume and k_{liq} is liquid phase mass transfer coefficient.

The two film theory defines the rate equation for direct mass transfer as

$$-\frac{dC}{dt} = \left[\frac{1}{\frac{1}{k_{Ag} a} + \frac{H_A}{k_{Al} a}} \right] (p_A - H_A C_A) \quad (5)$$

where H_A is the Henry law constant and C_A is the moles of oxygen dissolved per unit volume in the liquid phase.

The kinetics of the coagulation process is concerned with establishing the rate equation for the formation of flocs and also investigates the influence of pollutant concentration and temperature on the process mechanism. The rate at which the pollutant concentration decreases with time is expressed by n^{th} order general rate equation defined as (Marichamy and Ramasamy 2015)

$$-\left(\frac{dC}{dt}\right) = k \cdot C^n \quad (6)$$

where the variable C represents residual pollutant concentration in mg/L at the instantaneous time, k stands for the rate constant ($\text{min}^{-1} \cdot (\text{mg/L})^{(1-n)}$), n is the order of the process, and t (min) is operating time. The value of rate constant and process order is calculated using the kinetic data obtained from experiments. There are two approaches to estimate the kinetic parameters in the rate equation: the integral method of analysis and the differential method of analysis. The process order is assumed in the integral method, and after appropriate mathematical manipulations and integrations, a final equation between concentration term and time is obtained. The residual pollutant concentration versus time data obtained from the experiment is fitted with the final rate equation obtained. If the data satisfies the rate equation, the assumed order is correct. In the differential analysis method, the kinetic data are fitted directly to the rate equation without any integration. The rate equation defined by Eq. (6) is linearised by taking logarithm on both sides, and a plot is prepared between $\log_{10}\left(-\frac{dC}{dt}\right)$ variables along the ordinate axis and $\log_{10}(C)$ along the abscissa axis. The straight line slope gives the magnitude of process order (n), and the vertical axis intercept made by the trend line gives the magnitude of the rate constant. For most of the wastewater treatment methods, it was observed that the process obeyed the second order kinetic model. This means that the rate of decrease in pollutant load

per unit volume varies directly proportional to residual concentration square. The proportionality constant is called the rate constant, which indicates the speed of floc aggregation and pollutant depletion from the waste stream.

4.2 Development of Process Model

Modeling a process is useful in all engineering disciplines, basic sciences, process economics and biological sciences. The models are developed based on physical, chemical and mathematical laws. The dynamic characteristic of a system is understood by developing a process model relating the changes in one variable with respect to time. The standard of the proposed model is based on assumptions made, creativity and innovativeness of the engineers and scientists. The invalid assumptions impose restrictions on the model and significantly affect the predicted results. The solvability of the models is tested with the “degrees of freedom (DF)” of the system. If the number of variables equals the number of equations, then the DF value is zero, making the model easily solvable. If the number of variables is greater than or less than the number of equations, then it is concluded that the system is either over specified or under specified. The model developers shall think about the possible solution methodologies to simulate the model equations. The simulated results from the model equation should match with the real time process output. The worth of the equation depends on how far the model results match with the real world output.

4.3 Basics of RSM Modeling and ANN Modeling

In the early 1950's Response Surface Methodology (RSM), based on statistics and mathematics, was introduced as an analysis tool by Box and Wilson. This method is useful for optimising process variables to obtain the maximum or minimum response value. It is based on the design of the experiment's approach and helpful to study the effects of major independent variables on process outcome. The number of experiments to be conducted can be minimised with the design of the experiment concept. RSM is also used to develop and solve the model equations to obtain optimised process variables. RSM is used to find optimal process conditions, trouble shoot problems, identify weak points in the process and develop a process model having more robustness against external influences.

RSM investigate the effective correlations between the independent variables and response variables. The simplest model considered is the first order model defined by the expression

$$y = \alpha_0 + \alpha_1x_1 + \alpha_2x_2 + \varepsilon \tag{7}$$

where α_o is the constant term, $\alpha_1 \alpha_2$ the linear terms, and the error term.

A second order response surface model would be appropriate to represent the process if significant interactions between the process variables and curvature are obtained. It is expressed by the equation as

$$y = \alpha_o + \alpha_1 x_1 + \alpha_2 x_2 + \alpha_{11} x_1^2 + \alpha_{22} x_2^2 + \alpha_{12} x_1 x_2 + \varepsilon \quad (8)$$

where α_o is the constant term, $\alpha_1 \alpha_2$ are the linear terms, $\alpha_{11} \alpha_{22}$ are the quadratic terms and α_{12} is the interaction term. RSM approach is a sequential procedure because identifying the optimum point is done in sequences to move from the current point, which is far away from the exact stationary point. The positive sign for the coefficients indicates an increase in response value, whereas the negative sign indicates a decrease in the response value. The change in response variable value as a function of two independent variables is represented by 3-D response surface plots. Contour curves are the 2-D representation of response surface and are considered iso-response curves. The fitness quality of proposed models is tested with statistical parameters such as p-value, coefficient of determination (R^2) and F-value. The magnitude of the p-value is a measure of the effect of the independent variable on process response. It is based on testing the null hypothesis "coefficient term is zero," which means zero effect on process output. A lower p-value ($p < 0.05$) indicates that the variable profoundly affects the response variable. The R^2 square value explains the variation of predicted data from actual data. The response curve fits the real data when the R^2 value is high, and the ideal value is one. The predictive capability of the complete model is determined statistically with the help of the F-value. The larger the F-value, the better is the model forecasting ability. The null hypothesis is rejected if the F-value is large.

The most widely used experimental design for response optimisation is Central composite design (CCD) and Box-Behnken design. The CCD procedure gives a response surface curve that adequately fits the second order quadratic model. The curvature of the response surface is estimated by combining centre points with a group of star points. In CCD, the distance between each axial point (start point) and center is designated by the symbol alpha (α). This alpha value determines whether a design is rotatable and orthogonally blocked. The alpha value depends on the properties of response surface design and a number of factors describing the process. The equation defines the value of α

$$\alpha = (\text{number of factorial runs})^{0.25} \quad (9)$$

When full factorial is used then value of α is defined by the expression

$$\alpha = (2^k)^{0.25} \quad (10)$$

There are three types of central composite designs: Circumscribed, Inscribed, and Face Centered.

The second widely used procedure for process optimisation is the Box-Behnken design. The fractional factorial design is not available in this configuration, and hence it is considered as an independent quadratic design. The treatment combinations are located at the midpoint of each cube's edge and one at the center of the cube body. The number of runs required by the Box-Behnken design is 15 and 54 when the number of factors involved is 3 and 6, respectively. The equation calculates the number of experiments to be conducted according to this design

$$N = 2f^2 - 2f + Co \quad (11)$$

where f is the number of factors and Co is the center point of design space. The levels of the process variables are usually represented as coded variables such as -1 , 0 , $+1$, which indicates lower, middle and higher level values, respectively.

4.4 Objectives and Uses of RSM

RSM is useful for solving different types of optimisation problems in industries. The objective is to develop the process model equations, optimise the process conditions and enhance the process output. This objective is achieved by following the three steps: screening, improvement, and predicting the optimum. Screening refers to identifying the important factor influencing the process, whereas improvement cites the procedure to reach out the optimum by continuously changing the factor settings. The response surface methodology (RSM) is a mathematical strategy to elucidate the interrelationship between the independent variables with the dependent variables and explain the influence of these parameters on responses. There are six different general steps involved in the RSM technique: (1) identifying the major process factors and response under study (2) endorsing appropriate experimental design plan (3) performing regression analysis with the multivariable model of the process (4) pointing out the parameters significantly affecting process responses using analysis of variance (ANOVA) method (5) guessing whether screening of variables is necessary or not (6) conducting experiments at optimal conditions to verify the characteristics of the response.

4.5 Analysis and Transformation of Models

Analysis of variance (ANOVA) is a statistical approach used to test the quality of the model as a whole and also the nature of individual terms. To check whether the correct model is chosen or not, the descriptive statistics are tested along with other statistical tests and the significance of the parameters, variables and coefficients are

judged. The ideal starting point for the model is chosen based on the results of the fit summary table. The key parameters to look in fit summary table is:

- Mean which represents the sum of squares for the consequence of mean
- Linear measures the sequential sum of squares for the linear term. The addition of linear terms to the intercept and block effect and significance of this addition is tested with the aid of F-value magnitude
- The quadratic term indicates the sequential sum of squares for quadratic (A-squared, B-squared, etc.) terms. The importance of adding the quadratic terms in the model is verified with F-value. It is observed that the model prediction ability is improved when a small p-value ($\text{prob} > F$) is obtained from statistical tests.

5 Response Surface Design and Analysis of Variance (ANOVA)

The following parameters and plots are used to analyse and interpret the fitted models: Normal plots are used to highlight significant active factors. Residual plots are used to check the validity of normality and constant variance assumption. The fit of the proposed models could be improved by evaluating the response on a log scale and reported in the Box-Cox plot for power transformation. The linear term in a model explains the average effect of varying a control, whereas the interaction term studies the influence of altering a variable with the setting of another independent process variable. The quadratic terms (x^2) explain the effects of process factors on the curvature of the response curve. The purpose of ANOVA is to check if there is any deviation among the group of variables. The elementary proposition of ANOVA is to assess the magnitude of variation within the samples relative to the quantity of variation between the samples. There are two different approaches for ANOVA.

First is One-way (or single factor) ANOVA, in which only one factor is considered, and it is to be observed that varieties of samples can materialise inside that factor. The subsequent steps involved with this technique are: mean of each sample is obtained, the sum of squares for variance between the samples (SS) is then calculated, dividing SS obtains the mean square (MS) among the samples by degrees of freedom connecting the samples. In one way ANOVA, the F-statistic ratio is defined by the expression:

$$F = \frac{\text{variation between the sample means}}{\text{variation with in the samples}} \quad (12)$$

F-test could be used to assess the equality of variance. ANOVA compares the known variance (caused by input variables) to the unknown source of variance (mainly due to disturbance errors).

The two-way ANOVA test calculates an F value. It is used to test whether the means are significantly different or not. Two independent variables are used as input instead of one input variable, as in one-way ANOVA. The means and sum of squares

statistics are calculated for each combination of independent variables. The predictive stability of the model is gauged using Adjusted R^2 . For a good model, the predictive strength should be more than 10% if the significance level is set at 5%. The definitive relationship response value and input variable are confirmed if the model has a 10% relative improvement over the predictive strength. The ANOVA can be calculated using one of three types of sums of squares (SS). Type I or sequential SS calculations are done based on the order of adding the factors to the design. The process starts with the main effects, followed by the interactive effects. Type II or classical SS is followed when at least one multilevel categoric factor. The main effect SS calculation of factor is done by assuming that the factor is not a part of interactive effects. Type III or Partial SS corresponds to nil multilevel categoric factors and check for all other terms in the model before the SS is calculated for an individual term. ANOVA table for experimental design consists of the following terms:

- The residual, which shows the strange disparity in the response, lack of fit refers to missed observations by the model predictions
- sum of squares (SS) measures the squared differences between the accumulated average and the quantity of difference explained by the source
- degree of freedom used to calculate source’s sum of squares using the number of estimated variables
- p-value (Prob > F) explains the probability of getting the observed F-value if the null hypothesis is not false. The model equation and terms are significant if the Prob > F value is very small (should be less than 0.05)
- coefficient of variation is defined as the standard deviation expressed as mean% and estimated by dividing standard deviation with the mean and multiplying the result with 100
- PRESS stands for Predicted Residual Error Sum of Squares which measures the fitting capacity of the model to each point in the design. It is calculated by initially predicting the likelihood of other points except for the point under study.
- R squared is defined by the expression and appraises the quantity of discrepancy about the mean explained by the model

$$R^2 = 1 - \left[\frac{SS \text{ residual}}{SS \text{ residual} + SS \text{ model}} \right] \tag{13}$$

- Adjusted R^2 squared assesses the disparity around the mean, which is delineated by the model and adjusted for the number of terms present in the model. As the quota of model terms increases, there is a decrease in the adjusted R^2 square value. The expression defines it:

$$\text{Adjusted } R^2 = 1 - \left[\left(\frac{SS \text{ residual}}{df \text{ residual}} \right) / \frac{SS \text{ residual} + SS \text{ model}}{df \text{ residual} + df \text{ model}} \right] \tag{14}$$

- Predicted R^2 measures the quantity of deviation in new data elucidated by the model. It is defined as

$$\text{Predicted } R^2 = 1 - \left[\frac{\text{PRESS}}{SS_{\text{residual}} + SS_{\text{model}}} \right] \quad (15)$$

Either the data or the model may have problems if the predicted R^2 and adjusted R^2 is exceeding 0.2.

6 Types of Model Equations and Graphs in Response Surface Design

Model equations are used to predict the response values at a set of experimental conditions, and graphs are used to analyse the variation of output variables as a function of input variables. The most widely used models in process optimisation are the first order and second order models. The order of a model shows a trend followed by the experimental data. This factor explains how effective the model equation is to describe the data and predict an output. A linear model can explain the steady rate of change in the data. A quadratic model represented as a parabolic shaped curve can explain data's curvature. A polynomial model can describe a "peak-and-valley" trend in the data.

In the first order model, the cross product terms, which is an indication of response surface curvature, is ignored and consist only linear effect of the process variables. It is defined by

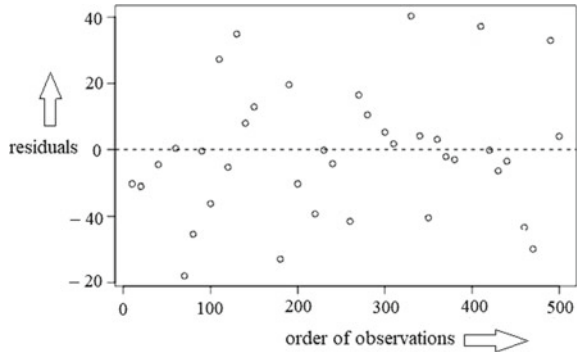
$$y = \alpha_0 + \alpha_1 x_1 + \alpha_2 x_2 + \varepsilon \quad (16)$$

where α_1 and α_2 are the linear terms, α_0 is the constant coefficient, and ε is the error or deviation variable. The variability between the model predicted value and the real time experimental value is called an error. This error should be less for the best model, and zero is the value for the ideal fitting model. The process is modeled as a first-order equation when the response changes linearly according to independent variable changes. The first order model is used to understand the orientation of flat planar surfaces with reference axis and is not suitable for finding maximum, minimum or saddle points for a function. For a small interval of x axis variable lying between $a \leq x \leq b$, the first order is suitable because the variation in function value is almost linear. The first order model is inadequate for response surfaces having curvature. A second order model is used to fit the response surface with curved shapes for such response surface designs.

Some of the widely used diagnostics plots are:

- Residuals versus Predicted plot: The persistent variance assumption is tested with this plot. A randomly scattered plot indicates that the residuals are spread across a constant range in the graph. A transformation is needed if the plot is showing an expanding variance pattern. The predicted values are taken along the horizontal X axis, and residuals are taken along the vertical Y axis. This plot helps us to

Fig. 2 Experimental run order affecting model residuals



determine whether a multiple regression model should be used or not. A well behaved plot should give a horizontal band around the residual = 0 line.

- Residuals versus Run order plot: This is a graph between residuals and experimental run order. The influence of lurking variables on output variables is checked using this plot. A random scatter plot should be obtained for a good model. If the data points are scattered above and below the reference line (residual = 0), the developed model equations are the best. A sample plot is shown in Fig. 2, which shows the random scattering of data points around the reference line.
- Predicted versus Actual plot: This plot of forecasted output values versus the real response values. It is used to check the presence of a value or group of values that the model cannot predict easily. The points should reside near the fitted line with narrow confidence interval width. Points located vertically, very far away from the line, represent the possibility of outliers.
- Contour plots: A graphical technique used to represent a 3-D surface on a 2-D graph format is called a contour curve. Contour curves are also called iso-response curve because it is obtained by plotting for constant response values. This plot is used to find the change in function value (Z) as a function of two independent variables, x and y. Let the contour function be $Z = f(x, y)$. The value of response variable 'Z' changes with respect to 'x' and 'y' variables (see Fig. 3).

The contour plot is plotted by taking independent variable 2 along the vertical axis and independent variable 1 along the horizontal axis. The response variable curves are represented by concentric circles, elliptical or linear shapes. The shape of contour curves gives a rough indication of the effects between the process variables. Circular shaped contour curves represent nil interaction between the independent variables, whereas elliptical contour curves indicate the best interactive effect between the input variables. Elliptical shaped contours are produced by a second order model containing interaction terms.

- 3D Response surface plots: This plot explains the relationship between a dependent variable and the two independent variables. It is useful to identify the desired operating conditions for the process in order to achieve optimised results. It has two components: predictor variable on the x- and y-axes and an output variable on the z-axis. A particular combination of x and y variables will give the peaks or

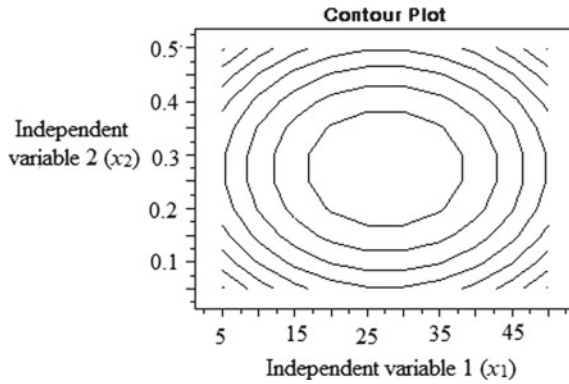


Fig. 3 Contour plot expressing the interactive effects between the two independent variables on process response

valleys, thus producing local maxima or minima. Different types of patterns occur in contour plots and 3D response surface plots. The point at which the maxima are obtained is called the critical point or stationary point, where the slope of the tangent plane is zero. In the minimax pattern, a decrease in the output is observed when the variables are either increased or decreased at the same time near the design center (see Fig. 4).

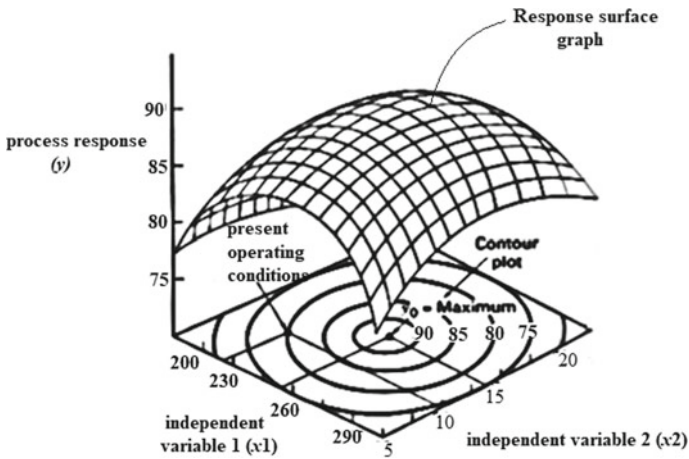


Fig. 4 Response surface graph illustrating the interaction effects between the two input variables on process response

6.1 Applications of RSM in Wastewater Treatment Domain

The optimisation is a mathematical technique which plays a major role in optimising waste handling treatment systems. Using RSM in the waste treatment realm is highly advantageous because it is flexible, can provide reliable results and is less time consuming. Apart from optimising the process conditions, this technique is used to analyse the effects of system variables on process output. Varieties of the industrial wastewater treatment process are optimised using the RSM technique. This chapter gives a brief overview of the usability, efficiency and drawbacks of RSM for process optimisation in waste handling treatment plants. A literature review has shown the widespread applications of RSM in the wastewater treatment unit. Modeling is the mathematical formulation of a system that relates dependent variables, independent variables and parameters in a process. The process model equations are used to understand the mechanism of the process, devise control strategies for automated systems, optimise the design and process variables, troubleshoot the process and in the economic analysis. In the textile wastewater treatment process, modeling and optimisation play a significant role in process synthesis and analysis. The model equations developed for the textile wastewater treatment process and the plant is used to analyse the effects of important process variables on treatment efficiency. The simulated results from the model equations are used to analyse the suitability of the treatment system for treating wastewater with specific characteristics.

Milk processing wastewater was successfully treated using a four compartmented multistage flexible fibre biofilm reactor (Abdulgader et al. 2020). The performance of this novel reactor is maximised at optimum operating conditions, which is obtained using RSM. Two important variables considered in this study is COD_{in} and HRT and 9 dependent response variables such as soluble and total COD (SCOD and TCOD), soluble and total BOD5 (SBOD5 and TBOD5), TSS, effluent pH, effluent turbidity, the retention time of sludge and substrate utilisation rate per unit mass were found from the experiments. The ANOVA results indicate that a quadratic regression model with lesser terms was better to elucidate the response surface for effluent pH of MS-FFBR.

In another study (Jadhav and Mahajan 2014), RSM was used as a tool to optimise the coagulation-flocculation process for turbid effluent treatment using a plant based coagulant prepared from *Coccinia indica*. The effects of coagulant dose, initial turbidity concentration, and pH of solution were studied using the central composite design method. A quadratic model having second order was developed to explain the progress of the coagulation process and analyse the interactive and non-interactive effects between the process variables. The worthiness of the proposed models was validated with the immensity of coefficient of determination (R^2) and adjusted R^2 , which had values of 0.941 and 0.926, respectively. This study concludes that RSM is an appropriate and ideal tool for optimising a process whose response depends on more than one stimulus variable.

Another author studied the applications of RSM for treating poultry slaughterhouse wastewater (PSW) which consists of organic matters, suspended solids,

dissolved nitrogen and detrimental nutrients (Williams et al. 2019). This study has utilised an Expanded Granular Sludge Bed (EGSB) to remove COD from PSW using hydraulic retention time (HRT) and organic loading rate (OLR). RSM augmented with a central composite design matrix was applied to identify the maximum achievement range of this reactor.

The applications of RSM is extended to slaughterhouse wastewater treatment because it contains varieties of pollutants, including organic matter (chemical oxygen demand (COD), biochemical oxygen demand (BOD)), total nitrogen, total suspended solids, total phosphorus, grease, and oil (Gökçek and Özdemir 2020). The process parameters such as initial pH, coagulants concentration, rate of rapid mixing and settling time were optimised using RSM to calculate the maximum removal % of process responses like COD, turbidity and suspended solids of the raw wastewater. Based on the response surface graph, the removal efficiency attained for COD, SS and turbidity removal was observed to be 75.25, 90.16, and 91.18%, respectively.

RSM was used to optimise the process variables for treating abattoir wastewater using Chito-protein coagulant extracted using crab shell (Okey-Onyesolua et al. 2020). To study the effects of pH, settling time, temperature and adsorbent storage on the removal of BOD, COD, turbidity and color from wastewater, RSM was used as an interlinking tool. The model predicted and experimental values had good correlations, indicating that the model equation developed using RSM is most suitable for understanding the underlying mechanism of process influencing factors.

The applications of RSM are also extended to the treatment of aqueous effluent from petroleum refinery plants (Singh and Kumar 2020). A central composite design matrix was applied to identify the best combination of the independent variables such as pH and coagulants to optimise the process output responses, including final pH, % of COD, turbidity, TDS and color removal from the targeted wastewater. ANOVA was employed to examine the statistical significance of the proposed models and their prediction ability. Second order quadratic model explained the relationship between the input and output variables.

The wastewater from the sunflower oil refinery industry was conditioned to achieve desired characteristics, and optimisation of the process variables was studied using the Box Behnken design (Sharma et al. 2020). This study highlighted the effects of current density, pH/H₂O₂ dosage and process time in removing COD, total organic carbon and dissolved organic carbon. The optimised condition for the electrocoagulation process was found to occur at 6.07 pH, and a current density of 5.69 mA/cm⁻² was applied for 18 min.

Modeling the process behavior and optimising the conditions were studied to treat petroleum industry aqueous effluent by Fe/Zn nanoparticles using RSM tools (Moghadam and Qaderi 2019). In this research, the critical point for the parameters phenol initial concentration, light source power, retention time, pH and the nano-catalysts concentration was estimated using RSM. The maximum removal of phenol 89% was found to occur at 5.23 pH, power of light equal to 43.53 W, feed phenol concentration of 50 ppm, 1.57 gm/lit nano concentration and process time of 58.6 min.

RSM was used to model and analyse the process for the treatment of cutting oil wastewater (Popović et al. 2019). The independent variables optimised were the

twisted tape aspect ratio and cross flow rate. The effects of varying the input variables were analysed by following the change in numerical values of the variable flux and specific energy consumption. The developed model equation concludes that the linear influence of aspect ratio and cross flow rate had a synergistic effect on the response flux. It was observed from the variable analysis that the aspect ratio's squared effect has statistical significance in process optimisation. The process modeling concept is also used in the treatment of textile dye wastewater in the packed-bed reactor (Devi et al. 2015), in the treatment of textile dye by adsorbing on organoclay using an artificial neural network (Elemen et al. 2012) and for the kinetic analysis of textile wastewater treatment using hybrid column upflow anaerobic fixed bed reactor (Sandhya and Swaminathan 2006).

7 Optimisation of the Process

The optimisation is a mathematical tool to identify the most economical design for a process and predict the efficient solution to a problem. In industrial processes, this approach is one of the major quantitative tools for decision making. The optimisation problem consists of three essential categories: the objective function to be optimised, equality constraints, and inequality constraints. The set of variables that satisfy equality and inequality constraints are called feasible solutions, whereas an optimal solution is defined as a set of values of process variables that satisfy both constraints. The method of solving the objective function depends on characteristics of the objective function, nature of the constraints and the number of dependent and independent variables involved in the development of process model equations.

8 Concept of Optimisation

The optimisation is the method of acquiring the supreme outcome for a given constraint. In the design, construction, operation and maintenance of any industrial process, engineers and scientists have to make crucial technical and managerial decisions at various stages. The utmost aim of all such decisions is to minimise the efforts, energy consumption, or maximise the desired output. Optimising a process or a system requires the following basic elements: An objective function is an indicator for quantitative performance measurer which should be either maximised or minimised. The system's behaviour is described by the predictive model, which is transformed to simultaneous equations and inequalities called constraints. The predictive model equations contain the variables that must be adjusted to satisfy the constraint equations. The optimisation algorithm is the major tool for process synthesis, process

analysis, design and retrofit. It is also useful for real time optimisation, scheduling and planning a process and process integration and intensification.

9 Methods for Optimisation

The optimisation of model equations is done either by analytical method, numerical method, or graphical method. For the function of a single variable, a test based on the second derivative is used to find the maxima or minima values. The single variable function is differentiated with respect to the independent variable, and the first order derivative is equated to zero. The solution of this equation gives the critical point or stationary point of the function. At this point to the curve, the tangent line's slope is zero because the tangent would appear as a straight line parallel to the horizontal axis. The first derivative is differentiated again to give the second derivative. The magnitude of the second derivative is evaluated at a critical point. If the second derivative is negative, then the function is maximised at the critical point or otherwise, if the second derivative yields a positive quantity at a critical point, then the function attains the minimum at the stationary point. The other methods, namely scanning and bracketing procedure, Newton method and Quasi-Newton methods, are followed for optimising single variable functions.

Newton's method uses a quadratic model equation as equivalent to a given function for minimisation. If the objective function is quadratic in nature, then the minimum is obtained in one iteration. This method converges slowly when the value of the second derivative approaches zero. The quasi-Newton method finds the points that give the first derivative of the function $f(x)$ are of opposite sign. This approach for predicting the functions with opposite signs is called the "regula falsi" method or false position. The quadratic interpolation method is a type of uni-dimensional minimisation technique using function values only. This method is based on equating the actual objective function to a quadratic equation and is more efficient than other methods if the first derivative is continuous. In the cubic interpolation method, the actual function is approximated as a third degree polynomial, and then the stationary point of the polynomial is calculated after differentiating it once and equating the resulting expression to zero. To estimate the maximum or minimum, either four values of the function or two function values and two derivative values are required.

The multivariable functions are frequently encountered in modeling a process by RSM. These functions are subjected to constraints or may not be constraint dependent. The methods that are used to optimise a multivariable function are the grid search method, Simplex search method, steepest descent method, conjugate gradient method etc. In the wastewater treatment domain, the proposed model equations are mostly quadratic. The Eigenvalues of the Hessian matrix are calculated to interpret the nature of function at a stationary point. The shape of the contour curve and Eigenvalue relations are used to examine the nature of the multivariable function. If the Eigenvalues of the Hessian matrix is equal, then the shape of contours are circles, whereas elliptical contours are formed for well-behaved functions. The necessary and

sufficient conditions for optimising a multivariable second order quadratic function is that: the function is differentiable twice at a critical point, the gradient (slope) of the function is zero at the stationary point, and the Hessian matrix is positive-definite for a minimum to exist and becomes a negative-definite for a maximum to exist.

10 Recent Development and Future Scope

RSM is one of the conventional methods to develop the model equations and optimise the process variables in the textile wastewater treatment process. The scientific community has explored the applications of artificial neural networks and genetic algorithm to process modeling and parameter optimisation. The model equations are also developed using multiple linear regression techniques, and the variables are optimised using an imperialist competitive algorithm. The artificial neural network model based on utilising Levenberg–Marquardt algorithm composed of the linear transfer function is also used in the adsorption treatment of textile effluents. The wastewater treatment plants performance is also evaluated using a black-box modeling approach based on artificial neural networking. The influent characteristics of the textile treatment plant are modeled with different meta-heuristic algorithms using a fuzzy interference system. The model prediction accuracy and sensitivity is improved by incorporating more terms and coefficients in the equation. In future, the development of advanced software modules, algorithm codes, artificial intelligence systems and machine learning tools would improve the quality of model equations and minimise the efforts to get the desired solution.

11 Conclusions

The textile industry utilised a large volume of water and is considered a water intensive unit. A large quantity of different waste characteristics is generated from the textile processing unit. Identifying a suitable treatment strategy is difficult because of the complicated nature of the wastewater produced. Dye compounds are considered the major pollutants in textile wastewater. The characteristics of effluents have detrimental effects on the environmental components because they decrease the oxygen solubility level in water bodies, prevent light penetration into the aquatic ecosystem and disturb the photochemical activity in water bodies. The volatile chemicals are easily evaporated and absorbed by cells, affecting normal biological activities such as respiration, osmoregulation, and reproduction. The partially treated effluent or the raw effluent without any treatment adversely affect the natural ecosystem and is responsible for chronic and acute health implications.

Various treatment techniques, namely adsorption, coagulation, ozonation, electrochemical degradation, membrane separation and ultra-filtration, are used to remove

the pollutants from textile wastewater. The treatment techniques are broadly classified into biological, chemical and physical methods. Biological treatment is cheaper than chemical and physical methods because the microorganisms are easily available and are cost-effective. An integrated design approach is the need of the hour for the efficient operation of the wastewater treatment unit. The process equipment is designed using the Physico-chemical characteristics of raw textile wastewater. The kinetic study is essential because the rate equation elucidates the rate of pollutant degradation. Process modeling aims to represent the interrelationship between the process variables and parameters by means of mathematical expression. The response surface method is used to develop a process model and calculate the optimised process conditions. The optimisation conditions are evaluated using a contour plot, 3-D response surface plot. The quality of the models is adjudged by the statistical significance of the parameters in the ANOVA table and coefficient of determination. The optimisation is done to predict the best set of independent variables to produce the desired optimum response for the developed model equation. The efficiency of the treatment process depends on selecting the major process variables, developing the model equation that truly reflects the system characteristics, analysing the interactive effects between the variables and selecting the optimised conditions for the process. The modeling of the wastewater treatment plant is important to understand the process behaviour and modify the process equipment configuration.

Conflict of Interest The authors declare no conflict of interest.

References

- Abdulgader M, JimmyYu Q, Zinatizadeh AA, Williams P, Rahimi Z (2020) Application of response surface methodology (RSM) for process analysis and optimisation of milk processing wastewater treatment using multistage flexible fiber biofilm reactor. *J Environ Chem Eng* 8(3):103793. <https://doi.org/10.1016/j.jece.2020.103797>
- Bravo AD, Mailier J, Martin C, Rodríguez J, Aceves-Lara CA, VandeWouwer A (2011) Model selection, identification and validation in anaerobic digestion: a review. *Water Res* 45(17):5347–5364. <https://doi.org/10.1016/j.watres.2011.08.059>
- Correia VM, Stephenson T, Judd SJ (1994) Characterisation of textile wastewaters—a review. *Environ Tech* 15(10):917–929. <https://doi.org/10.1080/09593339409385500>
- Devi S, Murugappan A, Kannan PR (2015) Textile dye wastewater treatment using freshwater algae in packed-bed reactor: modeling. *Desalin Water Treat* 57(38):17995–18002. <https://doi.org/10.1080/19443994.2015.1085910>
- Elemen S, Kumbasar EPA, Yapar S (2012) Modeling the adsorption of textile dye on organoclay using an artificial neural network. *Dyes Pigm* 95(1):102–111. <https://doi.org/10.1016/j.dyepig.2012.03.001>
- Gökçek ÖB, Özdemir S (2020) Optimisation of the coagulation–flocculation process for slaughterhouse wastewater using response surface methodology. *Clean Soil Air Water* 48:7(8):2000033. <https://doi.org/10.1002/clen.202000033>
- Hassaan MA, Nemr AE (2017) Health and environmental impacts of dyes: mini review. *Am J Environ Sci Engg* 1(3):64–67. <https://doi.org/10.11648/j.ajese.20170103.11>

- Holkar CR, Jadhav AJ, Pinjari DV, Mahamuni NM, Pandit AB (2016) A critical review on textile wastewater treatments: possible approaches. *J Environ Manage* 182:351–366. <https://doi.org/10.1016/j.jenvman.2016.07.090>
- Jadhav MV, Mahajan YS (2014) Application of response surface methodology to water/wastewater treatment using *Coccinia indica*. *Desalin Water Treat* 52(34):6403–6411. <https://doi.org/10.1080/19443994.2013.821043>
- Marichamy M, Ramasamy K (2015) Modelling the kinetics of coagulation process for tannery industry effluent treatment using *Moringa oleifera* seeds protein. *Desalin Water Treat* 57(32):14954–14964. <https://doi.org/10.1080/19443994.2015.1070294>
- Moghadam MT, Qaderi F (2019) Modeling of petroleum wastewater treatment by Fe/Zn nanoparticles using the response surface methodology and enhancing the efficiency by scavenger. *Results Phys* 15:102566. <https://doi.org/10.1016/j.rinp.2019.102566>
- Okey-Onyesolua CF, Chukwuma EC, Okoye CC, Onukwulia OD (2020) Response surface methodology optimisation of chito-protein synthesised from crab shell in treatment of abattoir wastewater. *Heliyon* 6(10):e05186. <https://doi.org/10.1016/j.heliyon.2020.e05186>
- Popović S, Karadžić M, Cakl J (2019) Optimisation of ultrafiltration of cutting oil wastewater enhanced by application of twisted tapes: response surface methodology approach. *J Clean Prod* 231(10):320–330. <https://doi.org/10.1016/j.jclepro.2019.05.184>
- Report on assessment of pollution from textile dyeing units in Tirupur, Tamil Nadu and measures taken to achieve zero liquid discharge, Central pollution control board, Zonal office (south), Bengaluru, Government of India. 2014 p 11. <https://cpcb.nic.in/openpdffile.php?id=UmVwb3J0RmlsZXMvNDEwXzE0OTU3MTQzMzZfbWVkaWFwaG90bzQ1MjJucGRm>
- Sandhya S, Swaminathan S (2006) Kinetic analysis of treatment of textile wastewater in hybrid column upflow anaerobic fixed bed reactor. *Chem Eng J* 122(1–2):87–92. <https://doi.org/10.1016/j.cej.2006.04.006>
- Sharma S, Aygun A, Simsek H (2020) Electrochemical treatment of sunflower oil refinery wastewater and optimisation of the parameters using response surface methodology. *Chemosphere* 249:126511. <https://doi.org/10.1016/j.chemosphere.2020.126511>
- Singh B, Kumar P (2020) Pre-treatment of petroleum refinery wastewater by coagulation and flocculation using mixed coagulant: optimisation of process parameters using response surface methodology (RSM). *J Water pro Eng* 36:101317. <https://doi.org/10.1016/j.jwpe.2020.101317>
- Williams Y, Basitere M, Ntwampe SKO, Ngongang M, Njoya M, Kaskote E (2019) Application of response surface methodology to optimise the COD removal efficiency of an EGSB reactor treating poultry slaughterhouse wastewater. *Water Pract Technol* 14(3):507–514. <https://doi.org/10.2166/wpt.2019.032>

UV-Chlorination and Treatment of Oily Wastewater in Batch Ozone Reactor



Thirugnanasambandham Karchiyappan and Rama Rao Karri

Abstract Among various industry wastewater, oily industry wastewater, cause extensive pollution to water and soil. This wastewater contains oily substances include phenols, petroleum hydrocarbons and polyaromatic hydrocarbons, which are toxic and can inhibit the growth of plants and animals. To human beings, they also bring mutagenic and carcinogenic risks. Hence, there is high priority need to develop a efficient technology to treat oily industry wastewater. This research study aims to optimize the operating parameters in the ozonation and UV-chlorination process to remove chemical oxygen demand (COD) from oily wastewater using response surface methodology (RSM). Three factors three levels Box-Behnken response surface design (BBD) is used for optimization and mathematical model development. pH, ozonation time and retention time are selected as process variables in the ozonation process. pH, UV irradiation and chlorine dose are selected as process variables in the UV-chlorination process. Significant quadratic polynomial modes are obtained with a high coefficient determination value ($R^2 = 0.90$ for COD). Numerical optimization is employed to achieve optimum conditions, resulting in >85% COD removal in both ozonation and UV-chlorination processes.

Keywords Oily wastewater · COD removal · Ozonation · UV chlorination · Model development · Optimization

T. Karchiyappan (✉)

Department of Molecular Engineering, Lodz University of Technology, Wolczanska 213, 90-924 Lodz, Poland

Department of Chemistry, ECET, Komarapalaam 637 303, India

R. R. Karri

Petroleum and Chemical Engineering, Faculty of Engineering, Universiti Teknologi Brunei, 1410 Bandar Seri Begawan, Brunei Darussalam

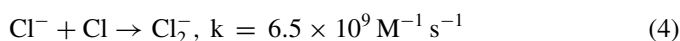
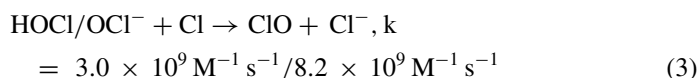
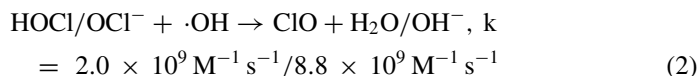
1 Introduction

Waters that do not present good quality represent a threat to human health due to the possibility of infectivity of populations through waterborne diseases (Mohan et al. 2007; Gotsi et al. 2005). One of the main sources of water pollution is the release of raw industry wastewater that has not undergone efficient treatment, thus constituting a potential load of pathogenic organisms excreted by infected individuals. Among various industry wastewater, oily industry wastewater, which can cause extensive pollution to water and soil. Oily wastewater is produced from various sources, e.g., oil/gas recovery, metal finishing, mining, transportation and oil refining (Aksu 2005). This wastewater contains oily substances include phenols, petroleum hydrocarbons and polyaromatic hydrocarbons, which are toxic and can inhibit the growth of plants and animals. To human beings, they also bring mutagenic and carcinogenic risks. Indian government regulations forbid direct disposal of oily wastewater, and oils in the wastewater should be removed to meet the discharge standard. Generally, oily industry wastewater contains oils in different forms, including free-floating oils, unstable dispersed oils and stable emulsified oils (Hameed and Ahmad 2009). Hence, there is critical to developing efficient technology to treat oily industry wastewater.

To eliminate emerging contaminants from wastewater and make wastewater reclamation possible, numerous investigations have focused on advanced oxidation processes (AOPs). Advanced oxidation processes (AOP) are technologies characterized by the generation of hydroxyl radicals, which are highly reactive and non-selective substances used to degrade toxic organic compounds present in wastewater. These AOPs for oily wastewater include electrochemical oxidation, Fenton oxidation, wet air oxidation, UV/H₂O₂, and photocatalytic degradation (Cooper 1993). Due to the high organic load of OMW, these processes generally require the addition of large amounts of reagents, which raises the problem of the production of putrescible sludge and the high cost of used products. Most AOPs degrade contaminants by generating highly reactive species, namely hydroxyl radical ($\cdot\text{OH}$), which have reduction potentials of 2.8 V. Combination of UV irradiation and chlorine (UV/chlorine) is a relatively new interested AOP in which UV/chlorine also generates other reactive species such as $\text{Cl}\cdot$ and Cl_2 , which are thought to have played important roles in the degradation of micropollutants (Ohea et al. 2004). Although the reduction potentials of $\text{Cl}\cdot$ (2.4 V) and Cl_2 (2.0 V) are lower than that of $\cdot\text{OH}$, they are more selective and can react with electron-rich moieties more rapidly than $\cdot\text{OH}$.

Ozonation is an alternative process for treating wastewater. Since ozone is a very powerful oxidant (2.07 V for ozone versus 2.8 V for hydroxyl radical) mainly used for the disinfection process, it has a strong cell lytic activity that can kill the microorganisms in the wastewater (Hermanowicz et al. 1999). Once dissolved in water, ozone reacts with many organic compounds in two ways: direct oxidation, as molecular ozone, or indirect reaction through the formation of secondary oxidants such as free radicals, particularly hydroxyl radicals. Moreover, under UV light, free chlorine can simultaneously produce $\cdot\text{OH}$ and reactive chlorine species (RCS), including chlorine ($\text{Cl}\cdot$), chlorine oxide ($\text{ClO}\cdot$) and dichloride anion ($\text{Cl}_2\cdot^-$) radicals (Eqs. 1–4).

Both $\cdot\text{OH}$ and RCS can decompose certain pollutants in wastewater (Gao et al. 2020; Nikravesh et al. 2020).



From the literature review, it is found that comparative treatment study of oily industry wastewater using ozonation and UV-chlorination is not yet studied in detail using statistical tools. The conventional optimization technique of changing one variable at a time to study the effects of variables on the response is time-consuming and expensive, particularly for multivariable systems. Statistical design of experiments includes response surface methodology (RSM) coupled with Behnken response surface design (BBD); it is one of the statistical tools mainly used for the modelling and investigation of multivariable systems in which several variables influence the response of interest. Hence, in this study, an attempt has been made to investigate the individual and interactive effects of ozonation and UV-chlorination process on the COD removal from oily industry wastewater using RSM coupled with three factors three levels Box-Behnken response surface design (BBD). This is the first study to compare the treatment efficiency of oily wastewater using ozonation and UV-chlorination process using the statistical tool.

2 Materials and Methods

2.1 Wastewater Source

The raw wastewater was obtained from a conventional oily wastewater treatment plant in Erode district, Tamil Nadu, India. Sample collection and characterization were performed according to the standard methods, and the initial parameters analyzed are given in Table 1. Standard solutions were purchased from Sigma-Aldrich, Chennai, Tamil Nadu. All other chemicals were at least of analytical grade and were used without further purification. All solutions were prepared with ultrapure water produced from a Milli-Q water purification system.

Table 1 Physico chemical properties of oily wastewater

Characteristics	Values
Turbidity, NTU	865
COD, mg/l	6500
pH	6
Conductivity, ms/cm	0.85
Total dissolved solids, mg/l	4500
Color, Pt-Co	75
BOD, mg/l	2758
TOC, mg/l	313

2.2 Experimental Setup

The ozonation of oily wastewater experimental setup (Ozone reactor) consisted of an oxygen concentrator, ozone generator with built-in oil-free compressor and reaction column. A controlled flow rate of 2 l/min of oxygen was used to produce 2 g/h of ozone. The reactor had a glass column of 54 cm height, an outer diameter of 3.8 cm, and an inner diameter of 2.8 cm and could hold 1000 mL of wastewater. It was provided with a sample port at various points, an ozone gas inlet at the bottom with an air diffuser over the inlet port to diffuse the oxygen/ozone gas mixture through the column, and a closed top with a collection port to collect the unreacted ozone gas venting it out. The experiments were carried out in various pH, ozonation time and retention times. The UV-chlorination equipment consists of a low-pressure UV Hg lamp was used for oily wastewater treatment. The average irradiation strength on the solution was calculated to be approximately $261 \mu\text{W cm}^{-2}$, using atrazine chemical actinometry. Before each experiment, the lamp was turned on for at least 30 min to stabilize the lamp output. The experiments were carried out in various pH, irradiation and chlorine doses. After both processes, the sample was withdrawn and filtered for COD determination. All the experiments were performed in triplicates, and the reported result is the mean of these triplicate measurements.

2.3 Experimental Procedure

The pH of the oily wastewater was adjusted using 1 N HCl and 1 N NaOH by pH meter. Chemical oxygen demand (COD) was measured following APHA standard methods. The removal of COD from oily wastewater is calculated as follows

$$RE = \left(\frac{c_0 - c_e}{c_0} \right) \times 100 \quad (5)$$

where c_0 and c_e are the initial and after treatment concentrations of COD.

2.4 Modeling Procedure

Design- Expert 8.0.7.1 (State-Ease Inc., Minneapolis, MN, USA) statistical package was employed for modelling (Three factors three-level Box-Behnken design (BBD)) and optimization of both ozonation and UV-chlorination process for oily wastewater treatment. The independent variables, namely pH (A_1), ozonation time (B_1) and retention time (C_1), were examined over COD removal (Y_1) in the ozonation process. Meanwhile, the independent variables, namely pH (A_2), irradiation (B_2) and chlorine dose (C_2), were examined over COD removal (Y_2) in the UV-chlorination process. Seventeen experiments were designed with five replications by BBD for each process. The correlation between the response and independent variables were evaluated by developing the second-order polynomial mathematical model, and the generalized form of equation was given below (Dong et al. 2011)

$$Y = \beta_0 + \sum_{j=1}^k \beta_j X_j + \sum_{j=1}^k \beta_{jj} X_j^2 + \sum_i \sum_{<j=2}^k \beta_{ij} X_i X_j + e_i \quad (6)$$

Later, the developed mathematical model was used to plot the three-dimensional response surface contour plots. Validation of the developed model was carried out by plotting actual versus predicted graphs and ANOVA analysis. Finally, numerical optimization was employed to optimize the process variables for the maximum COD removal from oily wastewater.

3 Results and Discussions

3.1 BBD Modeling

The BBD design with results of RSM experiments for ozonation and UV-chlorination process are shown in Table 2. To obtain second-order polynomial models, this experimental data were fitted to the various models (linear, interactive (2FI), quadratic and cubic). A sequential model sum of squares (Table 3) and model summary statistics (Table 4) was examined to determine model fitness. They indicate that linear and interactive (2FI) models were shown lower R², adjusted R², and predicted R² compared with second-order polynomial models (Murugesan et al. 2007). The cubic model was found to be aliased. Hence, the quadratic models incorporating linear, interactive and quadratic terms were chosen to describe process variables' effects on COD removal from oily wastewater. The developed second-order polynomial equation in terms of coded factors are given below

$$Y_1 = 91.71 - 0.23A_1 + 0.11B_1 + 0.36C_1 + 1.84A_1B_1 - 0.91A_1C_1 - 0.34B_1C_1 - 2.20A_1^2 - 0.87B_1^2 - 0.95C_1^2 \quad (7)$$

Table 2 BBD and their experimental results

S.No	A ₁	B ₁ (min)	C ₁ (min)	Y ₁ (%)	A ₂	B ₂ (mW/cm ²)	C ₃ (mM)	Y ₂ (%)
1	7	10	6	91.58	7	0.6	0.08	84.21
2	7	10	6	91.81	7	0.6	0.08	84.21
3	7	10	6	91.81	7	0.6	0.08	84.21
4	9	10	3	88.54	9	0.6	0.04	81.53
5	9	5	6	86.47	9	0.2	0.08	80.23
6	5	10	9	90.39	5	0.6	0.12	77.53
7	7	15	9	89.69	7	1	0.12	82.33
8	9	10	9	87.88	9	0.6	0.12	79.23
9	7	5	3	89.39	7	0.2	0.04	81.83
10	7	10	6	91.81	7	0.6	0.08	84.21
11	5	10	3	87.43	5	0.6	0.04	76.23
12	7	10	6	91.55	7	0.6	0.08	84.21
13	7	5	9	90.39	7	0.2	0.12	83.85
14	5	5	6	90.37	5	0.2	0.08	76.01
15	5	15	6	87.13	5	1	0.08	81.34
16	9	15	6	90.58	9	1	0.08	84.15
17	7	15	3	90.07	7	1	0.04	82.53

$$Y_2 = 84.21 + 1.75A_2 + 1.05B_2 + 0.10C_2 - 0.35A_2B_2 - 0.90A_2C_2 - 0.55B_2C_2 - 3.89A_2^2 + 0.11B_2^2 - 1.69C_2^2 \quad (8)$$

whereas Y_1 is COD removal in the ozonation process and Y_2 is COD removal in the UV-chlorination process. Moreover, A_1 , B_1 and C_1 are pH, ozonation time (min) and retention time (min). Whereas, A_2 , B_2 and C_2 are pH, UV/chlorination (mW/cm²) and chlorine dose (mM). Statistical analysis of the developed mathematical models (Y_1 and Y_2) was evaluated using ANOVA. The ANOVA for the model is shown in Table 5. The quadratic regression model showed that the determination coefficient (R^2) value is greater than 0.90, which shows that the model could explain 90% of the variations. Adj- R^2 should be close to R^2 for a good model; as shown in Table 5, adj- R^2 is greater than 0.95, implying that the developed model did not explain only less than 5.0% of the total variations. It also confirmed a high degree of correlation between the observed and predicted values. A low CV value indicated good reliability of the experiment's values (Moulai-Mostefa and Tir 2004). The corresponding variables would be more significant if the F-value becomes greater and the p-value becomes smaller. The results show that the developed model shows a high F-value and low p-value, which indicates the ability of the developed mathematical model. Also, the adequacy of the model is examined by constructing a diagnostic plot, namely

Table 3 Sequential model sum of squares for response

Source	Sum of squares	Df	Mean square	F value	Prob > F	Remarks
<i>Y₁</i>						
Mean	4807.83	1.00	4807.83	–	–	–
Linear	1.58	3.00	0.53	0.14	0.9319	–
2FI	17.26	3.00	5.75	1.89	0.1958	–
Quadratic	29.86	3.00	9.95	109.35	<0.0001	Suggested
Cubic	0.56	3.00	0.19	10.39	0.0233	Aliased
Residual	0.07	4.00	0.02	–	–	–
Total	4857.17	17.00	285.72	–	–	–
<i>Y₂</i>						
Mean versus total	113,299.99	1.00	113,299.99	–	–	–
Linear versus mean	33.57	3.00	11.19	1.49	0.2637	–
2FI versus linear	4.97	3.00	1.66	0.18	0.9085	–
Quadratic versus 2FI	79.06	3.00	26.35	13.49	0.0027	Suggested
Cubic versus quadratic	13.67	3.00	4.56	63,660,000.00	<0.0001	Aliased
Residual	0.00	4.00	0.00	–	–	–
Total	113,431.26	17.00	6672.43	–	–	–

Table 4 Model summary statistics for response

Model	Model summary statistics					
	Std.Dev	R ²	Adjusted R ²	Predicted R ²	PRESS	Remarks
<i>Y₁</i>						
Linear	1.9166	0.0321	–0.1913	–0.6737	82.6	–
2FI	1.7463	0.3819	0.0110	–0.7110	84.4	–
Quadratic	0.3017	0.9871	0.9705	0.8146	9.1473	Suggested
Cubic	0.1346	0.9985	0.9941		+	Aliased
<i>Y₂</i>						
Linear	2.7414	0.2558	0.0840	–0.3148	172.6	–
2FI	3.0451	0.2936	–0.1302	–1.6189	343.8	–
Quadratic	1.3974	0.8959	0.7620	–0.6662	218.7164	Suggested
Cubic	0.0000	1.0000	1.0000	–	+	Aliased

Table 5 ANOVA table for response

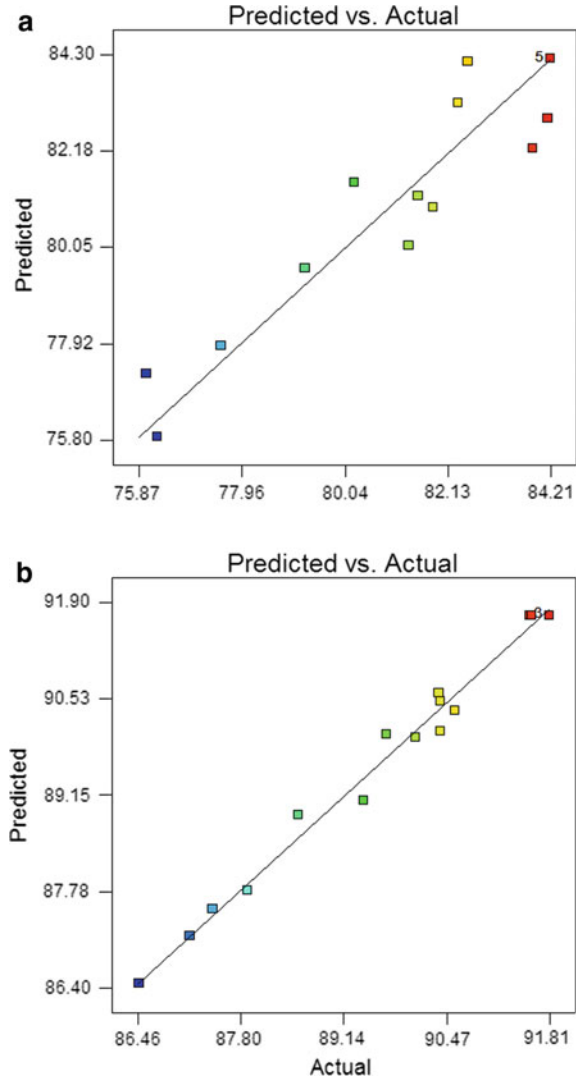
Source	Y1			Y2		
	Sum of squares	F value	P value	Sum of squares	F value	P value
Model	117.599	6.69108	0.0101	48.7004	59.4535	<0.0001
A	24.6051	12.5998	0.0093	0.42781	4.70046	0.0668
B	8.88311	4.54885	0.0704	0.09031	0.99228	0.3524
C	0.08405	0.04304	0.8416	1.0658	11.7102	0.0111
AB	0.49703	0.25452	0.6294	13.5056	148.389	<0.0001
AC	3.24	1.65913	0.2387	3.2761	35.9952	0.0005
BC	1.2321	0.63093	0.4531	0.4761	5.23101	0.0560
A ²	63.7551	32.6476	0.0007	20.3743	223.857	<0.0001
B ²	0.05448	0.0279	0.8721	3.22184	35.399	0.0006
C ²	12.0079	6.14899	0.0422	3.81802	41.9494	0.0003
CV%	5.83	–	–	7.68		
AP	23.69	–	–	28.87		

predicted versus actual plot (Fig. 1). The data points lie very close to the diagonal line depicts a good relationship between experimental and predicted data.

3.2 Effect of Process Variables on COD Removal

The relationship between process parameters and response (COD removal) are illustrated by the representation of surface contours plots generated by the developed mathematical models (Fig. 2). In this study, the model has more than two factors. So, the response surface contour plots are drawn by maintaining one factor at a constant level (in turn at its central level), whereas the other two factors were varied in their range. pH is selected as one of the variables and varies from acidic to alkaline (5–9). It was found that COD removal (76%) is observed in pH 5.9. As pH increased to alkaline conditions, COD removal decreased to 42%. Maximum COD removal (86%) is achieved at acidic pH (6.3). Compared to acidic pH 6.3, neutral and alkaline pH had less COD removals of 79% and 72%, respectively. This result implicates that acidic pH is favourable for COD removal. This phenomenon can be explained by the fact that the solubility of ozone is readily affected by pH. The influence of pH results from the relationship between oxidation potential and decomposition behaviour of ozone. In acidic pH, the ozone is available as molecular ozone, and in alkaline pH, it decomposes into secondary oxidants such as OH, HO₂, HO₃, and HO₄. OH is important and has the highest oxidation potential of 2.8 V (Garg and Prasad 2016). The oxidizing potential of ozone decreased from 2.08 V at acidic pH to 1.4 V in alkaline solutions. This indicates that the ozone reaction decreases with increasing pH resulting in the generation of secondary oxidants. Whereas UV-chlorination, COD

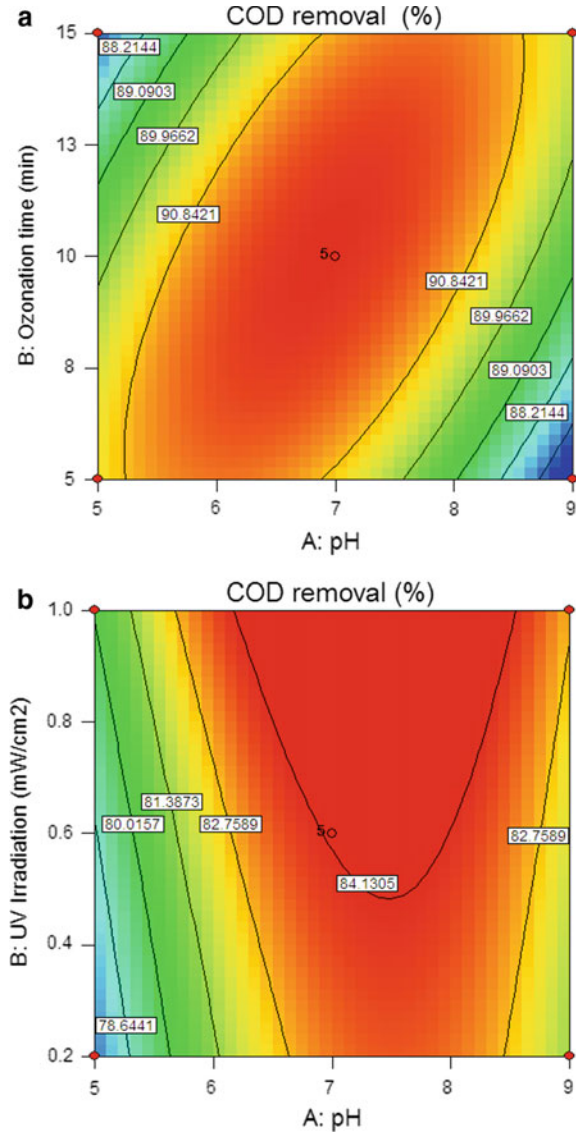
Fig. 1 Model adequacy plot



removal is increased up to pH of 6 (Fig. 2). After that, there is a drastic decrease in COD removal. In earlier studies, this is attributed to the higher quantum yields and the lower radical quenching rate in acidic conditions than in alkaline conditions. Also, it is reported that the OH quantum yield of UV/chlorine decreased more rapidly with increasing pH in acidic solutions than in basic solutions (Liu et al. 2017).

The effect of ozonation time on COD removal is shown in Fig. 2. Maximum COD removal (87%) is obtained at 8 min. As ozonation after 8 min increased, COD removal decreased up to 72%. It indicates that low ozonation time is in favour of COD removal. This result reveals that prolongation of the ozonation process causes

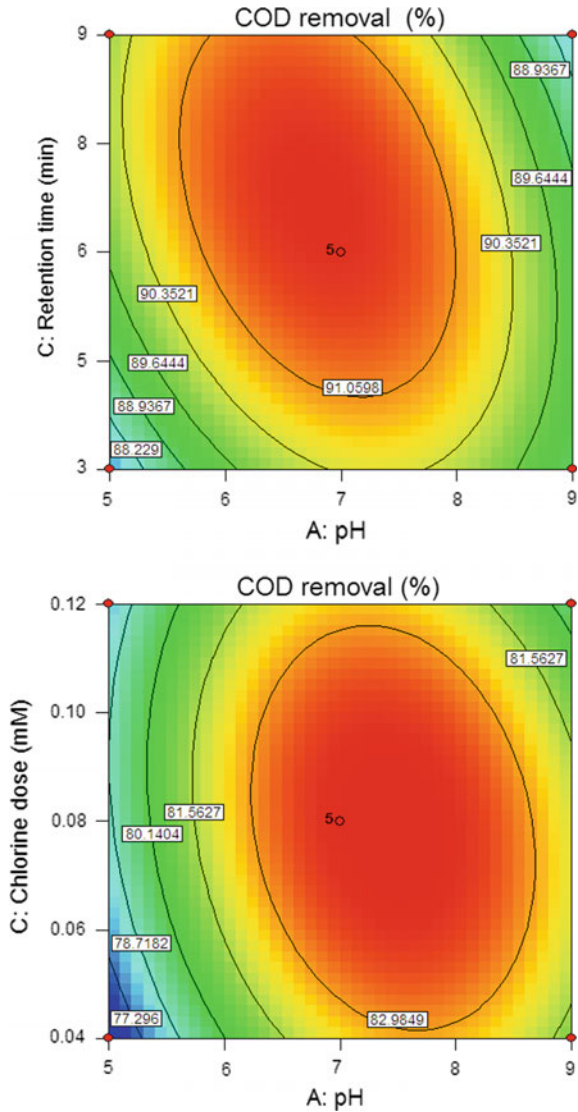
Fig. 2 Plots for COD removal (Ozonation time)



the ozone to gradually lose its ability to oxidize the organic molecules (Paz-Pino et al. 2014). Ozone first reacts with the soluble portion of the wastewater and then attacks the particulate fraction. With an increase in ozone time, more intracellular substances are released. The soluble portion has a screening effect on the particulate matter attacked by ozone, which results in little improvement in COD removal at higher ozone doses. UV irradiance and chlorine dose are two essential parameters of the UV/chlorination process. So, experiments are carried out with various UV

irradiance and chlorine dose, and the results are shown in Fig. 3. The results show that COD removal is increased with increasing UV irradiance and chlorine dose. This is because full photon absorbance would be reached at a higher chlorine dose and UV irradiance (Cardona et al. 2013). The effect of retention time on COD removal is shown in Fig. 4. Maximum COD reduction (80.5%) is obtained in a retention time of 7 min. As the retention time after 7 min increased, COD removal decreased to 70%. This may be due to the higher retention time that negatively affects COD removal (Israilides et al. 1997).

Fig. 3 Plots for COD removal (UV-chlorination)



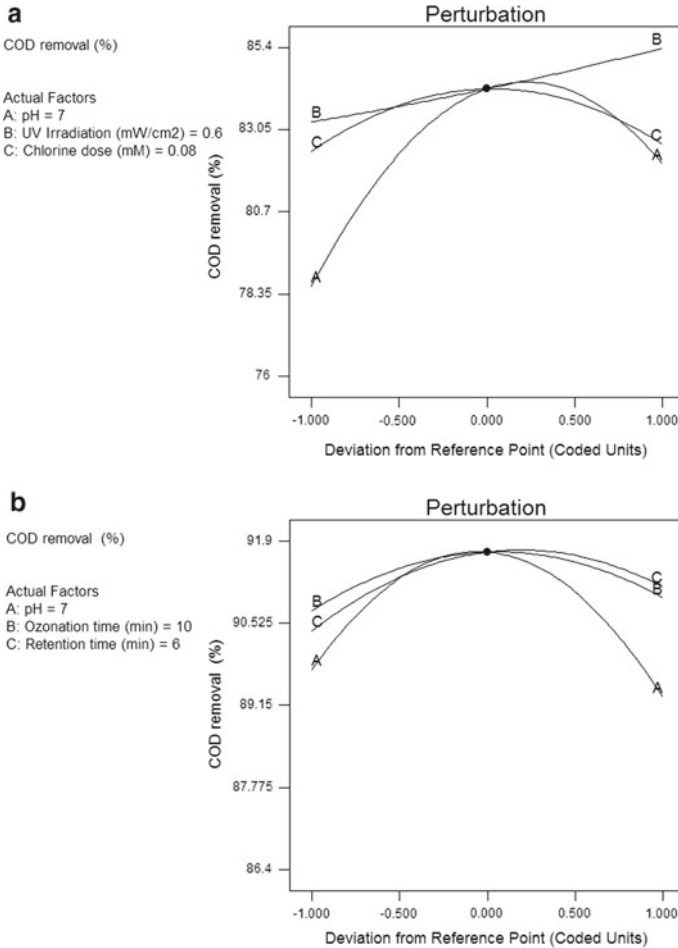


Fig. 4 Perturbation plot for COD removal

3.3 Optimization of Process Parameters for COD Removal

According to the BBD results, the optimal extraction conditions to obtain maximum COD removal are determined by Derringer’s desired function methodology. Optimum conditions for the ozonation process are found to be; pH of 6, ozonation time of 9 min and retention time of 7 min. Under these conditions, 92% of COD is removed. Optimum conditions for the UV-chlorination process are found to be; pH of 6, UV irradiation of 1 mW/cm² and chlorine dose of 0.07 mM. Under these conditions, 85% of COD is removed. The suitability of the optimized conditions for predicting the optimum response values is tested using the selected optimal conditions (Bellakhal et al. 2006). Additional experiments using the predicted optimum

Table 6 Comparative study of oily wastewater treatment

S. no.	Pollutant removal	Methods	References
1	COD removal	Ozonation-assisted electro-membrane hybrid reactor	Khalifa et al. (2021)
2	Oil removal	Ultrafiltration and ozone	Chang et al. (2001)
3	Oil removal	Chitosan, alum and PAC	Ahmad et al. (2006)
4	Oil removal	Coagulation/sand filter	Almojjly et al. (2018)
5	COD removal	Ozonation	Current study
6	COD removal	UV-chlorination	Current study

conditions for both the process and a mean value $L \pm 0.45\%$ ($N = 3$) (L may be Y_1 and Y_2) are obtained from the experimental, which agrees with the predicted values from Derringer's desirability function method.

3.4 Comparative Study of Oily Wastewater Treatment

To compare the study of oily wastewater treatment, various methods were examined and shown in Table 6 and shows the maximum efficiency of methods used in the current study.

4 Conclusion

Response surface methodology coupled with three factors three-level Box-Behnken design (BBD) was employed to optimize the process variables for ozonation and UV-chlorination process to remove chemical oxygen demand (COD) from oily wastewater. A second-order polynomial mathematical model was developed with a good coefficient of determination values ($R^2 > 0.95$) for both processes. Analysis of variance (ANOVA) showed the significant effect of each process variable on COD removal. Optimum conditions for this ozonation process were: pH of 6, ozonation time of 9 min, and retention time of 7 min. Under these conditions, 92% of COD was removed. Optimum conditions for this UV-chlorination process were found to be; pH of 6, UV irradiation of 1 mW/cm^2 and chlorine dose of 0.07 mM. Under these conditions, 85% of COD was removed. These results confirm the ability of the ozonation and UV-chlorination process as an effective technique to remove COD from oily wastewater.

References

- Ahmad AL, Sumathi S, Hameed BH (2006) Coagulation of residue oil and suspended solid in palm oil mill effluent by chitosan, alum and PAC. *Chem Eng J* 118:99–105
- Aksu Z (2005) Application of biosorption for the removal of organic pollutants: a review. *Process Biochem* 40:997–1026
- Almojjly A, Johnson D, Oatley-Radcliffe DL, Hilal N (2018) Removal of oil from oil-water emulsion by hybrid coagulation/sand filter as pre-treatment. *J Water Process Eng* 26:17–27
- Khalifa O, Banat F, Srinivasakannan C, AlMarzooqi F, Hasan SW (2021) Ozonation-assisted electro-membrane hybrid reactor for oily wastewater treatment: a methodological approach and synergy effects. *J Clean Prod* 289:125764
- Bellakhal N, Oturan MA, Dachraoui M (2006) Olive oil mill wastewater treatment by the electro-Fenton process. *Environ Chem* 3:345–349
- Cardona C, Machuca-Martínez F, Cabrales NM (2013) Treatment of vinasse by using electro-dissolution and chemical flocculation. *Ingeniería y Competitividad*. 15:191–200
- Chang I-S, Chung CM, Han SH (2001) Treatment of oily wastewater by ultrafiltration and ozone. *Desalination* 133(3):225–232
- Cooper PJ (1993) Removing colour from dyehouse waste waters—a critical review of technology available. *Soc Dyers Colour* 109:97
- Dong Y, Wang G, Jiang P, Zhang A, Yue L, Zhang X (2011) Simple preparation and catalytic properties of ZnO for ozonation degradation of phenol in water. *Chin Chem Lett* 22:209–212
- Gao YQ., Gao NY, Chen JX, Zhang J, Yin DQ (2020) Oxidation of β -blocker atenolol by a combination of UV light and chlorine: kinetics, degradation pathways and toxicity assessment. *Sep Purif Technol* 231:115927
- Garg KK, Prasad B (2016) Treatment of multicomponent aqueous solution of purified terephthalic acid wastewater by electrocoagulation process: optimization of process and analysis of sludge. *J Taiwan Inst Chem Eng* 60:383–393
- Gotsi M, Kalogerakis N, Psillakis E, Samaras P, Mantzavinos D (2005) Electrochemical oxidation of olive oil mill wastewaters. *Water Res* 39:4177–4187
- Hameed BH, Ahmad AA (2009) Batch adsorption of methylene blue from aqueous solution by garlic peel, an agricultural waste biomass. *J Hazard Mater* 164:870–875
- Hermanowicz W, Dojlido J, Dożańska W, Kozirowski B, Zerbe J (1999) (Arkady) Physical and chemical examination of water and wastewater, Warszawa (in Polish)
- Israilides CJ, Vlyssides AG, Mourafeti VN, Karvouni G (1997) Olive oil wastewater treatment with the use of an electrolysis system. *Bioresour Technol* 61:163–170
- Liu B, Qu F, Liang H, Gan Z, Yu H, Li G, Bruggen BV (2017) Algae-laden water treatment using ultrafiltration: individual and combined fouling effects of cells, debris, extracellular and intracellular organic matter. *J Membr Sci* 528:178–186
- Mohan N, Balasubramanian N, Basha CA (2007) Electrochemical oxidation of textile wastewater and its reuse. *J. Hazardous Materials*. 147:644–651
- Moulai-Mostefa N, Tir M (2004) Coupling flocculation with electroflotation for waste oil/water emulsion treatment. *Optim Operat Cond Desalin* 161:115–121
- Murugesan K, Dharmija A, Nam IH, Kim YM, Chang YS (2007) Decolourization of reactive black 5 by laccase: optimization by response surface methodology. *Dyes Pigment* 75:176–184
- Nikravesh B, Shomalnasab A, Nayyer A, Aghababaei N, Zarebi R, Ghanbari F (2020) UV/Chlorine process for dye degradation in aqueous solution: mechanism, affecting factors and toxicity evaluation for textile wastewater. *J Environ Chem Eng* 8(5):104244
- Ohea T, Watanabeb T, Wakabayashic T (2004) Mutagens in surfacewaters: a review. *Mutat Res* 567(2–3):109–149
- Paz-Pino OL, Barba LE, Cabrales NM (2014) Vinasse treatment by coupling of electro-dissolution, hetero-coagulation and anaerobic digestion. *Dyna* 8:187–195. *rev.fac.nac.minas*

Sol–gel Synthesis of Kaolin/TiO₂ Nanocomposites for Photocatalytic Degradation of Tannery Wastewater



S. Mustapha, J. O. Tijani, T. C. Egbosiuba, A. Sumaila, T. A. Amigun, A. B. Salihu, Y. O. Ibrahim, M. M. Ndamitso, and S. A. Abdulkareem

Abstract In this study, a TiO₂ immobilized on kaolin was synthesized by the sol–gel route. The surface morphology, chemical and phase composition of the kaolin, synthesized TiO₂ nanoparticles, and their nanocomposites were investigated using high-resolution scanning electron microscopy (HRSEM), RAMAN spectroscopy, high-resolution transmission electron microscopy (HRTEM) coupled with energy dispersive spectroscopy (EDX) and selected area electron diffraction (SAED). The influence of operational parameters such as irradiation time and catalyst dosage were evaluated. The influence of irradiation light on the degradation of chemical oxygen demand (COD) and total organic carbon (TOC) in tannery wastewater was found to be highest in 90 min, which follows a linear removal efficiency. It was evident that the photocatalytic degradation rate initially increases with catalyst loading and then decreases at high values. Almost complete decolourization was obtained upon 90 min of sunlight irradiation in the presence of kaolin/TiO₂ catalyst. The satisfactory stability in recyclability of photocatalyst indicates colour, COD and TOC abatement in tannery wastewater treatment. It is clear that photocatalysis has good potential to degrade organic pollutants. Thus, there is a need to determine the degradability performance on a commercial scale.

S. Mustapha (✉) · J. O. Tijani · A. Sumaila · M. M. Ndamitso
Department of Chemistry, Federal University of Technology, PMB 65, Bosso Campus, Minna, Nigeria

S. A. Abdulkareem
Department of Chemical Engineering, Federal University of Technology, PMB 65, Gidan Kwano Campus, Minna, Niger State, Nigeria

S. Mustapha · J. O. Tijani · T. C. Egbosiuba · A. Sumaila · Y. O. Ibrahim · M. M. Ndamitso · S. A. Abdulkareem
Nanotechnology Research Group, Africa Center of Excellence for Mycotoxin and Food Safety, Federal University of Technology, PMB 65, Minna, Niger State, Nigeria

T. A. Amigun
Department of Chemical and Geological Sciences, Al-Hikmah University, Ilorin, Nigeria

A. B. Salihu
Department of Chemical Sciences, Federal Polytechnic, Bida, Niger State, Nigeria

Keywords Immobilized · Synthesized · Operational parameter · Catalyst dosage · Organic pollutants

1 Introduction

Water pollution is one of the most concerning human health and sustainability challenges. Industrial sectors are principally responsible for thousands of organic and inorganic contaminants associated with wastewater released worldwide. These unregulated contaminants comprise pharmaceuticals, herbicides, and heavy metals. Organic and inorganic substances discharged from many industries such as metal plating, tanneries, mining, smelting, food processing, battery and smelting industries do not degrade into harmless end products, thus causing threats to humans and the environment (Engwa et al. 2019; Dehghani et al. 2021; Karri et al. 2021).

Various treatment technologies have been used to remove heavy metals from wastewater. These methods include coagulation/flocculation, ozonation, membrane filtration, photocatalyst, precipitation, and ion exchange (Crini and Lichtfouse 2019). Besides, most of these methods have their advantages and limitations in terms of capital cost, efficiency and operational conditions. However, the adsorption technique has been proposed as an alternative measure for removing heavy metals from wastewater (Nabbou et al. 2019; Khan et al. 2021; Mehmood et al. 2021; Lingamdinne et al. 2022). This method is considered to be simple, promising and effective for wastewater treatment due to its high adsorption capacity and insensitivity to heavy metals.

Nowadays, adsorbents like zeolites, activated carbon, nanoparticles, clay minerals and others are used for wastewater treatment. Currently, nanoparticles have received huge attention in treating wastewater globally (Mehmood et al. 2021). Some limitations in using these nanoparticles are the low adsorption capacity of hydrophobic pollutants related to its low surface area affecting the removal efficiency of contaminants. Other related issues of nanoparticles application in wastewater treatment are particle agglomeration and formation of suspension in water. Other practical problems are catalyst agglomeration and the formation of uniform suspension in water which makes it difficult to separate. This implies that removing these nanoparticles could require costly phase separation methods. It was reported by Mahvi et al. (2009) that the separation and recovery of TiO_2 nanoparticles from treated wastewater are expensive and time-consuming. They concluded that the depth of UV penetration was reduced due to strong absorption between TiO_2 and dye solution, and this problem could be solved by anchoring TiO_2 nanoparticles on the surface of the support adsorbent. But if these nanoparticles are embedded in clay minerals such as kaolin, bentonite and montmorillonite, the environmental problems will be reduced. Clay minerals are highly porous materials with a large surface area for physical and chemical reactions on their surfaces (Boruah et al. 2019). Therefore, their applications in adsorption processes are essential. Owing to these aforementioned merits, the interaction of nanoparticles with clay minerals will be of interest in solving separation problems of nanoparticles in water.

Furthermore, it is expected that the photocatalytic oxides coupled with clay favoured the photocatalyst via reduction of the bandgap due to the closeness oxides. Thus, the mechanical properties of photocatalyst enhance the photodegradation of pollutants in an aqueous solution (Silvestri and Foletto 2017; Ahmed et al. 2021). Various research articles reported the use of nanoparticles-clay composites to remove contaminants from wastewater (Mehmood et al. 2021). Among the studies carried out were the adsorption of methylene blue (MB) using titanium oxide/tungsten oxide/bentonite nanocomposites (Yang et al. 2015), synthesized clay/titanium oxide for the removal of lead, cadmium, copper and zinc ions from aqueous solution (Dukic et al. 2015), the use of titanium oxide/clay composites for removal of MB and cadmium ion (Aliou et al. 2018), the adsorption and photodegradation activities of titanium oxide/bentonite on the removal of dyes (Laysandr et al. 2017) and the photocatalytic effect using dyes on synthesized titanium oxide/clay nanocomposites (Mishra et al. 2017). To the best of our information, the photocatalysis application of kaolin as support to immobilized titanium oxide for the removal of total organic carbon (TOC) and chemical oxygen demand (COD) from tannery wastewater is scarce in the literature. In this present study, kaolin, TiO₂ and kaolin/TiO₂ were characterized by morphology, optical and structural properties. In addition, the influence of parameters such as time and catalyst dosage, the point of zero change effect on kaolin, TiO₂ and kaolin/TiO₂ and the effect of the photocatalytic properties in decolourization of tannery wastewater under sunlight have been demonstrated.

2 Materials and Methods

2.1 Materials

Raw kaolin was obtained from a clay deposit in Gbako Local Government Area in Niger State, Nigeria. The collected tannery wastewater from Majema Tannery industry, Manuri Road, Tudun Wada Area, Sokoto State was characterized for chemical oxygen demand (COD) using the method as described by the American Public Health Association (APHA) (2017), while total organic carbon (TOC) was determined using a TOC analyzer (model, Shimadzu, 5050A). Titanium tetraisopropoxide (TTIP, 97%), sodium hydroxide (NaOH, $\geq 97\%$), hydrochloric acid (HCl, 37%), and hydrogen peroxide (H₂O₂) were procured from Sigma Aldrich. All the reagents were analytical grade.

2.2 Kaolin Preparation

Exactly 20.0 g raw kaolin sample was weighed in a 250 cm³ beaker containing 5 cm³ H₂O₂, which acts as a bleaching agent and 20 cm³ of 1.0 M HCl to dissolve

undesirable soluble contents. The mixture was stirred with a glass rod for some time and allowed to stand for 12 h. Solution of three layers (water, finer particles and fine particles) was formed. The first and second layers (water and finer particles) were decanted from the solution into a separate 250 cm³ beaker, washed with de-ionized water many times until neutral (pH 7). The kaolin paste was dried at 105 °C for 5 h to evaporate the water and calcined at 450 °C for 3 h, crushed with mortar and pestle.

2.3 *TiO₂ Nanoparticle Preparation*

TiO₂ nanoparticles were prepared using the sol–gel method. A 5 cm³ of titanium isopropoxide was measured, added to 50 cm³ of de-ionized water in a 250 cm³ beaker and then stirred at 180 rpm for 1 h. The resultant mixture was adjusted to pH 7 using 0.1 M aqueous NaOH solution with continuous magnetic stirring at 180 rpm for 3 h. The mixture was washed copiously with de-ionized water to remove free ions, dried at 105 °C in an oven for 12 h, crushed and calcined at 450 °C for 3 h.

2.4 *TiO₂/Kaolin Preparation*

A 5.0 g beneficiated kaolin was weighed in a 200 cm³ beaker, and 50 cm³ of ionized water was stirred at 180 rpm for 30 min, and 1 cm³ of TTIP was added to the stirred kaolin suspension. The resultant kaolin/TiO₂ was adjusted until pH 7 and washed with de-ionized water to remove free soluble ions. The wet composite kaolin/TiO₂ was dried in an oven at 105 °C for 3 h and stored for catalysis.

2.5 *Point of Zero Charge*

The pH_{pzc} values for kaolin, TiO₂ and kaolin/TiO₂ were determined. Exactly 50 cm³ of 0.05 M HCl and 0.05 M NaOH solutions were added to kaolin (0.20 g), TiO₂ (0.20 g) and kaolin/TiO₂ (0.20 g) each for adjustment of pH values (2, 4, 6, 8, 10 and 12) at 25 °C prepared in three sets of six 250 cm³ conical flasks. The conical flasks were shaken using a rotary shaker at 200 rpm for 6 h. The dispersed samples were allowed to settle, and their final pH was determined.

2.6 *Photocatalytic Study*

The photocatalysis activities were performed under direct sunlight. A 100 cm³ of tannery wastewater was measured in a 250 cm³ beaker, 0.2 g of kaolin/TiO₂ catalyst

was introduced, and then placed under high-intensity sunlight. At different irradiation time intervals, samples were collected and analyzed using UV-visible spectroscopy. The removal efficiency of COD and TOC is expressed as follows:

$$\text{Removal efficiency}(E_r) = \frac{C_o - C_t}{C_o} \times 100 \quad (1)$$

where C_o and C_t are the initial concentration of pollutants and residual concentration of COD and TOC at different intervals of irradiation (0–150 min).

The extent of reusability of the kaolin/TiO₂ photocatalyst was determined in six consecutive experimental runs using deionized water several times until pH 7 was attained and dried at 105 °C for 12 h.

2.7 Characterization Techniques

The composition of kaolin, TiO₂ and kaolin/TiO₂ were determined by high-resolution scanning electron microscopy coupled with energy dispersive spectroscopy (HRSEM), RAMAN spectroscopy, UV-visible spectrophotometer, high-resolution transmission electron microscopy (HRTEM). The morphology of the samples was examined with HRTEM, a Zeiss Auriga model (USA) operated at a 20 kV of voltage, while HRTEM coupled with energy dispersed spectroscopy (EDX) was performed using a Zeiss Auriga model (USA) at an accelerating voltage of 20 kV. Raman spectroscopy was recorded at an ambient temperature in the wavenumber range of 300–2000 cm⁻¹. The UV-visible absorption spectra of the samples were examined using a UV-visible spectrophotometer, Shimadzu UV 1800.

3 Discussion

3.1 Characterization

The surface morphology of beneficiated kaolin was presented by HRSEM as seen in Plate 1a. The HRSEM image confirmed kaolin's hexagonal plates and stack appearance (see Fig. 1a). Also, the HRSEM image of kaolin revealed the large blocked and small pieces of kaolinite structure. The morphology of the synthesized TiO₂ nanoparticles calcined at 450 °C was characterized by HRSEM as presented in Fig. 1b. The anatase phase of TiO₂ nanoparticles exhibited agglomerated spherical shapes with an average size distribution of 14 nm. However, the discernable pores structure at the space between the TiO₂ nanoparticles is revealed at the surface of the synthesized particles. In Plate 1c, the HRSEM micrograph of kaolin/TiO₂ nanocomposites revealed a dispersed and block structure of TiO₂ nanoparticles on the surface.

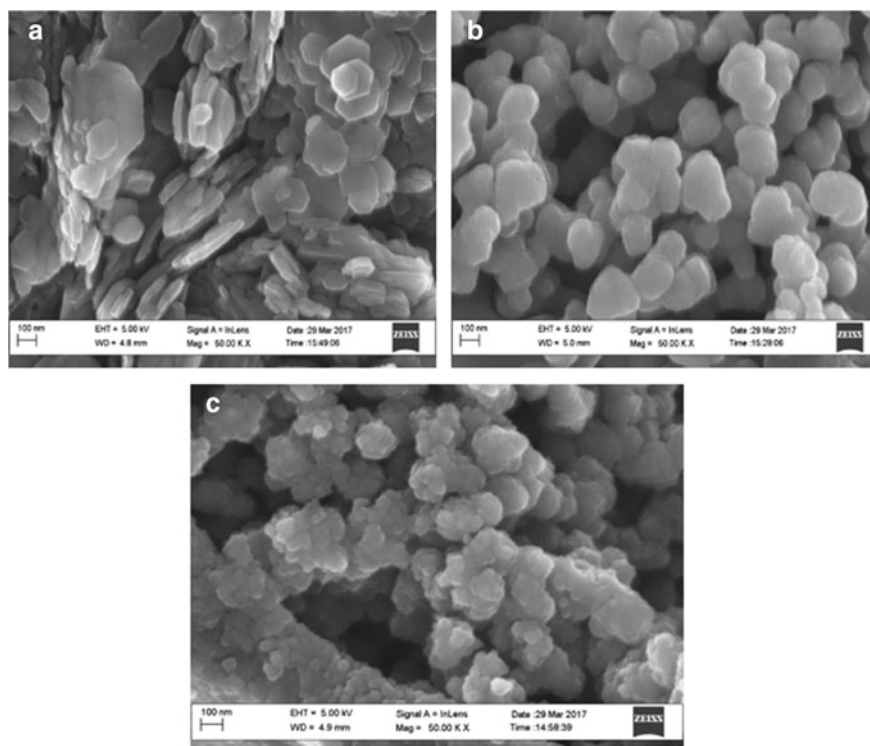


Fig. 1 HRSEM images of **a** beneficiated kaolin **b** TiO_2 nanoparticles and **c** kaolin/ TiO_2 nanocomposites at 450°C

The microstructure of kaolin was characterized by HRTEM and revealed a pseudo-hexagonal structure of kaolinite, as shown in Plate 2a. The EDX elemental analysis of kaolin was investigated. As shown in Fig. 2, O, Al, Si, Ti and Fe elements are apparently detected. The experimental percentage weight of O (54.96%), Al (19.84%) and Si (21.40%) from the EDX result are closely related to the percentage elemental composition of the theoretical structural formula of kaolin. The SAED result on the kaolin revealed the turbostratic arrangement of kaolinite oriented to one another (as seen in Fig. 3). The HRTEM structure of TiO_2 nanoparticles calcined at 450°C was presented in Fig. 2. It was revealed that the nanoparticles consist of a spherical like appearance with a size of 13.8 nm, in accordance with the HRSEM result. As seen in the HRTEM image (Fig. 2b), lattice fringes of anatase (0.346 nm), corresponding to the (101) plane, were evaluated.

Additionally, the EDX results of TiO_2 nanoparticles show the presence of dominant elements (Ti and O). The spectrum showed sharp peaks corresponding to Ti at 4.72 and 4.94 keV. The observed small peaks of Ni could be related to impurities. The SAED analysis as displayed in Plate 2b showed that the TiO_2 nanoparticles are

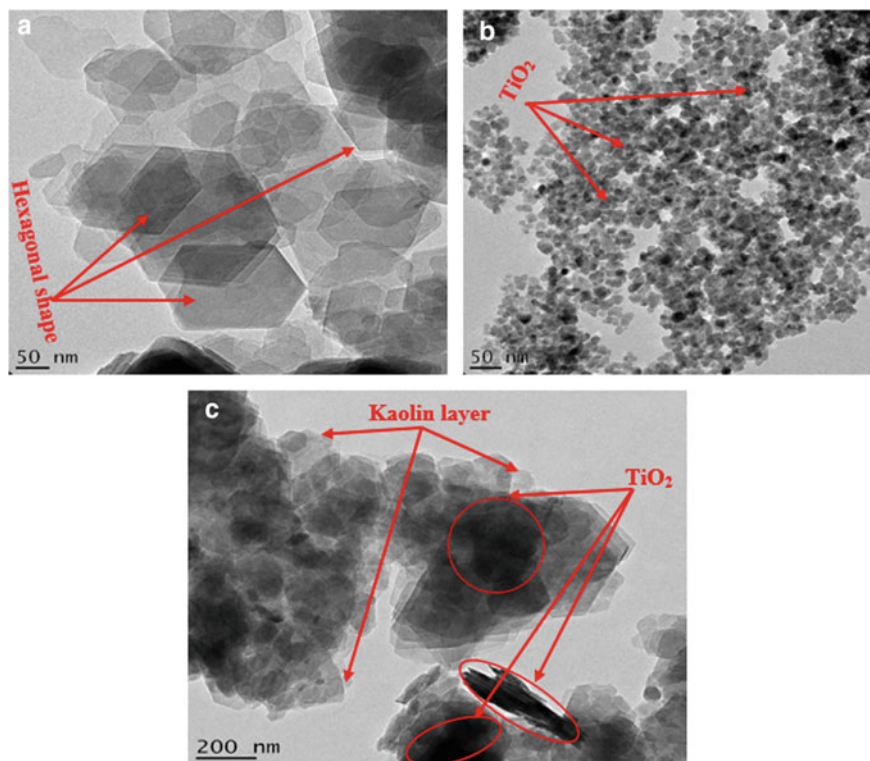


Fig. 2 HRTEM images of **a** beneficiated kaolin **b** TiO₂ nanoparticles and **c** kaolin/TiO₂ nanocomposites at 450 °C

crystalline with dotted concentric rings. TiO₂/kaolin nanocomposites were characterized by HRTEM microscopy. The image Fig. 2c showed the presence of layered kaolin and the elongated appearance of TiO₂ nanoparticles, indicating the embedment in the nanocomposites. The image displayed spherical TiO₂ nanoparticles, which showed lattice spacing of 0.35 and 0.24 nm characteristic of the (101) and (111) planes of the anatase phase. EDX analysis was performed to study the composition of the TiO₂/kaolin nanocomposites (Fig. 4), indicating the presence of C, O, Al, Si, Ti, Fe and Cu. However, the peaks of C is from the carbon holey grid used for the HRTEM study and besides Cu from impurities. The selected area of electron diffraction (SAED) analysis indicates that the nanocomposites are crystalline in nature (Fig. 5).

Kaolin has an intense peak at 472.46 cm⁻¹ related to the observed less intense peak for kaolin/TiO₂, whereas TiO₂ and kaolin/TiO₂ had similar significant vibration mode located at 367.19 and 512.41 cm⁻¹ (see Fig. 6). The band (472.46 cm⁻¹) is attributed to the bending mode of Si–O–Al (Rodrigues et al. 2016). The peak of kaolin/TiO₂

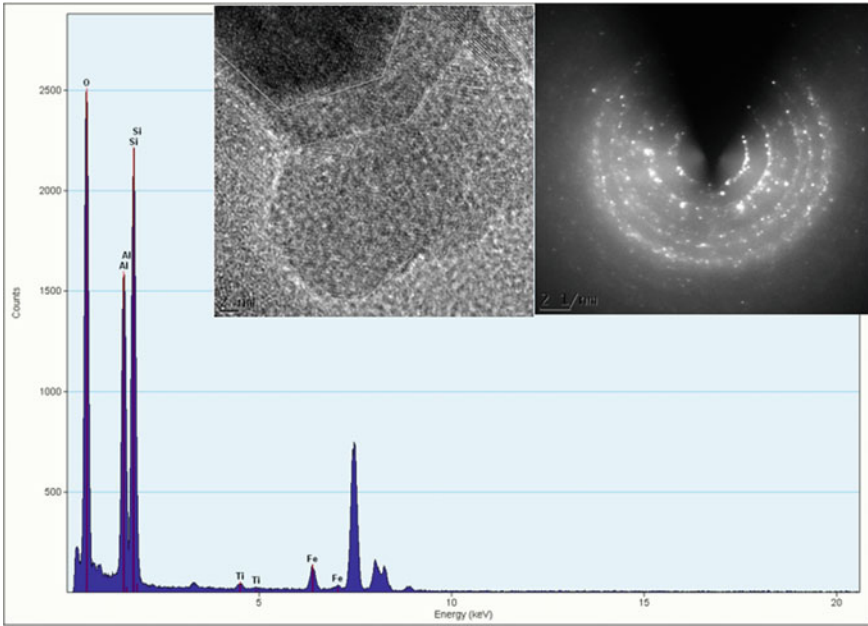


Fig. 3 EDX and SAED results for kaolin

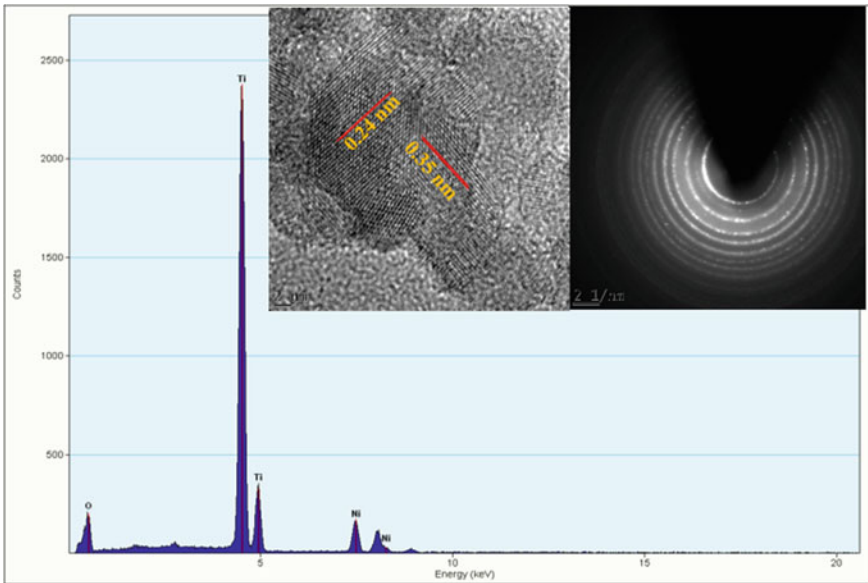


Fig. 4 EDX and SAED results for TiO₂ nanoparticles

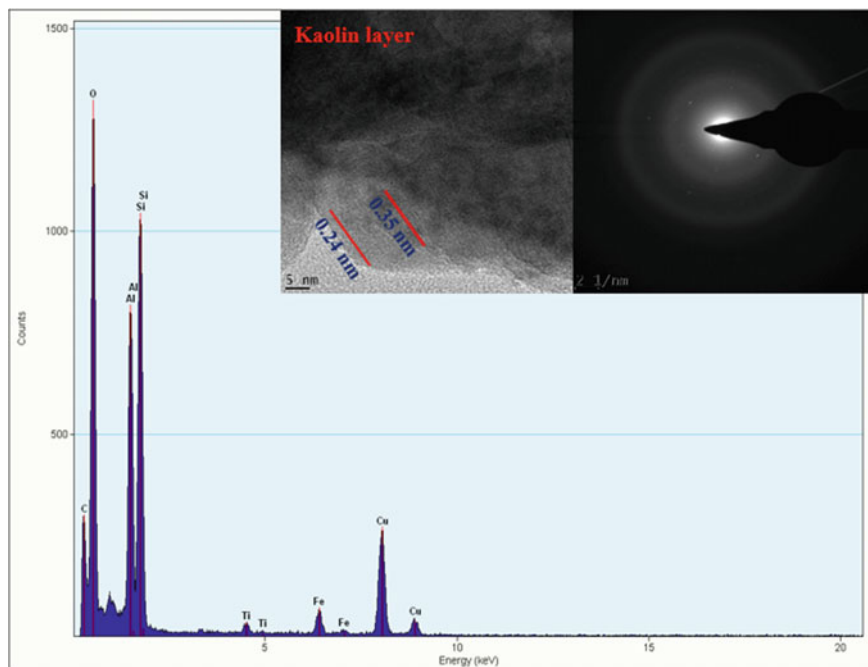


Fig. 5 EDX and SAED results for kaolin/TiO₂ nanocomposites

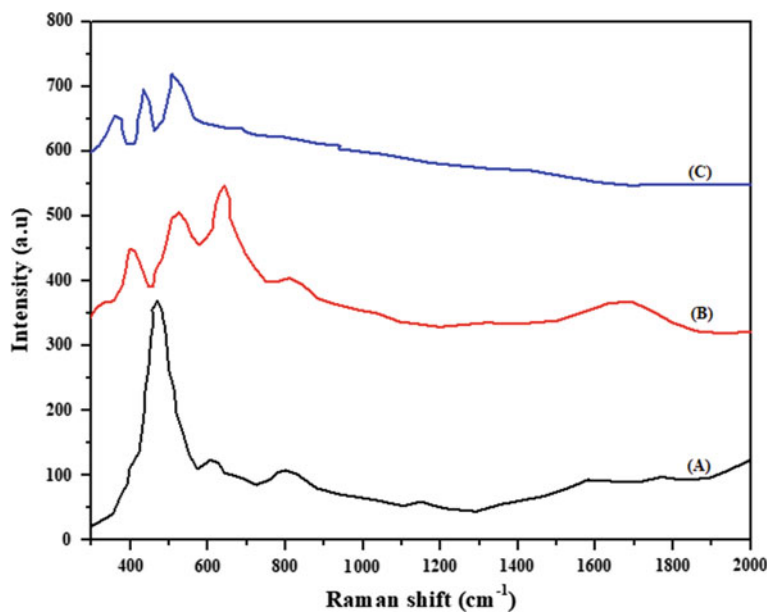


Fig. 6 The Raman spectra of kaolin, TiO₂ and kaolin/TiO₂

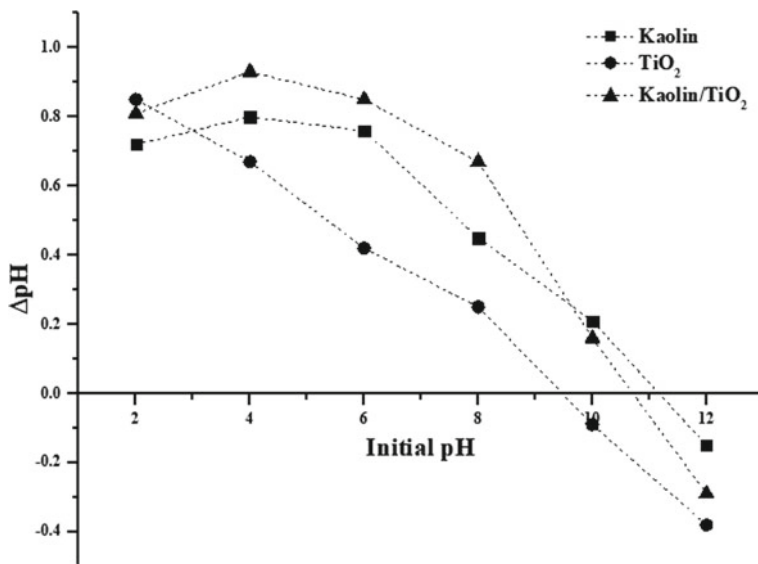


Fig. 7 Point of zero charge of kaolin, TiO₂ and kaolin/TiO₂

(512.41 cm⁻¹) indicated well-formed crystalline TiO₂ nanoparticles in the nanocomposites. The formation of peaks of TiO₂ nanoparticles in the nanocomposites was consistent with the TiO₂ structure.

Point of zero charge

The plots of change in pH against initial pH for kaolin, TiO₂ and kaolin/TiO₂ materials were depicted in Fig. 7. The kaolin revealed 11.09 pH_{pzc}, which is positive at pH 2–10.5, and negative at pH higher than the (pH_{pzc}). Figure 7 showed that the pure TiO₂ exhibited a positive surface charge at pH (9.44) lower than pH_{pzc} of kaolin, where it becomes a negatively charged surface below the pH_{pzc}. This indicated that the surface charge increased as the pH reduced. The kaolin/TiO₂ nanocomposites exhibited a pH_{pzc} of 10.72, and that the surface was positively charged below pH values of 10 and negatively charged surface at pH greater than 10.7. The positive charges of the kaolin, TiO₂ and kaolin/TiO₂ surfaces are believed to be responsible for contamination photodegradation of radicals in tannery wastewater. At greater pH_{pzc}, the negatively charged species in the wastewater would be repelled by the negatively charged kaolin, TiO₂ and kaolin/TiO₂ surfaces. This enables the contaminant species farther away from radicals, thus suggesting the photodegradation process become retarded at higher pH.

Effect of operational conditions

The efficient photocatalytic removal of TOC and COD under the influence of irradiation time and catalyst dosage was investigated.

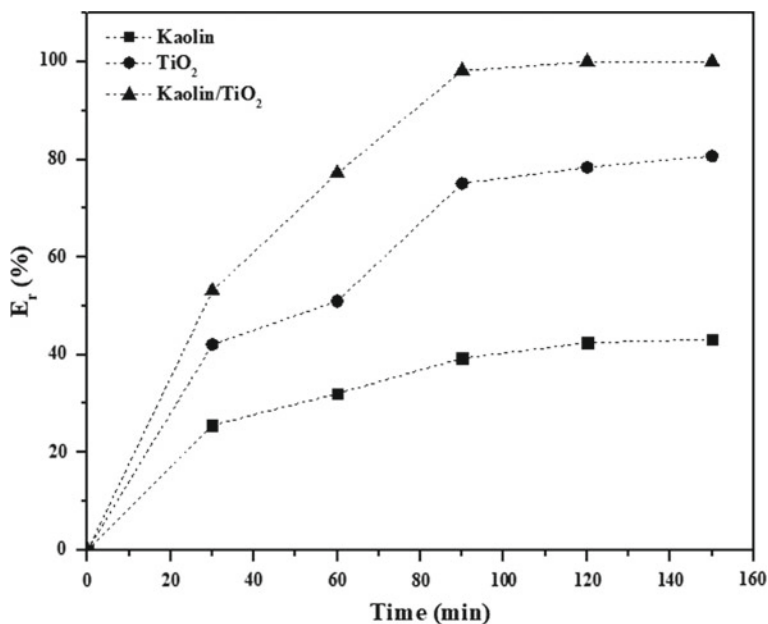


Fig. 8 Effect of time on photocatalytic removal of TOC in tannery wastewater using kaolin, TiO₂ and kaolin/TiO₂ (Dosage = 0.2 g, pH = and Temperature = 28 °C)

Effect of time

COD and TOC experiments' removal efficiency was performed at 0.20 g of the kaolin, TiO₂ and kaolin/TiO₂, each under sunlight at a different interval time (0 to 150 min) as depicted in Figs. 8 and 9. It was noticed that the removal efficiencies of the pollutants increase with time. After 90 and 120 min of reaction (maximal time), removal efficiency reached 100% compared to lower removal efficacies of kaolin and TiO₂. Furthermore, it can be seen from Figs. 8 and 9 that removal efficiencies of the sample n followed the trend: kaolin/TiO₂ > TiO₂ > kaolin, confirming that TiO₂ loaded improved the photocatalytic activity of kaolin/TiO₂.

Effect of catalyst dosage

The effect of time on the photodegradation of COD and TOC in tannery wastewater using kaolin, TiO₂ and kaolin/TiO₂ investigated over the range of 0.2 to 0.4 g are depicted in Figs. 10 and 11, respectively. An increase in dose and optimal dose with the maxima degradation of pollutant occurred. The results indicated that the removal efficiencies increase at constant concentrations of the pollutants by varying the adsorbent. The increase in removal efficiency could be attributed to the increased number of sites and available binding sites. It is noticed that the optimal dose, 0.40 g (100%), of the kaolin/TiO₂ photocatalyst is not far from that of 0.35 g (99.20%). This may have occurred due to the aggregation of adsorbent particles and repulsive force among the binding sites, leading to an increase in the binding sites.

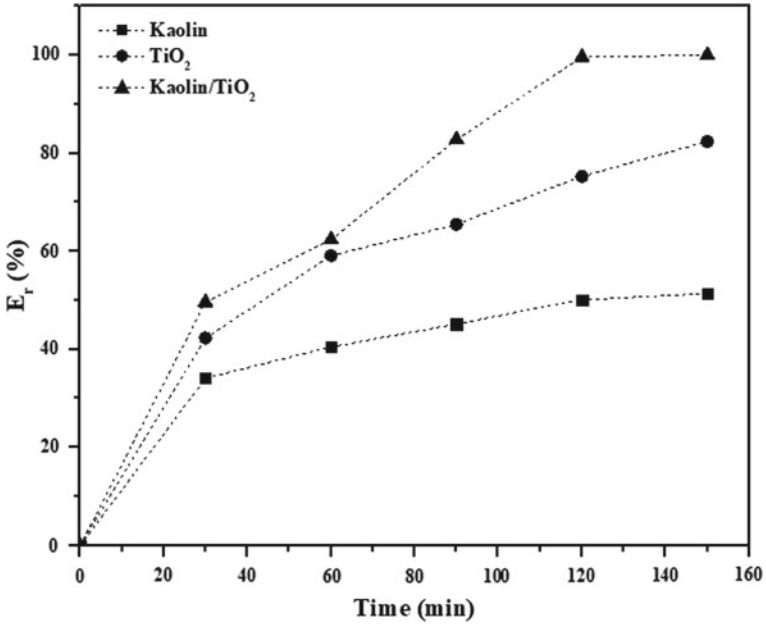


Fig. 9 Effect of time on photocatalytic removal of BOD in tannery wastewater using kaolin, TiO₂ and kaolin/TiO₂ (Dosage = 0.2 g, pH = and Temperature = 28 °C)

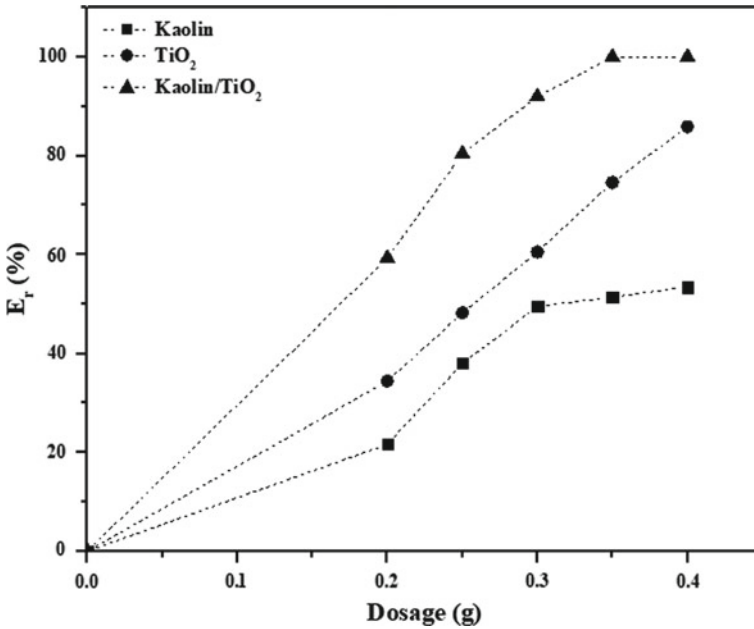


Fig. 10 Effect of dosage on photocatalytic removal of TOC in tannery wastewater using kaolin, TiO₂ and kaolin/TiO₂ (Time = 90 min, pH = and Temperature = 28 °C)

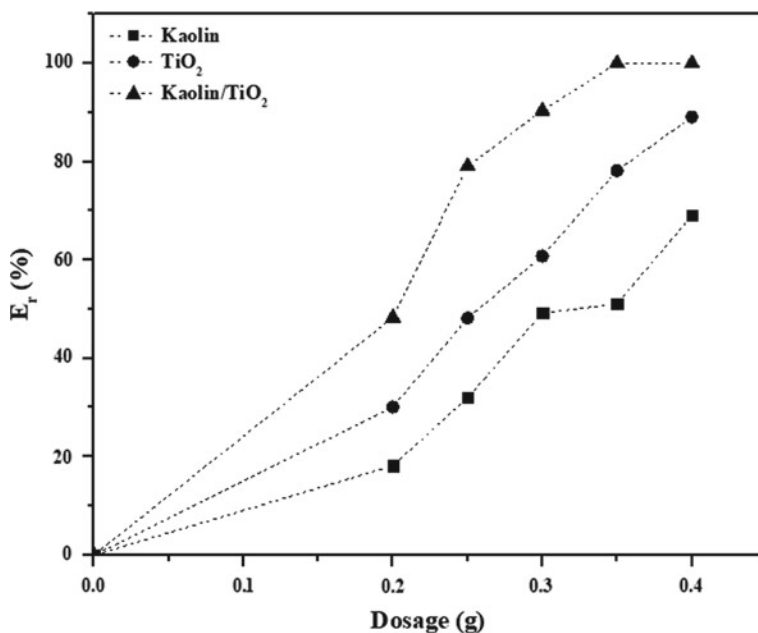


Fig. 11 Effect of dosage on photocatalytic removal of BOD in tannery wastewater using kaolin, TiO₂ and kaolin/TiO₂ (Time = 90 min, pH = and Temperature = 28 °C)

Discolourization of tannery wastewater

UV-visible absorption spectra of the tannery wastewater solution with kaolin, TiO₂ and kaolin/TiO₂ at a different time using λ_{max} are presented in Fig. 12. The % decolourization of tannery wastewater was performed at pH 8.4, 0.2 g of kaolin/TiO₂ photocatalyst and 50 cm³ of wastewater solution. The initial peaks of tannery wastewater decreased gradually by adding kaolin/TiO₂ and became smaller as time increased (30 to 90 min). The reduction of absorbance intensity of the sample showed the photodegradation of the wastewater under these conditions leading to the percentage reduction of COD and TOC. The percentage decolourization, 62.10% at 30 min, 75.50% at 60 min and 98.90% at 90 min, were achieved, corresponding to percentage reduction of COD and TOC. In this case, photodegradation was restricted to visible sunlight. At this point, the solution almost becomes colourless. The degradation of these pollutants confirmed the ability of TiO₂ nanoparticles, which enhanced photocatalytic efficiency by absorbing pollutants. A comparison between the present work and previous studies regarding the photodegradation of pollutants is presented in Table 1. The comparative study showed the efficacy of kaolin/TiO₂ for decolourization, TOC and BOD removal in real effluent (tannery wastewater). As it can be seen, the obtained maximum tannery wastewater discolourization was more favourable than most reported catalysts.

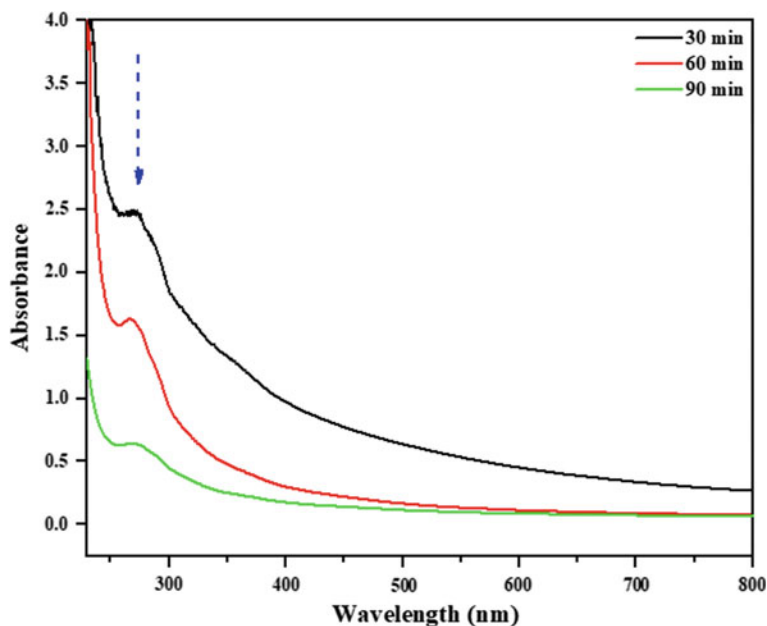


Fig. 12 Decolourization efficiency of tannery wastewater

The photocatalytic activity of kaolin/TiO₂ photocatalyst is related to the holes induced by releasing the electron from valance band to conduction band under UV light, as presented in Fig. 13. The conduction band electron decreased oxygen molecules produce superoxide radicals, and holes generated react with hydroxyl radicals. These forms of radicals serve as strong oxidative agents that degrade organic molecules.

During the interaction of kaolin/TiO₂ nanocomposites with tannery wastewater under sunlight, as depicted in Fig. 13, the photodegradation of pollutants involves adsorption of the photon, oxygen adsorption by the generation of superoxide radicals, generation of hydrogen atoms via photoelectrons, the yield of hydroxyl radicals and conversion of organic molecules by oxidation through hydroxyl radical attack. This result revealed that the photoactivity of kaolin/TiO₂ was due to the abundant surface oxygen vacancy and defects and the lower recombination of electron-hole of TiO₂ nanoparticles (Wang et al. 2011).

Kinetic study.

The kinetics of tannery wastewater using kaolin/TiO₂ photocatalyst were investigated by first-order model expression as follow:

$$\ln \frac{C_0}{C_t} = k_{app} t \quad (2)$$

Table 1 Comparison of pollutant removal with literature

Adsorbent	Experimental conditions	Characterization	Pollutant removal	Rate (k_{app})	Wastewater	Reference
TiO ₂ /Clay	Oxidating agent, concentration, time	BET, FTIR, XRD, TGA/DTA, SEM	Decolourization = 100% at 20 min COD = 98% at 45 min		Reactive blue 19	Hadjilataief et al. (2019)
ZnO/Clay	pH, catalyst, dosage, concentration, time	XRD, FTIR, BET, SEM, HRTEM-EDX	Decolourization = 97.18% at 60 min for MG, 100% at 70 min for CR	CR = 0.0146 min ⁻¹ MG = 0.0219 min ⁻¹	Malachite green (MG) Congo red (CR)	Hadjilataief et al. (2018)
Fungal biomass/TiO ₂ /UV	Time, dosage	SEM-EDX	Decolourization = 89% at 6 h COD = 73% at 6 h BOD = 86% at 6 h		Textile effluent	Blanco-Vargas et al. (2018)
Porous ceramic/TiO ₂	Time dosage	XRD, RAMAN, SEM	Decolourization = 83% at 5 h	0.00627 min ⁻¹	Rhodamine B	De Araujo-Scharnberg et al. (2020)
Polyaniline/TiO ₂	Time, pH	FE-SEM, TEM, FTIR, TG	Decolourization = 84% at 90 min		Azo dye	Gilja et al. (2017)
TiO ₂ /TPPS	Time, dosage	XRD, FTIR, SEM-EDX, UV-DRS	Decolourization = 99% at 50 min	0.0896 min ⁻¹	Eosin yellow dye	Manivannan et al. (2021)
TiO ₂ /Fe ₂ O ₃	Time	XRD, FE-SEM, PSD, XRF, XPS, DRS, BET	Decolourization = 64% at 540 min		Methylene blue	Retamoso et al. (2019)
Fe ₂ O ₃ /TiO ₂ /Clay	Time, pH, concentration	XRD, XRF, BET, SEM-EDX, DRS	Decolourization = 91% at 45 min		Acid orange 7 dye	Silvestri and Feletto (2017)
Biochar/TiO ₂		XRD, SEM, BET, FTIR			Methylene blue	Silvestri et al. (2020)

(continued)

Table 1 (continued)

Adsorbent	Experimental conditions	Characterization	Pollutant removal	Rate (k_{app})	Wastewater	Reference
Kaolin/TiO ₂	Time, dosage	HRSEM, HRTEM-EDX, RAMAN, UV-visible,	Decolourization = 98.90% at 90 min COD = 100% at 90 min TOC = 100% at 90 min	TOC - 0.03221 min ⁻¹ BOD = 0.0346 min ⁻¹	Tannery effluent	In this work

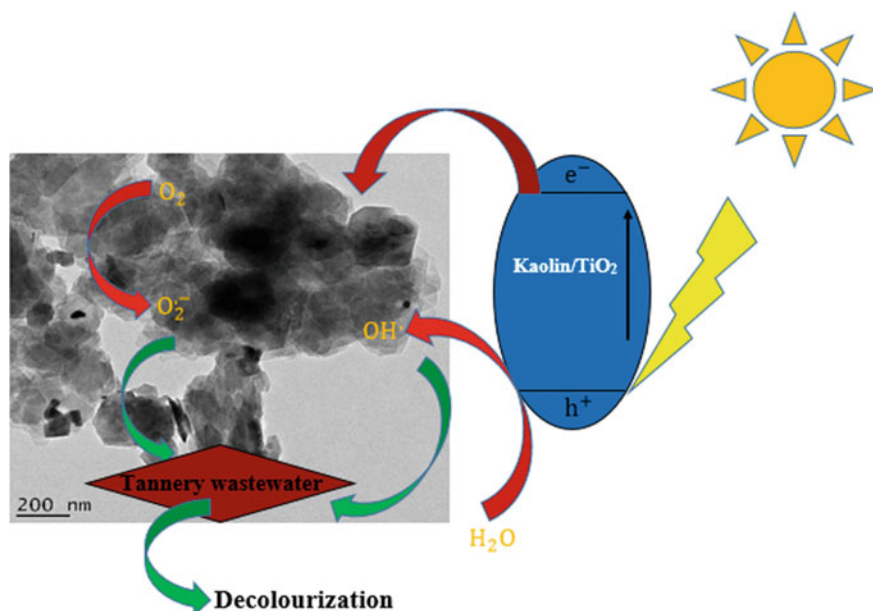


Fig. 13 The proposed mechanism of decolourization of tannery wastewater

where k_{app} is the apparent first-order rate constant (min^{-1}), C_o and C_t are the concentration of the pollutants at times 0 and t , respectively. The k_{app} values for COD and TOC degradation were calculated by plotting $\ln \frac{C_o}{C_t}$ against time (t) (see Figs. 14 and 15) and presented in Table 2.

The correlation coefficient (R^2) of the studies were greater than 0.98, indicating the difference between R^2 values and adjusted values less than 0.2. This revealed that the photodegradation of COD and TOC using kaolin/TiO₂ fitted well for apparent first-order kinetics. This observation corresponds to the finding of Hadjtaief et al. (2017).

3.2 Reusability Study

The stability of kaolin/TiO₂ was evaluated efficiently at optimum conditions for six cycles, and the results are depicted in Fig. 16. During cycles 1 to 3 of the photocatalyst, there was no significant change in the activities of the catalyst in terms of discolouration, removal of TOC and COD. However, the photocatalyst loses its removal efficiencies from the cycle. These results showed that kaolin/TiO₂ had easy and good recyclability.

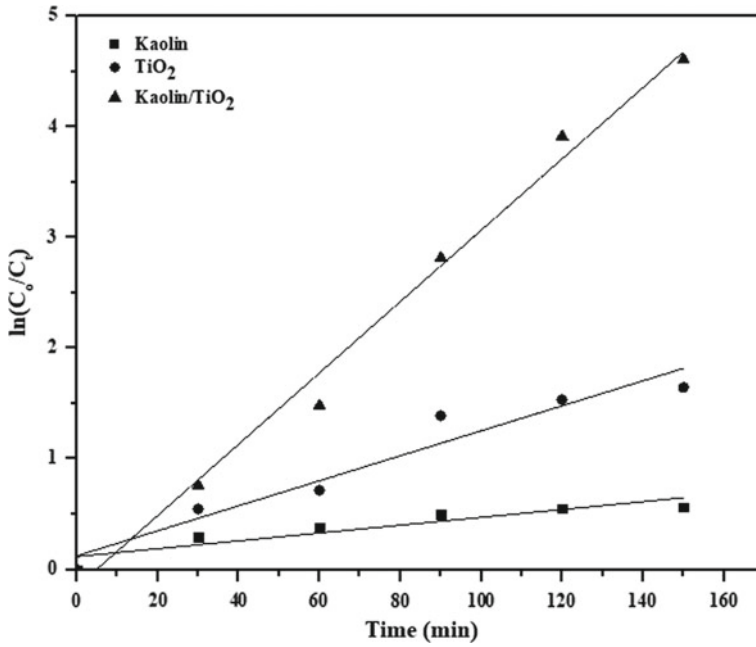


Fig. 14 The reaction kinetics for TOC removal in tannery wastewater

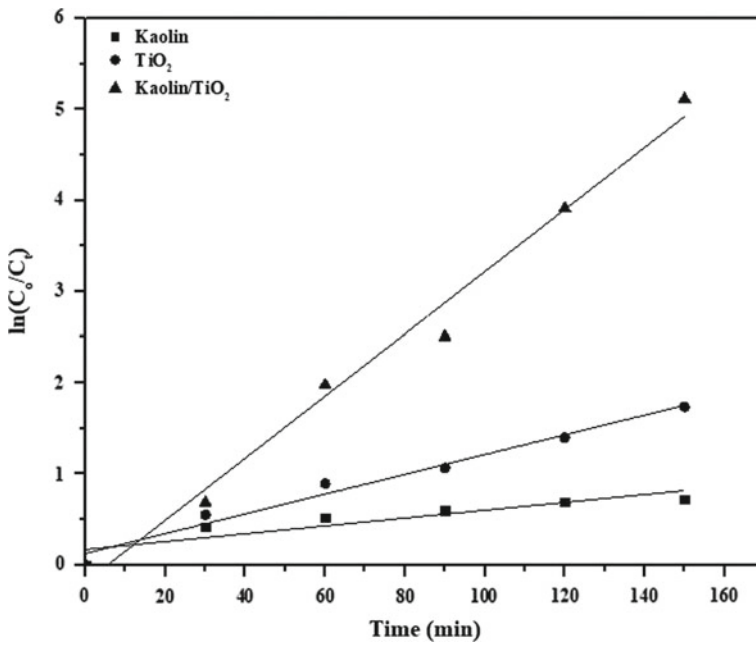
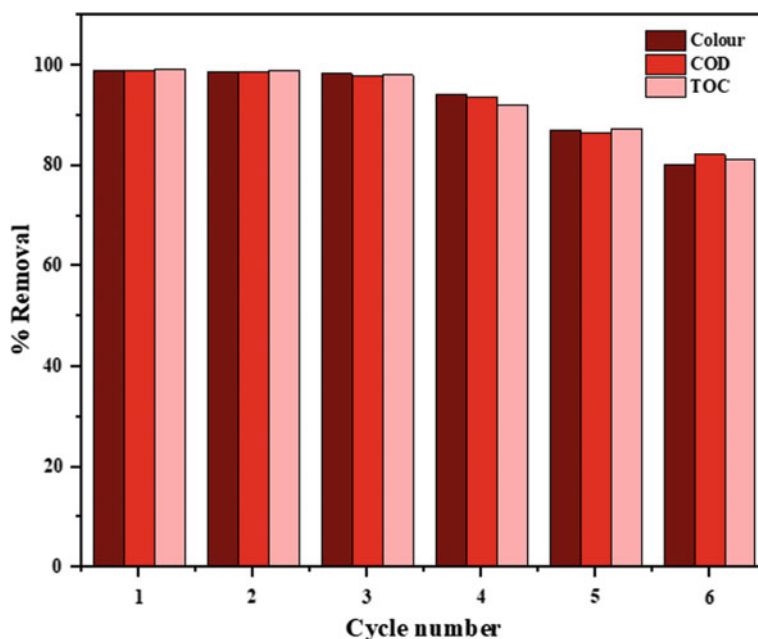


Fig. 15 The reaction kinetics for BOD removal in tannery wastewater

Table 2 Pseudo-first-order kinetic parameters for TOC and BOD removal

Parameter	Sample	k_{app}	R^2	Adjusted R^2
TOC	Kaolin	0.00354	0.92499	0.81951
	TiO ₂	0.01129	0.97034	0.92695
	Kaolin/TiO ₂	0.03221	0.99493	0.98735
BOD	Kaolin	0.00431	0.90841	0.78151
	TiO ₂	0.01066	0.98892	0.97245
	Kaolin/TiO ₂	0.0346	0.99329	0.98327

**Fig. 16** Photocatalysis reuse cycle for removal of colour, COD and TOC in tannery wastewater

4 Conclusions

The present study investigated the removal of COD and TOC in tannery wastewater under sunlight using kaolin, TiO₂ and kaolin/TiO₂. The nanoadsorbents were prepared using the sol-gel method and characterized using HRSEM, Raman spectroscopy, HRTEM-EDX and SAED, EDX. TEM and EDX confirmed the presence of TiO₂. The kaolin, TiO₂ and kaolin/TiO₂ were used to remove TOC and BOD in tannery wastewater. The removal efficiencies were found to be time and dosage-dependent. Almost a complete decolourization of tannery wastewater within 90 min under sunlight in the presence of kaolin/TiO₂ nanocomposites is confirmed. This

performance could be attributed to the synergistic between kaolin and TiO₂. The possible mechanism of discolouration of tannery wastewater was also discussed. The results indicate the feasibility of using kaolin/TiO₂ offer a new nanoadsorbent for water purification processes and photocatalytic discolourization of organic pollutants by natural solar radiations.

Declaration of Competing Interest The authors report no declarations of interest.

References

- Ahmed S, Khan FSA, Mubarak NM, Khalid M, Tan YH, Mazari SA, Karri RR, Abdullah EC (2021) Emerging pollutants and their removal using visible-light responsive photocatalysis—a comprehensive review. *J Environ Chem Eng* 9(6)
- Aliou Guillaume PL, Chelaru AM, Visa M, Lassine O (2018) Titanium Oxide-Clay as adsorbent and photocatalysts for wastewater treatment. *J Membr Sci Technol* 08(01)
- Blanco-Vargas A, Ramírez-Sierra CF, Duarte-Castañeda M, Beltrán-Villarraga M, Medina-Córdoba LK, Florido-Cuellar AE, Cardona-Bedoya JA, Campos-Pinilla C, Pedroza-Rodríguez AM (2018) A novel textile wastewater treatment using ligninolytic co-culture and photocatalysis with TiO₂. *Univ Sci* 23(3):437–464
- Boruah A, Rasheed A, Mendhe VA, Ganapathi S (2019) Specific surface area and pore size distribution in gas shales of Raniganj Basin, India. *J Petroleum Explor Produc Technol* 9(2):1041–1050
- Crini G, Lichtfouse E (2019) Advantages and disadvantages of techniques used for wastewater treatment. *Environ Chem Letters* 17(1):145–155
- de Araujo Scharnberg AR, de Loreto AC, Wermuth TB, Alves AK, Arcaro S, dos Santos PAM, Rodriguez ADAL (2020) Porous ceramic supported TiO₂ nanoparticles: enhanced photocatalytic activity for Rhodamine B degradation. *Boletín De La Sociedad Española De Cerámica y Vidrio* 59(6):230–238
- Dehghani MH, Omrani GA, Karri RR (2021) Solid Waste—sources, toxicity, and their consequences to human health. In *Soft computing techniques in solid waste and wastewater management*. Elsevier, pp 205–213. <https://doi.org/10.1016/B978-0-12-824463-0.00013-6>
- Dukic AB, Kumrić KR, Vukelić NS, Stojanović ZS, Stojmenović MD, Milošević SS, Matović LL (2015) Influence of ageing of milled clay and its composite with TiO₂ on the heavy metal adsorption characteristics. *Ceram Int* 41(3):5129–5137
- Engwa GA, Ferdinand PU, Nwalo FN, Unachukwu MN (2019) Mechanism and health effects of heavy metal toxicity in humans. In *Poisoning in the modern world-new tricks for an old dog?* IntechOpen.
- Gilja V, Novaković K, Travas-Sejdic J, Hrnjak-Murčić Z, Kraljić Roković M, Žic M (2017) Stability and synergistic effect of polyaniline/TiO₂ photocatalysts in degradation of azo dye in wastewater. *Nanomaterials* 7(12):412
- Hadjltaief HB, Zina MB, Galvez ME, Costa PD (2017) Photocatalytic degradation of methyl green dye in aqueous solution over natural clay-supported ZnO-TiO₂ catalysts. *J Photochem Photobiol A: Chem* 315:25–33
- Hadjltaief HB, Ameer SB, Da Costa P, Zina MB, Galvez ME (2018) Photocatalytic decolorization of cationic and anionic dyes over ZnO nanoparticle immobilized on natural Tunisian clay. *Appl Clay Sci* 152:148–157
- Hadjltaief HB, Gálvez ME, Zina MB, Da Costa P (2019) TiO₂/clay as a heterogeneous catalyst in photocatalytic/photochemical oxidation of anionic reactive blue 19. *Arab J Chem* 12(7):1454–1462

- Karri RR, Ravindran G, Dehghani MH (2021) Wastewater—sources, toxicity, and their consequences to human health. In *Soft computing techniques in solid waste and wastewater management*. Elsevier, pp 3–33. <https://doi.org/10.1016/B978-0-12-824463-0.00001-X>
- Khan FSA, Mubarak NM, Khalid M, Tan YH, Abdullah EC, Rahman ME, Karri RR (2021) A comprehensive review on micropollutants removal using carbon nanotubes-based adsorbents and membranes. *J Environ Chem Eng* 9(6)
- Laysandr aL, Sari MWMK, Soetaredjo FE, Foe K, Putro JN, Kurniawan A, Ju Y, Ismadji S (2017) Adsorption and photocatalytic performance of bentonite-titanium dioxide composites for methylene blue and rhodamine B decoloration. *Heliyon* 3(12):e00488
- Lingamdinne LP, Choi JS, Angaru GKR, Karri RR, Yang JK, Chang YY, Koduru JR (2022) Magnetic-watermelon rinds biochar for uranium-contaminated water treatment using an electromagnetic semi-batch column with removal mechanistic investigations. *Chemosphere* 286
- Mahvi AH, Ghanbarian M, Nasser S, Khairi A (2009) Mineralization and discoloration of textile wastewater by TiO₂ nanoparticles. *Desalination* 239(1–3):309–316
- Manivannan R, Ryu J, Son YA (2021) Photo discoloration of eosin yellow dye under visible light using TiO₂@TPPS nanocomposite synthesized via ultrasonic assisted method. *Colloids Surf A Physicochem Eng Asp* 608:125601
- Mehmood A, Khan FSA, Mubarak NM, Tan YH, Karri RR, Khalid M, Walvekar R, Abdullah EC, Nizamuddin S, Mazari SA (2021) Magnetic nanocomposites for sustainable water purification—a comprehensive review. *Environ Sci Pollut Res* 28(16):19563–19588
- Mishra A, Mehtav A, Sharma M, Basu S (2017) Enhanced heterogeneous photodegradation of VOC and dye using microwave synthesized TiO₂/Clay nanocomposites: a comparison study of different type of clays. *J Alloys Compd* 694:574–580
- Nabbou N, Belhachemi M, Boumelik M, Merzougui T, Lahcene D, Harek Y, Zorpas AA, Jeguirim M (2019) Removal of fluoride from groundwater using natural clay (kaolinite): optimization of adsorption conditions. *Comptes Rendus Chimie* 22(2–3):105–112
- Retamoso C, Escalona N, González M, Barrientos L, Allende-González P, Stancovich S, Serpell R, Fierro JLG, Lopez M (2019) Effect of particle size on the photocatalytic activity of modified rutile sand (TiO₂) for the discoloration of methylene blue in water. *J Photochem Photobiol, A* 378:136–141
- Rodrigues M, Souza AG, Santos IMG (2016) Brazilian kaolin wastes: synthesis of zeolite P at low-temperature. *Am Chem Sci J* 12(4):1–11
- Silvestri S, Foletto EL (2017) Preparation and characterization of Fe₂O₃/TiO₂/clay plates and their use as photocatalysts. *Ceram Int* 43(16):14057–14062
- Silvestri S, Stefanello N, Sulkovski AA, Foletto EL (2020) Preparation of TiO₂ supported on MDF biochar for simultaneous removal of methylene blue by adsorption and photocatalysis. *J Chem Technol Biotechnol* 95(10):2723–2729
- Wang C, Shi H, Zhang P, Li Y (2011) Synthesis and characterization of kaolinite/TiO₂ nano-photocatalysts. *Appl Clay Sci* 53(4):646–649
- Yang C, Zhu Y, Wang J, Li Z, Su X, Niu C (2015) Hydrothermal synthesis of TiO₂-WO₃-bentonite composites: Conventional versus ultrasonic pretreatments and their adsorption of methylene blue. *Appl Clay Sci* 105–106:243–251

Microbial Biofilm Reactor for Sustained Waste Water Treatment and Reuse



Shaon Ray Chaudhuri

Abstract Freshwater scarcity is a global problem that pertains to the ever-increasing population, contamination of freshwater by wastewater generated from different anthropogenic sources as well as misuse of freshwater for secondary (non-potable) applications. Later two issues could be addressed through the appropriate implementation of Microbial Technology in an eco-friendly way. The application will involve proper selection of the wastewater sources (for microbial isolation), their pollutant identification, selection of tailor made bacterial consortium/ isolates for treatment of the wastewater and converting the waste into reusable by-product. This is the current trend used for pilot scale wastewater treatment using biofilm bioreactors. This article talks about the few successful case studies implemented for different types of wastewater treatment (municipal/Agricultural runoff, petrochemical, tannery/mining industry and milk processing plant wastewater) in biofilm reactors that could run for years after being installed in the pilot scale. The processes are faster, sludge free and, in most cases, ensure complete reuse of treated water, hence preventing wastage of freshwater for non-potable applications. Biofilm based system makes them resistant to external perturbation, stable with enhanced efficiency. Through this approach, eco-friendly processes of wastewater treatment could be made self-sustainable.

Keywords Biofilm reactors · Tailor-made consortium · Wastewater · Biofertilizer · Non-potable application · Sludge free system

1 Introductory Background

Seventy-five percent of our planet, Earth, is covered with water, of which only 2.5% is suitable for consumption (freshwater). The population is rapidly growing, demanding more freshwater. However, our freshwater reserves are dwindling, with 40% of the world population (in 50 countries) threatened to face water scarcity by 2025 as per the United Nations report. The freshwater consumption in the United States per month

S. Ray Chaudhuri (✉)
Department of Microbiology, Tripura University, Kolkata, Suryamaninagar 799022, India
e-mail: shaonraychaudhuri@tripurauniv.in

is about $1.486 \times 10^{10} \text{ m}^3$. On average, about 10^6 m^3 of freshwater is used per day worldwide. While a portion of it is for potable purposes, the rest is wasted for non-potable application (that can be carried out using adequately treated wastewater). The major share of water consumption every day is used in agriculture (75 to 90%), which does not require fresh water. Freshwater is used directly for drinking, personal cleaning and indirectly (virtual water) through the products we use in our day to day lives. The lion's share of the virtual water (as proposed by Professor Tony Allen) goes for the food production (about $3.5 \text{ m}^3/\text{day}/\text{person}$), be it the grains ($1.12 \text{ m}^3/\text{kg}$), chocolate ($24 \text{ m}^3/\text{kg}$), or the meat ($15.4 \text{ m}^3/\text{kg}$) to name a few (The World Counts 2021). More than a billion people worldwide (mostly in developing countries) lack access to safe potable water.

The principal concern in front of mankind across the globe is ensuring the security of food, water, and energy. The limited freshwater resource is either misused for non-drinking purposes or contaminated due to anthropogenic reasons. To fulfil the demand for freshwater, it is essential to use freshwater judiciously and prevent its contamination through proper management. Hence, the wastewater could become valuable if adequately treated to prevent pollution and reused in the secondary application. Considering the amount of wastewater generated, the available treatment facility is substantially compromised (both in terms of quantity/capacity and quality of treatment) (Kaur et al. 2012). The quantity of wastewater is expected to rise with time, demanding more effluent treatment plant (ETP) installation. The existing treatment systems are affordable mostly by the large installations due to the cost involved in setting up and running the ETP (CPCB 2005a). In the absence of such facilities, the untreated or partially treated wastewater either pollutes the water bodies (Trivedy et al. 2001) due to discharge or is used for agriculture leading to employment generation, livelihood support from the sale of the produce but with a constant concern of occupational and environmental health hazard. About 49% of the annual groundwater recharged is used for irrigation, while 4.2% is used for the rest (domestic and industrial) of the activities (CGWB 2011), which is expected to rise to 6.7% by 2025. In addition, freshwater availability gradually decreases with a simultaneous increase in greywater generation (Bhardwaj 2005), calling for the rapid development of suitable water management technologies.

In India, the STPs are located on major river banks (CPCB 2005b), operating on the principle of Oxidation Pond/Activated Sludge/Up-flow Anaerobic Sludge Blanket/Waste Stabilization Ponds. The latter is considered the most suitable for developing nations with limited population and technological expertise (Shuval et al. 1986). Smaller industries in the same location often set up common ETP by implementing methods in isolation or different combinations (dissolved air floatation/dual media filter/activated carbon filter/sand filtration/tank stabilization/flash mixer/clarifier/flocculation/secondary clarifiers/Sludge drying beds). The cost for ETP set up for treating the entire volume of greywater would be of a different order of magnitude on the higher side (Kumar 2003). The step of ETP operation needing further attention is solid sewage handling which involves labour, energy, time and proper disposal. The lack of direct economic return and heavy investment is why local civic bodies have little interest in ETP/STP operation.

The large volume of wastewater and sewage is often sold for irrigation in places with a lack of alternative water sources (Bhamoriya 2004). This wastewater, due to its high N and P content, enhances the production of paddy, wheat, range of vegetables, flowers, fruits and fodder per unit land when supplemented with 50 or 75% of the prescribed quantity of chemical fertilizer (Strauss and Blumenthal 1990; Minhas and Samra 2004). The wastewater is also used for fish feed production during wastewater fed aquaculture at East Kolkata Wetland, India (Ray Chaudhuri et al. 2008). These activities are carried out in large chunks of land in countries like India (Sengupta 2008), generating employment (Minhas and Samra 2004) and nutritious food (Ray Chaudhuri et al. 2008; Ray Chaudhuri et al. 2007; Pradhan et al. 2008) while utilizing the plant growth nutrients in the wastewater and preventing the use of freshwater for non-potable application. However, there always remains a concern of environmental deterioration and health risks for the workers and the consumers of the produce (Satyawali and Balakrishnan 2008; Minhas et al. 2006; Tripathi et al. 2011). The integrated approach of utilizing wastewater for aquaculture (Ray Chaudhuri et al. 2008) and then using the treated water for agriculture (Ray Chaudhuri et al. 2008) resulted in safer produce which serves about one third of the population of the metropolitan (Kolkata) (Ray Chaudhuri et al. 2012). The science behind the purification of the wastewater has been investigated at length (Ray Chaudhuri and Thakur 2006; Adarsh et al. 2007; Chowdhury et al. 2008, 2011; Ray Chaudhuri et al. 2008; Yadav et al. 2010; Nasipuri et al. 2010; Chowdhury 2010; Mishra 2010; Nasipuri 2011) for understanding the ongoing process. An emergent behaviour was observed in the entire operation (Mishra 2010), a key feature of a complex system (Mukherjee et al. 2010). Based on this understanding, the system has been successfully replicated in Bangladesh (Khanam 2016; Khanam et al. 2016). The complexity of the ongoing practice at East Kolkata Wetland which treats the entire sewage of Kolkata generating a portion of its fish and vegetable demand along with ensuring environmental protection and employment, is represented in Fig. 1.

In India, in collaboration with the urban local bodies, the State Government is responsible for setting up and maintaining the sewage treatment plants. The funding for setting up the treatment plant and incentives for taking adequate measures for pollution reduction is also in place with contribution from the Central government. The statutory power for monitoring the operation/performance lies with the State Environmental Protection Agency (Pollution Control Board) as per the Water Act 1974, with adequate provision for using the treated water for irrigation. Different by-products are recovered during wastewater treatment (Satyawali and Balakrishnan 2008; Pant and Adholeya 2007). However, the notion of biological treatment alone being insufficient for optimum pollutant removal persists (Pant and Adholeya 2007), calling for elaborate ETP design. Conventional wastewater treatment involves physical, chemical and biological unit operations. The physical unit operations include screening, comminution, flow equalization, sedimentation, floatation, granular medium filtration. The chemical unit operation mostly involves chemical precipitation, adsorption, disinfection, dechlorination. The biological unit operation includes activated sludge, aeration lagoon, trickling filters, rotating biological contractors, pond stabilization, anaerobic digestion or biological nutrient removal

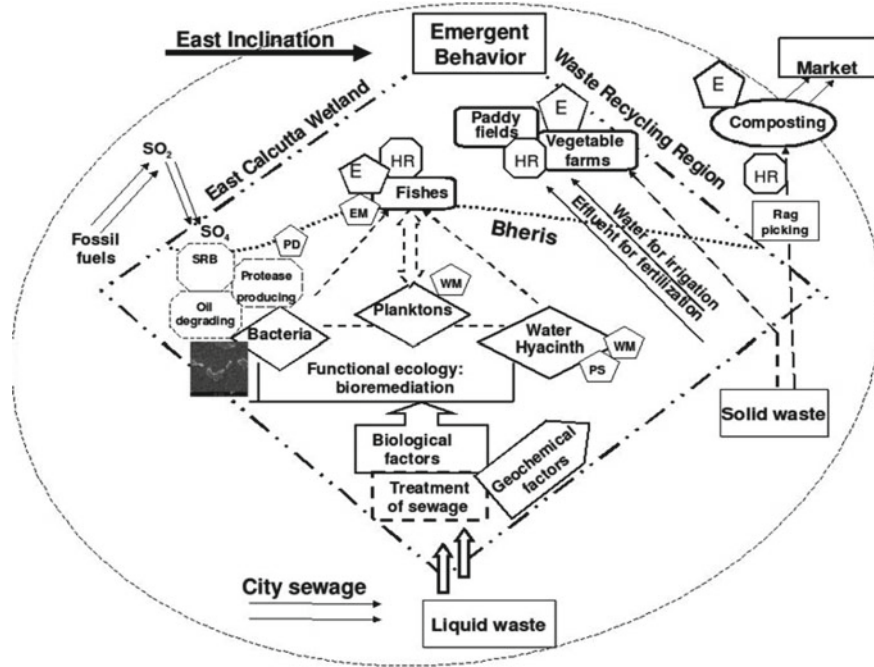


Fig. 1 The emergent behaviour observed in the ongoing integrated resource recovery system operating at East Kolkata Wetland where the city sewage is treated through indigenously designed wastewater fed aquaculture practice followed by using the sediment/silt and the treated water (with > 99% reduction in coliform count) for agricultural practices. It generates employment and revenue while protecting the environment. It involves close interaction among the microbes and plants in the region leading to detoxification and a perfect understanding of the aquaculture practice, which converts the nutrients in wastewater into fish feed (phytoplankton/zooplankton) to eliminate the expenditure of fish feed addition during fish cultivation. The abbreviations used in the figure are as follows: PD means Product Development, EM is Environment Management, WM stands for Waste Management, E is the abbreviated form of Economy Generation, and HR indicates Human Resource. Conceptualized by Prof Indranil Mukherjee and Dr Shaon Ray Chaudhuri while drawn by Dr Madhusmita Mishra from the West Bengal University of Technology (now renamed Maulana Abul Kalam Azad University of Technology West Bengal India)

(United Nations 2003). The treatment steps are selected based on the wastewater composition and volume. The different unit operations selected are used in combination to get the desired purification of the wastewater. Algal wastewater treatment and nutrient removal through constructed wetlands are economically viable options. Still, they need a large area for water treatment due to the prolonged hydraulic retention time with minimum energy requirement (Kadlec and Wallace 2009; Kadlec 2009). Land availability is a major problem in developing countries. Hence, a strong need is felt to develop rapid, eco-friendly biological processes with adequate scientific and technological intervention. The need based development of wastewater treatment technology is evident from ancient times (Chakraborty et al. 2018).

The approach for innovative rapid sludge free microbial wastewater treatment process development using microbial formulations has been established by the Microbial Technology Group, India, for different types of wastewater. The criterion for developing the microbial formulation involves the steps mentioned in the subsequent lines. The wastewater composition is analyzed to assess the pollutants to be treated (quantitative and qualitative assessment) as the first step towards consortium development. Microbial isolation is carried out using inoculum from environmental sites, selected based on two criteria, sites that receive point sources of the pollutant but do not show pollutant toxicity during quantitative estimation. The absence of elevated pollutant levels indicates the presence of potent bioremediants. The next step is selecting the medium for isolation of the microbes/consortium based on the literature. The microbial growth medium (based on the literature survey) for cultivating bacteria for bioremediation of the identified pollutant (in the wastewater) is used for strain/consortium enrichment. The pH and growth temperature are determined, keeping in mind these parameters in the environmental samples used for microbial isolation. The process of tailor made consortium development for sludge free wastewater treatment for different types of wastewater treatment are detailed in the subsequent sections.

2 Municipal/Agricultural Runoff Treatment Using Selectively Developed Consortium

The common pollutants present in municipal sewage and agricultural runoff are nitrates and phosphates. The origin of these is from the surface runoff (natural process of leaching from the soil, synthetic fertilizers leaching during agriculture), food products, animal excreta and manure, human excreta, detergents used for cleaning, leaching of industrial effluents like dairy effluent (farmyard runoff as well as milk processing plant runoff). The conventional sewage treatment process is an elaborate 240 h process using energy and labour (Saha et al. 2018). The essential plant growth nutrients in the wastewater are lost during the process. These include nitrates, ammonia and phosphate. While nitrogen fertilizer (urea) production needs immense energy, the phosphate reserves are rapidly depleted. The current trend is to recover these nutrients and reuse them for safe agricultural use. It is evident from the ongoing phosphate recovery practices (Ulrich and Frossard 2014; Chipako and Randall 2020; Alemayehu et al. 2020) from wastewater and human excreta. As mentioned earlier, wastewater based agricultural practices have a major concern of contaminating the produce, if used untreated, causing environmental hazards. The treatment of the generated wastewater needs immense expenditure for setting up the sewage treatment plant and hiring trained manpower for the labour intense operation, which is often not affordable by the concerned authority. There is a huge gap between the amount of wastewater generated and the available treatment facility. So there remains a need for the development of a rapid eco-friendly process.

The work started with screening for nitrate and phosphate reducing bacteria from different environmental origins. Thirty-two different sites were selected based on the point sources of pollutants received by them (DebRoy et al. 2012). Various kinds of water bodies like rivers, natural and artificial water bodies, marine coast, hot spring, rhizosphere of plants, algal mats and agricultural sites had been selected for sample collection (Fig. 2). In addition, microbial biofilms from nitrate containing wastewater treatment plants were also selected for bacterial isolation (Mishra et al. 2014). Next, the water samples were analyzed for their physicochemical properties. The sites that

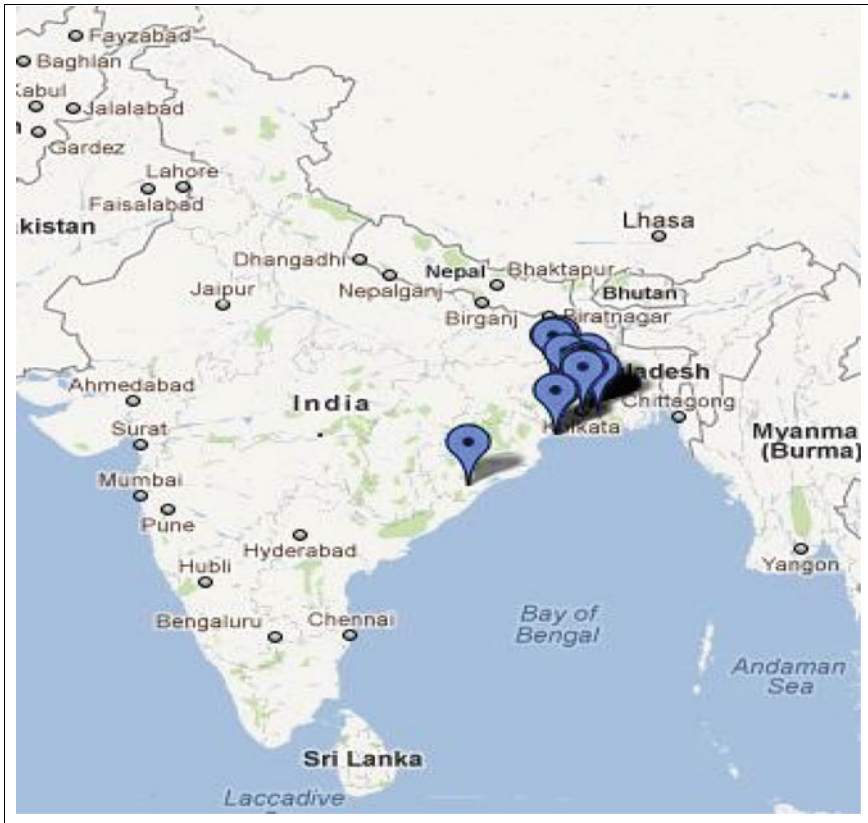


Fig. 2 Environmental screening for isolation of efficient microbes for wastewater treatment. The 1st three rows show site identification based on receiving point sources of nitrate and phosphate. The 4th row shows representative sites of sample collection from Mayurakshi (Tilpara barrage), Ultadanga over bridge, hot spring Agnikundu at Bakreshwar, wastewater canal next to Captain Bheri. The 5th row consists of images of the water plants whose rhizosphere were used to isolate microbes, namely Bulrush, Aquatic grass, water lily and water hyacinth. The 6th row consists of the enrichment techniques used like hay enrichment, air bubbling technique, Winogradsky column and plating techniques showing streaking of pure isolates on enriched medium with different concentrations (2000 mg/L) of nitrate and phosphate. The 7th row represents light microscopic images of the representative isolates



Fig. 2 (continued)

received point sources of nitrate and phosphate but did not show high concentrations of those pollutants were selected to isolate the bacteria for consortium development. The logic behind the selection was the assumption that there might be the presence of efficient pollutant reducers at those sites and hence a low level of pollutants inspite of receiving point sources. The purpose of the study was to sequester the essential nutrients during wastewater treatment. Microbes like *Beggiatoa*, *Thiomargarita* and *Thioploca* were known for nitrate accumulation (Mussmann et al. 2007; Otte et al. 1999; Schulz et al. 1999), while phosphate accumulation was well documented in domain bacteria (DebRoy et al. 2013a). The enrichment techniques were adopted based on the criterion for the enrichment of the nitrate accumulators. The growth medium for selective enrichment of nitrate and phosphate accumulators was based on literature survey. The samples used for cultivating the bacterial isolates from the selected sites, namely water, sediment, plants rhizosphere and algal mats, were

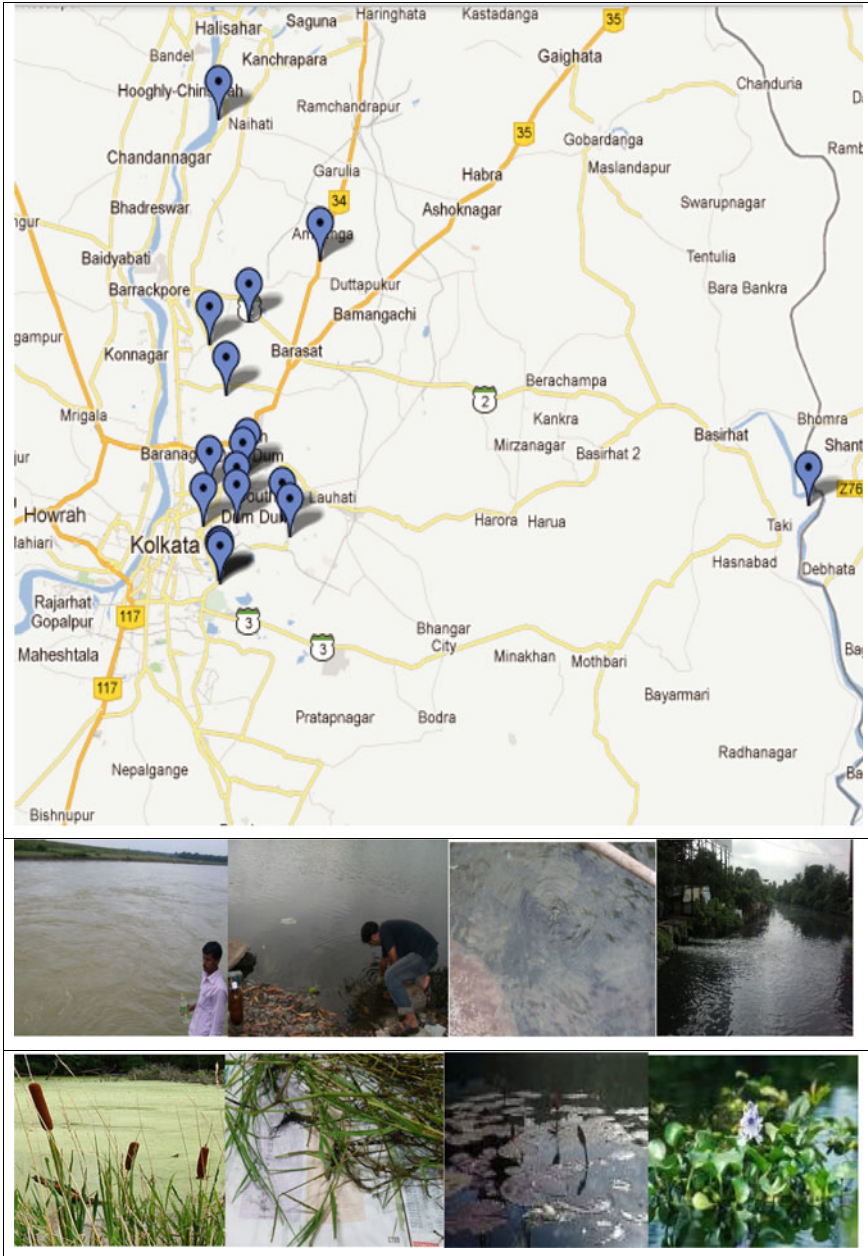


Fig. 2 (continued)

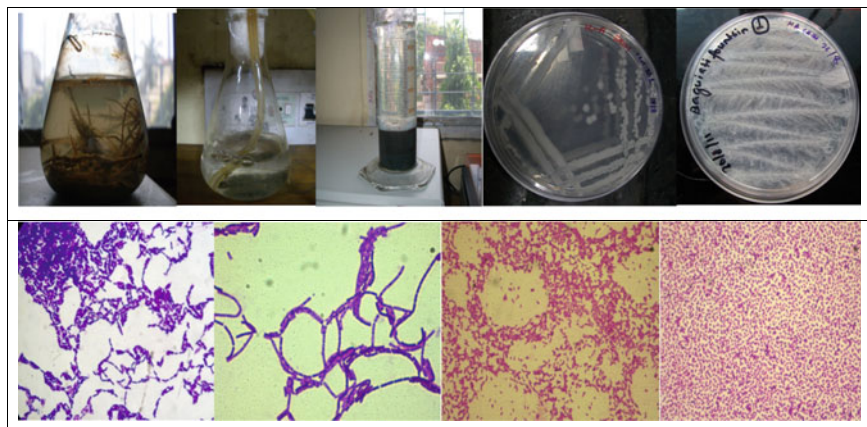


Fig. 2 (continued)

carried aseptically at room temperature for further processing, as shown below in Fig. 2.

From a total of 32 sites with different types of samples (water, sediment, algal slime, rhizosphere of plants) from each site, about 130 different isolates were purified on nitrate broth alone. On the assumption (based on the literature survey) that the nitrate accumulators might be filamentous, preliminary screening of the pure isolates was done to select the isolates that were bacilli or filamentous in shape. The selected 18 pure isolates and the other 6 isolates of the environmental origin from the laboratory stock were further selected for nitrate and phosphate removal from the medium. The isolates with maximum simultaneous nitrate and phosphate removing ability were selected to test the nitrate accumulating ability through cell lysis, followed by nitrate concentration assessment in the intracellular sap through the method of (Cataldo et al. 1975). Only one isolate (*Bacillus* sp. MCC0008) was found to accumulate nitrate intracellularly up to 1278.66–1302.122 ppm/gm of cell pellet wet weight when grown in nitrate broth with 1000 ppm of nitrate within 2 h of growth (Ray Chaudhuri et al. 2016a). Through Dissimilatory Nitrate Reduction to Ammonium and using nitrogenase enzyme, *Baggiatoa* is reported to accumulate 20,000 times more nitrate inside the vacuoles than the surrounding environment (Teske et al. 2006; Ruuskanen 2014). This strain was selected for consortium development.

Since phosphate removal is through polyphosphate accumulation in bacteria, the maximum phosphate removers (assessed through Daniges (Deniges 1920)) were selected for consortium development. The well characterized (DebRoy et al. 2013a, b, c; Ray Chaudhuri et al. 2016a) three selected isolates combined in definite proportion were used for simultaneous nitrate and phosphate removal from raw sewage canal water with agricultural runoff. The single unit operation process with minimal carbon source addition was scalable with little energy requirement. It was scaled upto 2.64 m³/day processing capacity with about 55 to 61% phosphate and 93% nitrate removal within 2 h (hydraulic retention time) with an associated Chemical

Oxygen Demand (240 mg/L) reduction of 91.8% and Biological Oxygen Demand (167.7 mg/L) reduction of 97.4% (Saha et al. 2018). Analysis of the different soluble and gaseous by-products formed during the metabolic pathway indicated the majority of the nitrogen to be accumulated as nitrate intracellularly in this low C/N ratio while showed higher ammonia production under high C/N ratio (nitrate broth). The finding was at par with available literature (Yoo et al. 1999). The bioreactor could run continuously for more than 200 days with little sludge generation before the system was dismantled. This is by far the fastest sewage treatment process (Ray Chaudhuri et al. 2017a). The accumulated nitrate and phosphate within the biomass could promote plant growth with the nutrient quality enhancement of mung bean seeds (Ray Chaudhuri and Thakur 2013). The treated wastewater with neutral pH (hence no phosphate precipitation) (Saha et al. 2018) was suitable for agriculture and aquaculture.

Adequate biotechnological intervention developed a single unit biofilm-based process for treating the sewage within 2 h without sludge formation using a tailor-made bacterial consortium from environmental origin suitable for secondary application. It reduces about 90% CO₂ equivalent gas emission due to a drastic reduction in energy consumption. In addition, it also saves investment on land for the installation of the ETP. Complete nitrate removal was reported from enriched (C/N) wastewater (Hao et al. 2013), but the current process could achieve similar results from low C/N rich wastewater within a very short time (Saha et al. 2018). Adopting this process can fill the gap between the amount of wastewater generated and the available processing capacity. It could also be introduced in existing ETP resulting in an enhanced treatment capacity.

3 Aquaculture Wastewater Treatment Using Single Unit Bacterial Biofilm System

The aquaculture industry is important for a countries economy. It uses a large volume of fresh water and generates a copious amount of wastewater. The system is extremely sensitive to elevated nitrogen concentration. The toxicity level for aquaculture is much lower than those permitted by Environmental Protection Agency for all other environmental purposes. The source of pollution is from the unutilized fish feed and the fish excreta (Cho and Bureau 1997; Axler et al. 1996). The major toxicity is due to ammonia (above 0.5 mg/L) and nitrite (above 0.02 mg/L), leading to reduced excretion, blood and tissue toxicity, lethargy, and finally, the mortality of fishes. The amount of organic waste produced is about 2.5 times fish production (Ackefors and Enell 1994). To avoid fish mortality, large volumes of freshwater are used for diluting the pollutants. This approach is becoming non-viable due to the fast depleting reserves of freshwater, necessitating the development of rapid, efficient, economic and eco-friendly aquaculture wastewater treatment processes (Goldburg and Triplett 1997; Porrello et al. 2003). Yet another contaminant released into the wastewater from aquaculture practice is phosphate (Piedrahita 2003), which must be removed

simultaneously. The existing treatment process is laborious to meet the strict guidelines according to the Water Resource Act and FAO (Moccia et al. 1997), making it unadoptable for the smaller agencies inspite of the extensive environmental damage caused by the discharge of untreated effluent (Doupe et al. 1999; Boyd et al. 2001). Innovative (but expensive) methods have been developed for minimizing pollution during fish cultivation (Mayer and McLean 1995). Biological treatment of aquaculture wastewater has been reported both under suspended (Barman et al. 2016; Lyles et al. 2008) as well as immobilized (Fei et al. 2019; Gogoi et al. 2021a, b) conditions within 7 days, 4 days, 24 h and 14 h (Gogoi et al. 2021a, b), respectively. The biofilm based system was found to show higher efficiency using a pure isolate of *Bacillus albus* AFFS01 from the sludge of aquaculture pond instead of a consortium developed using efficient ammonia removers (Fig. 3). It is not essential that consortium will always work better during environmental application. The efficiency of performance will depend on the interaction among the isolates.

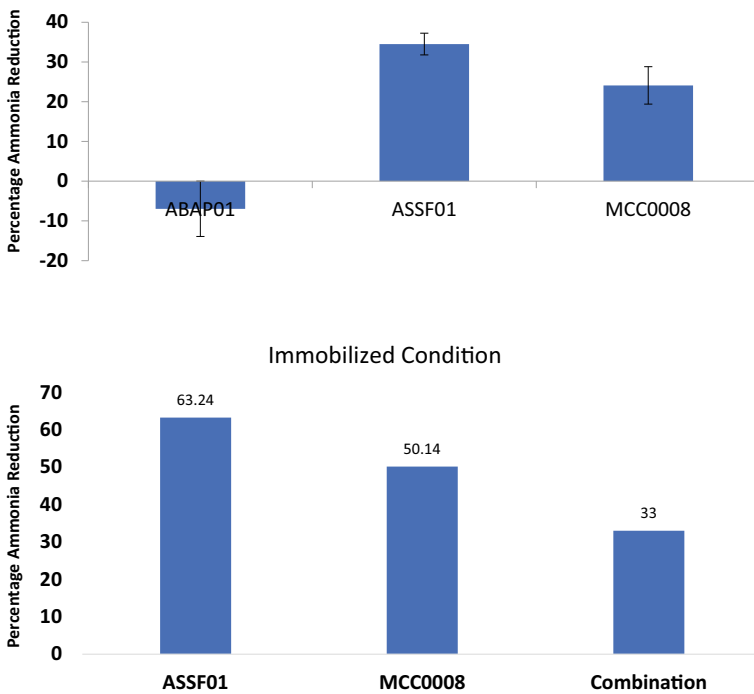


Fig. 3 Top graph—Percentage of ammonia reduction by three strains of genus *Bacillus* sp ABAP01 (Ammonia producer), ASSF01 and MCC0008 under the suspended condition of growth in nitrate broth. Bottom graph—Percentage ammonia reduction by two *Bacillus* strains ASSF01 and MCC0008 and their consortium (1:1). The graph shows a better ammonia reduction under an immobilized state by the pure isolates ASSF01. It also reveals an antagonistic interaction between ASSF01 and MCC0008

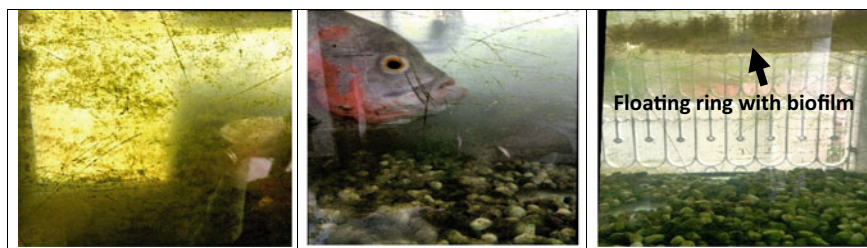


Fig. 4 Wall of the aquarium in absence and presence of the immobilized bacterial biofilm as floating rings on the surface of the water after one month of operation

The immobilized cells in the bioreactor could work efficiently for more than 20 months treating real effluent with maintained efficiency. The novel, sludge free microbial biofilm based approach developed by the Microbial Technology Group for treatment of aquaculture effluent tested at 15.43 L/day capacity at the laboratory scale in continuous mode (Gogoi et al. 2021a, b) was also found to be effective for refinery effluent treatment. Aquaculture effluent treatment is also required at a relatively smaller scale in the aquariums, which periodically involves labour for cleaning and freshwater replacement. The immobilized bacterial biofilm on raschig rings was found to drastically reduce algal growth on the aquarium walls (254 L) even after one month of operation without additional energy expenditure inspite of uneaten fish feed and sufficient sunlight, indicating efficient ammonia, nitrate and phosphate removal from the wastewater. This could alleviate the need for water replacement and clean regularly. The pictorial representation of the algal deposition on the walls of technology deployed and non-deployed aquarium, treated under identical conditions after one month of deployment in running aquarium is provided in Fig. 4.

4 Milk Processing Plant Wastewater Treatment Using Selectively Developed Consortium

The dairy industry produces 1.5 to 10 L of wastewater per litre of milk processed with composition dependent on the upstream operation. This kind of wastewater is C/N rich and, unless treated adequately, leads to the environmental deterioration (Biswas et al. 2019). Literature states that microbes lead to ammonification under a high C/N ratio instead of denitrification (Yoo et al. 1999). Since dairy wastewater is enriched and in large volume, biotransformation was attempted instead of bioremediation into ammonia-rich liquid fertilizer as ammonia is preferred over nitrate for plant growth (Nasholm et al. 2009). Through this approach, the plant growth nutrients (nitrate, nitrite, ammonia, phosphate, potassium, magnesium) in dairy wastewater could be completely reused along with the entire volume of treated water which could cut down on the loss of freshwater for agriculture. This would not

only cut down on the wastage of freshwater but will also prevent environmental pollution caused due to chemical fertilizer leaching. It would drastically reduce chemical fertilizer production, hence saving energy expenditure (used during urea production) and finite resources like rock phosphate. Unlike the application of untreated dairy wastewater, the treated wastewater would not harm the soil as the concentration of protein and lipids will be low, hence the associated Chemical Oxygen demand and Biological Oxygen Demand would be substantially reduced during the treatment. Based on the literature, the growth medium for cultivating the microbes for bioconversion was selected. The microbes known to be involved in ammonification, and preferably lacking denitrification, were selected for assessing their growth media and growth conditions. The activated sludge of Mother Dairy ETP at Dankuni, West Bengal, India, was used for bacterial strain isolation as per standard culture based procedure (Biswas et al. 2019). These organisms, along with other environmental isolates with nitrate, protein, phosphate reducing properties, were also considered for consortium development (Halder et al. 2020). The consortium with the highest ammonia producing ability was used for biofilm based reactor development. The performance of the consortium was enhanced under immobilized conditions. It is known that the cell density of the organism is higher in a biofilm, and so is the extracellular polymeric substances secreted by the cells. These factors lead to enhanced pollutant removal as a concentration gradient is created within the bulk liquid. The biofilm provides a higher actual hydraulic retention time as the pollutant diffuses from the bulk liquid through the extracellular polymeric substances to the cells in the biofilm. To understand the actual reason for performance enhancement in the current case, the consortium was tested for assessing its doubling time under the immobilized condition as per standard procedure (Gogoi et al. 2021b). The doubling time of the consortium in suspension culture was 78 min 56 s while the same under immobilized conditions was 17 min 10 s. The doubling time was determined as per the method reported by (Gogoi et al. 2021b). The determination of doubling time was done by allowing growth medium to pass through packed bed column with immobilized consortium at different flow rates (2.2 ml/min, 3.3 ml/min and 8.8 ml/min) under ambient condition.

The column was eluted with 25 times the bed volume with the bacterial growth medium. The fraction eluted were checked for scattering at 600 nm. The data was plotted with the elution time on the x axis while the optical density on the y axis. The data showed a doubling time of 17.6 min (at 2.2 ml/min), 17.16 min (3.3 ml/min) and 17.1 min (8.8 ml/min) for the different flow rates (Fig. 5). The average doubling time was 17.28 min, closest to 17.16 min at a flow rate of 3.3 ml/min. Hence the doubling time was taken as 17.16 min, equivalent to 17 min and 10 s. The doubling time was calculated by assessing the difference between the two peaks. It is assumed that the flow rate should be such that the eluted cells (after the cell divides) do not divide within the column. So every time that the cells divide, a peak is observed. Hence, the doubling time will be the gap between two subsequent peaks. The peak height increased with a slower flow rate, hence a longer retention time. It reflects the relative abundance of the cells getting eluted at a particular time.

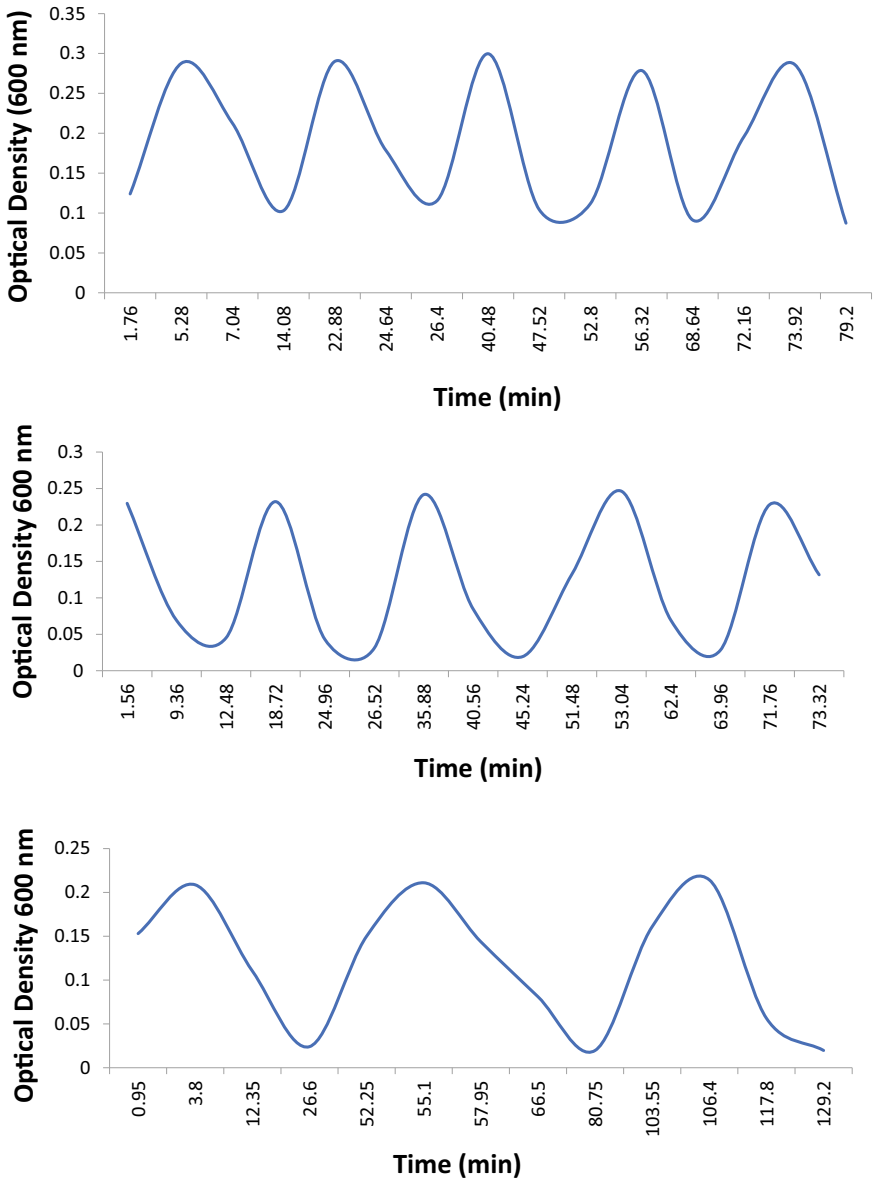


Fig. 5 Doubling time of the consortium revealed at a flow rate of 2.2, 3.3 and 8.8 ml

5 Selection of Microbial Growth Medium for Conversion

The consortium inside a packed bed biofilm reactor could convert the dairy wastewater into liquid biofertilizer within 16 h (Halder et al. 2020) with associated reduction of nitrate, phosphate, protein, lipid, chemical oxygen demand and biological oxygen demand and production of ammonia. The process was scaled up to 11 m³/day capacity with sustained efficiency (Gogoi et al. 2021c). The reactor starts performing from the first day of operation. Further analysis of the process revealed the desired reduction and production to occur within 4 h, making it's the fastest dairy wastewater conversion process. It enhanced yield of the economic crop at par with chemical fertilizer or higher than that as in the case of Mung bean, Black gram, Field pea, Maize, sugar cane, Ramie, Sorghum sudangrass, Aloe vera, lemongrass. It also sustained the cultivation of Cassava, Colocasia, Yam, Elephant foot yam and sweet potato. In the case of potato and yam bean, the yield was lower than chemical fertilizer grown produce but higher than convention biofertilizer based growth. But in all cases of the tuber crops, the carbohydrate content of the tubers was substantially less than chemical fertilizer grown plants. As per cited literature, it is expected due to the high nitrogen content of the fertilizer. Hence, this liquid biofertilizer not only alleviates the bottleneck of compromised production of the crop, but also produces diet tuber suitable for the diabetic and obese population. Using this tailored made microbial process, milk processing plant wastewater can be economically treated with more production of healthy, economic crop from a given area of land. A single unit operation with minimal energy expenditure, cuts down on the CO₂ equivalent gas emission from the operation of the plant by approximately 90%. Through this approach, the milk processing plant wastewater treatment can be converted into an economically affordable, eco-friendly, self-sustainable system that runs for years after charging the reactor. However, such a system could work only for the rural dairies with large farmlands in their vicinity. In the case of urban dairies, the transportation of the large volumes of liquid fertilizer from the point of production to the point of use might become a problem (economically not sustainable). Concentrating the fertilizer will result in loss of water, hence the replacement of freshwater for irrigation would not be possible anymore. Yet another treatment has been developed for the urban dairies. A bacterial consortium with 8 bacterial isolates mostly from the activated sludge of dairy ETP was found to efficiently bioremediate the milk processing plant wastewater within 20 h of hydraulic retention time to near discharge level (as per Central Pollution Control Board Norms). The phosphate and the ammonia concentration was just above the discharge level. The treated water was further treated for 48 h using a biofilm based microalgae bacterial mixed consortium. The nutrient was completely removed, making the treated water suitable for secondary application. It was accompanied by a significant increase in the biomass yield, lipid and carbohydrate content of the dried biomass compared to non-dairy wastewater treated samples. The conventional treatment takes about 105 to 120 h, while this process took 68 h with substantially reduced energy requirement. Hence, the urban dairies could adopt this two-unit operation with reduced energy and space requirement for effluent treatment with eco-friendly by-product generation (Biswas et al. 2021).

6 Petrochemical Wastewater Treatment Using Selectively Developed Consortium

A similar approach has also been adopted to develop a tailor-made bacterial consortium for petrochemical wastewater treatment. Bacteria isolated from the sludge and the effluent of different compartments of the ETP at a petrochemical industry terminal at Vishakhapatnam, India, were screened based on culture dependent method. The well characterized isolates were mixed in a definite proportion to develop the consortium. The consortium was immobilized to enhance the biological oxygen demand removal within a stipulated period. The immobilized consortium in a biofilm reactor was tested for its efficiency in pollutant removal in terms of reducing biological oxygen demand at a laboratory scale. Based on its performance, the system was scaled up to 12 m³/day capacity at the ETP of the petrochemical receiving terminal. The consortium with 31 isolates could remove the pollutant (as evident from the reduction in the biological oxygen demand) at the industrial scale within 18 h of hydraulic retention time from a moving bed biofilm reactor. After installation (which took about 10 days to become fully operational), the system could run for nearly 5 years without any breakdown at industrial site, making the industry Central Pollution Control Board compliant. The treated water could replace the purchase of freshwater for landscaping and firefighting storage to a substantial extent. This is another successful example of tailor-made consortium based sludge free wastewater treatment (Ray Chaudhuri et al. 2020; Biswas 2021).

The above examples establish that the innovative process of wastewater treatment using tailor-made consortium works for different kinds of wastewater with improved efficiency in an eco-friendly manner without sludge generation at different scales of operation with sustained performance. However, the consortium development could also be achieved by selecting the consortium directly from the environmental origin instead of combining individual isolates. Some examples are given below.

7 Enriched Consortium Based Treatment of Agricultural Runoff and Tannery/mining Effluent

As stated above, literature-based selection of growth medium and culture conditions was followed to enrich the consortium. To remove nitrate and phosphate from the agricultural runoff, nitrate broth was selected, and soil from East Kolkata Wetland (old dumping ground converted to agricultural land) was used as inoculum. The ongoing activity at the location ensured access to nitrate and phosphate. In contrast, the healthy growth of vegetables and fish in the location indicated a lack of nitrate and phosphate toxicity, hence the presence of strong bioremediants. The nitrate broth's anaerobic condition (nitrogen atmosphere) gave efficient consortium enrichment. In other experiments, biomass from nitrate reducing reactor was used as inoculum to develop a consortium under the aerobic condition in nitrate broth. The consortium

individually could remove nitrate and phosphate simultaneously from the solution. When the consortium was applied in a definite combination to the soil, it could prevent nitrate leaching from soil between 8 to 11 cm depth of soil (root zone). This nutrient was made available for the plants grown on that soil, resulting in promoting plant growth with yield enhancement (Ray Chaudhuri et al. 2016a, 2017b; Banerjee 2018). Hence the adverse effect of nutrient leaching during agriculture could be prevented while making the soil nitrate available to the plants over an extended period. The soil fertility was retained even after the cultivation was over.

Soluble sulphate reduction is required from wastewater from the tannery, mining industry, acid rain, to name a few. A similar approach was used for developing soluble sulphate reducing consortium in sulphate reducing bacteria specific medium using inoculum from wastewater fed aquaculture pond, waste dumping ground receiving the cities runoff (containing acid rain), mining effluent, raw sewage canal water, tannery effluent, hot springs to name a few. Multiple consortia were enriched and stabilized through repeated rounds of cultivation (Nasipuri 2011). Their efficiencies were compared (Nasipuri et al. 2010), and the most efficient consortium was further used for scale up operation (Ray Chaudhuri et al. 2016b), which revealed it to be the most efficient bio remedial system for soluble sulphate removal within 4 h of hydraulic retention time, showing similar efficiency for simulated wastewater, tannery effluent and mining effluent (Nasipuri 2011). Bioreactor design and minimal medium composition optimization made its adoption viable for pilot scale operation (Chanda et al. 2020).

This chapter details the criteria for a bacterial consortium based sludge free wastewater treatment.

8 Conclusion

Microbial technology can lead to efficient, economic, eco-friendly process development. The treatment systems developed are rapid, less energy consuming, stable with the generation of treated water suitable for the non-potable purpose. A comparative advantage of the developed wastewater treatment technologies reported in this chapter is tabulated (Table 1) below at a glance which is self-explanatory and summarizes the chapter.

Table 1 Wastewater treatment technologies developed by the Microbial Technology Group, India

Criterion	Dairy wastewater	Petrochemical wastewater	Municipal wastewater/ Agricultural runoff	Ammonia rich wastewater	Tannery/Mining effluent
Patent status	201,731,003,023 dt 27th January 2017	202,031,011,766 dt 18th March 2020	1179/KOL/2013 dt16 Oct 2013 351564 granted on 13th Nov 2020 (India); 1005753 granted on 24th Oct 2017 (Bangladesh)	202131002964 dt 21st January 2021	789/KOL/2011 dt June 10th, 2011; US8398856B2 ; US20120312743A1 341914 granted on 17th July 2020 (Indian)
Space requirement	25% of conventional	Similar	45% of conventional	50% of conventional	45% of conventional
Current HRT/ Conventional HRT	16 h/120 h	18 h/24 h (only biological)	2 h/240 h	14 h/24 h	4 h/12 h
Energy Requirement	10%	Less than conventional	20%	20%	20%
CO ₂ emission	90% less	Less than conventional	80%	80%	80%
Product	Liquid Biofertilizer	Irrigable water	Irrigable/ aquaculture suitable water	Irrigable/ aquaculture suitable water	For discharge
Microbial inoculum (actively functions)	1 time (more than 3 years)	1 time (more than 4 years)	1 time (more than 1.5 years)	1 time (more than 1.5 years)	1 time (more than 1.5 years)
Scale of operation	11 m ³ /day in 2 dairy farms	12 m ³ /day at EIPL Vishakhapatnam	2.64 m ³ /day at laboratory scale	0.041 m ³ /day at laboratory scale	2.64 m ³ /day at laboratory scale

(continued)

Table 1 (continued)

Criterion	Dairy wastewater	Petrochemical wastewater	Municipal wastewater/ Agricultural runoff	Ammonia rich wastewater	Tannery/Mining effluent
Scum Production	Scum free	Scum free	Scum free	Scum free	Largely scum free
Funding for Technology Development	BIRAC under the BIG scheme	MHRD under the FAST scheme	ICAR under National Fund Scheme	-	DAE under BRNS scheme
Recognition/Award	Visitor's Award 2019 Regional Climate Launchpad 2019	NASI-Reliance Industries Platinum Jubilee Award 2020	DST Lockheed Martin India Innovation Growth Program 2014	-	-

Acknowledgements The author acknowledges the effort put in by the research scholars and the trainee students of the Microbial Technology group, which led to the generation of the data reported here. The author is thankful to the granting agencies (University Grants Commission-Department of Atomic Energy, Government of India under the CRS scheme [UGC-DAE-CSR-KC/CRS/19/TE07/1069/1085]; Biotechnology Industry Research Assistance Council, Government of India under the Biotechnology Ignition Grant [BIRAC/KIIT0200/BIG-10/17]; Department of Atomic Energy (BRNS); Department of Biotechnology (DBT PDF in Life Sciences); Department of Science and Technology (FAST TRACK Scheme) and Ministry of Education under the Frontier Area of Science and Technology scheme [F.No 5-1/2014-TS.VII dt August 7 2014] which funded the work. The author is also thankful to the organizations (Tripura University; West Bengal University of Technology; Technology Business Incubator at KIIT, India; Centre of Excellence in Environmental Technology and Management at MAKAUT, WB, India; TBI KIIT, India; Gomati Cooperative Milk Producer's Union, India; OMFED, India; Mother Dairy, India; East India Petroleum Limited, Vishakhapatnam; Uranium Corporation of India Limited) which provided the infrastructure and resources for conducting these works.

References

- Ackefors H, Enell M (1994) The release of nutrients and organic matter from aquaculture systems in nordic countries. *J Appl Ichthyol* 10:225–242
- Adarsh VK, Mishra M, Chowdhury S, Sudarshan M, Thakur AR, Ray Chaudhuri S (2007) Studies on metal microbe interaction of three bacterial isolates from East Calcutta Wetland. *Online J Biol Sci* 7:80–88
- Alemayehu YA, Asfaw SL, Terfie TA (2020) Nutrient recovery options from human urine: a choice for large scale application. *Sustain Prod Consum* 24:219–231
- Axler R, Larsen C, Tikkanen C, McDonald M, Yokom S (1996) Water quality issues associated with aquaculture: a case study in mine pit lakes. *Water Environ Res* 68:995–997
- Banerjee S (2018) Understanding the effect of plant growth promoting bacteria (PGPB) formulation on nutritional quality of Mung bean seeds. PhD Thesis, Maulana Abul Kalam Azad University of Technology West Bengal, India
- Barman P, Kati A, Mandal AK, Bandyopadhyay PP, Mohapatra PK (2016) Biopotentiality of *Bacillus cereus* PB45 for nitrogenous waste detoxification in ex situ model. *Aquacult Int* 25:1167–1183
- Bhamoriya V (2004) Wastewater irrigation in Vadodara, Gujarat, India: economic catalyst for marginalized communities. In: Scott CA, Faruqui NI, Raschid-Sally L (eds) wastewater use in irrigated agriculture: confronting livelihood and environmental realities, CAB International in Association with International Water Management Institute and the International Development Research Centre, Colombo, Sri Lanka, Ottawa, Canada, pp 127–134
- Bhardwaj RM (2005) Status of wastewater generation and treatment in India. IWG-Env Joint Work Session on Water Statistics, Vienna. https://unstats.un.org/unsd/environment/envpdf/pap_wases3b6india.pdf. Accessed 27 July 2021
- Biswas T, Chatterjee D, Barman S, Chakraborty A, Halder N, Banerjee S, RayChaudhuri S (2019) Cultivable bacterial community analysis of dairy activated sludge for value addition to dairy waste water. *Microbiol Biotechnol Lett* 47:585–595
- Biswas T, Bhushan S, Prajapati SK, Ray Chaudhuri S (2021) An eco-friendly strategy for dairy wastewater remediation with high lipid microalgae-bacterial biomass production. *J Environ Manage* 286:112196
- BiswasT (2021) Development of tailor-made consortia for efficient effluent treatment. PhD Thesis, Tripura University, Tripura, India

- Boyd D, Wilson M, Howell T (2001) Recommendations for operational water quality monitoring at cage culture aquaculture operations. Environment Monitoring and Reporting Branch. Ministry of the Environment, Canada
- Cataldo DA, Maroon M, Schrader LE, Youngs VL (1975) Rapid colorimetric determination of nitrate in plant tissues by nitration of salicylic acid. *Commun Soil Sci Plant Anal* 6:71–80
- CGWB (2011) Ground Water Year Book-India 2010–11. Central Ground Water Board, Ministry of Water Resources. Government of India. <http://www.cgwb.gov.in/documents/Ground%20Water%20Year%20Book-2010-11.pdf>. Accessed 27 August 2021
- Chakraborty A, Bhowmik A, Jana S, Bharadwaj P, Das D, Das B, Agarwala BK, Ray Chaudhuri S (2018) Evolution of waste water treatment technology and impact of microbial technology in pollution minimization during natural fiber processing. *Curr Trend Fashion Technol Text Eng* 3:001–004
- Chanda C, Gogoi M, Mukherjee I, Ray Chaudhuri S (2020) Minimal medium optimization for soluble sulfate removal by tailor-made sulfate reducing bacterial consortium. *Bioremediat J* 24:251–264
- Ray Chaudhuri S, Mishra M, Nandy P, Thakur AR (2008) Waste management: a case study of ongoing traditional practices at East Calcutta Wetland. *Am J Agric Biol Sci* 3:315–320
- Chipako TL, Randall DG (2020) Investigating the feasibility and logistics of a decentralized urine treatment and resource recovery system. *J Water Process Eng* 37:101383
- Cho CY, Bureau DP (1997) Reduction of waste output from salmonid aquaculture through feeds and feeding. *Progress. Fish Cult* 59:155–160
- Chowdhury S, Mishra M, Adarsh VK, Mukherjee A, Thakur AR, Ray Chaudhuri S (2008) Novel metal accumulator and protease secretor microbes from East Calcutta Wetland. *Am J Biochem Biotechnol* 4:255–264
- Chowdhury S, Thakur AR, Ray Chaudhuri S (2011) Novel microbial consortium for laboratory scale lead removal from city effluent. *J Environ Sci Technol* 4:41–54
- Chowdhury S (2010) Tapping of multifunctional microbes from East Calcutta wetland. PhD Thesis, West Bengal University of Technology, West Bengal, India
- CPCB (2005a) Performance status of common effluent treatment plants in India. Central Pollution Control Board, India. <https://cpcb.nic.in/openpdffile.php?id=UmVwb3J0RmlsZXMvODQ4XzE1NTU0MDc4MjFfbWVkaWFwaG90bzMxNDQwLnBkZg==>. Accessed 27 August 2021
- CPCB (2005b) Parivesh Sewage Pollution–News Letter. Central Pollution Control Board, Ministry of Environment and Forests, Govt. of India, Parivesh Bhawan, East Arjun Nagar, Delhi 110 032 <http://cpcbenvi.nic.in/newsletter/sewagepollution/contentsewagepoll0205.htm>. Accessed 27 July 2021
- DebRoy S, Das S, Ghosh S, Banerjee S, Chatterjee D, Bhattacharjee A, Mukherjee I, Ray Chaudhuri S (2012) Isolation of nitrate and phosphate removing bacteria from various environmental sites. *OnLine J Biol Sci* 12:62–71
- DebRoy S, Bhattacharjee A, Thakur AR, RayChaudhuri S (2013a) Draft Genome of a nitrate and phosphate accumulating *Bacillus* sp. MCC0008. *Genome Announc* 1:e00189–e212
- DebRoy S, Mukherjee P, Roy S, Thakur AR, RayChaudhuri S (2013b) Draft Genome of a phosphate accumulating *Bacillus* sp. WBUNB004. *Genome Announc* 1:e00251–e312
- DebRoy S, Mukherjee P, Roy S, Thakur AR, RayChaudhuri S (2013c) Draft Genome of a nitrate and phosphate removing *Bacillus* sp. WBUNB009. *Genome Announc* 1:e00254–e312
- Deniges G (1920) Reaction de coloration extremement sensible des phosphates et des arseniates, ses Applications. *Acad Des Sci Compt Rend* 171:802–804
- Doupe RG, Alder J, Lymbery AJ (1999) Environmental and product quality in finfish aquaculture development: an example from inland Western Australia. *Aqua Res* 30:595–602
- Fei X, Sun S, He S, Huang J, Zhou W (2019) Application of a novel two-stage biofiltration system for simulated brackish aquaculture wastewater treatment. *Environ Sci Pollut Res Int* 27:636–646
- Gogoi M, Bhattacharya P, Bhushan S, Sen SK, Mukherjee I, Ray Chaudhuri S (2021a) Aquaculture effluent Treatment with ammonia remover *Bacillus albus* (ASSF01). *J Environ Chem Eng* 9:105697

- Gogoi M, Mukherjee I, Ray Chaudhuri S (2021b) Characterization of ammonia remover *Bacillus albus* (ASSF01) in terms of biofilm formation ability with application in aquaculture effluent treatment. *Environ Sci Pollut Res* (In press)
- Gogoi M, Biswas T, Biswal P, Saha T, Modak A, Gantayet LM, Nath R, Mukherjee I, Thakur AR, Sudarshan M, Ray Chaudhuri S (2021c) A novel strategy for microbial conversion of dairy wastewater into biofertilizer. *J Clean Prod* 293:126051
- Goldburg R, Triplett T (1997) Murky waters: environmental effects of aquaculture in the United States. Waste treatment methods in aquaculture. Environmental Defense Fund Publication Washington, Columbia, USA
- Halder N, Gogoi M, Sharmin J, Gupta M, Banerjee S, Biswas T, Agarwala BK, Gantayet LM, Sudarshan M, Mukherjee I, Roy A, Ray Chaudhuri S (2020) Microbial consortium-based conversion of dairy effluent into biofertilizer. *J Hazard Toxic Radioact Waste* 24:040190391–040190397
- Hao RX, Li SM, Li JB, Zhang QK, Liu F (2013) Water quality assessment for waste water reclamation using principal component analysis. *J Environ Inform* 21:45–54
- Kadlec RH (2009) Comparison of free water and horizontal subsurface treatment wetlands. *Ecol Eng* 35:159–174
- Kadlec RH, Wallace SD (2009) Treatment wetlands, 2nd edn. CRC Press Taylor & Francis Group, London, New York, pp 1–348
- Kaur R, Wani SP, Singh AK, Lal K (2012) Wastewater production, treatment and use in India. https://www.ais.unwater.org/ais/pluginfile.php/356/mod_page/content/128/CountryReport_India.pdf. Accessed 26 August 2021
- Khanam S, Mukherjee I, Thakur AR, Ray Chaudhuri S (2016) Successful technology transfer of waste water fed aquaculture from India to Bangladesh: a case study. In: Ray Chaudhuri S (ed) Life science: recent innovation and research. International Research Publication House, India, pp 351–368
- Khanam S (2016) An experimental study on scopes for transferring sewage fed aquaculture (Bheri) from Kolkata, India to Bangladesh. PhD Thesis, Maulana Abul Kalam Azad University of Technology West Bengal, West Bengal, India
- Kumar RM (2003) Financing of wastewater treatment projects. Infrastructure development finance corporation and confederation of Indian industries. Water Summit, 4–5 December, Hyderabad, India
- Lyles C, Boopathy R, Fontenot Q, Kilgen M (2008) Biological treatment of shrimp aquaculture wastewater using a sequencing batch reactor. *Appl Biochem Biotechnol* 151:474–479
- Mayer I, McLean E (1995) Bioengineering and biotechnological strategies for reduced waste aquaculture. *Water Sci Technol* 31:85–97
- Minhas PS, Sharma N, Yadav RK, Joshi PK (2006) Prevalence and control of pathogenic contamination in some sewage irrigated vegetable, forage and cereal grain crops. *Biores Technol* 97:1174–1178
- Minhas PS, Samra JS (2004) Wastewater use in peri-urban agriculture: impacts and opportunities. In: Minhas PS, Samra JS (eds) Bulletin No. 2, Central Soil Salinity Research Institute, Karnal, India, pp 1–75
- Mishra M (2010) Bioremediation studies using microbes from East Calcutta Wetland. PhD Thesis, West Bengal University of Technology, West Bengal, India
- Mishra M, Jain S, Thakur AR, Ray Chaudhuri S (2014) Microbial community in packed bed bioreactor involved in nitrate remediation from low level radioactive waste. *J Basic Microbiol* 54:198–203
- Moccia RD, Naylor S, Reid G (1997) An overview of aquaculture in Ontario. University of Guelph Extension Centre Fact Sheet. Canada, Publ. No 96–003
- Mukherjee I, Bhaumik P, Mishra M, Thakur AR, Ray Chaudhuri S (2010) Bheri- a unique example of biological complex system. *Online J Biol Sci* 10:1–10
- Mussmann M, Hu FZ, Richter M, de Beer D, Preisler A, Jorgensen BB, Huntemann M, Glockner FO, Amann R, Koopman WJ, Lasken RS, Janto B, Hogg J, Stoodley P, Boissy R, Ehrlich GD

- (2007) Insights into the genome of large sulfur bacteria revealed by analysis of single filaments. *PLoS Biol* 5:1923–1937
- Nasholm T, Kielland K, Ganeteg U (2009) Uptake of organic nitrogen by plants. *New Phytol* 182:31–48
- Nasipuri P, Pandit GG, Thakur AR, Ray Chaudhuri S (2010) Comparative study of soluble sulfate reduction by bacterial consortia from varied regions of India. *Am J Environ Sci* 6:152–158
- Nasipuri P (2011) Isolation and characterization of efficient sulfate reducing bacterial consortia from different environmental sites. PhD Thesis, West Bengal University of Technology, West Bengal, India
- Otte S, Kuenen JG, Nielsen LP, Paerl HW, Zopfi J, Schulz HN, Teske A, Strotmann B, Gallardo VA, Jorgensen BB (1999) Nitrogen, carbon, and sulfur metabolism in natural Thioploca samples. *Appl Environ Microbiol* 65:3148–3157
- Pant D, Adholeya A (2007) Biological approaches for treatment of distillery wastewater: a review. *Biores Technol* 98:2321–2334
- Piedrahita R (2003) Reducing the potential environmental impact of tank aquaculture effluents through intensification and recirculation. *Aquaculture* 226:35–44
- Porrello S, Ferrari G, Lenzi M, Persia E (2003) Ammonia variations in phytotreatment ponds of landbased fish farm wastewater. *Aquacult Eng* 219:485–494
- Pradhan A, Bhaumik P, Das S, Mishra M, Khanam M, Hoque BA, Mukherjee I, Thakur AR, Ray Chaudhuri S (2008) Phytoplankton diversity as indicator of water quality for fish cultivation. *Am J Environ Sci* 4:271–276
- Ray Chaudhuri S, Thakur AR (2006) Microbial genetic resource mapping of East Calcutta Wetland. *Curr Sci* 91:212–217
- Ray Chaudhuri S, Salodkar S, Sudarshan M, Thakur AR (2007) Integrated resource recovery at east calcutta wetland—how safe is these? *Am J Agric Biol Sci* 2:75–80
- Ray Chaudhuri S, Salodkar S, Sudarshan M, Mukherjee I, Thakur AR (2008) Role of water hyacinth mediated phytoremediation in waste water purification at East Calcutta wetland. *J Intgr Environ Sci* 5:53–62
- Ray Chaudhuri S, Mukherjee I, Ghosh D, Thakur AR (2012) East Kolkata Wetland: a multifunctional niche of international importance. *Online J Biol Sci* 12:80–88
- Ray Chaudhuri S, Thakur AR (2013) Method of improving elemental and nutritional content of plant seeds using *Bacillus* strain MCC0008 as a biofertilizer. Indian patent filed 1328/KOL/2013 (2013), PCT/IB2014/066010 (2014)
- Ray Chaudhuri S, Sharmin J, Banerjee S, Jayakrishnan U, Saha A, Mishra M, Ghosh M, Mukherjee I, Banerjee A, Jangid K, Sudarshan M, Chankraborty A, Ghosh S, Nath R, Banerjee M, Singh S, Saha AK, Thakur AR (2016a) Novel microbial system developed from low level radioactive waste treatment plant for environmental sustenance. In: Saleh HEDM, Rahman ROA (eds) *Management of Hazardous Wastes*, Intech, Croatia, pp 121–154
- Ray Chaudhuri S, Mukherjee I, Datta D, Chanda C, Krishnan GP, Bhatt S, Datta P, Bhushan S, Ghosh S, Bhattacharya P, Thakur AR, Roy D, Barat P (2016b) Developing tailor made microbial consortium for effluent remediation. In: Rahman ROA, Saleh MEDM (eds) *Nuclear material performance*, Intech, Croatia, pp 17–35
- Ray Chaudhuri S, Mukherjee I, Thakur AR (2017a) Microbial Consortium for nitrate and phosphate sequestration for environmental sustenance. Indian Patent 351564. November 13 (2020), 1005753. Bangladesh patent October 24 (2017a)
- Ray Chaudhuri S, Mishra M, De S, Samal B, Saha A, Banerjee S, Chakraborty A, Chakraborty A, Pardhiya S, Gola D, Chakraborty J, Ghosh S, Jangid K, Mukherjee I, Sudarshan M, Nath R, Thakur AR (2017b) Microbe-based strategy for plant nutrient management. In: Farooq R, Ahmed Z (eds) *Waste water treatment and reuse*, Intech, Croatia, pp 38–55
- Ray Chaudhuri S, Gantayet LM, Thakur AR (2020). Formulation of bacterial consortium for bioremediation of petrochemical wastewater. Indian patent filed 202031011766 (2020)
- Raychaudhuri S, Mishra M, Salodkar S, Sudarshan M, Thakur AR (2008) Traditional aquaculture practice at east calcutta wetland: the safety assessment. *Am J Environ Sci* 4:140–144

- Ruuskanen M (2014) The genus *Beggiatoa* and its effects on the nutrient cycles of the Baltic Sea. BSc Thesis. 10.13140/RG.2.1.4814.6329. https://www.researchgate.net/publication/300006271_The_genus_Beggiatoa_and_its_effects_on_the_nutrient_cycles_of_the_Baltic_Sea. Accessed 28 August 2021
- Saha A, Bhushan S, Mukherjee P, Chanda C, Bhaumik M, Ghosh M, Sharmin J, Datta P, Banerjee S, Barat P, Thakur AR, Gantayet LM, Mukherjee I, Ray Chaudhuri S (2018) Simultaneous sequestration of nitrate and phosphate from wastewater using a tailor-made bacterial consortium in biofilm bioreactor. *J Chem Technol Biotechnol* 93:1279–1289
- Satyawali Y, Balakrishnan M (2008) Wastewater treatment in molassesbased alcohol distilleries for COD and colour removal: a review. *J Environ Manage* 86:481–497
- Schulz HN, Brinkhoff T, Ferdelman TG, Hernandez Marine M, Teske A, Jorgensen BB (1999) Dense populations of a giant sulfur bacterium in Namibian shelf sediments. *Science* 284:493–495
- Sengupta AK (2008) WHO Guidelines for the safe use of wastewater, excreta and greywater, national workshop on sustainable sanitation, 19–20 May. New Delhi, India
- Shuval HI, Adin A, Fattal B, Rawitz E, Yekutieli P (1986) Wastewater irrigation in developing countries: health effects and technical solutions. Technical Paper No. 51. World Bank, Washington DC
- Strauss M, Blumenthal U (1990) Human waste use in agriculture and aquaculture: utilization practice and health perspectives. IRCWD Report No. 09/90. International Reference Centre for Waste Disposal, Duebendorf, Germany, pp 1–52
- Teske A, Nelson DC (2006) The genera *Beggiatoa* and *Thioploca*. In: Dworkin M, Falkow S, Rosenberg E, Schleifer KH (eds) *The Prokaryotes*. Springer, New York, pp 784–810
- The World Counts (2021) Tons of freshwater used. <https://www.theworldcounts.com/stories/average-daily-water-usage>. Accessed 27 August 2021
- Tripathi VK, Rajput TBS, Patel N, Lata Rao AR, Chandrasekharan H (2011) Dynamics of microorganisms under micro-irrigation system with municipal wastewater. International Symposium on Water for Agriculture, 17–19 January, Nagpur, India, pp 1–95
- Trivedy RK, Nakate SS (2001) Treatment of hospital waste and sewage in hyacinth ponds. In: Trivedy RK, Kaul S (eds) *Low cost wastewater treatment technologies*. ABD Publishers, Jaipur, India, pp 132–163
- Ulrich AE, Frossard E (2014) On the history of a reoccurring concept: phosphorus scarcity. *Sci Total Environ* 490:694–707
- United Nations (2003) Economic and Social Commission for Western Asia. Wastewater treatment technologies: A general review. University of Michigan, United Nations, New York. <https://www.worldcat.org/title/waste-water-treatment-technologies-a-general-review/oclc/55489914>. Accessed 28 August 2021
- Yadav JS, Chowdhury S, Ray Chaudhuri S (2010) Purification and characterization of an extracellular protease from *Pseudomonas aeruginosa* isolated from East Calcutta Wetland. *J Biol Sci* 10:424–431
- Yoo H, Ahn KH, Lee HJ, Lee KH, Kwak YJ, Song KG (1999) Nitrogen removal from synthetic waste water by simultaneous nitrification and denitrification (SND) via nitrite in an intermittently-aerated reactor. *Water Res* 33:145–154

Life Cycle Assessment of Emerging Technologies in Industrial Wastewater Treatment and Desalination



Arash Khosravi, Benyamin Bordbar, and Ali Ahmadi Orkomi

Abstract Today, water scarcity affects human activities and ecosystems in many countries worldwide, leading to emerging new technologies to supply water from unconventional resources or enhance the recycling and reuse of available wastewaters. While, these emerging technologies might have environmental impacts, which are big challenges for sustainable development. Analyzing environmental impacts can help find the best and most sustainable choices that have the least negative impacts on ecosystems, resources, and human health. Life Cycle Assessment (LCA) is a tool to analyze and assess the environmental impacts for sustainability studies. LCA is essential in policymaking for developing desalination projects, especially in restricted areas like the Persian Gulf. An LCA study involves a total inventory and impacts of the energy and materials required across the industry value chain of the product, process, or service. This chapter is discussed the sustainability concept and takes a look at the technologies used in industrial wastewater treatment and desalination from a sustainability point of view. The general contaminants of industrial wastewater and saline water are presented. In addition, the LCA concept, framework, approaches, and Life cycle Inventory (LCI) methodology are explained. Various impacts of conventional and emerging industrial wastewater treatment and desalination technologies are presented to compare the technologies. Furthermore, prospects and challenges are discussed as a summary for the water engineering community.

A. Khosravi (✉) · B. Bordbar
Sustainable Membrane Technology Research Group (SMTRG), Faculty of Petroleum, Gas and Petrochemical Engineering (FPGPE), Persian Gulf University (PGU), P.O. Box 75169-13817, Bushehr, Iran
e-mail: arash.khosravi@pgu.ac.ir

A. Ahmadi Orkomi
Department of Environmental Science and Engineering, Faculty of Natural Resources, University of Guilan, Guilan, Iran

1 Introduction

Water plays a significant and vital role in life on our planet, and all living species are dependent on it (Naushad 2018). It has been reported that less than 0.4% of water resources are accessible to drink, and it has been estimated until the next three decades. The water shortage will be increased by more than 50% (Naushad 2018; Bordbar et al. 2020). In addition, global warming intensifies water scarcity due to the melting of polar icecaps (Naushad 2018).

Most water bodies are not suitable due to inappropriate contaminants such as salinity, bio-organisms, oily components, and heavy metals. Furthermore, industries have a significant and notable role in the pollution of water sources. Industrial wastewater is contaminated with dangerous components such as chemicals, organic and inorganic pollutants, dyes, and in particular heavy metal ions like Pb, Hg, Cr, Co, Ni, and Cd that may cause harmful effects on humans, aquatic, and animal life if they enter into the food chain (Naushad et al. 2017; Dehghani et al. 2021; Karri et al. 2021). Therefore, water treatment and desalination methods are used to treat industrial wastewater and saline water resources to supply fresh water.

Nowadays, emerging technologies are appearing by improving and combining technologies or integrating them with renewable energy resources (Bordbar et al. 2020). However, these plants directly and indirectly impact the environment, human health, Natural resources, and energy resources such as greenhouse gases (GHG) emission, global warming, acidification, eutrophication, toxicity, and natural and energy resource depletion, etc. It is necessary to analyze and assess these impacts and reduce them by improving the technologies. Life Cycle Assessment (LCA) is a systematic tool to assess and calculate these impacts, and it is based on the Life Cycle Sustainability Assessment (LCSA) framework of sustainable development (Shahabi et al. 2017; Klöpffer 2008). Sustainability is included from three key pillars: Environment, Economy, and Social (EES) (Zhang et al. 2020). In addition, energy is considered as another important parameter of sustainability.

To make a process or product sustainable, balancing environmental, economic, energy, and social aspects is necessary. Various parameters affect these aspects in water treatment, such as applied technology (hybrid, ZLD, membrane-based, thermal process, chemical process), entrance feed (brackish, seawater, contaminants of wastewater), contaminants of waste discharge, and applied energy resources (Fossil fuels, renewable energy). It has been reported that conventional plants are the costliest ones. In membrane-based plants, the concentration of feed is important. For example, the costs of desalinating brackish water are lower than seawater due to less energy consumption and fewer equipment requirements (Gude 2016). In addition, due to the different economic, environmental, and policy contexts, the costs are influenced by the location of plants (Sachs 2013; Gude 2016). Treatment plants cause significant effects on the environment due to releasing pollutants in the air, water, and soil (Younos 2005). LCA assesses them in several midpoint and endpoint impacts. Energy is another issue of sustainability studies. It has been observed that energy consumption is better managed in large-scale plants. For example, it has been seen

that the average energy requirement is reduced by increasing the number of stages in Multi-Effect Distillation (MED) and Multi-Stage Flash (MSF) plants (Gude 2016).

This chapter is discussed the sustainability concept and takes a look at the technologies used in industrial wastewater treatment and desalination from a sustainability point of view. The contaminants of industrial wastewater and saline water are presented as an important factor in designing the plant and analyzing the impacts. In addition, the LCA concept, framework, approaches, and LCI methodology are explained. Impacts assessment is the main part of an LCA survey, while there are several midpoint and endpoint impacts. In this chapter, the studies on the impacts of emerging industrial wastewater treatment and desalination technologies are presented and compared to suggest the best technologies. Finally, future prospects and challenges are discussed to guide the water engineering community.

2 Sustainability in Industrial Wastewater Treatment and Desalination

Today, the phrases sustainability and sustainable development are frequently heard in media when a conflict occurs. Sustainability includes three key pillars: Economic, Environment, and Social (EES) (Zhang et al. 2020). The process that has the most negligible EES effects over the life cycle is sustainable (Jaafar et al. 2007). LCSA is the newest framework to analyze and predict the sustainability of a process (Ciroth et al. 2011; Klöpffer 2008). This framework consists of:

- LCC: Life Cycle Costing
- LCA: Life Cycle Assessment
- SLCA: Social Life Cycle Assessment.

However, the application of LCSA is related to the availability of the Life Cycle Inventory (LCI) database. It is hard and time-consuming to collect data, so many tools, principles, and guidelines assess the EES impacts at different life cycle stages (Zhang et al. 2020).

Sustainable development balances economic performance, social justice, and environmental conservation (Naushad 2018). First-time World Commission on Environment and Development (WCED) determines sustainable development as satisfying today's requirements without endangering future potentials (WCED 1991).

The costs of processes are depended on various parameters (Council 2008). For example, it has been seen that conventional water treatment processes are cost-efficient only where there are accessible ground and surface water sources with reasonable distance (Gude 2015). According to the reports, brackish water desalination is the lowest final cost of the water process. It has been seen that the end costs of conventional methods are twice, but they consume energy by 5–25 times more. In large populations and industrial regions, the technologies should be updated; in

this case, brackish or seawater treatment is a good choice, and due to the large-scale design, the energy usage becomes lower, especially for seawater desalination (Gude 2016). In areas with a large population with inaccessible water sources, end water costs and energy usage increase due to the transportation of raw water from a far distance. If seawater resource is accessible in these areas, seawater desalination is a good alternative. In this case, the energy usage and costs are comparable to conventional plants (Gude 2016).

Several European countries pay more water prices than other developed countries. It is due to different economic, environmental, and policy contexts. In developing countries, the government subsidizes the price of water (such as India and China). This causes excessive water consumption and is an unsustainable approach (Sachs 2013; Gude 2016). Several European countries have developed their water costs policy based on the environmental, socioeconomic, and full recovery of the costs in treatment plants. The removal of the water subsidy in Europe increased the price several times, and it was a solution to encourage people to consume less freshwater. In addition, because of huge investments in treatment infrastructure, the treatment costs and prices have fallen in Denmark and Germany (Gude 2016).

Energy consumption and environmental effects are important factors in water treatment. Energy consumption can be managed well in large-scale treatment systems. For example, by increasing the number of stages, energy usage will decrease in MED and MSF plants. As the same, Energy saving and water recovery will be improved by increasing the stages in membrane-based water treatment plants (Gude 2016).

Water treatment plants have notable direct and indirect effects on the environment and health. Fossil fuel consumption in these plants leads to air pollution and greenhouse gases (GHG) emissions that release CO, NO_x, and SO_x (Younos 2005). In addition, considerable amounts of chemical components such as anti-foams, anti-corrosion, anti-scaling, coagulants, and flocculants are used in pretreatment and post-pretreatment of the processes which are released into the river, groundwater, and sea affecting the ecosystem and water bodies (Lattemann and Höpner 2008; Qdais 2008) negatively. Furthermore, feed water's temperature and salinity may cause significant environmental challenges. It has been seen that conventional water treatment systems have more ecological impacts than membrane technologies, however, membrane water treatment plants have been used more chemical components in pre and post-treatment, and membrane cleaning steps (Gude 2016).

Technical, environmental, and economic issues are getting more attention than social issues, while installation and start-up of treatment plants have notable social effects. Lack of public reliance on water providers, making dust and noise pollution, and the effects on sea and beach can be considered social issues of water treatment plants (Gude 2016).

3 Contaminants of Industrial Wastewater and Seawater

The entrance of generated contaminants from agricultural, industrial, and commercial sources, landfills, and human activities pollutes the water bodies. Some industries are the main source of releasing toxic chemical components into the water streams. They include hydrometallurgy, mining, tanning, textiles, electroplating, dyeing, fertilizers, metallurgy, electrochemical and motor plants, metal fishing, and battery manufacturing (Olanipekun et al. 2014; Chen et al. 2015). Another source of water pollution is human activities due to the population increase, increasing landfills, generating sewage, deforestation, waste generation, and combustion (Owa 2013; Dehghani et al. 2021).

Contaminants are unwanted and frequently harmful and toxic components that decrease water quality. They can be originated from industries, natural resources, and mankind activities (Alqadami et al. 2016). In addition, salts are another undesirable contaminant found in seawater, brackish water, and other types of saline waters. The contaminants can be categorized into different types, such as heavy metals, organic and inorganic components, nutrients, dyes, biological substances, and salinity. These contaminants have been introduced in this section.

3.1 Heavy Metals

Industries are the major source of heavy metals discharge. Releasing heavy metals to nature is a dangerous environmental issues l which influences human health, plants, and animal life due to severe toxicity (Sharma et al. 2017). Due to bioaccumulation in living organisms, they can cause many diseases such as mutagenic disorders and cancer (Naushad 2018). Lead (Pb), mercury (Hg), nickel (Ni), arsenic (As), chromium (Cr), zinc (Zn), copper (Cu), cobalt (Co), cadmium (Cd), and antimony (Sb) are the main toxic heavy metals (Alqadami et al. 2017; Assadian and Beirami 2012; Ahmed et al. 2021). Today, developing countries are getting focused on removing toxic heavy metals to protect environments and human health (Ren et al. 2011).

Lead is an industrial heavy metal that is harmful to human health and is not biodegradable (Abdelwahab et al. 2015). It has been found in wastewater of metallurgy, refining, electronics, paint, and battery manufacturing industries. The most dangerous heavy metal is mercury. If it enters the food chain, bioaccumulation will happen easily. Mining, paper manufacturing, cement, and battery manufacturing are the sources of releasing mercury (da Cunha et al. 2016; Rahman and Singh 2016). Nickel is the raw material of alloys, steels, and battery manufacturing (Fukuzawa 2012). Combustion of fossil fuels and nickel production is a major source of releasing nickel into the environment (Naushad 2018). Cement, pesticides, color, and battery industries are the sources of releasing cadmium. The half-life of Cd has been predicted 10–30 years, and it is known as high-risk heavy metal (Bilal et al. 2016; Iqbal et al.

2016). Chromium is another toxic heavy metal, which has been found in tanning, electroplating, glass, and dyes industries (Dehghani et al. 2016). Arsenic is also a health-risk heavy metal found in deep areas of the earth (El-Moselhy et al. 2017). It enters the environment through natural and human activities, such as manufacturing glass, pesticides, mining, rural waste, and metallurgy (Jia et al. 2016; Hepp et al. 2017). Zinc is the common raw material in manufacturing due to its resistance to erosion. Zinc is used in electrical, metallurgy, and oil industries, and color industries to prevent erosion. Another heavy metal, which can be found in water sources, is copper. It has been found in wastewater of refining, mining, and electroplating industries. Cobalt is a metal that causes soil, water, and air pollution, and it may affect all living organisms by bioaccumulation. The main source of cobalt is mining, paints, and color industries. Antimony is known as high-risk toxic metal that is released by the burning of some commercial fuels, production of batteries, glycol, car parts, and coal mining (Naushad 2018).

3.2 *Dyes*

Around 10,000 different colors have been recognized and manufactured until now. It has been reported that near 700,000 tons of colors are produced annually and applied in several industrial sections categorized in cationic, anionic, and non-ionic dyes (Naushad 2018). In the production and manufacturing of products, dyes are entered into the environment by discharge effluents. Textile, food, paper, and tanning industries are the main sources of water pollution by dyes (Khan et al. 2020). If wastewaters that contain dyes enter the water sources, aquatic life will be endangered by chemical reactions (Zangeneh et al. 2015; Forgacs et al. 2004).

3.3 *Biological Contaminants and Microbes*

Biological contaminants, especially microbes, are another considerable parameter of water pollution caused by noxious microorganisms' activities in the water. The discharge of waste components by humans and animals causes waterborne pathogens. *Escherichia coli* (*E. coli*) is an important microorganism usually found in water. In addition, *E. coli* indicates the presence of other pathogens (especially *Vibrio cholerae*, *Salmonella typhi*, and *S. paratyphi*) in water. These contaminants lead to several diseases, and it is needed to control and remove them from water to protect humans and animals from toxic diseases (Ashbolt 2004; Fawell and Nieuwenhuijsen 2003).

3.4 *Undesirable Chemicals*

A group of noxious chemical materials is Endocrine-disrupting compounds (EDC). EDCs have various structures with a complex nature. The main source of EDCs is industrial wastewaters. Instructions have been set by organizations such as WHO, USEPA, and EU to determine a limitation amount for EDC in water. Removal of EDCs from wastewater is a key challenge due to the growth of industrial discharge effluent (Bolong et al. 2009).

Another root of water pollution is agricultural activities due to applying chemicals and pesticides. Agriculture has a significant role in environmental conflicts such as water shortage, pesticides release, soil erosion, water cycle changes, destroying aquatic life, food cycle changes, and releasing phosphorus and nitrogen components. The presence of nitrogen compounds in drinking water has a toxic effect on human health, causing disorders (Fawell and Nieuwenhuijsen 2003; Moss 2008).

3.5 *Oily Content*

Nowadays, the annual consumption of oil-based products is about 100 million tons (Abdullah et al. 2010). During drilling, extraction, oil production, and transportation by tankers, a high amount of oil is discharged to form oily waters. While, a small amount of oil content has significant impacts on human and aquatic life (Sabir 2015). The removal of oil content from oily water is a notable challenge in the oil industry, and this is a challenge for environmental experts. Regarding the regulations, the monthly average oil and grease concentration in the discharge stream should not exceed 40 ppm in the Persian Gulf region (Sabir 2015; Cambiella et al. 2006).

3.6 *Salinity*

The concentration of solved and dissolved salts in water is another environmental issue. It has been reported that more than 96% of water resources are saltwater (Gorjian and Ghobadian 2015). Dissolved solids and salt concentration in drinking water may cause diseases such as kidney failure. On the other hand, a saline hot spot may endanger the aquatic ecosystem, so there are strict environmental regulations for discharging the saline streams to avoid increasing the salt concentration by 10% in a 200 m distance from the discharge point.

Salinity is relevant to total dissolved solids (TDS) concentration, meaning higher salinity results in higher TDS. The salinity status of water are classified into the following categories (Mayer et al. 2005):

- Freshwater: salinity is less than 500 (mg/L TDS).
- Marginal water: salinity is between 500 and 1000 (mg/L TDS).

- Brackish water: salinity is between 1000 and 2000 (mg/L TDS).
- Moderately Saline water: salinity is between 2000 and 5000 (mg/L TDS).
- Saline water: salinity is between 5000 and 10,000 (mg/L TDS).
- Highly saline water: salinity is between 10,000 and 35,000 (mg/L TDS).
- Brine: salinity is over 35,000 (mg/L TDS).

4 Aspects of Life Cycle Assessment in Wastewater Treatment and Desalination

4.1 Goal and Scope

LCA is a systematic set of procedures, which analyzes and assesses environmental, economic, and social issues of products or processes. Triple sustainability pillars are related to the life cycle under the LCSA concept. Due to the purpose of projects, studies may include some or all of these three pillars (Guinée 2016). Environmental Life Cycle Assessment (ELCA), Life Cycle Costing (LCC), and Social Life Cycle Assessment (SLCA) are three forms of LCA (Traverso et al. 2012). ELCA is the most common indicator in studies, which was the early face of LCA in the early days of LCA appearance. The purposes of the LCA study include a comparison of products or processes, government policymaking, strategic planning, process improvement, marketing, consumer education, and product design (Demmers and Lewis 1996). LCA is a standardized methodology, which gives it its reliability and transparency. The ISO 14040 and 14,044 describe the four main steps of an LCA (Lee and Inaba 2004) as follows:

- Goal and scope definition
- Life cycle inventory analysis
- Life cycle impact assessment
- Life cycle interpretation.

The first step of an LCA is defining the goal and boundaries of the system. This step can affect the results of LCA and is named goal and scope by ISO 14040. This step includes determining goals of LCA, usage of results, and system boundaries that lead to defining a functional unit (Shaked et al. 2015). It should be clear that the purpose of LCA is based on which pillars of sustainability (environmental, economic, and social). The goal and scope of some studies in the literature are listed in Table 1.

Based on the system boundaries, the scope is determined. The scope determines the extent of the environmental, economic, and social impacts of components, raw materials, or the product, so there are a variety of scopes and system boundaries (ICCA 2020). Typical system boundaries are as follows:

- Cradle to grave: From raw material extraction through product use and disposal.
- Cradle to gate: From raw material extraction to the exit gate of the factory.

Table 1 A review of LCA in wastewater treatment and desalination. GWP: Global Warming Potential, AP: Acidification Potential, ODP: Ozone Depletion Potential, EP: Eutrophication Potential, POCP: Photochemical Oxidant Creation Potential, HTP: Human Toxicity Potential, ADP: Abiotic Depletion Potential, ETP: Ecotoxicity Potential, WD: Water Depletion, ERD: Energy Resource Depletion, LU: Land Use, MRD: Mineral Resources Depletion

No.	Process	Location	Software	LCIA Method	Functional Unit	Goal and Scopes		Impacts														Reference
						Mid-point	End-point	MRD	LU	ERD	WD	ETP	ADP	HTP	POCP	EP	ODP	AP	GWP			
1	RO	Sweden	GaBi	GaBi	NA	Environment, Cradle to cradle	✓	✓	✓	✓	✓	✓	✓	✓	✓	✓	✓	✓	✓	(Lundie et al., 2004)		
2	RO, MSF, MED	Spain	SimaPro	CML, Eco-points, Ecoindicator	45500 m ³ treated water	Environment, Cradle to grave	✓	✓	✓	✓	✓	✓	✓	✓	✓	✓	✓	✓	✓	(Ralyu et al., 2004b)		
3	RO, MSF, MED, renewable energy	Spain	SimaPro	CML, Eco-points, Ecoindicator	1 m ³ treated water	Environment, Cradle to gate	✓	✓	✓	✓	✓	✓	✓	✓	✓	✓	✓	✓	✓	(Ralyu et al., 2005a)		
4	RO, MSF, MED	Spain	SimaPro	CML, Eco-points, Ecoindicator, BUWAL, ETH-ESU	45500 m ³ treated water	Environment, Cradle to gate	✓	✓	✓	✓	✓	✓	✓	✓	✓	✓	✓	✓	✓	(Ralyu et al., 2004a)		
5	RO, MSF, MED	Spain	SimaPro	CML, Eco-points, Eco-indicator, BUWAL, ETH-ESU, IDEMAT	25000 hm ³ treated water	Environment, Cradle to gate	✓	✓	✓	✓	✓	✓	✓	✓	✓	✓	✓	✓	✓	(Ralyu et al., 2005b)		
6	RO	United States	WEST	NA	123 ML treated water	Environment, Cradle to gate	✓	✓	✓	✓	✓	✓	✓	✓	✓	✓	✓	✓	✓	(Stokes and Horvath, 2006)		
7	RO, MSF, MED	Spain	SimaPro	CML, Eco-points, Eco-indicator, BUWAL, ETH-ESU, IDEMAT, Ecoinvent	45500 m ³ treated water	Environment, Cradle to grave	✓	✓	✓	✓	✓	✓	✓	✓	✓	✓	✓	✓	✓	(Ralyu et al., 2004a)		
8	RO, UF	France	GaBi	IMPACT 2002+	1 m ³ treated water	Environment, Gate to gate	✓	✓	✓	✓	✓	✓	✓	✓	✓	✓	✓	✓	✓	(Vince et al., 2008a)		
9	RO	France		Ecoinvent, IMPACT 2002+	1 m ³ treated water	Economy, Cradle to gate	✓	✓	✓	✓	✓	✓	✓	✓	✓	✓	✓	✓	✓	(Vince et al., 2008b)		
10	RO	Spain	SimaPro	Ecoinvent	1 m ³ treated water	Environment, Cradle to gate	✓	✓	✓	✓	✓	✓	✓	✓	✓	✓	✓	✓	✓	(Muñoz and Fernández-Alba, 2008)		
11	NA	United States	SimaPro	Ecoinvent, ETH-ESU, BUWAL and	466 m ³ treated water	Environment, Cradle to gate	✓	✓	✓	✓	✓	✓	✓	✓	✓	✓	✓	✓	✓	(Lyons et al., 2009)		

(continued)

Table 1 (continued)

12	RO	Australia	Simapro	Franklin library, Eco-indicator the Australian Greenhouse Gas method	1 GL treated water	Environment, Cradle to gate	✓	✓	(Biswas, 2009)
13	Review, renewable energy	United States	WEST, and GaBi	EIO-LCA	1 m ³ treated water	Environment, Cradle to cradle	✓	✓	(Stokes and Honvath, 2009)
14	RO	Spain	USES-LCA	EDIP	1 m ³ treated water	Environment, Cradle to gate	✓	✓	(Muñoz et al., 2009)
15	RO	Spain	Simapro	Ecoinvent, CML, FEI indicator, CED	1 m ³ treated water	Environment, Cradle to gate	✓	✓	(Muñoz et al., 2010)
16	WWTP	Spain	SISOSTA QUA	CML	1 m ³ treated water	Environment, Cradle to cradle	✓	✓	(Pascualino et al., 2011)
17	RO	Spain	SISOSTA QUA	CML	1 m ³ treated water	Environment, Cradle to gate	✓	✓	(Meneses et al., 2010)
18	RO	Germany	GaBi	SETAC guidelines	1 m ³ treated water	Environment, economy, social, Cradle to gate	✓	✓	(Beery et al., 2010)
19	RO, RO-UF	Germany	GaBi	NA	1 m ³ treated water	Environment, economy, Cradle to gate	✓	✓	(Beery and Rejke, 2010)
20	RO	Germany	Excel	NA	1 m ² treated water	Environment, Cradle to gate	✓	✓	(Beery et al., 2011)
21	RO, MSF, MED	United States, SGP, Spain	Simapro	Ecoinvent	1 m ³ treated water	Environment, Cradle to gate	✓	✓	(Zhou et al., 2011a)
22	RO, Memstill	Spain	GaBi	Ecoindicator, CML, Ecoinvent	1 m ³ treated water	Environment, energy, Cradle to gate	✓	✓	(Tarnacki et al., 2011)
23	RO	United States	Simapro	CML, TRACI, US Ecoinvent	1 m ³ treated water	Environment, Cradle to gate	✓	✓	(Zhou et al., 2011b)
24	RO	Spain	CML, Ecoinvent	CML, Ecoinvent	1 m ² treated water	Environment, economy, Cradle to gate	✓	✓	(Salcedo et al., 2012)
25	PV RO, Solar still	United Arab Emirates	Simapro	Ecoinvent, Eco-indicator	1250 L/day treated water	Environment, Cradle to gate	✓	✓	(Jijakli et al., 2012)

(continued)

Table 1 (continued)

26	RO-Memstill	Spain		Eco-indicator, CML, Ecopoints, EcoInvent	1 m ³ treated water	Environment, Cradle to gate	✓	✓	✓	✓	✓	✓	✓	✓	(Tamacki et al., 2012)
27	RO, UF, NF Hybrid	United States	SimatPro	CML	1 m ³ treated water	Environment, Cradle to gate	✓	✓	✓	✓	✓	✓	✓	✓	(Hancock et al., 2012)
28	MSF, MED, VC, RO	United States	EIO-LCA	US EOI data	1 kWh energy	Environment, Cradle to gate economy.	✓	✓	✓	✓	✓	✓	✓	✓	(Norwood and Kammen, 2012)
29	Ion exchange, RO	South Africa	SimatPro	Ecoinvent, CML	1 ml boiler feed	Environment, Cradle to gate	✓	✓	✓	✓	✓	✓	✓	✓	(Ras and Von Bliotnitz, 2012)
30	UF, RO	Denmark	GaBi	EDIP	1 m ³ treated water	Environment, Cradle to gate	✓	✓	✓	✓	✓	✓	✓	✓	(Godskesen et al., 2013)
31	Solar RO	Spain		CML, Ecoindicator	NA	Environment, Cradle to gate	✓	✓	✓	✓	✓	✓	✓	✓	(Anipova et al., 2013)
32	RO, MSF	SGP	NA	USEtox	1 m ³ treated water	Environment, Cradle to gate	✓	✓	✓	✓	✓	✓	✓	✓	(Zhou et al., 2013)
33	RO, hybrid UF-RO	United Arab Emirates	SimatPro	Ecoindicator	1 m ³ treated water	Environment, Cradle to gate	✓	✓	✓	✓	✓	✓	✓	✓	(Al-Sarkal and Aralaf, 2013)
34	Tertiary treatment	Spanish MED sea	NA	Ecoinvent, CML	1 m ³ treated water	Environment, Cradle to gate	✓	✓	✓	✓	✓	✓	✓	✓	(Amores et al., 2013)
35	TVC-MED, MSF, RO, MVC	Italy	NA	EPD system framework	1m ³ treated water	Environment, Cradle to distribution	✓	✓	✓	✓	✓	✓	✓	✓	(Del Borghi et al., 2013)
36	RO	Australia	SimatPro	Australian database, IPCC	1 m ³ treated water	Environment, Cradle to gate	✓	✓	✓	✓	✓	✓	✓	✓	(Shahabi et al., 2015a)
37	RO renewable energy	Australia	SimatPro	Australian database, Ecoinvent, IPCC	1 m ³ treated water	Environment, Cradle to gate	✓	✓	✓	✓	✓	✓	✓	✓	(Shahabi et al., 2014)
38	WWTP	Denmark	SimatPro	ReCIPE	1 m ³ inlet water	Environment	✓	✓	✓	✓	✓	✓	✓	✓	(Niero et al., 2014)
39	WWTP	Australia		ReCIPE	1 year	Environment, Cradle to gate	✓	✓	✓	✓	✓	✓	✓	✓	(Lane et al., 2015)
40	FO	United States	SimatPro	TARCI	1 barrel O and G pit water	Environment, Cradle to gate economy	✓	✓	✓	✓	✓	✓	✓	✓	(Coday et al., 2015)

(continued)

Table 1 (continued)

41	RO	Australia	SimatPro	EOI-LCA, CML	1 m ³ treated water	Environment, economy, Cradle to gate	✓	✓	✓	✓	✓	✓	✓	✓	✓	✓	✓	✓	✓	✓	(Shahabi et al., 2015b)
42	RO	Australia	SimatPro	Ecoinvent, CML	1 m ³ treated water	Environment, economy, Cradle to gate	✓	✓	✓	✓	✓	✓	✓	✓	✓	✓	✓	✓	✓	✓	(Shahabi et al., 2015c)
43	RO	Iran	SimatPro	Ecological scarcity	1 ha tomato farm	Environment, economy, Cradle to gate	✓														(Karami et al., 2017)
44	RO, FO, RO-FO	Global	NA	NA	1 m ³ treated water	Economy, Cradle to gate	✓														(Linares et al., 2016)
45	MED, RO	China	GaBi	CML, USEtox model	1 m ³ treated water	Environment, Cradle to gate	✓	✓	✓	✓	✓	✓	✓	✓	✓	✓	✓	✓	✓	✓	(Li et al., 2016)
46	CDI	Taiwan	SimatPro	Ecoinvent, CML, CED	1 m ³ treated water	Environment, energy, Cradle to grave	✓	✓	✓	✓	✓	✓	✓	✓	✓	✓	✓	✓	✓	✓	(Yu et al., 2016)
47	RO, renewable energy	Tunisia	NA	Embodied Energy (EE) or Primary Energy Requirement (PER)	1 m ³ treated water	Environment, Cradle to gate	✓														(Cherif et al., 2016)
48	Renewable energy	United States	EXCEL	GT PRO, PEACE	Per unit of consumed energy	Environment, economy, Cradle to gate	✓	✓													(Cherchi et al., 2017)
49	Hybrid FO-NF	Australia	SimatPro	Ecoinvent	100000 m ³ treated water	Environment, economy, Cradle to gate	✓	✓	✓	✓	✓	✓	✓	✓	✓	✓	✓	✓	✓	✓	(Kim et al., 2017)
50	RO	Australia	NA	CML	1 m ³ treated water	Environment, economy, Cradle to gate	✓	✓	✓	✓	✓	✓	✓	✓	✓	✓	✓	✓	✓	✓	(Shahabi et al., 2017)
51	MDC	United States	GaBi	ILCD, Ecoinvent	1 L treated water	Environment, Cradle to grave	✓	✓	✓	✓	✓	✓	✓	✓	✓	✓	✓	✓	✓	✓	(Zhang et al., 2018)
52	RO, MSF	Kuwait		CML	1 ton of treated water	Environment, Cradle to gate	✓	✓	✓	✓	✓	✓	✓	✓	✓	✓	✓	✓	✓	✓	(Al-Shayji and Aleisa, 2018)
53	MSF, solar MED, RO, PV-RO	Kuwait	SimatPro	ELCD, CML	1 m ³ treated water	Environment, economy, Cradle to gate	✓	✓	✓	✓	✓	✓	✓	✓	✓	✓	✓	✓	✓	✓	(Aleisa and Al-Shayji, 2018)
54	NA	Israel	SimatPro	Ecoinvent, ILCD, AHP	1 year	Environment, economy, Cradle to cradle	✓	✓													(Ophir et al., 2019)

(continued)

Table 1 (continued)

55	ZLD, RO	Brazil	SimatPro	ReCiPe, CED, CML, EU25	1 m ³ treated water	Environment, Gate to gate	✓	✓	✓	✓	✓	(Ronquim et al., 2020)
56	RO	Persian Gulf	SimatPro	CML	1 m ³ treated water	Environment, Cradle to gate	✓	✓	✓	✓	✓	(Al-Kaabi and Mackey, 2019a)
57	MED	Northern Chile	GaBi	ReCiPe	1 m ³ treated water	Environment, Cradle to grave	✓	✓	✓	✓	✓	(Tarpani et al., 2019)
58	MSF, NF-MSF	Qatar	GaBi, VDS	ReCiPe	1 m ³ treated water	Environment, Cradle to grave	✓	✓	✓	✓	✓	(Mannan et al., 2019)
59	RO, MED, MSF, solar energy	Kuwait, Algeria, Abu Dhabi, Spain, United States, Australia, Chile	GaBi	ReCiPe	1 m ³ treated water	Environment, Cradle to gate	✓	✓	✓	✓	✓	(Alhaj and Al-Ghamdi, 2019)
60	MDS	Qatar	GaBi	ILCD	1 L treated water	Environment, Cradle to grave	✓	✓	✓	✓	✓	(Zhang et al., 2019)
61	RO	South Africa	SimatPro	ReCiPe	1 KL produce water	Environment, Cradle to grave	✓	✓	✓	✓	✓	(Goga et al., 2019)
62	RO	SGP		ReCiPe	1 m ³ treated water	Environment, Cradle to grave	✓	✓	✓	✓	✓	(Hsien et al., 2019)
63	RO	Qatar	GaBi	GaBi	1 m ³ treated water	Environment, Cradle to grave	✓	✓	✓	✓	✓	(Al-Kaabi and Mackey, 2019b)
64	Hybrid solar/wind RO-RED		GaBi	Ecoinvent	1 kWh energy	Environment, Cradle to gate	✓	✓	✓	✓	✓	(Tristán et al., 2020)
65	RO, Hybrid FO-RO, Hybrid UF-RO	Masig Island	WAVE, Hysys		-	Economy.	✓					(Pazouki et al., 2020)
66	ZLD	Europe	NA	NA	1 zero brine demo plant	Environment, Cradle to gate	✓					(Tsalidis et al., 2020)
67	RO	Malaysia	SimatPro	Ecoinvent	1 m ³ treated water	Environment, Cradle to grave		✓				(Abdul Ghani et al., 2020)

(continued)

- Gate to gate: Start in a point (for example, raw material input at the gate of a factory) and end at a point (for example, the final product exportation gate of the factory).

In addition, there are other approaches, such as Cradle to cradle, that complete LCA boundary. LCA researchers use cradle to cradle for the cradle to grave approach that at the end of life, the final product is recycled (ICCA 2020).

4.2 Functional Unit (FU)

The second step of LCA is determining functional units (Klöpffer and Grahl 2014). A functional unit is a reference unit that expresses the system's performance numerically. Also, all midpoint and endpoint indicators in an LCA study are reported based on the selected FU (Shaked et al. 2015). For example, in water treatment research, the goal is to produce treated water. FU can be one of the following examples:

- 1 m³ treated water
- 1000 glass bottles of treated water
- 5000 PET bottles of treated water
- 100 barrels of treated water.

The functional unit is the measurement basis of functions required to be supplied, such as fuel to provide 100 MJ energy, chemicals for pretreatment of 25,000 m³ saline water, etc. This is to certify that comparing different processes or products in LCSA is on an equal basis. In addition, this is determined by how to define system boundaries. Each plant includes several functions, emissions, waste discharges, and chemical and utility consumption. Determining system boundaries means which of them are included in the study. For example, the environmental impacts of brine may not be taken into account in studies on desalination if the cradle to gate or gate to gate boundaries are chosen. A process may produce several products, while the functional unit is defined to fairly devote each product's impacts (Zhang et al. 2020).

4.3 LCA Approach and Methodology

International Standard Organization has provided some standards for LCA, including ISO 14040 and 14,044, which are followed by most of the research approaches and methodologies (Naushad 2018).

Impacts are classified into three categories: primary impacts, which include on-site impacts during the process; secondary impacts that are caused by other activities such as supplying energy and raw materials; and tertiary impacts that are determined as the effects after the process, such as the impacts of product use (O'Connor and Hou 2020). Primary effects can be measured, and secondary effects can be evaluated, while

third-party effects are not measurable and only are presented by a unit-free value (Hauschild et al. 2017). Hence, Mid-point and End-point approaches are defined. The mid-point approach presents primary and secondary impacts in values with units, but the end-point approach reports a dimensionless value for impacts. The end-point analysis involves the environment, human health, and natural resources (Hauschild et al. 2017). At the same time, the impacts evaluated in the mid-point approach are presented in the next section. Determining the mid-point or end-point approach is important to choosing the LCA model. For example, CML, one of the most common life cycle impact assessment models, is a good choice for mid-point analysis, but it is not helpful for the end-point approach, while ReCiPe can be used for both mid-point and end-point analysis (Naushad 2018).

One of the LCA steps is Life Cycle Inventory Analysis (LCIA) that calculates the environmental impacts by determining each impact indicator from elementary flows in Life Cycle Inventory (LCI). LCIA includes the following steps:

Step 1: Choosing the relevant and suitable impact categories.

Step 2: Classification determines elementary flows into different impact categories.

Step 3: Characterization calculates potential impact indicators for each impact category.

Step 4: Normalization represents a relation of potential impact indicators to a reference.

Step 5: Grouping potential impact indicators based on specific rank or order.

Step 6: Weighting, which is assigning weights to each impact indicator due to relative importance.

Steps 1–3 are basic and mandatory steps of LCIA, and steps 4–6 are optional. Most LCIA studies only apply mandatory steps (Mu et al. 2020; Nieuwlaar 2004).

5 Environmental Impacts

5.1 Impact Assessment

Impacts assessment is the main part of an LCA survey. In this section, mid-point emissions are reported regarding the following impact indices (Hauschild et al. 2017):

- Global Warming Potential (GWP, or climate change)
- Ozone depletion
- Acidification
- Eutrophication
- Ecotoxicity
- Resources depletion
- Human toxicity
- Land use
- Water depletion

- Photochemical oxidation
- Particular matter formation
- Ionizing radiation
- Photochemical ozone formation.

In addition, end-point emissions are assessed into the three following impact categories (Hauschild et al. 2017):

- Natural resources
- Natural environment
- Human health.

In this chapter, these impacts are discussed under three categories: Environmental impacts, Impacts of resources, and, Impacts of Human health.

5.2 Global Warming Potential (GWP)

Global Warming Potential (GWP) impact (also known as Climate change) is the most noteworthy impact that reports greenhouse gases (GHG) emissions. CO₂ equivalent impact is reported in many LCA papers. This index also is called carbon footprint. In addition, the GWP index is also considered as an indicator to express the degree of development as well as energy loss. The primary effect of GHG is increasing infrared radiation adsorption, and the secondary effects are melting polar ices, increasing the sea level, and climate change (Hauschild et al. 2017). Figure 1 compares the global warming potential impacts of emerging industrial wastewater treatment and desalination technologies.

It has been found that the type of energy resources such as electricity and heat power has the most important effect on the GWP indicator. As shown in Fig. 1, the most negligible GWP impact is for Memstill® technology, which includes a solar still and membrane process with renewable energy power. The next one is RO technology with mixed electricity power included 98% wind power (Tarnacki et al. 2012). RO processes integrated with solar thermal energy that treated brackish and ocean water came in third and fourth, respectively (Stokes and Horvath 2009). The 5th is the RO process in Australia that uses wind power (Biswas 2009) and the 6th and 7th places are RO processes powered by photovoltaic energy (Stokes and Horvath 2009). All the characterizations of the third, fourth, sixth, and seventh plants are the same; therefore, it shows that solar thermal energy caused less GWP impact than PV resource and also, it has been revealed that wind power energy is a reliable low GWP effect resource.

The higher GWP emissions are for MSF and MED plants powered by natural gas (Raluy et al. 2004b) and the RO process, which consumes fossil fuels for electricity power (Biswas, 2009). This certifies that energy resource has the most prominent effect on GWP impact. To compare multiple processes as same as the functional unit, the scope of LCA should be the same. In this study, the scope of all studies is cradle

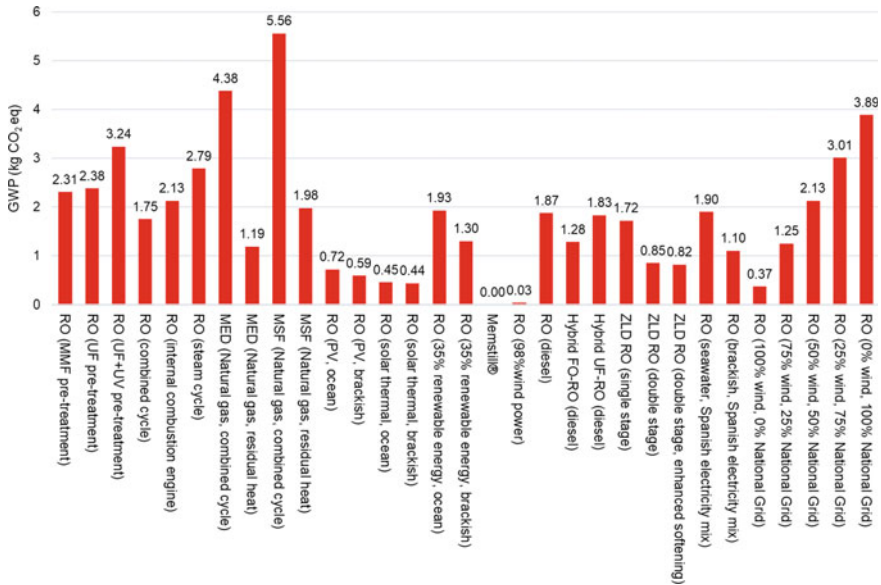


Fig. 1 Global warming potential impact of emerging industrial wastewater treatment and desalination technologies. FU = 1 m³ treated water (Raluy et al. 2004b; Beery and Repke 2010; Stokes and Horvath 2009; Tarnacki et al. 2012; Pazouki et al. 2021; Ronquim et al. 2020; Muñoz and Fernández-Alba 2008; Biswas 2009)

to grave except ZLD plants (ZLD RO (single-stage), ZLD RO (double stage), and ZLD RO (double stage, enhanced softening). The scope of these plants is the gate to gate; therefore, analyzed values would be higher if their scope was cradle to grave.

5.3 Acidification Potential (AP)

Acidification potential impact refers to the influence of total emissions of acidic species (such as SO_x, NO_x, HCl, HF, and NH₄ into the air). The release of these emissions causes acidification in water and soil and consequently facilitates corrosion (ICCA 2020). The development of technologies for acidic gaseous removal, especially SO₂, can improve air quality and, as a result, reduce the acidification of water and soil (Klöppfer and Grahl 2014). Figure 2 compares the potential acidification impact of some emerging wastewater treatment and desalination technologies. Acidification potential impact has been reported by kg SO_x equivalent.

As depicted in Fig. 2, Memstill® technology reports the least acidification impact, and after that, RO powered by 98% wind energy is the best one (Tarnacki et al. 2012). RO (solar thermal, brackish), RO (solar thermal, ocean), RO (PV, brackish), RO (PV, ocean) are placed in the next places (Stokes and Horvath 2009). The most acidification impact refers to RO (seawater, Spanish electricity mix), MED (Natural gas, residual

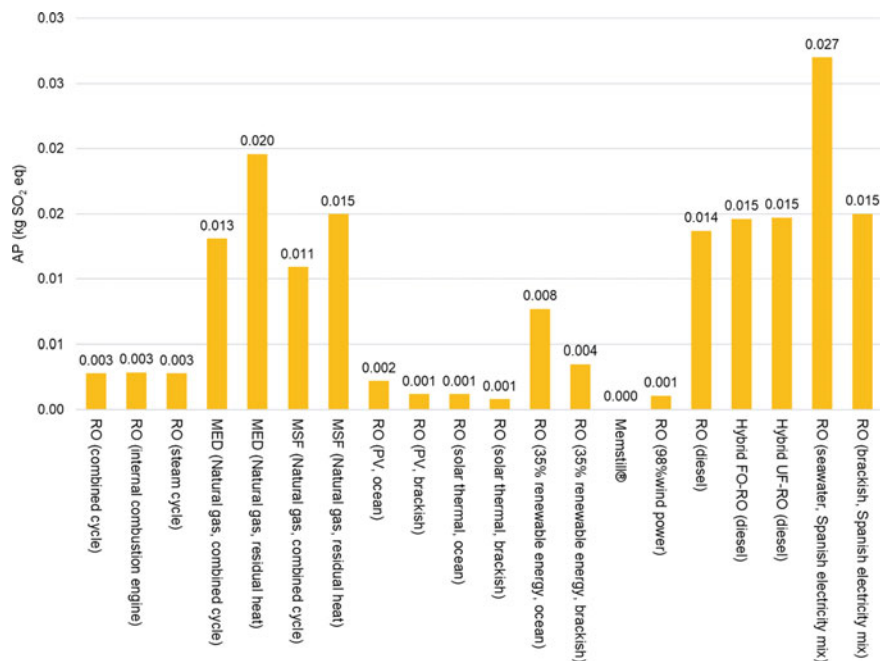


Fig. 2 Acidification potential impact of emerging industrial wastewater treatment and desalination technologies. FU = 1 m³ treated water (Raluy et al. 2004b; Stokes and Horvath 2009; Tarnacki et al. 2012; Pazouki et al. 2021; Muñoz and Fernández-Alba 2008)

heat), MSF (Natural gas, residual heat), and RO (brackish, Spanish electricity mix), respectively (Raluy et al. 2004b; Muñoz and Fernández-Alba 2008). This shows that the energy source has a significant impact in acidification because of SO_x emissions of power production and fossil combustion.

5.4 Eutrophication Potential (EP)

Eutrophication potential impact (also known as Nutrifcation Potential (NP)) refers to releasing limiting nutrients (P and N contained components) into the water resources and soil that causes overgrowth of algae (ICCA 2020). Overgrowth of algae destroys biomass at the water resources and changes the character of the water body. This impact can be divided into aquatic eutrophication and terrestrial eutrophication. Aquatic eutrophication includes components in wastewater that have not been treated well and the entrance of wastewater into the water resources. At the same time, terrestrial eutrophication refers to the effects of NO_x and NH₄ gases (Klöpffer and Grahl 2014). Marine Eutrophication impact reports these effects as kg N equivalent, and freshwater eutrophication impact has been reported by kg P equivalent.

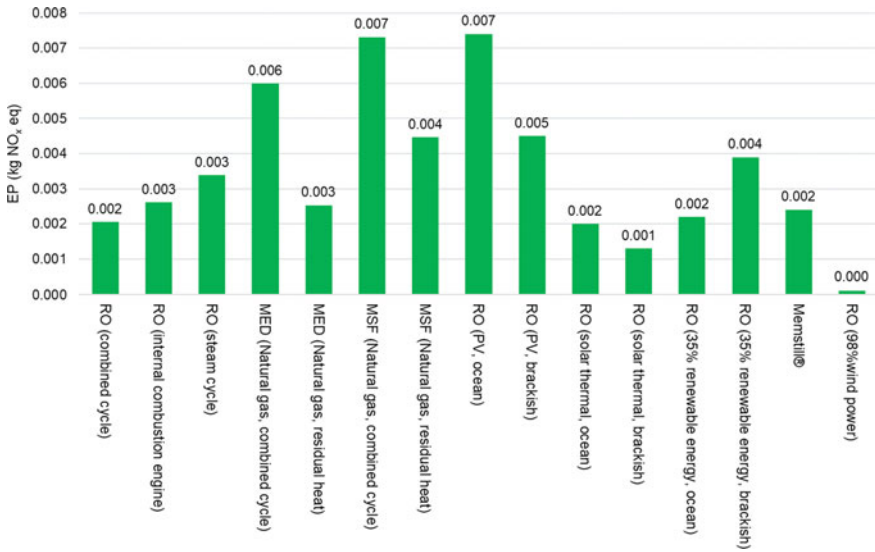


Fig. 3 Eutrophication potential impact of emerging industrial wastewater treatment and desalination technologies. FU = 1 m³ treated water (Raluy et al. 2004b; Stokes and Horvath 2009; Tarnacki et al. 2012)

According to Fig. 3, it has been found that the least NO_x emission is for RO process powered by 98% wind power, and solar thermal RO plants to treat brackish and ocean water were ranked second and third, respectively. RO integrated with the combined cycle is ranked fourth. Because, in addition to energy resources, the contaminants in disposed waste have a noticeable effect on NO_x emissions.

5.5 Ozone Depletion Potential (ODP)

Ozone depletion potential (ODP) includes the influences of releasing gases that destroy the ozone layer. The ozone layer is an artificial name for the middle part of the stratosphere, where the concentration of ozone is such that it prevents the passage of harmful UV to living cells. UV-B and C radiation can affect human health by leading to diseases such as skin cancer or lower crop yields (Baird 2012).

Trace components of HO_x and NO_x can cause a destructive reaction that causes ozone depletion. In addition, there was a challenge that supersonic airplanes could cause ozone layer depletion by NO₂ production in the 1970s. Then, the production of Freons and CFCs, by chlorine cycle as a refrigerant and spraying agents, caused Ozone depletion (Klöpffer and Grahl 2014). ODP impact reports these effects as CFC-11 equivalent.

Although the ozone depletion impact of water treatment plants has not been investigated in many studies, Fig. 4 compares a few processes. According to Fig. 4, it has

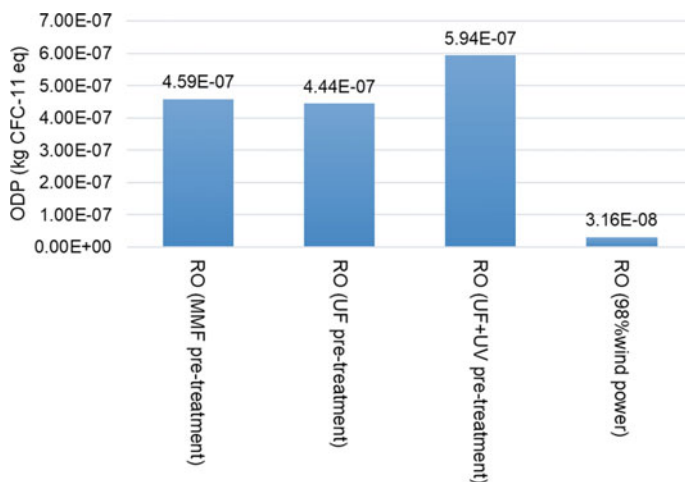


Fig. 4 Ozone layer depletion potential impact of emerging industrial wastewater treatment and desalination technologies. FU = 1 m³ treated water (Beery and Repke 2010; Tarnacki et al. 2012)

been found that the RO process by 98% wind power has the least ozone depletion impact. It can be concluded that the energy source is an essential factor in controlling and decreasing ozone depletion potential and CFC-11 eq amount. The next ranks are RO with UF pretreatment, RO with MMF pretreatment and RO with UF and UV pretreatment, respectively.

5.6 Ecotoxicity Potential (ETP)

Releasing toxic materials in the environment causes freshwater aquatic and marine aquatic ecotoxicity. The ecotoxicity potential (ETP) impact refers to the share of components that affect ecosystem substances. Heavy metals and organic pollutants are the main components (Tarnacki et al. 2012). This impact is divided into Freshwater Aquatic Ecotoxicity (FAETP) and Marine Aquatic Ecotoxicity (MAETP). Ecotoxicity impact reports these effects as 1, 4-DB equivalent.

Few of the above studies have investigated the ecotoxicity potential impact. In addition, differences in assessment method, scope and functional unit have made these studies incomparable. However, it has been observed that among the processes studied in the previous sections, the Memstill® process reports the lowest rate of ecotoxicity. In addition, the RO process powered by 98% wind power is in the next rank, indicating that the energy source plays a significant role in this impact category. The RO with UF pretreatment and RO with UF and UV pretreatment processes are also in the next ranks.

6 Impacts on Resources

6.1 *Water Depletion*

Freshwater is a vital resource, and water scarcity is a critical challenge today. LCA helps to determine a method to address water use correctly. The International Standardization Organization (ISO) determined a new concept to make an international standard for water footprint. The easiest way to define a water footprint is by applying water inventory analysis for the product of a process. By removing the amount of waste discharge from input water, the amounts of evaporated water, product use, and leakages are found, and consequently, water footprint can be defined and managed. LCA databases such as Ecoinvent, GaBi, etc., have determined water inventory analysis. It is noted that the inventories may be different depending on the database. These databases regularly just assess the input and output flows (Berger and Finkbeiner 2010).

In each process, requiring water is very important. The use of water affects the volume of water resources in the life cycle. Water depletion potential, also known as consumptive water footprint or water emissions footprint, represents the impacts of water usage. The main water resources are river, well, lake, and sea, subdivided into freshwater, saline water, and brackish water (ICCA 2020). The water consumption during the process, including the utility unit, has been assessed in this impact category, so the input water of plants has not been analyzed. Water depletion impact reports water use effects in m^3 .

6.2 *Energy Sources Depletion*

Energy sources depletion (also known as Cumulative Energy Demand (CED)) refers to total applied energy over the process. This can be divided into fossil energy and renewable energy called Fossil Energy Demand or fossil depletion, and Renewable Energy Demand, respectively.

Fossil Energy Demand involves impacts of applying fossil-based energy such as coal, petroleum derivatives, natural gas, etc. The unit of Fossil depletion impact is kg oil equivalent.

Renewable Energy Demand refers to the effects of applied renewable energy (non-fossil fuel-based), including geothermal, wind, hydro, wave, photovoltaic, and solar energy (ICCA 2020).

6.3 Land Use

Another notable indicator in developing countries is changing the land from its primary state (grassland, forest, etc.) to a new state that affects GHG emissions. The changing usage is also known as direct land use. Indirect land-use refers to secondary land-use change because of primary land-use change by moving the commercial product and grown in a new location that caused GHG changes in the new land (ICCA 2020). Land use impact is reported in m^2 .

7 Impacts on Human Health

The toxicity of materials on human health is not ignorable. Health safety should be assessed in each process and product. Human toxicity impact is one of the LCA indicators that refer to emissions and their effects on human health. Human toxicity and ecotoxicity have common resources, emissions, structure, and principles. Some emissions that release into the environment can endanger humans. In addition, during the production process, some emissions are released that endanger workers or consumers (Hauschild et al. 2017). The result of their influence on natural organisms is growing mortality, lowering mobility, lowering population growth, mutations, changing behavior, biomass changes, photosynthesis, etc. (Klöpffer and Grahl 2014). Human toxicity impact reports these effects as 1, 4-DB equivalent.

8 Future Prospects and Challenges

Industrial wastewater treatment and desalination technologies may cause severe environmental issues during their life cycle. Heavy metals, chemical components, biological components, salts, and other contaminants cannot be treated easily and can cause harmful and non-ignorable health issues by entering the food chain. In addition, water pollution destroys freshwater sources, and it accelerates water scarcity. Therefore, the governments should determine a policy and instructions to control the life cycle of water bodies. One of them is controlling and monitoring waste discharge of treatment plants (Naushad 2018). Another solution is to develop and build zero liquid discharge plants.

On the other hand, the energy source is a major parameter of environmental impacts. It has been seen that renewable energy resources are reliable and effective alternatives to fossil fuels to supply energy requirements in wastewater treatment and desalination plants. The chemical components impacts are lower than the impacts of the energy resources, but they are non-ignorable and should be considered in planning.

The LCA studies in the literature have not assessed the same environmental impacts. A few studies assessed the land use and salinity impacts. In addition, some of the studied system boundaries are incomplete. For example, the impacts of brine discharge have not been studied in many types of research with cradle to gate or gate to gate boundaries. New water treatment plants are built as collocated, cogeneration, and hybrid plants (Lee and Jepson 2021); Therefore, It is suggested that future studies focus on all dimensions of water-energy nexus impacts.

In addition to environmental aspects, economic and social impacts should be considered. Recently, LCA researchers have considered the LCSA framework for sustainability studies. Therefore, emerging LCA frameworks have a significant role in improving analyzing sustainability of industrial wastewater treatment and desalination plants.

References

- AbdelWahab NA, Ammar NS, Ibrahim HS (2015) Graft copolymerization of cellulose acetate for removal and recovery of lead ions from wastewater. *Int J Biol Macromol* 79:913–922
- Abdul Ghani L, Nazaran IS, Ali NA, Hanafiah MM (2020) Improving prediction accuracy of socio-human relationships in a small-scale desalination plant. *Sustainability* 12:6949
- Abdullah M, Rahmah AU, Man Z (2010) Physicochemical and sorption characteristics of Malaysian Ceiba pentandra (L.) Gaertn. as a natural oil sorbent. *J Hazard Mater* 177:683–691
- Ahmed S, Khan FSA, Mubarak NM, Khalid M, Tan YH, Mazari SA, Karri RR, Abdullah EC (2021) Emerging pollutants and their removal using visible-light responsive photocatalysis—a comprehensive review. *J Environ Chem Eng* 9
- Al-Kaabi AH, Mackey HR (2019a) Environmental assessment of intake alternatives for seawater reverse osmosis in the Arabian Gulf. *J Environ Manage* 242:22–30
- Al-Kaabi AH, Mackey HR (2019b) Life-cycle environmental impact assessment of the alternate subsurface intake designs for seawater reverse osmosis desalination. In: Kiss AA, Zondervan E, Lakerveld R, Özkan L (eds) *Computer aided chemical engineering*. Elsevier
- Al-Sarkal T, Arafat HA (2013) Ultrafiltration versus sedimentation-based pretreatment in Fujairah-1 RO plant: environmental impact study. *Desalination* 317:55–66
- Al-Shayji K, Aleisa E (2018) Characterizing the fossil fuel impacts in water desalination plants in Kuwait: A Life Cycle Assessment approach. *Energy* 158:681–692
- Aleisa E, Al-Shayji K (2018) Ecological–economic modeling to optimize a desalination policy: case study of an arid rentier state. *Desalination* 430:64–73
- Alhaj M, Al-Ghamdi SG (2019) Integrating concentrated solar power with seawater desalination technologies: a multi-regional environmental assessment. *Environ Res Lett* 14:074014
- Alqadami AA, Naushad M, Abdalla MA, Ahamad T, Alothman ZA, Alshehri SM, Ghfar AA (2017) Efficient removal of toxic metal ions from wastewater using a recyclable nanocomposite: a study of adsorption parameters and interaction mechanism. *J Clean Prod* 156:426–436
- Alqadami AA, Naushad M, Abdalla MA, Khan MR, Alothman ZA (2016) Adsorptive removal of toxic dye using Fe₃O₄-TSC nanocomposite: equilibrium, kinetic, and thermodynamic studies. *J Chem Eng Data* 61:3806–3813
- Amores MJ, Meneses M, Pasqualino J, Antón A, Castells F (2013) Environmental assessment of urban water cycle on Mediterranean conditions by LCA approach. *J Clean Prod* 43:84–92
- Antipova E, Boer D, Cabeza LF, Guillén-Gosálbez G, Jiménez L (2013) Uncovering relationships between environmental metrics in the multi-objective optimization of energy systems: a case study of a thermal solar Rankine reverse osmosis desalination plant. *Energy* 51:50–60

- Ashbolt NJ (2004) Microbial contamination of drinking water and disease outcomes in developing regions. *Toxicology* 198:229–238
- Assadian F, Beirami P (2012) An optimization model for removal of zinc from industrial wastewater. In: 2012 IEEE international conference on industrial engineering and engineering management, pp 136–140. IEEE
- Baird C (2012) *Environmental chemistry & solutions manual*. Freeman, W. H
- Beery M, Hortop A, Wozny G, Knops F, Repke J-U (2011) Carbon footprint of seawater reverse osmosis desalination pre-treatment: initial results from a new computational tool. *Desalin Water Treat* 31:164–171
- Beery M, Repke J-U (2010) Sustainability analysis of different SWRO pre-treatment alternatives. *Desalin Water Treat* 16:218–228
- Beery M, Wozny G, Repke J-U (2010) Sustainable design of different seawater reverse osmosis desalination pretreatment processes. In: Pierucci S, Ferraris GB (eds) *Computer aided chemical engineering*. Elsevier
- Berger M, Finkbeiner M (2010) Water footprinting: how to address water use in life cycle assessment? *Sustainability* 2:919–944
- Bilal M, Kazi TG, Afridi HI, Arain MB, Baig JA, Khan M, Khan N (2016) Application of conventional and modified cloud point extraction for simultaneous enrichment of cadmium, lead and copper in lake water and fish muscles. *J Ind Eng Chem* 40:137–144
- Biswas WK (2009) Life cycle assessment of seawater desalination in Western Australia. *World Acad Sci Eng Technol* 56:369–375
- Bolong N, Ismail A, Salim MR, Matsuura T (2009) A review of the effects of emerging contaminants in wastewater and options for their removal. *Desalination* 239:229–246
- Bordbar B, Khosravi A, Azin R (2020) A review on sustainable hybrid water treatment processes. In: 3rd international biennial conference on oil, gas, and petrochemical engineering (OGPC2020). Iran
- Cambiella A, Ortea E, Ríos G, Benito JM, Pazos C, Coca J (2006) Treatment of oil-in-water emulsions: performance of a sawdust bed filter. *J Hazard Mater* 131:195–199
- Chen C-S, Shih Y-J, Huang Y-H (2015) Remediation of lead (Pb (II)) wastewater through recovery of lead carbonate in a fluidized-bed homogeneous crystallization (FBHC) system. *Chem Eng J* 279:120–128
- Cherchi C, Badruzzaman M, Becker L, Jacangelo JG (2017) Natural gas and grid electricity for seawater desalination: an economic and environmental life-cycle comparison. *Desalination* 414:89–97
- Cherif H, Champenois G, Belhadj J (2016) Environmental life cycle analysis of a water pumping and desalination process powered by intermittent renewable energy sources. *Renew Sustain Energy Rev* 59:1504–1513
- Ciroth A, Finkbeiner M, Traverso M, Hildenbrand J, Kloepffer W, Mazijn B, Prakash S, Sonnemann G, Valdivia S, Ugaya CML (2011) Towards a life cycle sustainability assessment: making informed choices on products
- Coday BD, Miller-robbie L, Beaudry EG, Munakata-Marr J, Cath TY (2015) Life cycle and economic assessments of engineered osmosis and osmotic dilution for desalination of Haynesville shale pit water. *Desalination* 369:188–200
- Council NR (2008) *Desalination: a national perspective*. National Academies Press
- Da Cunha RC, Patrício PR, Vargas SJR, Da Silva LHM, Da Silva MCH (2016) Green recovery of mercury from domestic and industrial waste. *J Hazard Mater* 304:417–424
- Dehghani MH, Omrani GA, Karri RR (2021) Solid waste—sources, toxicity, and their consequences to human health. *Soft computing techniques in solid waste and wastewater management*. Elsevier. <https://doi.org/10.1016/B978-0-12-824463-0.00013-6>
- Dehghani MH, Sanaei D, Ali I, Bhatnagar A (2016) Removal of chromium (VI) from aqueous solution using treated waste newspaper as a low-cost adsorbent: kinetic modeling and isotherm studies. *J Mol Liq* 215:671–679

- Del Borghi A, Strazza C, Gallo M, Messineo S, Naso M (2013) Water supply and sustainability: life cycle assessment of water collection, treatment and distribution service. *Int J Life Cycle Assess* 18:1158–1168
- Demmers M, Lewis H (1996) Life cycle assessment: how relevant is it to Australia. Centre for design. Royal Melbourne Institute of Technology, Melbourne, Australia
- El-Moselhy MM, Ates A, Çelebi A (2017) Synthesis and characterization of hybrid iron oxide silicates for selective removal of arsenic oxyanions from contaminated water. *J Colloid Interface Sci* 488:335–347
- Fawell J, Nieuwenhuijsen MJ (2003) Contaminants in drinking water environmental pollution and health. *Br Med Bull* 68:199–208
- Forgacs E, Cserhati T, Oros G (2004) Removal of synthetic dyes from wastewaters: a review. *Environ Int* 30:953–971
- Fukuzawa R (2012) Climate change policy to foster pollution prevention and sustainable industrial practices—a case study of the global nickel industry. *Miner Eng* 39:196–205
- Gao L, Zhang J, Liu G (2021) Life cycle assessment for algae-based desalination system. *Desalination* 512
- Godskesen B, Hauschild M, Rygaard M, Zambrano K, Albrechtsen HJ (2013) Life-cycle and freshwater withdrawal impact assessment of water supply technologies. *Water Res* 47:2363–2374
- Goga T, Friedrich E, Buckley C (2019) Environmental life cycle assessment for potable water production—a case study of seawater desalination and mine-water reclamation in South Africa. *Water SA* 45:700–709
- Gorjian S, Ghobadian B (2015) Solar desalination: a sustainable solution to water crisis in Iran. *Renew Sustain Energy Rev* 48:571–584
- Gude VG (2015) Energy and water autarky of wastewater treatment and power generation systems. *Renew Sustain Energy Rev* 45:52–68
- Gude VG (2016) Desalination and sustainability—an appraisal and current perspective. *Water Res* 89:87–106
- Guinée J (2016) Life cycle sustainability assessment: what is it and what are its challenges? In: Clift R, Druckman A (eds) *Taking stock of industrial ecology*. Springer International Publishing, Cham
- Hancock NT, Black ND, Cath TY (2012) A comparative life cycle assessment of hybrid osmotic dilution desalination and established seawater desalination and wastewater reclamation processes. *Water Res* 46:1145–1154
- Hauschild MZ, Rosenbaum RK, Olsen SI (2017) *Life cycle assessment: theory and practice*. Springer International Publishing
- Hepp LU, Pratas JA, Graça MA (2017) Arsenic in stream waters is bioaccumulated but neither biomagnified through food webs nor biodispersed to land. *Ecotoxicol Environ Saf* 139:132–138
- Hsien C, Choong Low JS, Chan Fuchen S, Han TW (2019) Life cycle assessment of water supply in Singapore—a water-scarce urban city with multiple water sources. *Resour Conserv Recycl*, 151:104476
- Iqbal M, Iqbal N, Bhatti IA, Ahmad N, Zahid M (2016) Response surface methodology application in optimization of cadmium adsorption by shoe waste: a good option of waste mitigation by waste. *Ecol Eng* 88:265–275
- ICCA, I. C. O. C. A (2020) How to know if and when it's time to commission a life cycle assessment. International Council of Chemical Associations (ICCA)
- Jaafar I, Venkatachalam A, Joshi K, Ungureanu A, De Silva N, Dillon jr, O., Rouch, K. & Jawahir, I. (2007) Product design for sustainability: a new assessment methodology and case studies. *Environ Conscious Mech Des* 5:25–65
- Jia X, Gong D, Wang J, Huang F, Duan T, Zhang X (2016) Arsenic speciation in environmental waters by a new specific phosphine modified polymer microsphere preconcentration and HPLC–ICP-MS determination. *Talanta* 160:437–443

- Jijakli K, Arafat H, Kennedy S, Mande P, Theeyattuparampil VV (2012) How green solar desalination really is? Environmental assessment using life-cycle analysis (LCA) approach. *Desalination* 287:123–131
- Karami S, Karami E, Zand-parsa S (2017) Environmental and economic appraisal of agricultural water desalination use in South Iran: a comparative study of tomato production. *J Appl Water Eng Res* 5:91–102
- Karri RR, Ravindran G, Dehghani MH (2021) Wastewater—sources, toxicity, and their consequences to human health. Soft computing techniques in solid waste and wastewater management. Elsevier. <https://doi.org/10.1016/B978-0-12-824463-0.00001-X>
- Khan FSA, Mubarak NM, Tan YH, Karri RR, Khalid M, Walvekar R, Abdullah EC, Mazari SA, Nizamuddin S (2020) Magnetic nanoparticles incorporation into different substrates for dyes and heavy metals removal—a review. *Environ Sci Pollut Res* 27:43526–43541
- Kim JE, Phuntsho S, Chekli L, Hong S, Ghaffour N, Leiknes T, Choi JY, Shon HK (2017) Environmental and economic impacts of fertilizer drawn forward osmosis and nanofiltration hybrid system. *Desalination* 416:76–85
- Klöpffer W (2008) Life cycle sustainability assessment of products. *Int J Life Cycle Assess* 13:89–95
- Klöpffer W, Grahl B (2014) Life cycle assessment (LCA): a guide to best practice. John Wiley & Sons
- Lattemann S, Höpner T (2008) Environmental impact and impact assessment of seawater desalination. *Desalination*, 220;1–15. <https://doi.org/10.1016/j.desal.2007.03.009>
- Lane JL, De Haas DW, Lant PA (2015) The diverse environmental burden of city-scale urban water systems. *Water Res* 81:398–415
- Lee K-M, Inaba A (2004) Life cycle assessment: best practices of ISO 14040 series, Center for Ecodesign and LCA (CEL). Ajou University
- Lee K, Jepson W (2021) Environmental impact of desalination: a systematic review of life cycle assessment. *Desalination* 509:115066
- Li Y, Xiong W, Zhang W, Wang C, Wang P (2016) Life cycle assessment of water supply alternatives in water-receiving areas of the South-to-North water diversion project in China. *Water Res* 89:9–19
- Linares RV, Li Z, Yangali-Quintanilla V, Ghaffour N, Amy G, Leiknes T, Vrouwenvelder JS (2016) Life cycle cost of a hybrid forward osmosis–low pressure reverse osmosis system for seawater desalination and wastewater recovery. *Water Res* 88:225–234
- Lundie S, Peters GM, Beavis PC (2004) Life cycle assessment for sustainable metropolitan water systems planning. ACS Publications
- Lyons E, Zhang P, Benn T, Sharif F, Li K, Crittenden J, Costanza M, Chen YS (2009) Life cycle assessment of three water supply systems: importation, reclamation and desalination. *Water Supply* 9:439–448
- Mannan M, Alhaj M, Mabrouk AN, Al-Ghamdi SG (2019) Examining the life-cycle environmental impacts of desalination: a case study in the State of Qatar. *Desalination* 452:238–246
- Mayer X, Ruprecht J, Bari M (2005) Stream salinity status and trends in south-west Western Australia. Salinity and land use impacts. Department of environment
- Meneses M, Pasqualino JC, Céspedes-Sánchez R, Castells F (2010) Alternatives for reducing the environmental impact of the main residue from a desalination plant. *J Ind Ecol* 14:512–527
- Morsy KM, Mostafa MK, Abdalla KZ, Galal MM (2020) Life cycle assessment of upgrading primary wastewater treatment plants to secondary treatment including a circular economy approach. *Air Soil Water Res* 13:1178622120935857
- Moss B (2008) Water pollution by agriculture. *Philos Trans R Soc B Biol Sci* 363:659–666
- Mu D, Xin C, Zhou W (2020) Chapter 18—life cycle assessment and techno-economic analysis of algal biofuel production. In: Yousuf A (ed) *Microalgae cultivation for biofuels production*. Academic Press
- Mueller KE, Thomas JT, Johnson JX, Decarolis JF, Call DF (2020) Life cycle assessment of salinity gradient energy recovery using reverse electrodialysis. *J Ind Ecol*

- Muñoz I, Fernández-Alba AR (2008) Reducing the environmental impacts of reverse osmosis desalination by using brackish groundwater resources. *Water Res* 42:801–811
- Muñoz I, Milà-I-Canals L, Fernández-Alba AR (2010) Life cycle assessment of water supply plans in mediterranean Spain. *J Ind Ecol* 14:902–918
- Muñoz I, Rodríguez A, Rosal R, Fernández-Alba AR (2009) Life cycle assessment of urban wastewater reuse with ozonation as tertiary treatment: a focus on toxicity-related impacts. *Sci Total Environ* 407:1245–1256
- Naushad M (2018) Life cycle assessment of wastewater treatment. CRC Press
- Naushad M, Ahamad T, Al-Maswari BM, Alqadami AA, Alshehri SM (2017) Nickel ferrite bearing nitrogen-doped mesoporous carbon as efficient adsorbent for the removal of highly toxic metal ion from aqueous medium. *Chem Eng J* 330:1351–1360
- Niero M, Pizzol M, Bruun HG, Thomsen M (2014) Comparative life cycle assessment of wastewater treatment in Denmark including sensitivity and uncertainty analysis. *J Clean Prod* 68:25–35
- Nieuwlaar E (2004) Life cycle assessment and energy systems. In: Cleveland CJ (ed) *Encyclopedia of energy*. Elsevier, New York
- Norwood Z, Kammen D (2012) Life cycle analysis of distributed concentrating solar combined heat and power: economics, global warming potential and water. *Environ Res Lett* 7:044016
- O'Connor D, Hou D (2020) Sustainability assessment for remediation decision-making. Elsevier, Sustainable remediation of contaminated soil and groundwater
- Olanipekun O, Oyefusi A, Neelgund GM, Oki A (2014) Adsorption of lead over graphite oxide. *Spectrochim Acta Part Mol Biomol Spectrosc* 118:857–860
- Opher T, Friedler E, Shapira A (2019) Comparative life cycle sustainability assessment of urban water reuse at various centralization scales. *Int J Life Cycle Assess* 24:1319–1332
- Owa F (2013) Water pollution: sources, effects, control and management. *Mediterr J Soc Sci* 4:65–65
- Pasqualino JC, Meneses M, Castells F (2011) Life cycle assessment of urban wastewater reclamation and reuse alternatives. *J Ind Ecol* 15:49–63
- Pazouki P, Lu HR, El Hanandeh A, Biswas W, Bertone E, Helfer F, Stewart RA (2021) Comparative environmental life cycle assessment of alternative osmotic and mixing dilution desalination system configurations. *Desalination* 504
- Pazouki P, Stewart RA, Bertone E, Helfer F, Ghaffour N (2020) Life cycle cost of dilution desalination in off-grid locations: a study of water reuse integrated with seawater desalination technology. *Desalination* 491:114584
- Qdais HA (2008) Environmental impacts of the mega desalination project: the Red–Dead Sea conveyor. *Desalination*, 22016–23. <https://doi.org/10.1016/j.desal.2007.01.019>
- Rahman Z, Singh VP (2016) Full title: assessment of heavy metal contamination and Hg-resistant bacteria in surface I water from different regions of Delhi, India 2
- Raluy RG, Serra L, Uche J (2004a) Life cycle assessment of water production technologies—part 1: life cycle assessment of different commercial desalination technologies (MSF, MED, RO) (9 pp). *Int J Life Cycle Assess* 10:285–293
- Raluy RG, Serra L, Uche J (2005a) Life cycle assessment of desalination technologies integrated with renewable energies. *Desalination* 183:81–93
- Raluy RG, Serra L, Uche J, Valero A (2004b) Life-cycle assessment of desalination technologies integrated with energy production systems. *Desalination* 167:445–458
- Raluy RG, Serra L, Uche J, Valero A (2005b) Life Cycle assessment of water production technologies—part 2: reverse osmosis desalination versus the ebro river water transfer (9 pp). *Int J Life Cycle Assess* 10:346–354
- Ras C, Von Blottnitz H (2012) A comparative life cycle assessment of process water treatment technologies at the Secunda industrial complex, South Africa. *Water SA* 38:549–554
- Ren R-S, Jiang D-H, Shi F-E, Chen Y-N (2011) Notice of retraction: sorption equilibrium and kinetic studies of Cu (II) from wastewater with modified sepiolites. In: 2011 5th international conference on bioinformatics and biomedical engineering, pp 1–4. IEEE

- Ronquim FM, Sakamoto HM, Mierzwa J, Kulay L, Seckler MM (2020) Eco-efficiency analysis of desalination by precipitation integrated with reverse osmosis for zero liquid discharge in oil refineries. *J Clean Prod* 250:119547
- Sabir S (2015) Approach of cost-effective adsorbents for oil removal from oily water. *Crit Rev Environ Sci Technol* 45:1916–1945
- Sachs G (2013) Sustainable growth: taking a deep dive into water. Visited on 1:2018
- Salcedo R, Antipova E, Boer D, Jiménez L, Guillén-Gosálbez G (2012) Multi-objective optimization of solar Rankine cycles coupled with reverse osmosis desalination considering economic and life cycle environmental concerns. *Desalination* 286:358–371
- Shahabi MP, Anda M, Ho G (2015a) Influence of site-specific parameters on environmental impacts of desalination. *Desalin Water Treat* 55:2357–2363
- Shahabi MP, Mchugh A, Anda M, Ho G (2015b) Comparative economic and environmental assessments of centralised and decentralised seawater desalination options. *Desalination* 376:25–34
- Shahabi MP, Mchugh A, Anda M, Ho G (2014) Environmental life cycle assessment of seawater reverse osmosis desalination plant powered by renewable energy. *Renew Energy* 67:53–58
- Shahabi MP, Mchugh A, Anda M, Ho G (2017) A framework for planning sustainable seawater desalination water supply. *Sci Total Environ* 575:826–835
- Shahabi MP, Mchugh A, Ho G (2015c) Environmental and economic assessment of beach well intake versus open intake for seawater reverse osmosis desalination. *Desalination* 357:259–266
- Shaked S, Crettaz P, Saade-Sbeih M, Jolliet O, Jolliet A (2015) Environmental life cycle assessment. CRC Press
- Sharma G, Naushad M, Ala'a H, Kumar A, Khan MR, Kalia S, Bala M, Sharma A (2017) Fabrication and characterization of chitosan-crosslinked-poly (alginate) nanohydrogel for adsorptive removal of Cr (VI) metal ion from aqueous medium. *Int J Biol Macromol* 95:484–493
- Stokes J, Horvath A (2006) Life cycle energy assessment of alternative water supply systems (9 pp). *Int J Life Cycle Assess* 11:335–343
- Stokes JR, Horvath A (2009) Energy and air emission effects of water supply. *Environ Sci Technol* 43:2680–2687
- Tarnacki K, Meneses M, Melin T, Van Medevoort J, Jansen A (2012) Environmental assessment of desalination processes: reverse osmosis and Memstill®. *Desalination* 296:69–80
- Tarnacki KM, Melin T, Jansen AE, Van Medevoort J (2011) Comparison of environmental impact and energy efficiency of desalination processes by LCA. *Water Supply* 11:246–251
- Tarpani RRZ, Lapolli FR, Lobo Recio MÁ, Gallego-Schmid A (2021) Comparative life cycle assessment of three alternative techniques for increasing potable water supply in cities in the Global South. *J Clean Prod* 290
- Tarpani RRZ, Miralles-Cuevas S, Gallego-Schmid A, Cabrera-Reina A, Cornejo-Ponce L (2019) Environmental assessment of sustainable energy options for multi-effect distillation of brackish water in isolated communities. *J Clean Prod* 213:1371–1379
- Traverso M, Finkbeiner M, Jørgensen A, Schneider L (2012) Life cycle sustainability dashboard. *J Ind Ecol* 16:680–688
- Tristán C, Rumayor M, Dominguez-Ramos A, Fallanza M, Ibáñez R, Ortiz I (2020) Life cycle assessment of salinity gradient energy recovery by reverse electro dialysis in a seawater reverse osmosis desalination plant. *Sustain Energy Fuels* 4:4273–4284
- Tsalidis GA, Gallart JJE, Corberá JB, Blanco FC, Harris S, Korevaar G (2020) Social life cycle assessment of brine treatment and recovery technology: a social hotspot and site-specific evaluation. *Sustain Prod Consum* 22:77–87
- Vince F, Aoustin E, Bréant P, Marechal F (2008a) LCA tool for the environmental evaluation of potable water production. *Desalination* 220:37–56
- Vince F, Marechal F, Aoustin E, Bréant P (2008b) Multi-objective optimization of RO desalination plants. *Desalination* 222:96–118
- WCED, W. C. O. E. A. D (1991) Our common future. Oxford University Press, Oxford
- Younos T (2005) Environmental issues of desalination. *J Contemp Water Res Educ* 132:3

- Yu T-H, Shiu H-Y, Lee M, Chiueh P-T, Hou C-H (2016) Life cycle assessment of environmental impacts and energy demand for capacitive deionization technology. *Desalination* 399:53–60
- Zangeneh H, Zinatizadeh A, Habibi M, Akia M, Isa MH (2015) Photocatalytic oxidation of organic dyes and pollutants in wastewater using different modified titanium dioxides: a comparative review. *J Ind Eng Chem* 26:1–36
- Zhang J, Yuan H, Abu-Reesh IM, He Z, Yuan C (2019) Life cycle environmental impact comparison of bioelectrochemical systems for wastewater treatment. *Procedia CIRP* 80:382–388
- Zhang J, Yuan H, Deng Y, Zha Y, Abu-Reesh IM, He Z, Yuan C (2018) Life cycle assessment of a microbial desalination cell for sustainable wastewater treatment and saline water desalination. *J Clean Prod* 200:900–910
- Zhang X, Zhang L, Fung KY, Bakshi BR, Ng KM (2020) Sustainable product design: a life-cycle approach. *Chem Eng Sci* 217:115508
- Zhou J, Chang VWC, Fane AG (2011a) Environmental life cycle assessment of brackish water reverse osmosis desalination for different electricity production models. *Energy Environ Sci* 4:2267–2278
- Zhou J, ChanG VWC, Fane AG (2011b) Environmental life cycle assessment of reverse osmosis desalination: the influence of different life cycle impact assessment methods on the characterization results. *Desalination* 283:227–236
- Zhou J, Chang VWC, Fane AG (2013) An improved life cycle impact assessment (LCIA) approach for assessing aquatic eco-toxic impact of brine disposal from seawater desalination plants. *Desalination* 308:233–241

Photoelectrochemical Water Treatment of Sewage



Priya Chandulal Vithalani and Nikhil Sumantray Bhatt

Abstract Emerging industrial and human activities are depleting water and other environmental resources due to the massive production of synthetic complexes. Compounds present in sewage are resistant to degradation and have various toxicological properties, which generate various environmental issues. Many conventional methods based on physical, chemical and biological principles are applied to treat sewage. Currently, a combination of different conventional methods is in practice for effective treatment. The photoelectrochemical technique is a combination of light and electrical energy used in the treatment of sewage. In this technique, different types of metals and semiconductor types of photocatalyst are utilized to treat sewage due to its stability, efficiency and remediation performance. In the modified photocatalytic reactor, solar or artificial energy is applied for the oxidation of hazardous compounds which generate hydrogen. The modified photocatalyst has been employed in recent times for efficient treatment and refining hydrogen production. Recently, diverse photocatalytic reactors are designed for a large-scale treatment perspective. Photoelectrochemical reactors have an eco-friendly approach and are less harmful to the environment. Thus, recently researchers are focusing more on this technique from a treatment perspective.

Keywords Hydrogen production · Photocatalyst · Photocatalytic reactor · Photoelectrochemical technique · Sewage treatment · Synthetic complexes

1 Introduction

Water is an essential source for every lifeform on earth so, the removal of pollutants from water is a major concern. Generation of wastewater is estimated at 22,900 million litres per day (MLD) domestic wastewater and 13,500 MLD industrial wastewater in an urban area. Around 26% of wastewater is treated before discharge, and the rest is deposited as untreated. The sewage waste has two types: domestic,

P. C. Vithalani · N. S. Bhatt (✉)
Department of Biogas Research and Microbiology, Gujarat Vidyapith, Sadra, Gandhinagar,
Gujarat, India
e-mail: bhatt@gujaratvidyapith.org

and another is industrial. Domestic wastewater contains 70% organic content and 30% inorganic content. The major problem is the treatment of industrial sewage as it contains many hazardous persistent compounds that cannot be degraded naturally (Ahmed and Ismail 2018; Dehghani et al. 2021; Karri et al. 2021). As industrialization began, the production of synthetic compounds utilized a huge amount of water. Millions of tons of freshwater are utilized every year for synthetic organic compounds (SOCs) production. Textile industries; playing a major role in consuming 80% of total dyestuff production and creating a huge amount of wastewater. Wastewater containing dyes affects the photosynthetic ability of aquatic plants and provides a source for the growth of organisms, which causes deterioration of the ecosystem (Holkar et al. 2016). The waste contains many hazardous compounds such as heavy metals, petrochemical compounds, dyes, metals, stabilizers and thickeners (Feng et al. 2020). The discharge of this waste is having major concern as waste contains many hazardous complexes which have many toxicological properties. Rapid industrialization and globalization increase the demand for SOC. Production of SOC gives rise to pollution, which creates many health and sustainability issues (Orimolade and Arotiba 2020; Shukla 2020). Water is a frequent solvent thus, around 80% of diseases are water-borne, and 3.1% of death are caused due to polluted water. Among all pollution, water pollution is severe, and its consequence on people's health is poor (Ahmed and Ismail 2018; Dehghani et al. 2021; Karri et al. 2021). Organic compounds show different effects on humans, such as disturbance in the endocrine, reproductive, nervous, cardiovascular system, etc. The wastewater embedded with organic and inorganic compounds; utilized by microorganisms as nutrients affect the diversity and rate of photosynthesis of plants present in the water ecosystem (Arslan et al. 2017). These compounds have high stability and are resistant to degradation, consequently, it is necessary to remove them before discharge. Traditionally many physicochemical methods are developed, such as adsorption, precipitation, coagulation, electrochemical, advanced oxidation, and nanoparticles (Khan et al. 2021a, b; Mehmood et al. 2021).

Photoelectrochemical is an advanced oxidation process, majorly used to degrade toxic compounds present in wastewater. The combination of light and electrical energy plays a role inefficient treatment. This chapter consists of the basic overview, synthesis of photocatalyst, and large-scale treatment strategies.

2 Fundamental of Photoelectrochemical Treatment

Photoelectrochemical treatment is a modified version of the advanced oxidation process (AOP). The combination of photon energy and electrical energy is utilized for the treatment perspective. Electrochemical processes include various AOP, which can be applied individually or in combination. Majorly AOPs are dependent on the generation of free OH radicals, which are utilized to degrade SOC. In AOP; mainly two fundamentals are applied, one is the conversion of pollutant compounds into simple biodegradable compounds, which can be performed by direct or indirect

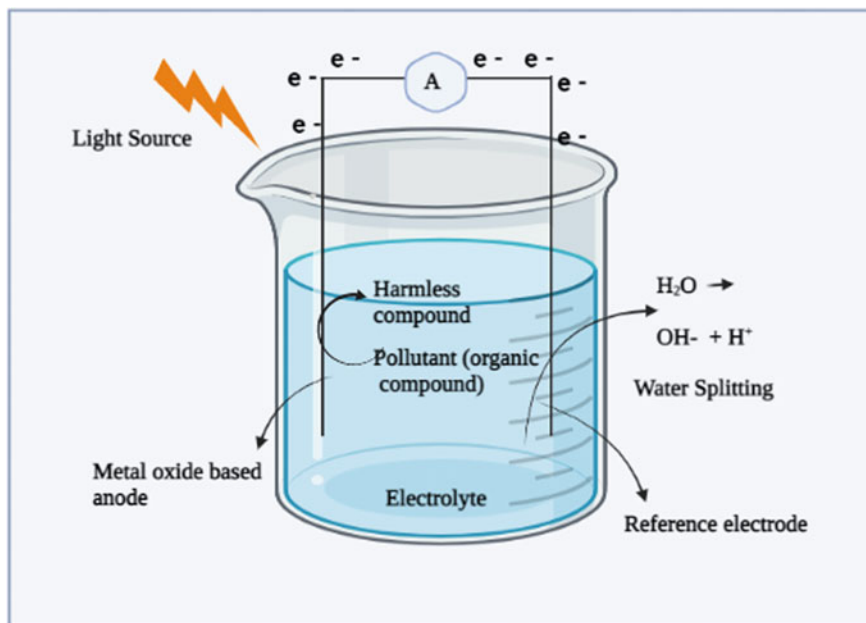


Fig. 1 Basic principle of photoelectrochemical treatment

transfer of an electron, known as an electrochemical conversion, and second is the mineralization of organic compounds by free radicals known as electrochemical combustion. Photo-assisted mediators are applied based on UV and visible wavelength range utilized in the photoelectrochemical process. Photo-assisted mediator activated by photon results in the formation of free OH radicals, which are utilized to oxidise organic compounds. Free radicals formed during the activation of metal nanostructures are used for the oxidation of organic compounds and conversion into simple organic compounds. Semi conductance-based catalysts are an important part of the treatment procedure. Metals have good conductance and efficiently generate free hydroxyl radicals, which are used to remediate different organic compounds (Radha and Sirisha 2018) (Fig. 1).

3 Photocatalytic Composites

Photocatalytic mediated degradation of toxic compounds has huge attention as it effectively solves environmental issues. Semiconductor-based catalysts, mainly TiO_2 and ZnO , are widely used to split water molecules. Metal-based composites are used due to high electronegativity and high energy band gap, which generates free radicals efficiently which are utilized for oxidation of organic compounds. Researchers are now trying combined metal-based composites synthesized by a combination of

different methods to increase efficiency (Ahmed et al. 2021). Composites having photocatalytic, antimicrobial properties and durability help resist water invasion and self-cleaning. TiO_2 mediated structures are widely used in photocatalytic treatment (Singh et al. 2018). Recently, easy availability, nontoxic nature, chemical stability, nanostructures are promising sources for environmental remediation. Numerous metal oxide-based semiconductors such as TiO_2 , ZnO , SnO_2 and ZrO_2 have been applied for a safer environment (Liu et al. 2015).

3.1 Methods for Preparation of Photocatalyst

Photocatalysts have great attention due to their efficiency in treating wastewater and remediation of carcinogenic compounds. Numerous reports are published regarding synthesis, characterization and photocatalytic activity. Physicochemical features and photocatalytic features are determined by the synthesis technique used for production. Different types of synthesis methods are described below.

3.1.1 Sol–Gel Method

Sol–gel processes are widely applied for the synthesis of photocatalysts as it is easy and feasible from a synthesis perspective. The main advantage of this method is homogenous mixing; enhancing polycrystalline particles and intermediate staged addition of dopants enhances the photocatalytic activity. The process incorporates the polymerization of precursor molecules, which is enhanced by a water molecule. The process consists of homogenization, aging, shaping and thermal treatment, which results in xerogel, further treatment results in gel formation. The sol–gel technique synthesised mixed oxide Fe_2O_3 and ZnO mediated photocatalyst (Hernández et al. 2007). Synthesis of TiO_2 based nanopowder was synthesized by sol–gel technique (Tobaldi et al. 2013).

3.1.2 Hydrothermal Method

This method is generally utilized for heterogeneous mixtures composites under high pressure and temperature condition. Hydrothermal mediated synthesis of BiOIO_3 was utilized for photocatalytic activity (Cui et al. 2016). Other Bi_2WO_6 composites were synthesized by the hydrothermal method (Phuruangrat et al. 2014). A combination of three metal oxides, $\text{Fe}_2\text{O}_3/\text{ZnFe}_2\text{O}_4/\text{ZnO}$ nanocomposite, was prepared by hydrothermal technique (Dhal et al. 2015).

3.1.3 Solvothermal Method

Chemical reactions are taking place at higher temperatures and pressure, water or any inorganic and organic solvents are utilized for the synthesis of composites. This method is a modification of hydrothermal processes. High temperature and pressure conditions are responsible for crystallization and result in metal oxide nanoparticles (Nunes et al. 2019). Silver and copper-based composites were synthesized by the solvothermal method (Deng et al. 2016). Solvothermal-based ZnO nanocomposites' characterization and activity were studied (Anu Ruba et al. 2019).

3.1.4 Direct Oxidation Method

Direct oxidation of metal oxide in hydrogen peroxide and other oxidizing agents is utilized, which directly oxidize metals. Direct oxidation of metals is performed in the anodic part. Direct anodic oxidation of titanium films with ethylene glycol was utilized to synthesise crystalline TiO₂ composites (Su et al. 2013).

3.1.5 Anodic Oxidation

Electrochemical anodic oxidation was utilized for the synthesis of TiO₂ based nanowires, nanotubes and nanorods. TiO₂ are synthesized in the presence of acidic electrolytes generation of Ti⁴⁺; secondly, high intensity of electric field results in exposure of Ti. Contact of Ti and electrolytes have resulted in nanotube generation (Zhang et al. 2014).

3.1.6 Sonochemical Method

A combination of ultra-sonication and chemicals is utilized for photocatalyst synthesis. Firstly, cadmium tungstate photocatalyst was synthesized by the sonochemical method. Cadmium nitrate hexahydrate and sodium tungstate dihydrate were utilized for synthesis (Hosseinpour-Mashkani and Sobhani-Nasab 2016). Dicarboxylate coordinate was utilized to synthesise cadmium coordination polymers by the sonochemical method (Hao et al. 2018). Crystalline TiO₂ based photocatalyst synthesized by sonochemical method (Kim et al. 2013).

3.1.7 Microwave Method

Microwave electromagnetic radiation is utilized for nanostructures formation. Microwave irradiation is induced interaction of chemical compounds by changing electric and magnetic fields, resulting in the formation of aggregated particles, leading to the synthesis of photocatalyst formation (Pan et al. 2013). TiO₂ and chloroplast

structured based nanoparticles with electron transfer were formed by microwave-assisted method (Xiao et al. 2019). TiO based powder and crystal structure were synthesized by microwave method (Falk et al. 2018).

3.1.8 Chemical Vapour Deposition (CVD)

This method is widely used in process technology as it requires thin-film semiconductors. Due to high pressure and vacuum, chemical reactions occur, which was used to synthesize metal-based thin-film semiconductors. Different categories of CVD techniques and their variants are utilized, such as horizontal- vertical chemical deposition, low- atmospheric pressure, plasma-photo and laser-assisted CVD. The metal integrated framework was possible through CVD, and the study presented; zeolitic imidazolate mediated thin film was synthesized, which had a uniform thickness even on a high aspect ratio. Unique properties of this metal framework were widely utilized in microelectronics (Stassen et al. 2016).

3.1.9 Physical Vapour Deposition (PVD)

PVD is also well-known technology for thin-film metal oxide framework synthesis. This technique is widely used in optic enhancement, visual upgrading, and many other fields. Deposition plasma ionization, improving target, improving bombardment, increasing deposition rate, and optimization of gases were utilized to improve the technique (Baptista et al. 2018). PVD-based platinum wires were synthesized, which have wide applications in nanotechnology (Dobrzański et al. 2016).

3.1.10 Electrodeposition

Electrodeposition has advantages overall methods such as high deposition rate, controllable and nontoxic. Electrodeposition was carried out directly and indirectly, directly through deposition of metals oxide and indirectly by deposition of intermediate metal hydroxides. Studies presented electrodeposition of copper oxide nanofilms as copper was widely used in capacitors, gas sensing, solar cell, field transistor, and biosensors (Wang et al. 2014). Electrodeposition carried out the synthesis of gold nanostructures (Worrall et al. 2016).

3.1.11 Electrosynthesis

Zinc oxide and manganese oxide-based composites were synthesized by the electrosynthesis method. This composite has better electrochemical behaviour and high conductance, which were utilized for wastewater treatment (Ameri et al. 2017). The

study revealed that electrosynthesis methods were utilized for a nanostructure formation which was used to absorb organic and inorganic compounds efficiently (Wang et al. 2020a, b).

3.1.12 Biological Synthesis

The biological approach of synthesis of nanoparticles is eco-friendly, cost-effective, and less harmful to the environment. Microorganisms such as bacteria, fungi, yeast, algae, actinomycetes are utilized for green nanotechnology. Microorganisms are a potential source for nanostructure synthesis and have application in the removal of dyes (Asgar et al. 2020). Biological synthesis of silver nanoparticles was carried out by *Chlorella vulgaris*, and photocatalytic efficiency was checked for methylene blue dye degradation. The results showed 96% degradation of methylene blue dye (100 ppm) in 3 h of incubation time (Rajkumar et al. 2021). Synthesis of nanostructures was carried out intracellularly by proteins, polysaccharides and extracellular synthesis was carried out by electron transfer mechanism (Gahlawat and Choudhury 2019).

3.2 Application of Metal Oxide Photocatalyst for Treatment Perspective

Anthropogenic activities of human beings are a major source of soil, water, and air pollution, which are alarming to the environment's health. Wastewater coming out from industries have many carcinogenic and toxic pollutants such as dyes, organic solvents, metals, high biological (BOD), and chemical oxygen demand (COD). Treatment of wastewater before discharge into the environment is a necessary task (Tahir et al. 2017). Various conventional methods are utilized, such as adsorption, precipitation, coagulation, membrane filtration, electrochemical, and advanced oxidation processes (Abebe et al. 2020). A combination of two or more two methods is required for efficient treatment in recent times. Photoelectrochemical have modified advanced oxidation processes, which are now applied more due to higher efficiency. ZnO, TiO₂, Fe₂O₃, CuO, and NiO mediated newly combined composites are applied in wastewater treatment (Liu et al. 2015). ZnO and TiO₂ based nanocomposites and their combination with other composites are common because of their easy synthesis, high efficiency and feasibility.

3.2.1 Zinc Oxide (ZnO)

ZnO has better stability and high photocatalytic activity thus, it is widely used in the treatment perspective. ZnO also shows better antimicrobial activity. An

extensive study indicates that controlled oxygen vacancies can manipulate ZnO's optical, surface, and electronic properties. ZnO has applications in different areas such as photocatalysis, gas sensor, biosensor, anti-bacterial agent, and supercapacitors. Synthesis of ZnO nanoparticles is carried out with chemical and physical approaches. Mechanical synthesis of ZnO nanostructure was carried out with desired characteristics (Wang et al. 2018a, b).

Now-a-days ZnO is utilized as nanostructures in photoelectrochemical and photochemical treatment. For the catalysis, under visible light junction must be developed. The ionic bond strength of Zn is higher, which shows low electronegativity. Combined with low band metal oxides composites, a junction enhances the absorbance of visible light. During heterojunctions formations, the up-down movement of semiconductors produces electrical energy, which activates photocatalytic reaction activity (Abebe et al. 2020). The co-precipitation method synthesised studies carried out with combine Ag/ZnO mediated photocatalyst. Photocatalysis activity was checked in a batch reactor, efficiency of ZnO combined with Ag was checked. The results show a decrease in BOD, COD of wastewater which concludes that the photocatalysis treatment efficiently degraded dyes present in wastewater. Microbial communities present in wastewater were eliminated with ZnO activity (Mesa et al. 2018). ZnO-based nanoparticles were synthesized by the chemical deposition method and applied on methylene blue dye degradation. The results showed 67% dye degradation with a concentration of photocatalyst 0.2 g/L in 2 h in UV irradiation (Ng et al. 2021). Six endocrine disrupters were removed using ZnO nanostructures. After the photocatalytic treatment, 80% of organic matter was removed, and concentration of endocrine disrupters was decreased, and the remaining concentration of 0–24% with different compounds were found (Vela et al. 2018).

3.2.2 Titanium Oxide (TiO₂)

TiO₂ is widely applied as a photocatalyst and promising material due to its high oxidation efficiency, no toxicity, photostability, and eco-friendly nature. As per research, TiO₂ is a great photocatalyst capable of removing organic pollutants present in wastewater under UV irradiation. TiO₂ can be activated through UV light due to lower wavelength (387 nm) and higher energy bandgap (3–3.2 eV). Due to the high success rate in the laboratory-scale study, nowadays, it is exploited in large scale studies (Daghrir et al. 2013). Fe₂O₃ and TiO₂ based mixed mesoporous nanostructure was formed by the sol–gel method (Palanisamy et al. 2013).

Similarly, with different methods, synthesis of TiO₂ was carried out and applied for degradation of various organic compounds and treatment of wastewater. TiO₂ based degradation mechanism was based on electron hole generation upon UV radiation. In reaction excitation, charge migration and redox reactions are taking place. The generation of free radicals (OH·) is responsible for the oxidation of organic compounds. The mechanism is described in Fig. 2. Metals getting energy through light and electrons moved from lower to higher energy levels, and sequential reactions were taking place for the generation of free radicals, which was important for

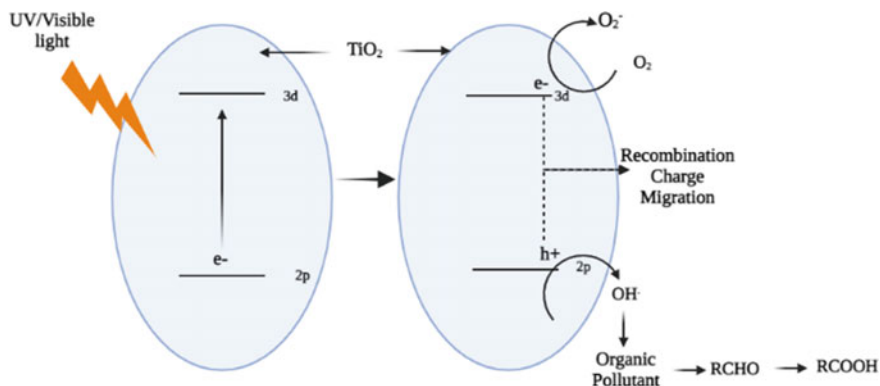
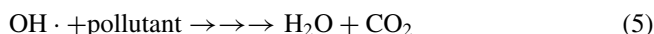
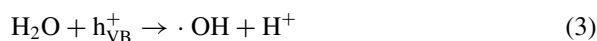


Fig. 2 Reaction mechanism of TiO_2 photocatalyst

removing organic pollutants (Nasirian et al. 2018). The chemical reaction is carried out by nanostructure are as follows.



TiO_2 was synthesized by a novel method UV-assisted thermal microwave method. The efficiency of the photocatalyst was checked in a batch photocatalytic reactor with the degradation of methyl orange dye. With different light sources, the degradation of methyl orange was checked. The result showed UV-C lamp was more efficient and degrades 98% of methyl orange (Nasirian and Mehrvar 2018). TiO_2 -Fe and biochar mediated heterogeneous composite was synthesized by thermal deposition single-step technique. The method was utilized to decrease the toxicity of metals and increase the absorbance of methylene blue dye molecules. Application of composites resulted in 377 mg/L of methylene blue removal after catalysis. The catalysts showed maximum stability, recyclability, and separability (Mian and Liu 2019).

3.2.3 Other Structured Materials

Bismuth Vanadate is now taking attention to photocatalytic-based wastewater treatment. Bismuth Vanadate is a nontoxic low-cost n-type semiconductor with a narrow energy gap (2.4 eV) and excellent photocatalytic capacity, stability, and photostability properties. Hydrothermal-based synthesis was widely utilized among all methods because structure and morphology are controlled through the thermal route. The first hydrothermal synthesis of bismuth vanadate was carried out by Roth and Waring (Orimolade and Arotiba 2020). Hydrothermally bismuth vanadate-based nanostructure was synthesized at different pH. Photocatalytic performance was checked with rhodamine B dye degradation. Maximum results were shown at pH 7, 70% degradation was found in 1 h under UV light irradiation (Lin et al. 2019).

Metal-based organic frameworks are also having an attraction for photocatalytic treatment of waste. Iron is a low-cost element of the earth having oxidation potential and photostability. The hydrothermal method-based iron-mediated framework was applied for the removal of tetracycline. Results showed 40% of the removal of tetracycline with 50 mg/L initial concentration (Wang et al. 2018a, b). Similarly, different iron-based metal frameworks were synthesized. Photocatalytic efficiency was performed with basic blue 41 degradations. The result observed that synthesized nanostructure can remove dye from colored wastewater, and the efficiency of the photocatalyst was not decreased up to three-cycle (Mahmoodi et al. 2018). Cadmium-based nanostructures also have a low bandgap with easy controllable morphology and potential toward visible light response. The main disadvantage of cadmium is intrinsic toxicity is a risk to human health and the environment (Regulacio and Han 2016). Nickle-based nanostructures were synthesized by the hydrothermal decomposition method. Nickle has a band gap (2.83 eV) that confirms photocatalytic properties. Photocatalytic efficiency was confirmed with 80% degradation of Rhodamine B (Motahari et al. 2014). Sonochemical method-based synthesis of silver tungstate nanostructure was having visible-light-driven photolysis. The photocatalytic efficiency was checked with Rhodamine B (100%), Acid red (94%), and Eriochrome cyanine (96%) removal of dye contaminant (Zinatloo-Ajabshir et al. 2020).

As nanostructures are applied for effective treatment. Nowadays, rather than using single metal oxide, a combination of different metal oxides is used to synthesise nanostructures. The metal oxide is efficiently used in photocatalytic treatment because band energy gap. Combined heterogeneous photocatalysts efficiently increase bandgap energy which enhances the photocatalytic activity of metals and enhances the removal rate of organic pollutants (Venkata et al. 2019). The physical vapour deposition method synthesised a combination of Ag and TiO₂ metal-based nanostructures. Photocatalytic efficiency was performed with 98% degradation of methylene blue in 120 min of UV radiation (Barrientos et al. 2018). In Table 1, different composites of nanostructures applied for photocatalytic treatment are mentioned.

Table 1 Nanoparticles and their composites for sewage treatment

Synthesis method	Nanocomposites	Result	References
Microbial (<i>Deinococcus radiodurans</i>)	Silver nanoparticles	Malachite green degradation (83%) and degradation ability > 64% after two cycle	Weng et al. (2020)
Sonochemical	Sliver tungstate	94% for Acid red 14 and 96% for Eriochrome cyanine R and 99% for Rhodamine B	Zinatloo-Ajabshir et al. (2020)
Microwave-assisted	Zinc- iron hybrid α -Fe ₂ O ₃ /ZnFe ₂ O ₄ /ZnO	99% removal of methylene blue and Malachite green in 32 and 24 min under solar light illumination	
Hydrothermal assisted	ZnO	99% Sulfamethoxazole removal	Makropoulou et al. (2020)
Plant-based (<i>Cannabis sativa</i> Leaf extract)	Zinc oxide & Sliver based zinc oxide (Ag/ZnO)	Methyl orange (96% with Ag/ZnO, 36% with ZnO) and Condo red (94% with Ag/ZnO, 34% with ZnO) removed	Chauhan et al. (2020)
Plant-based (<i>Syzygium Cumini</i>)	Zinc oxide	98% removal of Rhodamine B	Rafique et al. (2020)
Co-precipitation	Iron doped indium oxide	Removal of methylene blue, Rhodamine B, and Methyl orange 93, 95, and 93%, respectively	Jabeen et al. (2020)
Hydrothermal + (<i>A. linearis</i> plant leaf)	Cobalt oxide	20 ppm congo red removed 96% under visible light irradiation	Magdalane et al. (2019)
Microbial (<i>Cordyceps militaris</i>)	Zinc oxide	97% Methylene blue dye degradation	Li et al. (2019)
Enzyme based	NH ₂ -MIL-88B iron-based catalyst	(Possesses peroxidase activity) and removed 80% methylene blue in 45 min	He et al. (2018)
Microbial (<i>Aspergillus niger</i>)	Zinc oxide	90% of decolorization of Bismarck brown dye	Kalpna et al. (2018)

(continued)

Table 1 (continued)

Synthesis method	Nanocomposites	Result	References
Hydrothermal assisted	Tungsten trioxide	H ₂ evolution (288/ $\mu\text{mol h}^{-1}\text{g}^{-1}$)	Tahir et al. (2018)
Chemical	TiO ₂	5 ppm chromium removed in 15 in under UV light irradiation	Athanasekou et al. (2017)
Hydrothermal	Copper sulfide (CuS)	Removed 87% of methylene blue dye under visible light irradiation	Saranya et al. (2014)

3.3 Factors Affecting Photocatalysis Treatment

Photocatalytic efficiency is affected by various operational parameters such as contaminant concentration, pH, temperature, light intensity, nature of photocatalyst, the surface area of photocatalyst, irradiation time, and structure of photocatalyst (Kumar 2017). The initial concentration of organic pollutants is one of the major factors for photocatalytic degradation. The surface area aspect to a concentration of pollutants is the main factor for better treatment. The absorption capacity of photocatalyst plays an important role in removing pollutants (Zhu and Zhou 2019). The structure and morphology of nanoparticles are important factors for the removal of pollutants. The structure of nanoparticles depends on the synthesis method. So, an appropriate synthesis method is needed for controlled structure and morphology. The morphology of nanostructure is depended on the nature of metals and band energy gap (Shen et al. 2018). pH and temperature also play a vital role in nanostructure synthesis. A low temperature of the reaction shows higher catalytic efficiency. The pH of the medium plays a role in morphology and structure formation (Nie et al. 2017). Highly acidic or alkaline pH will affect the metal nanostructure and decrease the efficiency of the splitting mechanism. The light source is also affecting photocatalytic relations. The splitting of OH ions depends on the intensity and nature of light used for irradiation (Joy et al. 2018). Optimization of process parameters during the study will enhance photocatalytic activity. Optimization of methylene blue dye photocatalytic degradation was carried out by optimizing various process parameters. The maximum photocatalytic activity obtained in pH 3.5, catalytic dosage 0.9 g/L, 3.2 g/L methylene blue was degraded in 26 min with CuO-NiO combined photocatalyst (Senobari and Nezamzadeh-ejhieh 2018a, b). Another study carried out by same author, maximum result were obtained in pH 3.5, catalytic dosage 0.9 g/L, 3.2 g/L methylene blue was degraded in 83 min of reaction time with NiO-CdS combined photocatalyst (Senobari and Nezamzadeh-ejhieh 2018a). The results can conclude that combination of different metal oxide also play role in photocatalytic treatment. Similar study concluded that with increasing pH activity of photocatalysis increase

to some extent after that decrease the activity is seen. Intensity of light is important for generation of free radicals and adsorption mechanism. Photocatalytic efficiency depended on stability of photocatalyst (Yang et al. 2017).

4 Photoelectrochemical Technique for Sewage Treatment

In recent times, industrial development resulted in environmental pollution. A huge quantity of wastewater requires treatment before discharge. As wastewater contains many harmful substances which affect human and ecosystem health. Many conventional methods, such as precipitation, coagulation, membrane-based, electrochemical, advanced oxidation, and biological, are applied for treatment (Rajasulochana 2016). In recent times, treatment strategies have been applied for efficient treatment, a combination of more than two approaches. Photoelectrochemical is one of modified treatment of advanced oxidation processes. Fundamentals of this technique are described in the above section. As per fundamentals, metals-based structures play an important role in treatment. Visible or UV light irradiation is responsible for the generation of free radicals, which are helpful to oxidize organic pollutants. Nowadays, large-scale reactor studies are also performed for efficient and better treatment. Recently, different three-dimensional reactors are designed to treat and remediation of organic compounds. Instead of UV light irradiation, solar panels are utilized to reduce cost, efficient treatment, and reduce energy utilisation. A large-scale study requires high construction and treatment costs, so cost-effective strategies are applied. A three-dimensional photocatalytic reactor was studied for disinfection with photoelectrode made of granular activated carbon and titanium oxide. Results have shown granulated carbon; enhanced photocatalytic efficiency with UV radiation (Mesones et al. 2020). Recently researchers are focusing on hybrid reactor studies for efficient treatment of wastewater. Artificially synthesized composite made up from titanium oxide, graphene oxide, and graphitic carbon nitride immobilized on polystyrene film evaluated for degradation of remazol turquoise blue using photocatalytic airlift reactor. In 90 min reaction time, the results found 60% decolorization and 51% of degradation of dye by total organic carbon analysis. The same researcher carried the updated study with a photocatalytic airlift reactor, analyzing its performance. Results presented 92% total organic carbon reduction and 94% remazol turquoise blue dye decolorization in 2 h 10 min in the immobilized catalyst (Das and Mahalingam 2019, 2020). Zinc oxide capped polyethylene glycol (ZnO-PEG) and polypiperazine amide tight ultrafiltration membrane were utilized in the photocatalytic reactor to treat textile wastewater. The optimum operating condition of the reactor was pH 11, ZnO-PEG 0.1 g/L, more than 95% degradation of synthetic wastewater, and COD removal was observed with 75% dilution of industrial wastewater (Desa et al. 2019).

4.1 Photocatalytic Reactor for Treatment and Hydrogen Production

Various sources produce energy through wind, biomass, solar and nuclear assistance. Nuclear assisted H₂ production is now-a-days more utilized due to extreme energy generation, but it has risks to humans and the environment. Ecofriendly sources for H₂ production are needed to be applied for a sustainable environment (Wang et al. 2020a, b). Hydrogen is a clean energy source and has the potential to overcome the increasing energy demand. Treatment of wastewater with energy production is an alternative strategy for better and efficient treatment. Hydrogen (H₂) is the main energy source generated during wastewater treatment. Sustainable development leads to a focus on H₂ energy production from different natural and artificial substrates. Nowadays, demand is increasing as it is alternative, clean and green energy (El-Shafie et al. 2019). The schematic photocatalytic reactor design for hydrogen production and removal mechanism are shown in Fig. 3. Chemical-based methods for hydrogen production are photolysis, thermolysis, thermochemical water splitting and gasification. Many biological methods are applied for H₂ production like fermentation, an alternative method is microbial fuel cell (MFC). Biologically, MFC is important for wastewater treatment and hydrogen production. Non biologically, photoelectrochemical reactors are applied for hydrogen production (Rioja-Cabanillas et al. 2021). Wastewater is having great potential for energy generation. Researchers have quantified energy based on the COD of wastewater, and it is five times higher than the

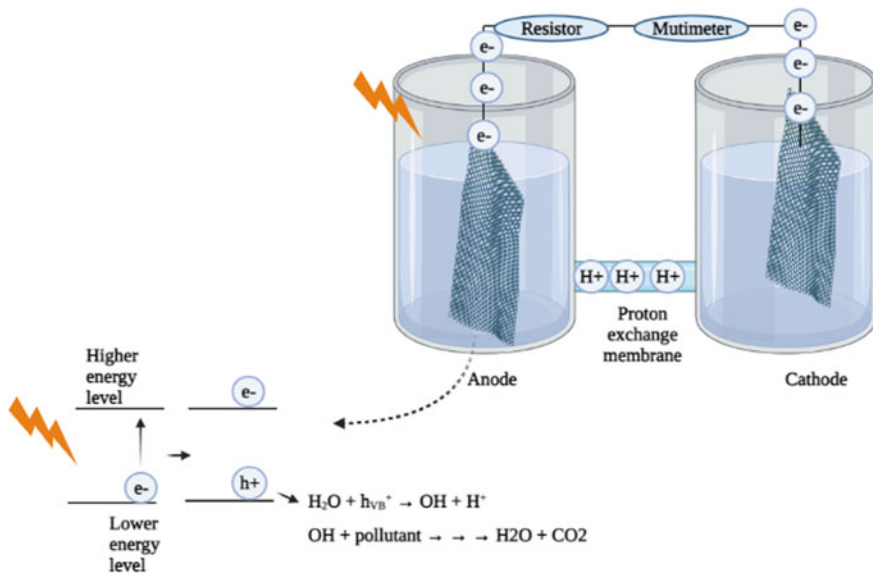


Fig. 3 Photocatalytic reactor design and mechanism of degradation and H₂ production

required energy for treatment. Photoelectrochemical and microbial-assisted photoelectrochemical reactors are now getting more attention due to higher efficiency in treatment and H_2 production. Microbes are utilized to oxidise organic compounds in the anaerobic condition in anodic part, and cathode aerobic condition helpful for water generation is utilized for better and efficient treatment. The utilization of nanostructure with microbes increases the efficiency of oxidation and remediation of organic compounds, which is a key entity for better treatment. (Islam et al. 2021). Photoexcitation of electron pair allows hydrogen production through charge transfer and recombination processes. To achieve photocatalytic water splitting, metal-based nanostructures are applied, which are helpful in the excitation and generation of free radicals, resulting in the removal of organic compounds and hydrogen production (Martino et al. 2021).

H_2 production with wastewater treatment is a novel approach in recent times. More research work is going on for efficient treatment and energy generation. Erbium-doped TiO_2 nanotubes are synthesized and applied in photocatalytic degradation of methylene blue. The results of photocatalytic efficiency showed 85% of methylene blue degradation after 180_{min} exposure to light. The H_2 production efficiency was observed at $17.39 \text{ mM}\cdot\text{hr}^{-1} \text{ cm}^{-2}$ (Cho et al. 2021). Highly toxic sulfide-containing wastewater was utilized for hydrogen production. CNT— $CdZnS/Fe_2O_3$ based nanostructures were applied for treatment and H_2 production. The highest hydrogen was produced, 2679 mmol/h, from wastewater (Anthony Raja and Preethi 2020). Hydrogen sulfide (H_2S) is a highly toxic gas, wastewater containing hydrogen sulfide was utilized for sulfide recovery and hydrogen production. Splitting of H_2S resulted in hydrogen production and 80 kJ/mol energy generation (Vikrant et al. 2019). Hybrid photocatalysis and peroxicoagulation were utilized for the removal of organic pollutants and the generation of electricity. The degradation rate was 11%, the maximum power density was $3.14 \text{ mW}\cdot\text{cm}^{-2}$, and an iron plate size of 30 cm^2 was obtained (Nordin et al. 2020). Integration of oxidation of photocatalyst and biodegradation approach was applied to treat CETP effluent. The reactor was set up with synthesized TiO_2 combined with activated carbon (AC) and biofilm. The results gained removal of COD, BOD, TSS, and ammonical nitrogen within 6_h were 61, 92, 88, and 50% respectively, and decolorization was 78% in the presence of solar light, TiO_2/AC , and biofilm (Chavan and Fulekar 2018). Lead tipped cobalt oxide-based nanowires were fabricated by a combination of hydrothermal and electrodeposition methods. Photoelectrochemical efficiency was checked, 70% of degradation of 60 mg/L concentration of reactive brilliant blue dye was obtained (Wang et al. 2019).

5 Conclusion

Rapid urbanization and industrialization for mankind are responsible for environmental issues. The demand for human beings is increasing day by day, leading to the production of new synthetic organic compounds, which results in deteriorating human and environmental health. The wastewater comes from different

industries, comprising many toxic pollutants affecting the whole ecosystem and causing many skins, cardiovascular, immunological, and developmental issues in animals and humans. Remediation of toxic compounds before discharging them into the ecosystem is crucial for all industrialists. Many conventional physical, chemical and biological methods are applied with advantages and disadvantages. Large-scale treatment perspective modification in existing treatment methods is important for better results. Photoelectrochemical is one of the modified and combined electrochemical and light energy methods. Combining these two methods exhibits great attention and is beneficial in large-scale studies. As per the literature study, photoelectrochemical methods have great potential for treating large level studies. Recently researchers have been focusing on resource recovery with the treatment of wastewater. Photoelectrochemical-based microbial fuel cells are good examples of efficient wastewater treatment with hydrogen production. So, microbial and photoelectrochemical-based fuel cells are developed for sewage treatment and hydrogen production, which has great attention in the research field.

6 Future Aspects

Treatment of wastewater plays an important role in overcoming air, water, and soil pollution. Sewage waste treatment is having difficulties due to the composition having many toxic, carcinogenic and mutagenic compounds. The discharge of waste directly into the ecosystem leads to disturbance in the ecosystem, food chain and causes many health issues. Remediation of organic compounds before discharging is crucial for a sustainable environment. Many different methods are already developed for the removal of such compounds. For the large-scale study, different researchers develop many reactors through the utilization of various methods, but methods developed have their pros and cons. Ultimately, modified methods are needed for better treatment. In the photoelectrochemical method, different nanostructure and composites are utilized, giving better results. Design, synthesis, morphology-based modified different metals and their utilization in treatment is one of the modifications. Several reactors are developed by applying different nanostructures, but it is not that effective. Researchers can modify reactor design and metal-based semiconductor design, giving better results from a treatment perspective. Researchers can combine two–three methods or utilize them sequentially for better efficiency in treatment and energy production. Wastewater treatment-based hydrogen generation is a sustainable approach for energy generation and has great potential to overcome the energy demand.

References

- Abebe B, Murthy HCA, Amare E (2020) Pre of environmental nanotechnology, monitoring & management, p 100336. <https://doi.org/10.1016/j.enmm.2020.100336>
- Ahmed S, Ismail S (2018) Water pollution and its source, effects & management: a case study of Delhi. *Int J Curr Adv Res* 7(2(L)):10436–10442
- Ahmed S, Khan FSA, Mubarak NM, Khalid M, Tan YH, Mazari SA, Karri RR, Abdullah EC (2021) Emerging pollutants and their removal using visible-light responsive photocatalysis—a comprehensive review. *J Environ Chem Eng* 9(6). <https://doi.org/10.1016/j.jece.2021.106643>
- Ameri B, Davarani SSH, Moazami HR, Darjazi H (2017) Cathodic Electrosynthesis of ZnMn₂O₄/Mn₃O₄ composite nanostructures for high performance supercapacitor applications. *J Alloy Compd* 720:408–416. <https://doi.org/10.1016/j.jallcom.2017.05.271>
- Anthony Raja M, Preethi V (2020) Photocatalytic hydrogen production using bench-scale trapezoidal photocatalytic reactor. *Int J Hydrog Energy* 45(13):7574–7583. <https://doi.org/10.1016/j.ijhydene.2019.08.204>
- Anu Ruba A, Johnny LM, Nirmala Jothi NS, Sagayaraj P (2019) Solvothermal synthesis, characterization and photocatalytic activity of ZnO nanoparticle. *Mater Today Proc* 8:94–98. <https://doi.org/10.1016/j.matpr.2019.02.085>
- Arslan M, Imran A, Khan QM, Afzal M (2017) Plant–bacteria partnerships for the remediation of persistent organic pollutants. *Environ Sci Pollut Res* 24(5):4322–4336. <https://doi.org/10.1007/s11356-015-4935-3>
- Asghar M, Habib S, Ali H, Saqib S (2020) Synthesis and characterization of microbial mediated cadmium oxide nanoparticles, pp 1–11. <https://doi.org/10.1002/jemt.23553>
- Athanasekou C, Romanos GE, Papageorgiou SK, Manolis GK, Katsaros F, Falaras P (2017) Photocatalytic degradation of hexavalent chromium emerging contaminant via advanced titanium dioxide nanostructures. *Chem Eng J* 318:171–180. <https://doi.org/10.1016/j.cej.2016.06.033>
- Baptista A, Silva F, Porteiro J, Míguez J, Pinto G (2018) Sputtering physical vapour deposition (PVD) coatings: a critical review on process improvement and market trend demands. *Coatings* 8(11). <https://doi.org/10.3390/COATINGS8110402>
- Barrientos L, Allende P, Laguna-Bercero MÁ, Pastrián J, Rodríguez-Becerra J, Cáceres-Jensen L (2018) Controlled Ag-TiO₂ heterojunction obtained by combining physical vapor deposition and bifunctional surface modifiers. *J Phys Chem Solids* 119:147–156. <https://doi.org/10.1016/j.jpcs.2018.03.046>
- Chauhan A, Verma R, Kumari S, Sharma A, Shandilya P, Li X, Batoo KM, Imran A, Kulshrestha S, Kumar R (2020) Photocatalytic dye degradation and antimicrobial activities of pure and Ag-doped ZnO using Cannabis sativa leaf extract. *Sci Rep* 10(1):1–16. <https://doi.org/10.1038/s41598-020-64419-0>
- Chavan A, Fulekar MH (2018) Integration of photocatalytic oxidation and biodegradation treatment processes to enhance degradation efficiency of CETP wastewater contaminants. *BioNanoScience* 8(3):761–768. <https://doi.org/10.1007/s12668-018-0534-3>
- Cho H, Joo H, Kim H, Kim JE, Kang KS, Yoon J (2021) Improved photoelectrochemical properties of TiO₂ nanotubes doped with Er and effects on hydrogen production from water splitting. *Chemosphere* 267:129289. <https://doi.org/10.1016/j.chemosphere.2020.129289>
- Cui DH, Zheng YF, Song XC (2016) Hydrothermal synthesis, characterization and photocatalytic properties of BiOIO₃ nanoplalelets. *J Exp Nanosci* 11(12):1000–1010. <https://doi.org/10.1080/17458080.2016.1193671>
- Daghrir R, Drogui P, Robert D (2013) Modified TiO₂ for environmental photocatalytic applications: a review. *Ind Eng Chem Res* 52(10):3581–3599. <https://doi.org/10.1021/ie303468t>
- Das S, Mahalingam H (2019) Dye degradation studies using immobilized pristine and waste polystyrene-TiO₂/rGO/g-C₃N₄ nanocomposite photocatalytic film in a novel airlift reactor under solar light. *J Environ Chem Eng* 7(5):103289. <https://doi.org/10.1016/j.jece.2019.103289>

- Das S, Mahalingam H (2020) Novel immobilized ternary photocatalytic polymer film based airlift reactor for efficient degradation of complex phthalocyanine dye wastewater. *J Hazard Mater* 383:121219. <https://doi.org/10.1016/j.jhazmat.2019.121219>
- Dehghani MH, Omrani GA, Karri RR (2021) Solid waste—sources, toxicity, and their consequences to human health. *Soft computing techniques in solid waste and wastewater management*, pp 205–213. Elsevier. <https://doi.org/10.1016/B978-0-12-824463-0.00013-6>
- Deng X, Wang C, Zhou E, Huang J, Shao M, Wei X, Liu X, Ding M, Xu X (2016) One-step solvothermal method to prepare Ag/Cu₂O composite with enhanced photocatalytic properties. *Nanoscale Res Lett* 11(1). <https://doi.org/10.1186/s11671-016-1246-7>
- Desa AL, Hairom NHH, Ng LY, Ng CY, Ahmad MK, Mohammad AW (2019) Industrial textile wastewater treatment via membrane photocatalytic reactor (MPR) in the presence of ZnO-PEG nanoparticles and tight ultrafiltration. *J Water Process Eng* 31:100872. <https://doi.org/10.1016/j.jwpe.2019.100872>
- Dhal JP, Mishra BG, Hota G (2015) Hydrothermal synthesis and enhanced photocatalytic activity of ternary Fe₂O₃/ZnFe₂O₄/ZnO nanocomposite through cascade electron transfer. *RSC Adv* 5(71):58072–58083. <https://doi.org/10.1039/c5ra05894e>
- Dobrzański LA, Szindler M, Pawlyta M, Szindler MM, Boryło P, Tomiczek B (2016) Synthesis of Pt nanowires with the participation of physical vapour deposition. *Open Phys* 14(1):159–165. <https://doi.org/10.1515/phys-2016-0017>
- El-Shafie M, Kambara S, Hayakawa Y (2019) Hydrogen production technologies overview. *J Power Energy Eng* 07(01):107–154. <https://doi.org/10.4236/jpee.2019.71007>
- Falk GS, Borlaf M, López-Muñoz MJ, Fariñas JC, Rodrigues Neto JB, Moreno R (2018) Microwave-assisted synthesis of TiO₂ nanoparticles: photocatalytic activity of powders and thin films. *J Nanoparticle Res* 20(2). <https://doi.org/10.1007/s11051-018-4140-7>
- Feng C, Yu L, Xiao Y, An C (2020) Environmental behavior and effects of pollutants in water. *J Chem*. <https://doi.org/10.1155/2020/2639389>
- Gahlawat G, Choudhury AR (2019) A review on the biosynthesis of metal and metal salt nanoparticles by microbes, pp 12944–12967. <https://doi.org/10.1039/c8ra10483b>
- Hao SY, Li YH, Zhu J, Cui GH (2018) Structures, luminescence and photocatalytic properties of two nanostructured cadmium(II) coordination polymers synthesized by sonochemical process. *Ultrason Sonochemistry* 40(Ii):68–77. <https://doi.org/10.1016/j.ultsonch.2017.06.028>
- He J, Zhang Y, Zhang X, Huang Y (2018) Highly efficient Fenton and enzyme-mimetic activities of NH₂-MIL-88B(Fe) metal organic framework for methylene blue degradation. *Sci Rep* 8(1):1–8. <https://doi.org/10.1038/s41598-018-23557-2>
- Hernández A, Maya L, Sánchez-Mora E, Sánchez EM (2007) Sol-gel synthesis, characterization and photocatalytic activity of mixed oxide ZnO-Fe₂O₃. *J Sol-Gel Sci Technol* 42(1):71–78. <https://doi.org/10.1007/s10971-006-1521-7>
- Holkar CR, Jadhav AJ, Pinjari DV, Mahamuni NM, Pandit AB (2016) A critical review on textile wastewater treatments: possible approaches. *J Environ Manage* 182:351–366. <https://doi.org/10.1016/j.jenvman.2016.07.090>
- Hosseinpour-Mashkani SM, Sobhani-Nasab A (2016) A simple sonochemical synthesis and characterization of CdWO₄ nanoparticles and its photocatalytic application. *J Mater Sci Mater Electron* 27(4):3240–3244. <https://doi.org/10.1007/s10854-015-4150-5>
- Islam AKMK, Dunlop PSM, Hewitt NJ, Lenihan R, Brandoni C (2021) Bio-hydrogen production from wastewater: a comparative study of low energy intensive production processes. *Clean Technol* 3(1):156–182. <https://doi.org/10.3390/cleantechnol3010010>
- Jabeen S, Iqbal J, Arshad A, Awan MS, Warsi MF (2020) (In_{1-x}Fe_x)₂O₃ nanostructures for photocatalytic degradation of various dyes. *Mater Chem Phys* 243. <https://doi.org/10.1016/j.matchemphys.2019.122516>
- Joy J, Mathew J, George SC (2018) Science direct Nanomaterials for photoelectrochemical water splitting: a review. *Int J Hydrogen Energy* 43(10):4804–4817. <https://doi.org/10.1016/j.ijhydene.2018.01.099>

- Kalpana VN, Kataru BAS, Sravani N, Vigneshwari T, Panneerselvam A, Devi Rajeswari V (2018) Biosynthesis of zinc oxide nanoparticles using culture filtrates of *Aspergillus niger*: antimicrobial textiles and dye degradation studies. *OpenNano* 3:48–55. <https://doi.org/10.1016/j.onano.2018.06.001>
- Karri RR, Ravindran G, Dehghani MH (2021) Wastewater—sources, toxicity, and their consequences to human health. *Soft computing techniques in solid waste and wastewater management*, pp 3–33. Elsevier. <https://doi.org/10.1016/B978-0-12-824463-0.00001-X>
- Kim TH, Rodríguez-González V, Gyawali G, Cho SH, Sekino T, Lee SW (2013) Synthesis of solar light responsive Fe, N co-doped TiO₂ photocatalyst by sonochemical method. *Catal Today* 212:75–80. <https://doi.org/10.1016/j.cattod.2012.09.014>
- Khan FS, Mubarak NM, Khalid M, Tan YH, Abdullah EC, Rahman ME, Karri RR (2021a) A comprehensive review on micropollutants removal using carbon nanotubes-based adsorbents and membranes. *J Environ Chem Eng* 9(6). <https://doi.org/10.1016/j.jece.2021.106647>
- Khan FS, Mubarak NM, Tan YH, Khalid M, Karri RR, Walvekar R, Abdullah EC, Nizamuddin S, Mazari SA (2021b) A comprehensive review on magnetic carbon nanotubes and carbon nanotube-based buckypaper for removal of heavy metals and dyes. *J Hazard Mater* 413. <https://doi.org/10.1016/j.jhazmat.2021.125375>
- Kumar A (2017) A review on the factors affecting the photocatalytic degradation of hazardous materials. *Mater Sci Eng Int J* 1(3). <https://doi.org/10.15406/mseij.2017.01.00018>
- Li JF, Rupa EJ, Hurh J, Huo Y, Chen L, Han Y, Ahn J, chan, Park, J. K., Lee, H. A., Mathiyalagan, R., & Yang, D. C. (2019) *Cordyceps militaris* fungus mediated Zinc Oxide nanoparticles for the photocatalytic degradation of Methylene blue dye. *Optik* 183:691–697. <https://doi.org/10.1016/j.ijleo.2019.02.081>
- Lin Y, Lu C, Wei C (2019) Microstructure and photocatalytic performance of BiVO₄ prepared by hydrothermal method. *J Alloy Compd* 781:56–63. <https://doi.org/10.1016/j.jallcom.2018.12.071>
- Liu Y, Sun L, Wu J, Fang T, Cai R, Wei A (2015) Preparation and photocatalytic activity of ZnO/Fe₂O₃ nanotube composites. *Mater Sci Eng B Solid-State Mater Adv Technol* 194:9–13. <https://doi.org/10.1016/j.mseb.2014.12.021>
- Magdalane CM, Kaviyarasu K, Arularasu MV, Kanimozhi K, Ramalingam G (2019) Structural and morphological properties of Co₃O₄ nanostructures: Investigation of low temperature oxidation for photocatalytic application for waste water treatment. *Surf Interfaces* 17:100369. <https://doi.org/10.1016/j.surf.2019.100369>
- Mahmoodi NM, Abdi J, Oveisi M, Alinia Asli M, Vossoughi M (2018) Metal-organic framework (MIL-100 (Fe)): synthesis, detailed photocatalytic dye degradation ability in colored textile wastewater and recycling. *Mater Res Bull* 100(2010):357–366. <https://doi.org/10.1016/j.matresbull.2017.12.033>
- Makropoulou T, Kortidis I, Davididou K, Motaung DE, Chatzisyseon E (2020) Photocatalytic facile ZnO nanostructures for the elimination of the antibiotic sulfamethoxazole in water. *J Water Process Eng* 36:101299. <https://doi.org/10.1016/j.jwpe.2020.101299>
- Martino M, Ruocco C, Meloni E, Pullumbi P, Palma V (2021) Main hydrogen production processes: an overview. *Catalysts* 11(5). <https://doi.org/10.3390/catal11050547>
- Mehmood A, Khan FSA, Mubarak NM, Tan YH, Karri RR, Khalid M, Walvekar R, Abdullah EC, Nizamuddin S, Mazari SA (2021) Magnetic nanocomposites for sustainable water purification—a comprehensive review. *Environ Sci Pollut Res* 28(16):19563–19588. <https://doi.org/10.1007/s11356-021-12589-3>
- Mesa JJM, Bolivar LGA, Alfonso H, Sarmiento R, Giovanna E, Martínez Á, Páez CJ, Lara MA, Antonio J, Santos N, Hidalgo C (2018) Urban wastewater treatment by using Ag/ZnO and Pt/TiO₂ photocatalysts
- Mesones S, Mena E, López Muñoz MJ, Adán C, Marugán J (2020) Synergistic and antagonistic effects in the photoelectrocatalytic disinfection of water with TiO₂ supported on activated carbon as a bipolar electrode in a novel 3D photoelectrochemical reactor. *Sep Purif Technol* 247:117002. <https://doi.org/10.1016/j.seppur.2020.117002>

- Mian MM, Liu G (2019) Sewage sludge-derived TiO₂/Fe/Fe₃C-biochar composite as an efficient heterogeneous catalyst for degradation of methylene blue. *Chemosphere* 215:101–114. <https://doi.org/10.1016/j.chemosphere.2018.10.027>
- Motahari F, Mozdianfard MR, Soofivand F, Salavati-Niasari M (2014) NiO nanostructures: synthesis, characterization and photocatalyst application in dye wastewater treatment. *RSC Adv* 4(53):27654–27660. <https://doi.org/10.1039/c4ra02697g>
- Nasirian M, Lin YP, Bustillo-Lecompte CF, Mehrvar M (2018) Enhancement of photocatalytic activity of titanium dioxide using non-metal doping methods under visible light: a review. *Int J Environ Sci Technol* 15(9):2009–2032. <https://doi.org/10.1007/s13762-017-1618-2>
- Nasirian M, Mehrvar M (2018) Photocatalytic degradation of aqueous Methyl Orange using nitrogen-doped TiO₂ photocatalyst prepared by novel method of ultraviolet-assisted thermal synthesis. *J Environ Sci (China)* 66:81–93. <https://doi.org/10.1016/j.jes.2017.05.032>
- Ng KH, Chen K, Cheng CK, Vo DVN (2021) Elimination of energy-consuming mechanical stirring: development of auto-suspending ZnO-based photocatalyst for organic wastewater treatment. *J Hazard Mater* 409(August):124532. <https://doi.org/10.1016/j.jhazmat.2020.124532>
- Nie Q, Yang L, Cao C, Zeng Y, Wang G, Wang C, Lin S (2017) Interface optimization of ZnO nanorod/CdS quantum dots heterostructure by a facile two-step low-temperature thermal treatment for improved photoelectrochemical water splitting. *Chem Eng J* 325:151–159. <https://doi.org/10.1016/j.cej.2017.05.021>
- Nordin N, Ho LN, Ong SA, Ibrahim AH, Abdul Rani AL, Lee SL, Ong YP (2020) Hydroxyl radical formation in the hybrid system of photocatalytic fuel cell and peroxi-coagulation process affected by iron plate and UV light. *Chemosphere* 244:125459. <https://doi.org/10.1016/j.chemosphere.2019.125459>
- Nunes D, Pimentel A, Santos L, Barquinha P, Pereira L, Fortunato E, Martins R (2019) Synthesis, design, and morphology of metal oxide nanostructures. In *Met Oxide Nanostructures*. <https://doi.org/10.1016/b978-0-12-811512-1.00002-3>
- Orimolade BO, Arotiba OA (2020) Bismuth vanadate in photoelectrocatalytic water treatment systems for the degradation of organics : a review on recent trends. *J Electroanal Chem* 878:114724. <https://doi.org/10.1016/j.jelechem.2020.114724>
- Palanisamy B, Babu CM, Sundaravel B, Anandan S, Murugesan V (2013) Sol-gel synthesis of mesoporous mixed Fe₂O₃/TiO₂ photocatalyst: application for degradation of 4-chlorophenol. *J Hazard Mater* 252–253:233–242. <https://doi.org/10.1016/j.jhazmat.2013.02.060>
- Pan L, Liu X, Sun Z, Sun CQ (2013) Nanophotocatalysts via microwave-assisted solution-phase synthesis for efficient photocatalysis. *J Mater Chem A* 1(29):8299–8326. <https://doi.org/10.1039/c3ta10981j>
- Phuruangrat A, Dumrongrojthanath P, Ekthammathat N, Thongtem S, Thongtem T (2014) Light-driven photocatalytic properties of Bi₂WO₆ nanoplates
- Radha KV, Sirisha K (2018) Electrochemical oxidation processes. *Adv Oxid Process Wastewater Treat Emerg Green Chem Technol* 359–373. <https://doi.org/10.1016/B978-0-12-810499-6.00011-5>
- Rafique M, Tahir R, Gillani SSA, Tahir MB, Shakil M, Iqbal T, Abdellahi MO (2020) Plant-mediated green synthesis of zinc oxide nanoparticles from *Syzygium Cumini* for seed germination and wastewater purification. *Int J Environ Anal Chem* 00(00):1–16. <https://doi.org/10.1080/03067319.2020.1715379>
- Rajasulochana P (2016) Comparison on efficiency of various techniques in treatment of waste and sewage water—a comprehensive review. *Resour-Effic Technol*. <https://doi.org/10.1016/j.refitt.2016.09.004>
- Rajkumar R, Ezhumalai G, Gnanadesigan M (2021) A green approach for the synthesis of silver nanoparticles by *Chlorella vulgaris* and its application in photocatalytic dye degradation activity. *Environ Technol Innov* 21:101282. <https://doi.org/10.1016/j.eti.2020.101282>
- Regulacio MD, Han MY (2016) Multinary I-III-VI₂ and I₂-II-IV-VI₄ semiconductor nanostructures for photocatalytic applications. *Acc Chem Res* 49(3):511–519. <https://doi.org/10.1021/acs.accounts.5b00535>

- Rioja-Cabanillas A, Valdesueiro D, Fernández-Ibáñez P, Byrne JA (2021) Hydrogen from wastewater by photocatalytic and photoelectrochemical treatment. *J Phys Energy* 3(1). <https://doi.org/10.1088/2515-7655/abceab>
- Saranya M, Santhosh C, Ramachandran R, Kollu P, Saravanan P, Vinoba M, Jeong SK, Grace AN (2014) Hydrothermal growth of CuS nanostructures and its photocatalytic properties. *Powder Technol* 252:25–32. <https://doi.org/10.1016/j.powtec.2013.10.031>
- Senobari S, Nezamzadeh-ejehieh A (2018a) A p-n junction NiO-CdS nanoparticles with enhanced photocatalytic activity: a response surface methodology study. *J Mol Liq*. <https://doi.org/10.1016/j.molliq.2018a.02.096>
- Senobari S, Nezamzadeh-ejehieh A (2018b) *Of Iran. J Mol Liq*. <https://doi.org/10.1016/j.molliq.2018b.04.028>
- Shen S, Chen J, Wang M, Sheng X, Chen X, Feng X, Mao SS (2018) Progress in materials science titanium dioxide nanostructures for photoelectrochemical applications. *Prog Mater Sci* 98(May):299–385. <https://doi.org/10.1016/j.pmatsci.2018.07.006>
- Shukla P (2020) Microbial nanotechnology for bioremediation of industrial wastewater, vol 11(November). <https://doi.org/10.3389/fmicb.2020.590631>
- Singh VP, Sandeep K, Kushwaha HS, Powar S, Vaish R (2018) Photocatalytic, hydrophobic and antimicrobial characteristics of ZnO nano needle embedded cement composites. *Constr Build Mater* 158:285–294. <https://doi.org/10.1016/j.conbuildmat.2017.10.035>
- Stassen I, Styles M, Grecni G, Van Gorp H, Vanderlinden W, De Feyter S, Falcaro P, De Vos D, Vereecken P, Ameloot R (2016) Chemical vapour deposition of zeolitic imidazolate framework thin films. *Nat Mater* 15(3):304–310. <https://doi.org/10.1038/nmat4509>
- Su Z, Zhang L, Jiang F, Hong M (2013) Formation of crystalline TiO₂ by anodic oxidation of titanium. *Prog Nat Sci Mater Int* 23(3):294–301. <https://doi.org/10.1016/j.pnsc.2013.04.004>
- Tahir MB, Nabi G, Rafique M, Khalid NR (2017) Nanostructured-based WO₃ photocatalysts: recent development, activity enhancement, perspectives and applications for wastewater treatment. *Int J Environ Sci Technol* 14(11):2519–2542. <https://doi.org/10.1007/s13762-017-1394-z>
- Tahir MB, Nabi G, Khalid NR (2018) Enhanced photocatalytic performance of visible-light active graphene-WO₃ nanostructures for hydrogen production. *Mater Sci Semicond Process* 84(April):36–41. <https://doi.org/10.1016/j.mssp.2018.05.006>
- Tobaldi DM, Pullar RC, Gualtieri AF, Seabra MP, Labrincha JA (2013) Sol-gel synthesis, characterization and photocatalytic activity of pure, W-, Ag- and W/Ag co-doped TiO₂ nanopowders. *Chem Eng J* 214:364–375. <https://doi.org/10.1016/j.cej.2012.11.018>
- Vela N, Calín M, Yáñez-Gascón MJ, Garrido I, Pérez-Lucas G, Fenoll J, Navarro S (2018) Photocatalytic oxidation of six endocrine disruptor chemicals in wastewater using ZnO at pilot plant scale under natural sunlight. *Environ Sci Pollut Res* 25(35):34995–35007. <https://doi.org/10.1007/s11356-018-1716-9>
- Venkata C, Raghava K, Shetti NP, Shim J, Aminabhavi TM, Dionysiou DD (2019) Science direct hetero-nanostructured metal oxide-based hybrid photocatalysts for enhanced photoelectrochemical water splitting e a review. *Int J Hydrog Energy*. <https://doi.org/10.1016/j.ijhydene.2019.02.109>
- Vikrant K, Kim KH, Deep A (2019) Photocatalytic mineralization of hydrogen sulfide as a dual-phase technique for hydrogen production and environmental remediation. *Appl Catal B: Environ* 259(July):118025. <https://doi.org/10.1016/j.apcatb.2019.118025>
- Wang D, Jia F, Wang H, Chen F, Fang Y, Dong W, Zeng G, Li X, Yang Q, Yuan X (2018a) Simultaneously efficient adsorption and photocatalytic degradation of tetracycline by Fe-based MOFs. *J Colloid Interface Sci* 519:273–284. <https://doi.org/10.1016/j.jcis.2018.02.067>
- Wang J, Chen R, Xiang L, Komarneni S (2018b) Synthesis, properties and applications of ZnO nanomaterials with oxygen vacancies: a review. *Ceram Int* 44(7):7357–7377. <https://doi.org/10.1016/j.ceramint.2018.02.013>
- Wang M, Wang G, Sun Z, Zhang Y, Xu D (2020a) Review of renewable energy-based hydrogen production processes for sustainable energy innovation. *Glob Energy Interconnect* 2(5):436–443. <https://doi.org/10.1016/j.gloei.2019.11.019>

- Wang X, Wu Q, Ma H, Ma C, Yu Z, Fu Y, Dong X (2019) Fabrication of PbO₂ tipped CO₃O₄ nanowires for efficient photoelectrochemical decolorization of dye (reactive brilliant blue KN-R) wastewater. *Sol Energy Mater Sol Cells* 191(1):381–388. <https://doi.org/10.1016/j.solmat.2018.12.005>
- Wang Y, Jiang T, Meng D, Yang J, Li Y, Ma Q, Han J (2014) Fabrication of nanostructured CuO films by electrodeposition and their photocatalytic properties. *Appl Surf Sci* 317:414–421. <https://doi.org/10.1016/j.apsusc.2014.08.144>
- Wang Z, Niu J, Xu Y, Wang L, Wang H, Liu H (2020b) Effects of AuCuB catalysts with porous nanostructures on electrosynthesis of ammonia. *ACS Sustain Chem Eng* 8(33):12588–12594. <https://doi.org/10.1021/acssuschemeng.0c03970>
- Weng Y, Li J, Ding X, Wang B, Dai S, Zhou Y, Pang R, Zhao Y, Xu H, Tian B, Hua Y (2020) Functionalized gold and Silver bimetallic nanoparticles using *Deinococcus radiodurans* protein extract mediate degradation of toxic dye malachite green. *Int J Nanomed* 15:1823–1835. <https://doi.org/10.2147/IJN.S236683>
- Worrall SD, Bissett MA, Hill PI, Rooney AP, Haigh SJ, Attfield MP, Dryfe RAW (2016) Metal-organic framework templated electrodeposition of functional gold nanostructures. *Electrochim Acta* 222:361–369. <https://doi.org/10.1016/j.electacta.2016.10.187>
- Xiao S, Zhang D, Pan D, Zhu W, Liu P, Cai Y, Li G, Li H (2019) A chloroplast structured photocatalyst enabled by microwave synthesis. *Nat Commun* 10(1):1–10. <https://doi.org/10.1038/s41467-019-09509-y>
- Yang C, Dong W, Cui G, Zhao Y, Shi X (2017) *Electrochimica Acta* Enhanced photocatalytic activity of PANI/TiO₂ due to their photosensitization-synergetic effect. *Electrochim Acta* 247:486–495. <https://doi.org/10.1016/j.electacta.2017.07.037>
- Zhang Q, Ma L, Shao M, Huang J, Ding M, Deng X, Wei X, Xu X (2014) Anodic oxidation synthesis of one-dimensional TiO₂ nanostructures for photocatalytic and field emission properties
- Zhu D, Zhou Q (2019) Environmental nanotechnology, monitoring & management action and mechanism of semiconductor photocatalysis on degradation of organic pollutants in water treatment : a review. *Environ Nanotechnol, Monit & Manag* 12(September):100255. <https://doi.org/10.1016/j.enmm.2019.100255>
- Zinatloo-Ajabshir S, Baladi M, Amiri O, Salavati-Niasari M (2020) Sonochemical synthesis and characterization of silver tungstate nanostructures as visible-light-driven photocatalyst for wastewater treatment. *Sep Purif Technol* 248(February):117062. <https://doi.org/10.1016/j.seppur.2020.117062>

Solar Energy in Water Treatment Processes—An Overview



Ashish Unnarkat, Ayush Bhavsar, Samyak Ostwal, Pancham Vashi,
and Swapnil Dharaskar

Abstract Water remains at the centre of human survival on the planet earth. Water availability and its consumption pattern in the world have drastically changed over the past few decades. The rising population and changes in the standard of living have put stress on the water bodies, and major countries around the globe are on the verge of facing serious water scarcity. Earth has an abundance of water but is not in usable form. It demands technologies that can provide fresh water for the people but must be economical, sustainable and less energy-intensive. Desalination is the solution, but the conventional techniques are energy-intensive processes and not eco-friendly. Solar energy has come out as a sustainable and greener energy source for carrying out desalination. Solar energy for desalination has been widely explored in recent times. Another major problem with developing countries is handling water-borne diseases, which lead to major health issues and fatalities. Solar energy comes to the rescue here, and its application for the disinfection of water will cater to the need for safe water, improving community health and providing a sustainable solution. The chapter presents a review on the application of solar energy in two broader domains of water treatment; (a) water desalination and (b) water disinfection. The chapter discusses the different types of solar integrated desalination technologies with their uniqueness and limitations. Recent developments for the most common desalination technologies of multi-stage flash (MSF), vapour compression (VC), multi-effect distillation (MED), and reverse osmosis (RO), and electro-dialysis (ED) are discussed. Solar energy-based technologies will prove to be an alternative to the current technologies in water treatment and disinfection, the price will remain the concern, but this will be overcome with the efforts and technological improvement in the field. Solar energy and its utilization in the water treatment process make its way as the potential solution for all safe and clean drinking water.

A. Unnarkat (✉) · A. Bhavsar · S. Ostwal · P. Vashi · S. Dharaskar
Department of Chemical Engineering, School of Technology, Pandit Deendayal Energy
University, Raisan, Gandhinagar, Gujarat 382426, India
e-mail: ashish.unnarkat@sot.pdpu.ac.in

S. Dharaskar
e-mail: Swapnil.dharaskar@sot.pdpu.ac.in

Keywords Desalination · Disinfection · Solar energy · Water treatment · Green energy · Sustainability

1 Introduction

1.1 *Water Scarcity and Treatment*

As the population of the world is on the rise so does the demand for fresh water. With the current climate change scenario across the globe and the deteriorating environmental conditions, water scarcity will pose a serious challenge to the survival of human race on the planet (Seckler et al. 1999). In the regions of Asia and Middle East, the ground water level is falling at an alarming rate and the water table is hugely disturbed. There is an urgent need to focus the attention of both professionals and policy makers to find sustainable solutions so as to fulfil the demand of fresh water for the growing population. Renewable energies like solar energy are widely explored as the primary source of energy in the water treatment process. Solar has been a clean and green energy solution and is available in abundance from the nature. Currently solar energy is in used two domains of water treatment, one being desalination of the sea water and second being water disinfection. The solar power driven water treatment processes has come as a novel and sustainable solution to address the issue of fresh and safe water for all (Pugsley et al. 2016; Chandrashekara and Yadav 2017; Ullah and Rasul 2019; Curto et al. 2021). Currently, the solar based water treatment processes are in great demand but the real time applications and the economics gives a major setback to the process. However, the solar based process are promising and can be viable for the large scale production and the water costs will then be significantly reduced. The efforts in the direction will make the technology more durable and available for the societal benefits (Foran 2007; Pugsley et al. 2016; Curto et al. 2021).

1.2 *Conventional Water Treatment Techniques for Desalination and Disinfection*

Natural sources of water are getting polluted with rapid industrialization and human activities. The increased demand and overuse of water in the urban areas have worsened the situation of the available water resources, and the conventional water treatment plants are overburdened. Over the decades, the conventional treatment included methods like coagulation-flocculation, sand filtration, sedimentation, ozonation and chlorine-based disinfection to gain freshwater (Sarkar et al. 2007). But in recent times, the water bodies are getting contaminated with industrial waste and toxins from human activities, the water quality is abrupt, making the conventional plants inefficient for quality assurance. The significant drop in feed water quality has impacted

the overall process. In the absence of a strong environmental protection framework and lawful practices, the contamination of water bodies is continuous in developing and underdeveloped nations. Several drawbacks or hardships in traditional water treatment plants are mentioned below:

- a. Pollution of water bodies by industries which consists of pharmaceutical wastes, toxins, chemicals and fertilizers used in agro-based industries are generally not affected and completely removed by the traditional and conventional methods of water treatment, and these require advanced techniques for the remediation (Xia et al. 2004; Radjenović et al. 2008).
- b. Separate biological treatment for removing the microorganism and bacteria's is to be incorporated. The case of the Mery-sur-Oise water treatment plant in France and the Cheng Ching Lake Water Works conventional water treatment plant are among those examples where algae and weeds were not removed from the water and caused several health issues (Yeh et al. 2000; Cyna et al. 2002).
- c. Water produced from traditional treatment plants may be too hard and must be softened further. Traditional softening processes such as cold and hot lime softening and pellet softening require intensive consumption of lime and acids and will produce large quantities of sludge (Bergman 1995).
- d. Chlorination methods that are used for disinfection remove viruses and bacteria, but prolonged exposure to the chlorinated water has severe health effects.

The conventional techniques for the desalination of water is through reverse osmosis (RO) desalination plants. However, the performance of RO membrane and its fouling resistance remains a challenging feature that deters its efficiency for the treatment. The water resources generally used for the desalination plants is sea water or blackish water. Seawater is generally rich in contaminants such as colloidal particulates, mineral salts, high microorganisms, natural organic material, oil and grease and hydrocarbons that require extensive pre-treatment plans (Bohn et al. 2009; Shekarchi and Shahnia 2019). If the pre-treatment process is not complete then these contaminants goes to the membrane unit and blocks the flow through the membrane and decrease the overall rejection. The pre-treatment processes that are widely preferred for the sea water RO plants is coagulation, flocculation, sedimentation, pH adjustment, chlorination, scale inhibition, dual media filter and dissolved air flotation, these are the conventional primary filtration methods employed in most of the water treatment plants. The pre-treatment provides the required feed water for the RO system though the parameters has to be tuned with the sea water quality (Amiri and Samiei 2007). The inconsistency in the quality of water, its flowrate, susceptibility of membranes to biofouling attacks and scaling are some of the shortcoming of the RO process that makes it slightly inefficient.

1.3 Application of Renewable Energy in Water Treatment

The use of domestic sources of renewable energy together with the implementation of energy-efficient technologies pave the way to sustainable solutions and overcome the dependency on conventional energy sources. These options would help curb the rise of greenhouse gas emissions and make countries less dependent on energy imports and face the repercussions of fossil fuel price fluctuations. The technological advances in the renewable energy sector will improve the economics. The renewable sources are available in abundance and will not face extinction as in the case of fossil fuels. This means that it would remain for the generations to come (Chandrashekara and Yadav 2017; Alnaimat et al. 2018; Zhang et al. 2018).

Renewable energy and energy-efficient technologies for water desalination can provide ideal solutions for large-scale desalination and treatment plants in both off-grid and on-grid areas. A large amount of energy that is required for the desalination can be provided from locally available renewable energy resources independent of whether they are directly produced and applied (e.g., solar thermal, geothermal direct use) or indirectly applied through an interim production of electricity (e.g., solar photovoltaic, electricity generation from wind or geothermal). This electricity can be used to power the desalination units. Coupling renewable energy with desalination technologies paves the way for meeting the demand for fresh water. Solar assisted water desalination and disinfection technologies and their classification if provided in Fig. 1.

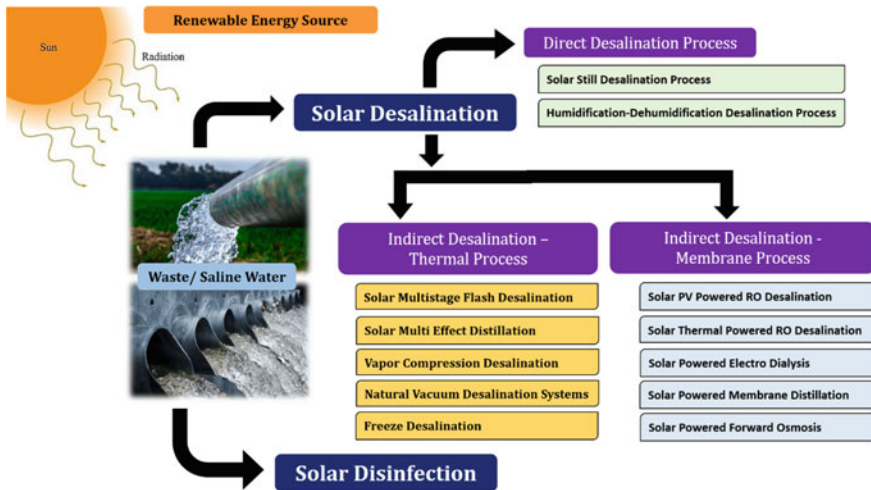


Fig. 1 Solar assisted water treatment

Water disinfection predominantly kills or deactivates the pathogens or microorganisms in the water. Mostly chlorine-based disinfections are prevailing in practice that is not eco-friendly. Chemical-based disinfection has environmental consequences and also health effects. Ozone is another method that is employed in disinfection; however, it's not an economically viable option on a larger application. Boiling is considered to be one of the most prevalent household methods for disinfection. This option needs high energy, and the generation itself puts the load on fossil fuels and ultimately to the GHG emissions. Hence, it can be inferred that using heat energy or other conventional methods for water disinfection is costly and degrades the environment to a great extent. Also, it rather toxifies the water (carcinogenic compound formation in chlorination method). Renewable sources such as solar energy give the best outputs in such cases. If used efficiently, it reduces the cost and is completely safe and environment friendly. Renewable energy-based water disinfection comes as the valued solution (Richards and Schäfer 2010).

1.4 Scope of Chapter

Desalination of the sea water to get the fresh drinkable water is the dire need of an hour with the water scarcity and environmental concerns are haunting the world with rising natural calamities and climate change. UNO has already alarmed regarding the same and said that about 1800 million people across the globe will face severe water scarcity in the coming decade (WHO and UNICEF 200AD 2000; Fewtrell 2014). However, the desalination process is an energy intensive process which will further increase the fossil fuel consumption that will add to GHG emissions. Salts easily dissolves in water and the ionic bonds break and the atoms are then surrounded by the water molecules around it forming a homogeneous solution. Energy and the technology to desalinate water are both expensive, and this means that desalinating water can be pretty costly. To remove salts from this solution is tough and requires a lot of energy. To make the desalination process green and sustainable it is advised to go for renewable sources of energy. The desalination technologies coupled with renewable energy sources will prove to be the sustainable solution.

In the case of water disinfection process the traditional methods become inefficient in certain cases and if solar energy is used instead of them, it may become the key to the lock of all problems. There are millions of cases reported of diseases like diarrhoea primarily due to unsafe and impure water. Apart, millions die every year due to lack of access to safe and clean water. The prevailing conventional methods of disinfection are ineffective over economic and environment reasons. Chemical treatment, heat pasteurization, and filtration, require facilities, materials, and fuel that may not be readily available or feasible at all the locations. Renewable energy sources provides an alternative treatment option using solar energy, to inactivate pathogens through pasteurization and radiation effects. In this chapter we have discussions about solar energy both in the process of desalination as well as in the process of

disinfection which could help researchers and experts to get all the required knowledge in this domain in a single content and further explore the research avenues. The chapter provides the perspectives on both the process and allied challenges in the domain (Abdel-Rehim and Lasheen 2005; Bohn et al. 2009; Shatat et al. 2013; Chandrashekara and Yadav 2017; Zhang et al. 2018).

2 Desalination

Solar energy based thermal desalination has been one of the novel approaches to applying renewable energy for getting fresh water. Solar energy-based desalination can either be categorized as a direct system where the solar energy is used directly to produce distillate in the solar collector or an indirect system where the solar system is combined with the other conventional desalination techniques; Multistage flash desalination, Vapor compression, Reverse osmosis, Membrane distillation and Electro dialysis. Solar energy is collected in the collectors while this is used in the desalination systems. Comparatively, the direct solar desalination needs larger areas and has less production rate than obtained with the indirect technologies. Both the technologies are discussed in the following paragraphs.

2.1 *Direct Desalination Systems*

2.1.1 **Solar Still Desalination Process**

Solar still method for desalination is one of the most economical and easiest ways to get fresh water from the sea feed water. In a solar still, the radiation directly falls on the sea feed water and provide the needed energy through solar radiation to evaporate the portion of feed water from the basin. The evaporated water gets collected at the top of the basin and eventually trickles down, condensing to be gathered as freshwater (Qiblawey and Banat 2008; Shekarchi and Shahnia 2019; Vigneswaran et al. 2019; Abd Elbar and Hassan 2020).

There are two different techniques employed in solar still water desalination. The first one employs the sun-tracking technique. In case the solar still rotates to capture the maximum amount of radiation. The possibility of receiving higher solar radiation increases with the movement of the solar still as it tracks the sun, and it leads towards higher production of fresh water. The second technique employs side mirrors; in this technique, the energy received from the sun is low; however, the presence of side mirrors causes multiple reflections and thereby secrete the energy in the still to a higher amount. Eventually, the higher energy causes higher evaporation and production rate (Kabeel and El-Said 2013, 2014).

Sohani et al. (2021) worked on innovative designs of solar still and has reported in-depth technical and economic analysis for the systems. They have investigated

the prevalent techniques, sun tracking and using side mirrors, and eight case studies were considered for the experimental studies. They have monitored multiple components like; water temperature in the basin, fresh water production, cumulative yield, produced distillate, efficiency, and cost per litre. The set-up consisted of a solar still and a flat plate solar collector. These are connected with the help of the pipeline. There were two different reservoirs, one reservoir for the salty water attached to the solar still and another for water above the solar collector. Even there was a space for accumulation of the fresh water. The black colour was painted at the bottom of the solar still, which helped absorb a higher level of solar radiation. The experimentation concluded that when both techniques were applied together, the peak water temperature increased by 7.6 °C in the passive mode. Also, the production rates were said to increase by 43.2% for passive mode and 34.3% when in active mode. The overall cost per litre of water is reduced with the employed techniques compared to the conventional systems (Sohani et al. 2021).

2.1.2 Humidification-Dehumidification Desalination Process

Solar humidification-dehumidification desalination systems have two different water and air cycles that go through the humidifier and dehumidifier sections. The feedwater goes through the dehumidifier and then to the humidifier column in the water cycle. The concentrated brine solution obtained after the evaporation of the feed water leaves the humidifier. The cycle of air and water between the two-column converts the feed water into fresh water. There can be an open or closed cycle for both water as well for air. The configurations and design of heaters, humidifiers, and dehumidifiers make the primary elements of the system (Shekarchi and Shahnia 2019).

Yamali et al. (2008) reported a solar desalination system using the humidification-dehumidification process and investigated the influence on operational parameters. The reported setup of humidification-dehumidification processes studied comprised of a double-pass flat plate solar air heater, a humidifier, a water storage tank and a dehumidifying exchanger. Figure 2 shows the experimental setup and the thermocouple locations.

The desalination process with the humidification-dehumidification process worked in three major steps. The ambient air passes through the double pass flat plate solar heater and gets preheated in the first part. The air gets preheated in the first pass, and the preheated air is completely heated in the second pass. The heated air then goes to the humidifier, which gets humidified by the salt water from the storage tank. The humidifier consisted of multiple pads and a sprayer at the top. The water trickles down from the humidifier and goes back to the sump. The pump attached to the bottom of the storage tank supplies the water to the humidifier. The remaining salt water from the humidifier goes back to storage and is recycled. Lastly, the humidified air goes into the dehumidifier, where the condensation occurs, and the fresh water is collected (Yamali and Solmus 2008).

In a similar work, Fath and Ghazy (2002) studied the performance of solar desalination using the humidification-dehumidification processes. The desalination system

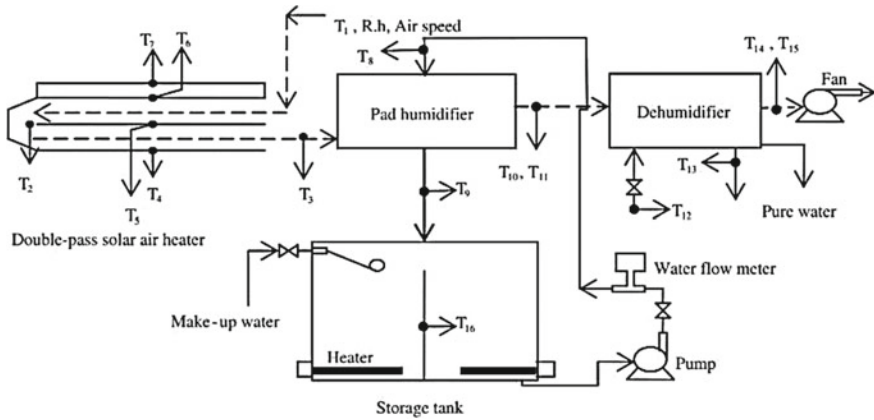


Fig. 2 Experimental set-up and thermocouple locations (Yamali and Solmus 2008)

used for the study consisted of a humidifier, dehumidifier, a circulating air-driving component, and a solar air heater. Different factors (environment, design and operational) affect the productivity of the desalination process. The environmental parameters were solar intensity, ambient temperature and wind speed, while design parameters included the solar heater insulation and the effectiveness of humidifier and dehumidifier. The operational parameters of the systems were water feed rate, air circulation rate and temperature. The increase in solar intensity and the ambient temperature improves productivity, while an increase in wind speed reduces the system productivity. The airflow rate improves the productivity only till 0.7 kg/s, beyond which no effect was observed. Overall it has been concluded that the system productivity is significantly influenced by the efficiency of the solar heater (Fathb and Ghazy 2002).

2.2 Indirect Desalination Systems—Thermal Process

Indirect solar desalination methods involves (1) collection of solar energy by using the conventional solar converting system and then (2) link it to a conventional desalination system. The electromagnetic solar radiation are converted to electricity using photovoltaic modules which then powers the desalination process. Desalination can be accomplished using multistage flash distillation, multiple effect evaporation, and/or vapor compression (Buros 2000).

2.2.1 Solar Multistage Flash Desalination

In a typical multi-stage flash desalination unit (MSF), the pressure in each unit was reduced steadily so that the feed water gets boiled repeatedly without adding more heat when it goes from one stage to another. MSF has been in use traditionally across the major regions around the globe, especially in the middle-east. In a multistage flash, desalination water is heated using the waste heat, and then it is flashed in different units by varying the saturation pressure. One such plant of 10,000 L capacity was installed and tested in 1983 at Safat, Kuwait. The detailed performance of this system is presented in the work by Moustafa et al. (1985). Solar multistage flash desalination will hold the major capital cost for solar energy collection and storage, including the solar panel collectors, PV modules, battery storage, and later for the desalination unit itself.

2.2.2 Solar Multi-effect Distillation

Preferably solar thermal plants are based on multi effect desalination for the reason being economical on energy consumption and has lower top brine temperature (TBT). Top brine temperature is an important part of the solar integrated techniques and regulating the TBT is essential to avoid the unstable operation. In a typical operation of multi effect distillation, water evaporates on the outside of the heated tubes in a single effect maintained at its saturation pressure. The evaporated water then moves on the next effect for additional vapor production. Sharaf et al. has reported the exergy and thermo-economic analysis for solar energy with different configurations of multi effect distillation desalination system. The comparison of multiple systems is presented for a case of 100 m³/day of product distillate (El-Nashar and Samad 1998; Sharaf et al. 2011).

2.2.3 Vapor Compression Desalination

In a vapour compression desalination system, the feed water is heated by an external source, and then it is flashed. The vapours derived from the flash are then sent for compression, either by mechanical-vapour compression or thermos-vapour compression leading to higher condensation pressure and higher temperature. The compressed vapours are then deployed for heating in the subsequent stages. Helal and Al-Malek (2006) has given a detailed design of a solar-assisted mechanical vapour compression desalination unit specific to the remote areas of UAE. Thermo-vapor compressor-assisted MED has a lower specific power and total water production cost than the mechanical vapour-assisted MED (Helal and Al-Malek 2006).

2.2.4 Natural Vacuum Desalination Systems

Using the vacuum pump, vacuum desalination systems employ a unique technique of producing fresh water vapours from the saline water source at low temperatures. However, the system needs higher energy to produce a vacuum. The consumption can be reduced by naturally creating a vacuum in the flow systems. These systems are more options for small scale applications. Maroo and Goswami (2009) has reported such systems that uses the gravitational force and the atmospheric pressure to create a vacuum naturally. Details presented the theoretical analysis of the single and dual-stage solar-based flash desalination working with a natural vacuum. In a typical two-stage low-temperature natural vacuum desalination system, the vapours formed in the first stage gets condensed in the heat exchanger placed in the second stage. The heat rejected in the process helps vaporise the water in the second stage. However, the vapours from the second stage are condensed using an external condenser. Dual stage water performance was better than that of the single-stage system (Maroo and Goswami 2009).

2.2.5 Freeze Desalination

Freeze desalination is one of the emerging technology that overcomes the limitations of membrane-based and thermal energy-based desalination processes. The freezing desalination system needs to cool down the feed water well below its freezing temperature causing the pure water to form ice crystals. There are three types of freeze desalination naming; direct contact freeze desalination, indirect contact freeze desalination and vacuum-operated freeze desalination (Lu and Xu 2010; Rane and Padiya 2011; Williams et al. 2013).

Direct Contact Freeze Desalination

Desalination by freezing processes is based on the fact that, ice crystals formed by freezing the saline water are basically of pure water. In contradiction to the distillation method, crystallization or the freezing method needs the phase change of water from liquid to solid and hence consumes the latent heat that makes the process energy intensive. In case of direct contact freeze desalination the liquid refrigerant (usually n-butane) is brought in direct contact with the saline feed water in a way that the heat from the saline water is taken up by the refrigerant leaving behind the pure water ice crystals. These ice crystals can be then removed and purified to get the fresh water (Lu and Xu 2010; Williams et al. 2013).

Indirect Contact Freeze Desalination

The indirect contact freezing process contains a wall or a physical barrier separating the seawater and the refrigerant used for cooling. The main difference in indirect freezing compared to direct contact freezing is that the saltwater and the refrigerant do not directly come into contact. Mechanical refrigeration or various other means cause the ice to form on the surface, which has to be then removed. Removing ice

from the heat transfer surface itself is a major drawback of this system (Lu and Xu 2010; Williams et al. 2013).

Vacuum Operated Freeze Desalination

In vacuum operated freeze desalination system, both the operation of evaporation and freezing are performed under vacuum. The feed water enters the system as the mix of ice and brine slurry, and water vapour are drawn out. At the start water is vaporized under high vacuum which in turn has a refrigerating effect that leads to ice crystals formation. These crystal are pure form of water that are melted and/or washed in the separate section. The compression of the vapour and driving the vacuum pump are the major heads of energy requirement for the system (Lu and Xu 2010).

2.2.6 Adsorption Desalination

In a typical arrangement the adsorption desalination system consists of (a) condenser, (b) adsorption beds (silica or zirconia) and (c) evaporator. This is a specific system where the water is having a double distillation effect. At first the adsorption cycle is undertaken by keeping the temperature low in the bed. The vapors from the evaporator are adsorbed in the bed. Secondly the water vapor so adsorbed is removed by increasing the temperature of the bed, this time circulating hot water. The removed vapors are now condensed to get the fresh water. First distillation effect is in the adsorption cycle and second in desorption cycle. Figure 3 gives the schematic of the adsorption desalination system that has two beds working alternate for adsorption and desorption cycle to get fresh water (Wu et al. 2010).

2.3 Indirect Desalination Systems—Membrane Process

2.3.1 Solar PV Powered RO Desalination

Reverse osmosis (RO) remains the demanding and dominating technology for water desalination. RO process needs the feed water to pass through the membrane module at high pressure, which is higher than the osmotic pressure of the membrane. The water passes under high pressure through the membrane module and rejects the salts. The rejection ratio of the salts is as high as 90%, while the water recovery is 50%. The primary attribute of Solar PV assisted RO desalination is a coupling of renewable energy in the operation of the RO desalination system. The membrane modules are prone to fouling and scaling. Sharon and Reddy (2015) has extensively reviewed the literature on Solar PV coupled RO systems that are installed across the globe. The quality of feed water, specifically salinity is the deciding factor for the life of the module and the required maintenance (Qtaishat and Banat 2013).

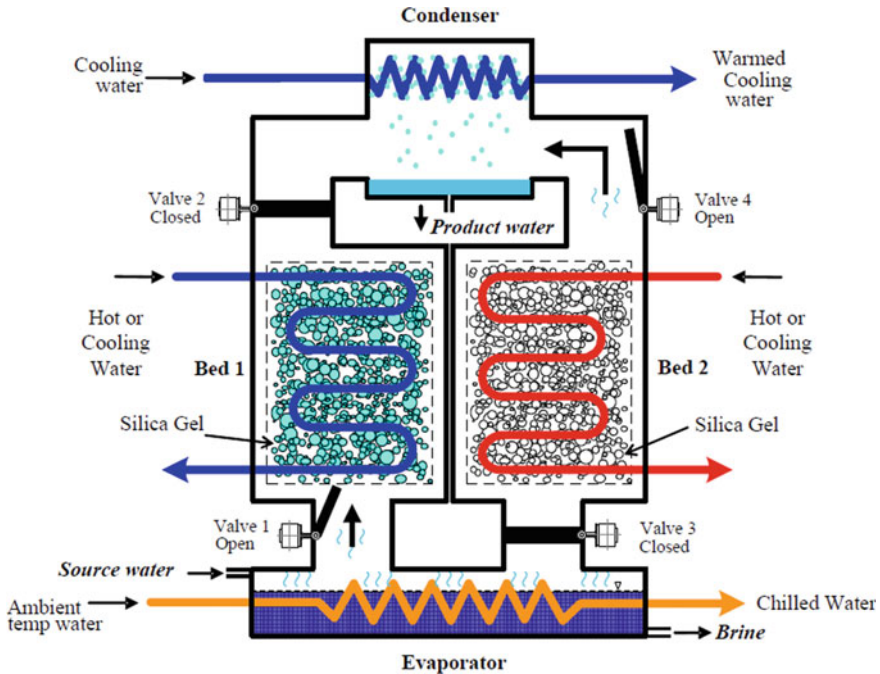


Fig. 3 Adsorption desalination system (Wu et al. 2010)

2.3.2 Solar Thermal Powered RO Desalination

As opposed to the solar PV in case of solar thermal powered RO desalination units, the energy produced by the solar is used to run the Organic Rankine Cycle which is then used to run the Reverse Osmosis unit. Solar thermal powered RO unit can be seen in the Fig. 4. Nafey et al. (2010) has studied on the thermos-economic analysis of solar thermal RO desalination unit where they explored the configurations for energy recovery. The study revealed that the energy recovery units positively reduced the production cost of water by 24% (Nafey et al. 2010; Sharaf et al. 2011).

2.3.3 Solar Powered Electro Dialysis (ED)

Dialysis is the process removing the excess waste. In case, salts are removed in the electro dialysis (ED) unit from the sea feed water. The ED unit comprise of compartments that are separated by cation and anion exchange membranes. These compartments are filled with the saline water. Under the influence of current across the membranes the positive ions are attracted towards the cation exchange membranes

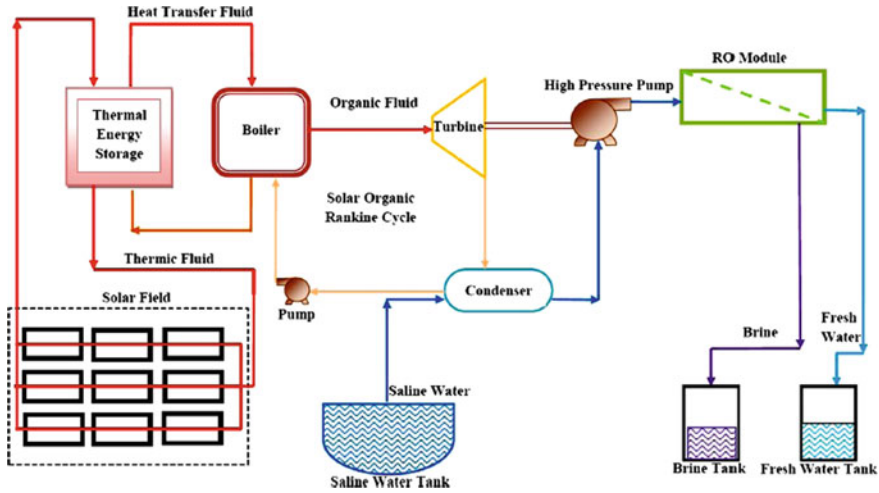


Fig. 4 Solar organic rankine cycle powered RO unit (Sharon and Reddy 2015)

while negative ions are attracted towards the anion exchange membrane. The accumulated ions across the membranes are removed leaving behind fresh water (Kuroda et al. 1987).

2.3.4 Solar Powered Membrane Distillation

Another set of membrane units that are coupled with solar is membrane distillation. In this process, water-vapour are only allowed to pass through the porous membrane. The hydrophobic membrane allows the separation due to the vapour pressure differences across the membrane. There are four types of membrane distillation processes: sweeping gas distillation, air gap membrane distillation, vacuum membrane distillation, and direct contact membrane distillation. Porosity, hydrophobicity and low thermal conductivity are the primary desired features for the membranes used in the process (Qtaishat and Banat 2013).

2.3.5 Solar Powered Forward Osmosis (FO)

Forward osmosis is a process in which the solvent molecules from the solution moves through the semi-permeable membrane towards the draw solution that is maintained at higher concentration than the feed solution. The higher osmotic pressure gradient yield high water fluxes and high feed water recoveries. McCutcheon et al. has presented a forward osmosis desalination process using ammonia and carbon dioxide system. The process used ammonium bicarbonate draw solution that extracted the water from a saline feed water across a semi-permeable polymeric

membrane. When the ammonium bicarbonate was moderately heated, it decomposed into ammonia and carbon dioxide gas that were separated and recycled as draw solutes and are left with the fresh product water. It is recommended that the membranes used in forward osmosis should be able to withstand higher internal concentration polarization (McCutcheon et al. 2005).

2.4 Challenges and Perspectives

Desalination is going to be a crucial technology in the coming decade. The advent of solar coupled desalination units has brought new hope to get the process green and sustainable. Table 1 gives the advantages and limitations of the different desalination systems. Solar based desalination technologies provide clean and safe water but come with certain challenges (Greenlee et al. 2009; Ali et al. 2011):

- (1) **Scaling**—Scaling remains the age-old problem dealing with the sea water. The depositions are hard to remove and hinder the overall desalination process. The higher temperature of operation leads to higher scale formation.
- (2) **Membrane Fouling**—Fouling refers to the degradation of the membrane surface by the rejected molecules and impurities from the feed solution. Fouling reduces the flux output, and permeate can be of poor quality.
- (3) **Corrosion**—The thermal process of desalination releases many gases during evaporation/flashing, which is the primary reason for corrosion. The performance of the heat transfer surface is greatly compromised because of corrosion.
- (4) **Brine Disposal**—Desalination units reject highly concentrated saline water. Disposal of this to the oceans or other water bodies severely hamper the marine ecosystem. The higher concentration affects the aquatic flora and fauna.

Solar based desalination is one of the promising technologies for getting freshwater. The efficacy of the units has to be tuned with the local aspects. Any small improvement in efficiency would be a step towards conserving environmental or energy resources. Material science has a lot to explore on the front of reducing corrosion. Research in the domain of corrosion-resistant coating or novel composites will be appreciated. Other domains of renewable energy should also be explored and should be coupled with the desalination unit. It can be wind and or geothermal. These sources can be location specific and should be considered while deploying the desalination technology. Energy is the prime factor of costing in the desalination units. Hence getting local energy solutions and small scale durable desalination units should be looked upon rigorously. Membrane fouling is always a concern; improving the fouling resistance by developing responsive membranes that can have longer is sought topic in water treatment. Desalination is not a perfect technology, and this can have health issues for human beings as well. Desalinated water can be damaging to the digestive system. One has to take due care to have the need mineral content for healthy water for the society. Lastly, it should be survival for all and not survival for

Table 1 Comparing the pros and cons of desalination techniques

Desalination technique	Advantages	Limitations
<i>Direct Desalination Techniques</i>		
Solar Still	<ul style="list-style-type: none"> • Simple setup • Easily deployable • Low cost of construction • Low maintenance cost • High-quality water 	<ul style="list-style-type: none"> • Bulky installation • Small scale production • Lower capacity • High labour cost • High water production cost • Needs large ground space
Solar HDH	<ul style="list-style-type: none"> • Simple • Low operation cost • Low maintenance cost • No need to pre-treatment • No scaling problem • Appropriate for remote areas and small units 	<ul style="list-style-type: none"> • Small scale production capacity • Low capacity • Lower gain to energy used
<i>Indirect Desalination Techniques—Thermal</i>		
Solar multi-stage flash desalination	<ul style="list-style-type: none"> • Suitable for large scale production • Wide quality of feed can be treated • High-quality water is obtained 	<ul style="list-style-type: none"> • High energy consumption • High possibility of Corrosion
Solar multi-effect distillation	<ul style="list-style-type: none"> • Comparatively low energy consumption • Lower temperatures operation possible • No pre-treatment required 	<ul style="list-style-type: none"> • High possibility of Corrosion • High energy consumption
Vapour compression desalination	<ul style="list-style-type: none"> • High efficiency • Low energy consumption • Suitable for low-capacity applications • High-quality water is obtained • Low scale formation and corrosion 	<ul style="list-style-type: none"> • Corrosion of compressor • High initial cost • Higher water production cost
Natural vacuum desalination systems	<ul style="list-style-type: none"> • A low-temperature heat source is sufficient 	<ul style="list-style-type: none"> • High structures are required • Need to removal non-condensable gases formed during evaporation of water
Freeze desalination	<ul style="list-style-type: none"> • The energy required is low • Reduced corrosion and scaling 	<ul style="list-style-type: none"> • Working with ice and water mixture is complex • Equipment is costlier • Freshwater is needed for washing off the salt on the surface of ice crystals before melting

(continued)

Table 1 (continued)

Desalination technique	Advantages	Limitations
Adsorption desalination	<ul style="list-style-type: none"> • Less fouling and corrosion • Less maintenance • High-quality water • Waste heat can be reused 	<ul style="list-style-type: none"> • Energy-intensive • High GHG emissions
<i>Indirect Desalination Techniques—Membrane</i>		
Solar RO	<ul style="list-style-type: none"> • Simple • Low EC • Suitable for very small to large scales • Ideal for remote areas • Permeate water quality with less than 500 ppm 	<ul style="list-style-type: none"> • Feed water quality matters • Needs pre-treatment of water • High-pressure pumps required • Fouling • High cost for unit and maintenance
Solar ED	<ul style="list-style-type: none"> • Operation at lower pressure in comparison to RO • Suitable for SFW with a salinity of less than 5000 ppm • Permeate water quality with less than 600 ppm 	<ul style="list-style-type: none"> • Needs pre-treatment and posttreatment for drinkable water production
Solar MSF	<ul style="list-style-type: none"> • Suitable for medium and large-scale desalination plants • Ideal for cogeneration from waste heat in power plants • No need for pre-treatment of water • Independent of SFW quality • Permeate water quality with less than 10 ppm 	<ul style="list-style-type: none"> • Consumes a high amount of thermal and electrical energies • Needs high top brine temperature (90–110 °C), high capital, and maintenance cost
Solar MED	<ul style="list-style-type: none"> • Suitable for medium and large-scale plants • Ideal for cogeneration from waste heat in power plants • No need for pre-treatment of water • Independent of SFW quality • Lower required top brine temperature (70 °C) • Permeate water quality with less than 10 ppm 	<ul style="list-style-type: none"> • Consumes a high amount of thermal and electrical energies • High capital and maintenance cost

Abbreviations: EC, energy consumption; GOR, gained output ratio; MED, multi-effect distillation; MSF, multi-stage flash; RO, reverse osmosis; SFW, saline feed water; WPC, water production

the fittest. The overall life cycle assessment of the brine and its impact assessment on the marine ecosystem should be taken to understand the effect of technology and move towards sustainability.

3 Solar Disinfection

3.1 *Need and Development of Solar Disinfection*

Consuming contaminated water poses a serious threat to human health worldwide. This is a grave problem specifically in third world countries and SAARC nations wherein healthcare resources and water treatment technologies are scarce. In developing countries, the primary source of water comes through rivers, side streams, ponds and lakes and these are also used for completing all the activities from agriculture to watering cattle to the daily requirements of the human race (WHO and UNICEF 200AD 2000). People in developing nations don't have any alternative sources apart, and the same sources are exploited for getting potable water for consumption. The water bodies are also getting polluted due to wide human activities and industrialization. Wherever the water distribution and treatment infrastructure is scarce, the same streams in the least treated form is used for consumption. The contamination caused seriously affects the health of flora, fauna and human beings. Specifically, children are the ones who are more susceptible to the ill effects of impure water.

Waterborne diseases infections come through a variety of bacteria, viruses and parasites. These come through a large group of causative agents and are followed by parasites and bacteria. Analysing these organisms require expensive analytical methods. However, as an indirect method, it is easier to check the organisms indicating the faecal pollution in the water. These organisms do not always transmit through the water but poor hygiene (Curtis et al. 2000).

Furthermore, secondary contamination of drinking water due to incorrect water storage and usage is frequently observed. Therefore, the need is sought for interventions to improve water quality while enhancing the general ways of hygiene. Waterborne diseases can be transmitted through multiple routes. Figure 5 showcases the possible transmission routes. Diarrhoea is a common problem that is caused by pathogens and easily transmits to humans through person-to-person contact, flies or through inadequate hygiene behaviour (e.g. not washing the hands). Improving hygiene itself has a considerable effect on the population's health. Apart from water treatment and improved water quality is necessary for building strong resistance to infections and curd the transmission (Ise et al. 1994; Swiss Federal Institute for Environmental Science and Technology (EAWAG) 2002).

As per the World Health Organization's evaluation, impure water and scarcity of freshwater supply are the predominant reason for around 80% of all the infectious diseases in the world. Water is essential for the cooling effect as well as excreting the

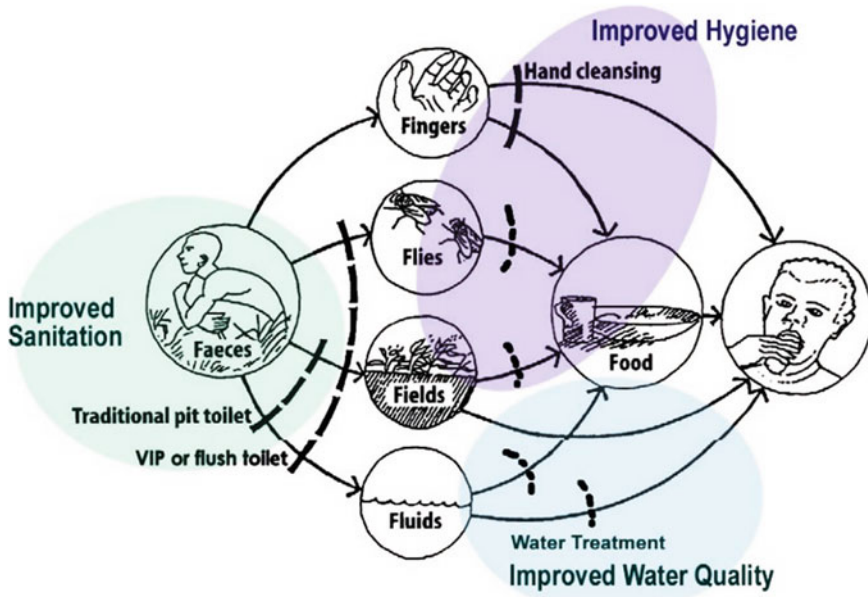


Fig. 5 General cycle showing transmission routes of diseases due to improper hygiene

toxins from the body. As per the United Nations Global Drinking Water Quality Index Development and Sensitivity Analysis Report, microbial load analysis and treatment are crucial factors ensuring the drinking water's safety (Rickwood and Carr 2007). Dissolved salts, alkalinity, toxic metals in water must also be taken for remediation and microbial loads. Photocatalytic degradation, Fenton process and other visible to UV light assisted processes to degrade the water pollutants (Herrera Melián et al. 2000; Rincón and Pulgarin 2004; Rizzo et al. 2014; Vyatskikh et al. 2018). Water bodies around the globe are under stress due to the rise in the population and the demands therein. Water disinfection is one of the essential components to reduce waterborne diseases. The advent of renewable energy-based water disinfection can lead to an economical way of providing safe water for all (Khan et al. 2015).

3.2 Implications of the Solar Disinfection (SODIS) Method

Solar Energy based disinfection popularly called the SODIS method employs the reactor that collects the solar radiation and cleanse the feed water. It is the simplest of water treatment technology that can be readily used at the household level. Primarily SODIS is for reducing the microbial load and improves the quality of drinking water thereby reducing the risk of contracting water borne disease. The quality of disinfection is dependent on the performance of the SODIS-reactor that is dependent

on the area for photon collection and the pathlength that the radiations has to be pass through the water. The solar assisted disinfection reactors are more opt for the isolated locations in emergency situations especially during the times of flooding or earthquake where the access to safe drinking water will be an issue. SODIS bags is a novel approach in the area which can be easily transported and stored. These bags can be made available for the personal usage and can be used for SODIS disinfection. These bags holds about 1–2 L of water (with low turbidity) and is let exposed to the sunlight for a certain time (recommended 6 h) depending on the site and weather conditions. SODIS is the simple and extremely low cost method for improving the microbial quality of drinking water. The method does not stand as the replacement for the access to safe drinking water as it does not ensure to complete remediation of water (Swiss Federal Institute for Environmental Science and Technology (EAWAG) 2002; Amin and Han 2009; Byrne et al. 2011; Verma and Prasad 2013; Dessie et al. 2014).

Mcguigan et al (1999) in his editorial note talked about the SODIS and use of sunlight to decontaminate drinking water in the developing countries. It was noted that how simple exposure to sunlight can be more economical, easier and simplest of an alternative to decontaminate the water. Similar system containing the array of transparent pipes facing to the sunlight would supply the water to complete village however the cost of installation, supply and the other factors disturbs the economics. It was noted that there is a strong synergy between the optical and thermal inactivation processes, temperature dictates the inactivation process. Table 2. provides the role of SODIS in inactivating different pathogens. (McGuigan et al. 1999).

Following factors should be ensured to enhance the efficiency of SODIS.

- Place the SODIS bags/PET bottles horizontally or at a flat angle facing the sun
- Use the raw water that has lower turbidity
- Place bottles on a sheet, roof top, or the ground which reflects sunlight
- Start exposing the bottles as early in the morning as possible, expose the bottle for about 6 h of bright sunlight
- Make sure that no shadow falls on the bottles.

In one such study Giannakis et al (2015) studied the environmental considerations on solar disinfection of waste water. The study was more focused on the effect analysis of different parameters like intensity of radiation, disturbance in the light delivery and the happenings during storage post-irradiation. It was concluded that based on the bacterial inactivation curves that when the illumination was intermittent it unevenly prolongs the exposure period. Hence extended illumination time is expected during such conditions. The disinfection kinetics was best described in the three phase; (a) first is induction/lag phase as the solar radiation begins (b) second is the monotonous inactivation period, this is prime phase where most inactivation is completed and (c) third is the tailing end when the rate is again lower towards closing. Overall it was understood from the study that tuning the parameters of the SODIS unit has to have a local oriented approach to make it more opt to the applications (Giannakis et al. 2015).

Table 2 Role of SODIS for various pathogens

Pathogens	Effect of SODIS
	<i>Load reduction >99%</i>
Bacteria	<ul style="list-style-type: none"> • E.coli • Vibrio cholera • Salmonella spp. • Shigella flexneri • Shigella dysenteriae • Campylobacter jejuni • Yersinia enterocolitica • Enterococcus faecalis Inactivation time of ~1 day
	<i>Load reduction</i>
Viruses	<ul style="list-style-type: none"> • Rotavirus 70–90% • Coliphages >90% • Encephalomyocarditis virus—Ineffective • Adenovirus—Ineffective • Polio virus—Ineffective Inactivation time of 1–2 day
	<i>Load reduction</i>
Protozoa	<ul style="list-style-type: none"> • Giardia >99% • Cryptosporidium 50–90% • Amoeba > 99% Inactivation time of up to 10 h to 3 day
	<i>Load reduction</i>
Fungi	<ul style="list-style-type: none"> • Ascaris suum > 90% • Fusarium solani ~70% • Candida albicans >90% Inactivation time of ~1 day

SODIS for waste water treatment plant was evaluated by Gutiérrez-Alfaro et al (2018). The evaluation was on the feasibility of integrating the solar disinfection technology along with the urban wastewater treatment plant having the processes based on microalgae biotechnology. The algal biotechnology consisted of an Up flow Anaerobic Sludge Blanket (UASB), High Rate Algal Ponds (HRAP) and a Dissolved Air Flotation (DAF). The author studied the efficiency of the SODIS process for the inactivation of *Escherichia coli*, *Enterococcus spp.* and *Clostridium perfringens* as indicator microorganisms with effect of irradiance and temperature. SODIS technology was found to be more effective for the two; *Escherichia coli*, *Enterococcus spp.* while DAF is better for *Clostridium perfringens*. It was concluded that the adding the SODIS unit with the WWTP improves the quality of treated water and increases the possibility of reuse (Gutiérrez-Alfaro et al. 2018).

SWINGS, a tie-up between the European Union and India for taking up projects on implementing the low-cost sustainable technologies for water treatment, disinfection and reuse targeting the population of rural India. Álvarez et al (2017) has reported on the SWINGS project on the constructed wetlands and solar-driven disinfection

technologies for rural India. The study focused to provide the sustainable wastewater treatment solution and reclamation of water resources. The study showcases the results from the two pilot plants one at Aligarh Muslim University, AMU and other at Indira Gandhi National Tribal University, IGNTU. The solar driven disinfection unit at IGNTU was able to produce the water quality that can be reused in for agriculture and irrigation purpose (Álvarez et al. 2017).

3.3 Visible Light Assisted Disinfection

Photocatalysis is the most cited way for pollutant degradation in water and wastewaters. Visible light holds a substantial range in the solar spectrum, making it more option to use it in water disinfection. Recently photocatalysts have been widely tested for their property of water disinfection. You et al. (2019) has given an extensive review on the topic of visible light active (VLA) photocatalysts for water disinfection. The review has reported the microbial disinfection efficiencies, recyclability characteristics, and disinfection mechanisms of different photocatalysts explored in the literature (You et al. 2019).

In a typical photo-catalytic mechanism, when the semiconductor material is irradiated with the visible light radiations, photons with higher energy than the bandgap of catalytic material are absorbed, and the electron from the valance band jumps to the conduction band. The process leaves behind a hole in the valence band and an electron in an excited state in the conduction band that is now available on the catalyst's surface. These electron-hole pair now acts as the base for generating radicals, hydroxyl and superoxide, through the reaction with oxidants and adsorbed water molecules. The reactive oxygen species so produced enter the microbial cells and cause inactivation. The susceptibility of different microbes to photocatalytic disinfection is not the same and is in this order: viruses > bacteria > yeasts > moulds (Bogdan et al. 2015). The precise mechanism for the inactivation is still not clear and can be further taken for research. Figure 6 gives the probable mechanism for the inactivation.

Although there is a wide pool of semiconductor materials, not all of them has the necessary properties to cause the inactivation of microbes. In recent times, the focus has been on developing semiconductor heterostructures that assist the charge transfer between the diverse photocatalysts. Doping with low-level impurities is another way to induce charge transfer.

3.4 Challenges and Perspectives

SODIS is undoubtedly one of the most simple, cheap and effective solutions for disinfecting the water and reducing the microbial load. The implications and outreach of the technology are high because the location does not constrain it.

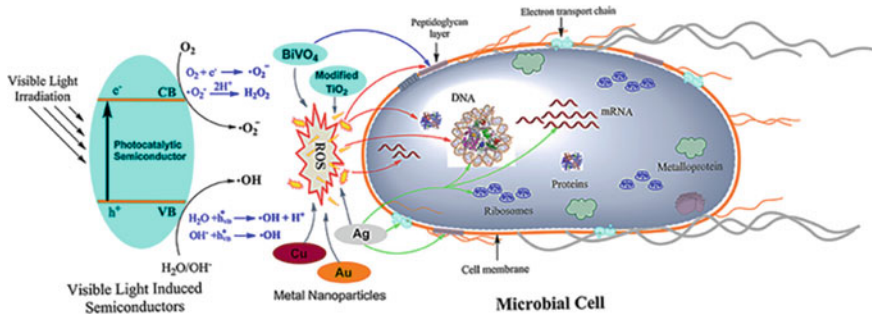


Fig. 6 The probable antimicrobial mechanisms of different photocatalytic semiconductors and their cellular targets. ROS—reactive oxygen species (You et al. 2019)

No process is full proof, and one needs to tune to the requirement of the process. Multiple parameters actually impact the SODIS process (Rincón and Pulgarin 2004; Blanco et al. 2009; Malato et al. 2009). These are.

- Water quality (pH, turbidity, chemical species)—the quality of water is crucial for the disinfection process. Content of any suspended solid particles, chemical species, organic matters or faecal material can add to the turbidity. The presence of these materials hinders the disinfection process. Some preliminary local filtration has to be carried out, be it sand filter/carbon filter to remove the unwanted materials before going for disinfection
- Nature of microorganism and microbial load—different organisms has different resistance, and the survival depends on the structure attacked during disinfection. The disinfectant can break through the cell wall/membrane and cause damage to the different elements of the cell (McGuigan et al. 1999; Byrne et al. 2011). This is the part of research where we need to look for the ability of SODIS and its limitations to handle some microbes.
- Exposure time for disinfection (refers to concentration and contact time). In abrupt weather conditions, when the sunlight will be less, the exposure time prolongs, and the disinfection process needs more time. Monitoring the microbial load is important in such cases.
- Temperature has a positive influence on disinfection. The disinfection efficiency improves with an increase in temperature. Developing the relation of sunlight intensity, exposure time, and microbial load concentration can set the guidelines for the applicants using the technology.
- Co-presence of other elements compounds might react or decompose during the process of disinfection and should be avoided. However, the disinfection process does not eliminate these components
- Monitoring the microbial load is crucial in understanding the progress and efficacy of the disinfection process. Faecal indicators reflect the presence of faecal contamination in the water and infer the load of microbes present. The

model organisms can be used to indicate pathogenic presence and behaviour, respectively.

4 Conclusion

Desalination and disinfection of water using solar-based technologies have added a newer avenue of looking at these processes. It is the step towards a sustainable and greener approach to get fresh, clean and safe water for all. Solar energy coupling with the desalination units has opened the arenas of innovative design and improved the efficacy of desalination so does the usage of renewable energy. Energy storage will dictate the future of these technologies. Solar energy comes as a feasible option for safe water, improving community health and providing a sustainable solution. Water disinfection has been conventionally done for cleaning water from micro-organisms in the water. However, chlorine-based and chemical-based disinfection that are common in practice has environmental concerns and health effects. Boiling remains as the energy intensive option. Solar-based disinfection has come out as the most efficient, eco-friendly, and economical water disinfection. Renewable energy-based water treatment will be the area of focus for the coming decades and will heavily impact the water remediation sector.

References

- Abd Elbar AR, Hassan H (2020) An experimental work on the performance of new integration of photovoltaic panel with solar still in semi-arid climate conditions. *Renew Energy* 146:1429–1443. <https://doi.org/10.1016/j.renene.2019.07.069>
- Abdel-Rehim ZS, Lasheen A (2005) Improving the performance of solar desalination systems. *Renew Energy* 30:1955–1971. <https://doi.org/10.1016/j.renene.2005.01.008>
- Ali MT, Fath HES, Armstrong PR (2011) A comprehensive techno-economical review of indirect solar desalination. *Renew Sustain Energy Rev* 15:4187–4199. <https://doi.org/10.1016/j.rser.2011.05.012>
- Alnaimat F, Klausner J, Mathew B (2018) Solar desalination. In: Eyvaz M, Yüksel E (eds) *Desalination and water treatment*. IntechOpen, pp 128–150
- Álvarez JA, Ávila C, Otter P, Kilian R, Istenič D, Rolletschek M, Molle P, Khalil N, Ameršek I, Mishra VK, Jorgensen C, Garfi A, Carvalho P, Brix H, Arias CA (2017) Constructed wetlands and solar-driven disinfection technologies for sustainable wastewater treatment and reclamation in rural India: SWINGS project. *Water Sci Technol* 76:1474–1489. <https://doi.org/10.2166/wst.2017.329>
- Amin MT, Han M (2009) Roof-harvested rainwater for potable purposes: application of solar disinfection (SODIS) and limitations. *Water Sci Technol* 60:419–431. <https://doi.org/10.2166/wst.2009.347>
- Amiri MC, Samiei M (2007) Enhancing permeate flux in a RO plant by controlling membrane fouling. *Desalination* 207:361–369. <https://doi.org/10.1016/j.desal.2006.08.011>
- Bergman RA (1995) Membrane softening versus lime softening in Florida: a cost comparison update. *Desalination* 102:11–24. [https://doi.org/10.1016/0011-9164\(95\)00036-2](https://doi.org/10.1016/0011-9164(95)00036-2)

- Blanco J, Malato S, Fernández-Ibañez P, Alarcón D, Gernjak W, Maldonado MI (2009) Review of feasible solar energy applications to water processes. *Renew Sustain Energy Rev* 13:1437–1445. <https://doi.org/10.1016/j.rser.2008.08.016>
- Bogdan J, Zarzyńska J, Pławińska-Czarnak J (2015) Comparison of infectious agents susceptibility to photocatalytic effects of nanosized titanium and zinc oxides: a practical approach. *Nanoscale Res Lett* 10:1–15. <https://doi.org/10.1186/s11671-015-1023-z>
- Bohn PW, Elimelech M, Georgiadis JG, Mariñas BJ, Mayes AM, Mayes AM (2009) Science and technology for water purification in the coming decades. *Nanosci Technol Collect Rev Nat J* 452:337–346. https://doi.org/10.1142/9789814287005_0035
- Buros OK (2000) *The ABCs of desalting*. MA: International Desalination Association, p. 30. Topsfield
- Byrne JA, Fernandez-Ibañez PA, Dunlop PSM, Alrousan DMA, Hamilton JWW (2011) Photocatalytic enhancement for solar disinfection of water: a review. *Int J Photoenergy* 2011. <https://doi.org/10.1155/2011/798051>
- Chandrashekhara M, Yadav A (2017) Water desalination system using solar heat: a review. *Renew Sustain Energy Rev* 67:1308–1330. <https://doi.org/10.1016/j.rser.2016.08.058>
- Curtis V, Cairncross S, Yonli R (2000) Review: domestic hygiene and diarrhoea—pinpointing the problem. *Trop Med Int Heal* 5:22–32. <https://doi.org/10.1046/j.1365-3156.2000.00512.x>
- Curto D, Franzitta V, Guercio A (2021) A review of the water desalination technologies. *Appl Sci* 11:1–36. <https://doi.org/10.3390/app11020670>
- Cyna B, Chagneau G, Bablon G, Tanghe N (2002) Two years of nanofiltration at the Méry-sur-Oise plant, France. *Desalination* 147:69–75. [https://doi.org/10.1016/S0011-9164\(02\)00578-7](https://doi.org/10.1016/S0011-9164(02)00578-7)
- Dessie A, Alemayehu E, Mekonen S, Legesse W, Kloos H, Ambelu A (2014) Solar disinfection: an approach for low-cost household water treatment technology in Southwestern Ethiopia. *J Environ Heal Sci Eng* 12:1–6. <https://doi.org/10.1186/2052-336X-12-25>
- El-Nashar AM, Samad M (1998) The solar desalination plant in Abu Dhabi: 13 years of performance and operation history. *Renew Energy* 14:263–274. [https://doi.org/10.1016/S0960-1481\(98\)00076-7](https://doi.org/10.1016/S0960-1481(98)00076-7)
- Fathb HES, Ghazy A (2002) Solar desalination using humidification—dehumidification technology. *Desalination* 142:119–133
- Fewtrell L (2014) Silver: water disinfection and toxicity. WHO, World Heal Organ, p 53
- Foran MM (2007) An analysis of the time to disinfection and the source water and environmental challenges in implementing a solar disinfection technology (SolAgua). *Dep Popul Int Heal* 50
- Giannakis S, Darakas E, Escalas-Cañellas A, Pulgarin C (2015) Environmental considerations on solar disinfection of wastewater and the subsequent bacterial (re)growth. *Photochem Photobiol Sci* 14:618–625. <https://doi.org/10.1039/c4pp00266k>
- Greenlee LF, Lawler DF, Freeman BD, Marrot B, Moulin P (2009) Reverse osmosis desalination: water sources, technology, and today's challenges. *Water Res* 43:2317–2348. <https://doi.org/10.1016/j.watres.2009.03.010>
- Gutiérrez-Alfaro S, Rueda-Márquez JJ, Perales JA, Manzano MA (2018) Combining sun-based technologies (microalgae and solar disinfection) for urban wastewater regeneration. *Sci Total Environ* 619–620:1049–1057. <https://doi.org/10.1016/j.scitotenv.2017.11.110>
- Helal AM, Al-Malek SA (2006) Design of a solar-assisted mechanical vapor compression (MVC) desalination unit for remote areas in the UAE. *Desalination* 197:273–300. <https://doi.org/10.1016/j.desal.2006.01.021>
- Herrera Melián JA, Doña Rodríguez JM, Viera Suárez A, Tello Rendón E, Valdés Do Campo C, Arana J, Pérez Peña J (2000) The photocatalytic disinfection of urban waste waters. *Chemosphere* 41:323–327. [https://doi.org/10.1016/S0045-6535\(99\)00502-0](https://doi.org/10.1016/S0045-6535(99)00502-0)
- Ise T, Tanabe Y, Sakuma F, Jordan O, Serrate E, Pena H (1994) Clinical evaluation and bacterial survey in infants and young children with diarrhoea in the Santa Cruz district, Bolivia. *J Trop Pediatr* 40:369–374. <https://doi.org/10.1093/tropej/40.6.369>

- Kabeel AE, El-Said EMS (2014) A hybrid solar desalination system of air humidification, dehumidification and water flashing evaporation: part II experimental investigation. *Desalination* 341:50–60. <https://doi.org/10.1016/j.desal.2014.02.035>
- Kabeel AE, El-Said EMS (2013) A hybrid solar desalination system of air humidification dehumidification and water flashing evaporation: a comparison among different configurations. *Desalination* 330:79–89. <https://doi.org/10.1016/j.desal.2013.10.004>
- Khan MZH, Al-Mamun MR, Majumder SC, Kamruzzaman M (2015) Water purification and disinfection by using solar energy: towards green energy challenge. *Aceh Int J Sci Technol* 4. <https://doi.org/10.13170/aijst.4.3.3019>
- Kuroda O, Takahashi S, Wakamatsu K, Itoh S, Kubota S, Kikuchi K, Eguchi T, Ikenaga Y, Sohma N, Nishinoiri K (1987) An electro dialysis sea water desalination system powered by photovoltaic cells. *Desalination* 65:161–169
- Lu Z, Xu L (2010) Freezing desalination process. In: Board IE (ed) *Thermal desalination processes*. UNESCO—Encyclopedia Life Support Systems
- Malato S, Fernández-Ibáñez P, Maldonado MI, Blanco J, Gernjak W (2009) Decontamination and disinfection of water by solar photocatalysis: recent overview and trends. *Catal Today* 147:1–59. <https://doi.org/10.1016/j.cattod.2009.06.018>
- Maroo SC, Goswami DY (2009) Theoretical analysis of a single-stage and two-stage solar driven flash desalination system based on passive vacuum generation. *Desalination* 249:635–646. <https://doi.org/10.1016/j.desal.2008.12.055>
- McCutcheon JR, McGinnis RL, Elimelech M (2005) A novel ammonia-carbon dioxide forward (direct) osmosis desalination process. *Desalination* 174:1–11. <https://doi.org/10.1016/j.desal.2004.11.002>
- McGuigan KG, Joyce TM, Conroy RM (1999) Solar disinfection: use of sunlight to decontaminate drinking water in developing countries. *J Med Microbiol* 48:785–787. <https://doi.org/10.1099/00222615-48-9-785>
- Moustafa SMA, Jarrar DI, El-Mansy H (1985) Performance of a self-regulating solar multistage flash desalination system. *Sol Energy* 35:333–340
- Nafeey AS, Sharaf MA, García-Rodríguez L (2010) Thermo-economic analysis of a combined solar organic Rankine cycle-reverse osmosis desalination process with different energy recovery configurations. *Desalination* 261:138–147. <https://doi.org/10.1016/j.desal.2010.05.017>
- Pugsley A, Zacharopoulos A, Mondol JD, Smyth M (2016) Global applicability of solar desalination. *Renew Energy* 88:200–219. <https://doi.org/10.1016/j.renene.2015.11.017>
- Qiblawey HM, Banat F (2008) Solar thermal desalination technologies. *Desalination* 220:633–644. <https://doi.org/10.1016/j.desal.2007.01.059>
- Qtaishat MR, Banat F (2013) Desalination by solar powered membrane distillation systems. *Desalination* 308:186–197. <https://doi.org/10.1016/j.desal.2012.01.021>
- Radjenović J, Petrović M, Ventura F, Barceló D (2008) Rejection of pharmaceuticals in nanofiltration and reverse osmosis membrane drinking water treatment. *Water Res* 42:3601–3610. <https://doi.org/10.1016/j.watres.2008.05.020>
- Rane MV, Padiya YS (2011) Heat pump operated freeze concentration system with tubular heat exchanger for seawater desalination. *Energy Sustain Dev* 15:184–191. <https://doi.org/10.1016/j.esd.2011.03.001>
- Richards BS, Schäfer AI (2010) Chapter 12 Renewable energy powered water treatment systems. *Sustain Sci Eng* 2:353–373. [https://doi.org/10.1016/S1871-2711\(09\)00212-8](https://doi.org/10.1016/S1871-2711(09)00212-8)
- Rickwood C, Carr. GM (2007) Global drinking water quality index development and sensitivity analysis report
- Rincón AG, Pulgarin C (2004) Field solar E. coli inactivation in the absence and presence of TiO₂: Is UV solar dose an appropriate parameter for standardization of water solar disinfection? *Sol Energy* 77:635–648. <https://doi.org/10.1016/j.solener.2004.08.002>
- Rizzo L, Della Sala A, Fiorentino A, Li Puma G (2014) Disinfection of urban wastewater by solar driven and UV lamp—TiO₂ photocatalysis: effect on a multi drug resistant Escherichia coli strain. *Water Res* 53:145–152. <https://doi.org/10.1016/j.watres.2014.01.020>

- Sarkar B, Venkateshwarlu N, Nageswara Rao R, Bhattacharjee C, Kale V (2007) Potable water production from pesticide contaminated surface water—a membrane based approach. *Desalination* 204:368–373. <https://doi.org/10.1016/j.desal.2006.02.041>
- Seckler D, Randolph B, Amarasinghe U (1999) Water Scarcity in the Twenty-first Century. *Int J Water Resour Dev* 15:29–42
- Sharaf MA, Nafey AS, García-Rodríguez L (2011) Exergy and thermo-economic analyses of a combined solar organic cycle with multi effect distillation (MED) desalination process. *Desalination* 272:135–147. <https://doi.org/10.1016/j.desal.2011.01.006>
- Sharon H, Reddy KS (2015) A review of solar energy driven desalination technologies. *Renew Sustain Energy Rev* 41:1080–1118. <https://doi.org/10.1016/j.rser.2014.09.002>
- Shatat M, Worall M, Riffat S (2013) Opportunities for solar water desalination worldwide: review. *Sustain Cities Soc* 9:67–80. <https://doi.org/10.1016/j.scs.2013.03.004>
- Shekarchi N, Shahnian F (2019) A comprehensive review of solar-driven desalination technologies for off-grid greenhouses. *Int J Energy Res* 43:1357–1386. <https://doi.org/10.1002/er.4268>
- Sohani A, Hoseinzadeh S, Berenjkari K (2021) Experimental analysis of innovative designs for solar still desalination technologies; An in-depth technical and economic assessment. *J Energy Storage* 33:101862. <https://doi.org/10.1016/j.est.2020.101862>
- Swiss Federal Institute for Environmental Science and Technology (EAWAG) (2002) Solar disinfection of water: a guide for the application of SODIS
- Ullah I, Rasul MG (2019) Recent developments in solar thermal desalination technologies: a review. *Energies* 12:119. <https://doi.org/10.3390/en12010119>
- Verma R, Prasad S (2013) Solar disinfection of water (SODIS): an approach of last century improving till today. In: *Hazardous waste management and healthcare in India*, p 3
- Vigneswaran VS, Kumaresan G, Dinakar BV, Kamal KK, Velraj R (2019) Augmenting the productivity of solar still using multiple PCMs as heat energy storage. *J Energy Storage* 26:101019. <https://doi.org/10.1016/j.est.2019.101019>
- Vyatskikh A, Kudo A, Delalande S, Greer JR (2018) Additive manufacturing of polymer-derived titania for one-step solar water purification. *Mater Today Commun* 15:288–293. <https://doi.org/10.1016/j.mtcomm.2018.02.010>
- WHO, UNICEF (200AD) Global water supply and sanitation assessment 2000 report
- Williams PM, Ahmad M, Connolly BS (2013) Freeze desalination: an assessment of an ice maker machine for desalting brines. *Desalination* 308:219–224. <https://doi.org/10.1016/j.desal.2012.07.037>
- Wu JW, Biggs MJ, Hu EJ (2010) Thermodynamic analysis of an adsorption-based desalination cycle. *Chem Eng Res Des* 88:1541–1547. <https://doi.org/10.1016/j.cherd.2010.04.004>
- Xia S, Li X, Liu R, Li G (2004) Study of reservoir water treatment by ultrafiltration for drinking water production. *Desalination* 167:23–26. <https://doi.org/10.1016/j.desal.2004.06.109>
- Yamali C, Solmus I (2008) A solar desalination system using humidification-dehumidification process: experimental study and comparison with the theoretical results. *Desalination* 220:538–551. <https://doi.org/10.1016/j.desal.2007.01.054>
- Yeh HH, Tseng IC, Kao SJ, Lai WL, Chen JJ, Wang GT, Lin SH (2000) Comparison of the finished water quality among an integrated membrane process, conventional and other advanced treatment processes. *Desalination* 131:237–244. [https://doi.org/10.1016/S0011-9164\(00\)90022-5](https://doi.org/10.1016/S0011-9164(00)90022-5)
- You J, Guo Y, Guo R, Liu X (2019) A review of visible light-active photocatalysts for water disinfection: features and prospects. *Chem Eng J* 373:624–641. <https://doi.org/10.1016/j.cej.2019.05.071>
- Zhang Y, Sivakumar M, Yang S, Enever K, Ramezani-pour M (2018) Application of solar energy in water treatment processes: a review. *Desalination* 428:116–145. <https://doi.org/10.1016/j.desal.2017.11.020>

Quantification of Potential Savings in Drinking Water Treatment Plants: Benchmarking Energy Efficiency



Shalini Nakkasunchi

Abstract The water industry accounts for about 30–40% of the total energy demand of the municipalities worldwide. This may vary from one facility to another based on the source, water quality, water storage, distance from the source, elevation, facility's age, and type of treatment techniques employed. Water abstraction and distribution are the highest energy consumption units among conventional water treatment facilities. Advanced treatment technologies, especially desalination (membrane and thermal) and disinfection technologies (ozone and ultraviolet), are the most energy consuming processes over the conventional treatment technologies. Various energy optimization measures such as the use of gravity for water transfer and distribution (where possible), selection of most energy and treatment efficient technologies, upgrading the treatment system and equipment (especially pumps), renewable energy generation at the facility, water conservation and restoration or protection of the potable water sources etc. can be employed to minimize the energy demand of the water treatment facilities. Application of these measures is challenging due to lack of adequate knowledge by the operational staff, lack of public awareness, investment cost involved, changes in future water treatment regulation with a growing population, pollutant load in the potable water bodies, etc. The current chapter discusses the possible energy intensive factors of the drinking water facilities with possible energy optimization measures and their limitations.

Keywords The treatment facility · Energy demand · Water abstraction · Water distribution · Water treatment · Energy efficiency

S. Nakkasunchi (✉)

Centre for Sustainable Technologies, Belfast School of Architecture and the Built Environment, Faculty of Computing, Engineering and the Built Environment, University of Ulster, County Antrim, Newtownabbey BT37 0QB, UK
e-mail: Nakkasunchi-S@ulster.ac.uk

1 Introduction

The water industry accounts for about 30–40% of the total energy demand of the municipalities worldwide (Biehl and Inman 2010; Copeland and Carter 2014). This is mainly due to energy demand at each stage of the water use cycle, i.e., raw water abstraction (from ground and surface water sources), treatment to potable grade and supply to the customers (GAO 2011). According to the World health organization (WHO), about 8% of the global population have no access to clean water (WHO 2017). Only 70% of the global population have access to clean water within the premises, and the rest need 30 min or above to collect from the source (WHO 2017; IEA 2020) (refer to Fig. 1). About 80% of the wastewater, including municipal and industrial wastewater, are discharged into the natural water bodies in addition to the agricultural runoff and storm waters leading to potable water source pollution (Kambole 2003; Lye 2009). These further increases energy demand for intensive treatment for potable use. Increased energy demand increases the carbon emissions from the water treatment facilities due to the continuous supply of electricity from

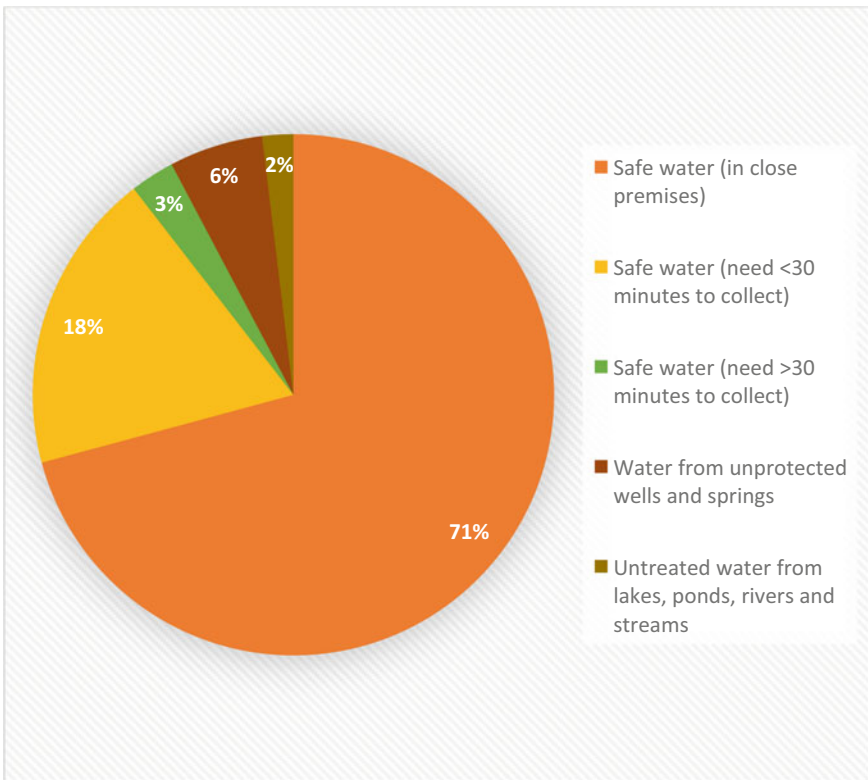


Fig. 1 Drinking water supply statistics from World Health Organization (WHO 2017)

gird, mainly generated from conventional fuel sources like coal, natural gas etc. (Presura and Robescu 2017). With an increase in population growth, water scarcity, stringent laws and environmental concerns, it is important to assess and optimize the energy demand of the water treatment facilities.

The energy demand of the drinking water treatment facilities varies based on the type of the water source (ground or surface), treatment technique employed (conventional or advanced), level of treatment etc. Section 2 describes various treatment techniques employed at the drinking water facility grouped under different stages based on the treatment intensity (level of treatment). This section also details the range (low to high) of the energy demand of the specific treatment stages and techniques. Section 3 discusses the key performance indicators to assess the energy demand of the drinking water treatment. Section 4 discusses the factors influencing the energy demand of the drinking water treatment facilities. Section 5 discusses the possible opportunities to reduce the energy demand of the drinking water treatment facilities. An overall conclusion of all the sections is given in the conclusion (Sect. 6).

2 Drinking Water Treatment and Its Energy Demand

The main role of the drinking water facilities is to treat the raw or source water to the potable level for human consumption. The drinking water facilities treat both surface water and groundwater to the required potable level based on the availability and quality of the resources available in the geographic location. The level of treatment given to the surface water is comparatively high over the groundwater due to higher pollutant loads (like organic and inorganic solids) in the surface waters due to various human, agricultural and industrial discharges (CDC 2015; Copeland and Carter 2014; OHIO 2021). Due to various waste discharges into the surface water bodies are highly susceptible to heavy metal pollution. Heavy metals such as chromium (Cr), cobalt (Co), copper (Cu), iron (Fe), magnesium (Mn), manganese (Mg), molybdenum (Mo), nickel (Ni), selenium (Se) and zinc (Zn) in minute quantities are beneficial for the human and environmental health. These, along with other heavy metals like arsenic (As), cadmium (Cd), chromium (Cr), lead (Pb), mercury (Hg) and silver (Ag) in larger quantities, are carcinogenic and toxic (Jarup 2003; Schwartzbord et al. 2013; Gleason et al. 2016). Removal of these heavy metals by typical drinking water treatment technics are ineffective (De Kwaadsteniet et al. 2013). Advanced treatment techniques such as adsorption (Cochrane et al. 2006; Davarnejad and Panahi 2016), electrochemical processes (Akbal and Camci 2011; Dharnaik and Ghosh 2014), ion exchange (Verma et al. 2008; Lai et al. 2016), membrane filtration (Landaburu-Aguirre et al. 2010; Rahmanian et al. 2011), solvent extraction (Lertlapwasin et al. 2010) etc., are the effective treatment techniques for the removal of heavy metals at a high operational cost due to high energy and material cost (Wołowiec et al. 2019). The level of treatment to the drinking water is categorized into different stages: raw water abstraction, screening, coagulation and flocculation, sedimentation, advanced treatment, filtration and disinfection. An overview of these stages and its energy

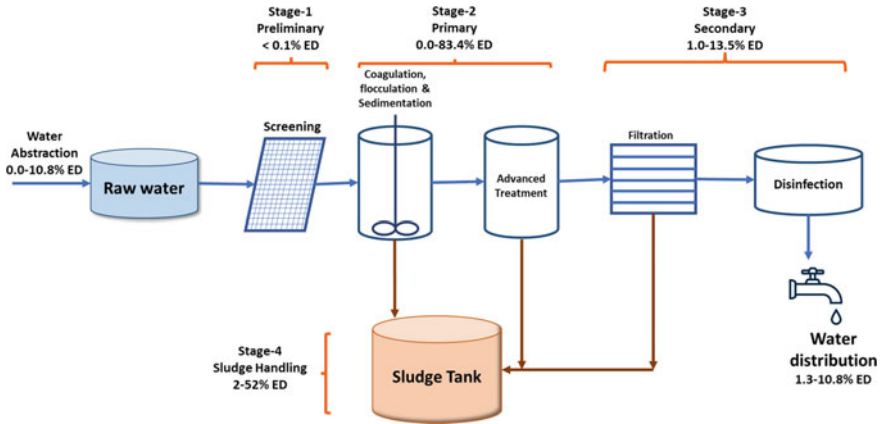


Fig. 2 Stages of drinking water treatment and its energy demand

demand are detailed below with the support of Fig. 2. The specific energy demand of the various stages involved in the drinking water facilities, i.e., water abstraction, water treatment and water distribution, are given in Table 1.

2.1 Water Abstraction

The surface water from sources like rivers, lakes, reservoirs, seas, oceans etc., are the most used drinking water source due to its easy access. The energy demand for surface water abstraction is highly dependent on the distance of water conveyance and the elevation profile of the water transfer location (Plappally and Leinhard 2012). The energy required for one cubic meter (m^3) of surface water abstraction for a kilometre (km) range between 0.0002 and 0.0073 kWh with an average energy demand of 0.0055 kWh (Stokes and Horvath 2009; Raluy et al. 2005; Plappally and Leinhard 2012).

Globally, about 25–40% of the drinking water is extracted from groundwater sources (NGWA 2016). Although the percentage of groundwater abstraction is lower than the surface water, the energy required to extract one cubic meter of groundwater is higher than that required for the surface water. The minimum energy required for water abstraction is 0.0027 kWh per meter of water lift. This value may increase to 0.64 kWh per every meter of water lift or above based on the water source and distance between the source and the treatment plant (Nelson et al. 2009; Rothausen and Conway 2011; Wang et al. 2012). The energy intensity of the groundwater abstraction is directly proportional to the water lift from the ground level (Plappally and Leinhard 2012).

Table 1 The energy demand of the water cycle at the drinking water treatment facility

Stage	Factor	Unit	Min	Max	Average	References
<i>Water abstraction</i>						
Water abstraction	Groundwater	kWh/m ³ /m	0.0027	0.64	0.137	Rothausen and Conway (2011), Nelson et al. (2009), Wang et al. (2012), Cohen et al. (2004), GAO (2011), Plappally and Leinhard (2012)
		kWh/m ³	0.14	3.3	0.77	Goldstein and Smith (2002), Rocheta and Peirson (2011), Plappally (2012a, b), McMahon and Price (2011), Fu and Zhong (2014), Gude et al. (2010), Gude (2011), Buonomenna (2013), Al-Karaghoul and Kazmerski (2013), CUWA (2012), Hu et al. (2013), Liu et al. (2013), Plappally (2012a, b), Sala and Serra (2004)
	Surface water	kWh/million gallons	–	–	1824	Goldstein and Smith (2002)
		kWh/m ³ /km	0.002	0.0073	0.0055	Plappally and Leinhard (2012), Stokes and Horvath (2009), Raluy et al. (2005), Muñoz et al. (2010)
		kWh/m ³	0.0002	1.74	0.60	Kenway et al. (2008), Fu and Zhong (2014), Gude et al. (2010), Gude (2011), Buonomenna (2013), Al-Karaghoul and Kazmerski (2013), CUWA (2012), Hu et al. (2013), Liu et al. (2013), Plappally (2012a, b), Sala and Serra (2004)
		kWh/annum ²	5.55×10^9	7.1×10^9	6.325×10^9	Maas (2010), Marsh 2008

(continued)

Table 1 (continued)

Stage	Factor	Unit	Min	Max	Average	References
	Unknown water source	kWh/m ³	0.04	2.4	0.5	Plappally and Leinhard (2012), Bukhary et al. (2020), Klein et al. (2005a, b), Sattenspiel and Wilson (2009), Gleick and Cooley (2009), Klein et al., (2005a, b), CEC (2005), CEC (2005) Sala (2007), Guillamón Álvarez (2007), Eltawil et al. (2008), Cramwincket al. (2006), Corominas (2009)
		kWh/million gallons	200	1800	1100	Arm and Phillips (2011)
	Overall water abstraction	kWh/m³	0.0002	3.3	0.623	
Water treatment						
Stage-1: Preliminary treatment	Screening	–	–	–	–	–
Stage-2: Primary treatment (conventional technologies)	Coagulation and Flocculation (Overall)	kWh/m ³	0.00015	0.42	0.042	Plappally and Leinhard 2012; Bukhary et al. (2020)
	Coagulation and Flocculation (Rapid mixing)	kWh/m ³	0.008	0.42	0.158	Plappally and Leinhard (2012), Khor et al. (2020), EPRI (2002)
	Coagulation and Flocculation (Slow mixing)	kWh/m ³	0.00084	0.00093	0.00089	Bukhary et al. (2020), Khor et al. (2020)
	Coagulation and Flocculation (Feed pump)	kWh/m ³	-	-	0.00063	Bukhary et al. (2020)
	Sedimentation/ Clarification	kWh/m ³	0.00012	0.035	0.015	Plappally and Leinhard (2012), Bukhary et al. (2020)
	Overall primary treatment	kWh/m³	0.00012	0.45	0.029	

(continued)

Table 1 (continued)

Stage	Factor	Unit	Min	Max	Average	References
Stage-2: Secondary treatment (Advanced technologies)	Reverse Osmosis (Brackish water)	kWh/m ³	1.0	2.5	1.75	Stokes and Horvath (2006)
	Reverse Osmosis (Sea/ocean water)	kWh/m ³	2.5	7.0	4.75	Siddiqi and Anadon (2011)
	Reverse Osmosis (Unknown water source)	kWh/m ³	0.36	8.5	2.93	IDA (2013), Plappally, (2012a, b), Sala and Serra (2004), Von Medeazza (2005)
	Reverse Osmosis (Overall)	kWh/m³	0.36	8.5	2.44	
	Nano filtration	kWh/m ³	–	–	0.92	IDA (2013)
	Electrodialysis	kWh/m ³	0.5	1.7	1.1	IDA (2013)
	Membrane technology (unknown)	kWh/m ³	0.26	0.40	0.33	Mika et al. (2018), WaterReuse Foundation (2015), Porse et al. (2020)
	Overall membrane technologies	kWh/m³	0.26	8.5	2.19	
	Multistage flash distillation	kWh/m ³	2.5	25.5	12.13	Siddiqi and Anadon (2011), DESWARE (2013)
	Multieffect distillation	kWh/m ³	6.5	11	8.75	DESWARE (2013)
Vapour compression	kWh/m ³	7	12	9.5	DESWARE, (2013)	

(continued)

Table 1 (continued)

Stage	Factor	Unit	Min	Max	Average	References
	Overall Thermal desalination	kWh/m³	2.5	25.5	10.63	
	Sea/ocean water desalination (unknown technology)	kWh/m ³	2.51	4	3.46	Mika et al. (2018), WasteReuse Foundation (2015), Porse et al. (2020), Rocheta and Peirson (2011)
	Desalination (unknown water source and technology)	kWh/m ³	3	5.9	4.93	Elimelech and Phillip, (2011a, b), Fu and Zhong (2014), Gude et al. (2010), Gude (2011), Buonomenna (2013), Al-Karaghoul and Kazmerski, (2013), CUWA (2012), Hu et al. (2013), Liu et al. (2013)
	Overall desalination/ Secondary treatment processes	kWh/m³	0.26	25.5	4.73	
Stage-3: Tertiary treatment	Disinfection	kWh/m ³	0.15	0.32	0.22	Bukhary et al. (2020), Klein et al. (2005a, b), CEC (2005)
Stage-4: Sludge treatment	Sludge dewatering (Filter press)	kWh/m ³	0.58	0.60	0.59	Bukhary et al. (2020)
	Overall surface water treatment	kWh/m³	0	1.24	0.60	ISAWWA (2012), Arm and Phillips (2011), Goldstein and Smith (2002)
	Overall ground water treatment	kWh/m³	0.48	0.79	0.63	ISAWWA (2012), Arm and Phillips (2011)

(continued)

Table 1 (continued)

Stage	Factor	Unit	Min	Max	Average	References
	Overall water treatment (unknown water source)	kWh/m ³	0.01	4.67	0.77	Wen et al. (2014) Smith et al. (2017), Plappally and Leinhard (2012), Bukhary et al. (2020), Klein et al. (2005a, b), Vadasarukkai and Gagnon 2015, ISAWWA (2012), Young (2015), Goldstein and Smith (2002), Meda et al. (2012), Smith et al. (2016), Friedrich (2002), Miller et al. (2013), Klein et al., (2005a, b), Arm and Phillips (2011), Mika et al. (2018), WaterReuse Foundation (2015), Porse et al. (2020), Marsh (2008), Kenway et al. (2008), EPA (2008), Gleick and Cooley (2009), CEC (2005), Sala (2007), Guillamón Álvarez (2007), Eltawil et al. (2008), Cramwincket al. (2006), Corominas (2009), Buckley et al. (2011)

(continued)

Table 1 (continued)

Stage	Factor	Unit	Min	Max	Average	References
Water distribution						
Water distribution	Residential and commercial buildings	kWh/m ³	0.12	0.39	0.27	Klein et al., (2005a, b), Arm and Phillips (2011), Klein et al. (2005a, b), CEC (2005), Sala (2007), Guillamón Alvarez (2007), Eltawil et al. (2008), Cramwincket al. (2006), Corominas (2009), Fu and Zhong (2014), Gude et al. (2010) Gude (2011), Buonomenna (2013), Al-Karaghoul and Kazmerski (2013) CUWA (2012), Hu et al. (2013), Liu et al. (2013)

Overall, irrespective of the water source, the energy intensity of the water abstraction for the drinking water facility ranges from 0.0002 kWh/m^3 to 3.3 kWh/m^3 (refer to Table 1) with an average value of 0.62 kWh/m^3 . This energy greatly varies from one plant to the other based on various factors detailed in Sect. 4.

2.2 Water Treatment

The quality of the groundwater greatly varies from the surface water. The surface water is highly polluted over the groundwater (GAO 2011) due to rain and storm water runoff, untreated or partially treated municipal and industrial wastewater etc. (Kambole 2003; Lye 2009; Karri et al. 2021) and require a higher level of treatment to meet the required/potable quality. The energy intensity of the surface and groundwater ranges between 0.00 and 1.24 kWh/m^3 and 0.48 – 0.79 kWh/m^3 with an average value of 0.60 kWh/m^3 and 0.63 kWh/m^3 , respectively. This proves that the energy intensity of the surface water treatment is high over the groundwater treatment (Arm and Phillips 2011; Plappally and Leinhard 2012; Bukhary et al. 2020). Further, the energy demand of individual treatment stage of drinking water differs based on the treatment technique employed. The drinking water treatment is categorized into five stages: preliminary, primary, secondary, tertiary, and sludge treatment.

2.2.1 Stage-1: Preliminary Treatment

The preliminary treatment of the drinking water involves the removal of the larger solids or debris using screens. Hence, this process is known as screening. This technique is employed mainly to avoid clogging or blockage in the pipelines and pumps at the drinking water facilities (NI Water 2007; GAO 2011; Wu et al. 2015). The energy required for this process is less than 1% of the plant's total energy.

2.2.2 Stage-2: Primary Treatment

Following the screening, water undergoes a chemical treatment called primary treatment. Here, water is supplied with the coagulants like alum, aluminium sulphate, ferrous sulphate, ferric chloride, sodium aluminate, activated silica, polymers etc., for the formation of flocs with the dissolved solids in the water under rapid or slow mixing of the coagulants with water. Mixing in the coagulation and flocculation tank enhances the formation of larger flocs, which are further allowed to settle in the sedimentation tank. The solids generated during the process are removed as sludge from the bottom of the sedimentation tank for further treatment, and the clarified water is transferred to the secondary or advanced treatment tanks or tertiary treatment tank, as per the requirement (GAO 2011; Plappally and Leinhard 2012; Wu et al. 2015).

Coagulation, flocculation and sedimentation are the most used conventional drinking water treatment techniques. These technologies are mainly adopted to remove some of the commonly found pollutants in the water (Jain et al. 2014). However, they are inefficient in removing other specific or emerging pollutants like personal care products, pharmaceuticals, pesticides from agricultural runoff, steroid hormones, other industrial compounds and natural organic matter (high concentrations). This is mainly due to change in these pollutants' physical and chemical characteristics from the common ones in the source water. Advanced treatment technologies such as ion exchange, adsorption, membrane technologies, solvent extraction, electrochemical processes etc., are some of the technologies used to remove specific pollutants from the source water (Jain et al. 2014; Park and Snyder 2020).

Adsorption is a highly used technique for removing the taste and odour causing compounds, disinfection by-products and its precursors and synthetic organic and inorganic chemicals/compounds (Jain et al. 2014). It is one of the effective and low-cost methods for removing specific pollutants (including virus) from the water. Commonly used adsorbents are activated carbon (Maneechakr and Karnjanakom 2017), biochar (Wang et al. 2018), clay (Bajda and Klapyta 2013; Bajda et al. 2015), nanomaterials (Gautam et al. 2014), organic polymers (He et al. 2017), reused sanding waste (Lim et al. 2009), zeolites (Petrus and Warchol 2005), water treatment residues (Ocinski et al. 2016; Jiao et al. 2017) etc. Factors such as temperature, pH and ionic strength of the source water and characteristics of the adsorption materials highly influence the removal of pollutants removed from the water (Joseph et al. 2019).

Ion exchange is one of the softening methods that are highly applicable for removing inorganic salts, organic solids and heavy metals from the water. This process involves the transfer of the feedwater over a packed bed called ion exchange resins, where the pollutant is removed by adsorbed onto the resin with the opposite charge. Based on the functional groups of the pollutants removed, the resins are classified as chelating ion exchange resin, anion exchange resin and cation exchange resin. These resins are either made of natural (zeolites) or synthetic (polymers) materials as per the quality of the raw and desired water (Sparks and Chase 2016; Kumar and Saravanan 2017).

Membrane technology is one of the highly efficient drinking water treatment techniques that uses pressure as a driving force for removing a wide range of selective contaminants from the water. Membranes are polymeric materials with varying pore sizes. Based on the pore size, membranes are characterized into porous (ultrafiltration and microfiltration), dense (reverse osmosis) and porous-dense membranes (nanofiltration) (Reif et al. 2013). The most used membrane technologies include reverse osmosis (Siddiqi and Anadon 2011), nanofiltration, microfiltration, electro dialysis (IDA 2013) etc. Reverse osmosis (RO) is one of the highly used seawater desalination technologies in the arid and semi-arid regions due to its ability in separating ions and high selective permeability (Reif et al. 2013). Nanofiltration (NF) is highly applicable for water with larger organic molecules and multivalent ions (Park and Snyder 2020).

Although membrane technologies are highly efficient in removing pollutants, they are energy intensive processes due to pressurized water supply through the

membrane for purification (Jacangelo et al. 1997; Plappally and Lienhard 2012; Zhang et al. 2016). The energy demand of these technologies ranges between 0.26 and 8.5 kWh/m³ treated water (Von Medeazza 2005; Mika et al. 2018; Porse et al. 2020). Among all the membrane technologies, the specific energy of RO technology (on average) is 2.19 kWh/m³, which is higher than the other membrane technologies. This is evident from Table 1.

Electrodialysis is applicable for the removal of ionic substances dissolved in the water. Over the other desalination processes like RO and NF, electrodialysis has high water recovery efficiency at low chemical and energy consumption (Hell and Lahnsteiner 2002). Multi-stage flash distillation is a water treatment technique employed for seawater desalination at high pressure by boiling seawater and then condensing with the incoming seawater to produce clean water. When run at low pressure using a series of evaporators and steam as a heat source to produce clean water, similar technology is called multi-effect distillation (Bragg-Sitton 2014). The process in which water vapor is compressed by mechanical or vacuum compression to produce water is called vapor compression (Garg 2019).

The total energy required for the conventional primary treatment processes is up to 1.5% of the total energy demand of the treatment plant and ranges between 0.00012 and 0.45 kWh/m³. The specific energy demand of the conventional process of the primary stage like coagulation and flocculation and sedimentation ranges between 0.00015 and 0.42 kWh/m³ and 0.00012–0.035 kWh/m³, respectively (Plappally and Leinhard 2012; Bukhary et al. 2020). Whereas the advanced primary water treatment may reach above 80%, with the highest being for thermal distillation processes due to high energy consumption to generate steam. The specific energy demand of the conventional and advanced treatment technologies (membrane and thermal) is given in Table 1.

2.2.3 Stage-3: Secondary Treatment

Any remaining solid particles from the primary treatment are largely removed from the water through the filtration process before its disinfection and distribution. Sand, gravel and activated carbon are the most used conventional filter media for drinking water filtration. This process also enhances the removal of colour and odour causing compounds from the water (GAO 2011; Plappally and Lienhard 2012; Zhang et al. 2016). Following the filtration, water is disinfected using controlled doses of chlorine to remove any pathogenic organisms before its distribution for human consumption (Ye et al. 2009; GAO 2011). In some cases, these conventional tertiary treatment techniques like sand filtration and chlorin disinfection are ineffective over organic and pathogen rich water. In such cases, the use of strong oxidants like ozone, hydrogen peroxide, and UV radiation can serve as a better option for removing organic pollutants and pathogens. This process is known as an advanced oxidation process. A single or combination of two or more oxidants can achieve good treatment efficiency and reduce costs involved in the process (Kumar et al. 2021; Verma et al. 2021). The nature of the pollutant, pH, and water temperature plays a vital role in these

processes (Kaur et al. 2020). The energy demand of the secondary treatment stages ranges between 1.0 and 13.5 kWh/m³ based on the type of treatment techniques employed and the quality of the water (Bukhary et al. 2020; Klein et al. 2005a, b; CEC 2005).

2.2.4 Stage-4: Sludge Treatment

Sludge generated during the primary and secondary treatment processes are further treated at the plant (dewatering and thickening) or are sent to the sludge treatment facilities for energy recovery before its disposal (to landfill). On average, around 10% of the total energy demand of the water treatment facility is towards sludge treatment (Bukhary et al. 2020).

2.3 Water Distribution

Treated water distribution is one of the highest energy consumption units of the water treatment facilities, which greatly varies based on the topography and the distance of the water transfer. The distribution system includes larger water pumps at the treatment facility, larger storage tanks (overhead), pipelines, valves, fire hydrants and water flow meters to measure water flow. Most water treatment facilities are designed to utilize gravity distribution for transferring treated water from the treatment facility to the consumers. The absence gravity distribution system may lead to high energy demand for water distribution (Smith and Liu 2017). The energy demand of this process ranges between 0.12 and 0.39 kWh/m³ (Klein et al. 2005a, b; Arm and Phillips 2011; Liu et al. 2013).

The highest energy demand among the water treatment stages is ranked for the primary advanced treatment techniques, especially thermal distillation and membrane technology. Water abstraction and distribution have an almost similar range of energy demand, which can be due to the water transfer distance from source to treatment plant and treatment plant to consumers.

3 Key Performance Indicator and Energy Benchmarking of Drinking Water Treatment Plant

No two water treatment plants have the same energy demand and are assessed using the same performance indicators. It is of significance to identify the key performance indicator (KPI) for the energy assessment of the water treatment facilities. The most used key energy performance indicators of water treatment facilities are,

Table 2 Key performance indicators for an energy assessment of the drinking water treatment plants

Key Performance Indicator (KPI)	Energy assessment parameter
kWh/m ³	Water treatment
kWh/m ³ /km	Surface water abstraction and treated water distribution
kWh/m ³ /m	Groundwater abstraction

- (i) Kilowatt hour per cubic meter (kWh/m³)
- (ii) Kilowatt hour per cubic meter per kilometre (kWh/m³/km)
- (iii) Kilowatt hour per cubic meter per metre (kWh/m³/m)
- (iv) Kilowatt hour per million gallons (kWh/mg).

Among these, kWh/m³ is the most used KPI for an energy assessment of the water treatment facilities globally. Whereas kWh/mg is the most used KPI for energy assessment in the United States. The KPI, kWh/m³/km, is highly suitable for addressing the energy demand of water abstraction from surface water sources as energy is required to transfer water from the source to the treatment facility, which highly varies based on distance water transfer. Whereas kWh/m³/m is highly suitable for accounting for the energy required for water abstraction from groundwater sources. Here, the energy is required to pump the water from the ground hence, the water source's depth from the ground level influences the energy required for the process. The KPIs suitable for an energy assessment of the water treatment facilities is given in Table 2.

The overall energy demand of the conventional water treatment facilities accounts for about 1.01–4.67 kWh/m³ with 0.01–1.24 kWh/m³ for surface water treatment and 0.48–0.79 kWh/m³ for groundwater treatment. This energy further increases to 8.5–25.5 kWh/m³ when advanced treatment technics like membrane filtration, thermal desalination etc., are applied for specific pollutant removals like inorganic salts and heavy metals. The energy required for water abstraction is larger than treated water distribution. This further varies based on the type of source and topography. The energy required for groundwater abstraction is approximately 85% higher than the energy required for surface water abstraction. This is evident from the numbers given in Table 1.

4 Factors Influencing Energy Demand of the Water Treatment Facilities and Its Optimization

Factors influencing the energy demand of the drinking water facility are the topography of the location (depth and distance water conveyed), source (ground or surface) and quality (organic or inorganic solids) of the water, type and level of treatment required etc. (GAO 2011; Gautam et al. 2014). These factors are further discussed below,

4.1 *Water Abstraction and Distribution*

The most used sources of water for potable use are surface water (like rivers, lakes, seawater etc.) and groundwater. The energy demand of water abstraction from ground and surface varies based on different factors. According to a study conducted by Wang et al. (2012), the energy demand of groundwater abstraction at two different locations in China, i.e., Shaanxi (0.64 kWh/m³) and Henan (0.30 kWh/m³), greatly vary from each other due to difference in the water lift at both the locations. Another study reported variation in the energy demand of the groundwater abstraction based on the change in the depth of groundwater (Cohen et al. 2004). Along with the water depth and lift, the volume of the water pumped and pump efficiency also plays a vital role in the energy intensity of groundwater abstraction (Bennett et al. 2010).

The specific energy of 3.3 kWh/m³ and 4.07 kWh/m³ of water transfer from surface water body to 450 km and 744 km was reported in Australia (Stokes and Horvath 2009) and Spain (Raluy et al. 2005; Munoz et al. 2010), respectively. This difference in the energy demand of the water transfer may be associated with the distance of water conveyance, topography/elevation profile of the location, friction and pipe diameter (Plappally and Lienhard 2012; Reardon et al. 2012). Generally, the energy intensity of groundwater abstraction is greater due to its elevation, which is unavoidable and may further increase with increasing elevation. Whereas, in the case of surface water, energy intensity is high when the water is transferred to a treatment plant or distributed to the consumers through an elevated path such as over the hilly locations or high-rise buildings (Arm and Phillips 2011). For example, the potable water demand of San Diego is supplied from the southern part of California over hundreds of miles through the Tehachapi Mountains. This water conveyance has been reported with large energy demand to the treatment facilities and great expenses to the customers for clean water access (GAO 2011). The use of gravity, where possible, can reduce the energy demand of the water transfer and distribution (Wu et al. 2015). The use of pressurized booster pumps for water distribution in high-rise buildings can reduce energy demand to some extent (Smith et al. 2017). Optimizing the hydraulic profile of the facility can reduce head losses, which in turn reduces the energy demand of the treatment facility (Capodaglio and Olsson 2020).

4.2 *Water Source and Quality*

The source water quality has a significant impact on the energy demand of the water treatment facilities. The water with a lower pollutant load may need less energy for treatment, whereas the water with a higher pollutant load may have high energy intensity due to the application of advanced treatment techniques, which may require energy for high pressure water pumping or mixing etc. The water source plays a vital role in the energy intensity of the water treatment. For example, the energy intensity of the Memphis city, which relies on groundwater, has less energy demand for water

treatment than Washington DC, which relies on surface water (GAO 2011). Most surface water available are highly polluted due to various anthropogenic activities like industries, agriculture runoff etc. (Wakeek et al. 2016).

There is also a possibility for the groundwater being highly polluted, especially with heavy metals due to runoffs from agricultural land or other sources and may need advanced treatment, which demands high energy (GAO 2011). Avoiding water abstraction from highly polluted water sources can reduce the energy intensity of the water treatment to a greater extent. In some cases, combining two or more water sources like surface and groundwater integrated treatment can reduce the energy involved in water treatment (Capodaglio and Olsson 2020).

4.3 Energy Audit

The first step in assessing the energy demand of the drinking water treatment facilities is by conducting an energy audit, which helps the treatment plant managers in identifying energy intensive factors at the plant (Capodaglio and Olsson 2020). The ASHRAE designed three levels of energy audits for an energy assessment. These are briefly discussed below (Greenberg 2011).

Level-1: Walkthrough a survey- This involves analysing the energy by visiting the plant to collect energy-related data from electricity bills, recorded process data (if available up to three years), basic energy measurements and interviewing the main decision makers at the plant. This helps in estimating the plant's energy use and provides possible low or no cost measures to improve the plant's energy efficiency. This also provides an energy benchmark for the plants to help choose and plan to implement the energy efficiency measures at the plant.

Level-2: Energy survey and analysis- It provides similar results to the Level-1 energy audit but in much more detail, which helps develop further control strategies for energy saving. A more detailed energy assessment is carried out in this level like energy demand of the different processes adopted by the plant, peak and off-peak energy data analysis, assessing the energy savings achieved by implementing energy saving measures etc. This further helps in much intense energy analysis.

Level-3: Detailed analysis of capital-intensive modifications- This is an intense analysis of energy data to plan the capital investment required to implement the energy efficiency measures at the plant. This may involve techno-economic modelling of the energy system to assess the suitability of the respective measures and the capital investment involved in applying such measures.

4.4 Maintenance and Equipment Upgrade

Maintenance of the treatment facility is one of the most significant factors for energy demand at the site. Regular maintenance of the treatment facility minimizes the

energy consumption at the plant. According to the energy assessment conducted by the American Society of Civil Engineers on the American water and wastewater treatment facilities, the use of old equipment (closer to the end of useful life) and infrastructure at most sites rank them with poor energy efficiency (GAO 2011). An improperly maintained, and old infrastructure is most energy inefficient. For example, an improperly maintained facility may have breaks or leaks within the water pipeline and may consume high energy to pump the water. According to a report published by the US Government Accountability Office on the energy needs of the water industry, about 50% of the water losses were identified due to the leakage in the pipelines. This further increased the energy demand of the water treatment facilities in transferring water from one point to other to meet the demand (OECD 2009; GAO 2011). The total energy lost by leakage in the water pipelines is largely unknown in most cases (Young 2015). It is impossible to visually identify any leaks and breaks in the water pipelines, as most infrastructure is underground. Identifying the specific location and severity of the leaks and breaks in the pipelines may require specific technology (Duffy 2017).

There are various acoustic and non-acoustic based technologies to detect leaks in the pipelines. The acoustic leak detection technology identifies the leakages in the pipeline by differentiating the water leak sound from the normal water flow sound. The most used acoustic water leak detection technologies are the listening rods, leak noise loggers, leak correlators etc. The non-acoustic leak detection technologies include infrared photography, ground penetrating radar technology, gas injection etc. (Li et al. 2015). The San Diego and south California water supplier, the San Diego County Water Authority, constantly monitors its pipelines for any leakages through fiber optic technology (GAO 2011). A drinking water treatment facility in Sydney, Australia, have achieved up to 38% of the energy saving in the water distribution by upgrading the flow monitoring device to minimize pipeline leakage (Brandt et al. 2012).

Among the various equipment used at the water treatment plants, pumps are the most energy intensive equipment, as water is pumped from the point of abstraction to various processes within the treatment plant and distribution. Varying flow rate and head at each stage of water pumping is the main cause of the energy demand. Minimizing the static head losses can reduce the significant energy demand of the treatment facility (Capodaglio and Olsson 2020). Further to this, the energy efficiency of the pumping system can be minimized by using the pumps at its designed speed. Most water treatment plants are designed to meet the future demands of water demand, which in some cases are over designed, and the operation of such a system may have high energy demand. Replacing larger and poor efficiency pumps with many small and energy efficient pumps to handle varying loads at the facility. Another energy efficient option to handle varying loads at the treatment plant is the use of variable frequency drive (VFD) pumps. VFD is highly suitable for the treatment facilities with varying load profiles, i.e., the treatment plants that do not have constant water demand. Constant speed pumps are highly suitable for the treatment plants with constant water demand (GAO, 2011). Application of VFD at the water collection system in Grobbendonk (Belgium) and at United Utilities in the UK saved

about 10–20% of the total energy associated with water pumping. Appropriate operation of the water valves, i.e., valve opening and closing according to the need, can reduce water leakage and associate energy in water pumping. Control of water flow between two water pumping stations in the Netherlands (Brakel and Bergambacht) reduce up to 19% of the energy demand of the water pumping system (Brandt et al. 2012). The right design and operation of the pumping system (pumps, valves, motors etc.) help reduce the energy demand of the pumping system at the treatment facility up to 50% (GAO 2011; Gautam et al. 2014).

4.5 Treatment and System Upgrade

The type of treatment technologies employed and the level of treatment given to the source water to achieve the desired quality of the potable water are the most significant factors for high energy intensity at the drinking water treatment facilities (GAO 2011). The level of the treatment given to the water is purely based on the quality of the source water (Majid et al. 2020). For example, desalination of the seawater and brackish groundwater have high energy demand compared to the surface water treatment (Arm and Phillips 2011). Selection of the water source that have low energy intensity or a combination of two or more water sources can serve as one of the energy efficient options, as it reduces the level of treatment to be given. For example, desalination of brackish groundwater can reduce the energy demand and operational cost of the system over seawater desalination due to its low salinity and low/no sediments (IAH 2015).

An overview of the energy demand of the varying treatment technologies are given in Fig. 3. Looking at the energy demand of the specific water treatment technologies,

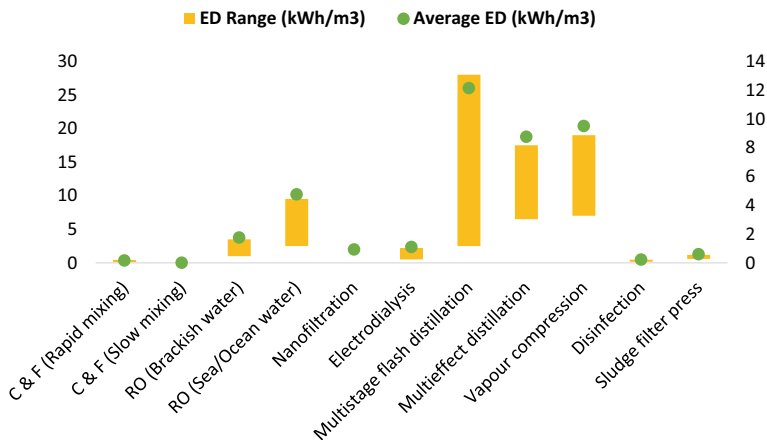


Fig. 3 Energy intensity of the different water treatment techniques (C & F = coagulation and flocculation; RO = Reverse osmosis)

the energy demand of the advanced treatment technologies is comparatively high over the conventional treatment technologies (evident from Fig. 3). A report published by US GAO (2011) on energy assessment of the water and wastewater treatment, use of the ultraviolet disinfection at the water treatment facilities in the US accounts for about 10–15% of the total energy demand the treatment facility. Similarly, filtration technology, especially membrane filtration, is the highest energy-intensive water treatment techniques due to the high-pressure water supply. The use of membrane materials that work under lower water pressure can minimize the energy associated with the membrane technologies (GAO, 2011).

It is of significance to optimize the treatment processes to achieve the desired water quality under reduced or no harmful treatment by-product production (like disinfection by-product formation), especially during chemical treatment (coagulation and disinfection) at reduced energy demand (Capodaglio and Olsson 2020). Application of dissolved air flotation can enhance the removal of the dissolved gases, which are not efficiently removed by conventional techniques like coagulation and sedimentation (Plappally and Lienhard 2012). The pollutant removal efficiency of the advanced water treatment technologies and their energy demand is interconnected with the pollutant removal by the conventional treatment technologies in the first place. Pre-treatment of the water using micro strainers, roughing filters, off-stream storage etc., can help to minimize the chemicals and energy used in the water treatment processes as it decreases the microbial activity in the water and reduces the organic matter and particulate matter in the water. Using an appropriate combination of treatment technologies based on the system requirement can reduce the energy associated with the water treatment (Capodaglio and Olsson 2020). Overall treatment process optimization can enhance the energy reduction of the system by up to 20% (CEE 2010; Copeland and Carter 2014).

Use control systems like online sensors or model-based control systems like supervisory control and data acquisition systems (SCADA). This system is operated centrally and helps monitor the energy intensive equipment and process with the possible operation of the equipment involved in the treatment automatically or by scheduling the operations (Capodaglio and Olsson 2020). Although the primary objective of the drinking water treatment facilities is to supply clean water to the consumers, it is also important for these facilities to have a good understanding of the energy consumption of the plant to minimize energy demand where possible (Gautam et al. 2014). Hence, hiring trained staff or providing training to the existing staff can further help identify the energy intensive process and timely application of the energy efficiency measures (Copeland and Carter 2014).

4.6 Renewable Energy Generation

There is a good scope of water treatment facilities to generate clean energy at the site using renewable energy resources like water flow, sun and wind. This reduces the carbon emission of the energy used at the plant, which is generated from fossil fuels.

According to a study conducted by Bukhary et al. (2020), a drinking water facility in the southwest of the US can generate 60% of the total energy demand of the facility by solar PV. Otay Water Treatment facility in San Diego generates clean energy using solar PV (945 kW) to meet the energy demand of the pumping system at the facility (GAO 2011). Solar energy generation at the treatment facilities is competitive with a reasonable payback but may need sufficient surface area to install the solar panels (Gautam et al. 2014).

The water system with large variation in the topography can replace the pressure reducing valves with the hydro turbines to generate electricity by utilizing the water flow (GAO 2011). Drinking water facility in Vienna, Austria, generates five times the energy consumed at the plant by hydropower turbine installation. Similarly, a drinking water facility in Athens, Greece, generates about 5 MW of electricity by diverting the treated water to a hydropower plant before its distribution to the consumers. Another drinking water facility in the north of Brussels, Belgium, generates about 18% of the total energy demand of the facility using hydropower turbines (Gautam et al. 2014). The drinking water network is also a good thermal and refrigeration energy recovery source. Research conducted by a drinking water facility in the Netherlands for thermal energy recovery proves that the water systems are potential enough for thermal/refrigeration energy recovery from the treated water with no impact on the treated water quality (van der Hoek et al. 2018).

4.7 Water Conservation and Others

Potable water resources available are not evenly distributed worldwide. Additionally, these resources are no longer potable due to various natural and anthropogenic activities and need a large amount of energy to treat them. It is challenging to supply - + -the clean water with increasing demand. In such a case, water conservation can serve as a direct and most effective energy saving measure for the water system. Reduction in water use reduces the energy involved in water pumping and treatment (Brandt et al. 2012; Wakeel et al. 2016). Some of the most effective water conservation measures include,

- *Suitable use-* Residential and commercial water consumers use potable water for all purposes, including the activities that may not need the potable water, such as landscaping or gardening. This increases water uses and, in turn, associated energy demand. Reclaimed water can reduce the energy involved in potable water generation (Young 2015). A large amount of hot water is used in the household in showers, dishwashing, cleaning. Avoiding hot water use where possible can reduce the associated energy etc. (GAO 2011). Setting up water use targets at local, regional and national levels can reduce the potable water use for various day to day activities. For example, In China, the government implemented a policy to save water in irrigation facilities by adopting advanced irrigation technologies

and efficient cropping structures. These measures are reported to save up to 17% of the water and energy involved in the agriculture sector (Li et al. 2016).

- *Improving household device efficiency*- using new or more efficient devices, i.e., efficient washing machines, dishwashers etc., in a residential building can save water and energy (Gautam et al. 2014).
- *Reduction in water leaks within the building*- timely identification and repair of the faulty toilet flushes and taps can reduce energy in pumping water due to water leakage (Gautam et al. 2014).
- *Use of toilet cisterns*- replacing the flush valves with the cisterns, especially with low capacity, can save water used in toilet flushing. Avoiding multiple flushing and use of flush friendly toilet paper can also save water to some extent (Gautam et al. 2014).
- *Rainwater harvesting*, where possible for non-potable water use like for landscaping, gardening, and toilet flushing can reduce water use (Gautam et al. 2014).
- *Community education*- conducting a water conservation program for the public by the involvement of the local communities helps in making the public understand the significance of water saving and, in turn, energy saving. This program may include all the above conservative measure discussion with the public in detail and helps them monitor any faults in the water distribution systems and plan for the supply of any future demands (Capodaglio and Olsson 2020).

Retrofitting and replacing the inefficient cisterns, pipes, taps etc., in the Mogale City, South Africa, reported about 30% of water (in turn energy) saving. Effective management of the groundwater resources and catchments can minimize the energy and operational cost of water treatment (Brandt et al. 2012; Capodaglio and Olsson 2020).

5 Barriers in Energy Optimization of the Drinking Water Treatment Facilities

Although many possible solutions are available for drinking water treatment facilities to optimise their energy, application these measures are limited due to various factors like costs associated, future changes in the regulations, lack of public awareness, lack of staff training, etc. (GAO 2011). For most water treatment facilities, energy management is secondary, as their primary aim is to supply potable water, complying with water regulations. For example, a drinking water treatment plant in San Diego opted ozonation for disinfection over other technologies (chlorination) due to its high disinfection efficiency and reduction of disinfection by-product formation (GAO 2011). Not many water treatment staff have adequate knowledge of energy management (including technologies and processes), especially in smaller treatment facilities. An operator with good knowledge of energy efficiency should be recruited to improve the energy efficiency of the treatment facilities, or appropriate training

should be provided to the existing staff. In some cases, the trained operators are hired on a part-time basis to help facilities to implement energy efficiency measures. The absence of the data available on the treatment plant energy demand can also limit the operators' decision-making on the energy efficiency measure implementation.

Most water treatment plants are old construction with a specific treatment technology for years. In such cases, the facility operators may alter or are reluctant to adopt new and more energy-efficient measures (technologies and processes) due to no appropriate evidence provided for its successful application at the water treatment facilities (GAO 2011; Capodaglio and Olsson 2020). In most cases, the application of the energy efficiency measures is cost intensive (especially for renewable energy systems) and exceeds the treatment facility's budget. Facilities with high payback or no cost recovery and high depreciation prices (for existing infrastructure) may delay implementing the energy efficiency measures (Gautam et al. 2014). Availability of energy incentives from the energy companies or the government can reduce the costs involved in implementing the energy efficiency measures (Nakkasunchi et al. 2021). Increasing pollutant loads in the source water may lead to stringent regulations in the future, further increasing the level of treatment given to the water. This may include more advanced treatment technologies like membrane filtration, ozonation etc., which are the highest energy consumers over the conventional techniques (GAO 2011).

6 Conclusion

The energy demand of the drinking water facility greatly varies from one facility to another based on various factors like level of treatment given to the source water, type of treatment technologies employed by the facilities, age of the treatment facility and equipment used, type of source water, pollutant load in the source water, location topography, facility maintenance etc. The energy demand of water sourcing can be minimized by a smart selection of the water sources based on the distance water travel and pollutant load. Use of gravity where possible in the water transfer and distribution can reduce energy to some extent in the water sourcing. The level of the water treatment and the treatment technologies employed at the facility is mainly dependent on the quality of the source water. Use of two or more sources of water where possible can minimize the energy intensity of the water treatment in regions with high pollutant load in the main water sources. Advanced treatment technologies are most energy consumers over the conventional ones, especially the membrane technology, ozonation, ultrafiltration etc. Despite their high energy intensity, these technologies are unavoidable in certain cases due to their high treatment efficiency. Selection of a good combination of the treatment technologies focusing on both treatment efficiency and energy minimization can serve as one of the better options for energy optimization. Upgrading the low energy efficient technologies and equipment with higher efficiency ones, especially in the case of the pumps use of varying frequency drivers, can minimize the energy demand of the treatment facility. Water

conservation and source water protection can reduce a greater amount of energy involved in the water treatment. Utilizing the topography and water flow rate in the water system, the water treatment facility can generate some energy required by the facility.

Along with this, the use of other renewable resources like sun and wind can also serve as the best option for energy generation at the facility. Most of the energy efficient solutions are limited in their application due to some factors like lack of adequate knowledge by the operational staff, high investments, considering energy as a secondary factor, lack of public awareness towards the energy associated with potable water supply, the possibility of changes in the future regulations due to increasing pollutant load in the water sources. Very limited data is available on the energy consumption of advanced technologies and their application at full-scale plants. Hence, further research is required in this aspect.

Acknowledgements The authors are thankful to Dr. Thiru Sambath and Dr. Rama Rao Karri for giving them this opportunity. This publication reflects only the authors' view and the Research Executive Agency, REA, is not responsible for any use that may be made of the information it contains.

References

- Akbal F, Camci S (2011) Copper, chromium and nickel removal from metal plating wastewater by electrocoagulation. *Desalination* 269:214–222
- Al- A, Kazmerski LL (2013) Energy consumption and water production cost of conventional and renewable-energy-powered desalination processes. *Renew Sustain Energy Rev* 24:343–356
- Arm S, Phillips C (2011) Chemical engineering for advanced aqueous radioactive materials separations. In: *Advanced separation techniques for nuclear fuel reprocessing and radioactive waste treatment*. Woodhead Publishing, pp 58–94
- Bajda T, Klapyta Z (2013) Adsorption of chromate from aqueous solutions by HDTMA-modified clinoptilolite, glauconite and montmorillonite. *Appl Clay Sci* 86:169–173
- Bajda T, Szala B, Solecka U (2015) Removal of lead and phosphate ions from aqueous solutions by organo-smectite. *Environ Technol* 36:2872–2883
- Bennett B, Park L, Wilkinson R (2010) Embedded energy in water studies: water agency and function component study and embedded energy—water load profiles. California Public Utilities Commission
- Biehl JW, Inman J (2010) *Am Water Works Assoc* 102:50
- Bragg-Sitton S (2014) Hybrid energy systems (HESs) using small modular reactors (SMRs) (No. INL/JOU-14-33543). Idaho National Laboratory (INL)
- Brandt MJ, Middleton RA, Wang S (2012) Energy efficiency in the water industry: a compendium of best practices and case studies-global report. Iwa Publishing
- Bukhary S, Batista J, Ahmad S (2020) An analysis of energy consumption and the use of renewables for a small drinking water treatment plant. *Water* 12(1):28
- Buckley C, Friedrich E, Von Blottnitz H (2011) Life-cycle assessments in the South African water sector: a review and future challenges. *Water Sa* 37(5):719–726
- Buonomenna MG (2013) Membrane processes for a sustainable industrial growth. *RSC Adv* 3(17):5694–5740

- Centre for Disease Control and Prevention (CDC) (2015) Water treatment: community water treatment. https://www.cdc.gov/healthywater/drinking/public/water_treatment.html. Accessed 20 Aug 2021
- California Energy Commission (CEC) California's water-energy relationship. Final staff report (2005)
- Capodaglio AG, Olsson G (2020) Energy issues in sustainable urban wastewater management: use, demand reduction and recovery in the urban water cycle. *Sustainability* 12(1):266
- Consortium for Energy Efficiency (2010) CEE National Municipal Water and Wastewater Facility Initiative, January 1, 2010, p 8
- Cochrane E, Lu S, Gibb S, Villaescusa I, Gibb S (2006) A comparison of low-cost biosorbents and commercial sorbents for the removal of copper from aqueous media. *J Hazard Mater* 137:198–206
- Cohen R, Nelson B, Wolff G (2004) Energy down the drain: the hidden costs of California's water supply. Natural Resources Defense Council, Pacific Institute
- Copeland C, Carter NT (2014) Energy-water nexus: the water sector's energy use
- Corominas MJ (2009) Agua y energía en el riego, en la época de la sostenibilidad, Comunicaciones de los invitados especiales. Paper presented at Jornadas de Ingeniería del Agua, Madrid
- Cramwinckel JF (2006) Water and energy nexus—Role of technology. *Re-thinking Water and Food Security*, p 309
- China Urban Water Association (CUWA) (2012). China urban water supply yearbook
- Davarnejad R, Panahi P (2016) Cu (II) removal from aqueous wastewaters by adsorption on the modified Henna with Fe₃O₄ nanoparticles using response surface methodology. *Sep Purif Technol* 158:286–292
- Duffy DP (2017) Successful water leak detection and audit methods. *Water World*. <https://www.waterworld.com/home/article/14070706/successful-water-leak-detection-and-audit-methods>. Accessed 20 Oct 2021
- Dharnaik AS, Ghosh PK (2014) Hexavalent chromium Cr(VI) removal by the electrochemical ion-exchange process. *Environ Technol* 35:2272–2279
- Electric Power Research Institute (2002) *Water & Sustainability (Vol. 4): US Electricity Consumption for Water Supply & Treatment- The Next Half Century*; Electric Power Research Institute Inc.: Palo Alto, CA
- Elimelech M, Phillip WA (2011a) The future of seawater desalination: energy, technology, and the environment. *Science* 333:712–717
- Elimelech M, Phillip WA (2011b). The future of seawater desalination: energy, technology, and the environment. *Science* 333(6043):712–717
- Eltawil MA, Zhengming Z, Yuan L (2008) Renewable energy powered desalination systems: technologies and economics-state of the art. In: Twelfth international water technology conference, IWTC12, pp 1–38
- EPA (2008) Energy: leveraging voluntary programs to save both water and energy. Environmental Protection Agency
- Friedrich E (2002) Life-cycle assessment as an environmental management tool in the production of potable water. *Water Sci Technol* 46(9):29–36
- Fu X, Zhong L (2014) Water-energy nexus of urban water systems for Chengdu's low-carbon blueprint. World Resources Institute, Beijing, China
- GAO U (2011) Energy-water nexus: amount of energy needed to supply, use and treat water is location-specific and can be reduced by certain technologies and approaches. Report to the ranking member committee on science, space and technology. US House of Representatives, Washington DC, pp 11–225
- Garg MC (2019) Renewable energy-powered membrane technology: cost analysis and energy consumption. In: *Current trends and future developments on (bio-) membranes*. Elsevier, pp 85–110
- Gautam RK, Sharma SK, Mahiya S, Chattopadhyaya MC (2014) Contamination of heavy metals in aquatic media: transport, toxicity and technologies for remediation
- Gleick PH, Cooley HS (2009) Energy implications of bottled water. *Environ Res Lett* 4(1):014009

- Goldstein R, Smith WEPRI (2002) Water & sustainability (volume 4): US electricity consumption for water supply & treatment-the next half century. Electric Power Research Institute
- Greenberg E (2011) Energy audits for water and wastewater treatment plants and pump stations. Continuing Education and Development, Inc.
- Gude VG, Nirmalakhandan N, Deng S (2010) Renewable and sustainable approaches for desalination. *Renew Sustain Energy Rev* 14(9):2641–2654
- Gude VG (2011) Energy consumption and recovery in reverse osmosis. *Desalin Water Treat* 36(1–3):239–260
- Guillamón Álvarez J (2007) Trasvase y desalación, las cifras y las cuentas. *Boletín*, (3)
- He Y, Liu QQ, Hu J, Zhao CX, Peng CJ, Yang Q, Wang HL, Liu HL (2017) Efficient removal of Pb(II) by amine functionalized porous organic polymer through post-synthetic modification. *Sep Purif Technol* 180:142–148
- Hell F, Lahnsteiner J (2002) The application of electrodialysis for drinking water treatment. In: Water resources quality. Springer, Berlin, Heidelberg, pp 315–327
- Hu G, Ou X, Zhang Q, Karplus VJ (2013) Analysis on energy–water nexus by Sankey diagram: the case of Beijing. *Desalin Water Treat* 51(19–21):4183–4193
- International Association of Hydrogeologists (IAH) (2015) Energy generation and groundwater. International Association of Hydrogeologists—Strategic overview series. <https://iah.org/wp-content/uploads/2015/11/IAH-Energy-Generation-Groundwater-Nov-2015.pdf>. Accessed 22 Oct 2021
- International Desalination Association (2013) IDA Desalination Yearbook 2012–2013
- IEA (2020) Introduction to the water-energy nexus, IEA, Paris. <https://www.iea.org/articles/introduction-to-the-water-energy-nexus>
- Jacangelo JG, Trussell RR, Watson M (1997) Role of membrane technology in drinking water treatment in the United States. *Desalination* 113(2–3):119–127
- Jain R, Camarillo MK, Stringfellow WT (2014) Drinking water security for engineers, planners, and managers. *Water Distrib Syst* 1–12
- Jiao J, Zhao JB, Pei YS (2017) Adsorption of Co(II) from aqueous solutions by water treatment residuals. *J Environ Sci* 52:232–239
- Joseph L, Jun BM, Flora JR, Park CM, Yoon Y (2019) Removal of heavy metals from water sources in the developing world using low-cost materials: a review. *Chemosphere* 229:142–159
- Karri RR, Ravindran G, Dehghani MH (2021) Wastewater—sources, toxicity, and their consequences to human health. In: Soft computing techniques in solid waste and wastewater management, Elsevier, pp 3–33
- Kaur R, Talan A, Tiwari B, Pilli S, Sellamuthu B, Tyagi RD (2020) Constructed wetlands for the removal of organic micro-pollutants. In: Current developments in biotechnology and bioengineering. Elsevier, pp 87–140
- Kenway SJ, Priestley A, Cook S, Seo S, Inman M, Gregory A, Hall M (2008) Energy use in the provision and consumption of urban water in Australia and New Zealand. Water Services Association of Australia (WSAA), Sydney, Australia
- Klein G, Krebs M, Hall V, O'Brien T, Blevins B (2005a) California's water-energy relationship. California Energy Commission: Sacramento, CA, USA
- Klein G, Krebs M, Hall V, O'Brien T, Blevins BB (2005b) California's water–energy relationship. California Energy Commission, pp 1–180
- Kumar PS, Saravanan A (2017) Sustainable wastewater treatments in textile sector. In: Sustainable fibres and textiles. Woodhead Publishing, pp 323–346
- Lai Y-C, Chang Y-R, Chen M-L, Lo Y-K, Lai J-Y, Lee D-J (2016) Poly(vinyl alcohol) and alginate cross-linked matrix with immobilized Prussian blue and ion exchange resin for cesium removal from waters. *Bioresour Technol* 214:192–198
- Landaburu J, Pongracz E, Peramaki P, Keiski RL (2010) Micellar-enhanced ultrafiltration for the removal of cadmium and zinc: Use of response surface methodology to improve understanding of process performance and optimization. *J Hazard Mater* 180:524–534

- Lertlapwasin R, Bhawawet N, Imyim A, Fuangswasdi S (2010) Ionic liquid extraction of heavy metal ions by 2-aminothiophenol in 1-butyl-3-methylimidazolium hexafluorophosphate and their association constants. *Sep Purif Technol* 72:70–76
- Li R, Huang H, Xin K, Tao T (2015) A review of methods for burst/leakage detection and location in water distribution systems. *Water Sci Technol Water Supply* 15(3):429–441
- Lim JW, Chang YY, Yang JK, Lee SM (2009) Adsorption of arsenic on the reused sanding wastes calcined at different temperatures. *Colloids Surf A Physicochem Eng Asp* 345:65–70
- Liu J, Zang C, Tian S, Liu J, Yang H, Jia S, You L, Liu B, Zhang M (2013) Water conservancy projects in China: achievements, challenges and way forward. *Glob Environ Chang* 23(3):633–643
- Maas C (2010) Ontario's water-energy nexus: will we find ourselves in hot water... or tap into opportunity? POLIS Project on Ecological Governance, University of Victoria
- Majid A, Cardenes I, Zorn C, Russell T, Colquhoun K, Bañares-Alcantara R, Hall JW (2020) An analysis of electricity consumption patterns in the water and wastewater sectors in South East England UK. *Water* 12(1):225
- Maneechakr P, Karnjanakom S (2017) Adsorption behaviour of Fe(II) and Cr(VI) on activated carbon: surface chemistry, isotherm, kinetic and thermodynamic studies. *J Chem Thermodyn* 106:104–112
- Marsh D (2008) The water-energy nexus: a comprehensive analysis in the context of New South Wales (Doctoral Dissertation). Sydney, University of Technology, Sydney, Australia, Faculty of Engineering and Information Technology
- McMahon JE, Price SK (2011) Water and energy interactions. *Annu Rev Environ Resour* 36:163–191
- Meda A, Lensch D, Schaum C, Cornel P, Lazarova V, Choo KH (2012) Energy and water: relations and recovery potential. *Water. Energy interactions in water reuse*, pp 21–35
- Miller LA, Ramaswami A, Ranjan R (2013) Contribution of water and wastewater infrastructures to urban energy metabolism and greenhouse gas emissions in cities in India. *J Environ Eng* 139(5):738–745
- Muñoz I, Milà L, Fernández AR (2010) Life cycle assessment of water supply plans in Mediterranean Spain: the Ebro River transfer versus the AGUA Programme. *J Ind Ecol* 14(6):902–918
- Nakkasunchi S, Hewitt NJ, Zoppi C, Brandoni C (2021) A review of energy optimization modelling tools for the decarbonization of wastewater treatment plants. *J Cleaner Product* 279:123811
- National Groundwater Association (NGWA) (2016) Facts about global groundwater usage. National Ground Water Association, <http://www.ngwa.org/Fundamentals/Documents/globalgroundwater-use-fact-sheet.pdf>
- Nelson GC, Robertson R, Msangi S, Zhu T, Liao X, Jawajar P (2009) Greenhouse gas mitigation: issues for Indian agriculture. *Intl Food Policy Res Inst*
- Northern Ireland Environment Agency (2020) Compliance with Drinking Water Quality Standards in Northern Ireland, 2019. <https://www.daera-ni.gov.uk/sites/default/files/publications/daera/Compliance%20with%20Drinking%20Water%20Standards%2C%202019.pdf>. Accessed 20 Aug 2021
- Ocinski D, Jacukowicz-Sobala I, Mazur P, Raczyk J, Kociolek-Balawejder E (2016) Water treatment residuals containing iron and manganese oxides for arsenic removal from water—characterization of physicochemical properties and adsorption studies. *Chem Eng J* 294:210–221
- OECD (2009) Managing water for all: an OECD perspective on pricing and financing. Organization for economic co-operation and development
- OHIO University (2021) The 4 steps of treating your community's water. <https://onlinemasters.ohio.edu/blog/the-4-steps-of-treating-your-communitys-water/>. Accessed 20 Aug 2021
- Park M, Snyder SA (2020) Attenuation of contaminants of emerging concerns by nanofiltration membrane: rejection mechanism and application in water reuse. In *Contaminants of Emerging Concern in Water and Wastewater* (pp. 177–206). Butterworth-Heinemann.
- Petrus R, Warchol JK (2005) Heavy metal removal by clinoptilolite. An equilibrium study in multi-component systems. *Water Res* 39:819–830

- Plappally A, Leinhard J (2012) Energy requirements for water production, treatment, end use, reclamation, and disposal. *Renew Sustain Energy Rev* 16:4818–4848
- Plappally AK, Lienhard JH (2012) *Renew Sustain Energy Rev* 16:4818
- Plappally AK (2012a) Energy requirements for water production, treatment, end use, reclamation, and disposal. *Renew Sustain Energy Rev* 16(7):4818–4848
- Plappally AK (2012b) Energy requirements for water production, treatment, end use, reclamation, and disposal. *Renew Sustain Energy Rev* 16(7):4818–4848
- Porse E, Mika KB, Escriva-Bou A, Fournier ED, Sanders KT, Spang E, Stokes-Draut J, Federico F, Gold M, Pincetl S (2020) Energy use for urban water management by utilities and households in Los Angeles. *Environ Res Commun* 2(1):015003
- Rahmanian B, Pakizeh M, Esfandyari M, Heshmatnezhad F, Maskooki A (2011) Fuzzy modeling and simulation for lead removal using micellar-enhanced ultrafiltration (MEUF). *J Hazard Mater* 192:585–592
- Raluy RG, Serra L, Uche J, Valero A (2005) Life cycle assessment of water production technologies-Part 2: reverse osmosis desalination versus the Ebro river water transfer (9 pp). *Int J Life Cycle Assess* 10(5):346–354
- Reardon DJ, Newell PL, Roohk DL (2012) Recycling conserves both water and energy. *Proc Water Environ Fed* 2012(13):3557–3564
- Reif R, Omil F, Lema JM (2013) Removal of pharmaceuticals by membrane bioreactor (MBR) technology. In: *Comprehensive analytical chemistry*, vol 62, Elsevier, pp 287–317
- Rocheta E, Peirson W (2011) Urban water supply in a carbon constrained Australia. UNSW Water Research Centre
- Rothausen SG, Conway D (2011) Greenhouse-gas emissions from energy use in the water sector. *Nat Clim Chang* 1(4):210–219
- Sala L, Serra M (2004) Towards sustainability in water recycling. *Water Sci Technol* 50(2):1–7
- Sala L (2007) Balances energéticos del ciclo de agua y experiencias de reutilización planificada en municipios de la Costa Brava. *Energía y Cambio Climático*, Universidad Politécnica, Valencia, Seminario Agua
- Sattenspiel BG, Wilson W (2009) The carbon footprint of water. Report by the Energy Foundation
- Siddiqi A, Anadon LD (2011) The water–energy nexus in Middle East and North Africa. *Energy Policy* 39:4529–4540
- Smith K, Liu S, Chang T (2016) Contribution of urban water supply to greenhouse gas emissions in China. *J Ind Ecol* 20(4):792–802
- Smith K, Liu S, Liu Y, Liu Y, Wu Y (2017) *Energy Build* 135:119
- Smith K, Liu S (2017) Energy for conventional water supply and wastewater treatment in urban China: a review. *Global Chall* 1(5):1600016
- Sparks T, Chase G (2016) Section 5-Solid–Liquid Filtration–Examples of Processes. In: *Filters and filtration handbook*, pp 297–359
- Stokes J, Horvath A (2006) Life cycle energy assessment of alternative water supply systems. *Int J Life Cycle Assess* 11:335–343
- Stokes JR, Horvath A (2009) Energy and air emission effects of water supply
- Vadasarukkai YS, Gagnon GA (2015) Application of low-mixing energy input for the coagulation process. *Water Res* 84:333–341
- van der Hoek JP, Mol S, Giorgi S, Ahmad JI, Liu G, Medema G (2018) Energy recovery from the water cycle: thermal energy from drinking water. *Energy* 162:977–987
- Verma V, Tewari S, Rai J (2008) Ion exchange during heavy metal bio-sorption from aqueous solution by dried biomass of macrophytes. *Bioresour Technol* 99:1932–1938
- Von Medeazza GM (2005) “Direct” and socially-induced environmental impacts of desalination. *Desalination* 185(1–3):57–70
- Wang J, Rothausen SG, Conway D, Zhang L, Xiong W, Holman IP, Li Y (2012) China’s water–energy nexus: greenhouse-gas emissions from groundwater use for agriculture. *Environ Res Lett* 7(1):014035

- Wang YY, Liu YX, Lu HH, Yang RQ, Yang SM (2018) Competitive adsorption of Pb(II), Cu(II), and Zn(II) ions onto hydroxyapatite-biochar nanocomposite in aqueous solutions. *J Solid State Chem* 261:53–61
- Wen H, Zhong L, Fu X, Spooner S (2014) Water energy nexus in the urban water source selection: a case study from Qingdao. World Resources Institute, Beijing
- Wołowiec M, Pruss A, Komorowska-Kaufman M, Lasocka-Gomuła I, Rzepa G, Bajda T (2019) The properties of sludge formed as a result of coagulation of backwash water from filters removing iron and manganese from groundwater. *SN Appl. Sci.* 1:639
- Wu K, Liu RP, Li T, Liu HJ, Peng JM, Qu JH (2013) Qu, JH Removal of arsenic(III) from aqueous solution using a low-cost by-product in Fe-removal plants-Fe-based backwashing sludge. *Chem Eng J* 226:393–401
- Ye B, Wang W, Yang L, Wei JXE (2009) *J Hazard Mater* 171:147
- Young R (2015) A survey of energy use in water companies. American Council for an Energy-Efficient Economy
- Zhang X, Qi Y, Wang Y, Wu J, Lin L, Peng H, Qi H, Yu X, Zhang Y (2016) *Renew Sustain Energy Rev* 64:660